

Dr. 1813 - 9

DOE/PO/10288-2(Vol.2)
(DE83016196)

WEST HACKBERRY STRATEGIC PETROLEUM RESERVE SITE BRINE
DISPOSAL MONITORING, YEAR I REPORT

Final Report. Volume II: Physical and Chemical Oceanography

February 1983

Work Performed Under Contract No. AC96-80PO10288

McNeese State University
Lake Charles, Louisiana

and

Texas A&M University
College Station, Texas

McNEESE STATE UNIVERSITY
LAKE CHARLES, LOUISIANA



U. S. DEPARTMENT OF ENERGY

DISCLAIMER

This report was prepared as an account of work sponsored by an agency of the United States Government. Neither the United States Government nor any agency Thereof, nor any of their employees, makes any warranty, express or implied, or assumes any legal liability or responsibility for the accuracy, completeness, or usefulness of any information, apparatus, product, or process disclosed, or represents that its use would not infringe privately owned rights. Reference herein to any specific commercial product, process, or service by trade name, trademark, manufacturer, or otherwise does not necessarily constitute or imply its endorsement, recommendation, or favoring by the United States Government or any agency thereof. The views and opinions of authors expressed herein do not necessarily state or reflect those of the United States Government or any agency thereof.

DISCLAIMER

Portions of this document may be illegible in electronic image products. Images are produced from the best available original document.

WEST HACKBERRY STRATEGIC PETROLEUM RESERVE SITE BRINE DISPOSAL MONITORING

YEAR I REPORT
FINAL REPORT

VOLUME II
PHYSICAL AND CHEMICAL OCEANOGRAPHY

EDITORS

L. R. DeRouen, Project Leader
R. W. Hann, Project Manager
D. M. Casserly, Technical Director
C. Giammona, Deputy Project Manager
V. J. Lascara, Field Coordinator

PRINCIPAL INVESTIGATORS

J. Beck, Special Pollutants
G. Gaston, Benthos
R. Ilg, Nekton
W. P. James, Hydrology and Hydrography
L. Jeffrey, Sediment and Water Quality
F. Kelly, Physical Oceanography
R. Maples, Phytoplankton
R. Randall, Hydrology and Hydrography
F. Slowey, Sediment Quality
S. Swetharanyam, Data Management
M. Vecchione, Zooplankton
D. Weston, Benthos
G. Wolff, Data Management

Prepared for the

DEPARTMENT OF ENERGY
STRATEGIC PETROLEUM RESERVE PROJECT MANAGEMENT OFFICE

Under

DOE CONTRACT NUMBER: DE-AC96-80PO10288

By

McNeese State University
Lake Charles, Louisiana

Texas A & M University
College Station, Texas
through the
Texas A & M
Research Foundation

February, 1983

TABLE OF CONTENTS

CHAPTER 1. INTRODUCTION	
1.1 Introduction	1-1
1.2 Characteristics of the SPR West Hackberry Study Area	1-6
1.3 Brine Discharge Data	1-12
CHAPTER 2. PHYSICAL OCEANOGRAPHY	
2.1 Introduction	2-1
2.2 Monthly Hydrographic Data	2-5
2.3 Meteorology and River Runoff	2-61
2.4 In situ Instrumentation	2-70
2.5 Discussion of Circulation and Hydrography in the West Hackberry Region	2-120
2.6 Summary and Conclusions	2-178
CHAPTER 3. ESTUARINE HYDROLOGY AND HYDROGRAPHY	
3.1 Introduction	3-1
3.2 Hydrology	3-5
3.3 Estuarine Hydrography	3-46
3.4 Summary of Results	3-73
3.5 Conclusions and Recommendations	3-76
CHAPTER 4. ANALYSIS OF DISCHARGE PLUME	
4.1 Introduction	4-1
4.2 Plume Measuring Equipment	4-7
4.3 Brine Plume Measurement Procedures	4-12
4.4 Areal Extent and Salinity of Measured Brine Plumes	4-20
4.5 Vertical Salinity Profiles	4-38

4.6 Vertical Dissolved Oxygen Profiles 4-55

4.7 Empirical Prediction of Plumes for the West
Hackberry Diffuser 4-71

4.8 Summary of Brine Plume Measurement Results 4-94

4.9 Conclusions and Recommendations 4-102

CHAPTER 5. WATER AND SEDIMENT QUALITY: SPECIAL POLLUTANT SURVEY

5.1 Water Quality Studies 5-1

5.2 Sediment Quality 5-38

5.3 Special Pollutant Survey 5-56

LIST OF TABLES

TABLE	PAGE
1-1 Longitude and latitude of West Hackberry offshore sampling stations	1-5
2-1 Latitude, longitude and LORAN C coordinates for the monthly offshore hydrographic sampling stations	2-7
2-2 In situ instrumentation information	2-70
2-3 Summary of monthly joint frequency distributions of speed and direction for site D	2-108
2-4 Average magnitude and direction of major axes of tidal current ellipses for site D	2-111
2-5 Average amplitude of the given tidal constituents for the current in Calcasieu Pass	2-112
2-6 Mean amplitude of tidal constituents along major axis of current ellipse	2-120
2-7 Mean current for period June 1, 1981 thru January 27, 1982 .	2-120
2-8 Comparison of advective length scales	2-121
3-1 Longitude and latitude for the ten estuarine stations	3-4
3-2 Drainage area contributing to ungauged surface runoff	3-15
3-3 Ungauged freshwater inflow expressed as a percent of total freshwater inflow	3-27
3-4 Salinity/Freshwater inflow regression analysis for Sabine . . .	3-30
3-5 Critical low flows for Calcasieu Lake and percent of time during dry period that flow is less than critical	3-33
3-6 Critical low flows for Sabine Lake and percent of time during dry period that flow is less than critical	3-34
3-7 Estimated salinity of the diverted water	3-37
3-8 Estimated change in salinity caused by pumping 70 cfs water . .	3-38
3-9 Estimated change in salinity caused by pumping 50 cfs water . .	3-39
3-10 Summary of model results	3-44

3-11	Average post disposal hydrographic data for Calcasieu Lake, raw water intake, and Sabine Lake	3-67
4-1	Summary of West Hackberry brine plume areal extent data	4-37
4-2	Summary of maximum measured distances from center of diffuser to above ambient salinity contours	4-39
4-3	Comparison of measured and computed vertical extent of brine plume	4-55
5-1	Average mean diameters and standard deviations of sediments	5-38
5-2	Summary of monthly total organic carbon concentrations	5-44
5-3	Summary of monthly pore water salinity for sediments	5-50
5-4	List of parameters to be measured in Special Pollutant sampling task	5-57
5-5	Major ion concentrations in water and sediment at the intake structure, brine pond and diffuser site	5-65
5-6	Total metal concentrations in water at the intake structure, brine pond and diffuser and sediments at the intake structure and diffuser site	5-67
5-7	Total metal concentration in selected benthic biota at the diffuser site	5-68
5-8	Concentrations of hydrocarbons in sediments collected at the intake structure and diffuser site	5-69
5-9	Pesticides and herbicides in water, sediment and selected biota at the intake structure, brine pond, and diffuser site	5-71

LIST OF FIGURES

FIGURE		PAGE
1-1	Area map of Texas-Louisiana showing inland and offshore station locations	1-2
1-2	Area map of Calcasieu Lake area in Louisiana showing station locations	1-6
1-3	Daily values for temperature, salinity, volume and salt loading of brine discharge	1-12
1-4	Mean salinities at surface, middle, and bottom depths along a west-east transect	1-14
1-5	Mean salinities at surface, middle, and bottom depths along a north-south transect	1-15
2-1	Locations of hydrographic stations and in situ instrumentation stations	2-5
2-2	Schematic of the Grundy CTD/DO profiling system	2-8
2-3	Hydrography for cross-shelf transect offshore Holly Beach . . .	2-18
2-4	Hydrography for alongshore transect offshore Holly Beach . . .	2-19
2-5	Hydrography for cross-shelf transect offshore Holly Beach . . .	2-21
2-6	Hydrography for alongshore transect offshore Holly Beach . . .	2-22
2-7	Hydrography for cross-shelf transect offshore Holly Beach . . .	2-25
2-8	Hydrography for alongshore transect offshore Holly Beach . . .	2-26
2-9	Hydrography for cross-shelf transect offshore Holly Beach . . .	2-30
2-10	Hydrography for alongshore transect offshore Holly Beach . . .	2-31
2-11	Hydrography for cross-shelf transect offshore Holly Beach . . .	2-34
2-12	Hydrography for alongshore transect offshore Holly Beach . . .	2-35
2-13	Temperature-salinity relationships for the surface and bottom water at diffuser and a control station	2-39

2-14	Temporal variation of bottom temperature at the diffuser site and the east control station	2-43
2-15	Temporal variation of bottom salinity at the diffuser site and the east control station	2-44
2-16	Temporal variation of bottom sigma-t at the diffuser site and the east control station	2-45
2-17	Temporal variation of bottom dissolved oxygen at the diffuser site, the east control and pump intake station	2-48
2-18	Vertical salinity profiles at stations 10A and 20 on July 16 and September 11, 1981	2-50
2-19	Vertical salinity profiles at stations 10A and 20 on October 12 and January 12, 1982	2-53
2-20	Vertical salinity profiles at stations 10A and 20 on February 11 and March 12, 1982	2-54
2-21	Vertical salinity profiles at stations 10A and 20 on April 27, 1982	2-55
2-22	Approximate frequency of frontal passages through the West Hackberry area	2-63
2-23	Preliminary 1981 daily Atchafalaya River stage data	2-67
2-24	Average daily streamflow for water years 1979 and 1980	2-68
2-25	Schematic diagram of instrumentation mooring and witness buoy configuration	2-72
2-26	Cross shelf comparison of near bottom salinities using 40-hour, low-pass filtered time series from meters NB, DB, and SB	2-77
2-27	Cross shelf comparison of near surface salinities using 40-hour, low-pass filtered time series from meters NB, DT, and ST	2-78
2-28	Alongshelf comparison of near bottom salinities using 40-hour, low-pass filtered time series from meters DB and WT .	2-79
2-29	Alongshelf comparison of near surface salinities using 40-hour, low-pass filtered time series from meters DT and WT .	2-81

2-30	Vertical comparison of salinities at site D using 40-hour low-pass filtered time series from meters DT and DB	2-82
2-31	Cross shelf comparison of near bottom temperature using 40-hour, low-pass filtered time series from meters NB, DB, and SB	2-87
2-32	Cross shelf comparison of near surface temperature using 40-hour, low-pass filtered time series from meters NB, DT, and SB	2-88
2-33	Alongshelf comparison of near bottom temperature using 40-hour, low-pass filtered time series from meters DB and WB . . .	2-89
2-34	Alongshelf comparison of near surface temperature using 40-hour, low-pass filtered time series from meters DT and WT . . .	2-90
2-35	Vertical comparison of temperature at site D using 40-hour, low-pass filtered time series from meters DT and DB	2-91
2-36	Autospectra for the alongshelf and cross shelf components of current at site D	2-95
2-37	Autospectra for the alongshelf and cross shelf components of current at site D	2-96
2-38	Monthly mean alongshelf and cross shelf components of near surface current for sites D, W and S together with the monthly mean alongshelf component of wind velocity	2-103
2-39	Monthly mean alongshelf and cross shelf components of near bottom current for sites D, W and S together with the monthly mean alongshelf component of wind velocity	2-104
2-40	Autospectra for the alongshelf and cross shelf components of near bottom current at West Hackberry site D	2-113
2-41	Autospectra for the alongshelf and cross shelf components of near bottom current at Bryan Mound site C	2-114
2-42	Autospectra, cross spectrum, cross phase and coherence squared for Bryan Mound site C versus West Hackberry site D cross shelf components of near bottom currents	2-116
2-43	Autospectra, cross spectrum, cross phase and coherence squared for Bryan Mound site C versus West Hackberry site D cross shelf components of near bottom currents	2-117

2-44	Sea-surface salinity on the Texas-Louisiana shelf based on GUS III observations	2-122
2-45	Coherence squared between alongshore wind stress at site A and currents at site C	2-126
2-46	Monthly mean alongshore component of current for top current meter at site A together with monthly mean alongshore component of wind stress based on NDBO wind data at site A	2-128
2-47	Monthly mean longshorement of current for the top current meter at site A together with monthly mean sea level	2-130
2-48a	Alongshore winds together with alongshore current components for the top meter at site B	2-131
2-48b	Alongshore winds together with alongshore current components for the top meter at site B	2-132
2-49a	Time-hodographs for monthly mean wind stress for Brownsville, Corpus Christi, Galveston	2-136
2-49b	Time-hodographs for monthly mean wind stress for Port Arthur, New Orleans and the oceanic 5° square	2-137
2-50	Alongshore components of mean wind stress estimated for Port Isabel, Port Arthur, Bryan Mound Disposal Region West Hackberry Brine Disposal Region and the region off Atchafalaya Bay	2-138
2-51a	Vertical sections of temperature across the shelf off Galveston for April	2-141
2-51b	Vertical sections of temperature across the shelf off Galveston for May	2-142
2-52	Monthly mean delta-T for the GUS II transect off San Luis Pass	2-143
2-53	Temperature at 43 m for the May 1963 cruise of GUS III	2-146
2-54	Sea surface salinity in the northwestern Gulf shelf region for May 30 - June 7, 1976	2-148
2-55	Schematic representation of the mean alongshore current direction on the Texas-Louisiana shelf for alternate months of the year	2-149

2-56	Coherence squared between alongshelf wind stress and current at West Hackberry site D	2-151
2-57	Comparison of 15 1/4-day means for alongshelf components of current at Bryan Mound site C	2-154
2-58	Monthly mean discharge from the Mississippi and Atchafalaya Rivers together based on water years 1976-1980 .	2-156
2-59	Monthly mean near surface salinity at the inshore location together with monthly mean sea-surface salinity for Galvestion Pier	2-157
2-60	Monthly mean near surface salinity at the inshore location together with monthly mean longshore component of current for top current meter at site A	2-159
2-61	Monthly mean sea-surface salinities for tide stations at Port Isabel, Port Aransas and Galvestion Pier	2-161
2-62a	Annual progressions of mean salinity and mean temperature for near surface and near bottom locations for inshore . . .	2-163
2-62b	Annual progressions of mean salinity and mean temperature for the offshore locations	2-164
2-63	Time-depth section for mean salinity and mean temperature, sigma-t, and vertical difference in sigma-t for the offshore location	2-165
2-64a	Vertical section of mean salinity and mean temperature for the Bryan Mound study region cross shelf transect	2-167
2-64b	Vertical section of sigma-t corresponding to 2-64a	2-169
2-65	Annual progression of mean temperature and salinity for near surface and near bottom depths in the vicinity of West Hackberry station 22	2-171
2-66	Vertical section of dissolved oxygen concentration for cross shelf transect in West Hackberry study region for July 16, 1981	2-175
3-1	Station locations for estuarine hydrology and hydrography stations	3-3
3-2	Location of gauging stations and ungauged drainage areas . . .	3-8

3-3	Flow-duration curve for Calcasieu Lake	3-10
3-4	Flow-duration curve for Calcasieu Lake during the low flow period from July thru November	3-11
3-5	Flow-duration curve for Sabine Lake	3-12
3-6	Flow-duration curve for Sabine Lake during the low flow period from July thru November	3-13
3-7	Water levels and salt water intrusion for the confined aquifers near Lake Charles, Louisiana	3-18
3-8	Coastal water table aquifer	3-20
3-9	Salt water intrusion caused by pumping groundwater from coastal water table aquifer	3-21
3-10	Salt water intrusion caused by evapotranspiration in the wetlands	3-22
3-11	Groundwater seepage into Calcasieu Lake	3-24
3-12	Groundwater flow net for the ICWW between Calcasieu and Sabine Lakes	3-26
3-13	Log-plot of average monthly gauged freshwater inflow into Lake Calcasieu and salinity in upper Calcasieu Lake for the low flow period of July thru November	3-31
3-14	Calcasieu Lake salinity model	3-41
3-15	Vertical salinity profiles at station E5 in Calcasieu Pass from May thru April 1981	3-42
3-16	Vertical salinity profiles at station E5 in Calcasieu Pass from September thru December 1981	3-46
3-17	Vertical salinity profiles at station E5 in Calcasieu Pass from January thru April 1982	3-55
3-18	Temporal variations of areal salinity for Calcasieu Lake, Sabine Lake, and the pump intake station	3-57
3-19	Temporal variation of areal average temperature for Calcasieu Lake, Sabine Lake, and the pump intake station	3-58
3-20	Temporal variation of areal average dissolved oxygen for Calcasieu Lake, Sabine Lake and pump intake station	3-70

4-1	Schematic of West Hackberry brine discharge operations	4-3
4-2	Schematic of brine plume characteristics	4-4
4-3	Schematic of plume tracking system	4-9
4-4	Detailed drawing of the towing sled	4-10
4-5	Schematic of brine plume measurement equipment	4-12
4-6	Example LORAN C chart used for brine plume measurements	4-15
4-7	Schematic of plume tracking course for West Hackberry	4-18
4-8	Isohaline contours for the West Hackberry brine plume on June 9, 1981	4-25
4-9	Above ambient isohaline contours for the West Hackberry brine plume on June 9, 1981	4-26
4-10	Isohaline contours for the West Hackberry brine plume on August 12, 1981	4-28
4-11	Above ambient isohaline contours for the West Hackberry brine plume on August 12, 1981	4-29
4-12	Isohaline contours for the West Hackberry brine plume on November 25, 1981	4-31
4-13	Above ambient isohaline contours for the West Hackberry brine plume on November 25, 1981	4-32
4-14	Ishaline contours for the West Hackberry brine plume on February 14, 1982	4-34
4-15	Above ambient isohaline contours for the West Hackberry brine plume on February 14, 1982	4-35
4-16	Vertical salinity profiles near the diffuser on June 9, 1981	4-42
4-17	Vertical salinity profiles near the diffuser on August 12, 1981	4-45
4-18	Vertical salinity profiles near the diffuser on November 25, 1981	4-48

4-19	Vertical salinity profiles near the diffuser on February 14, 1982	4-51
4-20	Vertical dissolved oxygen profiles near the diffuser on June 9, 1981	4-58
4-21	Vertical dissolved oxygen profiles near the diffuser on July 17, 1981	4-61
4-22	Vertical dissolved oxygen profiles near the diffuser on August 12, 1981	4-64
4-23	Vertical dissolved oxygen profiles near the diffuser on November 25, 1981	4-66
4-24	Vertical dissolved oxygen profiles near the diffuser on April 30, 1982	4-70
4-25	Schematic of ellipse used to predict areal extent of brine plume	4-74
4-26	The variation of the plume downstream length for the above ambient salinity contours	4-77
4-27	The variation of the plume width for the above ambient salinity contours	4-79
4-28	The variation of the plume upstream length for the above ambient salinity contours	4-80
4-29	The variation of the plume area inside the above ambient salinity contours	4-82
4-30	The comparison of the measured and predicted areal extent inside the above ambient salinity contours	4-83
4-31	Comparison of measured and predicted salinity plumes on August 12, 1981	4-85
4-32	Comparison of measured and predicted salinity plumes on November 25, 1981	4-86
4-33	Schematic showing division of diffuser area into sectors for use in exposure time computations	4-88
4-34	Twelve month percent exposure time rosette and distribution table for the +1 above ambient salinity contour	4-90

4-35	Twelve month percent exposure time rosette and distribution table for the +2 above ambient salinity contour	4-93
4-36	Twelve month percent exposure time rosette and distribution table for the +3 above ambient salinity contour	4-95
5-1	Inshore and offshore station locations for post-discharge used in water quality sampling	5-2
5-2	Changes in water column nitrite	5-7
5-3	Changes in water column nitrate	5-8
5-4	Changes in water column ammonia	5-9
5-5	Changes in water column phosphate phosphate	5-10
5-6	Changes in water column total phosphorus	5-11
5-7	Changes in water column silica	5-12
5-8	Changes in bottom water column dissolved oxygen	5-15
5-9	Changes in surface water column dissolved oxygen	5-16
5-10	Changes in turbidity	5-17
5-11	Changes in oil and grease	5-18
5-12	Changes in surface water column salinity	5-19
5-13	Changes in bottom water column salinity	5-20
5-14	Changes in bottom water column temperature	5-22
5-15	Changes in surface water column temperature	5-23
5-16	Changes in bottom water column pH	5-25
5-17	Changes in surface water column pH	5-26
5-18	Changes in sodium/potassium ion ratios in bottom water samples	5-28
5-19	Changes in sodium/potassium ion ratios in surface water samples	5-29

5-20	Changes in calcium/magnesium ion ratios in bottom water samples	5-30
5-21	Changes in calcium/magnesium ion ratios in surface water samples	5-31
5-22	Changes in chloride/sulfate ion ratios in bottom water samples	5-32
5-23	Changes in chloride/sulfate ion ratios in surface water samples	5-33
5-24	Changes in sodium/potassium ion ratios in sediment water samples	5-34
5-25	Changes in calcium/magnesium ion ratios in sediment water samples	5-35
5-26	Changes in chloride/sulfate ion ratios in sediment water samples	5-36
5-27	Variations of mean diameter of sediments with time in the estuarine area of the West Hackberry brine disposal area	5-40
5-28	Average mean grain size and respective standard deviations for West Hackberry stations	5-41
5-29	Variations of mean diameter of sediments of offshore stations M18, M10A, and M10	5-42
5-30	Monthly TOC values for West Hackberry sediments at offshore stations M10, M10A, and M18	5-45
5-31	Monthly TOC concentrations of estuarine sediments	5-46
5-32	Monthly variation of pore water salinity at offshore stations M18 and M10	5-48
5-33	Map of May 1981 pore water salinities	5-49
5-34	Map of November 1981 pore water salinities	5-51
5-35	Map of April 1982 pore water salinities	5-52

5-36	Monthly variations of pore water salinities for estuarine stations E1, E2, and E5	5-54
5-37	Monthly variations of pore water salinities for estuarine stations E3 and E4	5-55

CHAPTER 1

INTRODUCTION

1.1 Overview of the Strategic Petroleum Reserve Program

The Strategic Petroleum Reserve (SPR) is a program implemented by the U.S. Department of Energy (DOE) as mandated by Congress through the Energy Policy and Conservation Act of 1975. The purpose is to provide the United States with sufficient petroleum reserves to minimize the effects of any future oil supply interruption. In the Act, Congress declared the policy of the United States Government to provide for storing up to one billion barrels of crude oil and petroleum products.

Of several storage alternatives considered, underground storage in salt domes was most cost effective. The desired storage capacity required development of new caverns through the process known as "solution mining". Oil storage caverns are formed by injecting water into the salt deposits, and pumping out the resulting brine. This process requires a large volume of water, about 7 barrels of fresh water, or about 8 barrels of sea water, for every barrel of space created.

This project centers around the SPR site known as the West Hackberry salt dome and is currently designed to store 241 million barrels of crude oil. The dome is located in north-central Cameron Parish of southwestern Louisiana, approximately 20 mi (32.2 km) southwest of Lake Charles, Louisiana. The Sun terminal at

Nederland, Texas, serves as the oil supply and distribution terminal for West Hackberry. It is about 40 mi (64.4 km) west of the site.

At West Hackberry, the resultant brine from solution mining is disposed offshore through a pipeline and diffuser system. The seaward end of the brine disposal pipeline is located about 6.2 nm (11.4 km) offshore in 30 ft (9.1 m) of water. The diffuser section of the pipeline is approximately 3240 ft (987.5 m) long and has 55 brine discharge ports. The ports are spaced 60 ft (18.2 m) apart.

The National Pollutant Discharge Elimination System (NPDES) permit for discharging brine from this facility required that monitoring of the discharge be conducted in accordance with an EPA approved monitoring plan.

The study included a pre-discharge characterization and this post-discharge impact assessment. The objectives were to:

1. characterize the environment in terms of physical, chemical and biological attributes;
2. determine if significant adverse changes in ecosystem productivity and stability of the biological community are occurring as a result of brine discharge; and
3. determine the magnitude of any change observed.

An interdisciplinary team of scientists from McNeese State University made biological measurements of phytoplankton, zooplankton, nekton, and benthic organisms, as well as a special pollutant study. Texas A & M University scientists worked on characterizing the offshore

physical and chemical oceanography of the region as well as the estuarine hydrology and hydrography. Measurements were taken at 34 stations at the West Hackberry SPR site: 24 stations were located in the offshore area in the vicinity of the diffuser, and 10 stations were in the Calcasieu and Sabine estuarine systems. Table 1-1 and Figure 1-1 identify the approximate locations of these stations. Exact locations and number of sample sites for each task were based on task-specific requirements or instrument locations for a site.

Detecting impact from a point source discharge such as this is a difficult problem because of the many complicating natural variables that must be considered before a conclusion is reached; therefore it required a sampling scheme and data base that were suitable for rigorous statistical analyses. At the same time, however, a certain amount of latitude had to be left in the monitoring plan to allow for necessary adjustments and observing unusual environmental conditions or changes that might occur in the laboratory or field studies.

Studies described in this report were designed as follow-on studies to three months of pre-discharge characterization work at the West Hackberry site (DeRouen et al, 1982), and include data collected during the first year of brine leaching operations. The study design includes both before and after (base line and monitoring) comparisons as well as perturbed and unperturbed (impact and control) site comparisons. The basic sampling frequency in the plan called for

Table 1-1. Longitude and latitude of West Hackberry offshore sampling stations.

Station #	Latitude	Longitude	Loran C		Depth (ft.) (m)	
M-1	29°39'51.4"N	93°33'34.6"W	26522.4	46966.9	31	9.4
M-3	29°39'52.4"N	93°30'34.6"W	26550.6	46966.7	31	9.4
M-6	29°39'52.4"N	93°29'34.6"W	26560.0	46966.7	32	9.8
M-8	29°41'52.2"N	93°28'34.8"W	26580.0	46971.2	26	7.9
M-9	29°40'52.2"N	93°28'35.2"W	26574.8	46968.9	30	9.1
M-10	29°39'52.4"N	93°28'34.6"W	26568.8	46966.7	32	9.8
M-11	29°38'52.2"N	93°28'34.2"W	26564.6	46964.3	34	10.4
M-12	29°37'52.2"N	93°28'34.8"W	26559.6	46962.0	36	11.0
M-13	29°34'52.2"N	93°28'34.8"W	26544.0	46954.9	38	11.6
M-15	29°39'52.2"N	93°27'34.2"W	26579.4	46966.6	32	9.8
M-18	29°39'52.2"N	93°26'34.8"W	26588.4	46966.6	32	9.8
M-20	29°39'52.2"N	93°23'34.8"W	26617.0	46966.4	32	9.8
M-21	29°43'54.6"N	93°28'34.8"W	26598.8	46975.8	18	5.5
M-22	29°31'50.9"N	93°28'34.6"W	26528.9	46947.8	37	11.3
M-23	29°29'48.0"N	93°28'34.6"W	26513.2	46940.6	34	10.4
10-A	29°40'09.0"N	93°28'12.6"W	26574.3	46967.2	31	9.4
DN	29°40'39.6"N	93°28'12.6"W	26577.4	46968.4	30	9.1
DS	29°39'35.0"N	93°28'12.6"W	26572.3	46966.0	33	10.1
DE	29°40'09.0"N	93°27'36.0"W	26580.3	46967.1	31	9.4
DW	29°40'09.0"N	93°28'43.0"W	26569.5	46967.2	32	9.8
CS	29°40'50.0"N	93°18'12.0"W	26668.6	46966.4	33	10.1
NW	29°40'39.6"N	93°28'48.0"W	26571.5	46968.4	30	9.1
SW	29°39'37.2"N	93°28'48.0"W	26566.5	46966.1	33	10.1
NE	29°40'39.6"N	93°27'40.8"W	26582.5	46968.4	30	9.1
SE	29°39'37.2"N	93°27'36.0"W	26577.6	46966.1	32	9.8
Buoy P (E5)	29°46'11"N	93°20'38"W	in pass		20	6.0
D	29°39'54"N	93°28'44"W	46966.7	26568.8	32	9.8
S	29°27'07"N	93°26'00"W	46936.5	26530.2	41	12.5
N	29°42'50"N	93°28'24"W	46973.4	26585.8	21	6.4
W	29°38'30"N	93°40'00"W	46963.7	26454.8	31	9.4
E-1	30°03'32"N	93°26'09"W				
E-2	30°03'05"N	93°18'41"W				
E-3	29°51'33"N	93°22'00"W				
E-4	29°51'20"N	93°18'47"W				
E-5	29°46'11"N	93°20'38"W				
E-6	30°03'47"N	93°20'55"W				
E-7	30°03'35"N	93°41'55"W				
E-8	29°57'32"N	93°42'40"W				
E-9	29°54'07"N	93°48'13"W				
E-10	29°51'45"N	93°55'06"W				

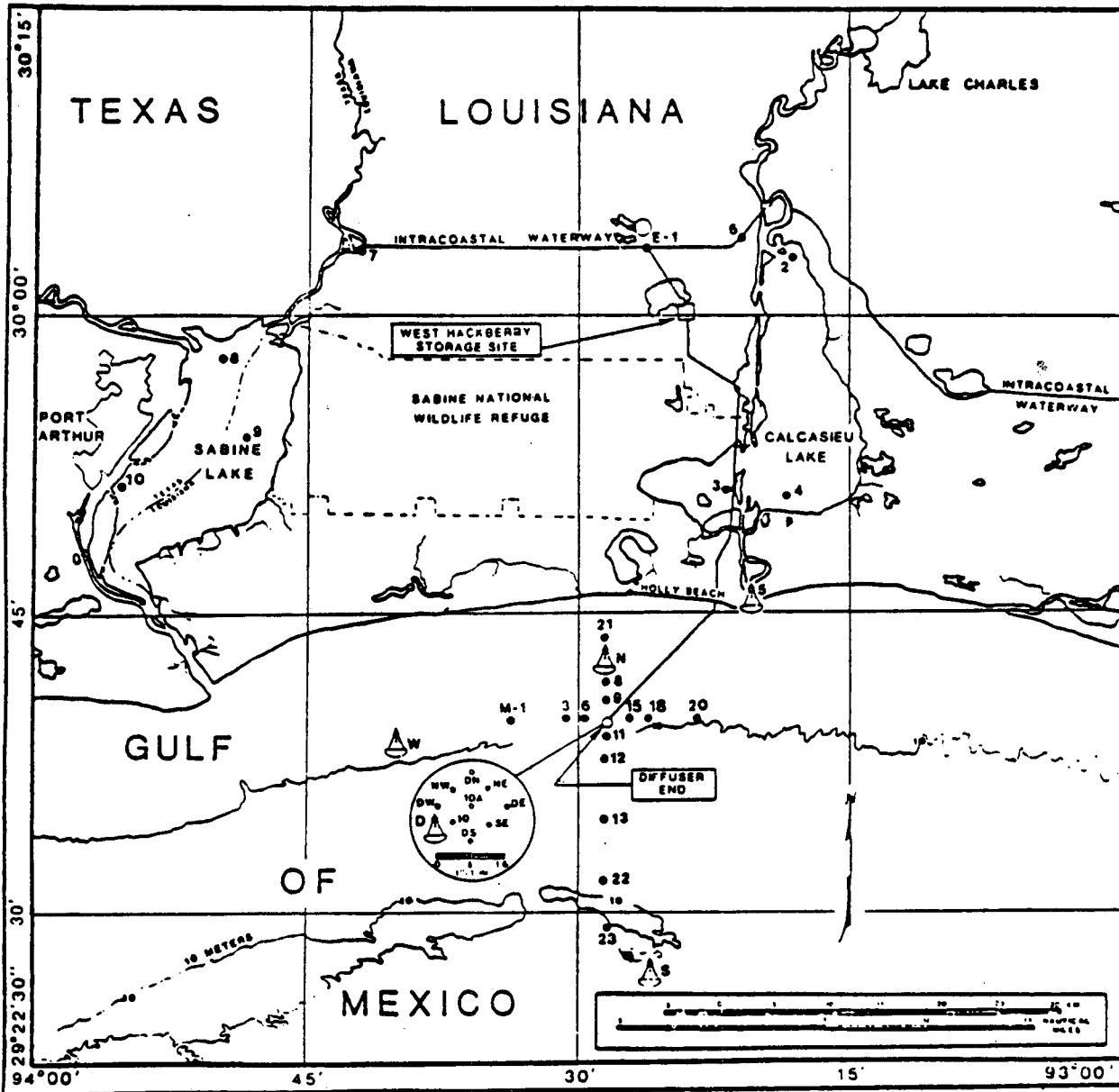


Figure 1-1. Area map of Texas-Louisiana showing inland and offshore station locations of West Hackberry brine discharge studies.

monthly data collecting activities although physical oceanographic and hydrologic data were collected with continuously recording in situ instrumentation.

1.2 Brine Discharge Data

Daily values for temperature, salinity, volume and salt loading of brine discharge are plotted in Figure 1-2. On May 14, 1982 with 31 of 55 ports open, intermittent discharge began at approximately 50,000 bbl/day and 30 ‰ salinity. Both discharge rate and salinity gradually increased to near 600,000 bbl/day and 220 ‰ by mid-June and continued at this level until late August. From late August to mid-September pumps at West Hackberry were non-operational, no brine was discharged. Disposal rates returned to pre-non-operational levels for a short period and then became intermittent (with pumps operating for a portion of each day) from mid-September through mid-October. During this period discharge volumes were approximately one-half of the June-August values. Flow rates were then increased and stabilized at nearly 500,000 bbl/day from late October through December 1981. Once again intermittent flow, resulting in reduced daily discharge volumes, occurred during January 1982. Flow then returned to approximately 500,000 bbl/day rates until late February. Study period maximum discharge rates, approximately 750,000 bbl/day, were attained in late February and continued through late April. During this time an additional 19 diffuser ports were uncapped bringing the total to 50 open ports. In late April, eight ports were re-capped due to maintain desired exit velocities.

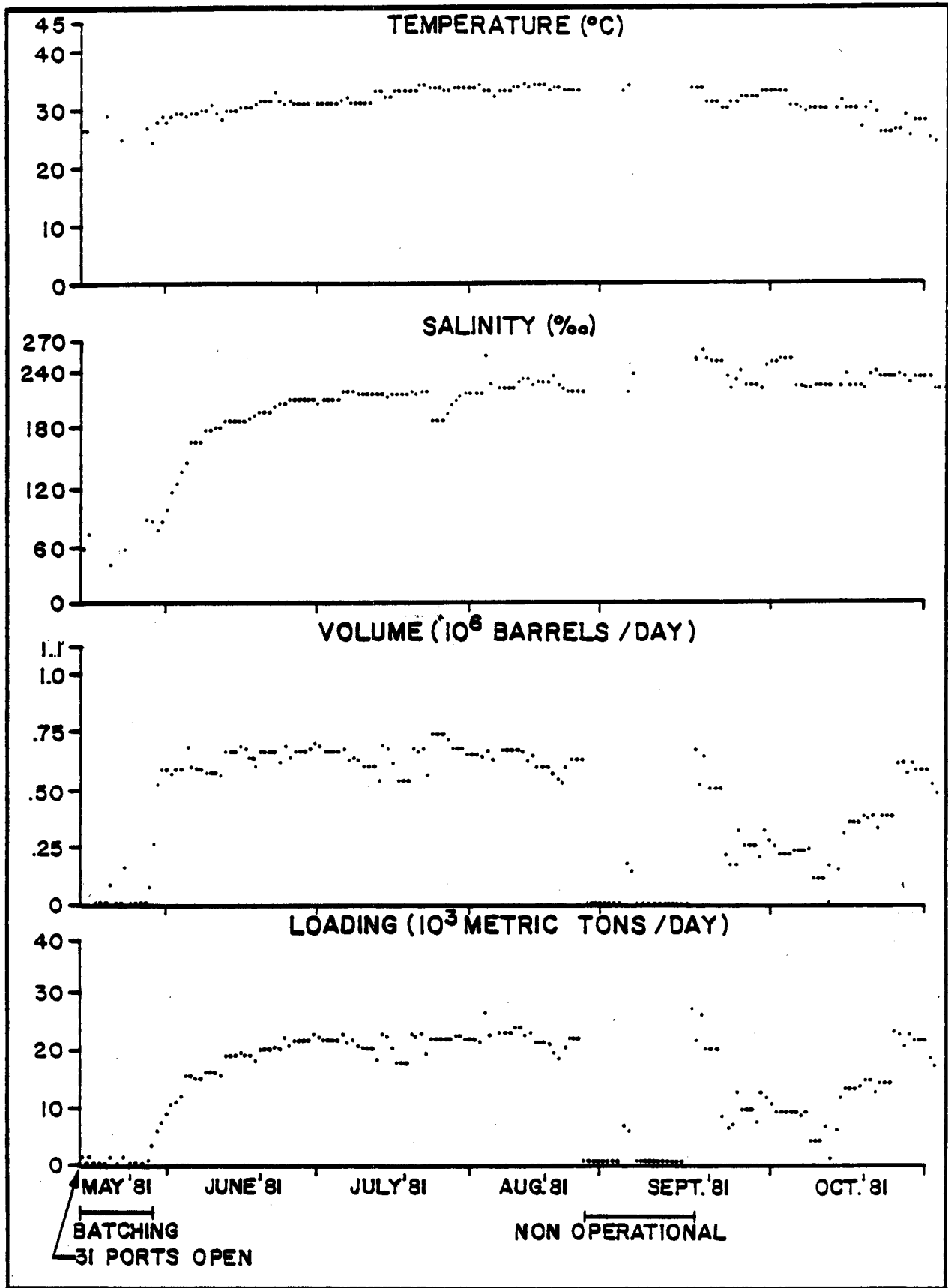


Figure 1-2. Daily values for temperature, salinity, volume and salt loading of brine discharge from May 1981 through April 1982.

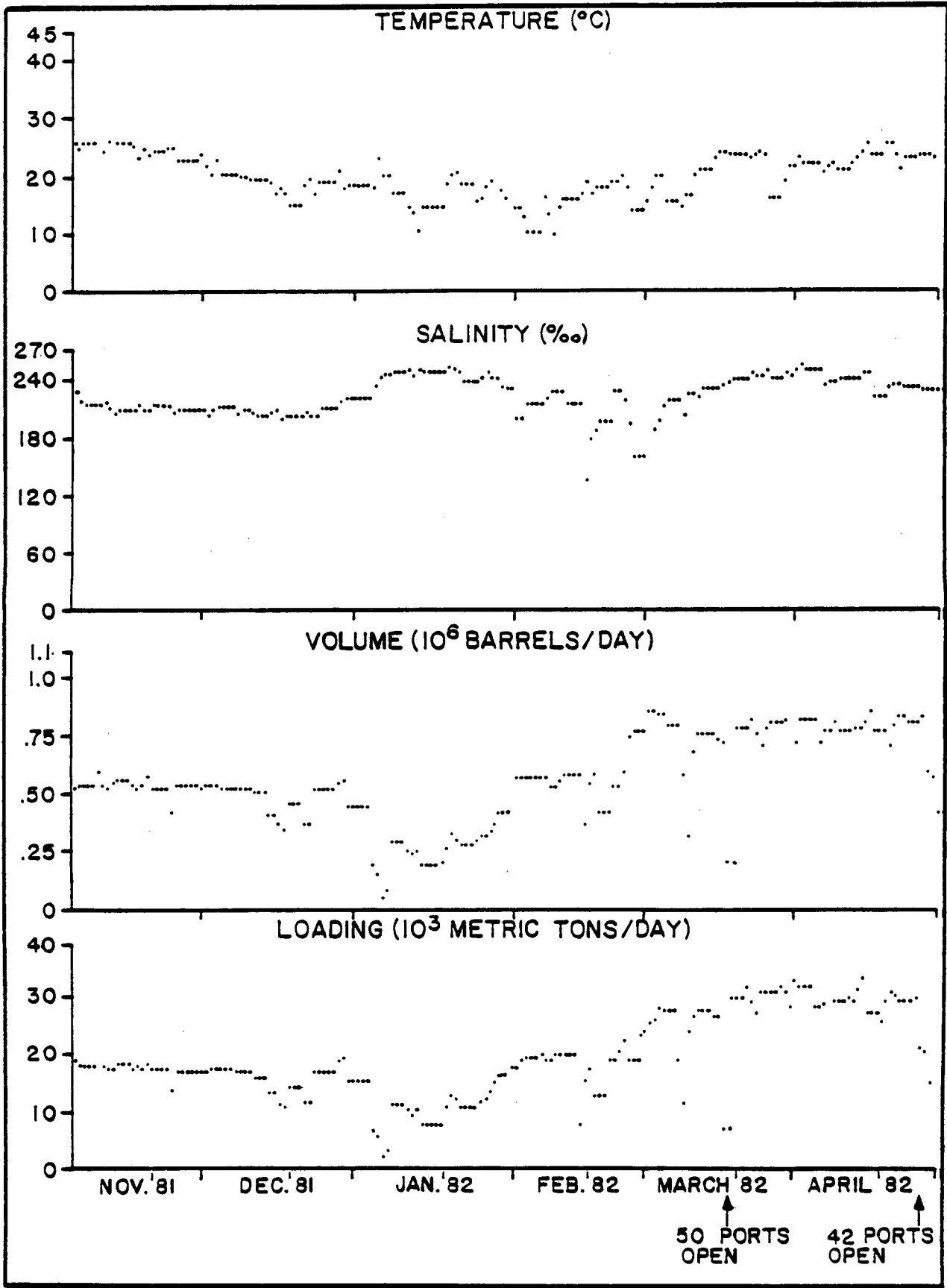


Figure 1-2. Continued.

Generally, brine discharge volumes have not been at a constant rate during the study. Periods have occurred in which flow became either intermittent or discontinued. During the 12-month study period, the daily discharge averaged 529,000 bbl of 216 ‰ brine equalling a loading of over 18,000 metric tons of salt per day. These values are substantially lower than design capacities of 1.1 million bbl per day and 260 ‰ resulting in 47,000 metric tons of brine disposed per day.

In the following chapters, the specific hypotheses, sampling designs, statistical analyses, results, and interpretations of the post discharge phase (May 1981 - April 1982) are detailed for each task.

CHAPTER 2

PHYSICAL OCEANOGRAPHY

F. J. Kelly, J. D. Cochran, R. E. Randall and J. E. Schmitz
Texas A&M University
College Station, Texas 77843

2.1 Introduction

In this chapter, the meteorological and physical oceanographic data collected from May 1981 through April 1982 at the West Hackberry brine disposal site are presented, analyzed and compared with similar data collected at the Bryan Mound diffuser site (Kelly et al., 1982a). This period encompasses the first year of brine discharge operations. A short pre-discharge study was conducted from late January 1981 through April 1981 as part of the present monitoring effort (Kelly et al., 1982b), and longer pre-discharge studies of the physical oceanography of the area were made by others from October 1977 through October 1978 (Waddell and Hamilton, 1981) and from July 1978 through June 1979 (Frey et al., 1981). The general geography, climatology, historical data base, etc. for the study area have been well described in these previous reports.

The objectives of the physical oceanographic study are:

1. to characterize the magnitude of naturally occurring variations of salinity, temperature, density and current velocity;
2. to define ambient conditions for various times of the year;
3. to document the magnitude and extent of the brine plume when detectable;
4. to determine the relative importance of forcing factors such

as wind stress, river runoff, tides, etc., on the density structure and circulation;

5. to provide current velocity and hydrographic data in a format which can readily be used by other components of this project in the analysis and interpretation of their data.

To meet these objectives this study has utilized both monthly hydrographic sampling and continuously recording in situ instrumentation. Figure 2-1 shows the locations of the hydrographic stations and in situ instrument sites. The grid of hydrographic stations provides detailed information about the spatial distribution of hydrographic variables, but since the stations are sampled monthly, temporal resolution is limited to seasonal changes. The in situ instrumentation, on the other hand, provides very fine resolution of temporal changes but coarse estimates of spatial distributions and gradients. Together, the two sampling methods provide a fairly comprehensive picture of the physical oceanography of the study area. Details of the methods and instrumentation are discussed in sections 2.2 and 2.4 and also in the West Hackberry Field and Laboratory Procedure Manual (Kelly et al., 1981a; Randall and James, 1981).

The hydrographic data collected during the first year of brine discharge operations are analyzed in section 2.2 by means of vertical sections, temperature-salinity relationships and vertical profiles. The effect of river runoff is quite evident in the hydrographic data. Although the streamflow data for water year 1981 were received too late for inclusion in this report, some preliminary river stage data have been obtained. In section 2.3 a qualitative comparison is made between this river stage data and streamflow data for previous years.

Section 2.3 also discusses the meteorological time series data collected in the study area by NOAA/NDBO. In section 2.4 the time series of current velocity, temperature and salinity are presented. Comparisons are made between the diffuser site and the other sites in the area, and also between the West Hackberry and Bryan Mound diffuser sites. Spectral analyses and harmonic tidal analyses are used to quantify the time/frequency scales of importance, the effect of local wind forcing, and the amount of coherence between the diffuser site and the other sites.

An important result of this section is that there is little coherence between the local alongshelf components of wind stress and current at periods longer than about 4 days at the West Hackberry site. This implies that much of the long period (low frequency) water movement is part of a larger scale or regional circulation pattern. In section 2.5 the large scale seasonal circulation and hydrography at both the West Hackberry and Bryan Mound sites are discussed and contrasted.

A complete set of vertical sections, monthly statistics, monthly wind and current roses and monthly time series plots of meteorological and oceanographic data have been placed in Appendix A, along with other large groups of figures such as results of spectral and harmonic analyses and expanded plots of current velocity, temperature and salinity for days on which the plume was mapped (see Chapter 4). It is hoped that the variety of methods used to present the data and the high degree of resolution in the figures will achieve the last objective stated above, i.e. present data in a readily usable format. Appendix B contains the results of study by Mr. William Ulm in which

a census was made of the volume of water on the Louisiana and Texas continental shelves for various ranges of temperature and salinity. It is felt that since some biological organisms show a preference for particular ranges of temperature and salinity, this study may be useful to other investigators, and may provide a perspective from which the hydrographic observations at West Hackberry and especially the magnitude (volume) of plume induced changes can be viewed.

There are numerous areas of investigation which should be pursued given the large data base which has been collected; however, this report is intended to be responsive to the Department of Energy's need for timely dissemination of the results of studies concerning the impact of its brine disposal activities on the ocean environment. Therefore, some compromises had to be made about the scope of various analyses. The analyses of the data from the wave/tide meter have been delayed because of hardware problems and will be included in a future report. A detailed analysis of the data from Site P (or station E-5) in Calcasieu Pass has not been made because of delays in receiving streamflow data and remote sensing images and because of time constraints in the preparation of this report. However, the basic statistics, time series plots, and analyses of tidal currents for Site P data are included in Appendix A.

2.2 Monthly Offshore Hydrographic Data

2.2.1 Sampling Station Locations

The monthly hydrography of the coastal waters off Holly Beach, Louisiana, has been evaluated using conductivity, temperature, depth, and dissolved oxygen (CTD/DO) data which were collected at the fifteen offshore stations shown in Figure 2-1. The offshore stations are

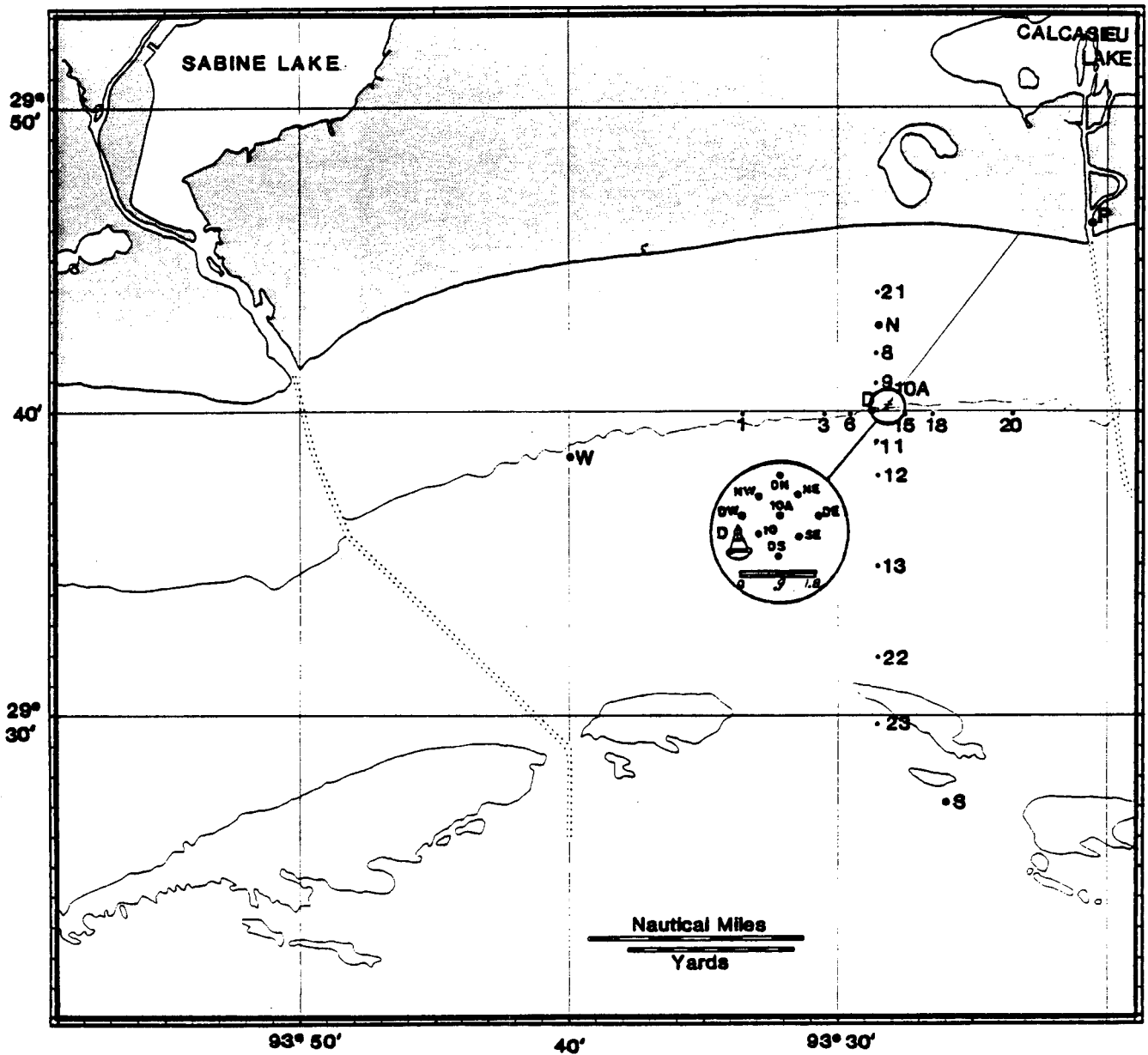


Figure 2-1. Locations of hydrographic stations and in situ instrumentation stations at the West Hackberry brine disposal site.

arranged in an alongshelf transect (stations 20, 18, 15, 10A, 6, 3, and 1) and a cross-shelf transect which includes stations 21, 8, 9, 10A, 11, 12, 13, 22, and 23. The latitude and longitude and the LORAN C coordinates for the offshore stations are tabulated in Table 2-1. The offshore hydrographic data were collected synoptically once a month during a one-day (about 10 hours) cruise.

2.2.2 Data Collection Equipment

The primary instrument used for measuring the offshore hydrographic data was the Grundy CTD/DO instrument (Figure 2-2) which consists of a Grundy Model 9400-1 CTD system, a Grundy Model 8400 digital data logger, a Hewlett Packard Model 85 computer, and a General Oceanic rosette sampler. The model 9400-1 CTD system measures conductivity inductively over the range of 0 to 60 mmho/cm and temperature is measured by a platinum resistance thermometer with a range of -2°C to 35°C . The pressure, or depth, is measured by a bonded strain-gage transducer over the range of 0 to 100 m. The dissolved oxygen sensor has a range of 0 to 15 mg/l. The accuracy of the conductivity, temperature, depth, and dissolved oxygen sensors is ± 0.03 mmho/cm, $\pm 0.02^{\circ}\text{C}$, ± 1.5 m, and ± 0.3 mg/l respectively. The conductivity is converted to salinity and accuracy for salinity is then ± 0.02 o/oo.

The Grundy Model 8400 is a general purpose digital data logger designed to digitize and accept input signals. It also provides the capability of varying the data sampling period from 0.1 second to 10 seconds. For this application, the data logger was interfaced with a Hewlett Packard Model 85 computer. The HP85 computer is capable of recording the data on cassette tape or printing the data on 10.8 cm

Table 2-1. Latitude, longitude and LORAN C coordinates for the monthly offshore hydrographic sampling stations.

Station Number	North Latitude	West Longitude	LORAN C	
1	29°39'51.4"	93°33'34.6"	26522.4	46966.9
3	29°39'52.4"	93°30'34.6"	26551.1	46966.7
6	29°39'52.4"	93°29'34.6"	26560.3	46966.7
8	29°41'52.2"	93°28'34.8"	26580.0	46971.2
9	29°40'52.2"	93°28'34.2"	26574.8	46968.9
10A	29°40'09.0"	93°28'12.6"	26574.5	46967.2
11	29°38'52.2"	93°28'34.2"	26564.6	46964.3
12	29°37'52.2"	93°28'34.8"	26559.6	46962.0
13	29°34'52.2"	93°28'34.8"	26544.0	46954.9
15	29°39'52.2"	93°27'34.2"	26579.4	46966.6
18	29°39'52.2"	93°26'34.8"	26588.4	46966.6
20	29°39'52.2"	93°23'34.8"	26617.0	46966.4
21	29°43'54.6"	93°28'34.8"	26590.8	46975.8
22	29°31'50.9"	93°28'34.6"	26528.9	46947.8
23	29°29'48.0"	93°28'34.6"	26513.2	46940.6

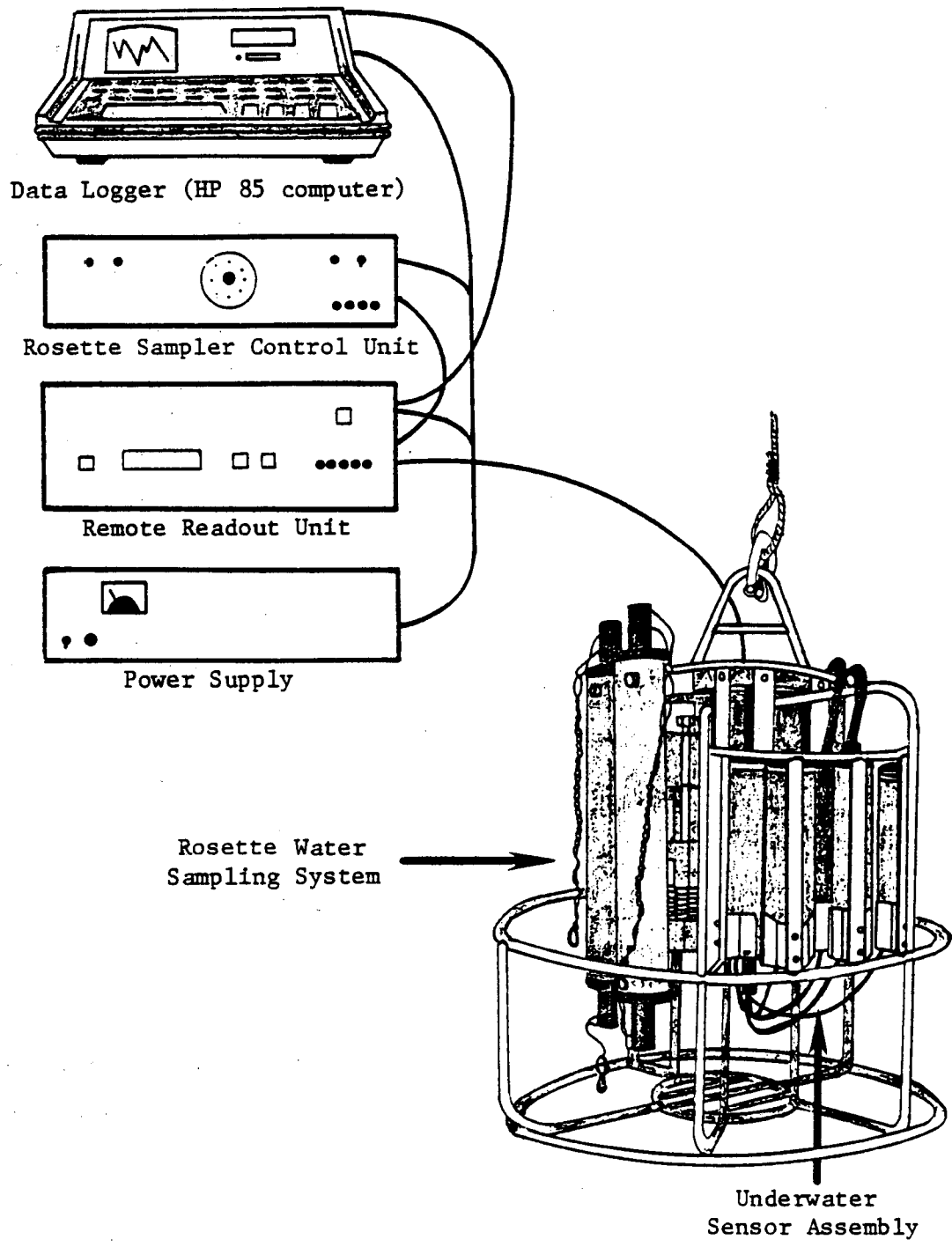


Figure 2-2. Schematic of the Grundy CTD/DO profiling system.

wide thermal paper. The data are also visually displayed on a 12.7 cm diagonal CRT screen. Appropriate computer software were written in BASIC for data recording, analysis, and graphic display.

The Hydrolab 8000 CTD/DO instrument was used as a backup for the Grundy system, and it was also used for estuarine hydrography studies (Chapter 3) and the brine plume investigations (Chapter 4). The Hydrolab CTD/DO instrument consists of a data transmitting unit (probe), the data bus cable (conductor cable), and the data control unit (remote readout). The probe is capable of measuring conductivity (0 to 200 mmho/cm), depth (0 to 200 m), temperature (-5°C to +45°C), dissolved oxygen (0 to 20 mg/l), and pH/ORP. The latter parameter is used in the water quality component of the project. The accuracy of the conductivity sensor (four electrode type) is +/-0.5% of full scale which is 200 mmho/cm at 25°C, and this corresponds to +/-1 mmho/cm or +/-0.7 o/oo. The accuracy of the conductivity sensor was improved to at least +/-0.5 o/oo by calibrating it with standard solutions using a Grundy laboratory salinometer which has an accuracy of +/-0.003 o/oo (Grundy, 1978). The temperature, depth, and dissolved oxygen sensors have accuracies of +/-0.2°C, +/-1 m, and +/-0.2 mg/l, respectively.

The procedure for collecting the monthly hydrographic data was to begin at station 21 (Figure 2-1) and proceed directly offshore along the cross-shelf transect to station 23. At each station, the Grundy and Hydrolab CTD/DO instruments were simultaneously lowered to the bottom while the Grundy CTD data were continuously recorded. When the instruments were on the bottom, the Grundy sampling period was changed and the instruments were raised to 1 m above the bottom, every 3 m thereafter, and 1 m below the surface. The instrument had to be

stopped at each depth to allow the dissolved oxygen sensor to stabilize. When the DO sensor stabilized, the Hydrolab CTD/DO data were recorded in a bound field data book and the Grundy data were recorded on cassette tape. In addition to the CTD/DO data, water samples were taken at 1 m above the bottom and 1 m below the surface. These samples were chemically fixed aboard ship and returned to the laboratory where a Winkler laboratory analysis was performed to determine dissolved oxygen content. These data were used to correct the dissolved oxygen data obtained from the Grundy and Hydrolab CTD/DO instruments. When the cross-shelf transect was completed, the ship proceeded to station 1 (Figure 2-1) and began sampling the alongshelf transect to station 20. This sampling procedure normally required 8 to 10 hours. The data collected were recorded in a bound data book and on a cassette magnetic tape, and after completion of the cruise, the data were returned to the laboratory for calibration corrections and further analysis. Additional information on the procedures and equipment is contained in the West Hackberry Field and Laboratory Procedures Manual, (Randall and James, 1981).

2.2.3 Instrument Calibration Procedures

The conductivity sensor on the Grundy Model 9400-1 and the Hydrolab Model 8000 were compared to the results of a Grundy Model 6230N laboratory salinometer which has an accuracy of ± 0.003 o/oo. The sensors on both instruments measure conductivity which is converted to salinity. The calibration of the Hydrolab Model 8000 was performed before and after each cruise. This calibration was accomplished by making standard solutions whose salinity values covered the range of salinities expected in the study area. In the

laboratory, the standard solutions were poured into the calibration cup surrounding the sensors and the conductivity was recorded and converted to salinity. The same samples were then processed through the laboratory salinometer. A calibration curve was obtained from the data and used to correct all the salinity data measured with the Hydrolab instrument.

The Grundy Model 9400-1 is much larger and required a much larger bath (approximately 1 m x 1 m x 1 m) to completely immerse the instrument for calibration. This instrument was calibrated in such a large bath in November 1981. The conductivity values were converted to salinity and water samples were processed through the Model 6230N laboratory salinometer for comparison. The results showed the Model 9400-1 conductivity sensor was within the specified accuracy limit (± 0.02 o/oo) so no calibration corrections to the Model 9400-1 salinity data were made. The Grundy salinity data were routinely compared with the calibrated Hydrolab 8000 salinity results to determine if the Grundy salinity was staying near the accuracy specification or if it needed recalibration.

The temperature sensors on the Grundy Model 9400-1 and the Hydrolab 8000 were calibrated against a Brooklyn Thermometer Co. mercury-in-glass thermometer which has an accuracy of $\pm 0.03^{\circ}\text{C}$. Calibration results showed the temperature sensors for the Model 9400-1 and Model 8000 were within their accuracy specifications. Therefore, no corrections were made to temperature data from either the Grundy or the Hydrolab instruments.

The depth sensors were checked for zero readings at the surface and compared to depth sounder readings at the bottom. If significant

errors at either depth were observed, an average correction to the data was determined and applied. The Grundy Model 9400-1 depth readings did not require any correction during the study period. The Hydrolab 8000 depth sensor frequently had a small zero offset which was applied to the corresponding data.

The Hydrolab Model 8000 dissolved oxygen (DO) sensor was calibrated before and after each field cruise. The DO sensor was adjusted to read the DO value for water saturated air at the local atmospheric conditions as described in the operations manual (Hydrolab, 1980). After the field data were collected, they were then corrected for salinity and temperature effects. During the collection of DO data, selected water samples at the same location as the DO sensor were collected and chemically fixed aboard the research vessel. These samples were brought back to the laboratory and analyzed using the Winkler titration procedures. The resulting data were then plotted, and a linear curve fit to the data was determined. Finally, the data were corrected based upon these calibration results.

The Grundy Model 9400-1 dissolved oxygen sensor did not have a fast enough response time such that the data recorded on the downcast were valid. Therefore, the DO data were collected on the upcast when the sensor was stopped a 1 m above the bottom, every 3 m, and 1 m below the surface.

A different pre-calibration procedure was used for the Grundy DO sensor. This procedure checks the sensor in deoxygenated water and 100% saturated water. In order to deoxygenate the water, it was purged with nitrogen with the Grundy sensor immersed. This was followed by bubbling air through the water until 100% saturation was

reached. With this initial calibration check, the sensor was sent to the field and selected samples were collected, chemically fixed in the field, and brought back to the laboratory where Winkler titration analyses were conducted to obtain a calibration curve. This curve was then used as previously described to correct the DO data.

2.2.4 Field Data Conversion Techniques

The conductivity data from the Grundy Model 9400-1 was converted to salinity using the equation of Daniel and Collias (1971):

$$S = -0.505 + 1115.294 C + 3680.067 C^2 - 35.412 CT \\ - 120.291 C^2T + 0.860 CT^2 - 0.011 CT^3 + 0.048 C^2T^3$$

where C is the conductivity in mhos/cm (rather than the usual millimhos/cm) and T is the temperature in degrees Celcius. Since the calibration of the Grundy instrument indicated that it was within the accuracy specifications (+/- .02 o/oo), no further corrections were made to the data.

A similar procedure was used to convert the Hydrolab Model 8000 conductivity data. The Hydrolab Model 8000 instrument has an internal temperature compensation circuit which corrects the conductivity such that it is the conductivity at 25°C. These data were then converted to salinity using an equation by Weyl (1964):

$$S = 1.80655 \times 10^3 \frac{\log_{10} C - 0.57627}{0.892}$$

where C is the conductivity in mmho/cm at 25°C. After the salinity was determined, it was corrected according to the calibration results previously described. A detailed description of these procedures is

given in the laboratory and procedures manual (Randall and James, 1981).

The temperature data from both the Grundy and Hydrolab instruments were used as read from the instruments since calibration results indicated the data were within the accuracy specifications of +/-0.2°C. The depth data from the Grundy instrument was used as read from the instrument. However, the Hydrolab depth data frequently required a correction which was determined by a surface (zero depth) reading and a bottom reading which was checked with the ship's depth sounder.

The salinity, temperature and depth data were used to compute the density of the water column in the customary oceanographic form of sigma-t (σ_t) which is defined as:

$$\sigma_t = (\rho - 1.0) \times 10^3$$

where the density (ρ) is expressed in gm/cm³. Sigma-t values were computed from salinity, temperature, and depth data using the equation of LaFond (1951).

The dissolved oxygen data collected in the field were first corrected for the effects of salinity and temperature and then further corrected with the results of a comparison of the data obtained from the Winkler analysis of water samples collected at the same time and location. The Grundy Model 5175 dissolved oxygen sensor automatically corrects for temperature effects and the salinity effects were corrected by using the following equation:

$$DO_A = DO_M = \frac{1.0 - (S/36.11)(DO_f - DO_s)}{DO_f}$$

where DO_A is the actual dissolved oxygen, DO_M is the measured DO, S is the salinity of the sample, DO_f is the DO of saturated freshwater at 760 mm pressure at the temperature of the sample, and DO_s is the DO of saturated sea water (36.11 o/oo) at 760 mm pressure at the same temperature as the sample. Winkler analysis of water samples taken at 1 m above the bottom and below the surface were compared with the Grundy data at the same locations. A linear correction equation was determined and used to correct all the dissolved oxygen data. For the Hydrolab Model 8000 instrument, the field data must be corrected for both temperature and salinity which was accomplished with a computer interpolation scheme for the dissolved oxygen correction nomograph in the Hydrolab 8000 operations manual (Hydrolab, 1980). The data were further corrected by comparing the data with results of the Winkler analysis of selected samples as previously described for the Grundy instrument.

2.2.5 Vertical Cross-sections of Temperature, Salinity, Sigma-t, and Dissolved Oxygen

2.2.5.1 Introduction

Vertical cross-sections of temperature, salinity, sigma-t, and dissolved oxygen were constructed from monthly hydrographic data collected along a cross-shelf and an alongshelf transect during the period from January 1981 through April 1982. All of these cross-sections are contained in Appendix A.1; the cross-sections for January through April 1981 have been described in a previous report (Kelly, et al., 1982b). The discussion in this section will focus on the period May 1981 through April 1982 when brine was being discharged through the West Hackberry diffuser the center of which is located at

station 10A.

2.2.5.2 Spring 1981 (April through June)

On April 10, 1981, prior to brine discharge, the isopleths of temperature, salinity, sigma-t, and dissolved oxygen were nearly vertical with the largest variation occurring in the cross-shelf direction as shown in Appendix Figure A-4. The temperature decreased from about 22°C at the station 21 which is nearest shore to about 20°C at station 23 which is farthest offshore. The salinity increased from near 26 o/oo to 33 o/oo and dissolved oxygen increased from near 7 mg/l to near 8 mg/l. The vertical variation of all parameters was small as evidenced by the vertical orientation of the isopleths. The alongshelf variation from station 1 to 20 was also small.

Brine discharge began in May 1981 on an intermittent basis but the amount of brine being discharge during the May 21 monthly hydrographic cruise was not known. The vertical cross-section data are illustrated in Appendix Figures A-6 and A-7. The cross-shelf transect shows the temperature variation was nearly isothermal (24°C) in the vertical and horizontal directions. However, the salinity data show the existence of some stratification in the bottom waters in the vicinity of the diffuser (station 10A) with the salinity increasing with depth from 27 o/oo to near 30 o/oo. The dissolved oxygen isopleths were also horizontal and decreased with depth in the bottom 4 m from near 7 mg/l to 5 mg/l. The alongshelf transect which was measured in the afternoon, after the cross-shelf transect, shows the temperature was isothermal, near 24.5°C, and the near bottom salinity was stratified with isohalines varying from 27 o/oo to 30 o/oo. The dissolved oxygen alongshelf data indicate a strong gradient of

dissolved oxygen in the same layer as the salinity stratification where the dissolved oxygen decreased with depth from near 8 to 5 mg/l along the transect west of the diffuser and 9 to 7 mg/l along the transect east of the diffuser.

The major event occurring every spring is the large runoff of fresher water from the Mississippi River and the local Calcasieu Lake. This annual event causes strong salinity stratification which is normally followed by a dissolved oxygen depletion in the near bottom waters. This was reported by Frey et al. (1981) in their predisposal study from June 1978 through June 1979. The vertical cross-section data for June 8, 1981 are shown in Figures 2-3 and 2-4. The cross-shelf transect data show the temperature increased to near 28°C with little variation in the vertical or horizontal direction. The effect of increased fresh-water runoff is clearly evident in the strong middepth salinity and density stratification. In Figure 2-3, the isohalines at station 10A increased with depth from 22 o/oo at 3 m to 30 o/oo at 1 m above the bottom. On this day, brine was being discharged at a rate of 23,580 barrels/hr, and the average salinity and temperature of the brine were 176 o/oo and 30°C. The isohalines show no indication of the brine discharge. Isopycnals increased as expected from 13 to 18 sigma-t units. Figure 2-4 shows that the vertical variation at stations 1, 3, 6, 10A, 15, and 18 was the same and that essentially no horizontal variation was present. The dissolved oxygen isopleths decreased from 6 to 4 mg/l near the diffuser on the cross-shelf transect and from 7 to 4 mg/l on the alongshelf transect. Thus, the vertical cross-sections of the spring hydrographic data show that the isopleths of temperature, salinity,

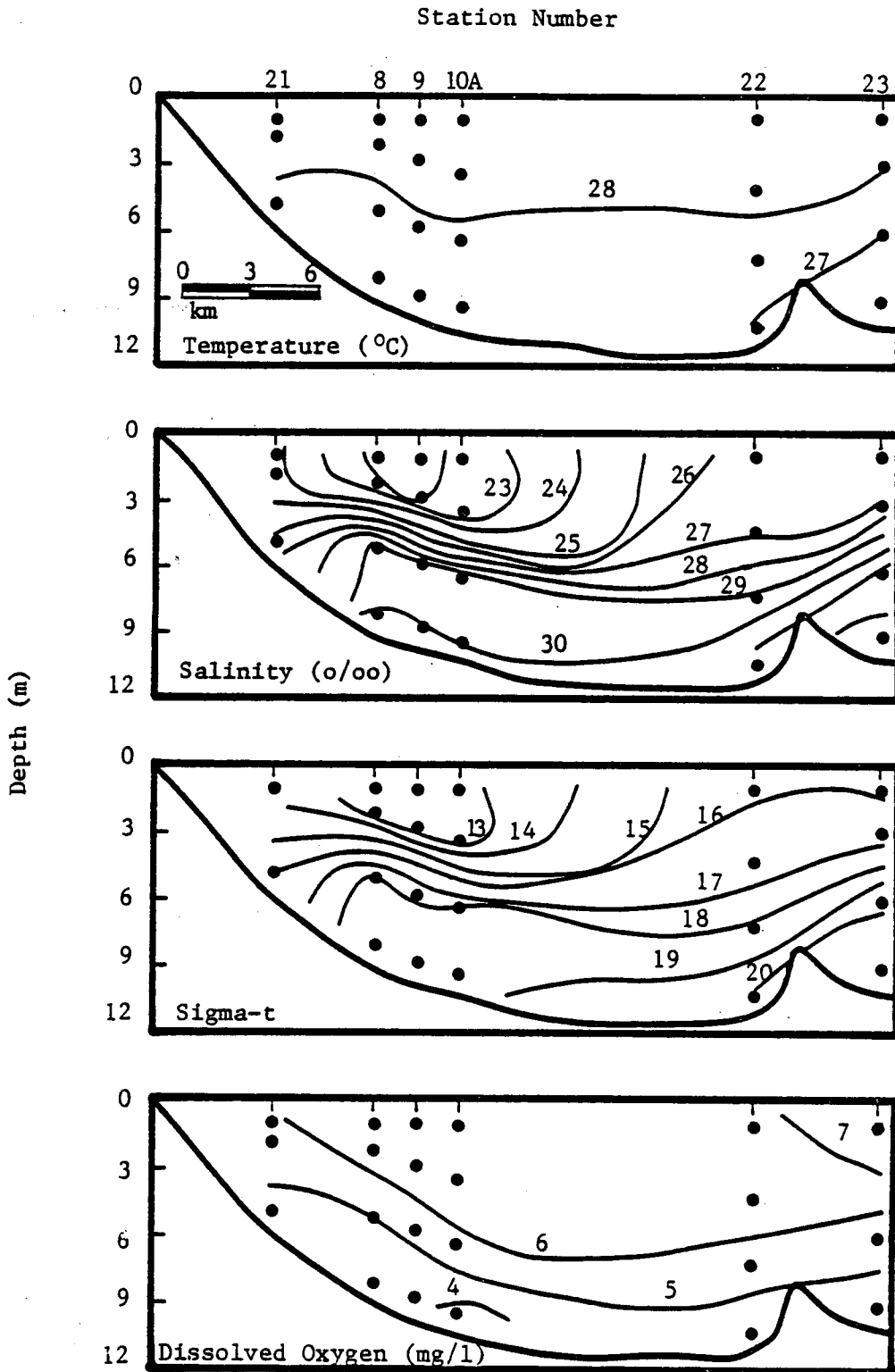


Figure 2-3. Hydrography for cross-shelf transect offshore Holly Beach, Louisiana on June 8, 1981.

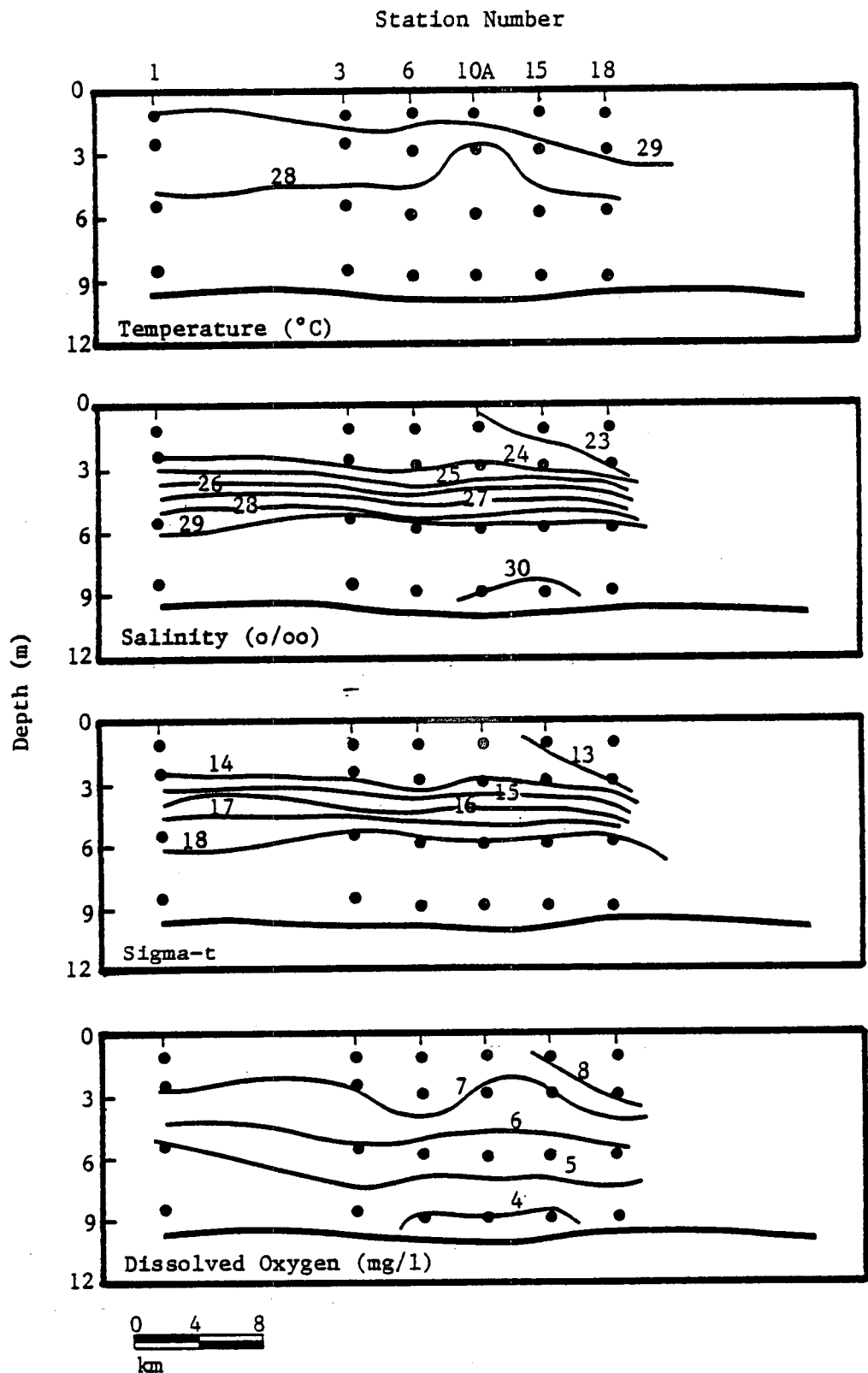


Figure 2-4. Hydrography for alongshelf transect offshore Holly Beach, Louisiana on June 8, 1981.

sigma-t, and dissolved oxygen were nearly vertical in early April with salinity, sigma-t, and dissolved oxygen increasing and temperature decreasing with distance offshore; the alongshelf data showed small variations. In May and June, the isopleths became nearly horizontal resulting in vertical gradients of all parameters. The vertical temperature gradients were slight, but the salinity and density (sigma-t) gradients were strong. The isopleths of dissolved oxygen show the dissolved oxygen gradient was moderate. Brine discharge began in May 1981 on an intermittent basis, but the hydrographic data show very little effect, which is attributed to the intermittent operations and low brine salinities.

2.2.5.3 Summer 1981 (July through September)

The summer of 1981 continued to experience the effects of the fresher water entering the area as a result of the spring runoff, and Figures 2-5 and 2-6 illustrate the hydrographic data collected on July 1, 1981. The temperature data indicate that a small thermocline was present beginning near the diffuser site (station 10A) and extending offshore. The isohalines show the strongest vertical variation in salinity for the year with a 12 o/oo isohaline at the surface and a 26 o/oo near the bottom at the diffuser site. A vertical gradient of 16 o/oo existed at station 13 which is 9 km offshore of station 10A. The associated vertical density gradient at the diffuser site and at station 13 was 12 sigma-t units. The isohaline and isopycnals were nearly horizontal on the cross-shelf transect except for a slight inclination in the upper half of the water column. Thus, the salinity stratification was spread over the entire cross-shelf transect. The alongshelf transect, Figure 2-6, shows the vertical temperature

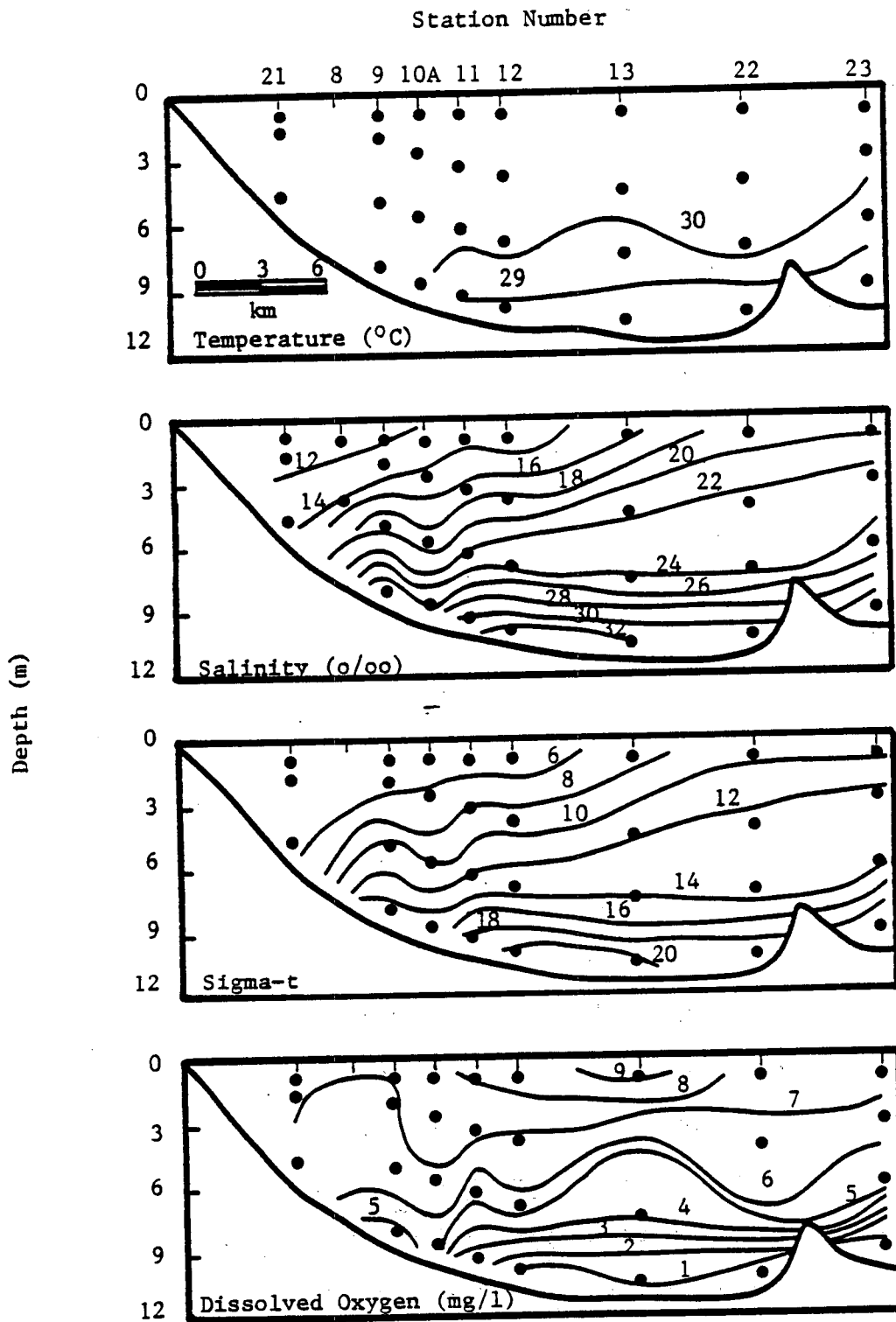


Figure 2-5. Hydrography for cross-shelf transect offshore Holly Beach, Louisiana on July 1, 1981.

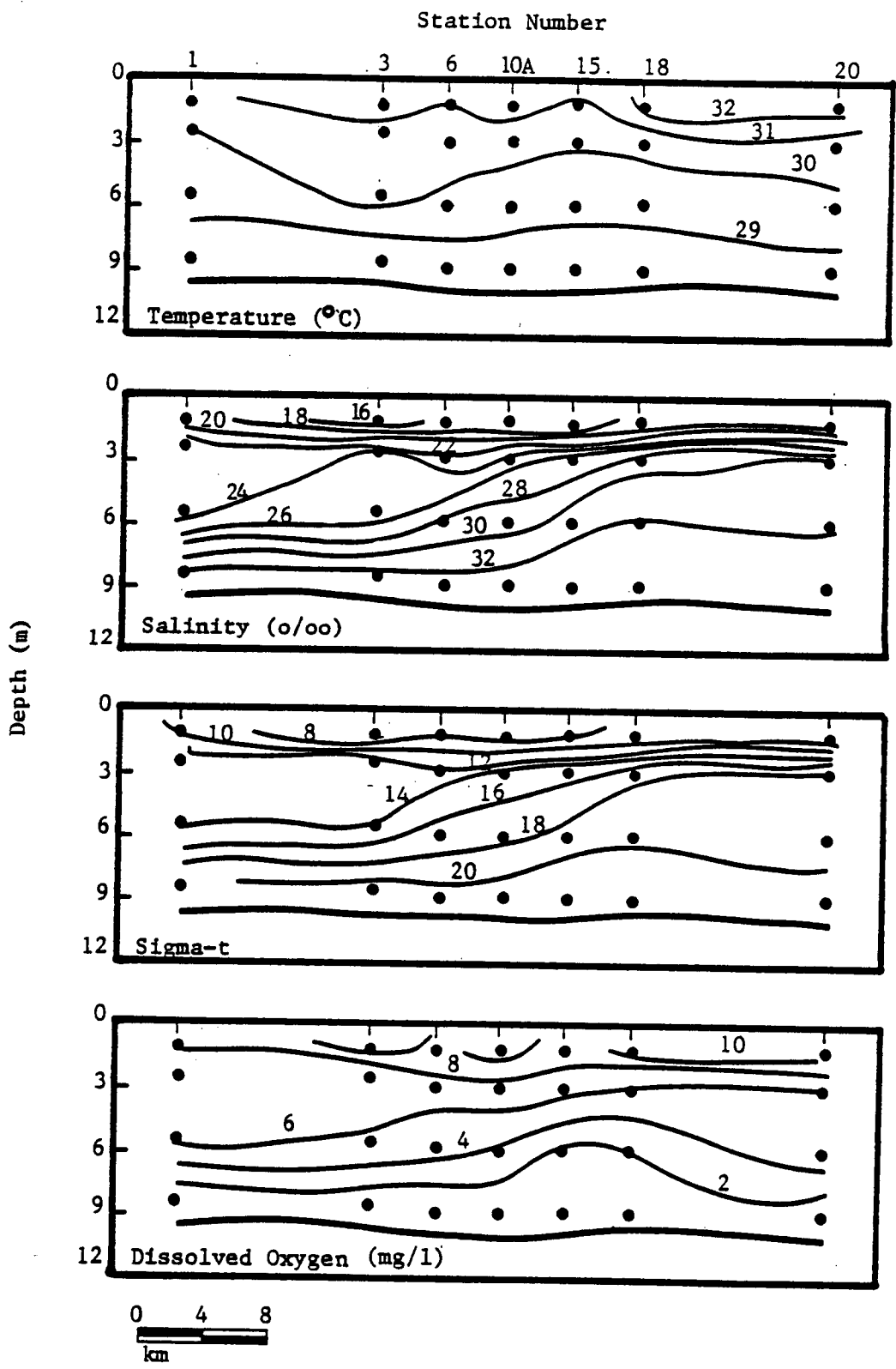


Figure 2-6. Hydrography for alongshelf transect offshore Holly Beach, Louisiana on July 1, 1981.

variation increased to near 2°C with the addition of a 31°C isotherm which is attributed to afternoon heating effect, but otherwise the thermocline was nearly the same along the entire transect.

The salinity data in Figures 2-5 and 2-6 show the isohalines on the east side of the diffuser increased from 20 o/oo at 1 m below the surface to 26 o/oo at 3 m and further increased to 32 o/oo near the bottom. On the west side, they increased from 18 o/oo at 1 m below the surface to 26 o/oo at 6 m and 32 o/oo near the bottom. Therefore, a strong pycnocline was present between 1 and 3 m depths on the east side of the diffuser. West of the diffuser, the data showed a strong pycnocline occurred between 1 and 3 m depths and again between 6 and 9 m. On this day, 205 o/oo brine was being discharged at an average discharge rate of 28,129 barrels/hr. The larger density gradient on the west side of the diffuser is not believed to be the result of brine discharge because its effects are usually a more abrupt change in the isohalines around the diffuser as has been documented at the Bryan Mound site (Kelly et al., 1982a) and in this report.

The dissolved oxygen data collected on July 1 show the first instance of anoxia in the bottom waters where the dissolved oxygen was less than 2 mg/l. The cross-shelf transect shows the 1 mg/l isopleth covered the sea floor (approximately 1 m above the bottom) from station 12 to station 23. Isopleths of 3 and 4 mg/l reached the diffuser site (station 10A) but were apparently broken down by the mixing resulting from the brine discharge. The alongshelf transect dissolved oxygen data show the 2 mg/l isopleth extended along the entire transect, and the mixing effect of the brine discharge was evidenced by the dropping of the 6 mg/l isopleth on the west side of

the diffuser. The anoxia in the bottom waters was expected to occur in these waters because of a similar occurrence reported in the summer of 1978 by Frey et al. (1981). Such an event in 1979 was not documented off Holly Beach, but it is suspected that it did occur in July of 1979 because the anoxia condition was detected at the Bryan Mound site by Harper and McKinney, 1980; Slowey, 1980; Harper et al., 1981).

On July 16, 1981, an additional cruise was conducted to again determine the extent of the anoxia conditions. These data are plotted in Appendix Figures A-16 and A-17. These figures show the conditions were similar to those found on July 1. The slight thermocline (approximately 2°C) and strong halocline (10 o/oo) were still present. The 2 mg/l dissolved oxygen isopleth was present over the entire cross-shelf and alongshelf transects and there was less evidence of brine discharge causing a breakdown in the anoxia conditions near the diffuser.

The thermocline was absent in the August cruise and the salinity stratification weakened. The anoxia conditions also began to breakdown as shown by the cross-shelf and alongshelf data illustrated in Figures 2-7 and 2-8. The temperature data show the water column was isothermal near 30.8°C. The salinity and sigma-t data show the isohalines and isopycnals were nearly horizontal, and the vertical differences decreased to nearly 2 o/oo and 2 sigma-t units respectively. Brine was being discharged at an average rate of 27,360 barrels/hr at an average salinity of 218 o/oo. The only evidence of the effect of brine discharge in the hydrographic data was the small increase in salinity at station 10A in Figure 2-8.

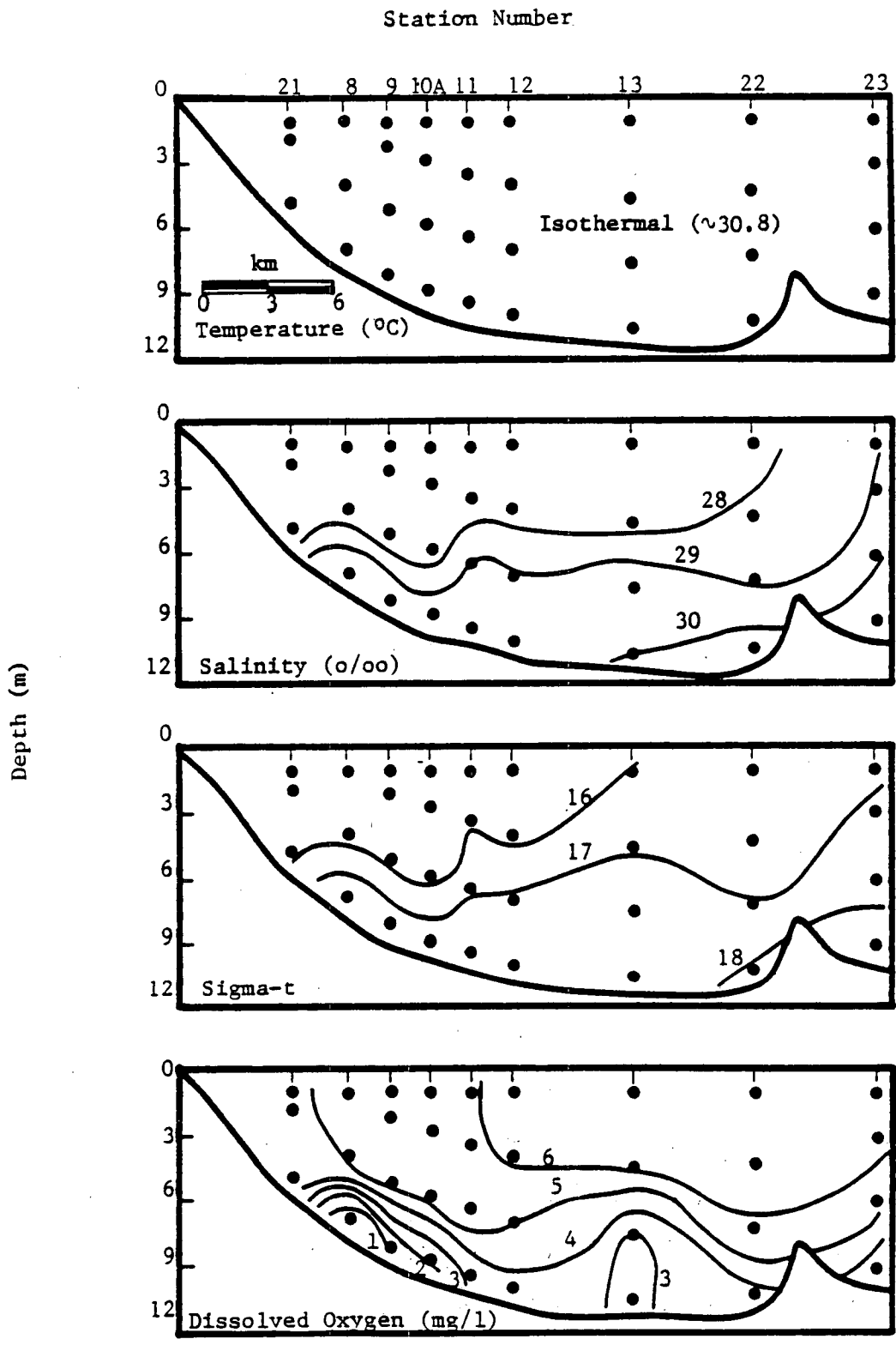


Figure 2-7. Hydrography for cross-shelf transect offshore Holly Beach, Louisiana on August 7, 1981.

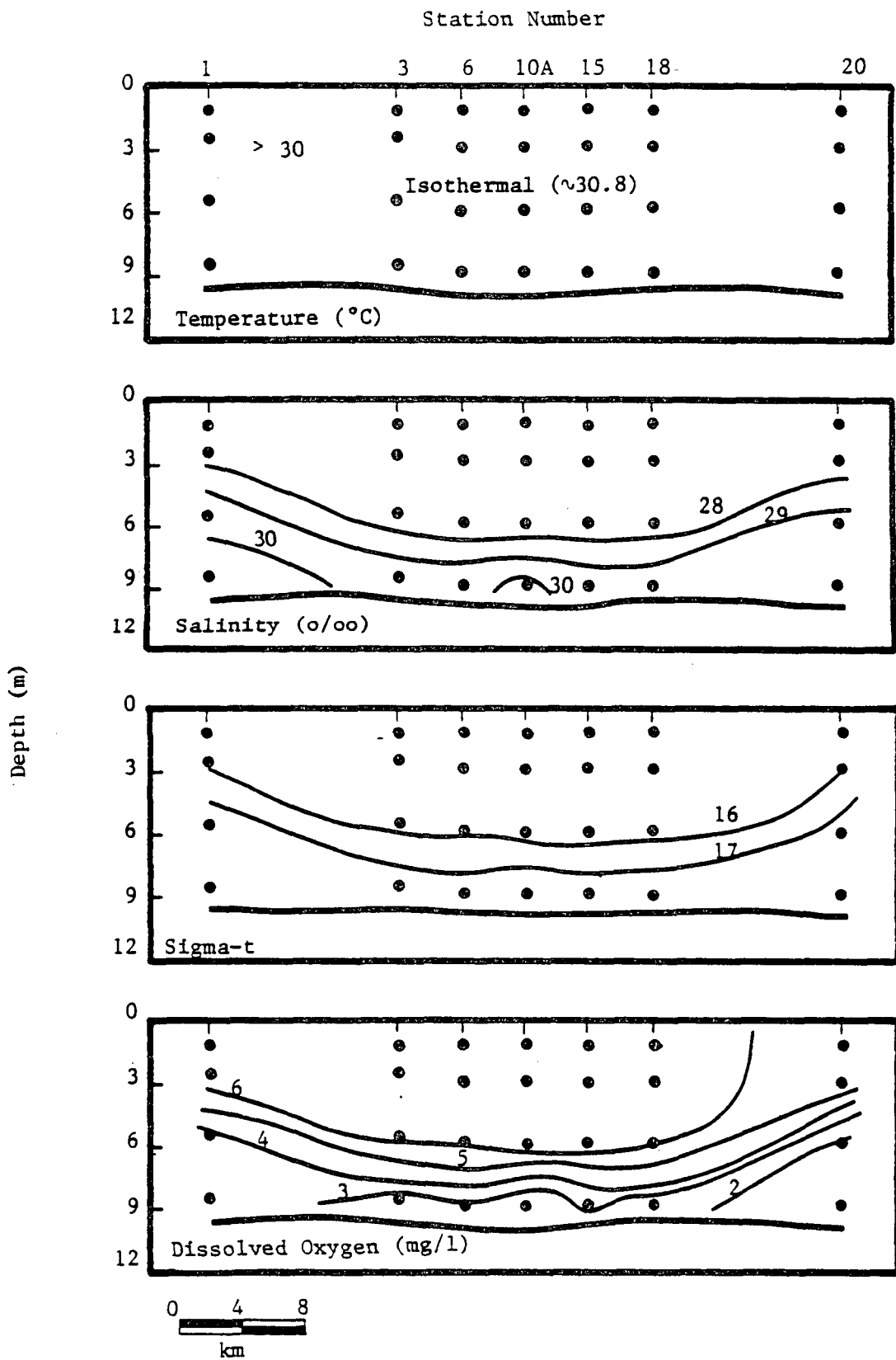


Figure 2-8. Hydrography for alongshelf transect offshore Holly Beach, Louisiana on August 7, 1981.

The dissolved oxygen data show the anoxia condition was beginning to breakdown. The cross-shelf transect shows the 2 mg/l isopleth was limited to the bottom waters midway between station 8 and 9 to station 10A, and the 4 mg/l isopleth extended over the entire cross-shelf transect. The alongshelf transect was measured in the afternoon, and the 2 mg/l isopleth was only present near station 20. The 3 and 4 mg/l isopleths extended the entire length of the transect, and there was no apparent effect of the brine on the dissolved oxygen isopleths. The anoxia conditions broke down inshore of station 21 which is 4 km from the shore and offshore of station 11.

The next hydrographic cruise during the summer was conducted on September 11, 1981, and the results are illustrated in Appendix Figures A-20 and A-21. The brine diffuser had not been operational since August 24, 1981. The temperature data shows the water column was still isothermal, but the temperature had decreased to near 28.7°C. The isohalines became nearly vertical and increased from 23 o/oo inshore (station 21) to 28 o/oo midway between stations 12 and 13. The isopycnals were similar to the isohalines and also indicated there was no vertical stratification.

The dissolved oxygen isopleths show the 1 mg/l isopleth was not present, but there was still a region near the bottom between stations 8 and 12 where the dissolved oxygen was below 4 mg/l. Since the brine was not being discharged at this time, it could not be the cause of the slow recovery of the dissolved oxygen to conditions similar to that measured at the offshore stations. Therefore, it is assumed that some biological demand was causing the depressed oxygen region.

2.2.5.4 Fall 1981 (October through December)

Brine discharge began again on September 15, 1981, but it was on an intermittent basis which continued into October. On October 2, when the hydrographic cruise was conducted, the brine was being discharged at an average rate and salinity of 24,100 barrels/hr and 250 o/oo. The vertical cross-sections of this data are illustrated in Appendix Figures A-22 and A-23. The temperature continued to decrease, but a near isothermal condition (approximately 28°C) still existed. However, fresher water had entered the study area, and the isohalines were nearly horizontal with the salinity increasing from a near surface value of 23 o/oo at station 10A to 29 o/oo near the bottom. The 29 o/oo isohaline at the bottom of station 10A is attributed to the brine discharge. The alongshelf transect, Appendix Figure A-23, shows the effect of the brine discharge more clearly when the 27 and 28 o/oo isohalines appear as convex lines at the bottom of station 10A. It is believed that the 27 and 28 o/oo contours would not have occurred if the brine was not being discharged.

The cross-shelf transect of dissolved oxygen data show a 3 mg/l isopleth was still present and that it had moved a little further offshore between stations 11 and 13 than where it was located in September. The alongshelf transect was measured in the afternoon, and it shows that station 10A was no longer anoxic.

In November the brine discharge operation was almost continuous, and on November 18, brine was being discharged at an average rate, salinity, and temperature of 21,979 barrels/hr, 210 o/oo, and 25°C. The November hydrographic cruise was conducted on this date, and the cross-shelf and alongshelf transects are illustrated in Figures 2-9

and 2-10 respectively. The temperature data indicate the water column had returned to a near isothermal condition at 20°C. The bottom isotherm of 20°C is the result of bottom measurements which may have been affected by the surrounding sediments or a slight temperature increase of 0.1 or 0.2°C due to the warmer (25°C) brine discharge. For example, the bottom temperature at stations 1 and 20 was 19.9°C, and at stations 3, 6, 10A, and 15, it was 20.2, 20.1, 19.9, and 20.2°C respectively. The resolution of the temperature sensor is 0.1°C, and consequently it is not possible to definitely conclude that the observed small temperature increase was caused by the brine discharge.

The salinity and density data on this date clearly show the existence of the brine discharge near the bottom. The isohalines of 31 to 36 o/oo in the cross-shelf transect (Figure 2-9) and 31 to 34 o/oo in the alongshelf transect (Figure 2-10) were caused by the brine discharge. This 31 o/oo isohaline shows the brine plume extends from station 9 offshore to near station 13, and in the alongshelf direction it extends from midway between stations 3 and 6 to midway between stations 15 and 18. The cross-shelf length of the isohaline is 10 km and the alongshelf length is 13 km. The vertical extent is exaggerated due to the linear interpolation.

The dissolved oxygen data show no evidence of anoxia and the lowest dissolved oxygen isopleth is 6 mg/l in the cross-shelf transect, Figure 2-9. For the alongshelf transect, isopleths of 4 and 5 mg/l are shown on the west side of the diffuser, and these low values may be caused by the sediment surrounding the sensor when it was setting on the bottom. The data for both transects indicate the brine discharge caused the dissolved oxygen to be mixed in the

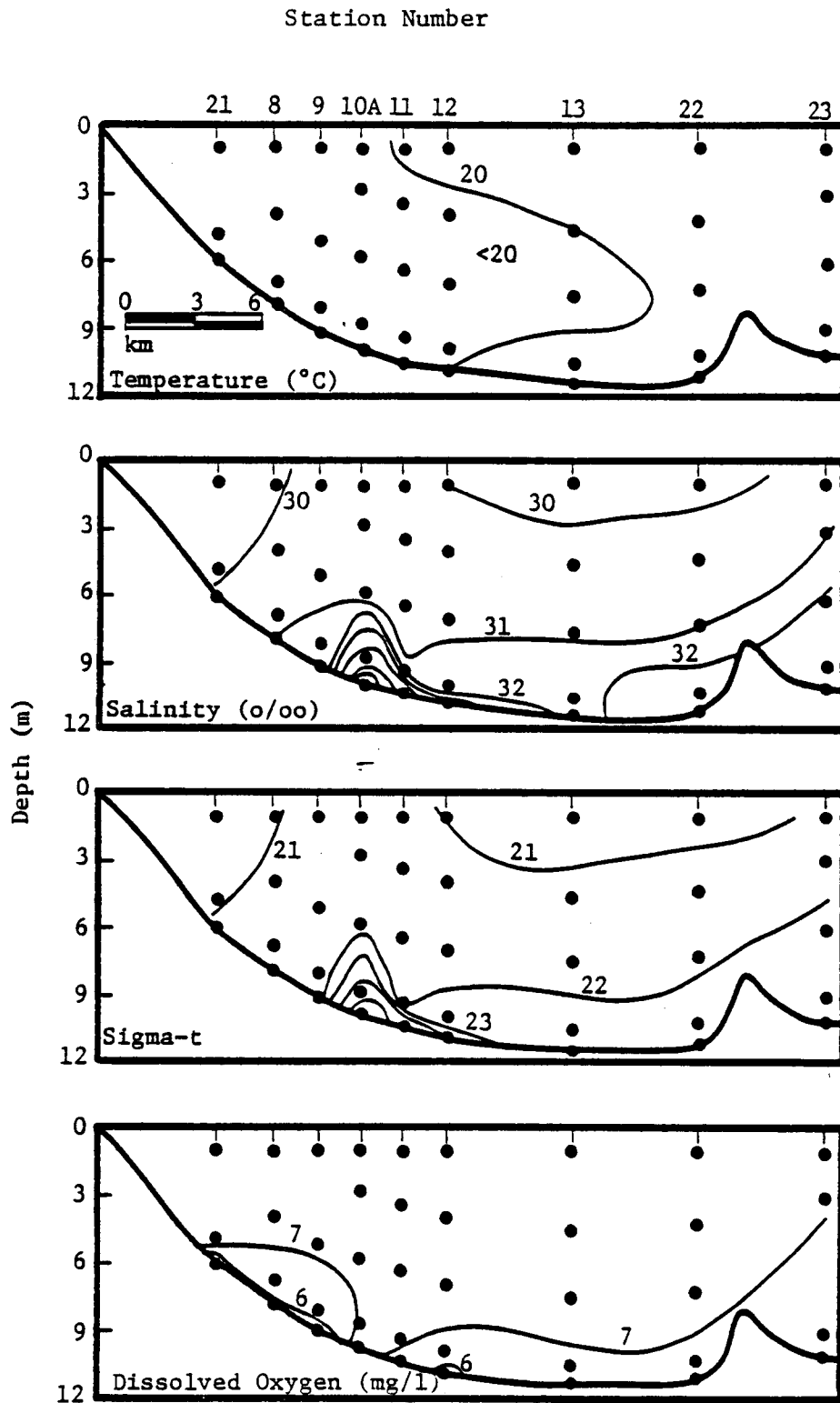


Figure 2-9. Hydrography for cross-shelf transect offshore Holly Beach, Louisiana on November 18, 1981.

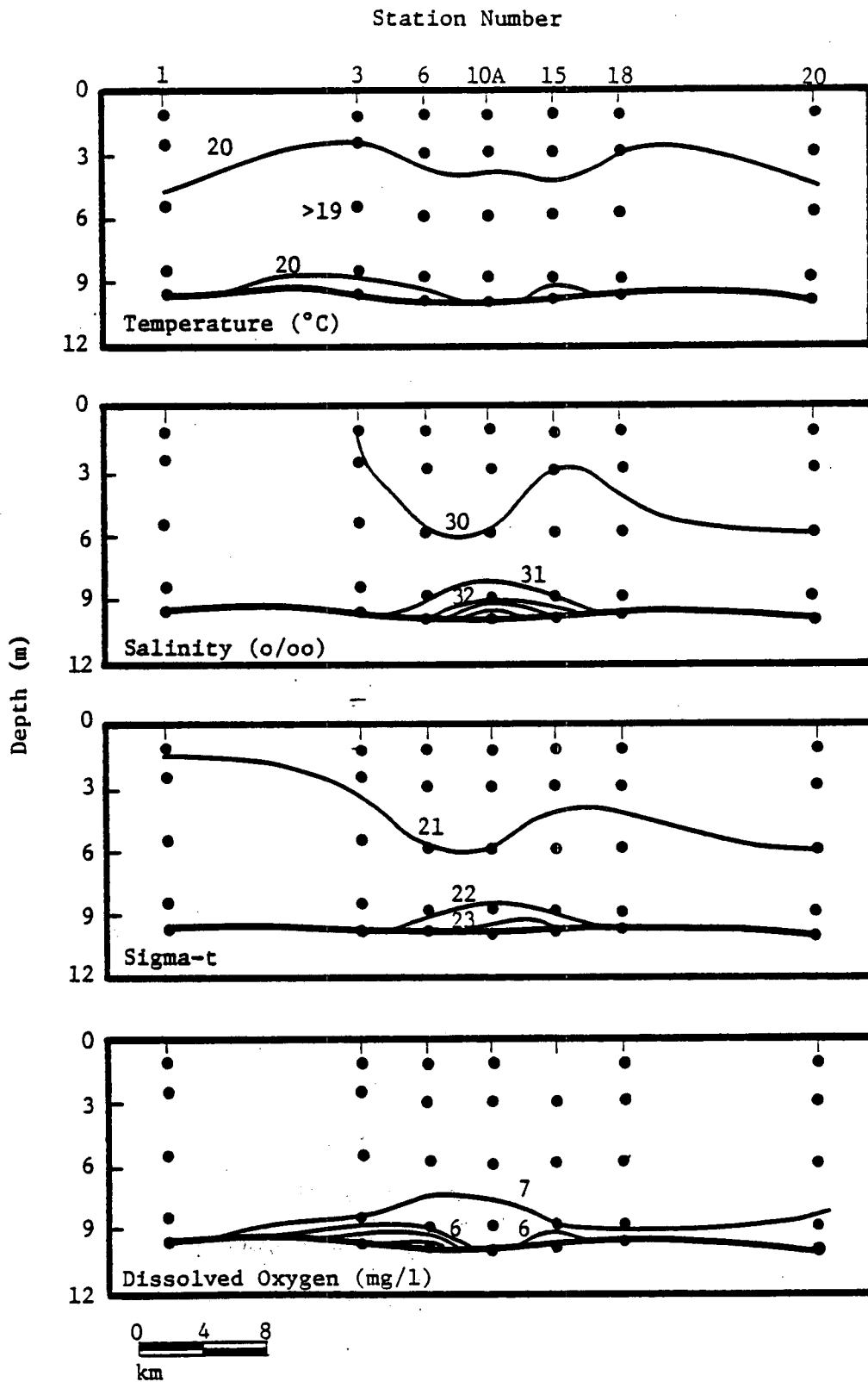


Figure 2-10. Hydrography for alongshelf transect offshore Holly Beach, Louisiana on November 18, 1981.

vicinity of the diffuser as evidenced by the discontinuous nature of the 6 and 7 mg/l isopleths in the cross-shelf transect and the 6 mg/l isopleth in the alongshelf transect.

The next hydrographic cruise was conducted on December 2, 1981, when brine was being discharged at an average rate, salinity, and temperature of 21,681 barrels/hr, 210 o/oo, and 21°C respectively. Appendix Figures A-27 and A-28 illustrate the data for this date. The isotherms were essentially horizontal and the temperature increased from 18.9°C to 20.9°C at station 10A while slightly warmer water was found offshore at station 23. The salinity and sigma-t data show the existence of some salinity stratification near middepth where the isohalines were near horizontal and increased from 30 to 32 o/oo. The bottom isohalines show the extent of the brine discharge was between stations 9 and 11 in the cross-shelf direction and between stations 6 and 15 in the alongshelf direction. The overall dissolved oxygen continued to increase with values near 8 mg/l at the surface and near 7 mg/l at the bottom. Both transects showed a slight increase in the bottom dissolved oxygen at the diffuser site compared to the surrounding bottom measurements.

2.2.5.5 Winter 1982 (January through March)

The brine discharge was again intermittent during January 1982 which was evident in the January 22 hydrographic data. On this date, brine was discharged for only fourteen of the possible twenty-four hours at an average rate, salinity, and temperature of 22,563 barrels/hr, 240 o/oo, and 18°C. The hydrographic data for this date are illustrated in Appendix Figures A-28 and A-29. The cross-shelf data show the isotherms were nearly vertical with the temperature

increasing from near 10°C inshore to near 13°C offshore, and the alongshelf data show the temperature was between 10 and 11°C along the entire transect.

The salinity and sigma-t cross-shelf data show the isohalines and isopycnals were nearly at 45° with the fresher water near the shore. The isohalines increased from 26 o/oo near stations 8 and 21 to 33 o/oo near station 13 at the surface. There was no indication that brine was being discharged during the time the cross-shelf data was being collected. The alongshelf transect (Appendix Figure A-29) shows a definite brine plume effect with isohalines 34 and 35 o/oo which extended from midway between station 10A and 14 to just beyond station 6. A rather strong density gradient was also located in the upper 3 m of the water column for the entire alongshelf transect where the isohalines and isopycnals increased from 27 to 29 o/oo and 22 to 23 sigma-t units.

The dissolved oxygen data show the dissolved oxygen decreased from 10 mg/l near the surface at station 10A to near 8 mg/l at the bottom. The isopleths were near horizontal, and the alongshelf data showed no indication of increased dissolved oxygen in the diffuser area as previously detected.

The February hydrographic data are illustrated in Figures 2-11 and 2-12. Brine was being discharged on a continuous basis with an average rate, salinity, and temperature of 23,000 barrels/hr, 229 o/oo, and 14°C. The cross-shelf data (Figure 2-11) show the isopleths of temperature, salinity, and sigma-t were vertical, and consequently, the water column was well mixed in the vertical direction. The 10 and 11°C isotherms were located near stations 21 and 9 respectively, and

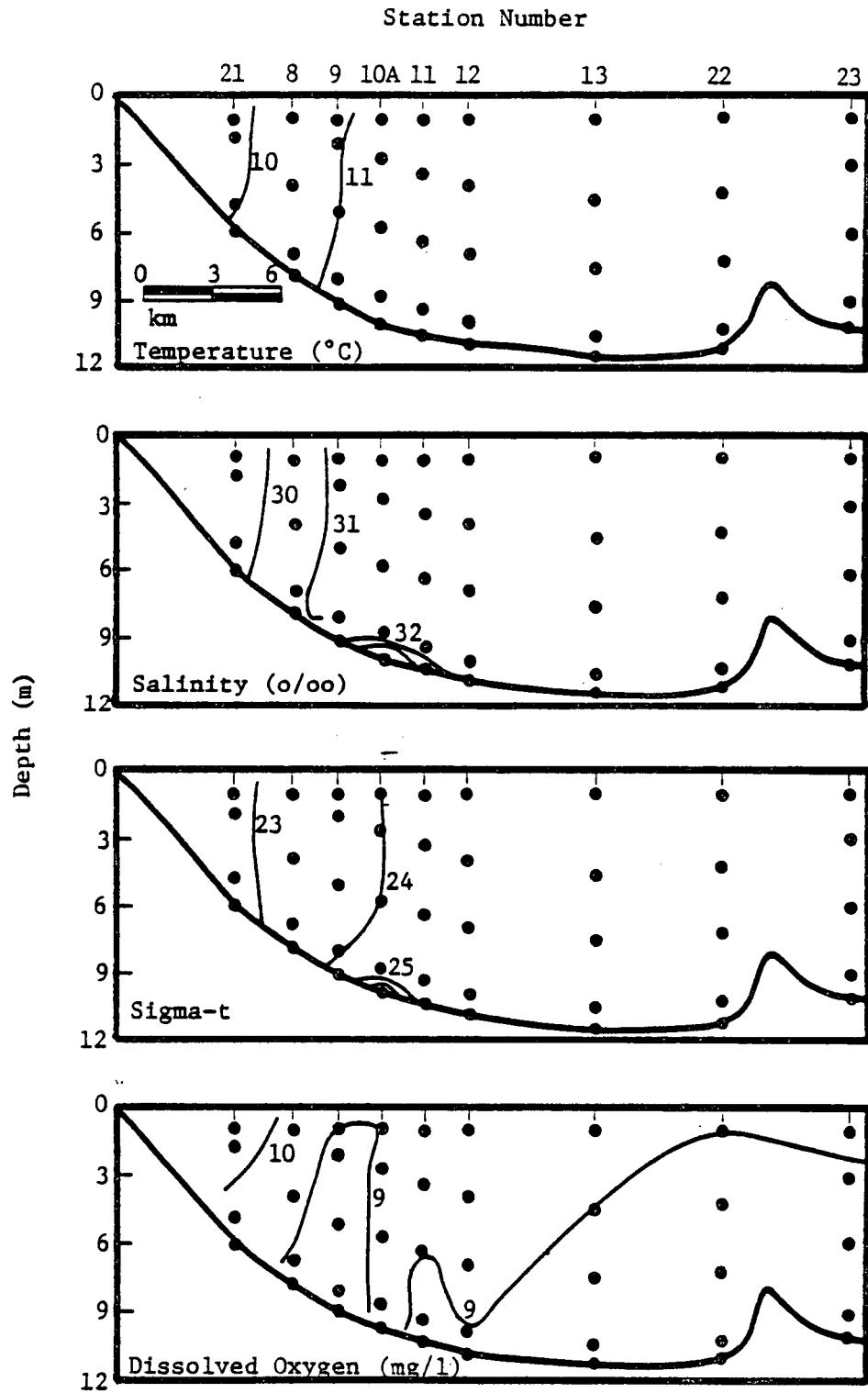


Figure 2-11. Hydrography for cross-shelf transect offshore Holly Beach, Louisiana on February 11, 1982.

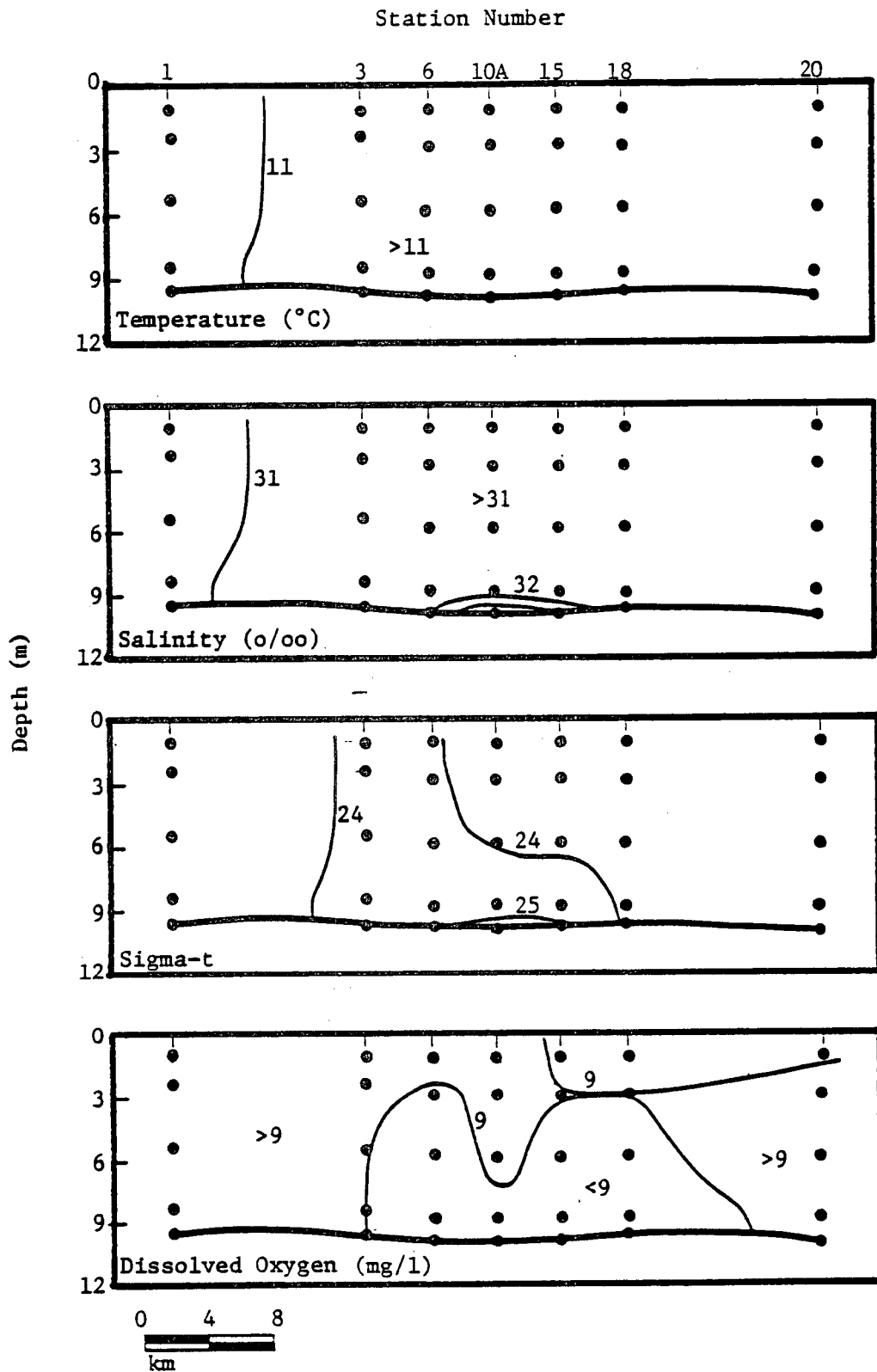


Figure 2-12. Hydrography for alongshelf transect offshore Holly Beach, Louisiana on February 11, 1982.

the temperature increased with distance offshore but remained below 12°C. Isohalines of 30 and 31 o/oo were also vertical and similarly located as the isotherms with salinity increasing in the offshore direction but remaining less than 32 o/oo. The brine plume is clearly shown in Figure 2-11 by the convex isohalines of 32 and 33 o/oo extending from near station 9 to midway between stations 11 and 12, and they also show the plume was within 1 m of the bottom. The dissolved oxygen isopleths show the dissolved oxygen was near 9 mg/l except for close to the shore where it was near 10 mg/l.

The alongshelf transect (Figure 2-12) shows there was a small increase in temperature from west to east and that the temperature was near 11°C from top to bottom. The salinity data indicate the salinity also increased slightly from west to east and was well mixed from top to bottom at near 31 o/oo except at the bottom of stations 6 through 14. Here, isohalines of 32 and 33 o/oo were detected which was the result of the brine discharge. The dissolved oxygen data is confusing, but it basically indicates the dissolved oxygen was near 9 mg/l from top to bottom for this transect.

The late winter hydrographic cruise was conducted on March 12, 1982, and the data are plotted in Appendix Figures A-32 and A-33. On this day, the brine salinity was 232 o/oo, and it was being discharged at an average rate of 31,283 barrels/hr at a temperature of 21°C. The temperature data indicate the overall warming of the water column was continuing with the temperature being near 16°C.

The cross-shelf salinity data show the isohalines were nearly at an angle of 45° and increasing from 26 o/oo inshore to 30 o/oo offshore. As previously observed, the brine plume was detected by the

convex isohalines centered over station 10A which increased from 30 to 32 o/oo and were contained between stations 9 and 11. The alongshelf transect indicates the salinity front shown in the cross-shelf data had moved further offshore, but show the brine plume was not as clearly evident as in the cross-shelf data. The dissolved oxygen data indicate the amount of dissolved oxygen in the water was nearly the same as in February with a value near 9 mg/l except inshore where it was near 10 mg/l.

The final hydrographic cruise for the first year of postdisposal studies was conducted on April 27, 1982. Although these data really belong with a discussion of spring data, it is discussed here because the other spring months were not included in the first year study. The results of the April 27, 1982 hydrographic data are illustrated in Appendix Figures A-34 and A-35. These data show no thermal stratification was present with the temperature near 21°C.

The salinity data indicate the beginning of the spring runoff, with the presence of strong vertical salinity and density gradients. At station 10A, the isohalines and isopycnals were near horizontal in the cross-shelf and alongshelf transects with values increasing from surface to bottom of 20 to 29 o/oo and 13 to 20 sigma-t units respectively. The brine plume was again observed in the near bottom waters as convex contours of 29 and 30 o/oo, or 20 and 21 sigma-t units. The dissolved oxygen isopleths also show the increased variation with depth with values decreasing from near 9 mg/l at the surface to near 7 mg/l at the bottom.

2.2.6 Comparison of Temperature-Salinity Relationships for the Surface and Bottom Water at the Diffuser and Control Station

The temperature-salinity relationship for the surface and bottom waters at the West Hackberry diffuser site (station 10A) and the control station (station 20) which is 7.6 km east of the diffuser is shown in Figure 2-13. The May 1981 data are marked with the number 5 which show the surface temperature and salinity were 24.1°C and 26.2 o/oo at station 10A and 24.6°C and 26.4 o/oo at station 20. The surface waters warmed and freshened through July with a minimum salinity of 16.2 o/oo at 10A and 19.7 o/oo at station 20 and a maximum temperature of 31.5°C at 10A and 32.3°C at station 20. The waters at both stations were more saline in August reaching a salinity of near 27.5 o/oo and attained a maximum temperature of 30.8°C. Station 10A freshened to 21.9 o/oo in October, and it was followed by station 20 at 20.2 o/oo. The surface waters at both stations began to cool in September and by October they had decreased to 28°C. The November data indicate the surface waters continued to cool to 20.5°C, but they had become more saline with values near 30 o/oo at both stations. In December and January, the temperatures continued to decline to a minimum value of 10.2°C and 11.0°C at stations 10A and 20 while the salinity decreased to 24.9 o/oo at station 10A and 28.7 o/oo at station 20. The temperature began to climb after January, and it reached a value of nearly 11.4°C at both stations. The salinity increased to its maximum value of 31.3 o/oo and 31.4 o/oo at stations 10A and 20 respectively. In March and April, the surface waters freshened and the temperatures increased. By April, the salinity had

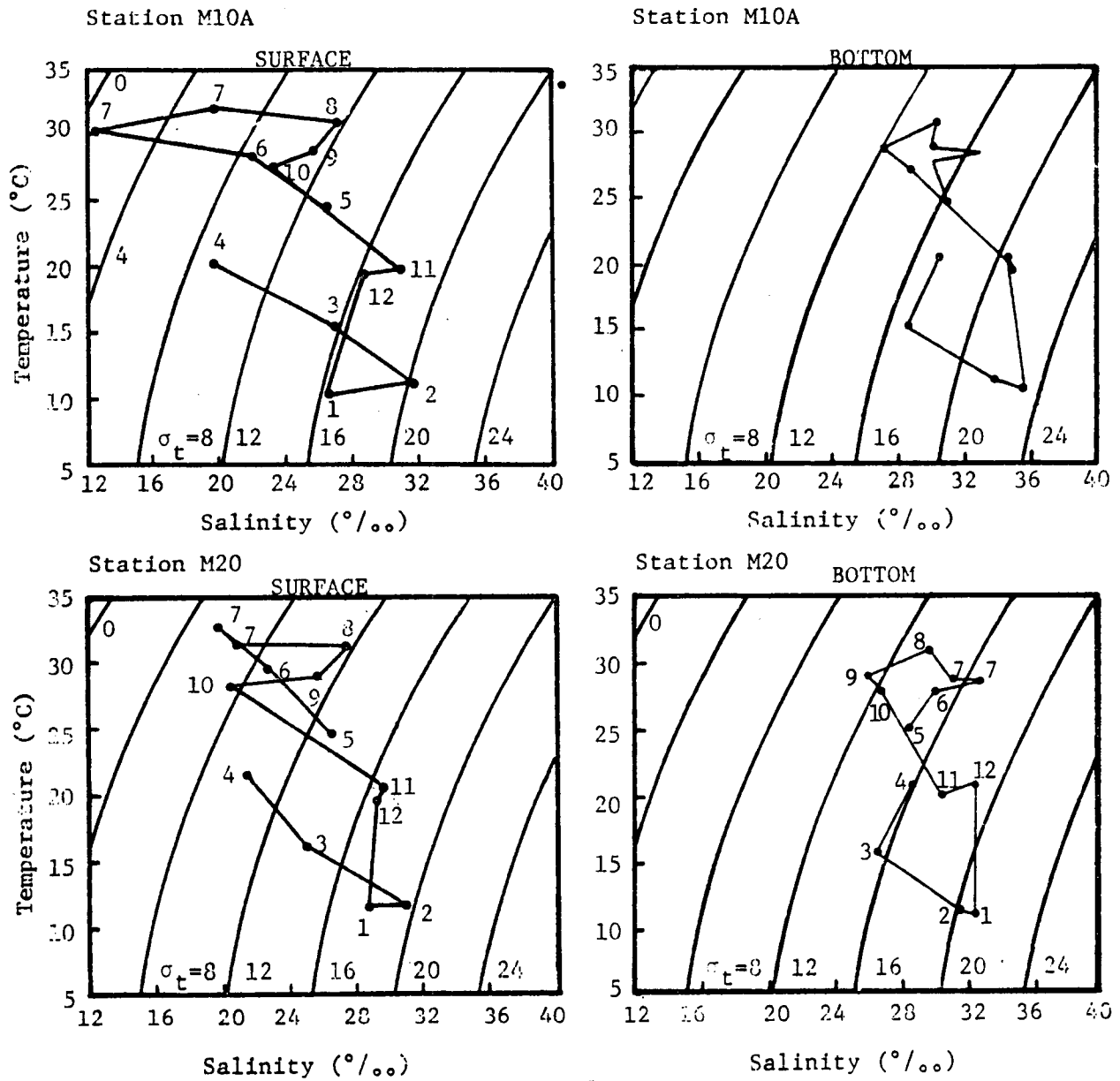


Figure 2-13. Temperature-salinity relationships for the surface (1 m below surface) and bottom water at the diffuser (station M10A) and at a control station (M20). Isopleths of sigma-t are also shown. The numbers alongside each data point indicate the month of the year from 5/81 to 4/82.

decreased to 19.4 and 21.2 o/oo at station 10A and 20 respectively, and the temperature rose to nearly 21.9°C. In summary, the surface temperature-salinity relationships show the temperature reached a maximum in August and a minimum in January with a range from 10.2 to 32.3°C. The temperature at the two stations agreed very well and the largest difference was 0.8°C in July 1981. The data showed the maximum salinity was 31.4 o/oo in February and the minimum (16.2 o/oo) occurred in July 1981. The agreement between the two stations for salinity was not as good as found in the case of temperature and the maximum variation was 3.8 o/oo in January.

The bottom waters at station 10A receive the highest brine concentrations being discharged, and station 20 was not expected to be impacted by the brine. So a comparison of the bottom data is made to evaluate the maximum effects on the bottom waters. The May data indicate the bottom waters at the two stations were near 24.9°C and the salinity was 28.2 o/oo at station 20 and 30.6 o/oo at station 10A indicating an increased salinity due to brine discharge. From June through July the temperature increased, and the salinities were in close agreement showing little effect of brine discharge as a result of low brine salinities. In August the bottom temperature reached a maximum of 30.8°C, and the salinities were essentially the same (approximately 30 o/oo) at both stations. The brine diffuser was not operating in September and the bottom salinity reached its minimum value of 26.7 o/oo and 26.0 o/oo at stations 10A and 20 respectively. In November, the bottom temperature decreased to 19.9°C at both stations while the salinity at stations 10A and 20 was 34.9 and 30.3 o/oo. The higher salinity at station 10A was clearly caused by the

brine discharge. Similar results were obtained in December with the salinity at station 20 increasing to 32.4 o/oo. The January data shows the minimum temperature was reached at 10.7°C, and the maximum salinity of 35.4 o/oo at station 10A was also measured while it was 32.3 o/oo at station 20. Again, this was attributed to the brine discharge. The February and March temperatures increased and the salinities decreased. Station 10A was near 2 o/oo greater than the salinity measured at station 20 which was again attributed to the brine discharge. The April data showed the temperature had reached 20.5°C, and the salinity was 30.4 o/oo at station 10A and 28.6 o/oo at station 20. Thus, the bottom temperature-salinity relationships show that the bottom temperature was very nearly identical at station 10A and 20. The maximum temperature was 30.8°C (August) and the minimum was 10.7°C in January. At station 20, the maximum and minimum salinity was 32.7 o/oo (July) and 26.0 o/oo (September) with a range of 6.7 o/oo. In contrast, the salinity range at station 10A was 8.7 o/oo while the maximum and minimum values were 35.4 o/oo (January) and 26.7 o/oo (September). The increase in the range of salinity at station 10A compared to station 20 is attributed to the brine discharge.

2.2.7 Temporal Variation of Bottom Hydrographic Data at the Diffuser Site and Control Station

The temporal variation of the bottom temperature, salinity, sigma-t, and dissolved oxygen which were measured at the diffuser site (station 10A) and at the east control station (station 20) are compared. The maximum impact of the brine discharge is expected to occur in the vicinity of the diffuser which is represented by

measurements at station 10A. It was also expected that the brine plume would not reach station 20, and therefore it was selected as the control station.

The temporal variation of temperature from May 1981 through April 1982 at stations 10A and 20 is illustrated in Figure 2-14. These data show that the difference in the temperature at stations 10A and 20 was very small, in fact the maximum difference was 0.2°C. These data show the intrayear bottom temperature variation was from 30.8°C to 10.7°C with the maximum and minimum occurring in August and January respectively. During the days when the temperature measurements were taken the average brine temperature difference was only 3.7°C above the ambient temperature. Therefore it is reasonable to expect that the data would show there was no temperature increase in the bottom waters. Consequently, it can be stated that a thermal plume has not resulted from the brine discharge.

Brine has been discharged near station 10A, and consequently the bottom waters at this location should be near the highest salinity. Since the brine is much more dense than the ambient sea water, it falls to the bottom and forms a brine plume which is advected away and diluted by the ambient sea water. In Chapter 4 of this report it has been shown that the above ambient salinity plume did not reach the control station during the first year of discharge. Thus, a comparison of the bottom salinity at stations 10A and 20 should show the maximum effect of the brine discharge on increasing the salinity of the local Gulf waters.

Figures 2-15 and 2-16 show the temporal variation of bottom salinity and density (σ_t) at the diffuser site (station 10A) and

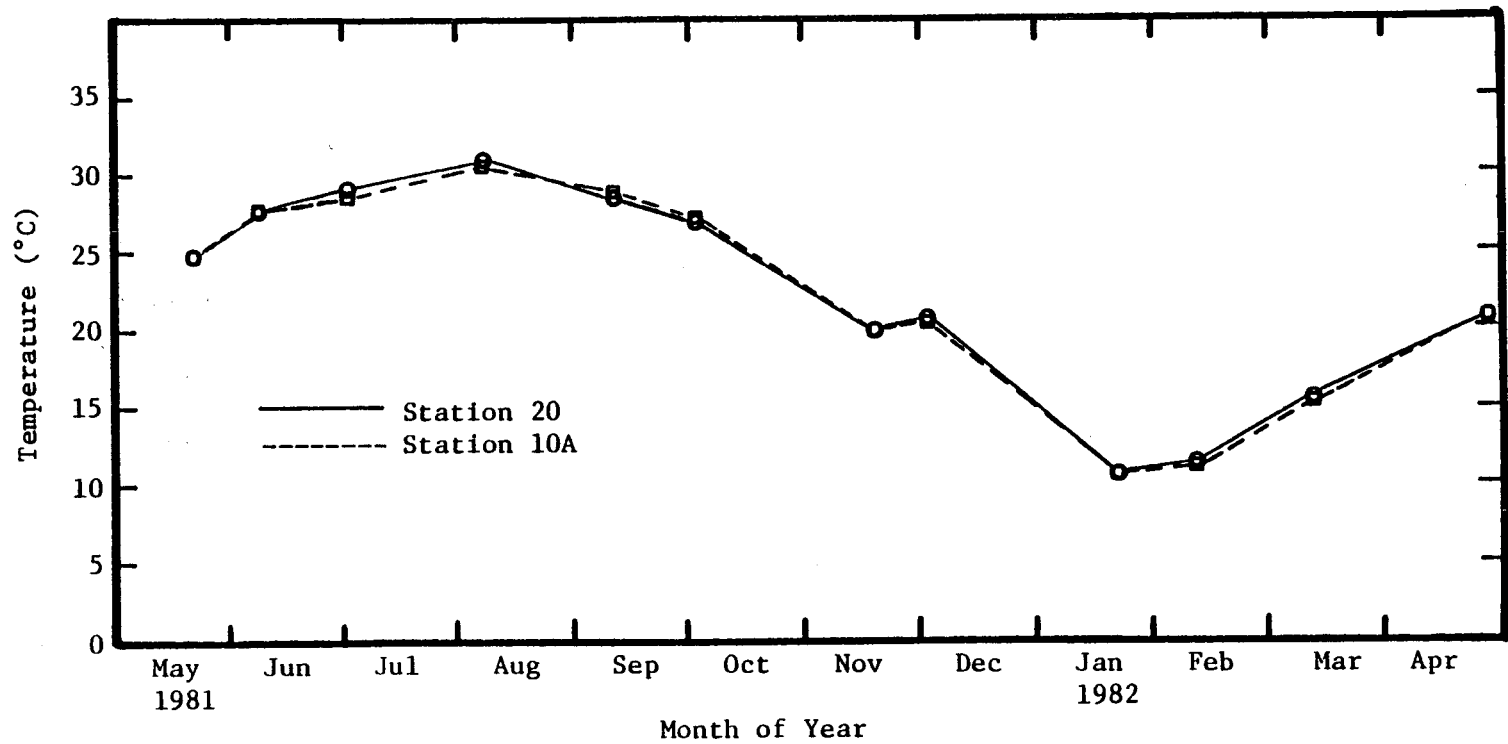


Figure 2-14. Temporal variation of bottom temperature at the diffuser site (station 10A) and the east control station (station 20).

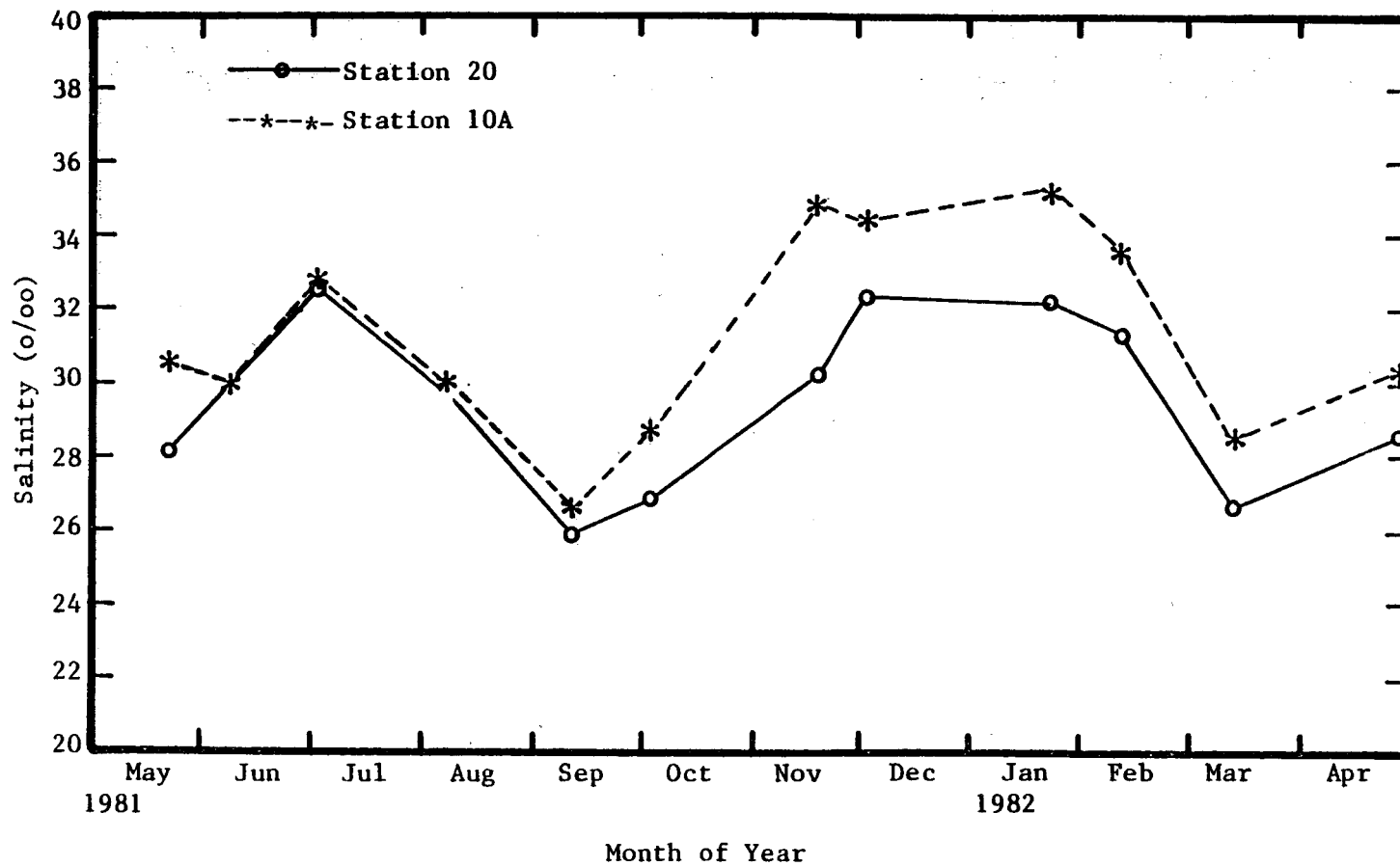


Figure 2-15. Temporal variation of bottom salinity at the diffuser site (station 10A) and the east control station (station 20).

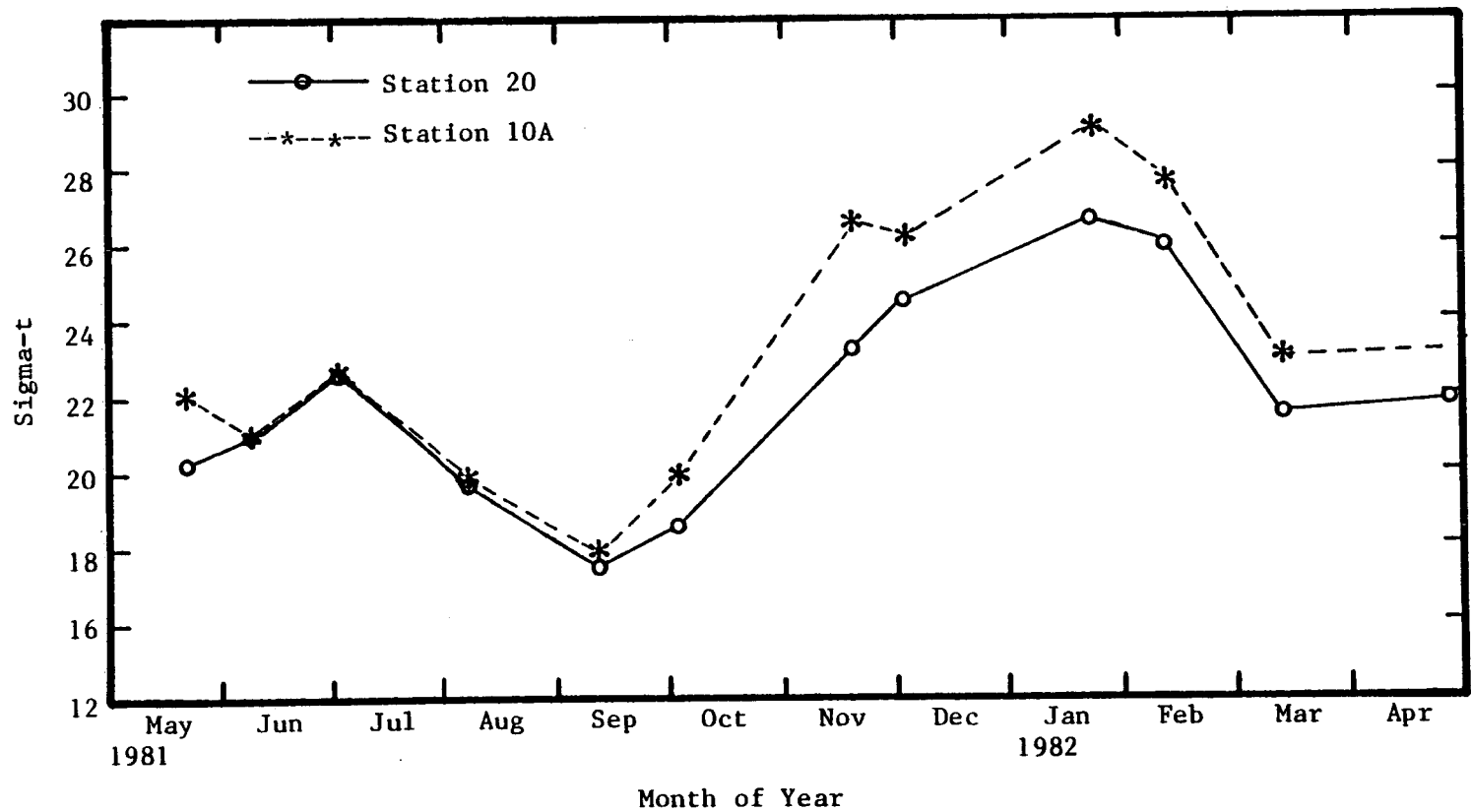


Figure 2-16. Temporal variation of bottom sigma-t at the diffuser site (station 10A) and the east control station (station 20).

the control station 20. The variation in density follow closely the salinity variation and thus only the salinity variation is described in detail. The May data show the salinity at station 10A was 30.6 o/oo while the value at station 20 was 28.2 o/oo. The 2.4 o/oo salinity difference is attributed to the brine discharge. From June through September, the difference in salinity was less than 1 o/oo and this indicated there was essentially no effect of brine discharge on the salinity of the bottom waters. In June, July, and August the average brine salinity was 176 o/oo, 205 o/oo, and 218 o/oo which is low compared to the 100% saturated condition of 263 o/oo. The low brine salinity and the fact that the bottom measurement were taken 1 m above the bottom are probably the reason for the small salinity differences. The September data was collected on a day when the diffuser was not operating. The salinity differences from November 1981 through February 1982 were always greater than 2.0 o/oo with a maximum value of 4.6 o/oo recorded in November. All of these differences are attributed to the brine discharge whose salinity was between 210 and 250 o/oo. The March and April data show a 1.8 o/oo salinity difference was measured and it also is attributed to the brine discharge.

The temporal salinity data show the bottom salinity range was 35.4 to 26.7 o/oo at station 10A and 32.7 to 26.0 o/oo at station 20, and the increased range was caused by the brine discharge. On the days of the hydrographic cruises the maximum salinity difference was 4.6 o/oo and it is expected that the salinity differences at stations away from 10A would be less.

The temporal variation of the bottom dissolved oxygen at stations

10A and 20 are illustrated in Figure 2-17. In May 1981 the dissolved oxygen at station 10A was 3.9 mg/l which was much lower than the 5.7 mg/l value at station 20. The bottom dissolved oxygen was the same in June at station 10A but had decreased to 4.3 mg/l at station 20. The July 1, 1981 data show the bottom waters went anoxic at both station 10A and 20 and remained anoxic through the August 7 cruise with dissolved oxygen values of 2 mg/l or less. Brine was not being discharged in September when the dissolved oxygen climbed to 3.3 and 5.9 mg/l at stations 10A and 20 respectively. The dissolved oxygen reached values between 6 and 8 mg/l at both stations from October through January 1982. Except for October the station 10A dissolved oxygen was higher by an average of 0.4 mg/l than that at station 20. In February the highest values were measured as 8.9 and 9.2 mg/l at stations 10A and 20 respectively. By April the dissolved oxygen had reached values of 6.7 and 6.2 mg/l at stations 10A and 20.

In summary, the temporal bottom dissolved oxygen data show an annual cycle in which the dissolved oxygen decreased in the spring and reached anoxic conditions (near 0 mg/l) at the beginning of the summer. The anoxic conditions (less than 2 mg/l) remained until late summer when the dissolved oxygen began to increase and reached values near 7.0 mg/l in mid fall (November). The maximum dissolved oxygen was reached in the winter (February) with a value near 9.0 mg/l. Early spring saw the dissolved oxygen values decreasing to near 6.0 mg/l. During the months of May 1981, June 1981, July 1981, September 1981, October 1981, February 1982, and March 1982 the station 10A bottom dissolved oxygen was less than that at station 20 by an average of 0.6 mg/l excluding September because no brine was being discharged.

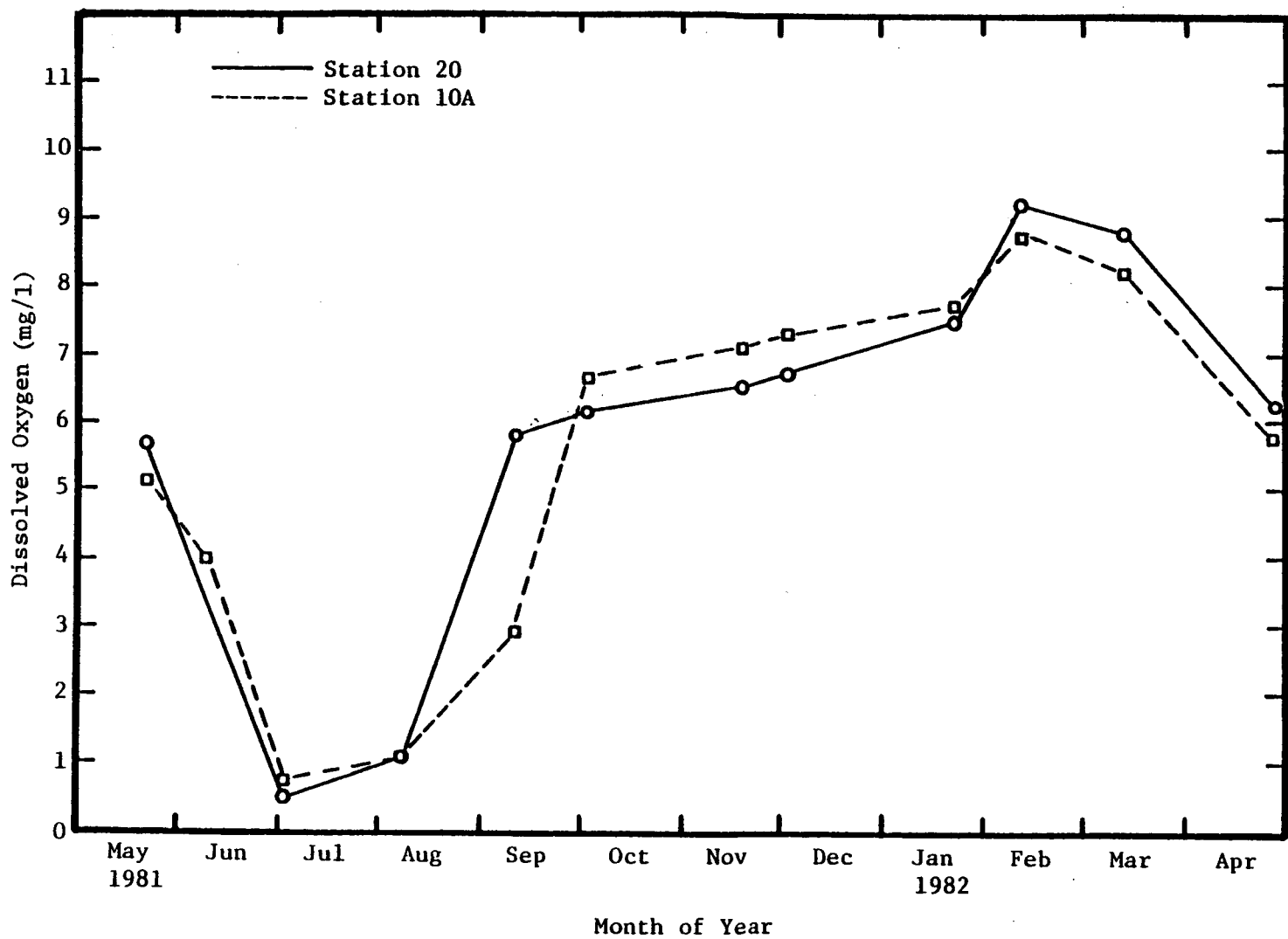


Figure 2-17. Temporal variation of bottom dissolved oxygen at the diffuser site (station 10A) and the east control station (station 20).

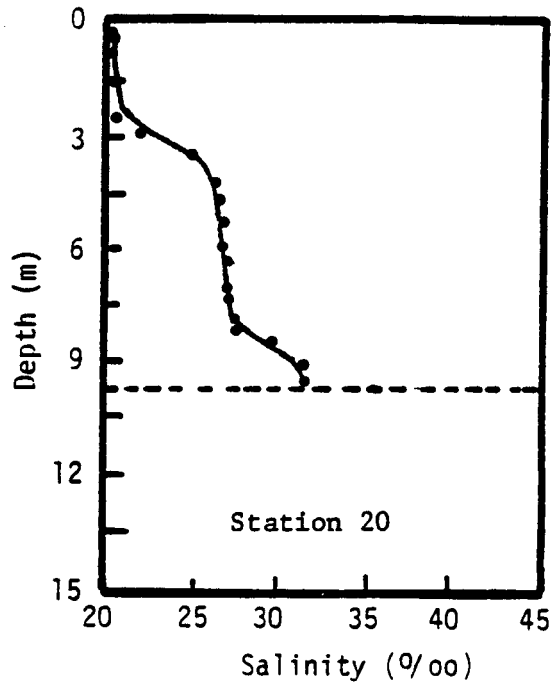
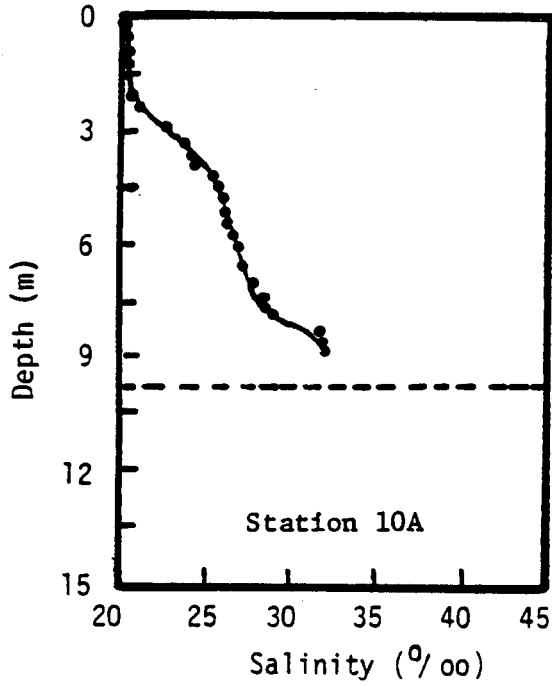
During August, November, December, January, and April 1982 the station 10A dissolved oxygen was greater than that at station 20 by an average of 0.5 mg/l. Thus, it is concluded from this data that the brine discharge had little effect on increasing or decreasing the dissolved oxygen in the bottom waters.

2.2.8 Vertical Salinity Profiles at the Diffuser Site and Control Station

The Grundy CTD/DO profiling instrument was used to collect the hydrographic data on most of the cruises. This instrument is capable of rapidly sampling all parameters, and thus the data can be used to show the detailed structure of the water column. The temperature of the water column in these coastal waters does not change very much as shown in previous sections. The dissolved oxygen sensor has a slow response time, and therefore the fast sampling frequency was not a great asset. Since salinity is the more important physical property in the density stratification and in describing the brine plume coverage, the available vertical profiles are described.

Vertical profiles of salinity at station 10A and station 20 are shown in Figure 2-18 for the hydrographic cruise on July 16 and September 11, 1981. At station 20, the salinity profile shows the presence of fresher water in the first 2 meters and a sharp halocline at the 3 m depth. Then, the water column was nearly isohaline from 4 to 8 m where a second sharp halocline was present and the salinity increased from 27 o/oo to 31 o/oo. The last meter of depth saw the salinity increase from 31 to nearly 32 o/oo. In comparison, the profile at station 10A shows the same depth of fresher water was present at the surface, but a more gradual halocline was observed from

July 16, 1981



September 11, 1981

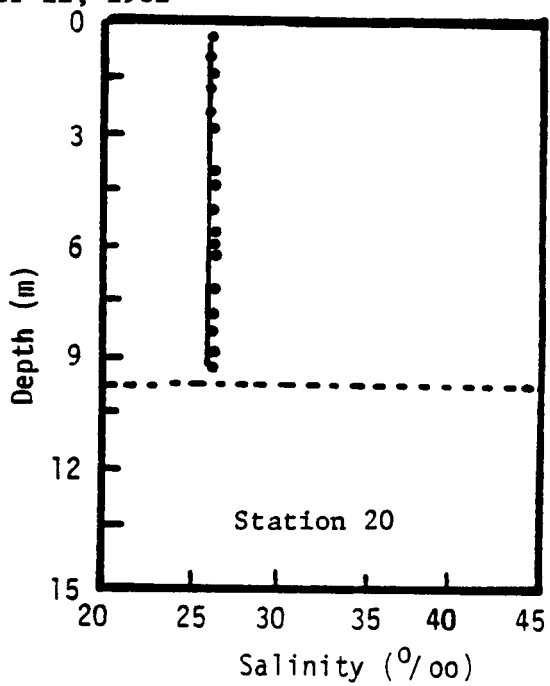
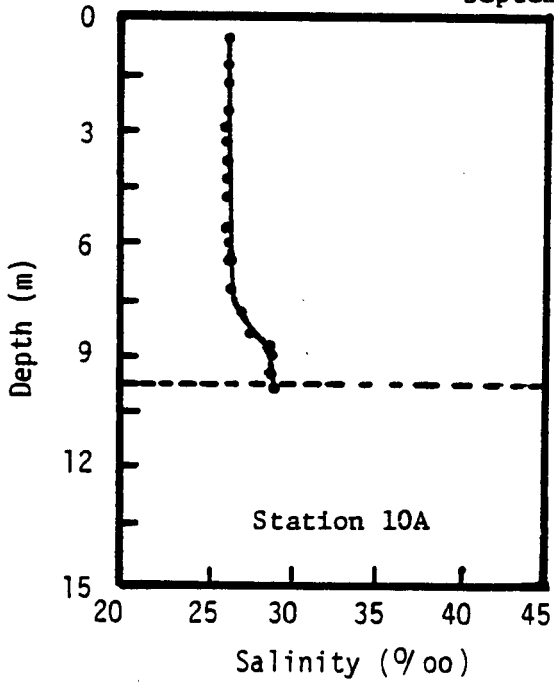


Figure 2-18. Vertical salinity profiles at stations 10A and 20 on July 16 and September 11, 1981.

near 2.5 to 8 m where it sharply increased from 30 to near 32 o/oo. Brine was being discharged on this day at a rate of 24,848 barrels/hr and salinity of 212 o/oo, but the profile did not appear to show any effects such as a higher bottom salinity or deviation from the profile observed at station 20.

The September 11 profiles show the water column at station 20 was essentially isohaline near 27 o/oo. At station 10A the profile was similarly isohaline to 7.5 m where a moderate halocline caused the salinity to increase to near 29 o/oo at the bottom. This deviation from the control station profile would normally have been attributed to the brine discharge but none was being discharged on that day. The cause of the halocline was a salinity front which partially penetrated the diffuser location, and this can be seen in the vertical cross sections for this date (Appendix Figure A-20).

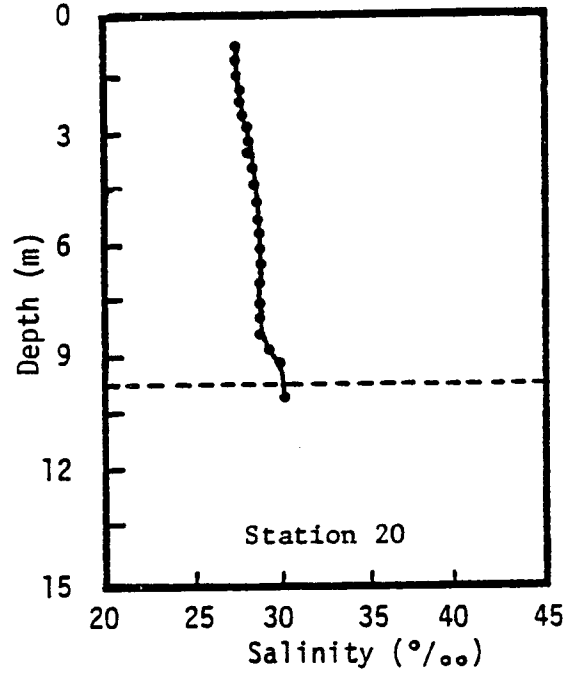
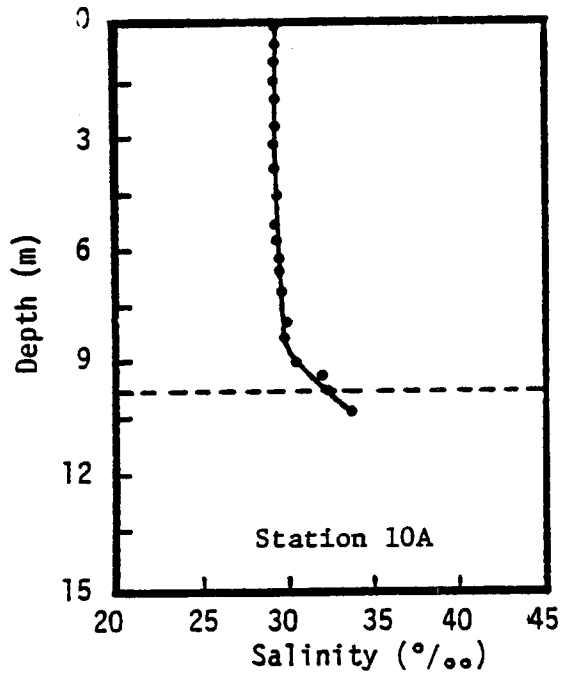
The vertical profiles for October 12 and January 21, 1982 are shown in Figure 2-19. The October 12 data show a very slight increase in salinity occurred from the surface to near the 8 m depth. At this depth there was a very slight increase in salinity at station 20, but a very sharp increase was observed at station 10 which is attributed to the brine plume. Brine was discharged at an average rate and salinity of 21,500 barrels/hr and 221 o/oo on this date. On January 21, 1982 the profiles show a layer of fresh water was contained in the upper 3 m of the water column. At station 20 it was isohaline from 3 m to the bottom. However, the station 10A profile showed a rapid increase in salinity beginning at 9 m which was similarly attributed to the discharge of brine which was at a rate of 22,250 barrels/hr and salinity of 249 o/oo.

The vertical salinity profiles for February 11 and March 12, 1982 are illustrated in Figure 2-20. The brine discharge rate was 23,000 and 31,283 barrels/hr and the brine salinity was 229 and 232 o/oo on these dates respectively. The February profiles show nearly isohaline conditions from the surface to the bottom at station 20, but at station 10A an abrupt change is shown beginning at a depth of 8 meters where the salinity increased from near 31 to 35 o/oo. In March the profiles were again nearly isohaline except from 7.5 m to the bottom at station 10A. In both cases the deviation from the station 20 profiles near the bottom was caused by the presence of the brine plume.

The April 27, 1982 vertical profiles are shown in Figure 2-21, and the brine discharge rate and salinity were 30,870 barrels/hr and 228 o/oo. A particular set of profiles demonstrates the capability of the Grundy profiler in defining the location of the strong haloclines. The station 20 profile shows a deep layer of fresher water to a depth of 5.5 m where a sharp halocline resulted in a salinity increase from near 26 o/oo to 33 o/oo, and from 7 m to the bottom, isohaline conditions were present. In contrast, the profile at station 10A shows that the layer of fresher water was only 3 m deep, and from that depth to the bottom, the halocline was unusually constant. The sharp halocline at station 20 was not observed. Therefore it is believed that the brine discharge altered the salinity profile up to a depth of near 7 m.

In summary, these vertical profiles demonstrate the capability of the Grundy profiling instrument to define the detailed salinity structure of the water column which is very important during late

October 12, 1981



January 21, 1982

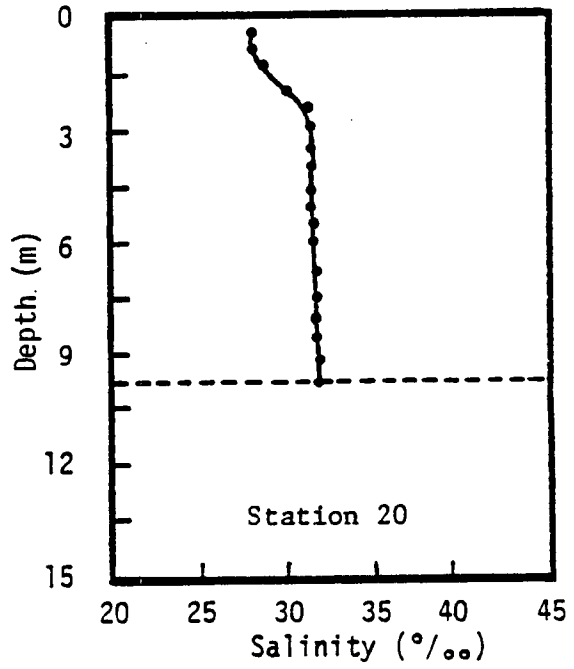
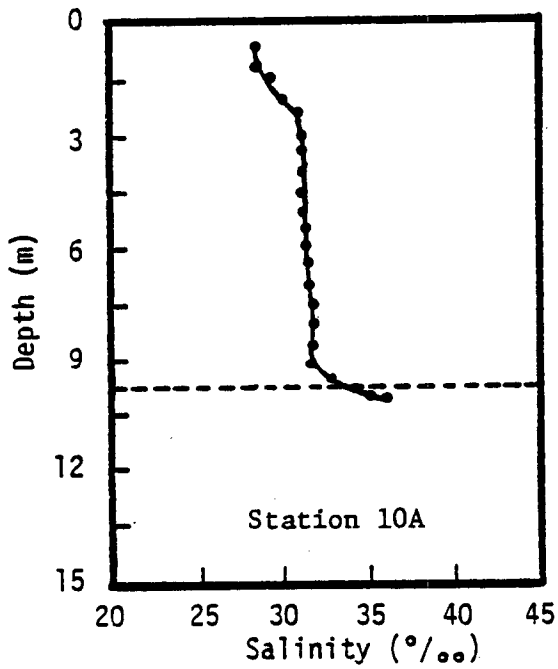
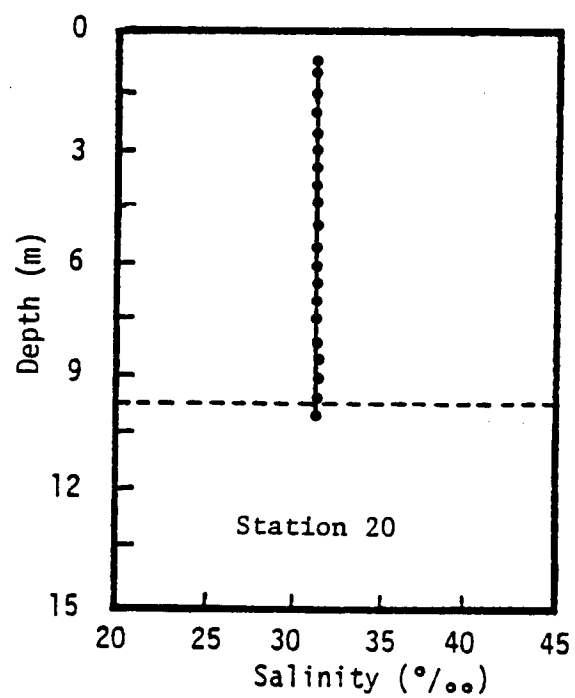
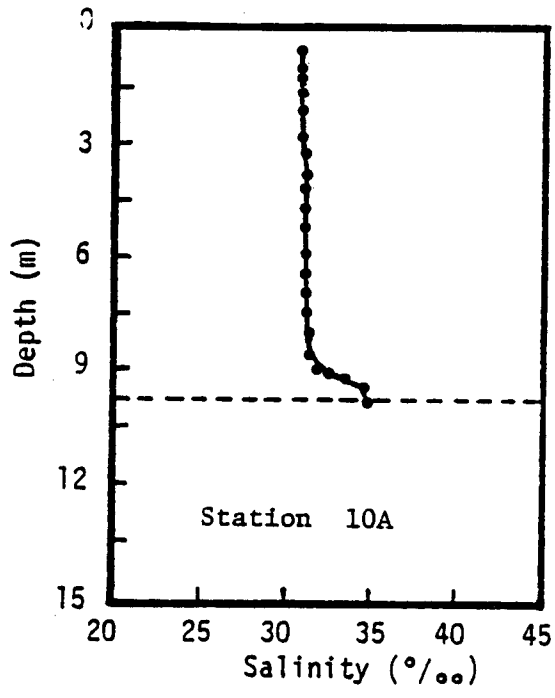


Figure 2-19. Vertical salinity profiles at stations 10A and 20 on October 12, 1981 and January 21, 1982.

February 11, 1982



March 12, 1982

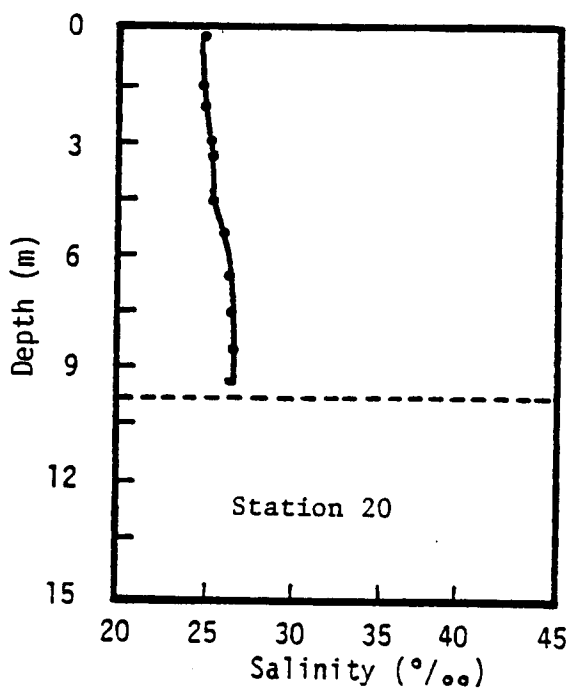
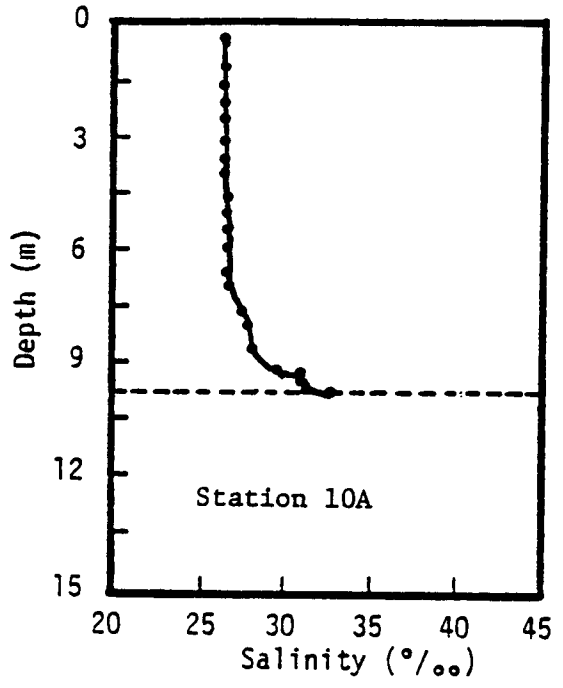


Figure 2-20 Vertical salinity profiles at station 10A and 20 on February 11 and March 12, 1982.

April 27, 1982

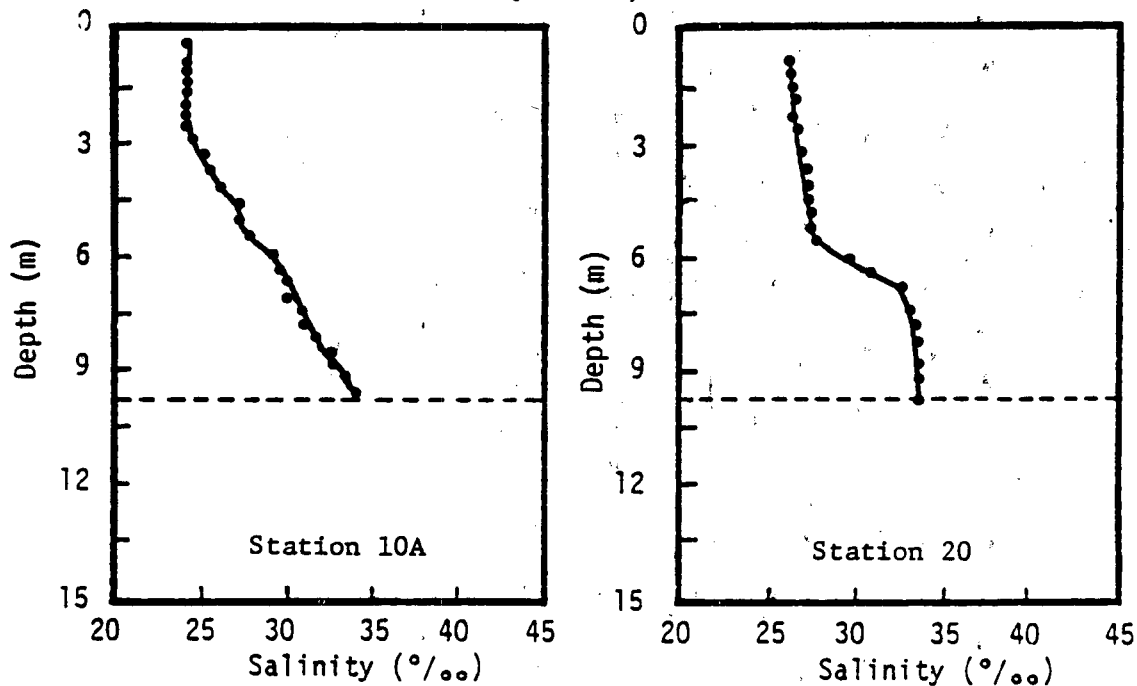


Figure 2-21. Vertical salinity profiles at stations 10A and 20 on April 27, 1982.

spring, early summer, and early fall when the water column structure is normally highly stratified. It has also demonstrated the effect of the brine discharge on the bottom waters. The data has shown the brine discharge effect can reach a depth of approximately 3 m above the bottom. The problems which salinity fronts can cause for the interpretation of the data was also demonstrated.

2.2.9 Summary of Monthly Hydrographic Data

Hydrographic data for the coastal waters offshore of Holly Beach, Louisiana were collected on a one-day cruise each month at fifteen stations which were arranged in a cross-shelf and an alongshelf transect intersecting at the diffuser. Data have been described for the period May 1981 through April 1982 and during this period a brine solution was being discharged into the same coastal waters at the intersection of the two transects.

The hydrographic data in the spring of 1981 show the isopleths of temperature, salinity, sigma-t, and dissolved oxygen were vertical in April, and as the annual spring runoff began these isopleths became nearly horizontal in May and June. The vertical temperature gradients were slight, but the salinity and sigma-t gradients were strong, indicating the existence of stratification. The dissolved oxygen isopleths show a moderate gradient with the overall values decreasing. The cross-shelf variation of the hydrographic parameters was the largest and small variations were detected in the alongshelf direction. The effect of the brine discharge was small which was attributed to the intermittent operation and low brine salinities.

The summer of 1981 hydrographic data showed the salinity and density stratification was the strongest with a 14 o/oo vertical

salinity gradient at the diffuser site in July. The salinity stratification was spread over the entire cross-shelf transect and, presumably, the area. At the same time the bottom waters became nearly depleted of oxygen (less than 2 mg/l). The salinity stratification and anoxic conditions persisted over the entire area through August. Late summer (September) data show the anoxic conditions began to breakdown as well as the salinity stratification. The existence of anoxic bottom waters is not unusual in the area, and a similar event was reported in the summer of 1978 by Frey, et al. (1981). Harper, et al., (1981) and Slowey (1980) also detected anoxic conditions in 1979 at the Bryan Mound brine disposal site. The effect of the brine discharge was very small other than showing the breakdown of isopleths of dissolved oxygen near the diffuser which was presumably caused by jet mixing.

The fall 1981 hydrographic data show the area waters experienced a freshening trend in early fall and became more saline in the late fall. The salinity stratification was moderate, and the dissolved oxygen returned to normal levels. The effect of the brine discharge was more clearly shown in the form of convex isohalines and isopycnals near the diffuser site on both transects.

During the winter of 1982 the area water showed moderate stratification at times which is attributed to the passing of weather frontal systems. The dissolved oxygen reached its highest values (approximately 9.0 mg/l) while the temperature reached its lowest values (approximately 10°C). The effects of the brine discharge continued to be most evident in the vertical sections of salinity and sigma-t data with convex isohalines and isopycnals near the diffuser

and within 4 m or less of the bottom. There appeared to be no effect of the brine on the temperature data and only a slight effect on the dissolved oxygen.

The temperature-salinity relationship for the diffuser site (station 10A) and a control station (station 20) showed the surface temperature reached a maximum in August and a minimum in January with a range from 10.2 to 32.2°C. The surface salinity was a maximum in February 1982 with a value of 31.4 o/oo and the minimum of 16.2 o/oo occurred in July 1981. The bottom data show that the maximum and minimum temperatures were 30.8°C in August and 10.7°C in January. In the case of salinity, the diffuser site showed a range of 8.7 o/oo with the maximum (35.4 o/oo) occurring in January and the minimum (26.7 o/oo) occurring in September. The range at the control station was 6.7 o/oo and the maximum and minimum values were 32.7 o/oo (July) and 26.0 (September). The increased range in salinity at the diffuser site is attributed to the brine discharge, but the brine discharge does not appear to affect the ambient water temperature.

The temporal variation of the bottom temperature at the diffuser site and a control station show that the intrayear bottom temperature variation was from 30.8°C (August) to 10.7°C (January). The average temperature difference between the brine and ambient bottom temperature was only 3.7°C, and thus it is reasonable to expect no measureable increase in the temperature of the bottom waters.

The temporal variation of the bottom salinity at the diffuser site and control station show that the salinity ranged from 35.4 to 26.7 o/oo at the diffuser site and 32.7 to 26.0 o/oo at the control station. The maximum salinity difference between the diffuser and

control stations was 4.6 o/oo, and it is expected that the salinity difference would be less at stations further away from the diffuser. The increased range of salinity at the diffuser site was caused by the brine discharge.

The temporal variation in dissolved oxygen showed an annual cycle where the dissolved oxygen maximum was 9.2 mg/l in February 1982, and the minimum was near zero in July and August 1981. The anoxic conditions covered the entire area from the shore to 30 km offshore and 8 km east and west of the diffuser. The temporal variation showed the bottom dissolved oxygen at the diffuser site was 0.5 mg/l higher than at the control station some of the time and vice versa. Therefore, the temporal data indicate the brine discharge had little effect on increasing or decreasing the bottom water dissolved oxygen.

Vertical salinity profiles at the diffuser site and the control station were described which show the detailed salinity structure of the water column. These data indicate the water column structure was highly variable in the late spring, early summer, and early fall. The data also demonstrated that the effect of the brine discharge could be interpreted as a sharp deviation of the diffuser site salinity profile compared to the profile measured at a control station. Results of the salinity profiles indicated the brine plume at the diffuser site extended as high as 3 m above the bottom.

2.3 Meteorology and River Runoff

Hourly time series of wind velocity, barometric pressure and air temperature are recorded by the NOAA Data Buoy Office with instruments atop fixed structures in the West Hackberry brine diffuser area. From February 1981 through March 1982 instrument package 42010 was active

and deployed at a height of 35° above the water on an oil platform located about 5 nm east of the diffuser site (Lat. 29°39.5' N, Long. 93°23.3' W.)

In December 1981, the construction of a fixed tower (monopole platform) was completed at the West Hackberry diffuser site (Lat. 29°40.27' N, Long. 93°28.15' W). Instrument package 42011 was installed on top of this tower at a height of 32 ft above the water. The data for the two meteorological instrument sites overlap for the period December 1981 through March 1982 and, as might be expected, are virtually identical because of their proximity. Therefore, the data from 42010 through 1981 have been joined with the data from 42011 beginning in 1982 to form one long time series for use in the analyses discussed in the next section.

The data have been analyzed in several different ways to better interpret the meteorological effects on the circulation in the study area: monthly average values of orthogonal components of wind velocity, monthly joint frequency distributions of wind speed and direction (wind roses), monthly time series plots of each parameter and finally spectral analyses of wind stress versus currents. Details concerning the methods of data processing and filtering are described by Kelly and Randall (1980) and in Appendix A, sections A.2, A.3 and A.4.

For ease in comparison with current meter data, the wind velocity data have been converted to the oceanographic direction convention, i.e. the direction towards which the wind blows. Time has been expressed in Central Standard Time (CST) for working purposes, that is, to facilitate discussion among the various investigators and for

comparison with events and cruise observations which are naturally remembered in the local time units.

The monthly time series plots, Figures A-110 through A-124 and wind roses, Figures A-37 through A-51 show that the meteorology over the study area during the period May 1981 through April 1982 followed a typical annual cycle but was mild in terms of frequency and intensity of storms. In addition, the wind roses and time series plots for the West Hackberry study area are quite similar to those for the Bryan Mound study area (Kelly et al., 1982a) which indicates a high degree of (qualitative) coherence in the wind field over the whole Texas/Louisiana shelf. A quantitative comparison between the wind velocities at the two sites is presently being conducted.

The meteorological data for the period February 1981 through April 1981 have already been described by Kelly et al. (1982b), but the data from this period have been included in Appendix A for completeness.

From May 1981 through July 1981 the wind shifted clockwise and blew more predominantly from the south instead of the southeast, and the most frequent speed range dropped from 6-8 m/s to 4-6 m/s. In August 1981 the most frequent speed range remained 4-6 m/s but the frequency of southerly wind decreased to 25%, the same as southeasterly, as a result of a counterclockwise shift in the mean wind direction in the latter half of August (Figure A-116). In September the counterclockwise shift continued. Easterly winds were most frequently recorded, and the most frequent speed range increased to 6-8 m/s. The frequency of frontal passages through the area increased in October with a resulting increase in the percentage of

wind speeds greater than 8 m/s; however, 6-8 m/s was still the most frequent speed range. Southeasterly winds were most frequent, occurring about 43% of the time.

From November 1981 through March 1982 the frequency of frontal passages and northers increased, and northerly winds became either the most frequent or second most frequent, with percentages between about 20 and 25%. Southwestely, westerly and northwesterly winds were seldom recorded during these months. The most frequent speed range varied between 4-6 m/s and 6-8 m/s; their combined total usually was near 50%. The percentage of speeds in excess of 8 m/s was clearly greater than in the summer and early fall months. In April 1982 the frequency of frontal passages decreased and winds shifted to mostly easterly and southeasterly and the 4-6 m/s speed range, at 40%, was most frequent.

In January 1982 (Figure A-131) there were several cold air outbreaks with air temperatures below 0°C. However, they were relatively short lived, and temperatures below 0°C persisted for less than a day.

The winds associated with northers rarely exceeded 14 m/s, and in general the monthly frequency of frontal passages was below normal for 1981 and the first half of 1982. Figure 2-22 shows the mean monthly frequency of frontal passages for the period 1965-1972 (DiMego et al., 1976) together with the years 1981 and early 1982 which clearly have lower values. There were no hurricanes in the northwestern Gulf of Mexico in 1981. A tropical storm during June 10-11 had little effect at the West Hackberry site.

Basic statistics for the alongshelf and cross-shelf orthogonal

	1965-1972*	1981	1982
JAN	9	7	5
FEB	9.5	6	4
MAR	8	6	3
APR	6.5	5	5
MAY	4.5	4	1
JUN	2	2	
JUL	2	0	
AUG	2	2	
SEPT	3	5	
OCT	6	5	
NOV	7	6	
DEC	9	6	

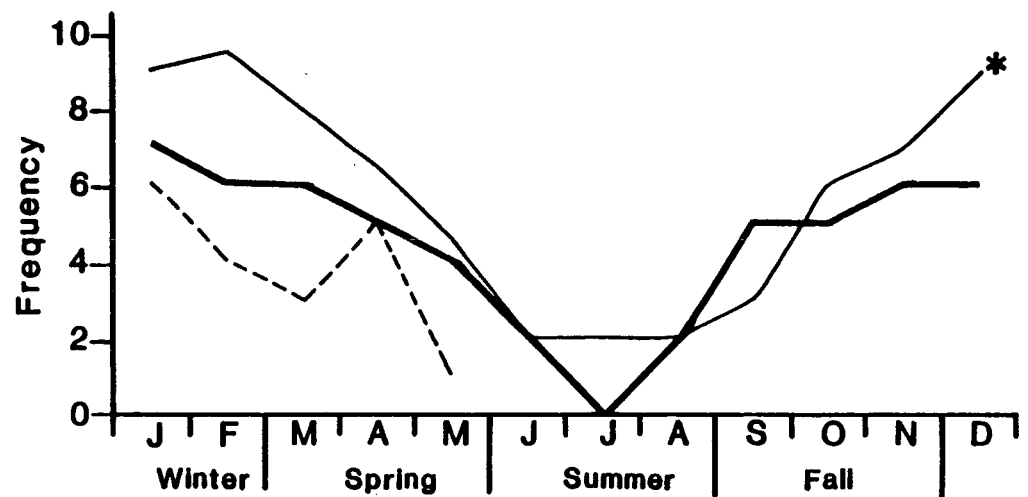


Figure 2-22. Approximate frequency of frontal passages through the West Hackberry area for the period 1965 - 1972 compared with 1981 and early 1982.

components of wind velocity are listed in Table A-1. Section A.2 describes the details of the computations. In coastal areas currents respond to the mean alongshelf component of the wind stress (see sections 2.4 and 2.5). The response time is probably on the order of an inertial period, or about one day. Thus the monthly mean alongshelf component of current and wind should agree qualitatively in terms of magnitude and sign. This was found to be true at Bryan Mound (Kelly et al., 1982a). However, at West Hackberry the mean alongshelf component of wind was always downcoast (negative) while the mean alongshelf component of near surface current was upcoast (positive) in July 1981. (c.f. Tables A-1 and A-2). It is not surprising that the mean alongshelf component of wind was downcoast in July at West Hackberry since the local topography is oriented approximately east-west and the two most frequent directions of wind in July were towards the north (onshore) and towards the northwest (onshore and downcoast). At Bryan Mound a virtually identical wind field produced an upcoast component of alongshelf wind since there the local topography is oriented approximately 55° clockwise from true north. A corresponding upcoast current was recorded at Bryan Mound, which apparently persisted past the West Hackberry site despite the opposing direction of wind. This difference between the two brine disposal sites is further discussed in section 2.5.

As can be seen in the hydrographic data of section 2.2 and in the results of previous studies (Wadell and Hamilton, 1981; Frey et al., 1981) there are usually pronounced decreases in salinity during the spring and again during the late summer of each year. Kelly and Randall (1980) showed that the Mississippi-Atchafalaya river system is

the principal source of fresher water along the Texas/Louisiana coast and that other Louisiana and Texas rivers may augment the fresher water in the inner coastal zone during certain times of the year. In 1979, a year of major floods, this streamflow effected pronounced changes in the density structure, circulation, chemical nutrients, and biology along the Louisiana and Texas coast at least as far westward as the Bryan Mound site (Kelly and Randall, 1980; Frey et al., 1981; Harper et al., 1981; Waddell and Hamilton, 1981). At the West Hackberry site the strong stratification associated with the streamflow appears to be more usual and persistent than at Bryan Mound and may actually be an annual event. The strong stratification reduces vertical mixing and oxygen replenishment in the near bottom waters and hypoxic/anoxic conditions often exist. Therefore, the analysis of streamflow data is necessary for a proper interpretation of the data collected for this study area.

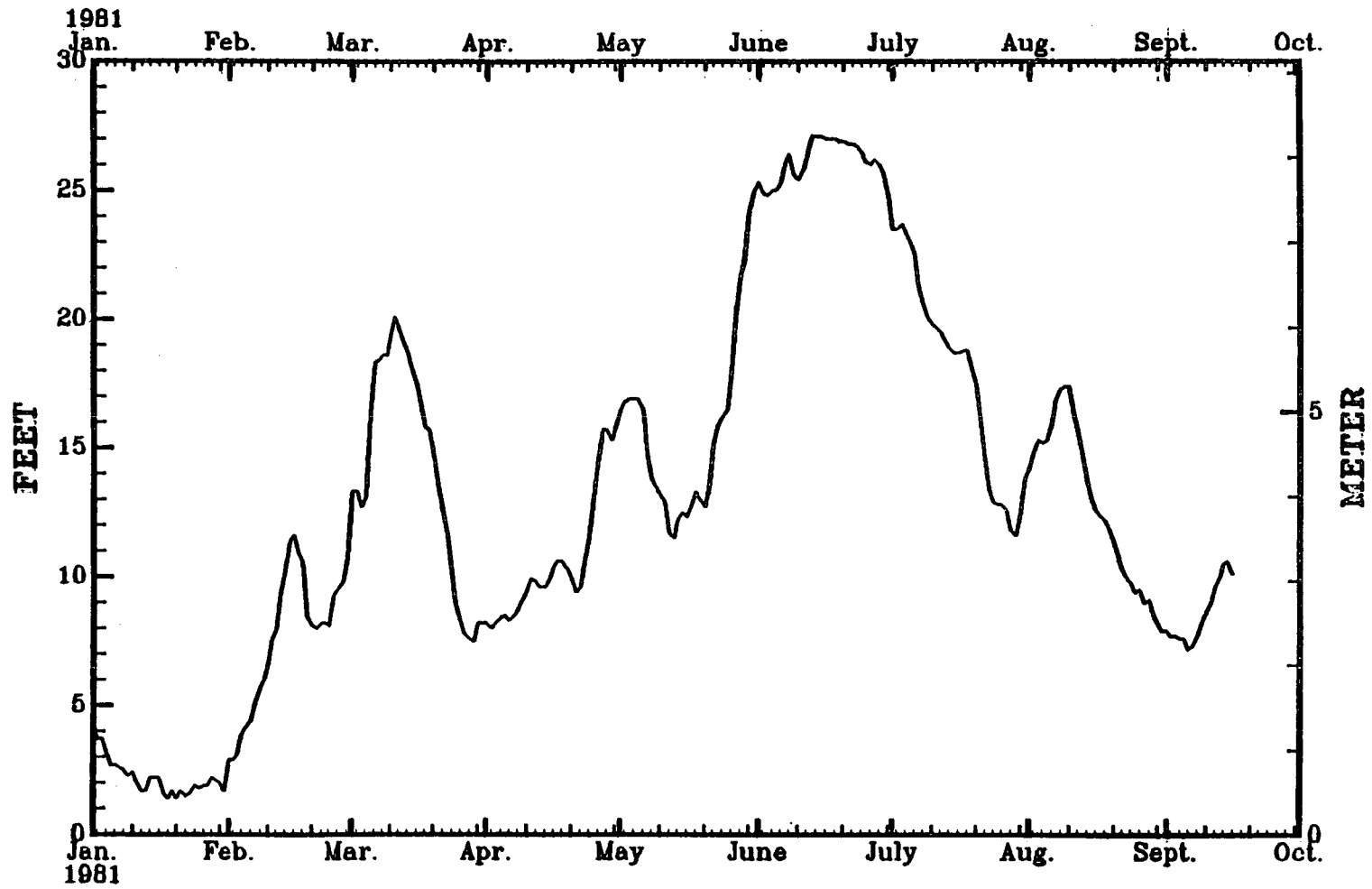
Kelly et al. (1981b) have analyzed the streamflow data for 54 rivers and streams which contribute fresh water to the Louisiana-Texas Gulf waters from the Mississippi to the Rio Grande. Their analysis is based on water years 1977 through 1980. (A water year covers the period from October 1 of the preceding year through September 30 of the given year.) They concluded that the periods in which relatively fresh water enters the study area in the winter and spring (January through June) are qualitatively correlated with periods of increased streamflow from rivers, primarily the Mississippi and Atchafalaya, allowing for a phase lag. However, the low salinity in about September of each year corresponds to the period of lowest streamflow. Kelly and Randall (1980) have shown that during the summer months

there is a region of low salinity trapped west of the Mississippi delta by predominantly northeastward surface currents. Low salinity water from this region propagates rapidly southwestward along the Texas-Louisiana coast when the average alongshelf component of wind, and thus the surface current, reverses to southwestward flow in middle to late August. Thus the low salinity water which is advected through the study area in September corresponds to a current shift rather than increased streamflow.

The streamflow data for water year 1981 were not available in time for inclusion in this report. However, preliminary Atchafalaya river stage data at Simmesport have been obtained (Wiseman, personal communication) for a qualitative assessment of the streamflow in 1981. Simmesport is where the Atchafalaya breaks off from the Mississippi. The river stage data are shown in Figure 2-23; it is emphasized that this is preliminary data and subject to change. Streamflow (volume flow) is proportional to river stage, but the function is not quite linear. Flood stage at Simmesport is 47 ft. For comparison, Figure 2-24 shows the streamflow for water years 1979 and 1980 for the Mississippi-Atchafalaya system (heavy line with shading underneath) and the total of all rivers from the Mississippi to the San Bernard, just west of Freeport, Texas (light line). For a complete description of the gaging stations and methods used, see Kelly et al. (1981).

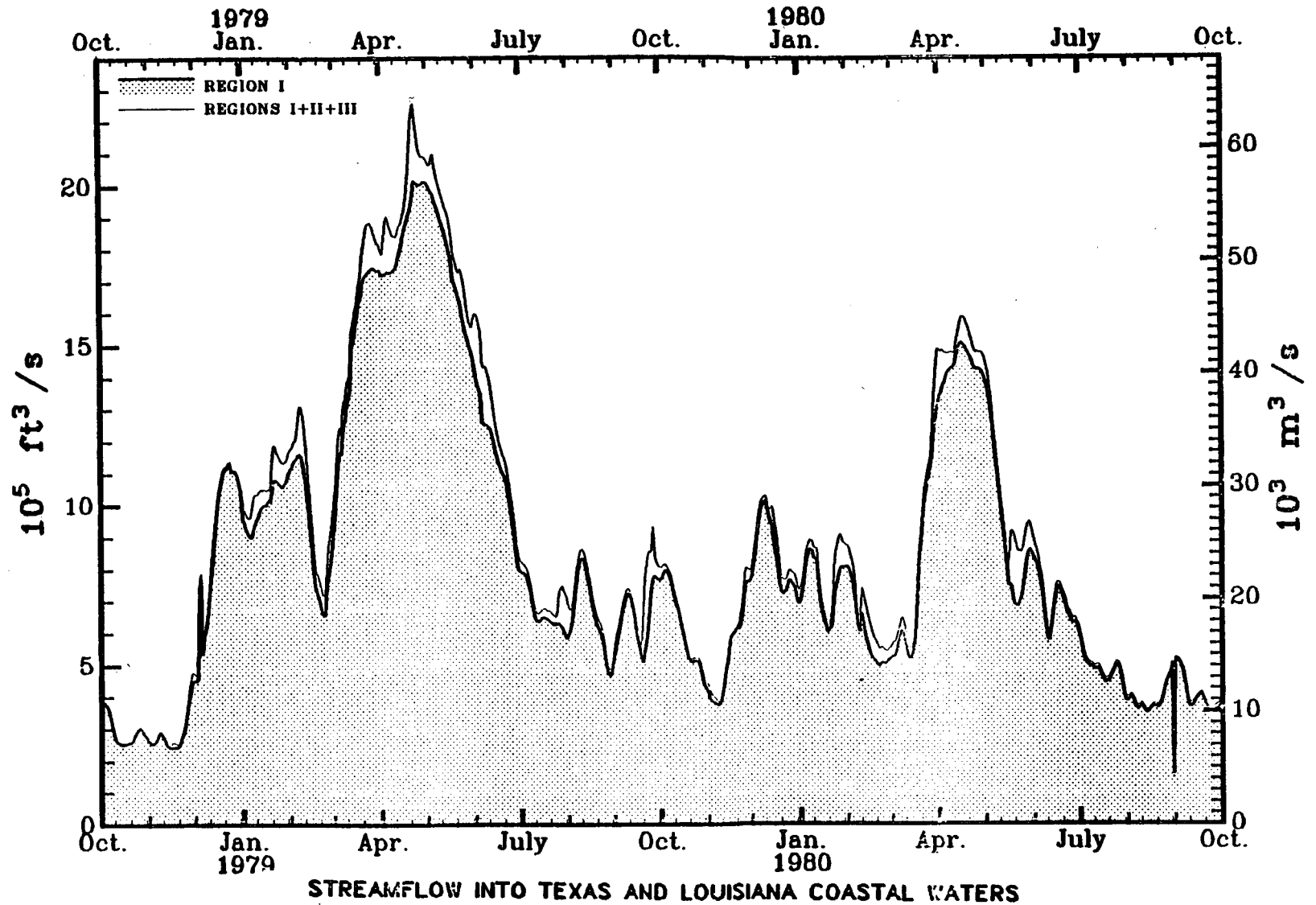
Two important points can be inferred from these figures. The first is that 1981 was a year of relatively low discharge, since the peak stage of about 27 ft (Figure 2-23) is well below the flood stage of 47 ft. The second point is that the major peak in the 1981 stage data occurred in June whereas the major peaks in streamflow in 1979

2-67



SIMMESPORT RIVER STAGES

Figure 2-23. Preliminary 1981 daily Atchafalaya River stage data at Simmesport.



STREAMFLOW INTO TEXAS AND LOUISIANA COASTAL WATERS

Figure 2-24. Average daily streamflow for water years 1979 and 1980 the total of all rivers from the Mississippi to the San Bernard, just west of Freeport Texas (light line) (from Kelly et al., 1981).

and 1980 (Figure 2-24) occurred in late April. Thus, it should be expected that advection of low salinity through the study area should occur in late June and July 1981, and that compared to the previous years of this study, the resulting vertical salinity gradients should be weaker. The results from the hydrographic surveys and in situ recording instruments are in agreement with these expectations.

2.4 In situ Instrumentation

2.4.1 Experimental Design

Time series of current velocity, temperature and salinity (conductivity) are recorded at five sites designated D, N, P, S, and W (Figure 2-1). All sites but N have meters at two depths, 3.7 m below the surface and 1.8 m above the bottom, hereafter referred to as Top and Bottom respectively. Site N has only one meter, placed 1.8 m above the bottom. Sites D and P also have water level/wave recorders (not discussed in this report). Table 2-2 lists the coordinates and other information about each site.

Sites W and D form an alongshelf transect to study the coherence of water properties and currents in the alongshelf direction. Site W, together with sites N and D, help determine the relative effects and extent of outflow from Sabine and Calcasieu Passes. Site W, which is located about 10 nm west of site D and lies on the same depth contour as site D, helps to define ambient conditions since site D may be affected by the brine plume.

Sites N and S, together with site D, form a cross-shelf transect. While the principal direction of current flow is alongshelf, the strongest gradients in water properties are usually in the cross-shelf direction. The purpose of sites N and S is to help differentiate

Table 2-2. In situ instrumentation information.

Site Name	Inst.	Water Depth (ft)	Inst. Depth (ft)	Coordinates	Comments
DT	CM	30	12	29°39.90'N, 93°28.73'W	Site D is located about 900 ft west of the end of the diffuser
DB	CM	30	24	" "	
DL	W/T	30	29	" "	
DZ	VNB CM	30	28.5	" "	
NB	CM	21	16	29°42.84'N, 93°28.40'W	3 nm north of the diffuser
PT	CM	21	12	29°46.18'N, 93°20.64'W	East side of Calcasieu Pass
PB	CM	21	15	" "	
PL	W/T	21	20	" "	
ST	CM	41	12	29°27.12'N, 93°26.00'W	13 nm south of the diffuser
SB	CM	41	35	" "	
WT	CM	31	12	29°38.50'N, 93°40.00'W	10 nm west of the diffuser
WB	CM	31	25	" "	

CM = current meter

VNB CM = very near bottom current meter

W/T = wave/tide meter

plume effects from natural variations, especially during upwelling favorable conditions. Higher salinity water lies offshore of the diffuser area, and during periods of onshore flow along the bottom, there is a natural increase in salinity values. The choice of a location for site S was complicated by the presence of a ridge line (Sabine Bank) about 10 nm south of the diffuser and the presence of a shipping fairway between the diffuser and the ridge. Given these practical constraints, the best location for site S was determined to be on the south side of a break in the ridge, about 13 nm south of the diffuser. Site S monitors the higher salinity waters offshore of the diffuser which can be advected into the diffuser region. Site N has only a single instrument because of the depth (6.2 m) and lies about 3 nm north of the diffuser. It monitors the waters inshore of the diffuser and defines the strength of cross-shelf gradients and the shoreward extent of cross-shelf flow.

Site P (E-5) is located on the east side of Calcasieu Pass about 100 m north of the red U.S.C.G. channel marker buoy and is as close to the main channel as is practical. The water depth at site P is about 6.4 m (21 ft) and the channel is dredged to a depth of about 12 m (40 ft). While the data are probably representative of flow through the Pass on the average, extreme values which are recorded may be less than extreme values which actually occur in other parts of the channel. The purpose of site P is to provide data which can link the estuarine and marine portions of this study.

The current meters are ENDECO Type 174 meters with temperature and conductivity sensors, and Figure 2-25 shows a typical mooring configuration. Each site is protected by a large witness buoy which

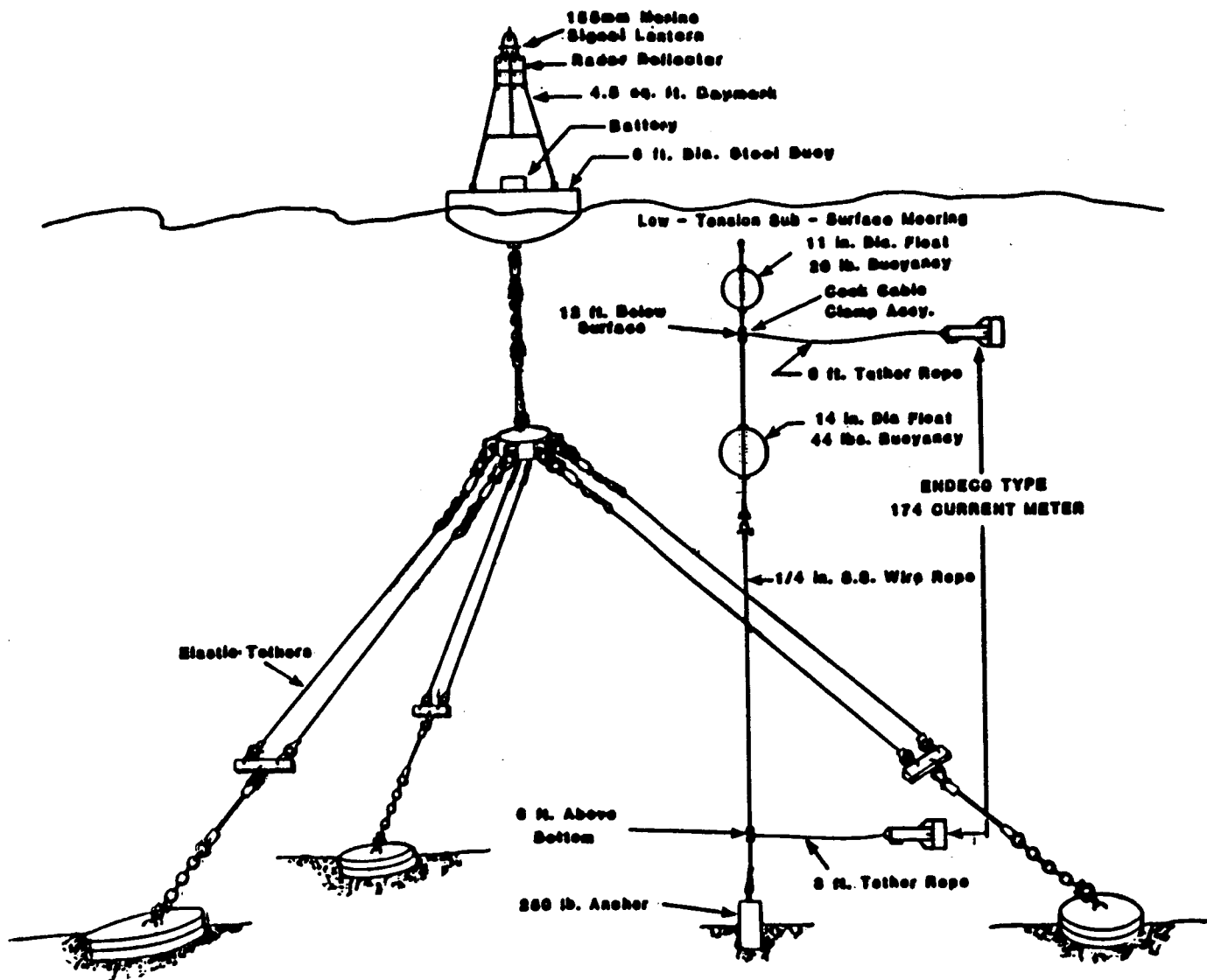


Figure 2-25. Schematic diagram of instrumentation mooring and witness buoy configuration.

utilizes the elastically tethered mooring concept to reduce the buoy's watch circle to less than 5% of the water depth. Problems with commercial fishing, which plagued earlier investigations in this area, have been minimized with this combination of instrument mooring and witness buoy. Instruments are replaced about every four weeks to minimize the effect of biofouling which is quite strong in this area. A detailed description of the instrument characteristics, data quality assurance procedures, and field procedures are given in the West Hackberry Field and Laboratory Procedures Manual (Kelly et al., 1981) and in other reports (e.g. Kelly and Randall, 1980).

2.4.2 Data Processing Methods

The time series of raw data (speed, direction, temperature, and conductivity) for each deployment period are carefully edited to eliminate spikes or other obviously bad data points. Current velocity data are then resolved into orthogonal components oriented parallel and perpendicular to the local isobaths. For sites D, N, and S, the parallel direction is approximately $086^{\circ}\text{T} - 266^{\circ}\text{T}$; for site W, it is approximately $075^{\circ}\text{T} - 255^{\circ}\text{T}$; The alongpass direction for site P is approximately $356^{\circ}\text{T} - 176^{\circ}\text{T}$. Temperature and conductivity data are used to calculate salinity according to the equation of Daniel and Collias (1971), a low order polynomial which is computationally efficient and quite sufficient for the accuracies of the instrument. A two-hour, low-pass, symmetric Lanczos filter is then applied to each of the time series: alongshelf current, cross-shelf current, temperature and salinity. Several different raw data sample intervals are used depending on a meter's location. Top meters have a 3-minute sample interval; bottom meters have a 5-minute interval; and meters at

site P have a 2-minute interval.

Two-hour low-pass filters have been designed to produce an identical response for each of the different sample intervals. The filters have a -6 db point at two hours and a sharpness which results in 1.5 hours being lost from each end of the record. The filtered series are then subsampled to a half-hourly interval. The resulting half-hour series from each deployment period are then joined end-to-end to form a single long series for each parameter. Short gaps are filled by linear interpolation. Gaps greater than about one day in duration are not filled and thus determine how long the joining process can be carried on before a new series must begin. Tables A-11 through A-15 list the dates for each deployment period along with notes about the data quality for each period.

The joined series are next filtered with a three-hour low-pass filter and subsampled to hourly intervals, and then filtered with a forty-hour low-pass filter and subsampled to six-hourly intervals. Both filters are symmetric Lanczos filters and have sharpnesses which result in a loss of eight hours and four days of data, respectively, from each end of the record. The forty-hour low-pass filter is designed to eliminate all fluctuations of a daily nature such as tides, inertial oscillations, etc. The subsequent analyses to be discussed utilize the three-hour and forty-hour, low-pass filtered time series. The above time series operations were performed using the FESTSA software package (Brooks, 1976).

The time series have been analyzed by a variety of methods. First, basic statistics were computed for monthly intervals for each series, and the results are listed in the Tables of Appendix A in

section A.2. Next, joint frequency distributions of speed and direction were computed for both wind velocity and current velocity over monthly intervals and rose diagrams were plotted. These results are shown in section A.3. Monthly plots of the meteorological time series (section A.4) and the oceanographic time series (section A.5) were constructed. For vector time series, the monthly plots show both the three-hour and the forty-hour low-pass filtered series of each orthogonal component and a stick vector series which is reconstructed at six-hourly intervals from the forty-hour, low-passed orthogonal components. For scalar time series, the three-hour low-passed data have been plotted. Harmonic analyses for 29-day intervals have been performed for the currents at sites D and P. A modified version of the program by Dennis and Long (1971) has been used, and the parameters of the tidal current ellipse have been computed (Doodson and Warburg, 1941). Tables of the complete results are given in section A.6. Next, autospectra, cross-spectra, phase and coherence squared were computed for selected individual series and pairs of series. The method used is the classical Fourier transform of the autocorrelation function (e.g. Jenkins and Watts, 1968). Section A.8 shows the results of the spectral computations. Finally, section A.7 shows time series plots of the site D, bottom data for each day on which a plume mapping cruise was conducted. These plots are provided primarily for reference purposes in the discussion in Chapter 4.

An introduction is provided for each section in Appendix A which gives additional details about the method of analysis used to obtain the results of that particular section and how to interpret the tables or plots. In the discussions in this chapter, selected figures from

the Appendix are used along with special summary plots to elucidate the main points of interest.

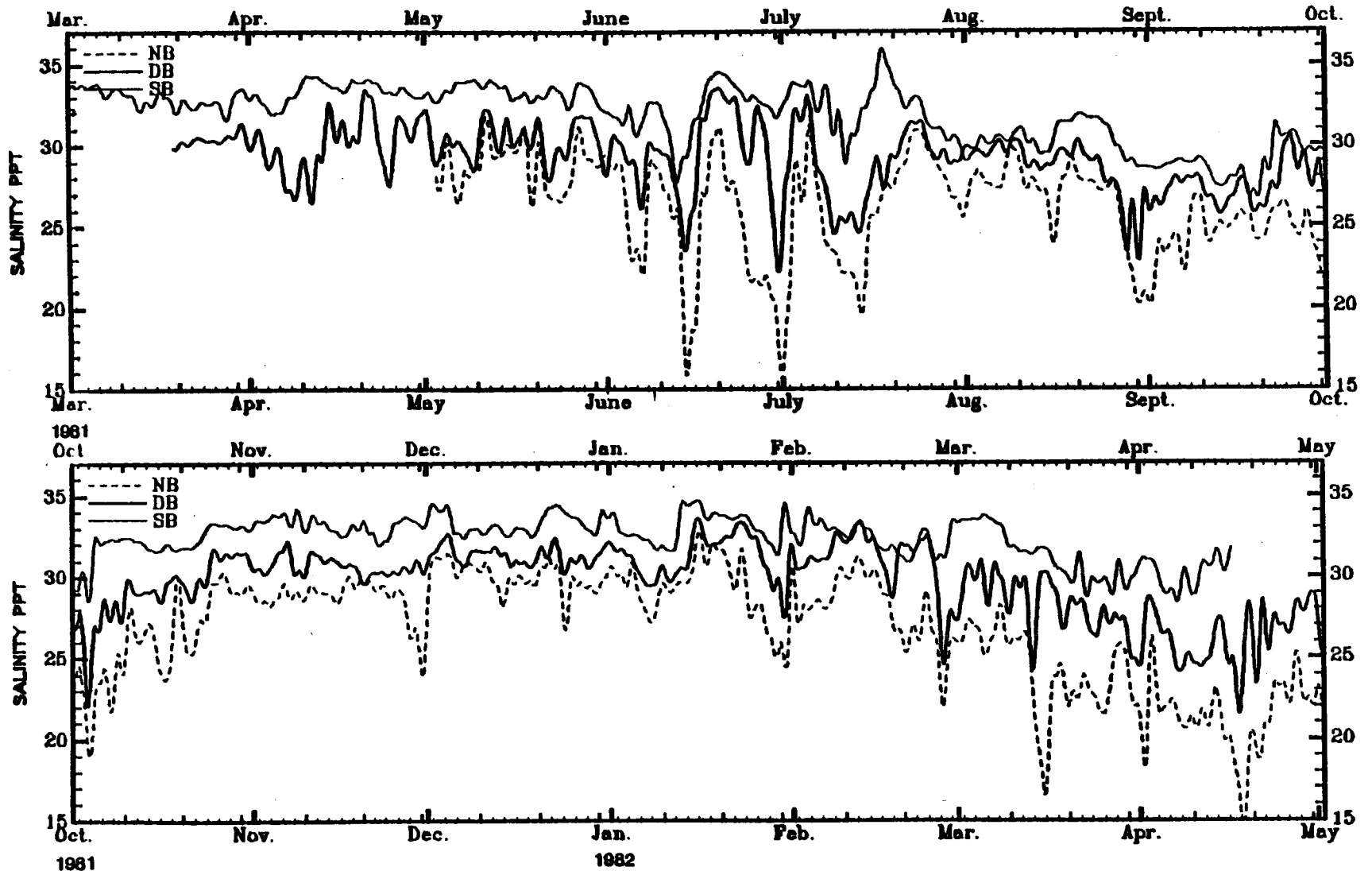
2.4.3 Salinity and Temperature

The description of the hydrography of the study area can be amplified using the time series of salinity and temperature collected at sites D, N, S, and W. We start with the forty-hour, low-pass filtered series in which fluctuations with periods shorter than forty hours have been eliminated. These series are similar to daily averages. (A block average, i.e. hourly, daily, monthly, etc., is a type of filter, but it has a poor response function.) Figures 2-26 through 2-30 show the variation of salinity in cross-shelf, alongshelf and vertical directions as a function of time.

Figure 2-26 shows the near bottom salinity recorded at sites N, D, and S, a cross-shelf direction. The most striking feature in this figure is the magnitude of change which can occur in just a few days, as for example in the latter half of June 1981. Changes of up to about 10 o/oo at DB

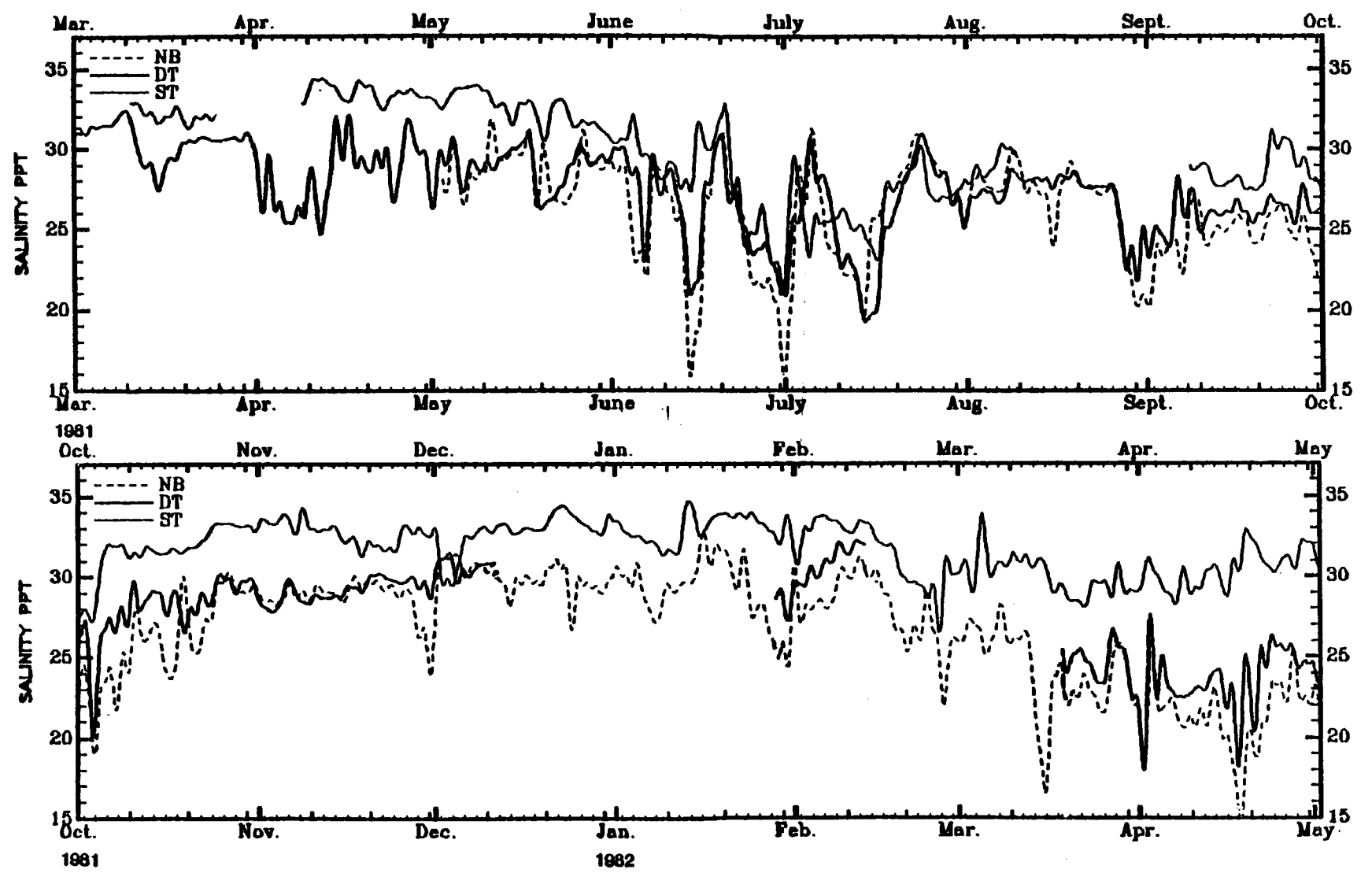
and up to about 15 o/oo at NB occurred within a period of about four days. These changes were not isolated or random fluctuations at a single site, but rather were related to events which affected the whole study area as evidenced by the correlation of the fluctuations among all three sites. Also, note that the fluctuations are the least intense at SB and the most intense at NB. A second feature of Figure 2-26 is the persistent cross-shelf stratification. NB was almost always less saline than DB which was almost always less saline than SB. The difference in salinity between SB and NB exceeded 15 o/oo at times in June 1981 and March - April 1982. There is a noticeable

2-77



BOTTOM SALINITIES, CROSS SHELF COMPARISON USING NB,DB,SB

Figure 2-26. Cross-shelf comparison of near bottom salinities using 40-hour, low-pass filtered time series from meters NR, DB, and SB.



SURFACE SALINITY, CROSS-SHELF COMPARISON USING NB,DT,ST

Figure 2-27. Cross-shelf comparison of near surface salinities using 40-hour, low-pass filtered time series from meters NB, DT, and ST.

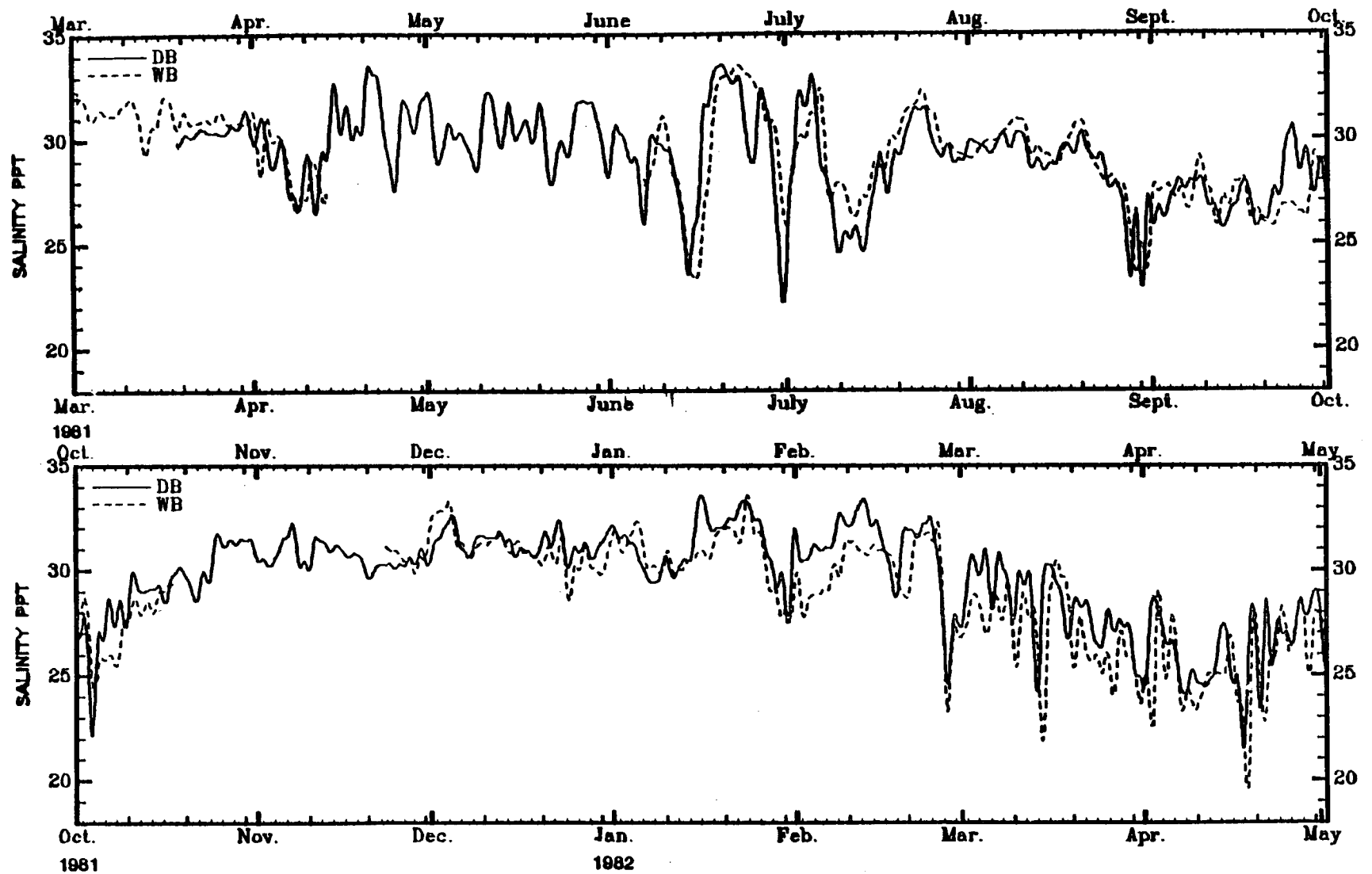
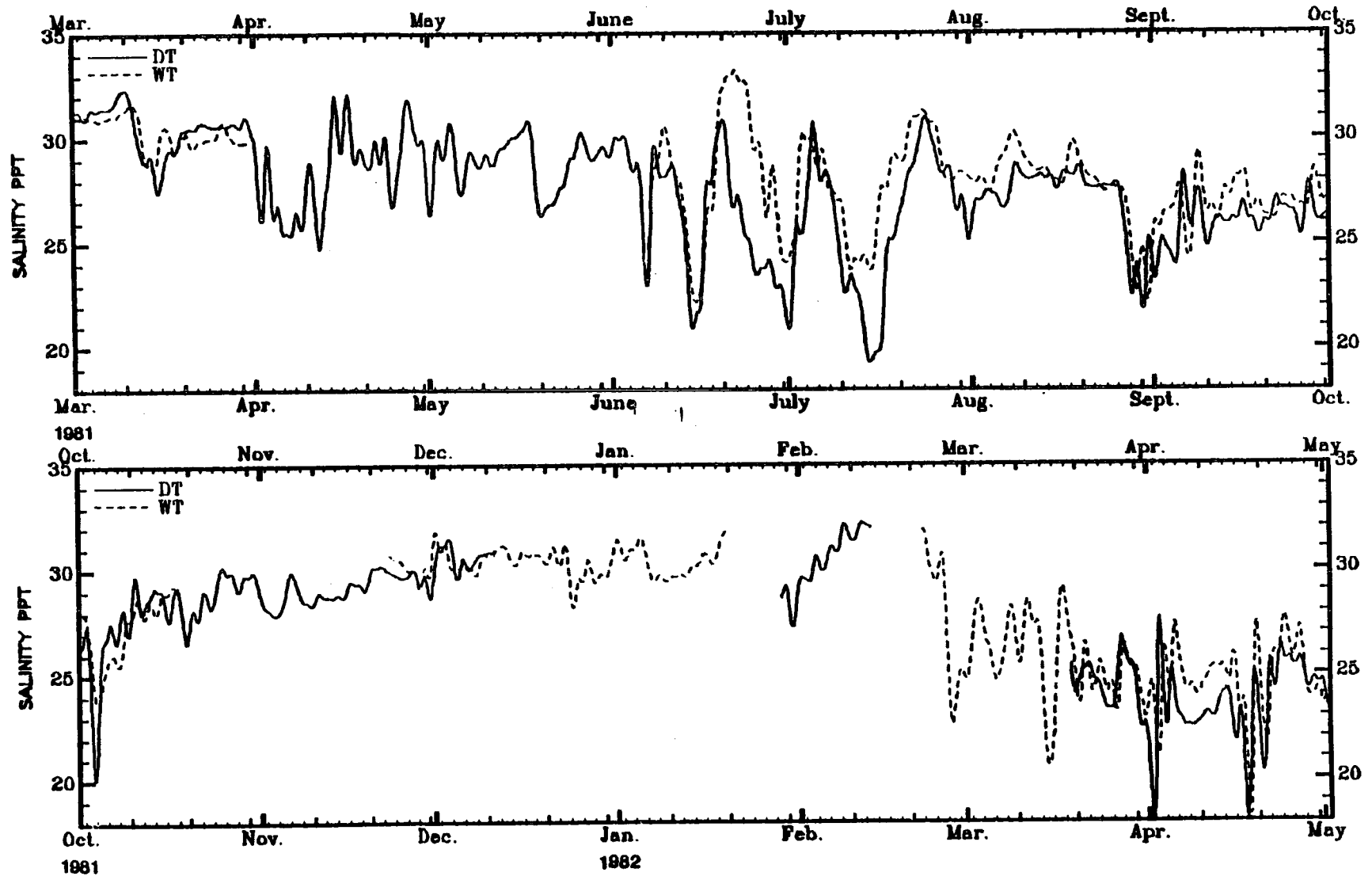
**BOTTOM SALINITY, ALONGSHELF COMPARISON USING DB,WB**

Figure 2-28. Alongshelf comparison of near bottom salinities using 40-hour, low-pass filtered time series from meters DB and WB.





SURFACE SALINITY, ALONGSHELF COMPARISON USING DT,WT

Figure 2-29. Alongshelf comparison of near surface salinities using 40-hour, low-pass filtered time series from meters DT and WT.

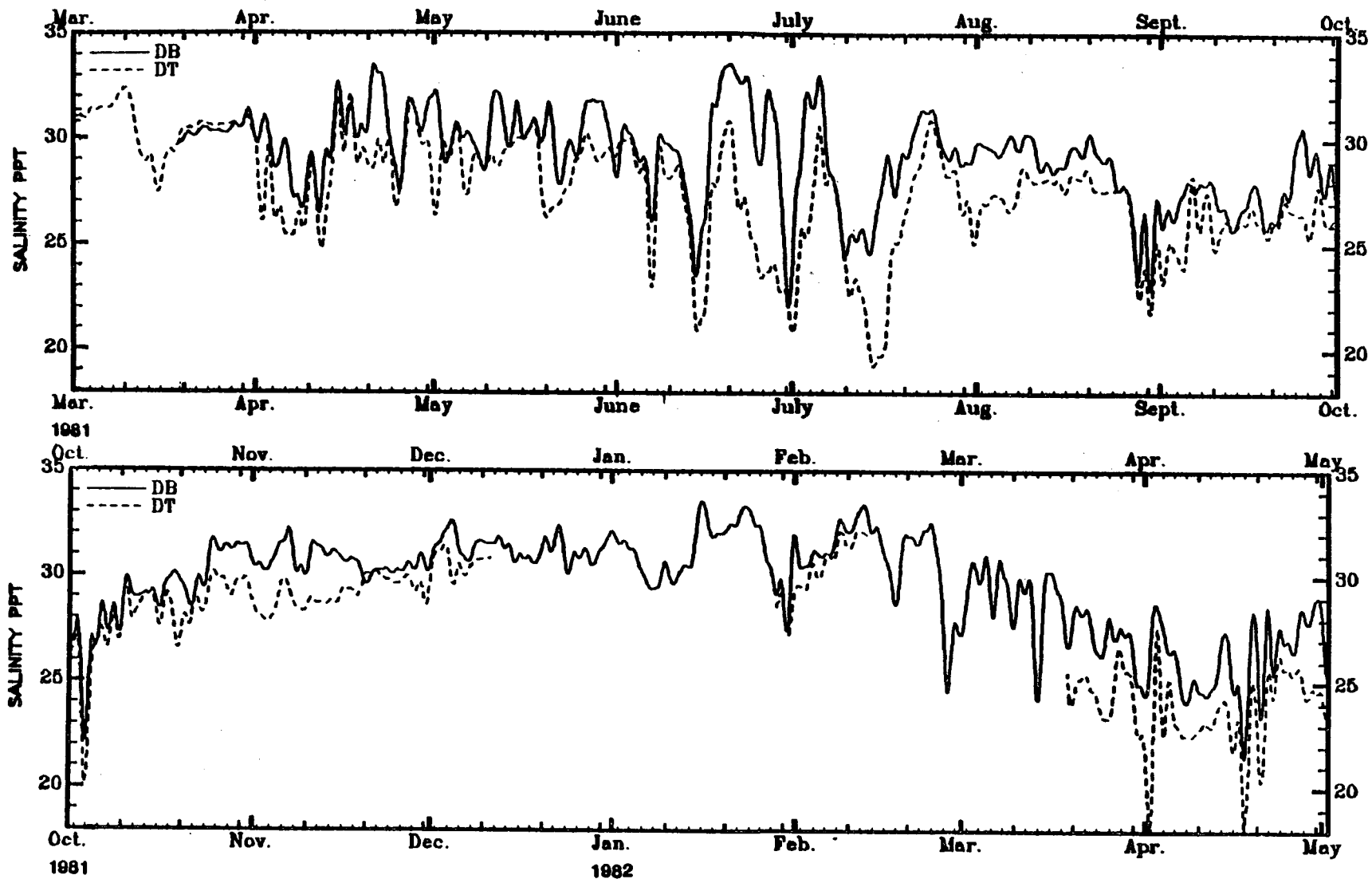
**SALINITY, VERTICAL COMPARISON USING DT,DB**

Figure 2-30. Vertical comparison of salinities at Site D using 40-hour, low-pass filtered time series from meters DT and DB.

difference in the spring/summer decrease in salinity between 1981 and 1982. It was shown in section 2.3 that in 1981 river discharge did not reach a maximum until early June, i.e. later than normal, and that the volume of discharge was relatively low. Figure 2-26 shows that in 1981 there were abrupt decreases in salinity in June and July 1981, but these were of relatively short duration. In 1982, however, salinity began to gradually decrease in March and this trend continued at least through the end of this reporting period. Presumably, the spring increase in river discharge followed a more typical pattern in 1982, and in the next report, when the rest of the data for 1982 are available, the persistence and extent of salinity stratification should be compared for the two years. There were also noticeable decreases in salinity in late August 1981 and early October 1981. As discussed in section 2.3, river discharge is at a minimum during this period, and these decreases are related to increased westward advection of relatively fresh water along the coast from a residual pool of brackish water to the east.

The relative salinities recorded at the three sites give some indication of the magnitude and position of frontal zones in the area. When NB and DB have similar salinity values, the front lies offshore of site D and when DB and SB have similar values, the front lies inshore of site D. The time series show that on May 21, 1981 a salinity front lay offshore of site D with a 5 o/oo change between DB and SB. The vertical section (Figure A-10) for the hydrographic data on this date shows the details of this front. However, this kind of inference must be made cautiously. Strong cross-shelf stratification is indicated for July 16, 1981, but as the vertical section for this

date (Figure A-16) shows there is actually strong vertical stratification; much of the change in near bottom salinity from NB to SB is related to the increase in depth. In fact, the vertical section indicates an upwelling situation in which relatively high salinity water is being advected inshore in a thin, near bottom layer. Between July 16 and July 20, 1981, there is an increase in bottom salinity at all three sites, but especially at SB, and the cross-shelf component of near bottom current at site D during this time is onshore (Figure A-147). Weak cross-shelf stratification between NB and DB is indicated for January 21, 1982. The vertical sections for these dates (Figures A-18 and A-28) are in agreement with these interpretations.

Figure 2-27 shows the near surface salinities recorded at sites N, D, and S. (Meter NB is used for both top and bottom comparisons with the other sites.)

An interesting feature in this figure is that during the periods of large fluctuation in salinity in June and July 1981, the surface salinity difference among the three sites is small. This is consistent with the strong vertical stratification and horizontally oriented isopleths of salinity noted in the vertical section for July 16, 1981 (Figure A-16). The low salinity water in the upper half of the water column thus extends more than 19 nm offshore during this period. During most of the period covered by Figure 2-27, however, the near surface salinities at DT and NB are similar in magnitude while those at ST are higher, and large fluctuations in salinity are greatly attenuated at ST. The onset of lower surface salinity conditions beginning in March 1982 is confined to DT and NB, at least through the end of the period covered in this report. Salinity fronts

associated with the advection of lower salinity water through the study area thus are usually confined to a region inshore of ST except during the peak effect of the spring river runoff and during periods of upwelling.

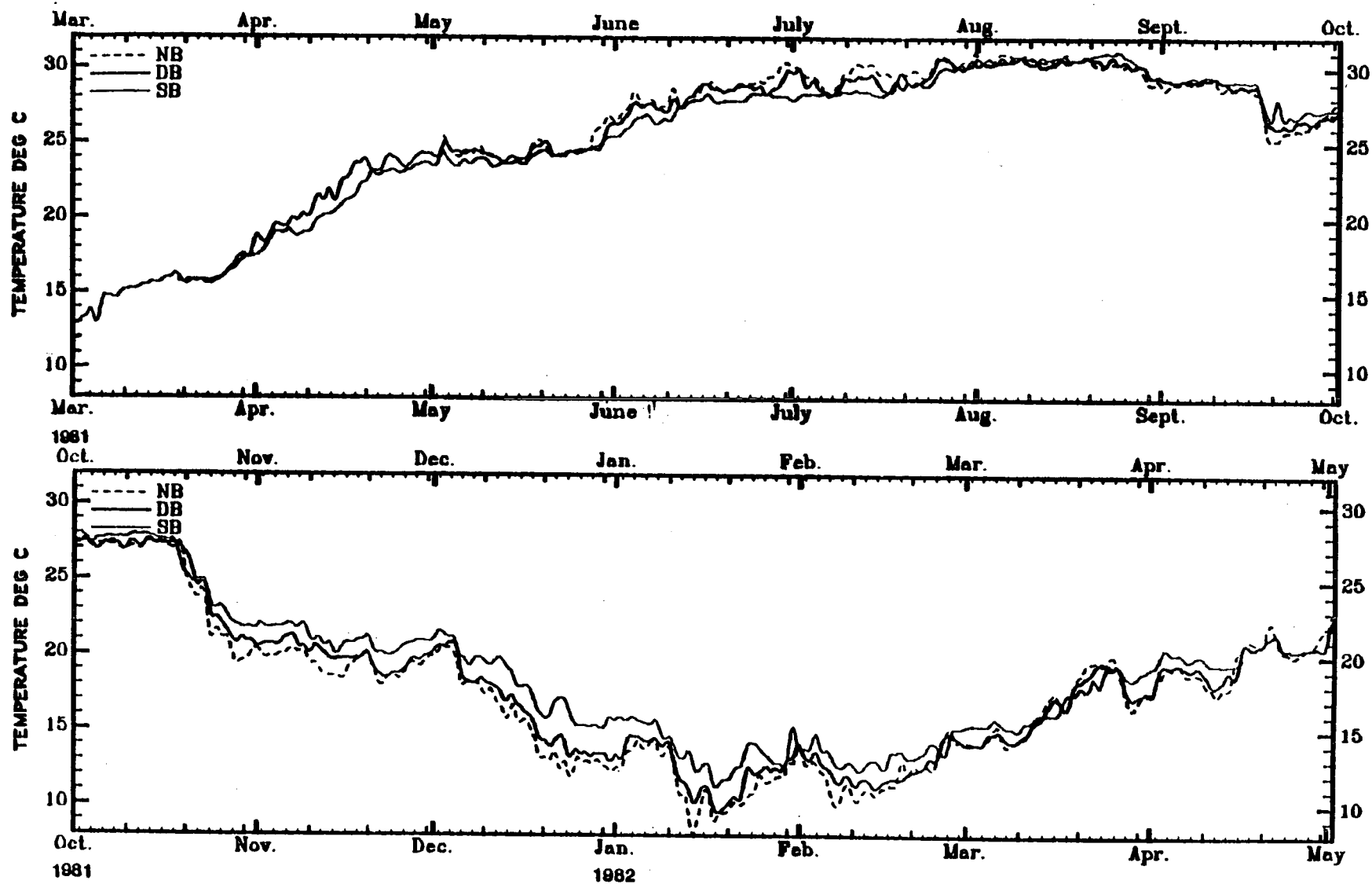
In an alongshelf direction, the near bottom salinity field is quite homogeneous. Figure 2-28 compares the values recorded at sites S and W which are separated by about 10 nm. The fluctuations at each site track each other closely most of the time, and changes at WB often lag those at DB by about two to three days. As noted in Chapter 4, plume effects at the distance of site D from the diffuser (about 275 m) are usually confined to a distance of less than two meters above the bottom for discharge rates which occurred during the period of this report. The near bottom meter at site D is moored at a nominal depth of about 1.8 m above the bottom and thus should not be significantly biased by plume effects. The close agreement most of the time between the salinity values recorded by the DB meter and the WB meter (which clearly is not influenced by the plume) is in agreement with the above hypothesis. However, there are several events/periods when the salinity at DB is obviously higher than at WB: September 23-28, 1981, January 15-17, 1982, the first half of the month of February 1982, and at various times during March 1982. The difference is typically about 2 o/oo except for September 25, 1981 when the difference reaches 4 o/oo. It cannot be determined to what extent these increases at DB are due to natural changes and to what extent they might be plume induced, but a statement can be made about an upper bound on the magnitude of possible plume effects recorded by the DB meter: typically less than 2 o/oo if any. Figure 2-28 also

shows that natural fluctuations in near bottom salinity are often much larger than 2 o/oo. Several fluctuations were recorded which exceeded 10 o/oo in less than about 5 days.

An alongshelf comparison of surface salinities using DT and WT is shown in Figure 2-29. Gaps in the data for each site limit the periods which can be compared. The most interesting period is mid-June through July 1981 when strong salinity stratification existed, as noted above. It appears that there were also significant surface salinity variations in an alongshelf direction during this period and that variations in the density field, which are governed principally by salinity variations, were complex and covered a large portion of the inner continental shelf along this part of the Louisiana coast.

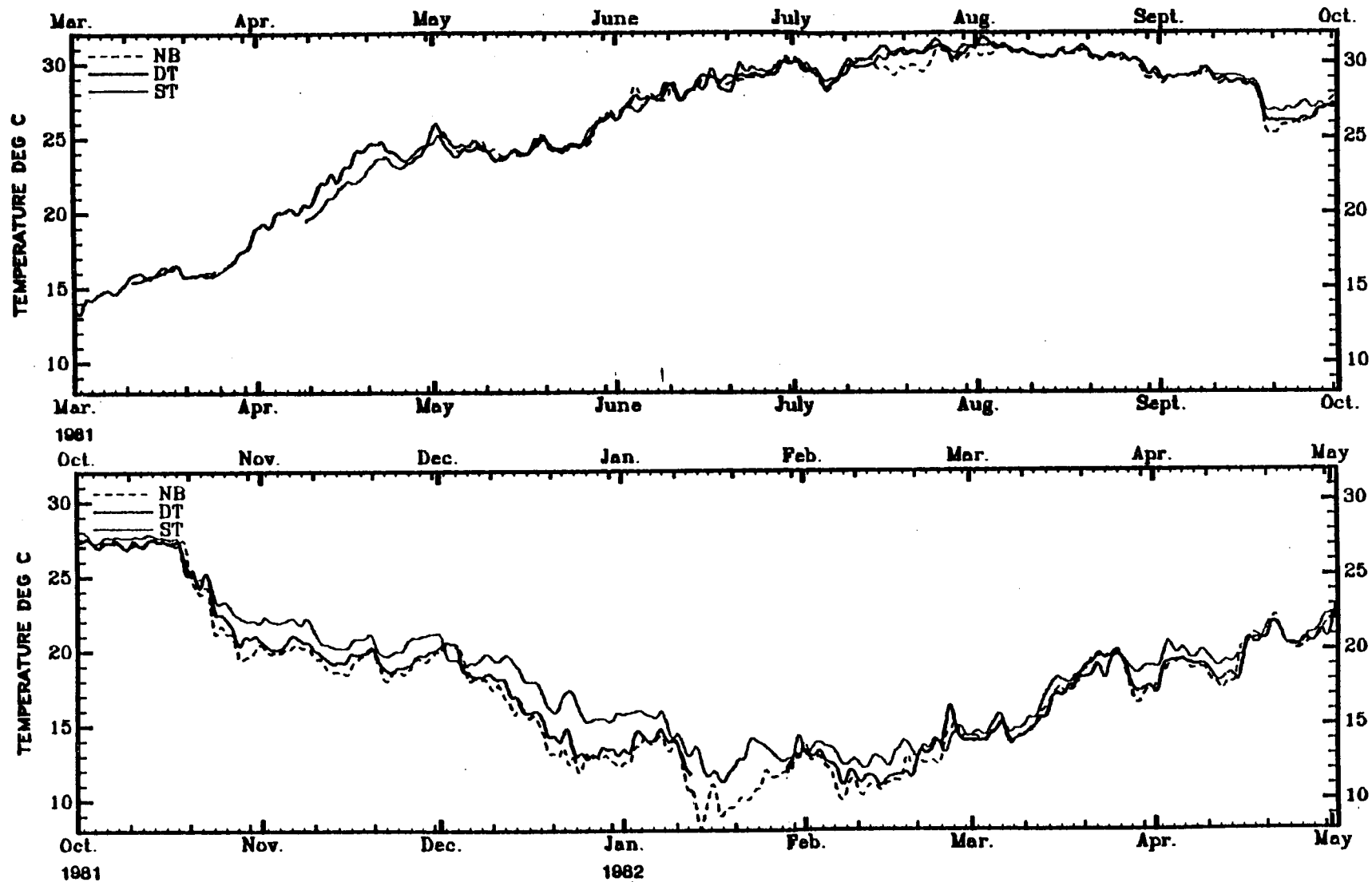
Figure 2-30 shows the vertical salinity stratification at site D. Again, the most interesting period is during June and July 1981. Vertical salinity differences changed from near zero to up to 9 o/oo in very short periods of time. During the rest of the period of Figure 2-30, however, vertical salinity differences were on the order of 2 to 4 o/oo with considerable temporal dependence.

Figures 2-31 through 2-35 show the variation of temperature in cross-shelf, alongshelf and vertical directions as a function of time. The cross-shelf comparison of near bottom temperatures (Figure 2-31) shows the large annual temperature cycle typical for this area, which reaches a minimum in mid-January and a maximum in mid-August. Near bottom temperatures increase rapidly in March and April, level off in May, and then continue to warm gradually through August. SB is typically about 2°C colder than the inshore sites during this period.



BOTTOM TEMPERATURE, CROSS SHELF COMPARISON USING NB,DB,SB

Figure 2-31. Cross-shelf comparison of near bottom temperature using 40-hour, low-pass filtered time series from meters NB, DB, and SB.



SURFACE TEMPERATURE, CROSS SHELF COMPARISON USING NB,DT,ST

Figure 2-32. Cross-shelf comparison of near surface temperature using 40-hour, low-pass filtered time series from meters NB, DT and SB.

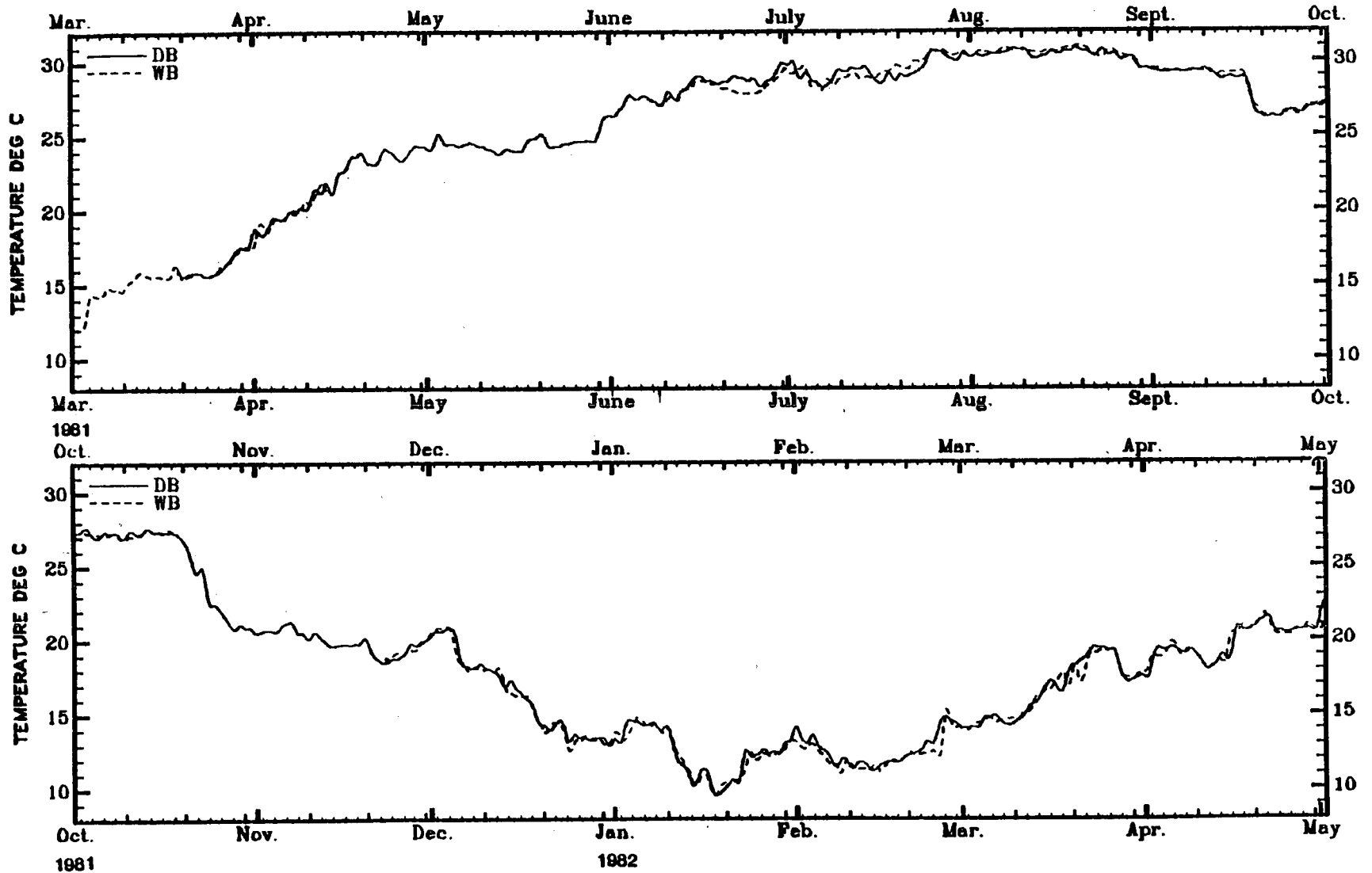
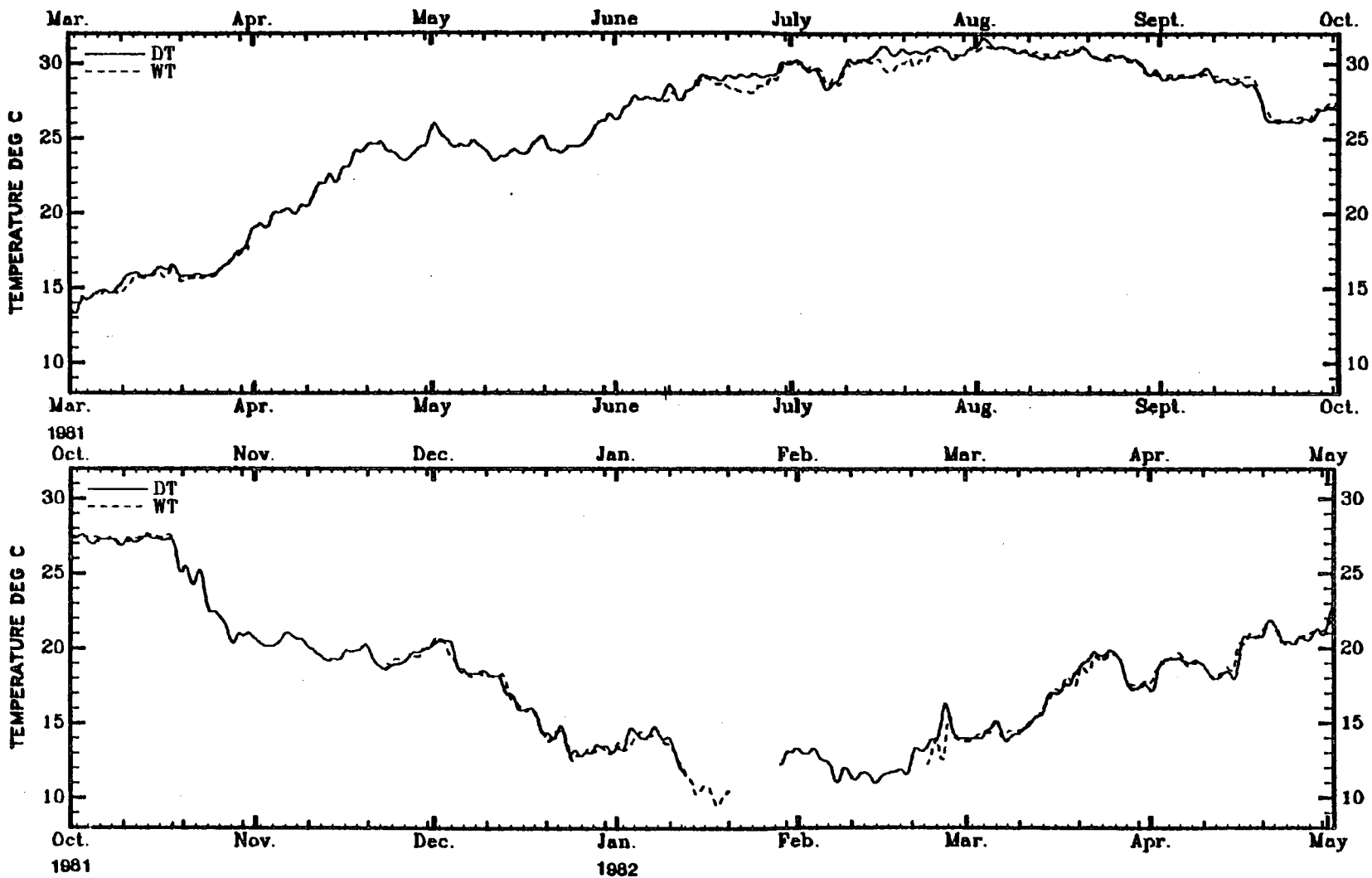
**BOTTOM TEMPERATURE, ALONGSHELF COMPARISON USING DB,WB**

Figure 2-33. Alongshelf comparison of near bottom temperature using 40-hour, low-pass filtered time series from meters DB and WB.



SURFACE TEMPERATURE, ALONGSHELF COMPARISON USING DT,WT

Figure 2-34. Alongshelf comparison of near surface temperature using 40-hour, low-pass filtered time series from meters DT and WT.

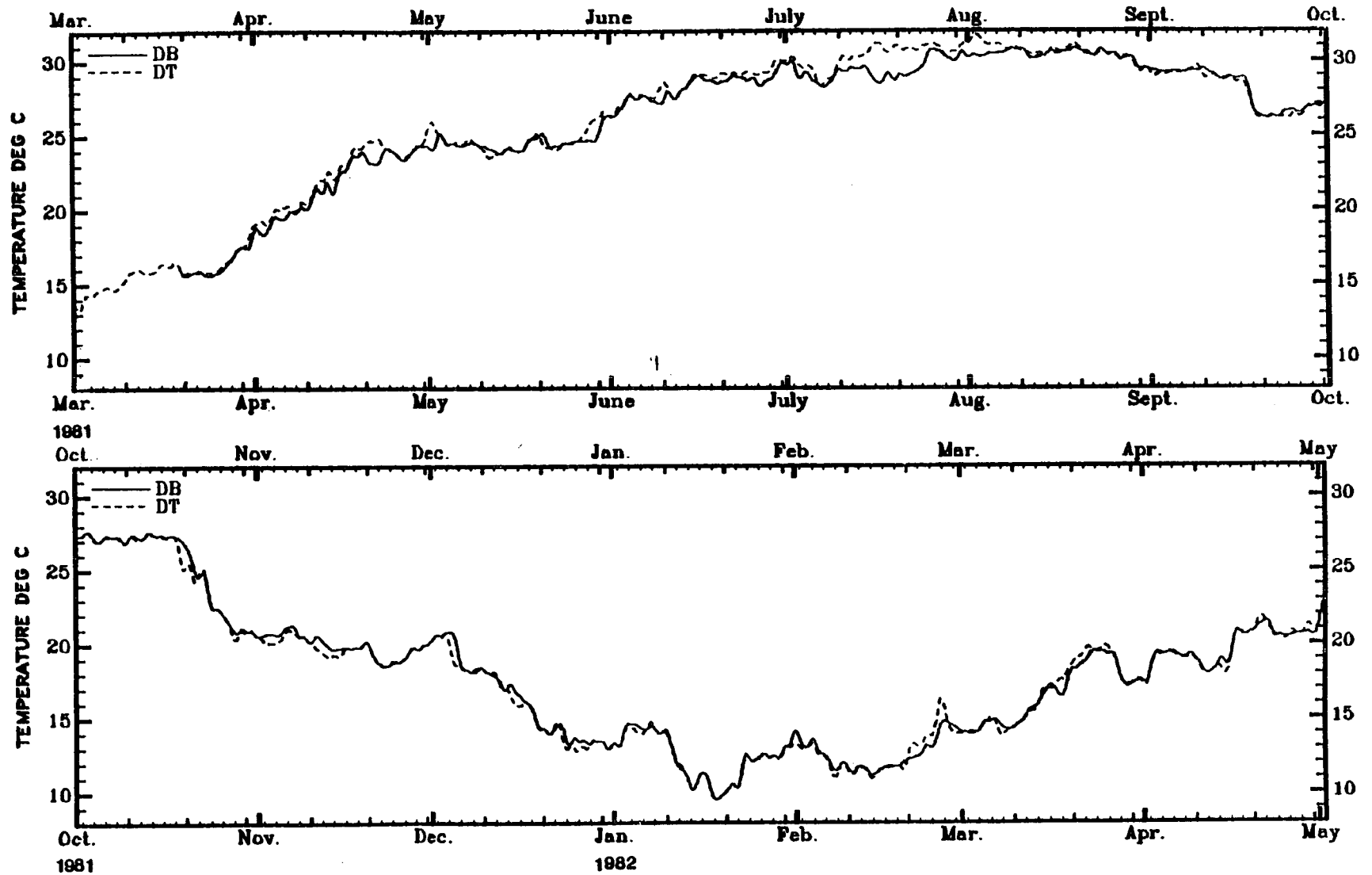
**TEMPERATURE, VERTICAL COMPARISON USING DT, DB**

Figure 2-35. Vertical comparison of temperature at site D using 40-hour, low-pass filtered time series from meters DT and DB.

Cooling takes place from late August to mid-January. During the cooling period, SB is warmer than the shallower inshore sites, and the cross-shelf bottom temperature difference is stronger, about 3 to 4°C. Cooling of the water column occurs more episodically than warming since cooling of surface water decreases vertical stability. The various periods of pronounced cooling, e.g. September 18-20, 1981; October 20-25, 1981; December 5-7, 1981; January 10-14, 1982; etc., can be correlated with the passages of cold fronts through the area (Figures A-117 through A-121).

The cross-shelf comparison of near surface temperatures is shown in Figure 2-32. The annual cycle for surface temperature is similar to bottom temperature except that the maximum of about 31°C is reached in late July/early August. Surface cross-shelf temperature differences are smaller during the warming period than at the bottom after about April. During the cooling period, the near surface conditions are almost identical to those just discussed for the near bottom conditions.

In the alongshelf direction, there is virtually no difference between the temperature at sites D and W (Figures 2-33 and 2-34) except during June and July 1981 when there was strong stratification and frontal zone activity associated with salinity. A difference between sites D and W of up to about 1°C occurred during this time.

Vertical temperature variations at site D (Figure 2-35) are small (less than 1°C) most of the time except in July and early August 1981 when a difference of up to 3°C was recorded. During the warming period, the near surface temperature is slightly warmer than the near bottom temperature and during the cooling period, it is slightly

cooler. There is no evidence of a thermal effect from brine discharge operations in any of the in situ data recorded thus far.

The above discussion of salinity and temperature variations was based on data from which short period fluctuations had been removed. Figures A-146 and A-147 show the bottom temperature and salinity with daily fluctuations included for the months of June and July 1981, the months in which the greatest fluctuations occurred. The main point is that large variations in salinity, up to 8 o/oo on June 16, 1981, can occur in less than one day. Changes on the order of 5 o/oo are not uncommon. Daily temperature fluctuations are usually less than 1°C.

Tables A-2 and A-3 show the basic statistics of temperature and salinity for each month using hourly time series which have been filtered with a three-hour low-pass filter. The annual cycle of monthly mean values is consistent with that discussed in section 2.2, but because it is based on continuous time series, it is more quantitative. This data is further discussed in section 2.5 and compared with other monthly mean salinity data along the Texas-Louisiana coast. June and July have the greatest standard deviation about the mean for salinity which is consistent with the high degree of variability noted above for these months. For DB the lowest salinity value recorded was 19.7 o/oo (August 30, 1981) and the highest was 34.2 o/oo (February 11, 1982). The lowest temperature value was 9.4°C (February 15, 1981 and January 18, 1982) and the highest was 31.0°C (July 25, 1981).

2.4.4 Currents

2.4.4.1 Frequency Domain (Spectral) Characterization

There are a variety of paths along which the discussion of the

current observations at West Hackberry can proceed. We have chosen to begin in the frequency domain, using the results of spectral analyses to show the distribution of variance (which is proportional to kinetic energy for current spectra) as a function of frequency for site D. For the DB location, there is more than one year of continuous data, but for DT there are two gaps, one of about three days duration (July 30 - August 2, 1981) and the other of about eight days duration (January 17-24, 1981). It will be shown that the coherence between sites D and W is very strong, and so these gaps in the DT record have been filled with data from WT in order to obtain a continuous record of at least one year's duration. The result is a common one-year period of data, April 29, 1981 - April 28, 1982, for the Top and Bottom instrument locations at site D.

Autospectra were computed for the alongshelf and cross-shelf components of current using the year long records, and the results are shown in Figures 2-36 and 2-37. The left and right frames in each figure show the total spectrum and the spectrum from 0.6 to 3.0 cycles/day, respectively, which were computed using three-hour, low-pass filtered time series of hourly values. The middle frame shows the spectrum from 0 to 0.5 cycles/day, computed from forty-hour, low-pass filtered series of six-hourly data.

All spectral computations discussed in this report were done by the Blackman-Tukey method (1958) in which estimates of spectral density are obtained from the Fourier Transform of the autocovariance function. A cosine (Tukey) correlation lag window was used in all cases. The spectrum ordinate units are variance units per cycle per day, where the variance units are those appropriate for the time

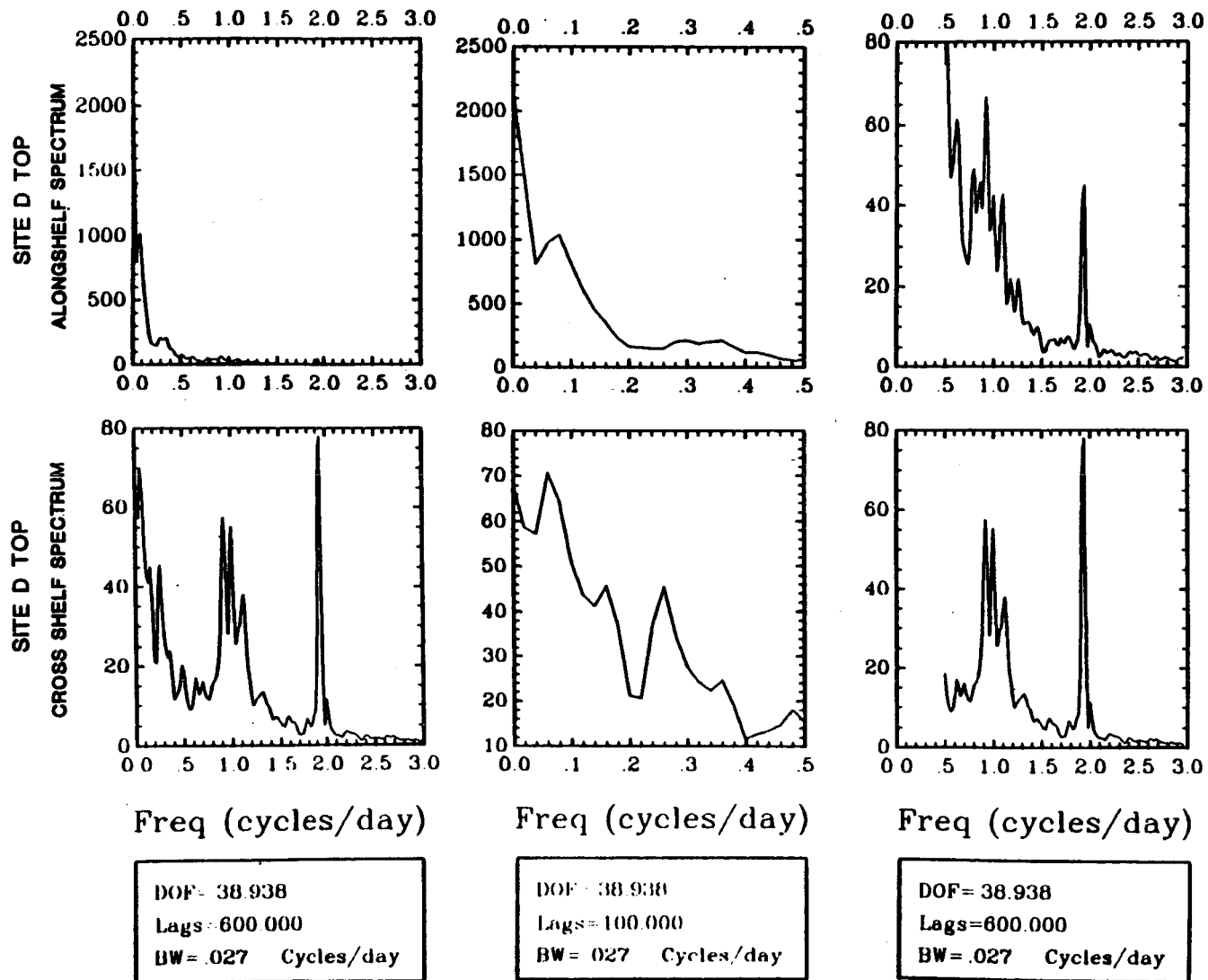


Figure 2-36. Autospectra for the alongshelf and cross-shelf components of current at site D, top for the one-year period April 29, 1981 through April 28, 1982. Left frame is complete spectrum; middle frame is the spectrum from 0.0 to 0.5 cpd; and right frame is the spectrum from 0.5 to 3.0 cpd. Ordinate units are $\text{cm}^2/\text{s}^2/\text{cycle}/\text{day}$.

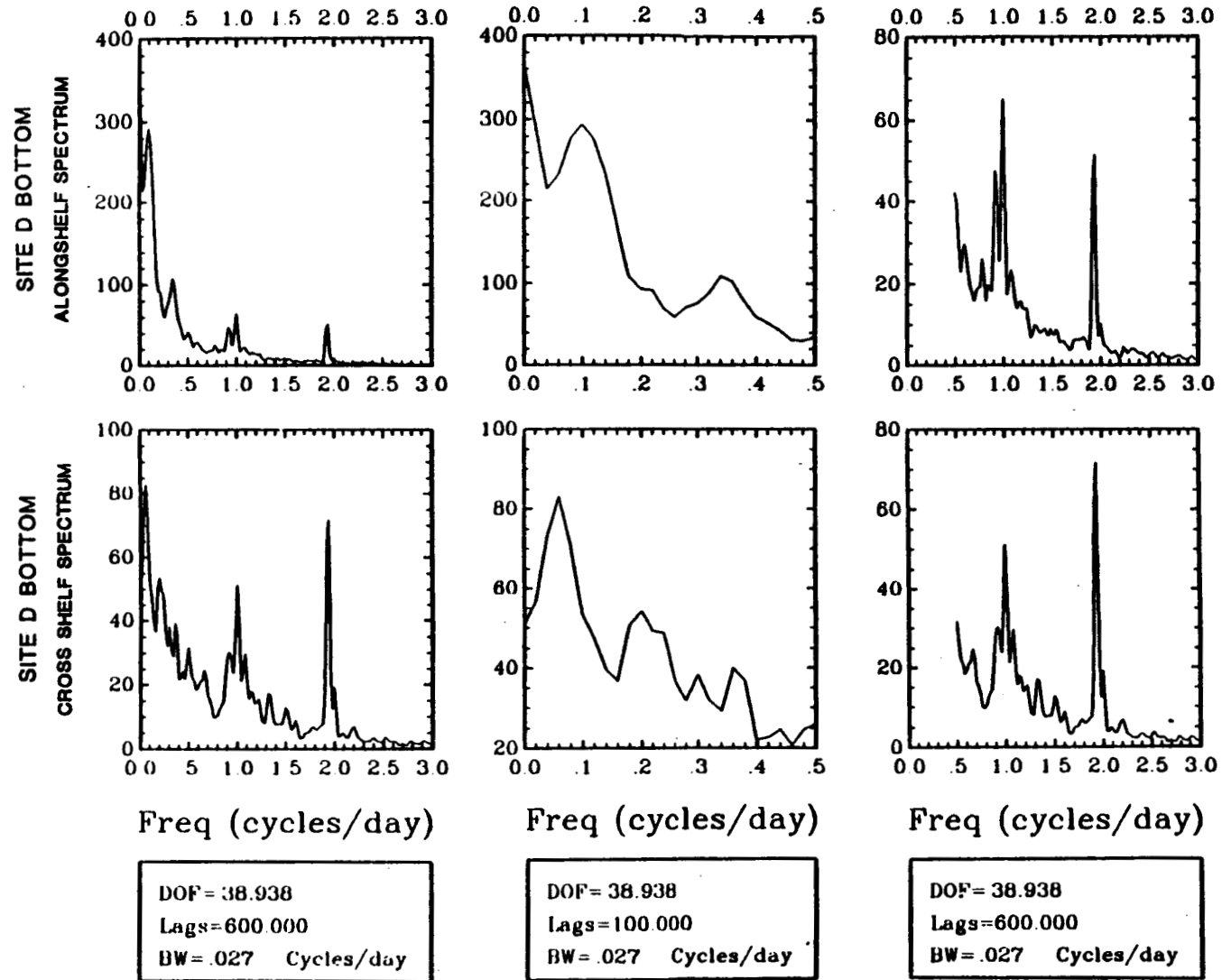


Figure 2-37. Autospectra for the alongshelf and cross-shelf components of current at site D, bottom for the one-year period April 29, 1981 through April 28, 1982. Left frame is complete spectrum; middle frame is the spectrum from 0.0 to 0.5 cpd; and right frame is the spectrum from 0.5 to 3.0 cpd. Ordinate units are $\text{cm}^2/\text{s}^2/\text{cycle}/\text{day}$.

series in question. Root-mean-square estimates of a variable in a particular frequency band can be obtained by multiplying the spectrum estimate in that band by the effective bandwidth given in the Figure and taking the square root of the product. In cross-spectral computations, the 95% significance level for coherence squared is the level below which would fall 95% of the coherence estimates between truly uncorrelated variates. (Note: the significance level is not a confidence interval.) Negative phase means the "Y" series lags the "X" series.

Because of the length of the records used to obtain the results shown in Figure 2-36, there is relatively good resolution near the low frequency end of the spectrum. For DT, the alongshelf component has an order of magnitude more energy than the cross-shelf component at frequencies below 0.5 cycles per day. However, the spectra of both components are similar in that they have a peak in the 0.06 to 0.08 cpd band (16.7 to 12.5 days) and smaller peaks between 0.25 cpd and 0.38 cpd (4 to 2.6 days). The peaks in the cross-shelf component occur at a slightly lower frequency than those in the alongshelf component. Energy in the tidal range is small compared to the lower frequencies for the alongshelf component, but for the cross-shelf component the energy in the tidal range has the same magnitude as the lower frequencies. For DB, the alongshelf component again has significantly more energy than the cross-shelf component. The alongshelf component has a major peak at 0.1 cpd (10 days) and a smaller one at 0.34 (2.9 days) while the cross-shelf component has its major peak at 0.06 cpd (16.7 days) and secondary peaks at 0.2, 0.3, and 0.36 cpd (5, 3.3, and 2.8 days respectively). Energy in the high

frequency range is of the same order of magnitude as for DT which means it is a significant part of the cross-shelf spectrum, but is a relatively smaller part of the alongshelf spectrum.

We next investigate the spatial coherence of the current field by cross-spectral analyses between currents at site D and currents at the other sites. Data gaps in the records from the other sites dictated the pairs of series which could be analyzed. There was no long period of good data common to all sites, and so each analysis is for a different period. Generally, however, there was a record of reasonable length for the summer/fall period and another for the winter/spring period for each instrument location at sites N, S, and W. For each such record, the matching period of data from site D was extracted and the cross-spectral analysis was performed. The results are shown in Appendix A.8. Because of the shortness of the records, two trials of each cross-spectral analysis are shown, one using a maximum lag number of about 10% of the record length and the other about 20%. The former produces a smoother spectral estimate with smaller variance and greater degrees of freedom but wider bandwidth and larger bias. Both were included so that the reader can see the effect of the tradeoff between variance and bandwidth (Jenkins and Watts, 1968).

The coherence of the alongshelf component of current in the alongshelf direction is very strong according to the estimates for three periods of DT versus WT (Figures A-266 through A-268) and two periods of DB versus WB (Figures A-271 and 272). Coherence squared estimates are well above the 95% significance level in all cases. The coherence of the alongshelf component in the cross-shelf direction is

evaluated for two periods each of DT versus ST (Figures A-269 and A-270), DB versus SB (Figures A-275 and A-276), and DB versus NB (Figures A-273 and A-274). Again, the coherence squares estimates are high at almost all frequencies. It should also be noted that in the autospectra for each location, there is a significant increase in the energy in the 0.3 to 4 cpd band relative to the lower frequencies in records which span the winter months and particularly in records for near bottom locations (c.f Figures A-271 and A-272).

The coherence of the cross-shelf component of current in the alongshelf direction is shown for three periods of DT versus WT (Figures A-282 through A-283) and two periods of DB versus WB (Figures A-277 through A-279). For the near bottom records, the cross-shelf component is highly coherent in the alongshelf direction at frequencies below about 0.34 cpd. For the near surface records, the coherence is weaker and more variable with the time of year, but nevertheless, it is significantly coherent in one or two low frequency bands for each comparison. To evaluate the coherence of the cross-shelf component in a cross-shelf direction, two periods each of DT versus ST (Figures A-280 and A-281), DB versus SB (Figures A-286 and A-287) and DB versus NB (Figures A-284 and A-285) are examined. For DT versus ST, there is no significant coherence for the record covering the April-August 1981 period, but the record for the December 1981 - May 1982 period has a strong peak between about 0.2 and 0.3 cpd. For the cases of DB versus NB and SB, three out of four exhibit strong coherence at frequencies above about 0.3 or 0.35 cpd. The fourth case, DB versus SB for November 1981 - April 1982, shows weak coherence at several frequencies over the 0 to 0.4 cpd range.

In summary, the alongshelf component of the current field is strongly coherent in both alongshelf and cross-shelf directions over distances of about 18 km and 30 km respectively. The cross-shelf component of the current field is also coherent much of the time in the alongshelf direction. The coherence for the near bottom currents is strong at frequencies below about 0.34 cpd and is more consistent than the near surface currents. In the cross-shelf direction, the coherence of the cross-shelf component of near bottom current tends to be high at the higher frequencies, i.e. above about 0.3 cpd, but for the near surface current it is high only in one of the two cases and only in the 0.2 to 0.3 cpd band.

We have examined the characteristics of the currents in the frequency domain and found that most of the energy is contained in the lower frequencies in the alongshelf component and that the alongshelf component is spatially coherent throughout the study region. We next examine the role of the local wind field in driving the currents. An uninterrupted wind velocity record is available for the period June 24, 1981 - April 25, 1982 if the data from NDBO #42010 through December 31, 1981 is joined to the data from NDBO #42011 beginning January 1, 1982 (See Section 2.3). Wind stress was computed for the hourly values using a drag coefficient computed by the linear expression of Wu (1980). The time series of the alongshelf and cross-shelf components of wind stress were then filtered with three-hour and forty-hour low-pass filters which have characteristics identical to those used for currents. The results of cross-spectral computations between the wind stress and currents at site D are shown in Figures A-288 through 293. Because the wind stress is computed

using the square of the wind speed, it has a more impulse like character and its spectrum must be computed with a wide bandwidth to get a stable variance estimate. Figure A-288 a, b, and c show the results of spectral computations using maximum autocorrelation lag numbers of 5%, 10%, and 20% of the record length (i.e. wide bandwidth to narrow bandwidth). With a 5% maximum lag number, most of the oscillations in the estimate of the spectrum of alongshelf stress (Figure A-288 b, c) are smoothed out, but the peaks near 0.16 cpd and 0.36 cpd survive. Thus, a lag number of 60 (5%) was used for all the results to be discussed.

Figures A-288 and 289 show that the alongshelf component of wind stress is coherent with the alongshelf component of near surface and bottom currents mostly between 0.25 and 0.45 cpd with a significant peak at 0.36 cpd. Coherence at about 0.13 cpd and below 0.06 cpd is weak. The lack of strong coherence at low frequencies is surprising since most of the energy in the alongshelf components of currents and wind is contained in the low frequency region. At Bryan Mound, strong coherence was found between the alongshelf wind stress and current (Kelly et al., 1982a) which is typical for inner continental shelf regions (Allen, 1980; Winant, 1980).

For the combination of alongshelf stress and cross-shelf surface current there is a weak coherence at frequencies below about 0.14 cpd, but for alongshelf stress versus cross-shelf bottom current there is no coherence. Furthermore, there is no coherence between the cross-shelf component of wind stress and the alongshelf components of surface or bottom current.

The relative lack of coherence between the alongshelf components

of local wind stress and current implies that the low frequency fluctuations of current in the diffuser area are driven by some other mechanism such as density fluctuations from river runoff or are part of a larger scale circulation system, which in turn may be driven by the wind in a large scale sense.

2.4.4.2 Time Domain Characterization

In the time domain we can analyze currents by several methods. The first is a plot of time series data. Appendix A.5 shows all time series data collected with the ENDECO 174 instruments plotted on a monthly basis. These will not be discussed in detail but are the fundamental reference source of data. All other analyses, both spectral and temporal, operate on the data shown in Appendix A.4 to extract and quantify features of interest. A second method of temporal analysis is the computation of basic statistics for some interval of time, in this case monthly. Since the preceding analysis has demonstrated that most of the energy in the currents is contained in the low frequency region, we now examine the monthly mean value of current versus time. Figures 2-38 and 2-39 show graphs of the monthly mean value of the orthogonal components of surface current and bottom current respectively. The mean values were extracted from the tables of basic statistics in Appendix A.2. The monthly mean value of the alongshelf component of wind velocity is also plotted. Open circles are used to indicate months for which the total amount of missing data exceeds 10% of the month. Thus, anomalies with open circles should be interpreted with caution.

For the near surface currents (Figure 2-38), the mean alongshelf component is downcoast (towards the SW) in all months except July when

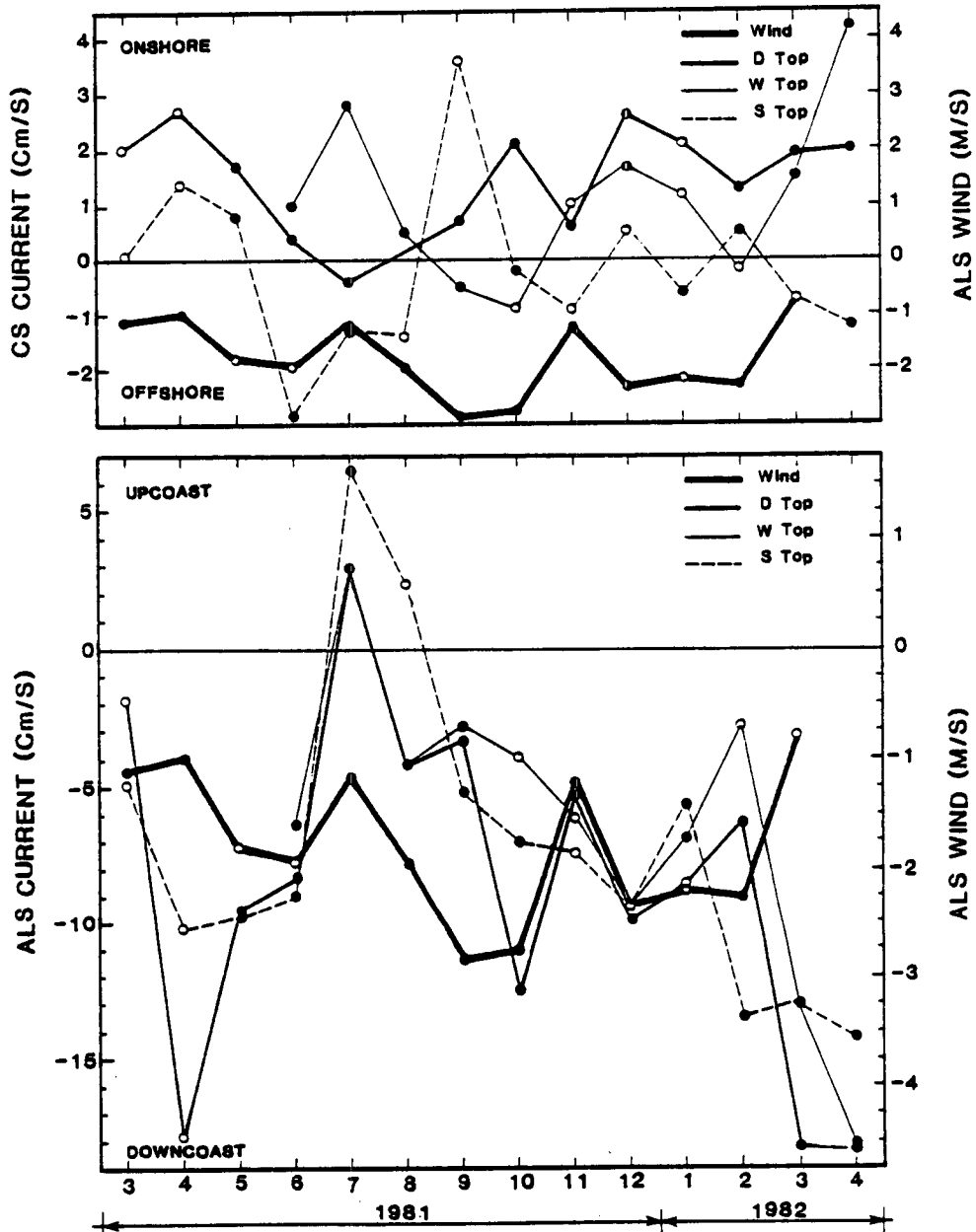


Figure 2-38. Monthly mean alongshelf and cross-shelf components of near surface current for sites D, W and S together with the monthly mean alongshelf component of wind velocity.

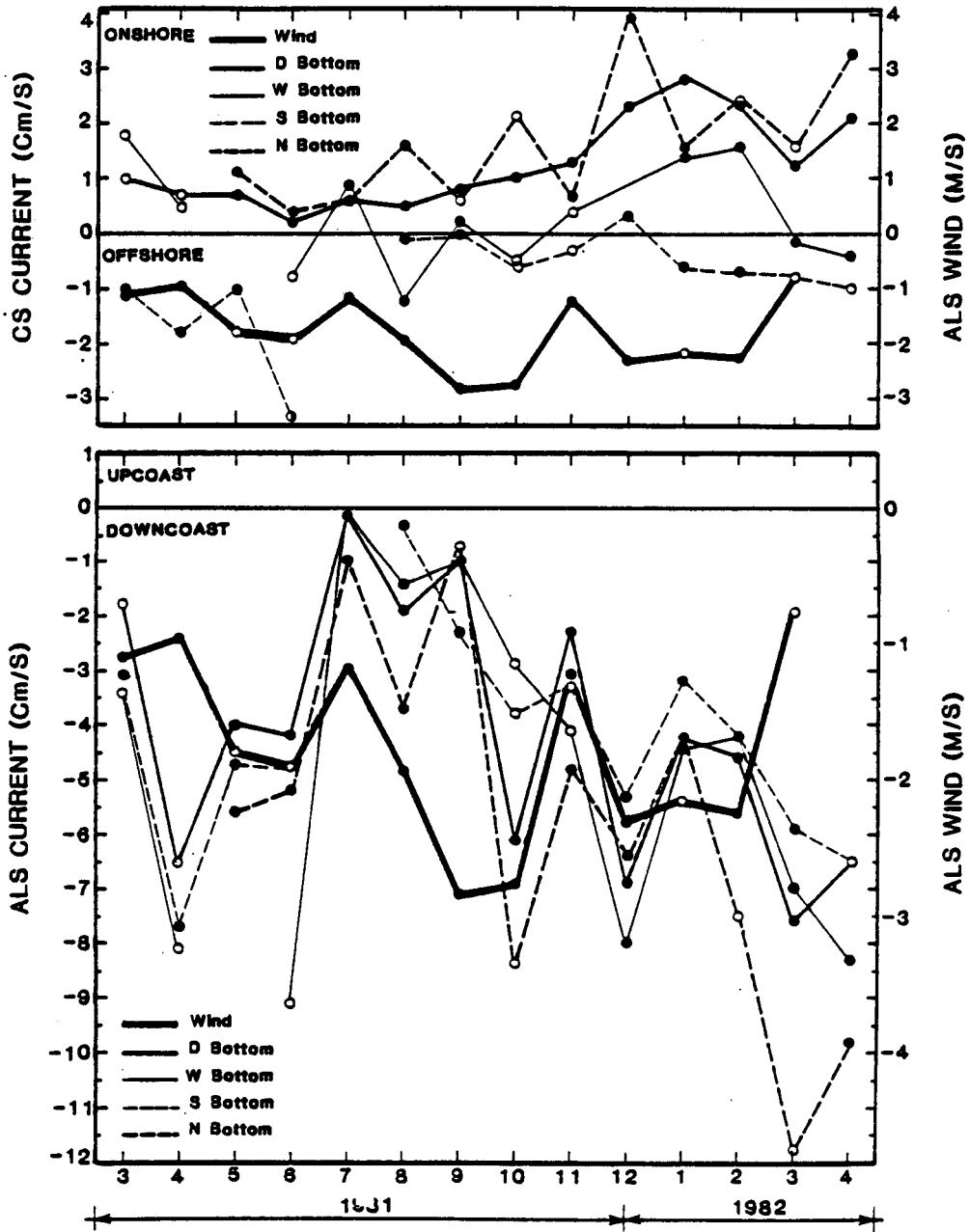


Figure 2-39. Monthly mean alongshelf and cross-shelf components of near bottom current for sites D, W and S together with the monthly mean alongshelf component of wind velocity.

DT, WT, and ST all indicate an upcoast flow. The upcoast flow indicated in August for ST is based on just two weeks of data (Figure A-205). The strong coherence of the alongshelf current among the various sites, which was demonstrated in the spectral analyses, is reflected in both trend and magnitude for DT, ST, and WT. The greatest difference among the monthly means for the three sites occurs in October 1981 and March 1982. Data gaps in the ST and WT records, however, limit the number of months which can be quantitatively intercompared. The DT record has the fewest gaps. As previously noted, it can be considered representative for the area. The strongest mean surface flow occurred in April of each year at about -18 cm/s (downcoast). The mean alongshelf component of wind is downcoast in all months, even in July 1981. Changes in the magnitude of the mean monthly wind do not appear to be related to changes in the mean monthly current, which is consistent with the results of the spectral analyses.

The monthly, mean, cross-shelf, surface current is also shown in Figure 2-38. For DT, which is fairly continuous from April 1981 onward, the mean cross-shelf current was onshore in all months except July 1981 when it was weakly offshore. The offshore direction is consistent with the upcoast direction of the alongshelf component in that month, but if upwelling was occurring, it was not driven by the local alongshelf component of wind. Again, the alongshelf component of wind bears little relation to the cross-shelf currents. The visual correlation among the mean cross-shelf surface currents for DT, ST, and WT appears low as might be expected from the discussion in Section 2.4.4.1.

The mean, alongshelf bottom currents were downcoast in all months (Figure 2-39) including July 1981; the magnitude of the downcoast flow in July was, however, near zero. There is a strong coherence of the alongshelf flow among the sites. For the cross-shelf component of bottom current, the mean value was onshore in all months for both DB and NB. Site WB tracks DB somewhat with about a 1 cm/s offset. The mean cross-shelf current at SB was offshore in all months but December 1981. Fluctuations in the mean alongshelf component of wind are somewhat more related to fluctuations in the mean alongshelf component of bottom current except in April - May and September. The mean alongshelf wind and cross-shelf bottom current appear unrelated.

A third way of examining currents in the time domain is by a joint frequency distribution of speed and direction. This method is particularly useful for brine disposal study because the plume's extent and orientation is related to the magnitude and direction of the current (See Section 4.0). Since the current records for site D have the fewest gaps, we will restrict the discussion to this site. Appendix A.3 shows the monthly joint probability distribution of speed and direction for each site along with a corresponding current rose which is a graphic representation of the tabular data. In order to summarize section A.3, we have extracted the following from each month's data: most frequent speed range and percentage of observations in that range, most frequent direction sector and percentage of observations in that sector, average speed for all observations, percentage of calms (defined to be less than 2 cm/s), and total number of observations. The average speed is a scalar average not a vector average, that is the sign (or direction) is not

taken into account.

Table 2-3 shows the summary data. The data are consistent with the monthly (vector) means discussed above but give some additional information masked by the vector averaging process. The following points are noted. For DT and DB the most frequent direction sector was west in all months but July 1981 when it was east at DT and north at DB. However, the percentage of observations in July in these sectors was a relatively low 25% or less, which indicates other sectors also had a significant percentage of the observed directions. The months of April 1981 and March-April 1982 which had high overall average speeds for DT also had the highest percentage of observations in the west direction sector. For DB these were also months of relatively high speed and frequent west flow, but the contrast with other months is not as pronounced as for DT and the values are lower than for DT. Strong vertical velocity shear is implied during these months. While July 1981 had the lowest monthly (vector) mean flow, the lowest monthly (scalar) mean flow occurred in September 1981, about 8 cm/s for both DT and DB. The percentage of calms, which is defined to be less than 2 cm/s, was greater than about 5% only in August, September, and November 1981. (The months of January - March 1981 are ignored because of the low number of observations in those months). The time series plots for these months (Appendix A.5) show, however, that prolonged calm conditions did not occur. Speeds less than 2 cm/s were of short duration and distributed throughout the given month. The low average currents in those months just made occurrences of speeds less than 2 cm/s more frequent. Finally, if we average the overall (scalar) mean speeds for the twelve month period

Table 2-3. Summary of monthly joint frequency distributions of speed and direction (current roses, Appendix A.3) for site D, top and bottom.

D TOP	J	F	M	A	M	J	J	A	S	O	N	D	J	F	M	A
MOST FREQUENT SPEED RANGE	5-10	5-10	5-10	20-25	10-15	10-15	10-15	5-10	5-10	10-15	5-10	5-10	10-15	10-15	30-40	30-40
PER CENT OCCURRENCE	38.9	31.0	32.5	22.2	25.7	18.6	29.0	32.3	38.6	26.2	30.0	26.2	36.8	28.3	17.7	21.7
MOST FREQUENT DIRECTION SECTOR	W	W	W	W	W	W	E	W	W	W	W	W	W	W	W	W
PER CENT OCCURRENCE	30.3	34.4	32.5	73.3	45.8	35.0	25.9	33.0	30.6	57.5	33.9	51.5	48.8	40.5	59.4	58.8
TOTAL AVERAGE SPEED (CM/S)	7.9	10.6	9.3	21.3	17.2	20.1	15.7	11.1	8.5	15.3	9.6	15.7	16.0	15.6	23.3	22.2
PER CENT CALM	9.0	6.4	2.4	0.3	1.9	2.2	1.4	5.1	7.4	2.0	10.6	1.6	1.3	2.2	2.7	1.5
NUMBER OF OBSERVATIONS	244	672	123	622	744	720	711	705	720	744	720	744	541	672	744	720

D BOTTOM	J	F	M	A	M	J	J	A	S	O	N	D	J	F	M	A
MOST FREQUENT SPEED RANGE	2-5	2-5	2-5	5-10	5-10	5-10	5-10	5-10	5-10	10-15	5-10	5-10	10-15	10-15	5-10	10-15
PER CENT OCCURRENCE	50.8	29.8	31.3	34.2	33.7	28.6	32.4	34.1	37.8	33.1	44.9	28.1	30.9	27.8	24.5	27.1
MOST FREQUENT DIRECTION SECTOR	W	W	W	W	W	W	N	W	W	W	W	W	W	W	W	W
PER CENT OCCURRENCE	12.3	29.5	22.9	44.4	28.4	29.2	17.9	21.0	18.8	34.3	26.1	37.4	29.3	38.4	39.7	31.7
TOTAL AVERAGE SPEED (CM/S)	3.6	7.4	9.6	10.8	11.8	12.7	10.5	9.4	7.8	11.1	9.0	13.0	11.7	11.1	12.7	14.4
PER CENT CALM	32.4	18.3	5.2	2.1	2.6	3.2	2.8	8.6	11.1	3.4	4.9	1.5	2.7	2.7	4.0	1.7
NUMBER OF OBSERVATIONS	244	383	406	430	744	720	744	744	720	744	720	744	744	672	744	720

of March 1981 - April 1982 we get 15.9 cm/s for DT and 11.3 cm/s for DB.

2.4.4.3 Harmonic Tidal Analysis

The current spectra discussed in section 2.4.4.1 have pronounced peaks at the diurnal and semidiurnal frequencies. However, details of the tidal constituents contributing to the peaks were not resolved. In order to get a quantitative estimate of the various tidal constituents, half-hourly current vector series have been analyzed by the harmonic method for various 29-day periods. A modified version of the computer program developed by Dennis and Long (1971) was used, which in turn is a computerized version of the method described by Schureman (1941). In addition, the parameters of the tidal current ellipse were computed (Doodson and Warburg, 1941). The results are shown in the tables in Appendix A.6. All tidal components either computed or inferred by the program are listed for reference purpose, but only the K_1 , O_1 , M_2 , N_2 , and S_2 are significant in the study region. The analyses were performed for site D which is considered representative of the offshore sites and for site P which is a strong tidal pass (channel).

For site D the results for the K_1 and O_1 tidal constituents may be biased at times by effects from inertial oscillations and, in the summer months, sea breeze effects. The periods of the K_1 and O_1 constituents are 23.9 hours and 25.8 hours. The inertial period for the latitude of site D is 24.9 hours, and the period of sea breeze effects is, of course, 24 hours. Baroclinic effects (internal tides) may increase variability among the various month's estimates during periods of large scale stratification. Despite these complications

the results are reasonably consistent. Table 2-4 shows the average magnitude and orientation of the major axis of the tidal ellipse for each of the five constituents at site D. In general, the amplitudes of the individual tidal constituents in the study area are small, that is on the order of 1 to 3 cm/s. The sense of rotation is predominantly clockwise for diurnal tidal currents and counterclockwise for semidiurnal tidal currents. The current ellipses are typically very eccentric. Table 2-5 shows the average tidal amplitudes for site P.

2.4.4.4 Comparison of the Near Bottom Currents at West Hackberry and Bryan Mound

It is interesting to make comparisons between the West Hackberry and Bryan Mound diffuser sites because the latter has a larger and longer running data base associated with brine disposal operations. In addition, the Bryan Mound diffuser is located 20 km offshore in 9.4 meters of water. Since the near bottom currents are a major factor in determining the dispersion of the brine, a comparison of the near bottom currents at the two sites is useful. During the period June 6, 1981 - January 22, 1982 good near bottom current velocity records were collected at both sites. Figures 2-40 and 2-41 show the spectra for the orthogonal components at DB and CB, respectively, for the 231-day period. The left frame shows the total spectrum; and the middle and right frames show the low and high frequency parts, respectively.

There is considerably less energy in the low frequency part of the spectrum at DB than CB in both alongshelf and cross-shelf components. However, at frequencies above 0.5 cpd the alongshelf components of CB and DB have about equal amounts of energy, and for

Table 2-4. Average magnitude (cm/s) and direction (degrees clockwise from north) of major axes of tidal current ellipses for site D, top and bottom, along with average eccentricity of the ellipses and the number instances of each sense of rotation (from Appendix A.6).

D TOP	A	DIR	ECC	ROTATION		
				CW	CCW	LIN
K(1)	2.08	141.5	0.818	9	3	1
O(1)	2.28	139.1	0.874	11	2	
M(2)	2.88	143.1	0.911		13	
N(2)	1.07	138.8	0.934	3	10	
S(2)	1.12	141.5	0.905	3	9	1

D BOTTOM	A	DIR	ECC	ROTATION		
				CW	CCW	LIN
K(1)	2.81	130.7	0.887	8	4	1
O(1)	2.05	123.1	0.925	7	5	1
M(2)	2.91	137.1	0.879		13	
N(2)	0.97	135.6	0.887	5	8	
S(2)	1.30	141.2	0.940		10	3

Table 2-5. Average amplitude of the given tidal constituents for the current in Calcasieu Pass. Orientation of the pass is approximately 356°T - 176°T (from Appendix A.6).

TIDAL COMPONENT	P TOP	P BOTTOM
K(1)	41.55	32.40
O(1)	34.80	28.37
M(2)	35.21	29.42
N(2)	10.72	7.88
S(2)	11.11	10.46

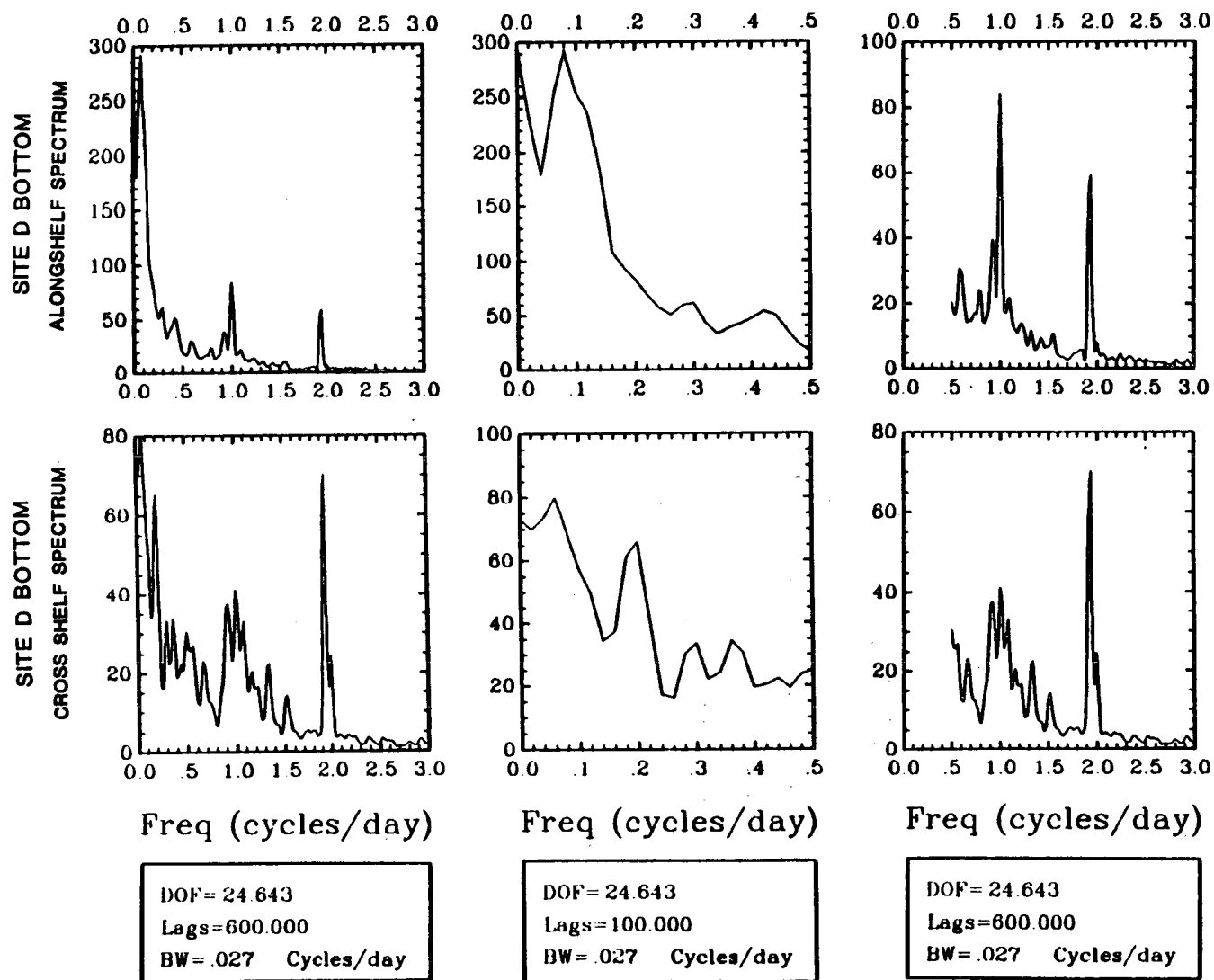


Figure 2-40. Autospectra for the alongshelf and cross-shelf components of near bottom current at West Hackberry site D for the 231-day period from June 6, 1981 through January 22, 1982. Left frame is complete spectrum; middle frame is the spectrum from 0.0 to 0.5 cpd; right frame is the spectrum from 0.5 to 3.0 cpd. Ordinate units are $\text{cm}^2/\text{s}^2/\text{cycle}/\text{day}$.

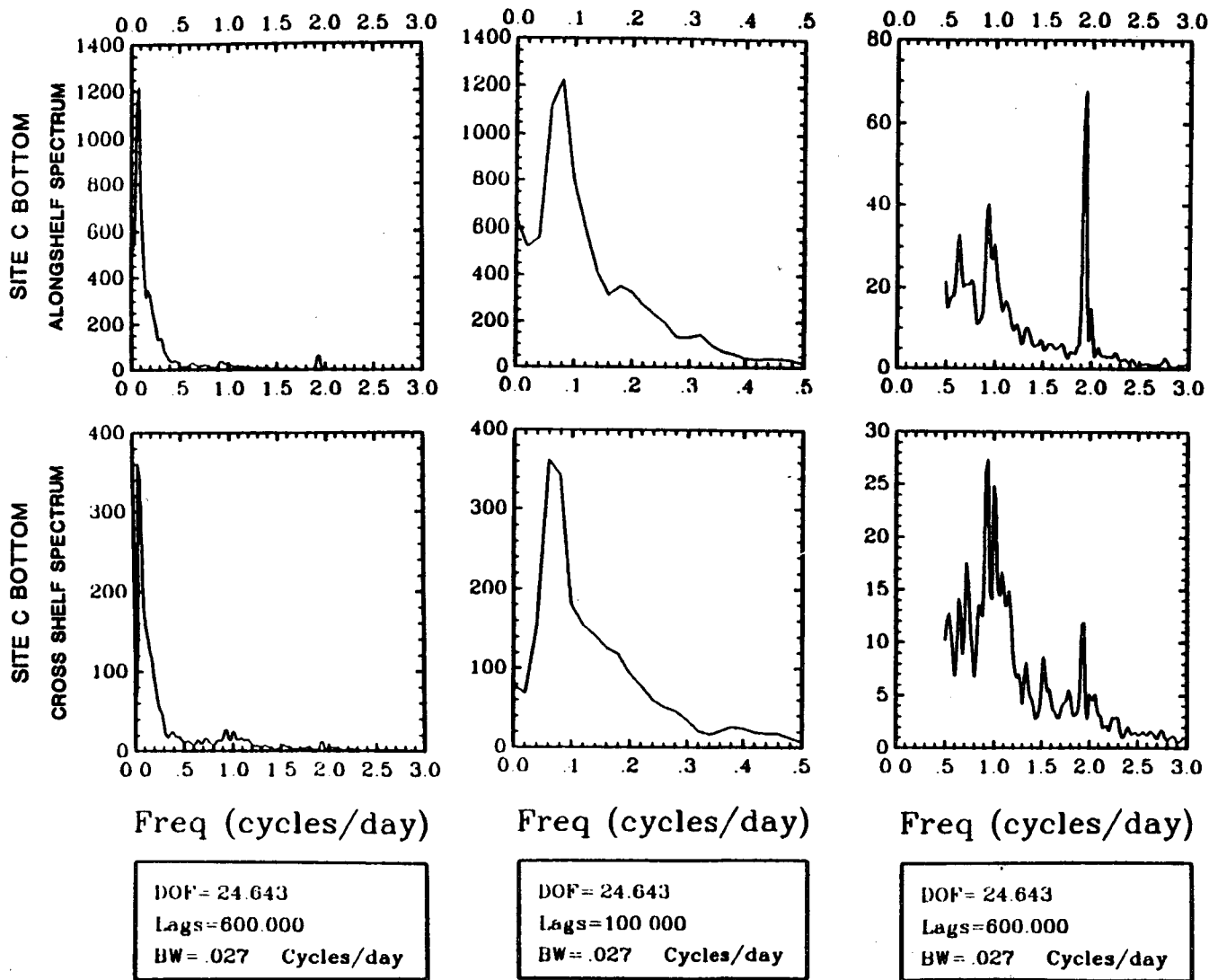
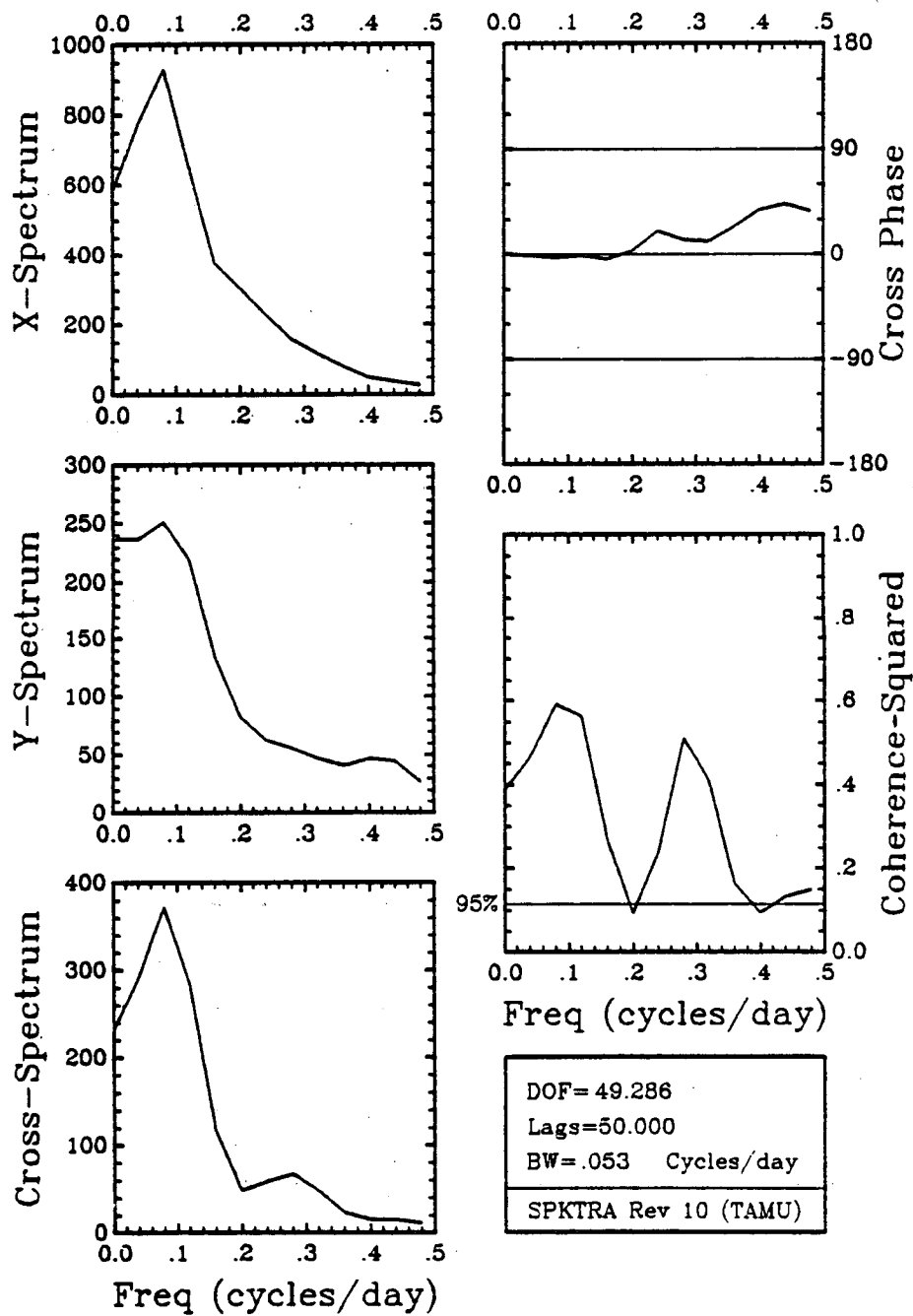


Figure 2-41. Autospectra for the alongshelf and cross-shelf components of near bottom current at Bryan Mound site C for the 231-day period from June 6, 1981 through January 22, 1982. Left frame is complete spectrum; middle frame is the spectrum from 0.0 to 0.5 cpd; right frame is the spectrum from 0.5 to 3.0 cpd. Ordinate units are $\text{cm}^2/\text{s}^2/\text{cycle}/\text{day}$.

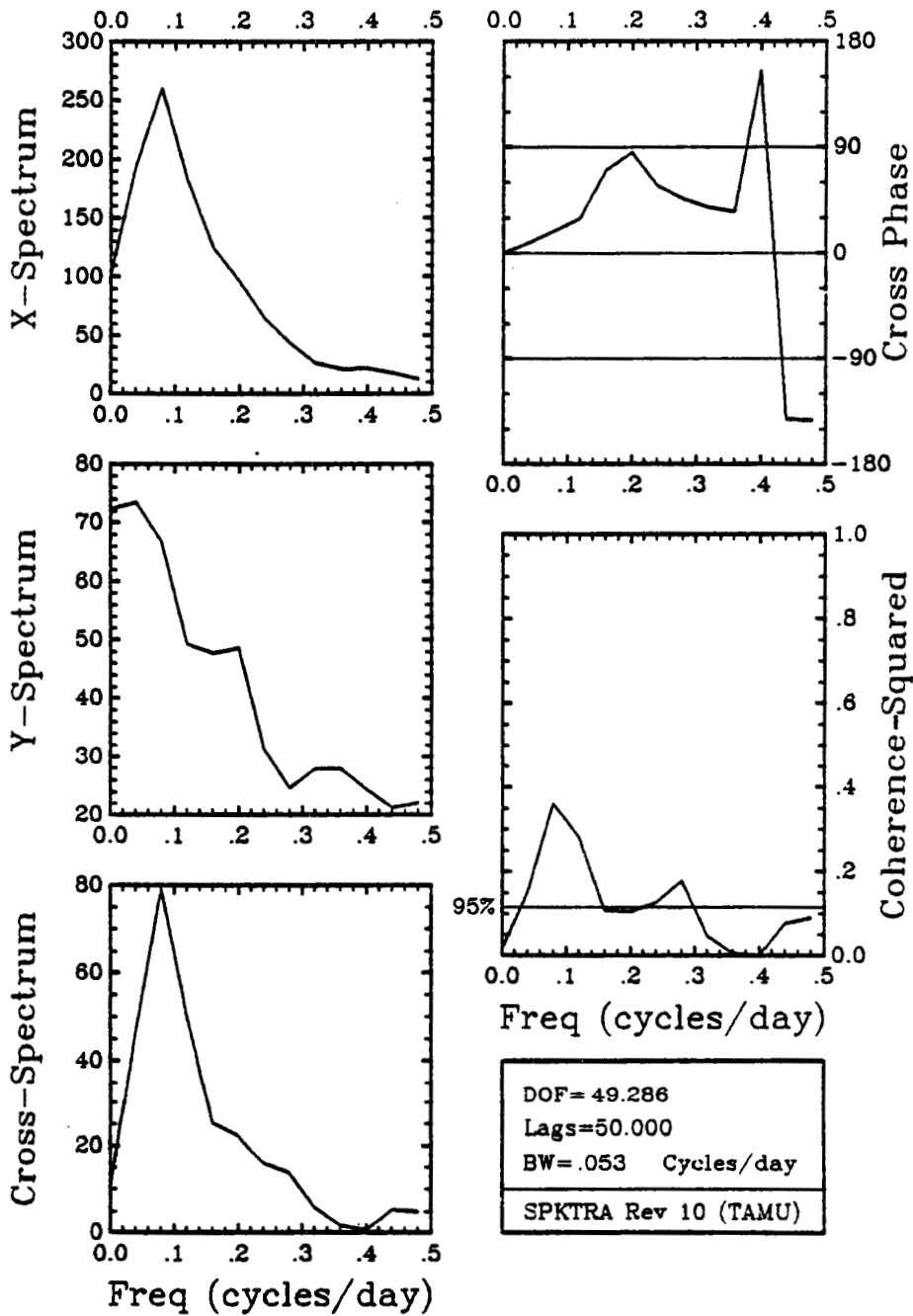
the cross-shelf component DB appears to have slightly more energy. Because of the much greater energy at low frequencies at CB, the energy in the tidal bands is a very small percentage of the total spectrum for both components. At DB the tidal energy is a major part of the cross-shelf spectrum and a "noticeable" part of the alongshelf spectrum. In section 2.4.4.1 it was shown that there was strong correlation of the currents in the West Hackberry study area in the alongshelf direction. The West Hackberry and Bryan Mound sites are separated by a distance of about 200 km. We have investigated the coherence between the near bottom currents of the two sites using the series of the above 231-day period. The results are shown in Figures 2-42 and 2-43. Strong coherence exists between the alongshelf components at periods of about 10 days and 3.3 days, and, somewhat surprisingly, there is also significant coherence between the cross-shelf components at 10 days and some weak coherence at 3.5 days. The Bryan Mound currents were found to be correlated with the alongshelf component of wind stress at low frequencies; the Bryan Mound and West Hackberry currents are correlated at low frequencies, but the alongshelf wind stress and currents at West Hackberry are not correlated at low frequencies. This supports the idea that low frequency current fluctuations currents at West Hackberry are determined in part by large scale, i.e. non-local, processes.

Any time series can be decomposed into three parts: a mean component, one or more deterministic components and a stochastic residual. The deterministic components are those which can be determined precisely for all time, for example a linear trend or sinusoidal signal. For currents, the tidal components are



X_(CB ALS) VS Y_(DB ALS) (06JUN81-22JAN82, 924,3)

Figure 2-42. Autospectra, cross-spectrum, cross-phase and coherence-squared for Bryan Mound site X versus West Hackberry site Y alongshelf components of near bottom current for the 231-day period from June 6, 1981 through January 22, 1982. Ordinate units are $\text{cm}^2/\text{s}^2/\text{cycle}/\text{day}$. Negative phase means Y lags X.



X(cs cs) VS Y(ds cs) (06JUN81-22JAN82, 924,3)

Figure 2-43. Autospectra, cross-spectrum, cross-phase and coherence-squared for Bryan Mound site C (X) versus West Hackberry site D (Y) cross-shelf components of near bottom current for the 231-day period from June 6, 1981 through January 22, 1982. Ordinate units are $\text{cm}^2/\text{s}^2/\text{cycle}/\text{day}$. Negative phase means y lags X.

deterministic. The stochastic residual, or short memory part, has some degree of randomness and cannot be predicted precisely even with an infinitely long past history, but adjacent values in time are to some degree related. The instantaneous current for each component can thus be expressed as

$$q(t) = Q + \sum_{i=1}^N A_i (\omega_i t + \theta_i) + q_r(t)$$

where Q is a constant equal to the mean value of the series, A_i , ω_i , and θ_i are the amplitude frequency and phase of the i -th tidal constituent and $q_r(t)$ is the stochastic residual.

Following the method of Gaboury and Stolzenbach (1979) we have determined the advective length scale associated with each of the above parts. An advective length scale is computed from the product of a velocity scale (units of L/T) and a time scale (units of T). The advective length scale is a measure of the distance travelled by a water parcel over the given time scale at the given velocity scale. We estimate the tidal advective scale as $[A_T T_T]$, where T_T is one half the tidal period and A_T is the average tidal amplitude for the record, computed as in section 2.4.4.3. The advective length scale of the stochastic residual is estimated as $[\sigma_r T_x]$, where σ_r is the standard deviation of the residual current about the mean and T_x is the length of time between current reversals. T_x , in turn, is estimated from the second derivative of the autocorrelation function, $\rho''(0)$, (Ingraham, 1976). The advective scale of the mean current is estimated as $[V T_x]$, where V is the mean of the series. Finally, it is of interest to compare the advective length scales to a diffusive length scale which can be estimated as $[E_H T_x]$. We have taken the diffusion coefficient,

E_H , as $100 \text{ ft}^2/\text{s}$ (Gaboury and Stolzenbach, 1979).

Table 2-6 shows the average tidal amplitudes for each site and Table 2-7 shows the mean of the alongshelf and cross-shelf current for each site over the period of the record. Table 2-8 shows the results of computing the advective length scales as discussed above. The exact value of a given length scale should not be given much significance since the time scale, T_x , can be estimated in a variety of ways, each giving a different value. The relative magnitudes (or ratios) between the various scales is what is significant. It can be seen that at site C the residual component of current is almost an order of magnitude greater than the other factors affecting the plume and several times greater than at site D. Although the mean current is slightly larger at site D than site C, the time scale T_x is shorter at D than C. It is concluded that at site D, the advective length scale is only two to three times greater than the tidal and mean scales. Therefore, the tidal and mean currents have a more significant role in plume advection at site D. The effect of diffusion is smaller for the assumed diffusion coefficient than the other factors at both sites.

2.5 Discussion of Circulation and Hydrography in the West Hackberry Region

2.5.1 Introduction

The West Hackberry brine disposal region (Figure 2-1) lies within the narrow brackish wedge that extends to the west from the Mississippi and Atchafalaya Rivers along the Louisiana and Texas coasts. Figure 2-44 shows the near surface salinity distributions encountered by GUS III (Temple et al., 1977; Kelly and Randall, 1980)

Table 2-6. Mean amplitude of tidal constituents along major axis of current ellipse.

	Site D	Site C
\bar{K}_1	2.6 cm/s	1.9 cm/s
\bar{O}_1	2.3	2.1
\bar{M}_2	3.0	2.6
N_2	0.9	0.9
S_2	1.5	1.1

Table 2-7. Mean current for period June 1, 1981 through January 27, 1982.

	Site D		Site C	
	Alongshelf	Cross-Shelf	Alongshelf	Cross-Shelf
Mean				
Standard				
Deviation	-3.3	1.2	-2.3	-0.3 cm/s
of				
Residual	7.50	4.65	12.77	6.74

Table 2-8. Comparison of advective length scales.

	Site C	Site D
$[A_T T_T]$ Diurnal	0.9 km	1.1 km
$[A_T T_T]$ Semidiurnal	0.6	0.7
$[\bar{V} T_x]$ Alongshelf	1.5	1.3
$[\bar{V} T_x]$ Cross-shelf	0.2	0.3
$[\sigma_r T_x]$ Alongshelf	8.3	3.0
$[\sigma_r T_x]$ Cross-shelf	3.2	1.3
$[E_H T_X]^{1/2}$ Alongshelf	0.8	0.6
$[E_H T_X]^{1/2}$ Cross-shelf	0.7	0.5

T_x = Average length of time between current reversals
(estimated from $\rho''(0)$)

T_T = Half of tidal period

E_H = Horizontal diffusion coefficient

\bar{V} = Mean current

σ_r = Standard deviation of residual

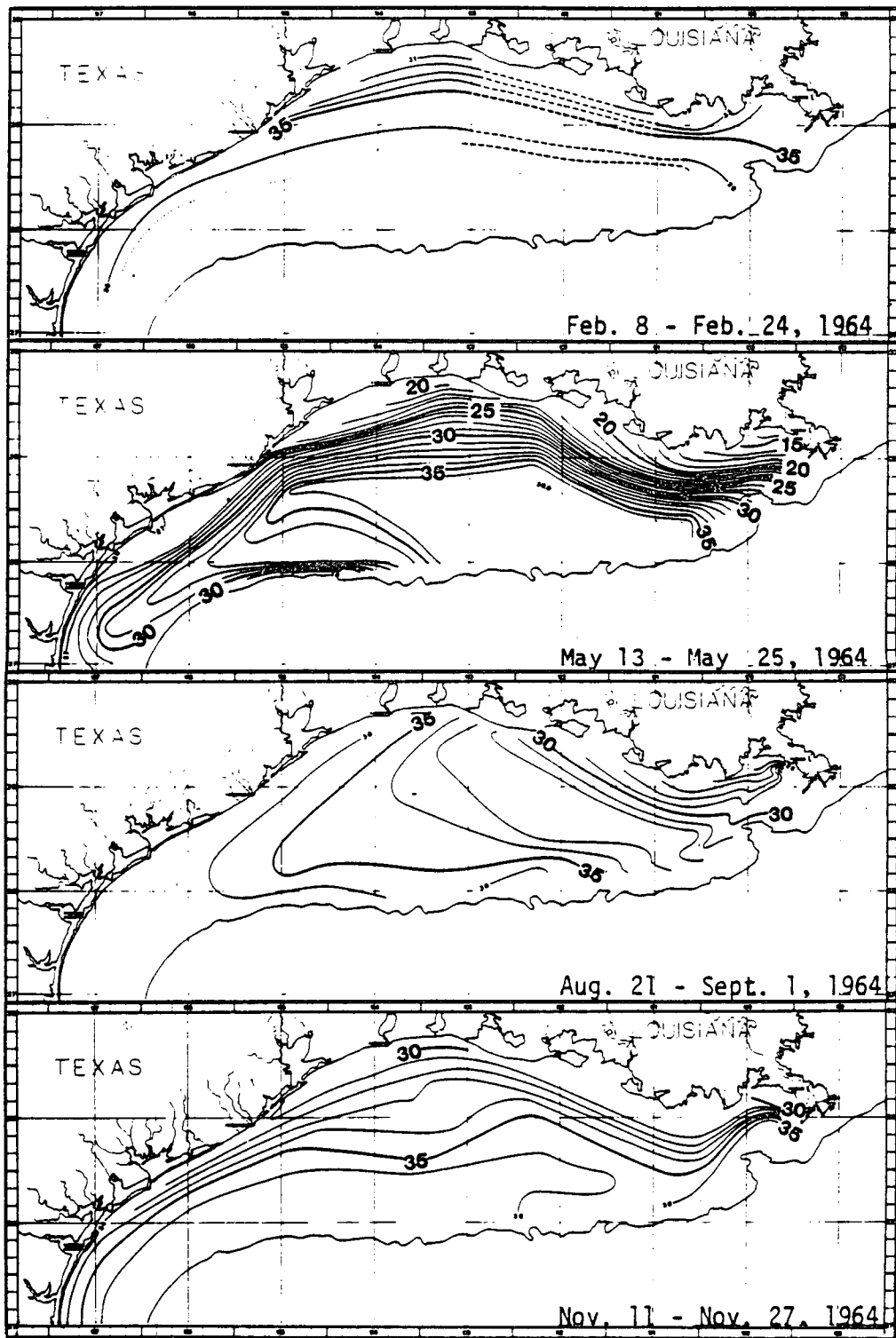


Figure 2-44. Sea-surface salinity (o/oo) on the Texas-Louisiana shelf based on GUS III observations made in February, May, August, and November 1964.

along the Texas-Louisiana coast during a month in each season in 1964, distributions which seem to be fairly typical. Except in summer, the wedge is present as far west and south as the lower Texas coast. In summer, the wedge extends only along the Louisiana coast, being displaced along the Texas coast by water of the considerably higher salinities typical of the adjacent offshore regions. The salinity pattern suggests, correctly as we shall show, that there is a downcoast (westward and southward) flow which prevails along the coast from August or September until about June along much of the inner portion of the Texas-Louisiana Shelf.

As in most coastal regions, local wind stress may be expected to be a major driving mechanism for currents of subtidal frequency (e.g., Winant, 1979, 1980). The mechanism we envisage is that at some distance beyond the frictional boundary layer, 10 km or so out from the coast, Ekman transport due to the alongshelf component of wind stress constitutes a flow toward or away from the coastline. Depending on the sense of the alongshelf component, water at the coast is either piled up to produce downwelling or reduced in level to produce upwelling. If the resulting slope in the sea surface is to be maintained, the pressure force associated with it must be balanced, most probably by the Coriolis force due to down or upcoast water movement: the slope's pressure force may be geostrophically balanced. For such a balance, the current must be in the same direction as the alongshelf wind stress. The alongshelf current may become steady as a result of bottom friction.

Haline forcing may also be an important mechanism for the flow along the Louisiana-Texas coast. A coastal band or wedge of brackish

water due to runoff or, once initiated, to brackish water advection, may be stabilized if the resulting sea-surface slope (or better, the associated pressure-gradient force) is balanced by the Coriolis force due to a current flowing with the coast on its right.

In addition to the local forcing due to the wind or to fresh-water runoff (and its advection), the flow along a coast may be driven by a third mechanism, the forces involved in a circulation of larger than the local scale. This circulation is in turn built up by the action of wind and runoff at other locations along the coast. Often such circulations appear to have dimensions comparable to those of the shelf adjacent to the coast under consideration. Of course, the circulation in any area (here, the West Hackberry region is considered) is the resultant of all of the driving mechanisms acting together.

We wish to provide a fairly comprehensive picture of the hydrography, the characteristics and distributions of waters as they vary through the year at the West Hackberry brine disposal region and the circulation there, a picture that is essential in determining the fate of brine pumped into the Gulf at the diffuser site (Site D, Figure 2-1.) In the following discussions, because of the limited data series from the West Hackberry brine disposal region, we consider first the circulation and hydrography in the better known Bryan Mound brine disposal region and general ideas about the Texas-Louisiana coastal shelf circulations developed as a result of the Bryan Mound studies (Kelly, et al., 1982). Then we compare the limited information we have assembled on currents and hydrography for the West Hackberry region, trying to show how it fits in with what we know

about the larger-scale coastal and shelf circulation.

2.5.2 Circulation of the Texas-Louisiana Shelf, especially the Inner Shelf

The quantitative relationship between wind stress and currents in the Bryan Mound region has been studied by determining the coherence and phase between wind stress and currents for frequencies ranging from 0 to 0.5 cycles per day. An unbroken series of wind measurements at Bryan Mound site A together with current measurements at Bryan Mound site C extending from April 5 to July 3, 1980 (89 days) provides the basic information. The stress τ was determined by use of the equation $\tau = \rho C_d U^2$ where ρ is the density, U the wind speed, and C_d the drag coefficient for which the values given by Wu (1980) were adopted. Significant coherence-squared is found between the alongshelf wind stress and the alongshelf current component near the surface except near 0.35 c.p.d., that is, a period of 2.8 days (Figure 2-45a). (In view of the length of the current record, coherences at frequency below about 0.08 are not significant.) Significant coherence-squared is also found between the alongshelf stress and alongshelf current near the bottom (Figure 2-45b). Similarly, the coherence-squared between the alongshelf stress and the cross-shelf current near the bottom is significant over much of the range of frequency investigated (Figure 2-45c). The latter coherence is in accord with the view that up or downwelling is involved in the driving of the alongshelf current by wind stress. The coherence between the alongshelf stress and the near-surface cross-shelf current component was significant in only a few frequency intervals (Figure 2-45d). Possibly, the low coherence results from the complexity of currents near the strong and convoluted

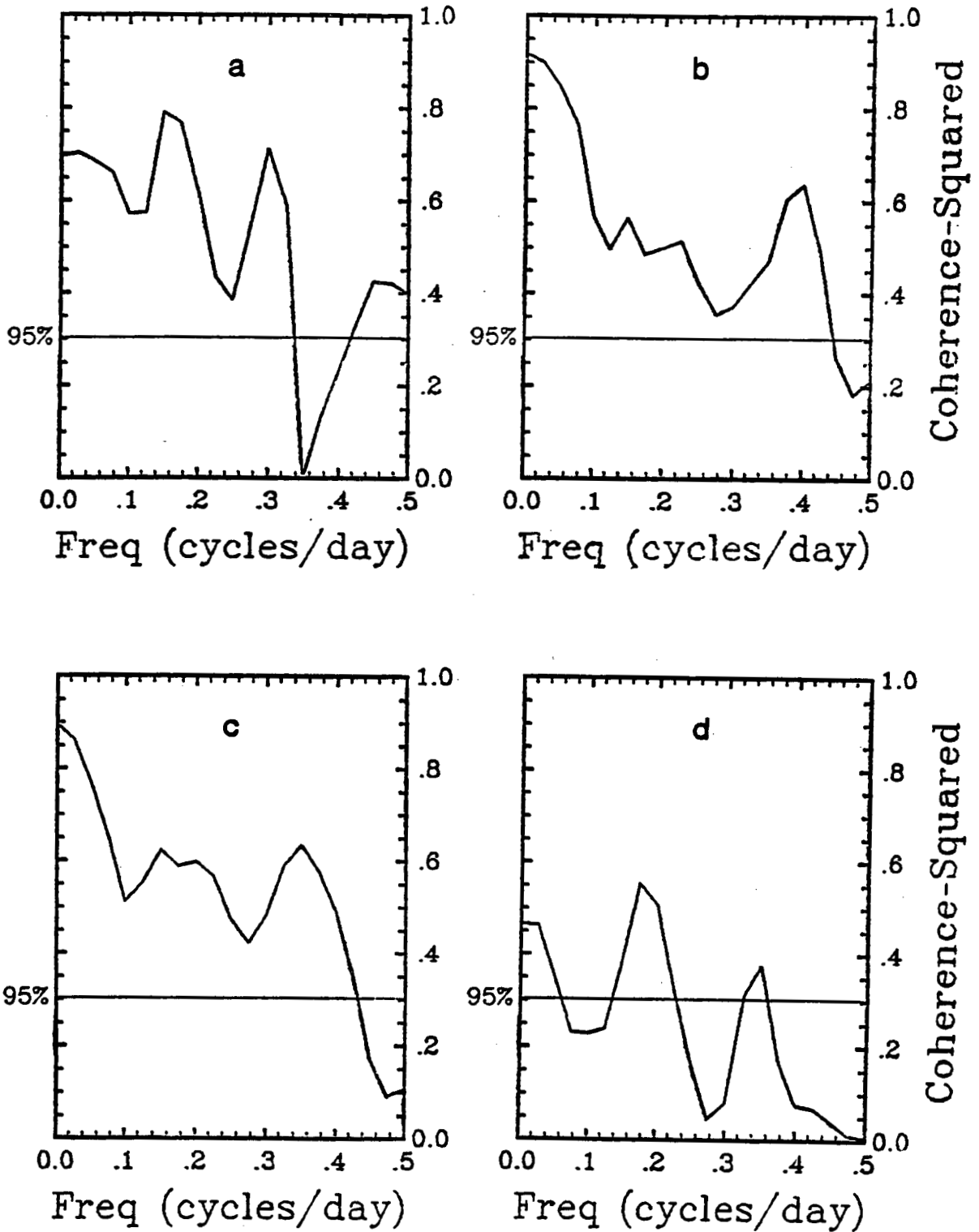


Figure 2-45. Coherence-squared between alongshelf wind stress at Bryan Mound site A and currents at Bryan Mound site C, (a) alongshelf component at the top meter, (b) alongshelf component at the bottom meter, (c) cross-shelf component at the bottom meter, and (d) cross-shelf component at the top meter. (See also Figures 1-52 through 1-55.)

zone of large salinity gradient near the surface.

As Winant (1979) has noted in reviewing wind-induced coastal current measurements, currents lag an imposed wind stress by a time on the order of one inertial period. Phases in the spectral analysis for the Bryan Mound study region indicate lags that often are even less than the inertial period (at 29°, the inertial period is 23.3 hr.)

Since the detailed data required for spectral analysis are available in only a few places, one must turn to monthly means in comparing the annual progression of currents, wind stress, and salinities observed in the Bryan Mound brine disposal study region with corresponding values found at other locations along the Texas-Louisiana coast. The annual progressions of current and wind stress in the study area are considered first.

Since the alongshelf components of wind stress and current exhibit the high degree of coherence indicated in Figure 2-45, it is not surprising to find a close correspondence between the monthly mean alongshelf components of wind stress for Bryan Mound site A and current at site A (or site B if site A was not in operation), as Figure 2-46 shows. Both the wind and current records used in averaging extend from the earliest available time in 1978 to September 1981. The mean stress component was computed by obtaining the vector mean wind stress at the NDBO buoy at site A for each month and then obtaining the alongshelf component. The components of current and wind stress are, according to our information, directed downcoast (southwestward) from September until May (wind stress) or June (current) upcoast in July, with magnitudes for the latter being considerably smaller than in the downcoast period. For the transition

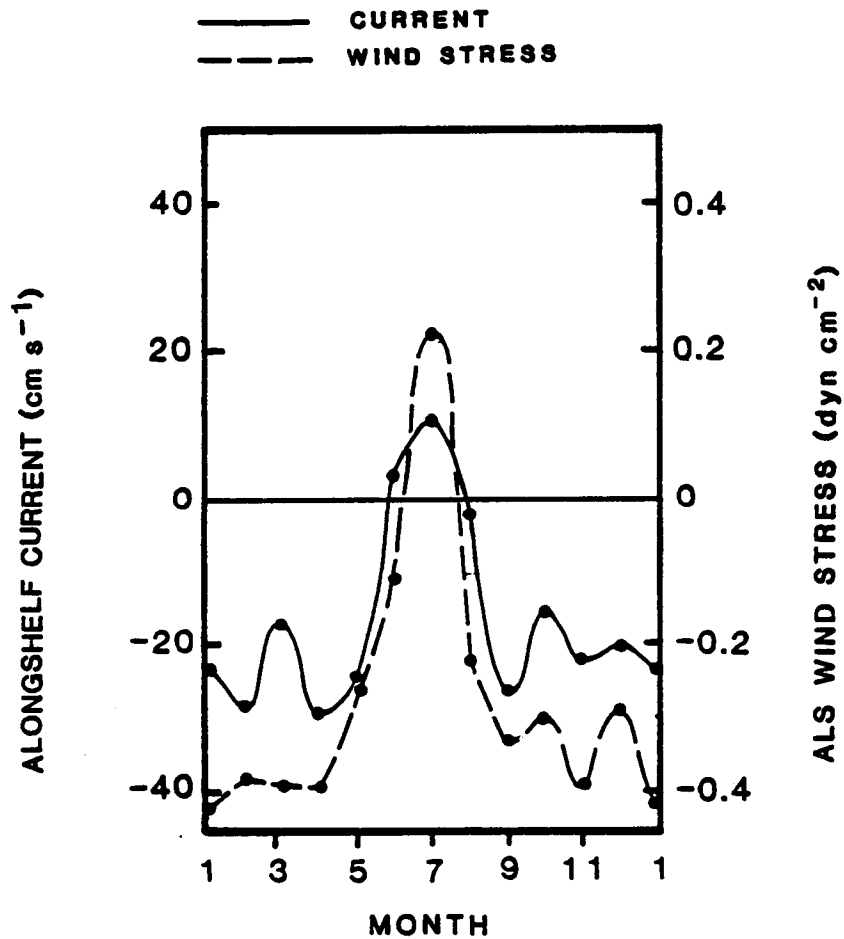


Figure 2-46. Monthly mean alongshelf component of current (cm s⁻¹) for top current meter at Bryan Mound site A together with monthly mean alongshelf component of wind stress (dyn cm⁻²) based on NDBO wind data at site A.

months of June and August, the mean current components are close to zero while the mean stress components are negative (downcoast) but not large. Although the correspondence between current and stress is thus not perfect, it is strong. Since the Bryan Mound current data form by far the longest series along the Texas-Louisiana coast of which we are aware, and are among the longest we find in coastal current literature in general, we feel that the annual progression of current in the study region is among the best known of any coastal region.

Further evidence for the above annual progression of the Texas coastal currents is provided by the degree of agreement between the alongshelf current means and the monthly mean sea level at Galveston Pier when the latter is corrected for steric level (Figure 2-47). The correction used is based on the monthly mean temperature-depth relationship at the outer edge of the continental shelf. The temperature-depth data used are from the GUS III cruises reported by Temple et al. (1977). Significant agreement between sea level and alongshelf current is of course implied by the mechanism relating wind stress and current which was outlined above.

Earlier work based on drift bottle data has found similar annual progression in currents along much of the Texas-Louisiana coast. Harrington (1971) stated on the basis of drift bottle data then available (Kimsey and Temple, 1963 and 1964, primarily) that:

1. Currents between September and April for the most part are longshore westward along the Louisiana coast and southwestward along the Texas coast.
2. A reversal of this system usually starts around May or June when currents become irregular and obliquely onshore.

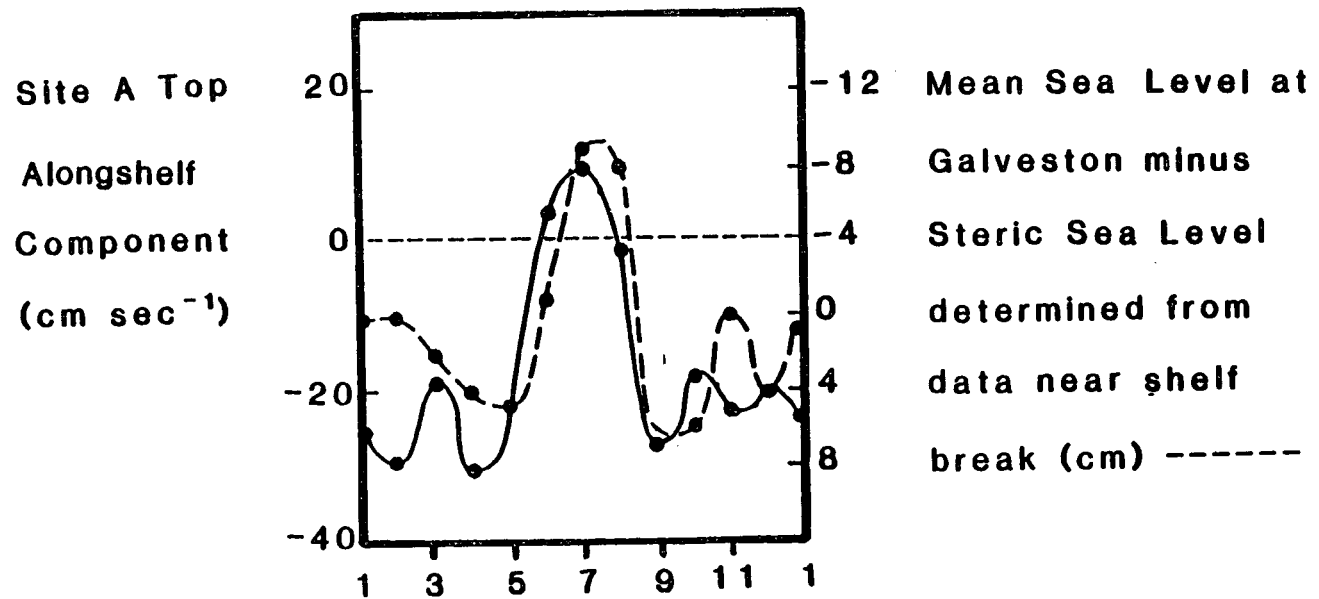
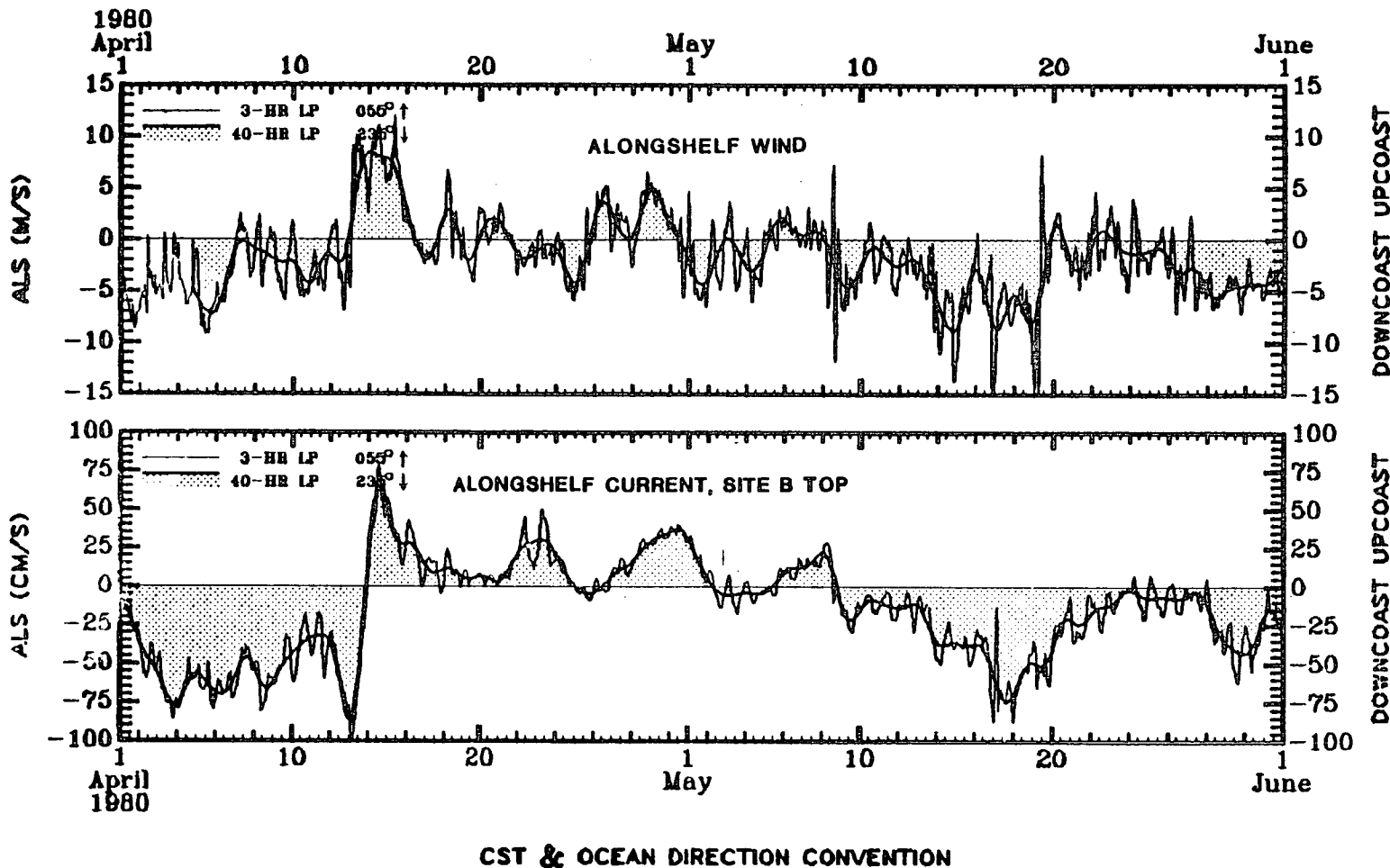


Figure 2-47. Monthly mean alongshelf component of current (cm/s⁻¹) for the top current meter at Bryan Mound site A together with monthly mean sea level at Galveston pier (1951-1960) corrected for steric sea level.



2-131

Figure 2-48a. Alongshelf winds together with alongshelf current components for the top meter at Bryan Mound site B during April and May 1980.

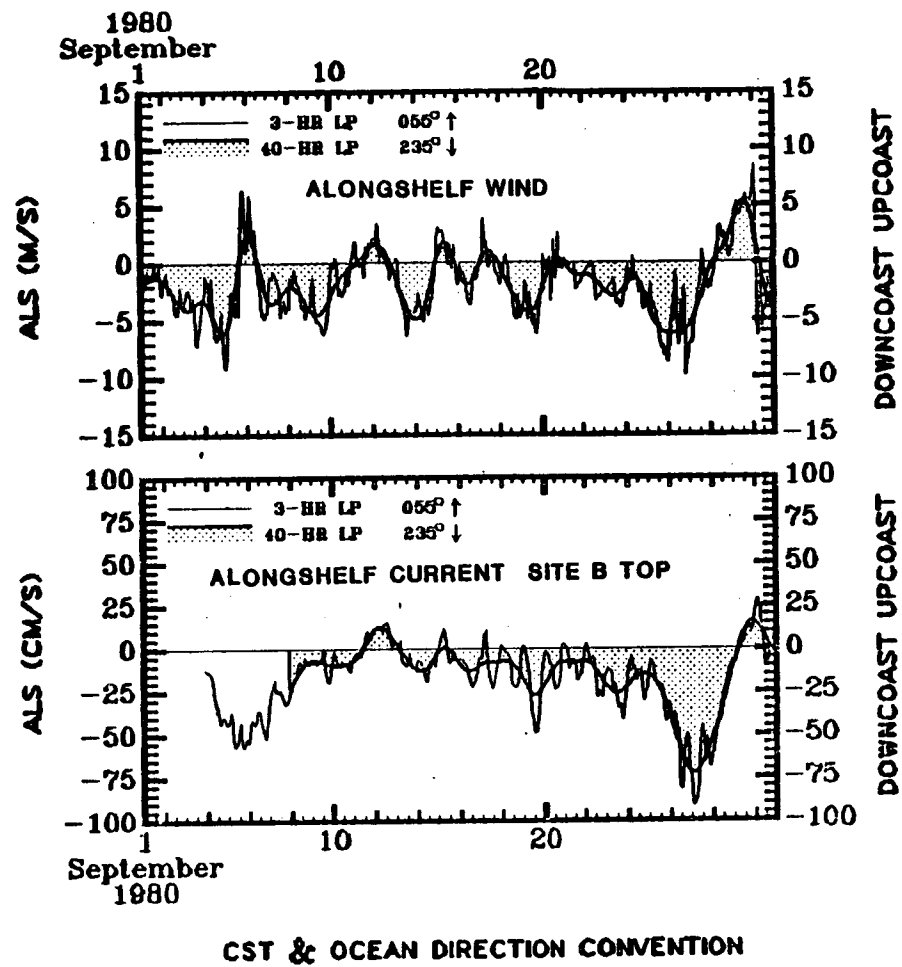


Figure 2-48b. Alongshelf winds together with alongshelf current components for the top meter at Bryan Mound site B during September 1980.

3. By July, currents are strong northeasterly or easterly; this reversal usually prevails for a short period of time, and by mid-August, the flow has returned to westward.

Hunter et al. (1974) in discussing their study of drifters released along the south Texas coast (south of 28°N) concluded that "in accordance with seasonal variations in wind direction, southward drift is best developed during winter, whereas northward drift is best developed during summer. Southward drift is best developed in the northern part of the study region and northward drift is best developed in the south due to variations in the orientation of the shoreline relative to the predominant southeasterly winds." Hill et al. (1975), in a companion study of drifters released along the north central Texas coast (27°30'N to 95°W), note that "a seasonal change of drift patterns from northward drift in summer to south or southwesterly drift in winter was found to be common to both areas (the south and the north-central Texas coast regions). However, southward drift is more extensive in the fall and spring along the north-central Texas coast than off the south Texas (coast)." Thus, it is clear that the Bryan Mound brine disposal study area currents are a part of a rather extensive current regime.

Further support that the Bryan Mound study area currents are part of an extensive system is provided by the Bryan Mound current records. Careful study reveals that the current is often more persistent than the wind. Figure 2-48 shows examples of this situation for the top current meter at site B in April - May and in September 1980. (The site B top current meter has unbroken measurements for those periods.) Clearly, the current at those times remains downcoast on many

occasions when the wind stress component shows alternation in direction. Often the alongshelf current component does exhibit modulation related to wind reversal, but not reversal. Evidently, the current is not simply a response to the local wind.

That the downcoast current system which dominates the study region has a southern limit was first suggested by the convergence indicated by the resultant current charts based on ships' drift data (USN, 1946). Leipper (1954) was the first to comment on the convergence. The latter was recognized before drift bottle studies, and the clear pictures of the coastal low-salinity band from the GUS III cruises had made it evident that a downcoast current existed during much of the year. A convergence near 27°N has been suggested by Bullard (1942) and Watson (1968) on the basis of geological information. This convergence may be due to littoral drift rather than to coastal currents, but is certainly suggestive of the latter.

Further light may be brought to bear on the extent of the current regime that includes the downcoast flow in the Bryan Mound area by considering the annual progression of wind stress at a number of locations along the Texas-Louisiana coast. Since longshore current is driven by the alongshelf stress component, the latter must be determined for a number of locations along the coast. Hunter et al. (1974), Smith (1980) and others recognized the importance of stress and coastal orientation, although they did not look at its effect over the whole Texas-Louisiana coast.

One may represent the annual variation of a vector by means of a "time hodograph" showing the positions of the heads of the monthly mean vectors. Such hodographs have been determined for a number of

locations near the Texas-Louisiana coast and for the 5-degree quadrangle in the Gulf of Mexico from 25° to 30°N and from 90° to 95°W. The locations utilized are airports where ten years of reliable data are readily available (U.S. Dept. of Commerce Weather Bureau pamphlets, undated but probably issued in 1962). Information for the oceanic 5-degree quadrangle are based on ships' observations (U.S. Dept. of Commerce, 1973). These are usually considered to be rather low quality, but in the quadrangle considered observations are numerous and represent many decades.

Figure 2-49 gives the hodographs. Although these vary considerably in scope, they exhibit some general patterns and trends. Many of the hodographs have a "figure-8" form, that for the 5-degree quadrangle being the most clearly marked. The spring-summer mean stresses are in the mean from the southeast while the fall-winter means are near zero or from the southeast, the latter direction seeming to become stronger as one proceeds from Brownsville toward the northwest. The scope of the hodographs for Port Arthur and New Orleans are notably smaller than at other locations, perhaps because wind at these more inland positions are usually weaker than along the coast or over water. The changes in the mean vector from July or August to September and from February or March to April are generally large.

Since there appears to be some regular geographic change among the hodographs with apparently only small changes over distances of 50 to 100 km, it seems to be possible to obtain fairly good approximations for a number of locations along the coast (Figure 2-50). The locations are chosen because of nearby current

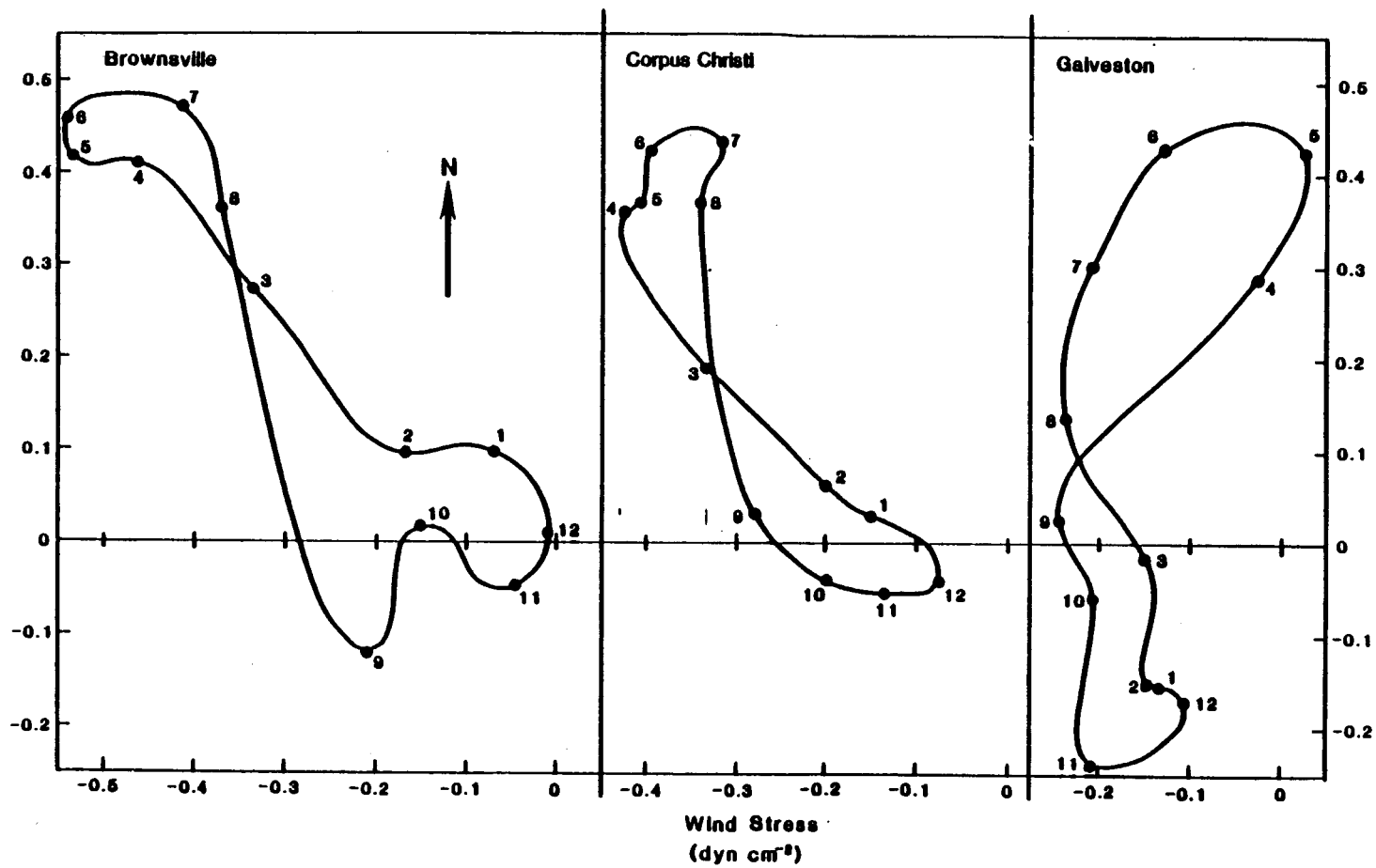


Figure 2-49a. Time-hodographs for monthly mean wind stress for Brownsville (BRV), Corpus Christi (CCH), Galveston (GLV).

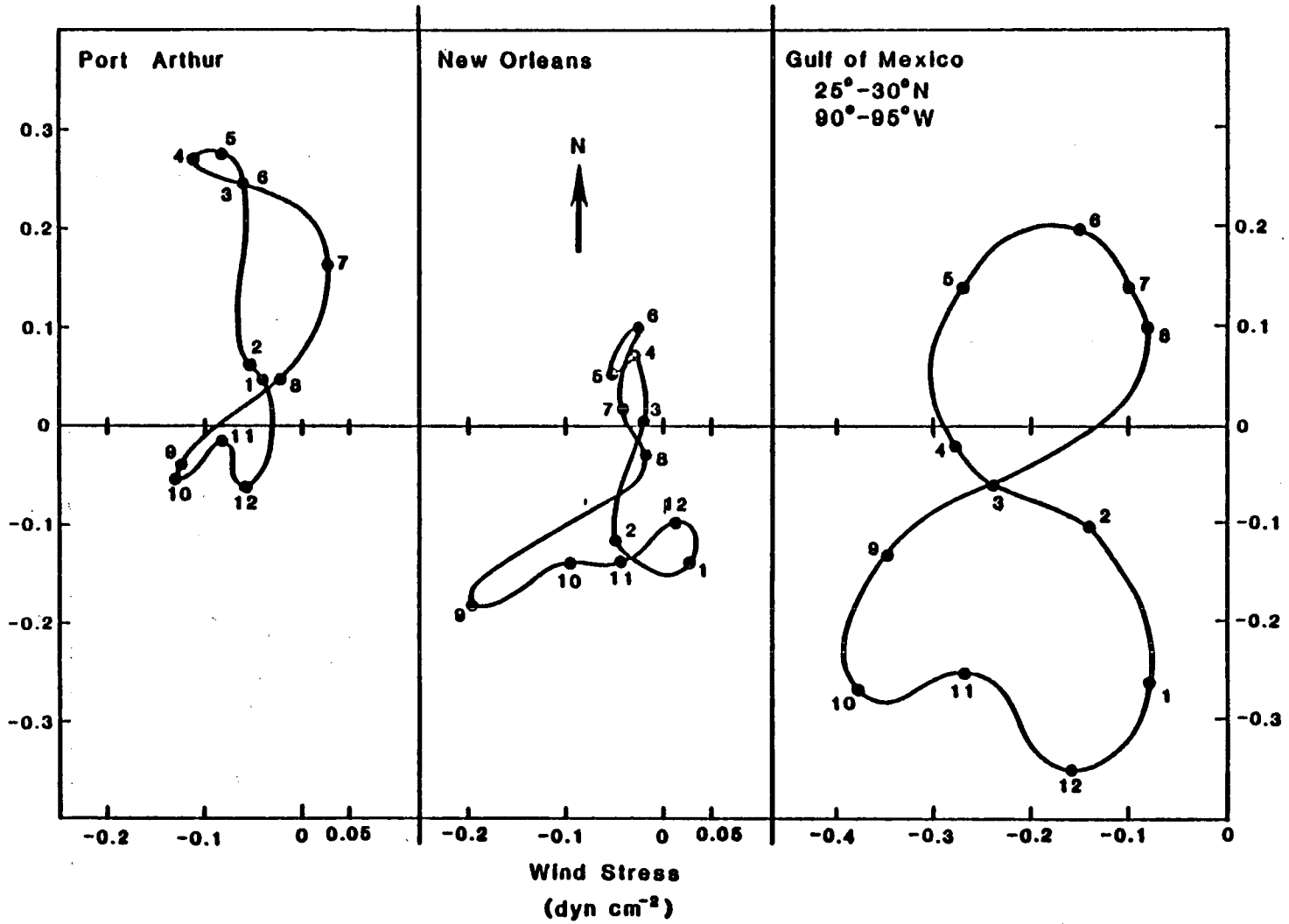


Figure 2-49b. Time-hodographs for monthly mean wind stress for Port Arthur (POR), New Orleans (NOR), and the oceanic 5° square from 25° to 30°N, and from 90° to 95°W.

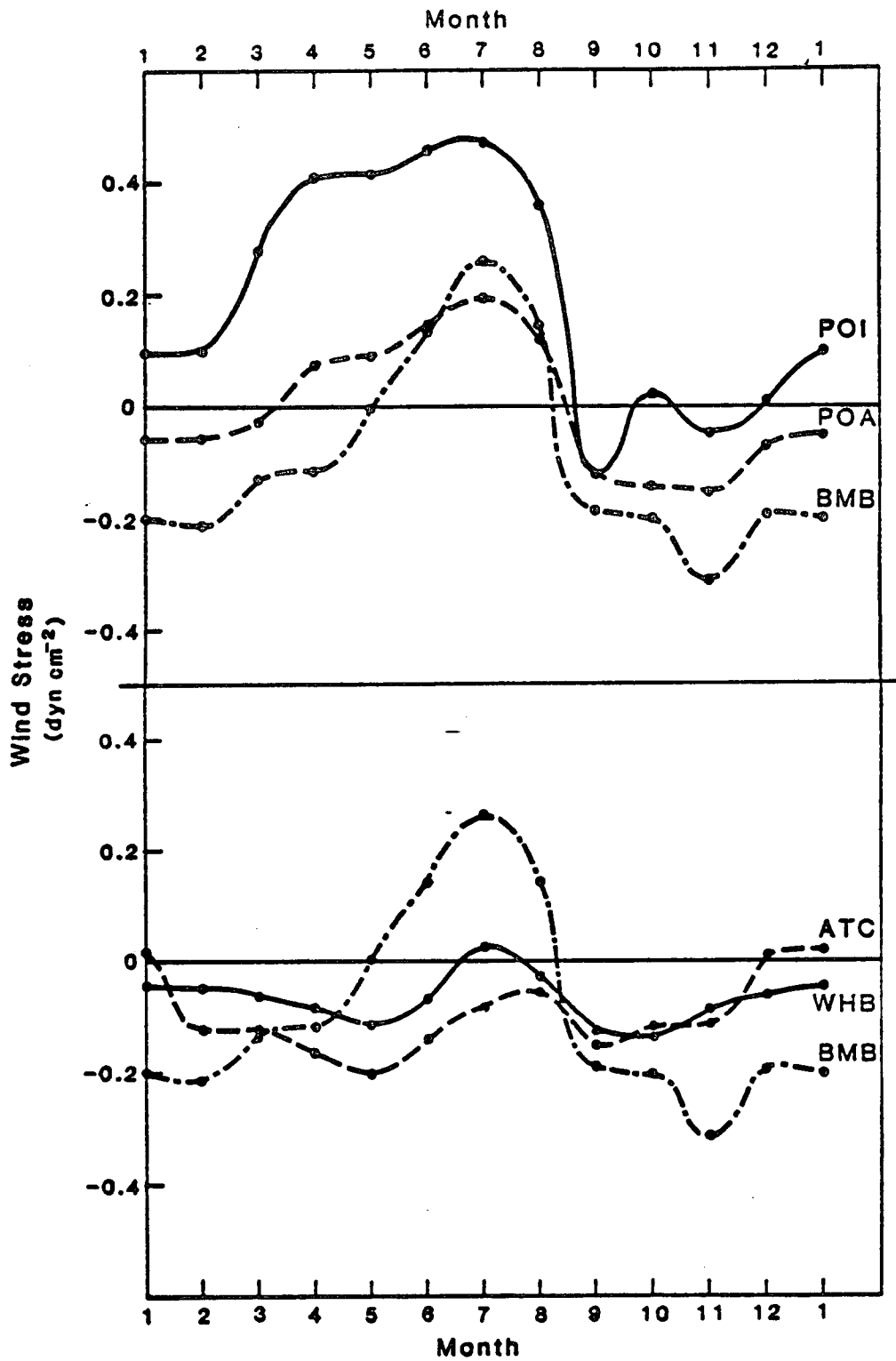


Figure 2-50. Alongshelf components of mean wind stress estimated for Port Isabel (POI), Port Aransas (POA), Bryan Mound Disposal Region (BMB), West Hackberry Brine Disposal Region (WHB) and the region off Atchafalaya Bay (ATC) (Morgan City offing).

measurements or to provide information at fairly regular intervals along the coast.

The alongshelf wind stress components along the coast imply the existence of the convergence to the west or south of the downcoast flow. Watson and Behrens (1970), Hunter et al. (1974) and Smith (1980) have noted this implication. The components imply that the mean convergence position moves from somewhere between Port Aransas and Brownsville in January to a position east of the Calcasieu River in July. The convergence has retreated to the vicinity of its January position by mid-September. That the convergence does not correspond exactly with its position as implied by the wind stress has been noted both by Watson and Behrens (1970) and by Hunter et al. (1974). The latter say that the "southward drift is more extensive than can be explained by the relation of local wind direction to shoreline direction."

The alongshelf stress components imply a divergence in currents between the Calcasieu River and the offing of Morgan City, Louisiana, in December and January. There is an upcoast stress component off Morgan City in those months. However, it should be emphasized that there is no direct evidence of either an upcoast flow or divergence in those months.

The downcoast flow regime which has been described above appears to be the coastal portion of a closed cyclonic circulation over much of the Texas-Louisiana Shelf. There are various lines of evidence which support the presence of such a cyclonic gyre. First, there are many vertical temperature sections across the shelf off Galveston which exhibit a doming of isotherms over the outer portion of the

shelf during April, May, or June. Figure 2-51 shows such sections (copied from Etter and Cochrane, 1975) for April and May. Further, more conclusive evidence of the existence of flow on the inner shelf and upcoast flow over the outer shelf on the slope is provided by the GUS III data (Temple et al., 1977): Average thermosteric anomaly (related to specific volume, the reciprocal of density) fields along the GUS III line running south southeast from San Luis Pass exhibit a mound of lower values over the central or outer shelf in all months except for July and August when upwelling and upcoast flow prevail along the Texas coast (Figure 2-52). The same situation is found along most of the GUS III lines. Further, the same mound of lower specific volume (higher density) over the outer shelf has been encountered by Wiseman and Chuang (personal communication) in meridional sections crossing the shelf off the Sabine River and at about 93°W in January, February, March and April 1982.

Another view better illustrating the extent of the cyclonic feature is provided by the map (Figure 2-53) of temperature at 43 m as observed from GUS III in May 1964. The long narrow region of low temperature just inside the 183 m (100 fm) line represents a cold ridge forming the center of a cyclonic circulation (Figure 1-65). Csanady (1979) and others have presented evidence that away from a frictional coastal boundary region (and outside of top and bottom Ekman layers) currents over shelf regions tend to be in geostrophic balance. Thus qualitative estimates, at least, of the current system are provided by the density distribution which is dominated by temperature except in shallow near-shore waters.

A second line of evidence for a cyclonic circulation, given the

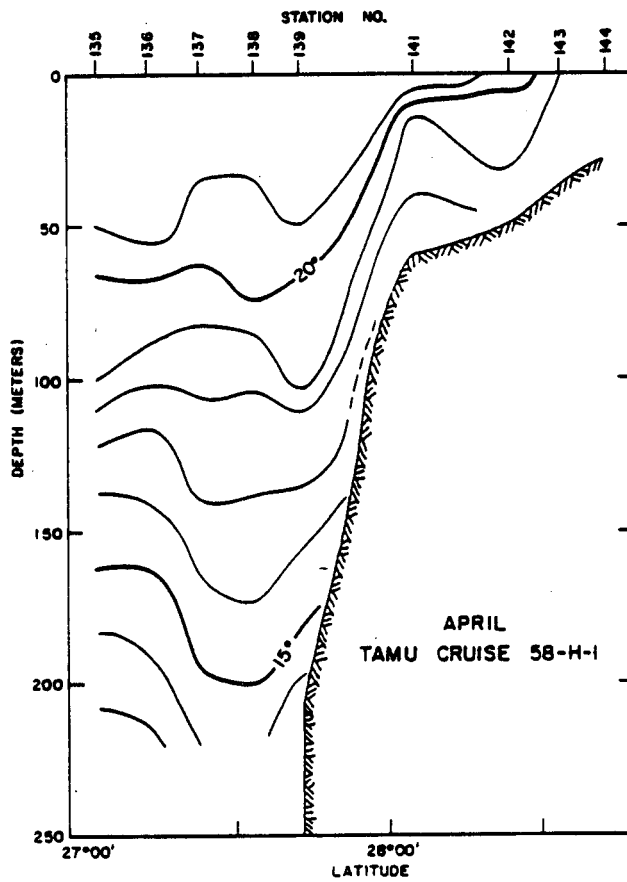


Figure 2-51a. Vertical sections of temperature across the shelf off Galveston for April (from Etter and Cochrane, 1975).

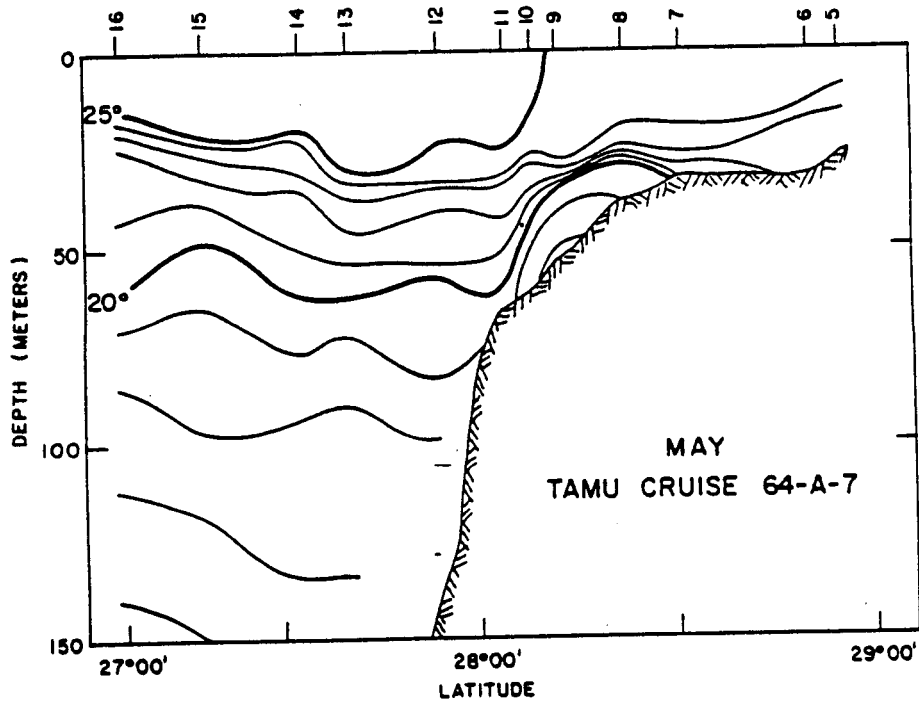
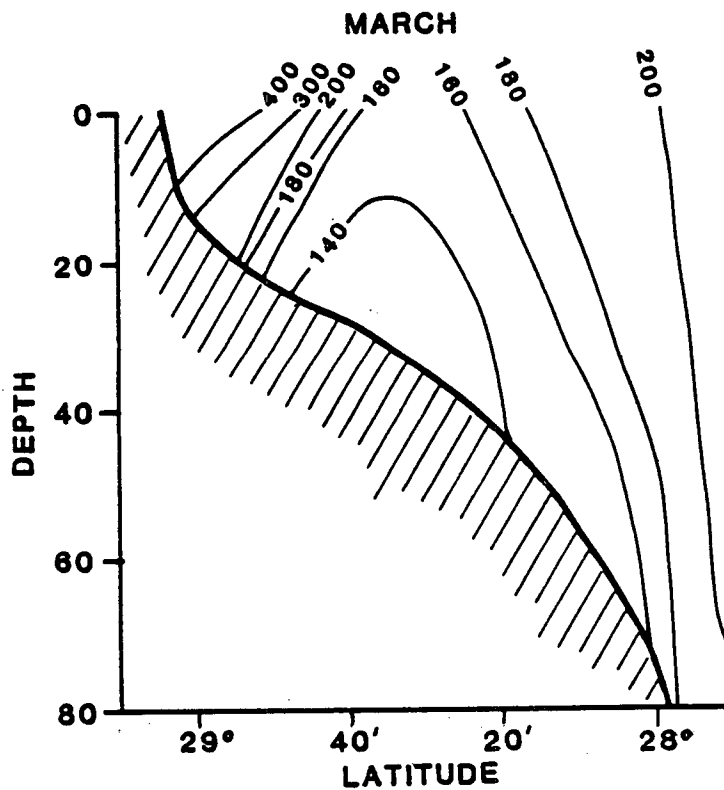
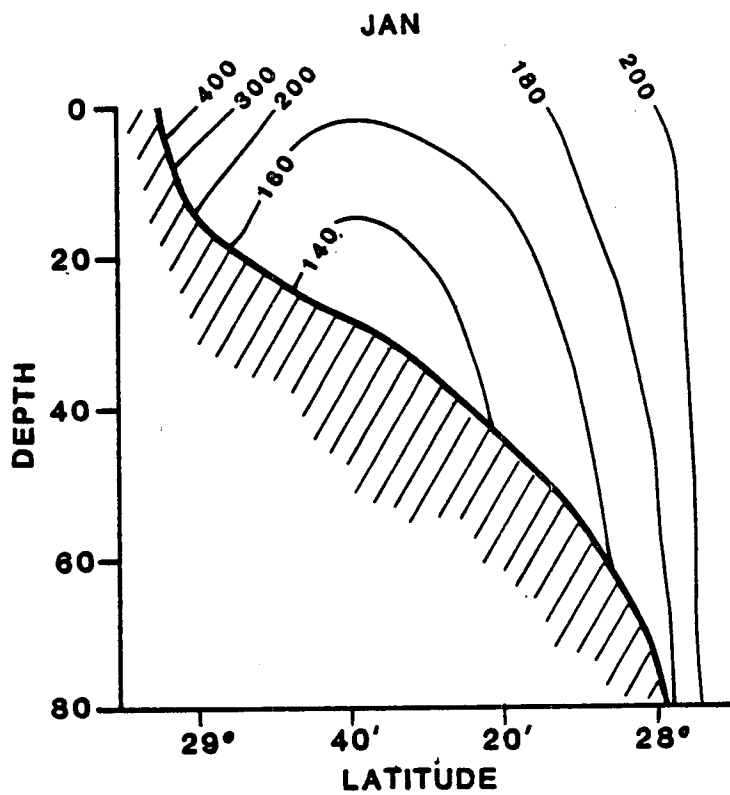
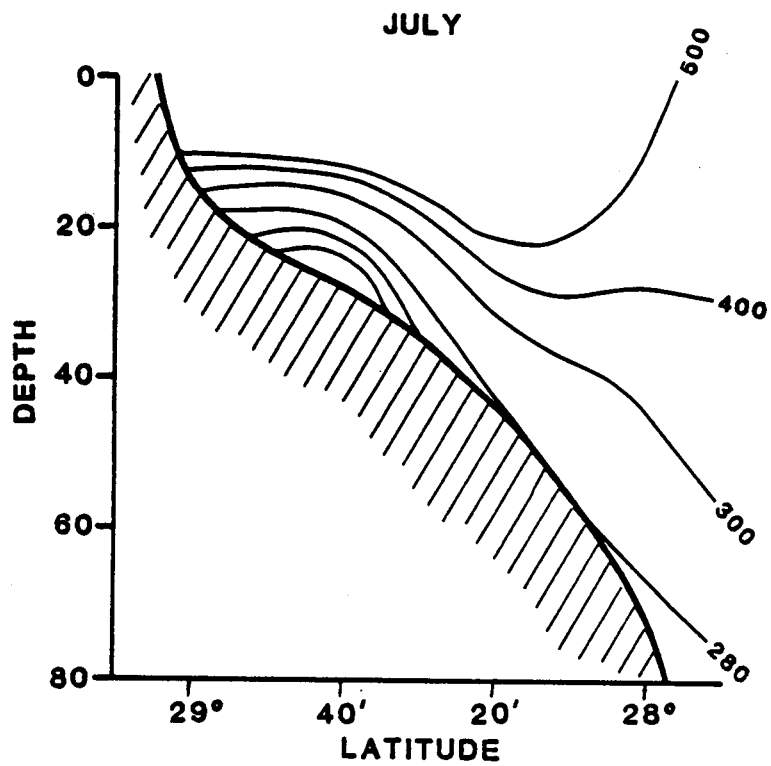
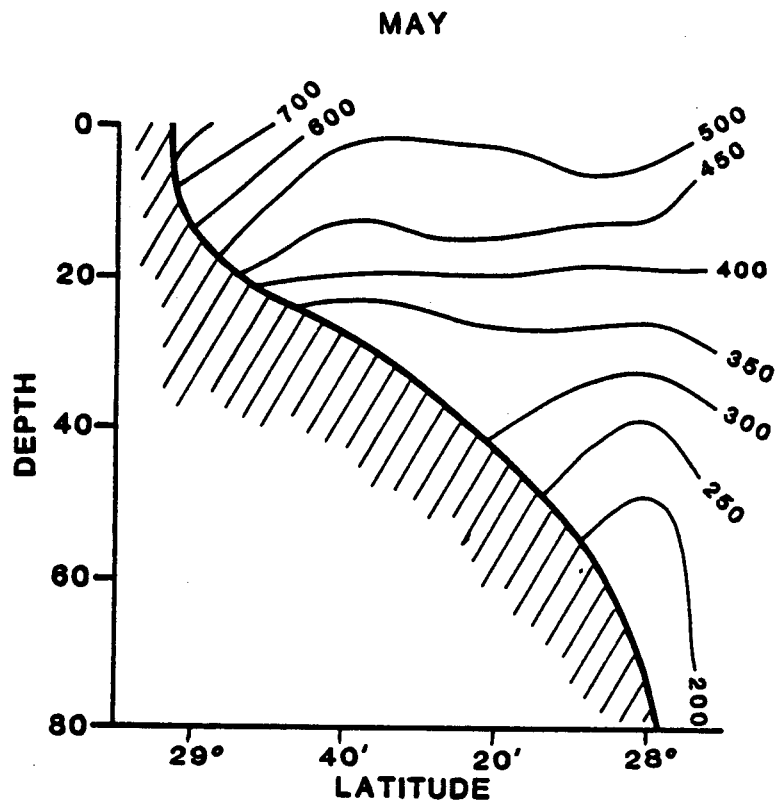


Figure 2-51b. Vertical sections of temperature across the shelf off Galveston for May (from Etter and Cochrane, 1975).



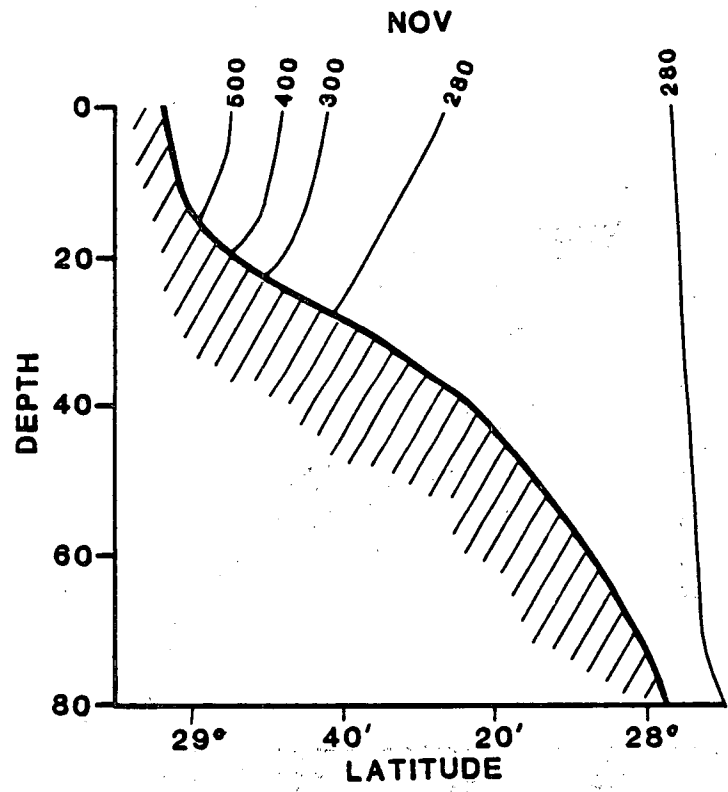
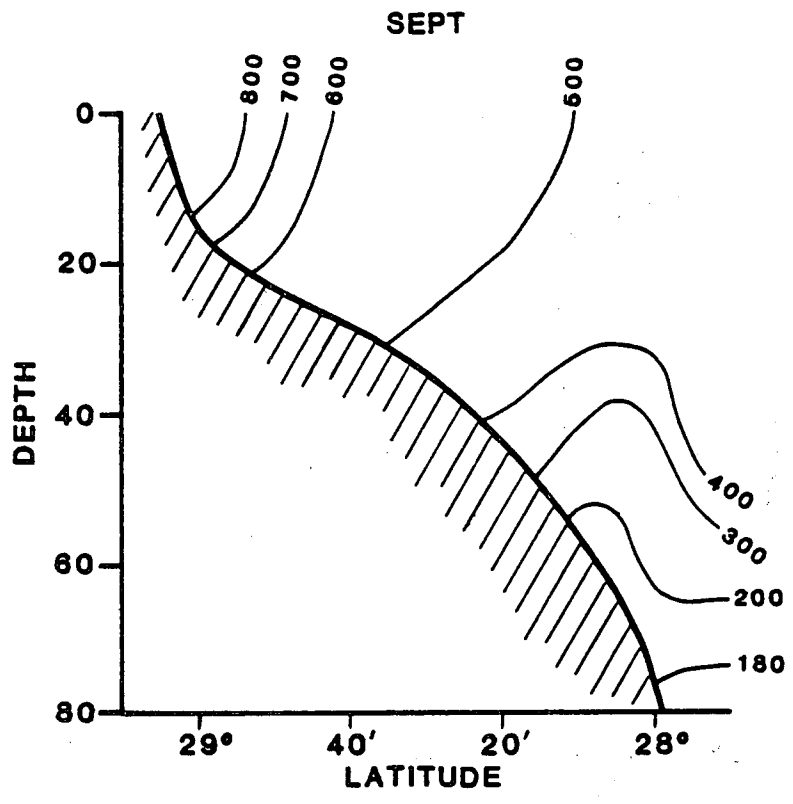
a.

Figure 2-52. Monthly mean δ_T (a specific volume parameter) for the GUS II transect off San Luis Pass for a) January and March, b) May and July, c) September and November.



b.

Figure 2-52. Continued.



c.

Figure 2-52. Continued.

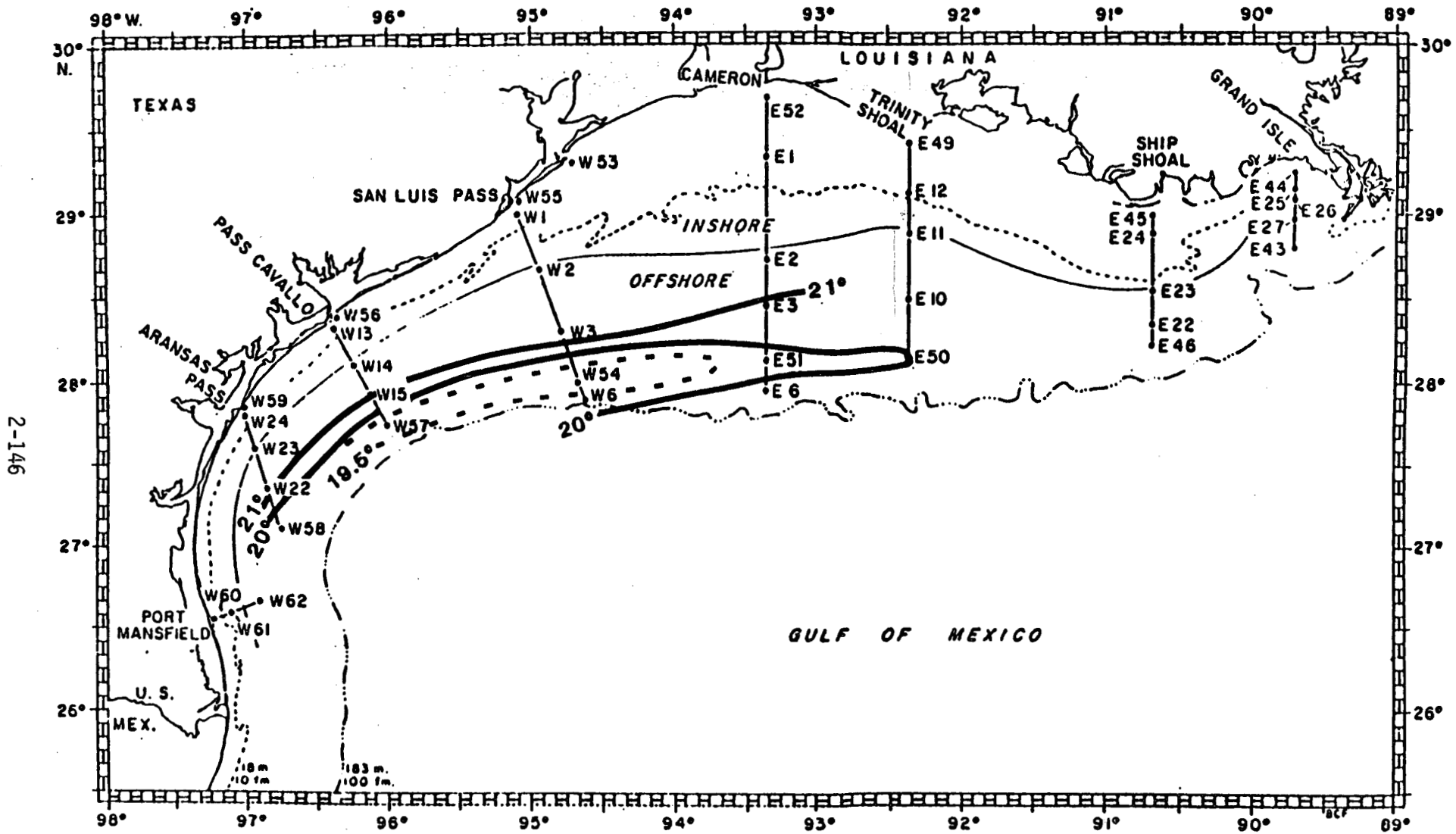


Figure 2-53. Temperature at 43 m for the May 1963 cruise of GUS III.

prevalence during much of the year of downcoast flow near the coast, is the fact that eastward currents have been found to predominate at the edge of the shelf near such reef structures as the Flower Gardens (McGrail and Carnes, personal communication).

Surface salinities provide some further evidence of a cyclonic circulation. Smith (1979) showed from the rather closely spaced stations off the south Texas coast that the low salinity tongue which extends along the coast toward the southwest appears to turn eastward (away from the coast) near 27°N (Figure 2-54). That low-salinity surface water moves offshore near 27°N is also indicated by the surface salinities from the GUS III cruise of May 1964 which Figure 2-44 shows.

On the basis of the wind stress components, observed currents, surface salinity distributions, and density distribution over the outer shelf, we tentatively propose the monthly average surface currents on the Texas-Louisiana Shelf shown in Figure 2-55. The convergence and divergence positions discussed above are shown by means of the alongshelf wind vectors in the figure. The divergence and eastward flow off Morgan City in January are suspect as already noted. Very probably, a downcoast flow driven by the Mississippi discharge overrides, close to the shore, the wind-induced flow which is shown in the figure.

The east side of the cyclonic circulation is the most speculative part of the picture in all months. Perhaps the flow is directed inshore in some months by water moving along the west side of the Mississippi Trough. The pattern shown for July is based on the salinity for that month shown in Figure 2-44 and the information from

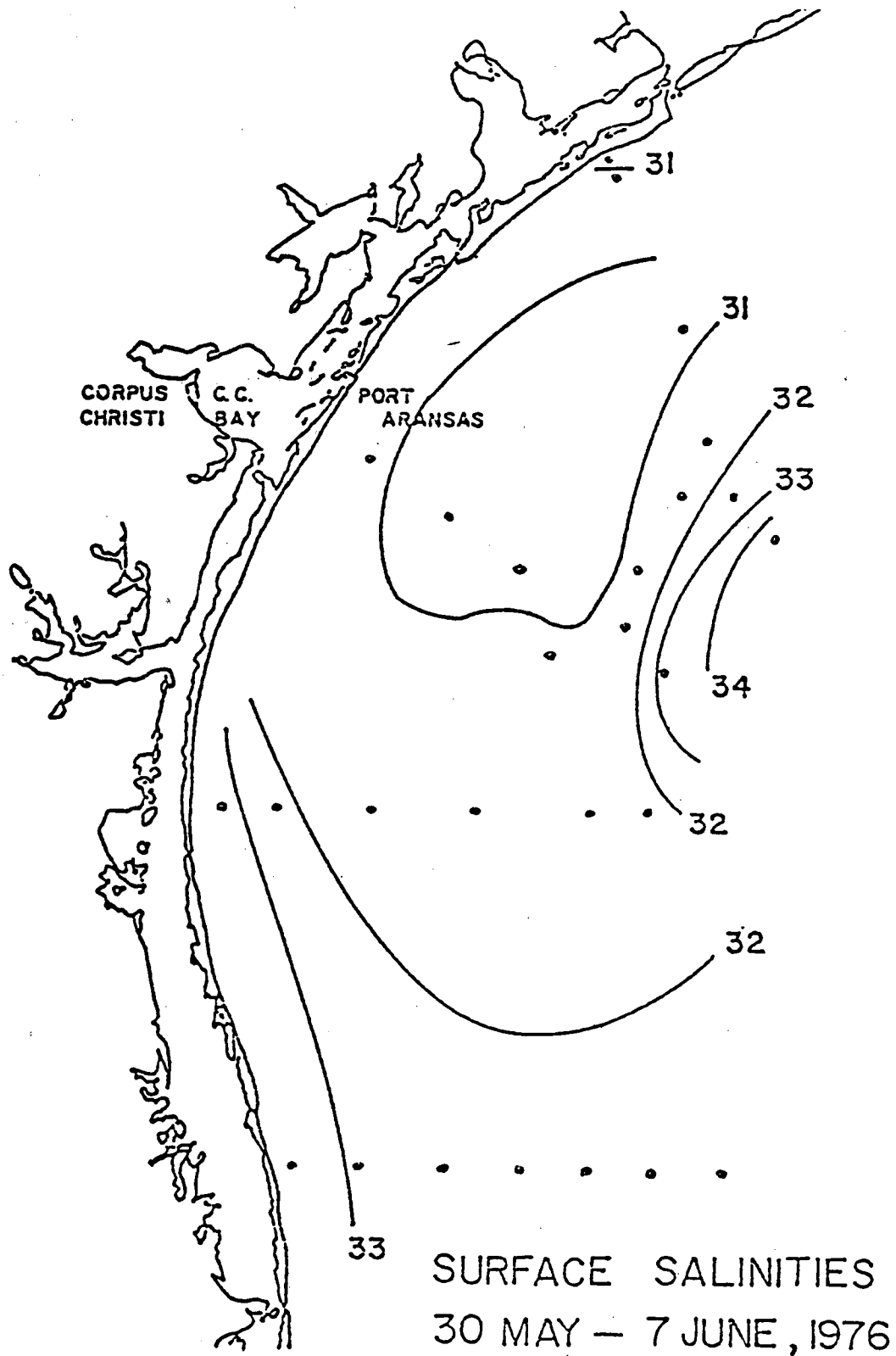


Figure 2-54. Sea surface salinity in the northwestern Gulf shelf region for May 30 - June 7, 1976 (from Smith, 1979).

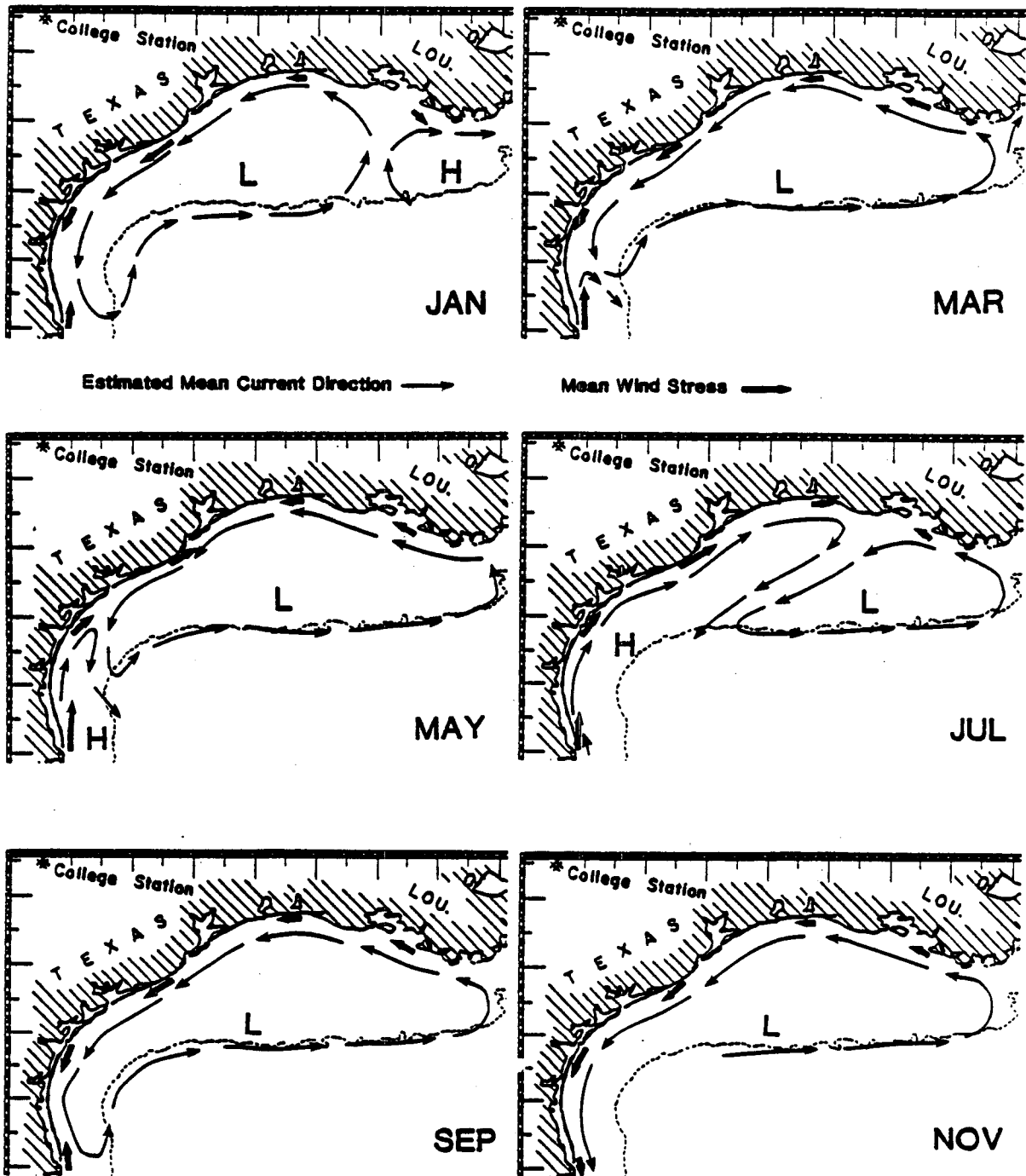


Figure 2-55. Schematic representation of the mean alongshelf current direction on the Texas-Louisiana Shelf for alternate months of the year. The sense of the mean alongshelf wind stress component is also shown.

McGrail and Carnes (personal communication) that eastward flow prevails at the Flower Garden Reefs (shelf edge off Galveston) throughout the year.

Although a mean cyclonic circulation over the shelf is envisioned for much of the year, it should be noted that the salinity of the waters which are present along the coast and then in the offshore part of the cyclone are increased in value by diffusion. The waters turning in toward the coast at the end of its circuit is joined by new, low-salinity water from the Mississippi and Atchafalaya Rivers.

2.5.3 Circulation in the West Hackberry Brine Disposal Region

We may begin our discussion of the circulation in the West Hackberry region by presenting the coherence-squared between the alongshore component of wind stress and the alongshelf component of the current for the top current meter (Figure 2-56a) at site D. Using Wu's (1980) values of drag coefficients, we computed the wind stress as explained in the previous section. The time interval considered runs from June 24, 1981 through April 25, 1982 (306 days). The coherence-squared is definitely significant within the range 0.25 to 0.4 cycle day⁻¹ (periods from 4 to 2 days respectively). This may be compared to the coherence-squared between alongshelf stress and alongshelf current for the top meter at Bryan Mound site (Figure 2-45a) which is significant over a wider range of frequencies (or periods), in particular, significant coherence is formed at the Bryan Mound site for frequencies below 0.25 cycle day⁻¹ (period longer than four days). We do not understand the lack of coherence between alongshelf stress and currents at West Hackberry site D. It may be that at such low frequencies, the alongshelf current is driven

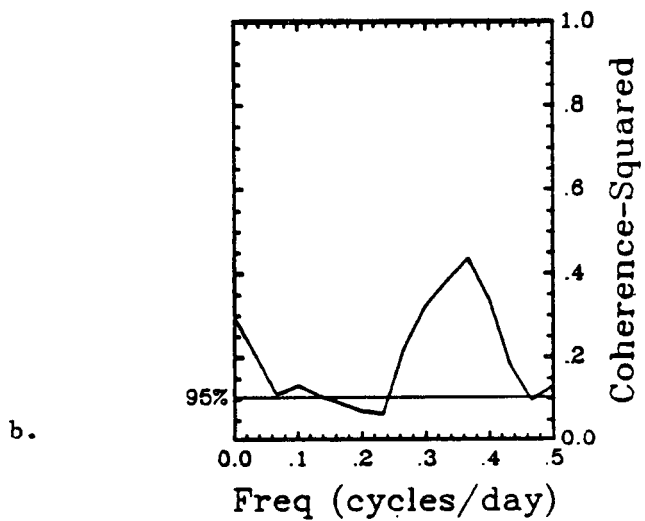
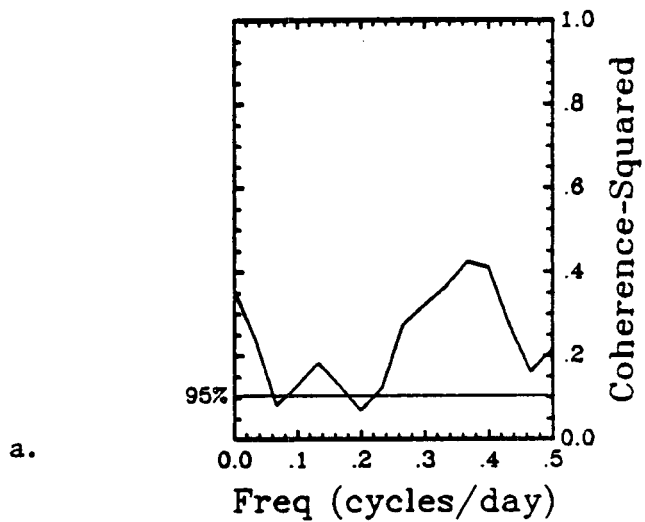


Figure 2-56. Coherence-squared between alongshelf wind stress and current at West Hackberry site D for the period from June 24, 1981 through April 25, 1982 for a) alongshelf component at top meter and b) alongshelf component at bottom meter.

primarily by the relatively fresh water of the Mississippi. Driving by such a density contrast might be expected to be larger in the West Hackberry region than in the Bryan Mound region.

The phase corresponding to the coherence-squared just discussed is, within the range of frequency where significant coherence is found, a slightly negative, but mainly close to zero. This means that the current lags the wind by less than an inertial period. Both the significant coherence and the small negative phase in the range of periods from 2 to 4 days are in agreement with analyses made at most inner shelf locations (Winnant, 1979, 1980).

Another probable influence on currents in the West Hackberry region is the larger-scale circulation in the inner shelf region. As noted above, the large-scale circulation seems to influence the currents in the Bryan Mound region. A suggestion of such influence in the West Hackberry region appears when the 15 1/4-day means of alongshelf current at the top current meter there are plotted together with those for Bryan Mound (Figure 2-57). There is a considerable resemblance between the records. The West Hackberry currents (Figure 2-56) at low frequencies are according to the coherence analysis less responsive to wind stress than those in the Bryan Mound region, yet the 15 1/4 day means at West Hackberry resemble the corresponding Bryan Mound means. It seems probable that the lower-frequency currents represented in the 15 1/4-day averages participate in a larger-scale circulation.

In particular, it should be pointed out that the 15 1/4-day means for the top meter at Site D in the study region exhibit upcoast flow in June and July just as do those Bryan Mound region which is quite a

long way downcoast where the coastal orientation and prevailing winds lead, for the average conditions shown in Figures 2-50 and 2-51, to a much larger mean upcoast wind stress component. The wind records actually taken in July at Site D (West Hackberry) show only short, weak periods of upcoast wind component. The upcoast current component (Figure 2-57) in July was evidently not driven by local wind, but represents a participation in a widespread occurrence of upcoast flow. The upcoast flow is of particular interest because it is normally associated with upwelling along the coast farther west.

The mean alongshelf speeds at Site C (Bryan Mound) are appreciably larger than those at Site D (West Hackberry). The speeds at all of the Bryan Mound current-measurement sites are comparable; on the other hand, the speeds at Site D in the West Hackberry region are stronger than those at Site S also there. It appears, therefore, that the currents of the Bryan Mound region are indeed faster than those of the West Hackberry region. For the sample in Figure 2-57, the ratio of downcoast speed at Bryan Mound to downcoast speed at West Hackberry values is 2.0.

2.5.4 Hydrography of the Texas-Louisiana Inner Shelf Region

It is clear from the sea-surface salinity distributions for four months of 1964 shown in Figure 2-44 that the discharge from the Mississippi and Atchafalaya Rivers plays an important role. It is also noteworthy that the picture of coastal currents suggested by the sea-surface salinity is consistent with the description of coastal circulation of subtidal frequency developed above. From September until May, June, or July, downcoast, or westward, flow prevails along the coast from the Mississippi Delta nearly to Brownsville. During

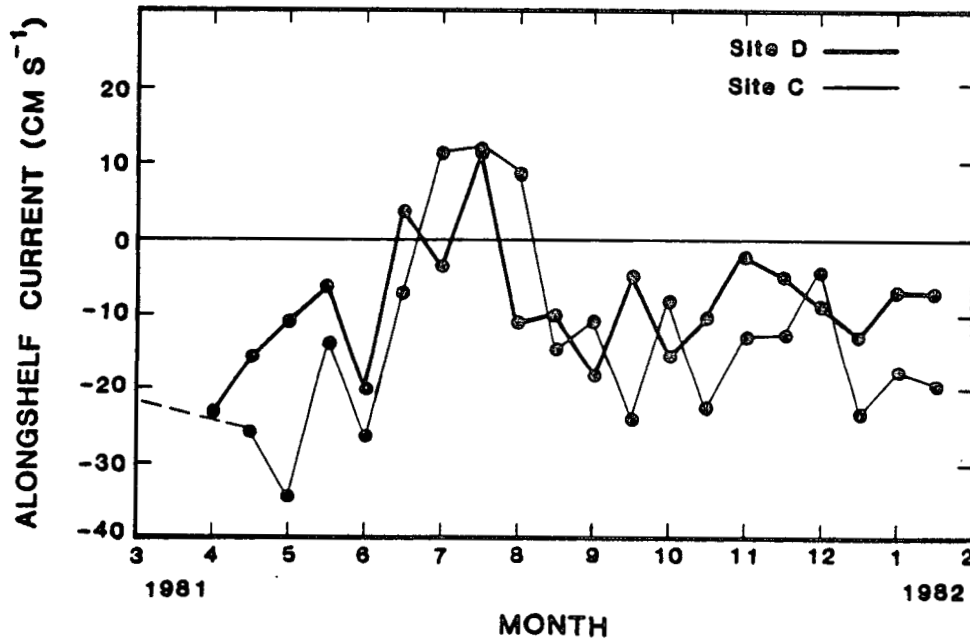


Figure 2-57. Comparison of 15 1/4-day means for alongshelf components of current at the top current meter for Bryan Mound site C and West Hackberry site D.

the spring, in response to change in the prevailing wind direction, upwelling and upcoast flow develops off Brownsville and propagates upcoast to reach the West Hackberry disposal region in weakened form by July. The brackish coastal wedge is replaced along the Texas coast by water nearly as saline as that of the deep Gulf.

The mean monthly discharge from the Mississippi-Atchafalaya system for the years 1976-1980 is shown in Figure 2-58. The maximum mean discharge in April is well over twice the minimum in August-November. The discharge from the Mississippi-Atchafalaya system is larger by a factor of at least ten than that of the rivers west of the Atchafalaya to the Rio Grande combined.

The temperature and salinity measurements taken in the Bryan Mound studies, together with the GUS III data (Temple et al., 1977), constitute a fairly extensive information base for studying the hydrography of the inner shelf.

Figure 2-59 shows the monthly mean near surface salinity based on the data from Bryan Mound Station 14, together with the GUS III Station W-1 which was located just off San Luis Pass. The combined data set (here after called the inshore location) represents five to eight years. The mean salinity has strong minima in May - June and in September. Separating these minima is a strong maximum in July. That the pattern truly indicates a recurring annual progression is supported by the monthly mean surface salinity for the long series of observations taken at Galveston Pier (U.S. Dept. of Commerce, 1973) which exhibits a quite similar pattern. Except in August, the Galveston Pier values are lower, probably because Station 14 is about 10 km offshore. The minimum in June at the inshore location seems to

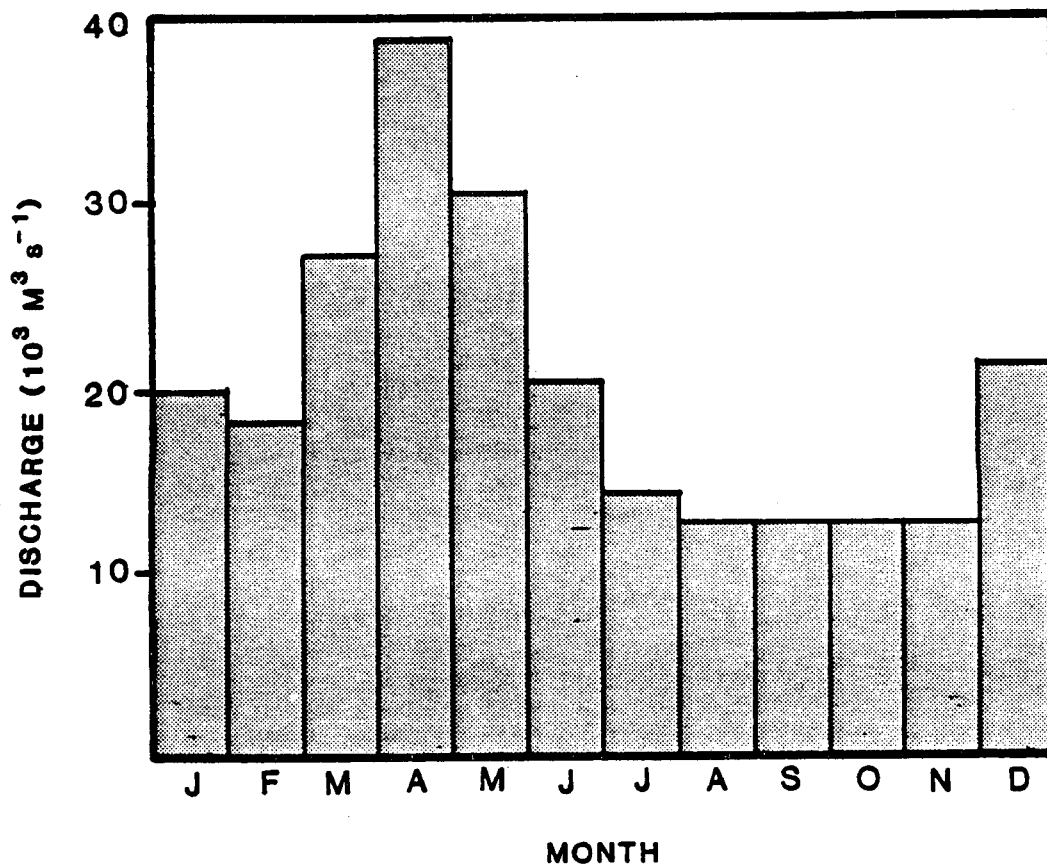


Figure 2-58. Monthly mean discharge ($10^3 \text{ m}^3 \text{ s}^{-1}$) from the Mississippi and Atchafalaya Rivers together based on water years 1976-1980 (incl).

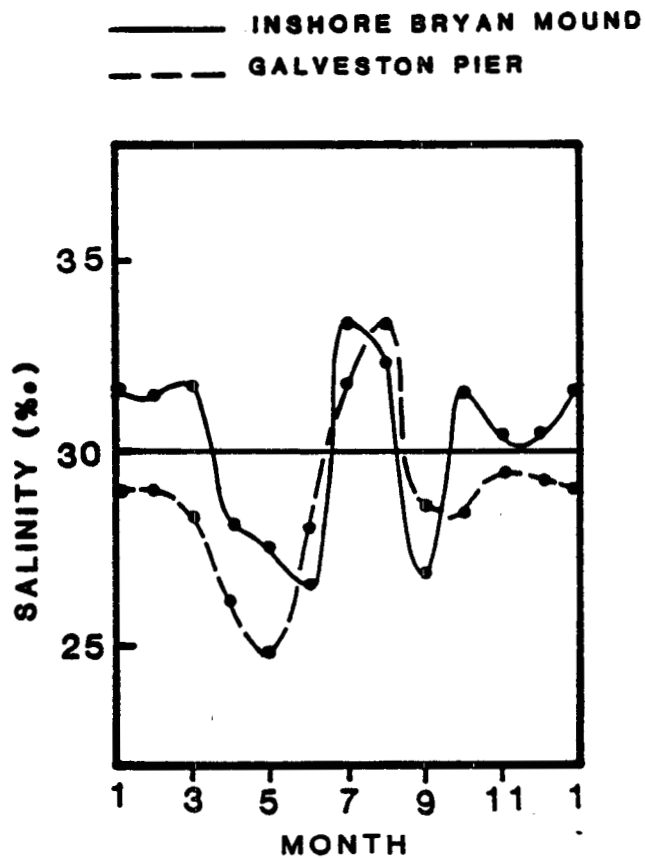


Figure 2-59. Monthly mean near-surface salinity (o/oo) at the inshore location (Bryan Mound sta. 14 and GUS III sta. W-1 data) together with monthly mean sea-surface salinity for Galveston Pier (very long term mean).

be due to exceptional local runoff in that month.

The relationship between mean inshore salinity and the mean current at Bryan Mound site A (or B, if A is missing or incomplete) is given in Figure 2-60. The currents are consonant with the picture that the minimum salinity of May - June represents the arrival of the accumulation of fresh water due to the discharge maximum of the Atchafalaya and Mississippi Rivers in April. As already noted, local runoff may contribute to the June minimum. The upwelling and upcoast flow in July is in agreement with the high salinity for that month. The renewed downcoast flow in September agrees with the lower salinity in that month. The salinity seems to result largely from the return of fresh water from a pool off Louisiana east of 92° W which is present in July and August. The high salinity in the period from October to April seems to be due to the depletion of the eastern brackish pool and the lower discharge from the Mississippi and Atchafalaya Rivers during that portion of the downcoast current phase.

Some idea of the way in which diffusion and the varying wind forcing along the coast influence the coastal salinity distribution is provided by the monthly mean salinities for tide stations along the coast. Trying to use stations as near as possible to the open Gulf, we have chosen to look at the 10-year means for Galveston Pier, Port Aransas, and Port Isabel (U.S. Dept. of Commerce, 1973). That the salinity at Galveston Pier and Port Aransas are dominated by the coastal rather than local estuarine processes or direct runoff, is suggested by the essential agreement of the Galveston Pier values with those for Bryan Mound station 14 given in Figure 2-16 and a similar agreement of Port Aransas values with the means of determinations

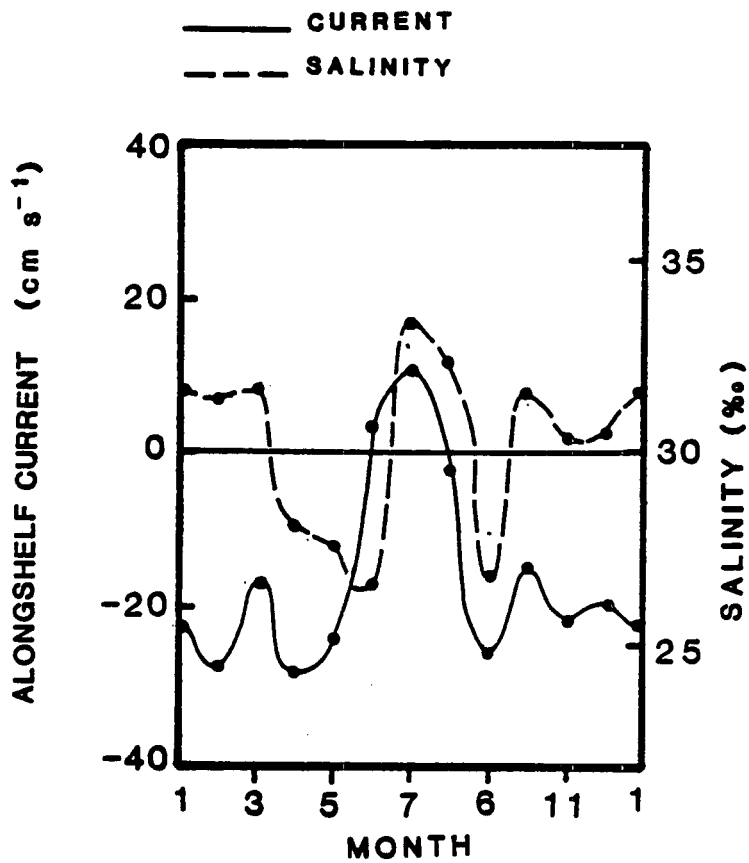


Figure 2-60. Monthly mean near-surface salinity (o/oo) at the inshore location (Bryan Mound sta. 14 and GUS III sta. W-1 data) together with monthly mean alongshelf component of current (cm s⁻¹) for top current meter at site A.

reported by Smith (1980) for the Port Aransas offing.

The mean monthly salinities for the tide stations (Figure 2-61) show similar progressions through the year with a distinct maximum in July or August and minimums in October and except for Port Isabel in May. Evidently, the maximum is due to upwelling and upcoast advection. It appears earliest at Port Isabel as the alongshelf wind stress component (Figure 2-50) implies. However, the increase is not so early as the advent of mean upcoast wind components, probably because downcoast movement of quite low salinity water during May intermittantly, or even predominantly in some years, reaches as far as Port Isabel. The minimum in May is due to the maximum of Mississippi-Atchafalaya runoff in April and the downcoast flow still prevailing along much of the coast in May. The absence of a distinct minimum at Port Isabel in May must result from the upwelling and upcoast flow which upcoast wind components prevailing then produce. The October minimum is caused by the downcoast currents that are reestablished in September.

To provide a more complete picture of the annual progressions in the hydrography of the coastal regions, we present in Figures 2-62 through 2-64 various representations of monthly mean temperatures, salinities and densities for the Bryan Mound study region. Although these figures may "speak for themselves," some brief discussion may be helpful. Comparisons with the West Hackberry region will be made later.

Figure 2-62a shows the annual progression of salinity and temperature for the inshore location together with a representation of both progressions in a T-S diagram. The T-S curve is a sort of

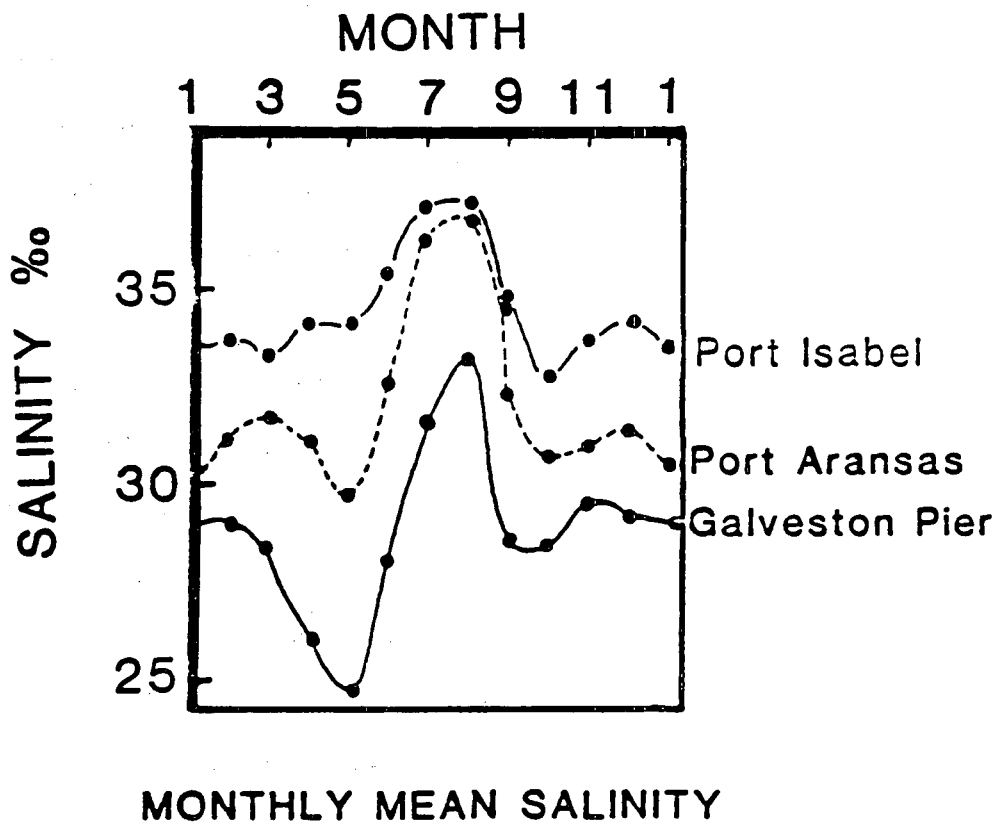


Figure 2-61. Monthly mean sea-surface salinities for tide stations at Port Isabel, Port Aransas, and Galveston Pier (U.S. Dept. of Commerce, 1962).

Lissajou figure resulting from the individual cycles. Figure 2-62b shows the same parameter, but for an "offshore location," Bryan Mound Station 36, together with GUS III Station W-2.

The near surface salinity at the offshore location is, as might be expected, higher than that at the inshore location, except in July when upwelling is strong. The near bottom salinity at the inshore location (Figure 2-62a), shows the same minima and maxima as are found at the surface, but the salinity is always higher. The salinity near the surface at the offshore location (Figure 2-62b) also shows the same pattern of maxima and minimum, but with higher values than near the surface inshore. However, the pattern disappears in the near bottom, offshore observations.

The progression of mean temperatures at all of the locations and depths are similar. The curves for both locations cross over in February and September, approximately, indicating that bottom temperatures are higher than those at the sea surface from late September until March. Maxima at the two locations are nearly the same, but, as might be expected, lower temperatures occur in winter at the shallower, inshore location. One of the most interesting features of the temperature progressions is the leveling in June at the offshore location. The near bottom temperature is even lower in July than in June. This feature is evidently due to upwelling which is clearly more intense at the offshore station. (The fact that lower temperature and salinity occur together provides strong evidence for upwelling.)

Figure 2-63 gives the annual progression of salinity, temperature, and sigma-t at the offshore location in the form of a

2-163

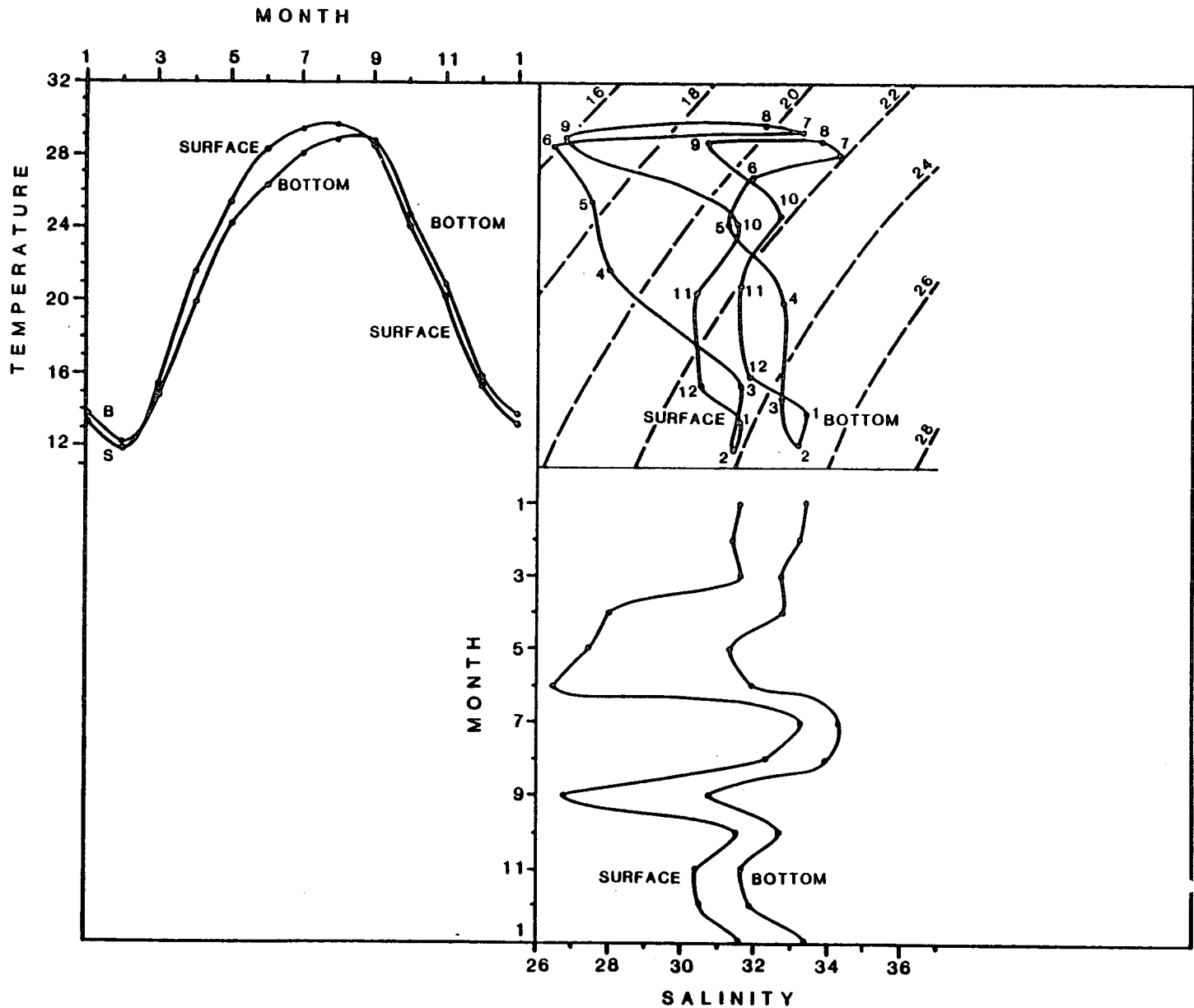


Figure 2-62a. Annual progressions of mean salinity (o/oo) and mean temperature (°C) for near-surface and near-bottom locations for the inshore location (Bryan Mound sta. 14 and GUS III sta. W-1 data). Corresponding monthly temperature and salinity values are shown in a T-S diagram in which σ_t lines are entered.

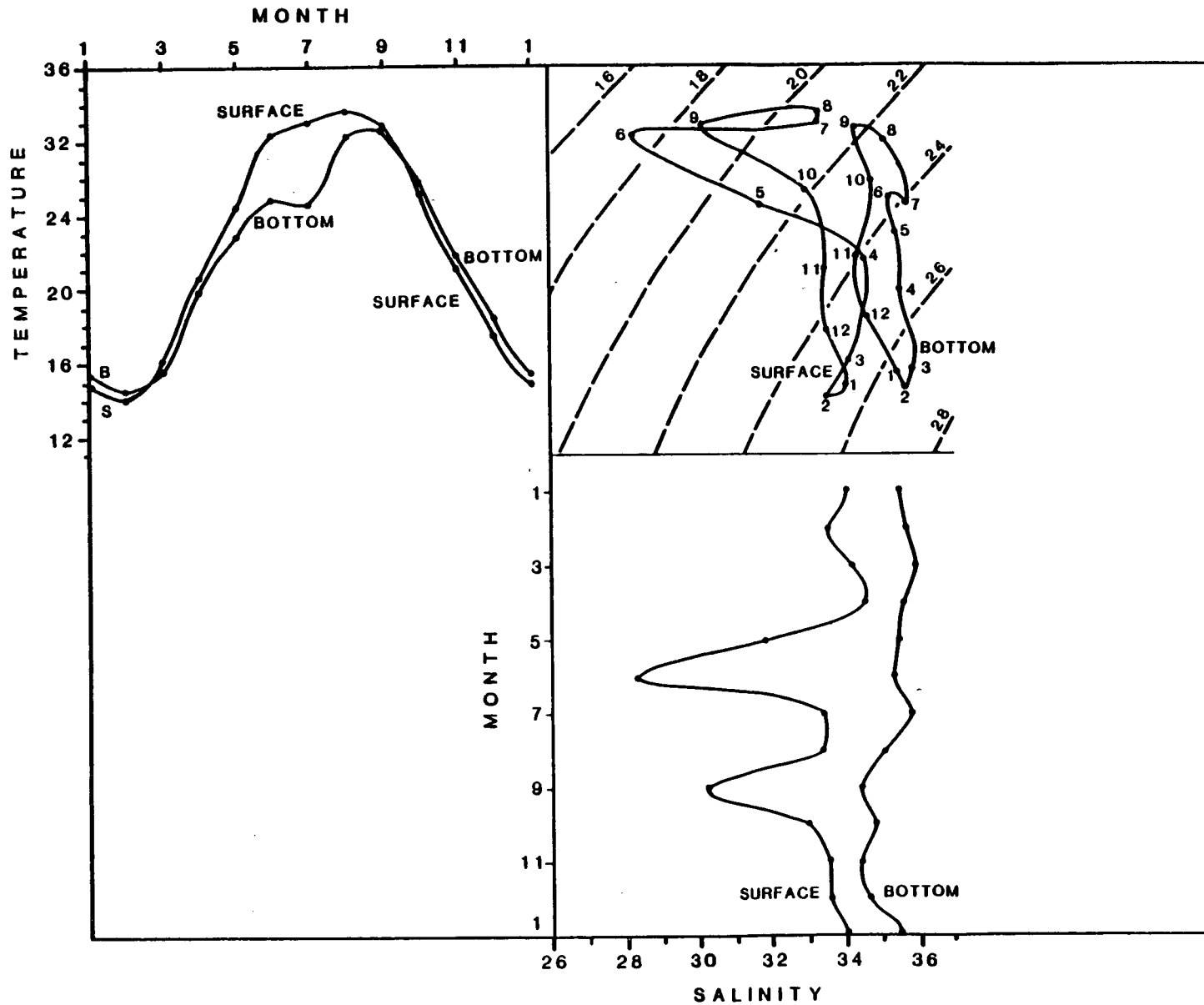
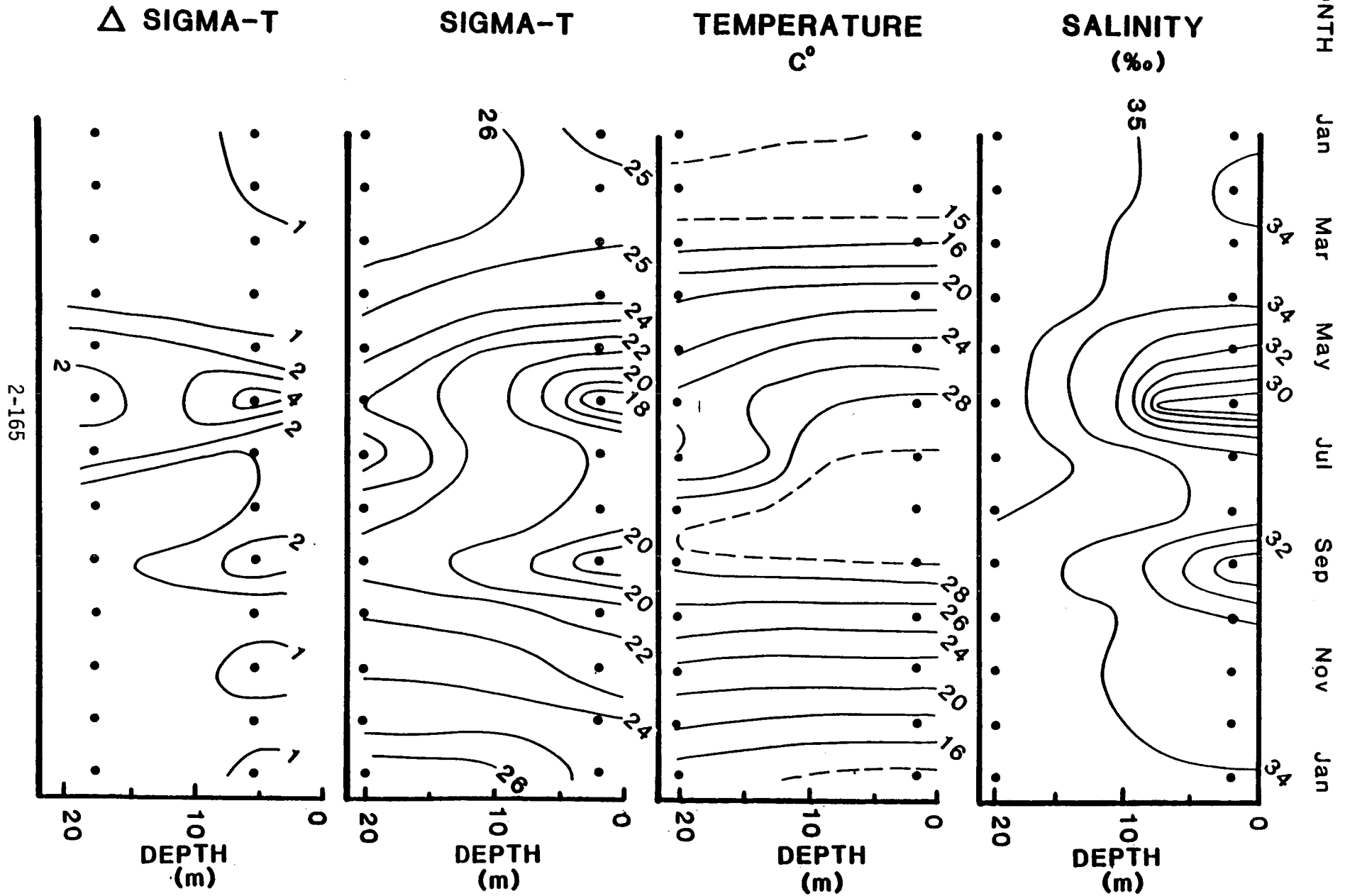


Figure 2-62b. Annual progressions of mean salinity (o/oo) and mean temperature ($^{\circ}$ C) for near-surface and near-bottom locations for the offshore location (Bryan Mound sta. 36 and GUS III sta. W-2 data). Corresponding monthly temperature and salinity values are shown in a T-S diagram in which σ_t lines are entered.



2-165

Figure 2-63. Time-depth section for mean salinity (o/oo) and mean temperature ($^{\circ}$ C), σ_t , and vertical difference in σ_t ($\Delta\sigma_t$) for the offshore location.

time-depth section. Since only three depths are sampled, the detail in the vertical is rather poorly resolved. The minima of salinity in June and September are clearly marked. It is noteworthy that the means at least show that some degree of salinity stratification is present throughout the year. It is greatest in June when the minimum is present at the sea surface. Although surface salinity is nearly as low in September, the bottom salinity is lower than in June. The lower bottom salinities persist until January. For this reason, the weakest salinity stratification is found on the average in November and December.

The time-depth section for temperature makes it clear that nearly isothermal conditions are commonly present except in June and July. A slight negative gradient of temperature is, as noted above, present from October until March. The effect of upwelling is seen in the levelling of isotherms in June; and, as already noted, the bottom temperature falls in July.

The sigma-t section is seen to be strongly influenced by salinity (as well as by temperature). Although the sigma-t section gives information regarding vertical stability, a more explicit representation is provided in a section based on the vertical differences in sigma-t. (Keep in mind that vertical resolution is not very good.) The difference section shows that, on the average, stability is very small in December, but also small in April, and, indeed, not very large in the upwelling month of August. The highest stability occurs in June when the lowest surface salinity is present. The upper layers are also quite stable in September.

Figure 2-64a shows mean temperature and salinity sections for

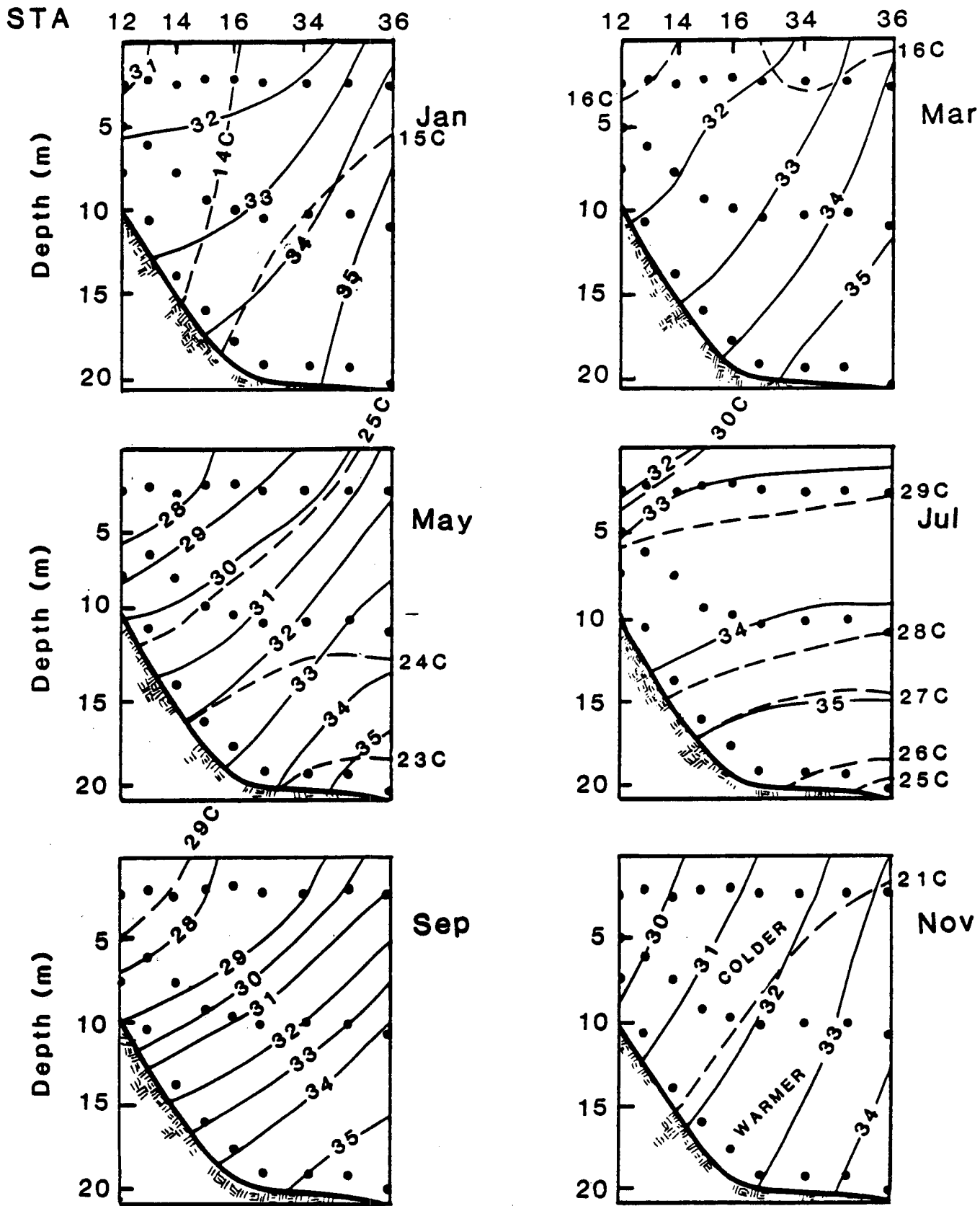


Figure 2-64a. Vertical section of mean salinity (o/oo) and mean temperature (°C) for the Bryan Mound study region cross-shelf transect.

every other month along the transect normal to shore which passes across the diffuser site. The sections show that the fresh-water band (present except in July, of course), as might be expected, takes, on the average, the form of a wedge pressed against the shore. In July, when upwelling is at its maximum, the salinity is relatively high and is not much less at the top than at the bottom.

Figure 2-64b shows the sigma-t values corresponding to the salinities and temperatures of Figure 1-64a. The isopycnals in the section provide a measure of mean stability. They also, through the hydrostatic equation, give some idea of the pressure field and, consequently, since there is a tendency toward geostrophic balance, some indication of the velocity field normal to the section. If the near bottom current is zero, the sections all indicate downcoast flow. The indications provided by the section are, with the exception of July, roughly in accord with the means for the measurements by the top current meter at Bryan Mound site A (or B, as specified above). Why the July indications are not in accord with current measurements is not clear. It must be noted, of course, that the current measurements are made almost continually, while the hydrographic observations are taken, at most, on two occasions each month. Possibly frictional forces or accelerations are relatively strong during upwelling.

2.5.5 Hydrography of the West Hackberry Brine Disposal Region

Although a climatological picture of the hydrography of the West Hackberry region cannot yet be put on as firm a basis as that in the preceding section for the Bryan Mound region (Figures 2-62 through 2-64), we attempt here to obtain a first approximation to the annual progression of temperature and salinity in the form shown in Figure

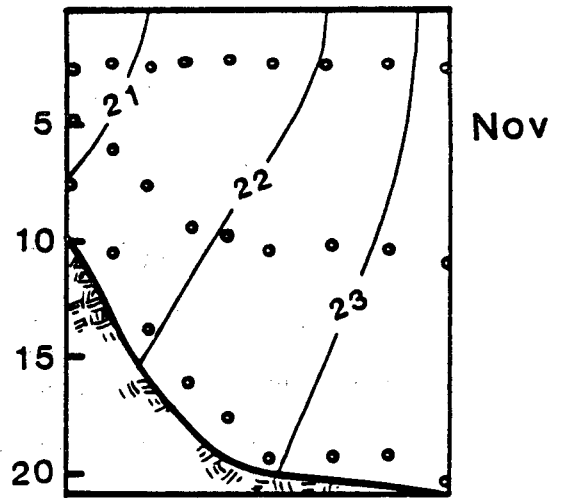
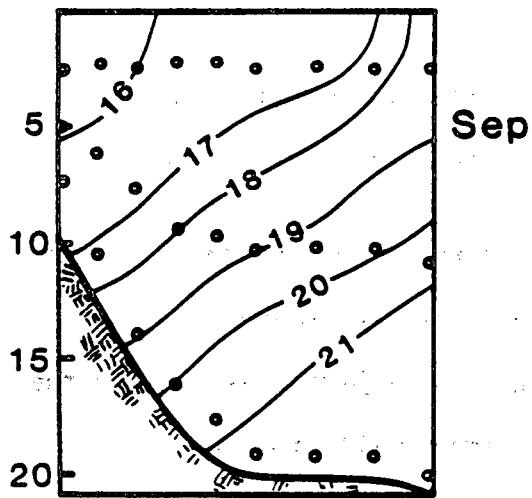
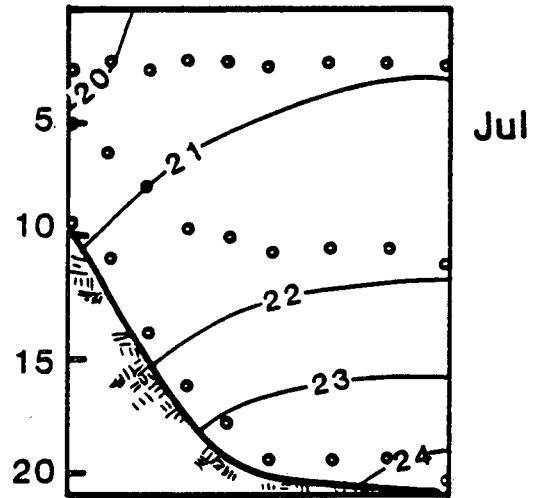
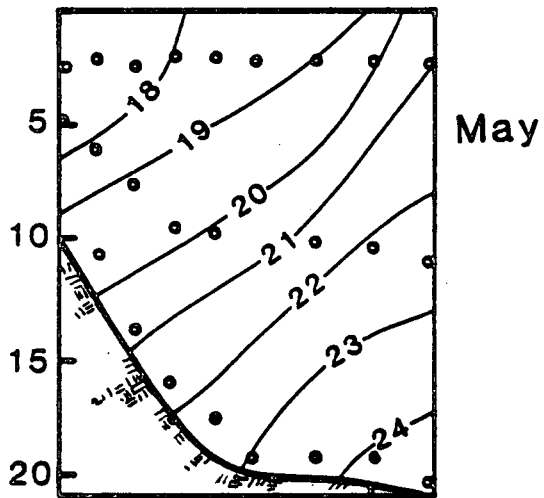
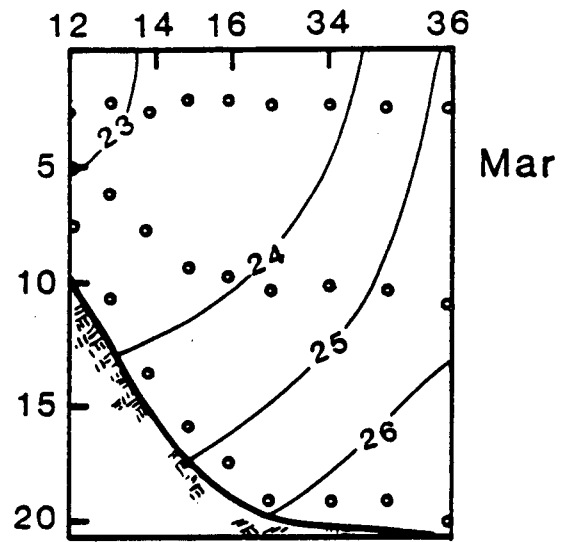
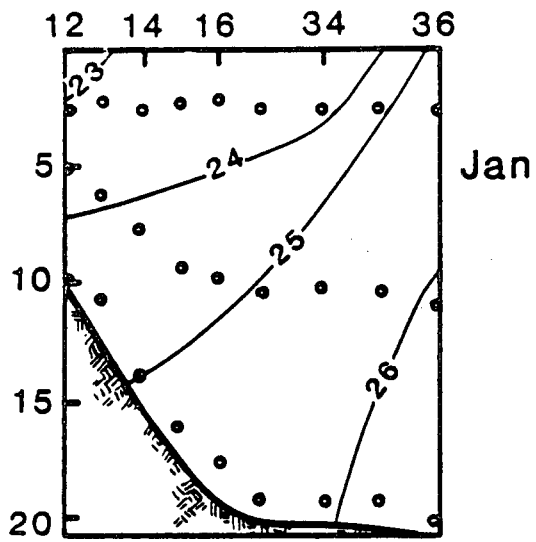


Figure 2-64b. Vertical section of σ_t corresponding to 2-64a.

2-62. Means of temperature and salinity based on values at West Hackberry station 22 and at GUS III station E1, slightly farther offshore are presented in Figure 2-65. The mean of the latter positions is comparable to a position between the onshore and offshore locations in the Bryan Mound region (Figures 2-62a and 2-62b, respectively). Since the sample for Figure 2-65 is quite small, the means can only suggest the annual progression. The fact that more "Mississippi" water is now discharged by the Atchafalaya River than there was in the period of GUS III cruises (1963-1965) must be kept in mind.

The mean temperatures at the sea surface at the West Hackberry offshore location (Figure 2-65) are similar to those of the Bryan Mound region (Figure 2-62b). A winter minimum similar to that of the inshore location in the Bryan Mound region, about 12°C, is not quite as low as the minimum at Bryan Mound. The relatively low bottom temperature in June and July is suggestive of upwelling but certainly not conclusive.

The range of mean salinity at the sea surface in the West Hackberry region is similar to that in the Bryan Mound region. Although the West Hackberry region is much closer to the sources of Mississippi water, the salinity minimum at West Hackberry differs by an insignificant amount from the minimum at the corresponding Bryan Mound location. Perhaps the years sampled at West Hackberry lead to this somewhat surprising situation. The highest of the monthly mean salinities at West Hackberry is close to 34 o/oo, as it also is at the Bryan Mound offshore location. The monthly means for the deepest salinity determination at West Hackberry have a range similar to that

2-171

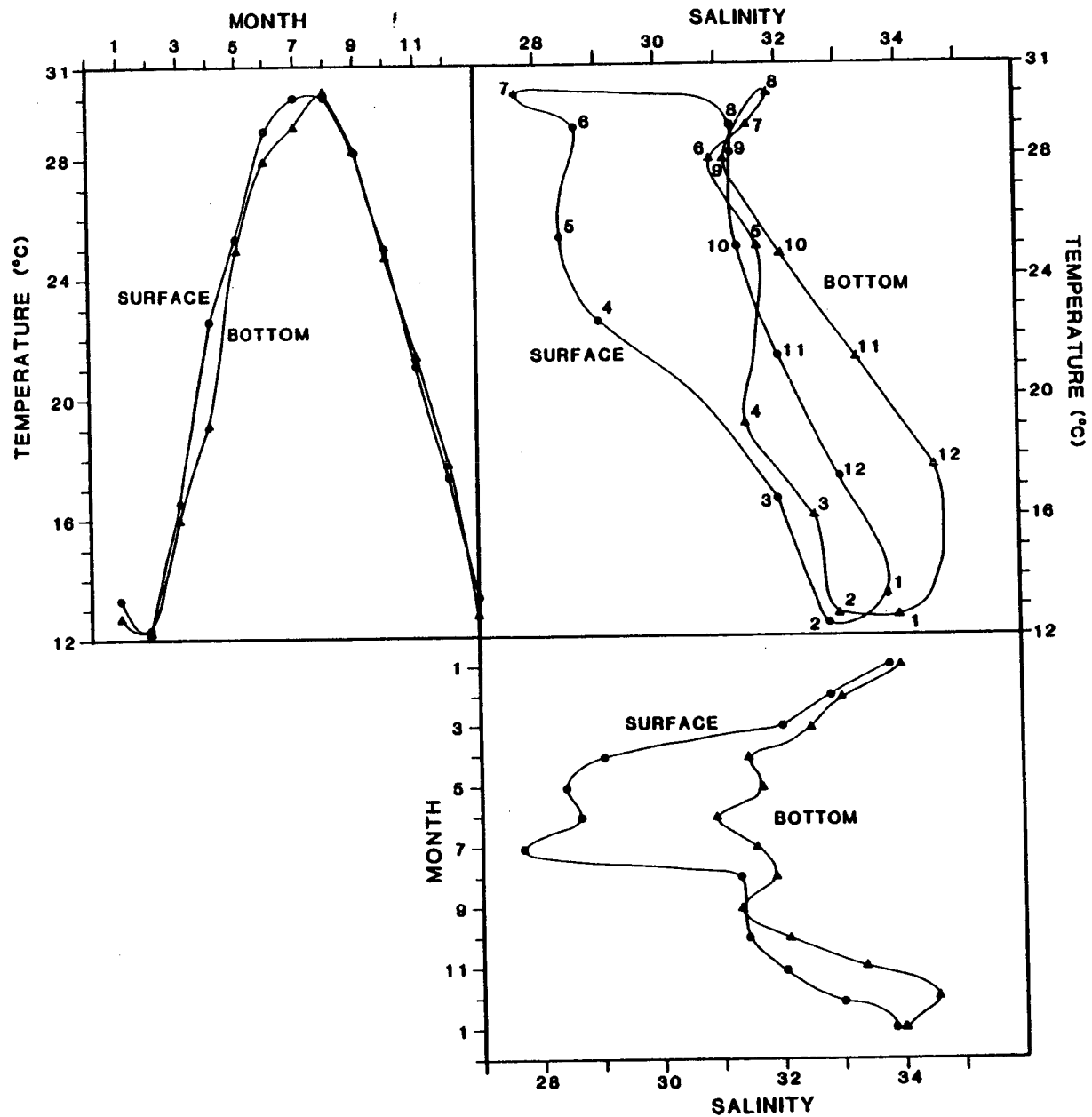


Figure 2-65. Annual progression of mean temperature (°C) and salinity (o/oo) for near-surface and near-bottom depths in the vicinity of West Hackberry station 22. Means are based on data from station 22 and GUS III station E1. The means are also entered in a T - S diagram.

for corresponding determinations at the Bryan Mound inshore location. At West Hackberry in January, February, and March, there is little difference in mean salinity from the top to the bottom of the water column. On the other hand, the monthly mean near surface salinity in the Bryan Mound region is not as high as the mean at the bottom during those months. The occurrence of vertical homogeneity in winter is interesting and may indicate a different mixing regime, but the small sample for the West Hackberry location leaves doubt that the occurrence represents the true mean condition.

The mean salinity at the West Hackberry location seems to vary through the year in a quite different fashion from that at Bryan Mound locations. The decrease from the winter maximum in January begins earlier, as one might expect, because the West Hackberry site is closer to the Atchafalaya and Mississippi River mouths. The means for the West Hackberry region during April, May, and June fall between the offshore and onshore means for the Bryan Mound region (Figures 2-62a and 2-62b). The apparent persistence of low salinity in the July mean seems to be due to the low salinities observed at the West Hackberry site in 1981. The Mississippi river stage was high at Simmesport in July 1981, indicating an unusually large discharge for that month.

The low value in July is surprising for another reason. During the latter halves of June and July, as Figure 2-57 shows, the top current meter at site D registered a net upcoast (eastward) flow. If the currents have a significant baroclinic component and are roughly geostrophic, an adjustment in mass structure like that during upwelling is to be expected. However, such a change certainly does not appear in the top and bottom salinity means. The winds observed

at the location in July 1981 seem too weak to make upwelling predominate during the periods of net upcoast flow. Still, the estimated climatological mean wind stress (Figure 2-50) off West Hackberry for July does indicate a small degree of upwelling to be normal at that time.

Possibly the strong rise in the August mean salinity is a result of upwelling or upwelling together with advection from the west. However, the expected effect of upwelling on the annual progression at the West Hackberry disposal site would not lead to a maximum salinity like that appearing in the Bryan Mound region during July and August (Figures 2-62a and 2-62b).

From the difference in salinity between top and bottom-depth means, one may gain some idea of the vertical stability at the locations considered. (Note that sigma-t lines are entered in the T-S coordinate regions of the figures.) Comparisons of the two disposal sites suggest that the differences in mean vertical stability between the sites is not significant for most months. However, at West Hackberry, the period of high vertical stability is not interrupted by an upwelling phase in July and August as it is at the Bryan Mound site.

Examination of salinities along the offshore section (Figure 2-1) indicates that the brine from the diffuser has a considerably greater influence on the salinity field in the West Hackberry region than does the brine from the Bryan Mound diffuser. This is in spite of generally lower output rates at West Hackberry. Two possible explanations are the lower upper layer current speeds at West Hackberry site (Figure 2-57) and the longer duration of high stability

conditions at the West Hackberry site.

A very interesting feature of the hydrography of the West Hackberry disposal region is the appearance in May or June of a nearly anoxic bottom layer. Figure 2-66 shows the very low oxygen concentrations encountered in July 1981. This sort of occurrence has been noted earlier for the central Louisiana coast by Fotheringham, et al. (1979) and others. As the latter have noted, the appearance of the hypoxic conditions seems to be an annual occurrence. The onset of the conditions seems to lag the arrival of low-salinity surface water by a number of days. Quite stable conditions seem to persist in the region until autumn, as we have already noted. Upwelling, because it is weak, does not lead to the large reduction in stability that occurs in the Bryan Mound region during June or July. The persistent high stability in the West Hackberry region may account for the duration of hypoxic conditions. In 1981 low dissolved oxygen values were encountered from May until November.

The extent of the hypoxic layer in the offshore direction is not known. In July 1981 (Figure 2-66) it was present at West Hackberry station 23 which is about 25 km offshore. However examination of Texas A&M hydrographic stations taken just off the Texas-Louisiana continental shelf has not turned up low oxygen concentrations in layers that might be related to the bottom layers on the inner shelf.

The western limit for the hypoxic layer is also unknown, although the feature has been observed in the Bryan Mound region. It appears there, with the advent of low-salinity water from the Mississippi or Atchafalaya or shortly thereafter. The oxygen concentrations encountered are not as low as those at West Hackberry. Harper, et al.

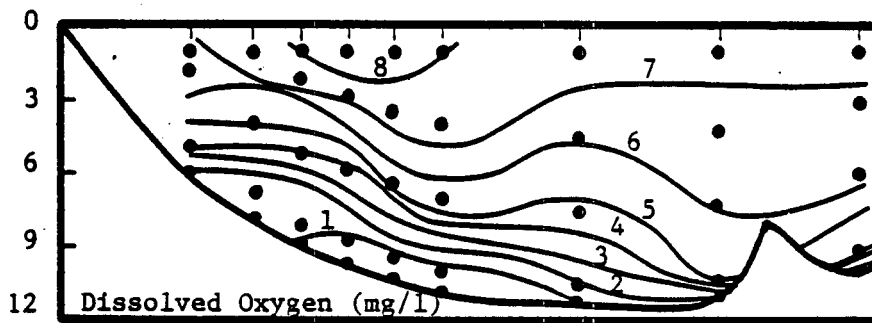


Figure 2-66. Vertical section of dissolved oxygen concentration (ml l^{-1}) for cross-shelf transect in West Hackberry study region for July 16, 1981.

(1981) reported the occurrence of a hypoxic layer off Freeport (in the Bryan Mound region) in May-July 1979. Records for 1982 show that the layer was fairly strong in June, but had disappeared in July. Temperatures and salinities in July indicated that rather strong upwelling had occurred. Offshore water had been brought in and the strong stratification of June had disappeared.

It may be useful to review a few comparisons between the West Hackberry and Bryan Mound study regions. In the West Hackberry region:

1. the average current in the upper layers is considerably weaker (about one half);
2. average upwelling intensity is considerably less (in June, July, and August);
3. strong stratification (stability) consequently persists from spring into fall (no interruption due to upwelling occurs in summer); and
4. perhaps because of the smaller velocity shear between upper and lower layers and the longer duration of strong stratification, the effect of brine disposal on salinity distribution is more evident.

All of the comparisons suggest that the West Hackberry region is more vulnerable to environmental injury, either natural or induced by man, than is the Bryan Mound study region.

2.6 Summary and Conclusions

The monthly hydrographic cruises and in situ recorded time series of temperature and salinity together provide a coherent picture of the spatial distribution of the hydrographic variables and their temporal variation in the West Hackberry study area. Temperature has a large annual cycle with small short period variability. The lowest bottom temperature at the

diffuser site was 9.4°C in January and the highest was 31.0°C in July. Cross-shelf temperature differences are 2°C or less when the water column is warming and 3 -to 4°C when it is cooling. Vertical temperature differences are less than 1°C most of the time, but in July and August top to bottom differences increase to about 3°C. No effect on the natural ambient water temperature from brine discharge was measured.

Cross-shelf salinity differences persisted throughout most of the study period and exceeded 15% at times in June 1981 and March-April 1982. Vertical salinity stratification at the diffuser site was very strong in July 1981 reaching a maximum of 14 o/oo. Temporal variations in ambient bottom salinity were up 10 o/oo over a few days and up to 8 o/oo in less than one day. The annual spring decrease in salinity began in June 1981, later than normal because of a late maximum in Mississippi/Atchafalaya river discharge. In 1982, a decreasing trend in salinity began in March. The lowest ambient bottom salinity recorded at the diffuser site was 19.7 o/oo; the highest was 32.7 o/oo.

Salinity effects from brine discharge were clearly detected by both the hydrographic surveys and the in situ, near bottom meter at the diffuser site. Salinity differences between the diffuser site and the control site, at 1.0 m to 1.8 m above the bottom, indicate a maximum above ambient salinity increase of 4.6 o/oo, and a typical increase of about 3 o/oo. Vertical profiles indicate that salinity effects from brine discharge can reach a height of 3 m above the bottom near the diffuser.

Because of the low magnitude of short term temperature variability, density fluctuations and gradients are primarily determined by salinity.

Variation in dissolved oxygen near the bottom had an annual cycle with a maximum of 9.2 mg/l in February 1982 and a minimum of almost zero in July

and August 1981. The hypoxic/anoxic conditions near the bottom covered the entire study area from the shore to 30 km offshore and 8 km east and west of the diffuser. Very close to the diffuser, there was an increase in dissolved oxygen during the anoxic period, apparently as a result of mixing induced by the discharge jets. The anoxia is apparently related to the strong salinity stratification and may be an annual event.

Currents were studied by a variety of methods. Most of the energy in the currents is contained in the lower frequencies (longer periods) of the alongshelf component. The cross-shelf component has much less energy than the alongshelf component. Currents were found to be very coherent in an alongshelf direction throughout the study area, and indeed, even as far as Bryan Mound site. Periods near 10 days and 3 days were the most strongly coherent.

The alongshelf component of local wind stress was found to be coherent with the alongshelf top and bottom currents, but only near a period of 3 days. At periods near 10 days, there was no significant coherence.

The monthly mean alongshelf current was downcoast in all months except July 1981 at the surface. The mean upcoast current in July 1981 was in opposition to the mean alongshelf wind which was downcoast in all months including July 1981.

A comparison of the West Hackberry and Bryan Mound diffuser sites shows that the residual component of bottom current is much stronger at Bryan Mound. The tidal constituents at both sites are similar and have amplitudes of 2 to 3 cm/s. The long term mean bottom currents are slightly stronger at West Hackberry. The average current in the upper layers is weaker at West Hackberry (about one half). Average upwelling intensity is less at West Hackberry and strong stratification persists from spring to

fall. These conditions suggest that the West Hackberry region may be more vulnerable than the Bryan Mound region, particularly during the summer months.

CHAPTER 3

ESTUARINE HYDROLOGY AND HYDROGRAPHY

Wesley P. James and Robert E. Randall
Texas A&M University
College Station, Texas 77843

3.1 Introduction

The West Hackberry site of the Department of Energy's Strategic Petroleum Reserve Program began discharging brine into the Cameron, Louisiana coastal waters in May 1981. The brine discharge is the result of leaching and filling of storage caverns in the West Hackberry underground salt dome. The leaching process and subsequent withdrawal of crude oil requires large volumes of raw water which are obtained from the nearby Intracoastal Waterway (ICWW). The purpose of this chapter is to estimate the impact of the water diversion on the water resources of the area and to determine the impact of brine discharge on the estuarine environment of Lake Sabine, Intracoastal Waterway, and Lake Calcasieu.

A predisposal study of estuarine hydrology and hydrography of the Lake Calcasieu, ICWW and Lake Sabine was conducted by the authors from January through April 1981; the results of that study were also reported in 1981 (Randall and James, 1981a). Prior to this study, Environmental Impact Statement was published by the Department of Energy (DOE, 1978). Estuarine hydrographic data have also been collected by the Louisiana State Wildlife Commission in the late 1960's and mid 1970 and reports have been published by Barrett (1971) and Barrett et al. (1978). The data from these studies, and other available literature, along with the data collected from January through April 1981, are discussed in this chapter.

For this postdisposal study, data were collected at ten estuarine stations shown in Figure 3-1 and whose latitude and longitude are tabulated in Table 3-1. Three stations (E2, E2, and E4) are located in Lake Calcasieu where conductivity, temperature, depth, and dissolved oxygen (CTD/DO) were measured monthly, and temperature and pressure were measured continuously at station E2. There are three stations (E1, E6, and E7) located in the ICWW where monthly CTD/DO data and continuous water pressure and temperature data were collected. Stations E8, E9, and E10 are located in Lake Sabine with monthly CTD/DO data having been collected at all three stations and continuous pressure and temperature data at E8. A final station (E5) is located in Calcasieu Pass and monthly CTD/DO data was collected there as well as a continuous current velocity, salinity, temperature, and pressure data which are discussed in Chapter 2 of this report.

The data collected at the stations shown in Figure 3-1 are analyzed and described in the following sections of this chapter. The general organization of the remainder of this chapter is to discuss the impact of the water diversion for the leaching process in the section entitled "Hydrology" and to characterize the estuarine environment and describe the impact, if any, of the brine discharge on the same environment in section entitled "Estuarine Hydrography."

3.2 Hydrology

The West Hackberry SPR project has been pumping approximately 1.4 cms (50 cfs, 0.77 million barrels per day (MBD)) of water from the ICWW this past year. The maximum pumping rate during the life of the project has been estimated at 1.98 cms (70 cfs, 1.08 MBD). The pumping site is located in the ICWW approximately 9.66 km (6 mi) west of

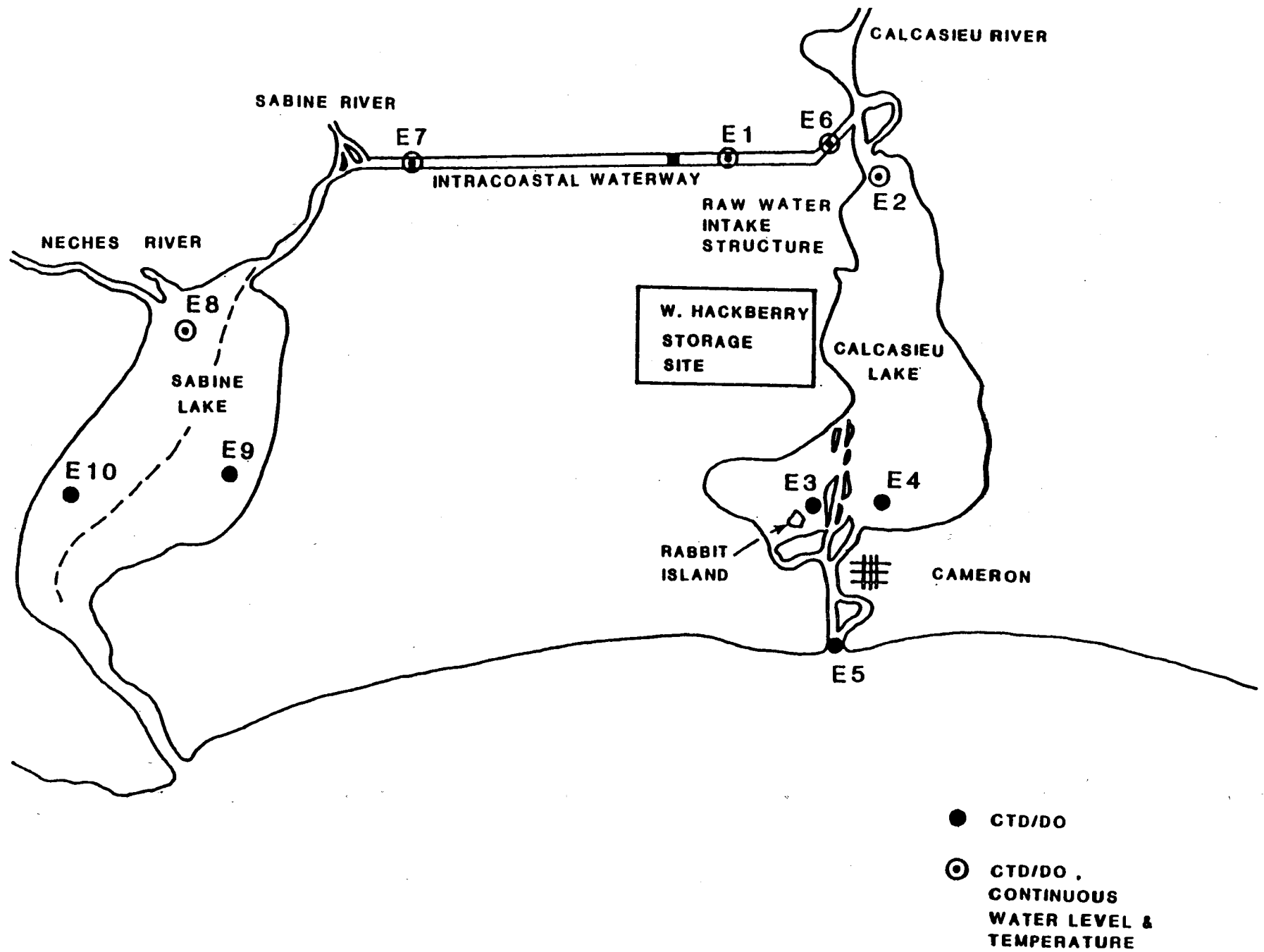


Figure 3-1. Station locations for estuarine hydrology and hydrography stations.

Table 3-1. Latitude and longitude for the ten estuarine stations at the West Hackberry site.

Station #	Latitude	Longitude
E1	30°03'32" N	93°26'09" W
E2	30°03'05" N	93°18'41" W
E3	29°51'33" N	93°22'00" W
E4	29°51'20" N	93°18'47" W
E5	29°46'11" N	93°20'38" W
E6	30°03'47" N	93°20'55" W
E7	30°03'35" N	93°41'55" W
E8	29°57'32" N	93°42'40" W
E9	29°54'07" N	93°48'13" N
E10	29°51'45" N	93°55'06" W

Calcasieu River and 27.37 km (17 mi) east of Sabine River. The removal of the relatively freshwater in the ICWW from the Calcasieu-Sabine system could change salinity levels in other parts of the system. In addition to increasing salinity levels in Calcasieu and Sabine Lakes, the project could potentially affect the salinity levels in Calcasieu River, groundwater, and freshwater marsh areas. The impact of pumping water from the ICWW on the water resources of the area will be evaluated in this section of the report.

The specific objectives of this phase of the study were:

1. Install water level recorders with conductivity and temperature sensors for continuous time series observations at estuarine stations E-1, E-2, E-6, E-7, and E-8 (see Figure 3-1).
2. Identify conditions for critical period of the year when the project might affect the salinity in the estuaries.
3. Estimate the impact that the project might have on the water resources of the area.

3.2.1 Water Level Recorders

Water level recorders were installed at five sampling stations in the Calcasieu-Sabine system. Station E-1 is located at the raw water pump intake structure on the ICWW approximately 8.0 km (5.0 statute mi) west of the Ellender Bridge, station E-2 is located at the north end of Calcasieu Lake near West Pass, station E-6 is located in the ICWW at Ellender Bridge, station E-7 is located about 1000 ft (300 m) north of the confluence of the ICWW and the Sabine River, and station E-8 is located in the north end of Sabine Lake about 1.8 km (1.2 statute mi) south of the ICWW.

The instrument that was initially used on the project was Sea Data Corporation TDR-1. This instrument measured and recorded temperature and pressure. Sea Data added conductivity to the instrument and the TDR-1 instruments were replaced by CTDR-1 instruments. The instruments were serviced monthly. The data are recorded on tape wafers which are read with a Sea Data Micro-reader and transferred to the Texas A&M computer for processing. The conductivity sensors are calibrated before the instruments are deployed in the field and again after they are returned to the laboratory. Depth and temperature are also checked during calibration. Pressure readings are converted to water depth after the data has been corrected for changes in atmospheric pressure observed at Lake Charles airport. Time series plots of depth and pressure are included in Appendix Figures C-1 through C-5. The plots are not complete. The recorder head on several of the instruments had shifted and we were not able to read the data. These tapes have been sent to Sea Data Corporation and they are reading the tapes for us.

3.2.2 Freshwater Inflow

Freshwater inflow is important in that it affects the salinity levels in Calcasieu and Sabine levels in Calcasieu and Sabine Lakes. During periods of high freshwater inflow the salinity in the lakes will be relatively low, while during periods of low freshwater inflow the salinity in the lakes will be relatively high. The effect of water diversion on the salinity levels in Calcasieu and Sabine Lakes will be greatest during low freshwater inflow periods. Freshwater flow into the Calcasieu-Sabine system is discussed as measured or gauged flow and ungauged flow in the following sections.

3.2.2.1 Gauged Flow

Surface waters in the major rivers and streams entering the Calcasieu and Sabine system have been measured by the U.S. Geological Survey. Excellent records are available for the gauged freshwater inflow into the system from October 1967 to the present time. The following gauging stations were utilized in this study:

- A. Calcasieu River near Kinder, LA
- B. Beckwith Creek near Quincy, LA
- C. Bear Head Creek near Starks, LA
- D. Sabine River near Ruliff, TX
- E. Cow Bayou near Mauriceville, TX
- F. Neches River at Everdale, TX
- G. Village Creek near Kountze, TX
- H. Pine Island Bayou near Sour Lake, TX

Gauging station locations are shown in Figure 3-2. The letters (A through H) in Figure 3-2 refer to the letters in the above list of gauging stations.

The average monthly freshwater inflow in cfs entering the Calcasieu system is tabulated in Appendix Table C-1 for the period October 1967 through September 1981. The table includes gauged flows in the Calcasieu River with a drainage area of 4,303 km² (1,700 mi²), Beckwith Creek with a drainage area of 383 km² (148 mi²) and Bear Head Creek with a drainage area of 458 km² (177 mi²). The total gauged inflow or sum of the three stations from a drainage area of 5,244 km² (2,055 mi²) is also included in the table. It can be observed that the average monthly total gauged freshwater inflow for

3-8

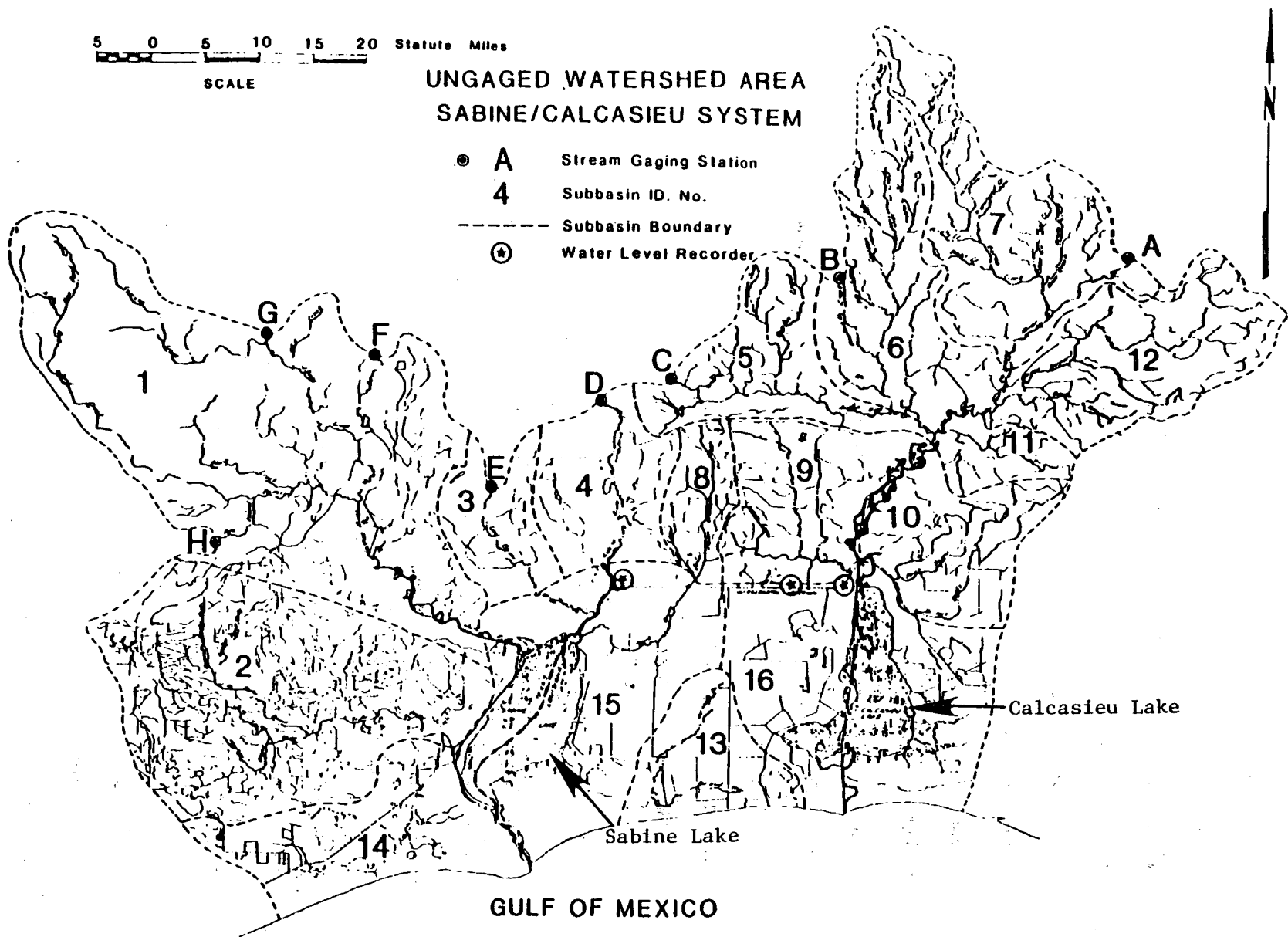


Figure 3-2. Location of gauging stations and ungauged drainage areas.

Calcasieu Lake is often (33% of the time) less than 11.3 cms (400 cfs) during the period July through November. The minimum average monthly gauged freshwater inflow to Calcasieu Lake during the period of record was 7.25 cms (256 cfs) in October 1978. Figure 3-3 is the flow-duration curve for Calcasieu Lake. The curve is based on the total monthly average gauged inflow listed in Appendix Table C-1. Flow duration curve for the low flow period of July through November is shown in Figure 3-4. During the low flow period the total average monthly gauged freshwater inflow to Calcasieu Lake ranged from 256 to 8200 cfs (7.3 to 232 cms). The average monthly gauged inflow is less than 600 cfs (17 cms) 50% of the time during the low flow period.

The average monthly gauged freshwater inflow to Sabine Lake is tabulated in Appendix Table C-2. Total drainage area of the gauged inflow is 18,560 mi² (48,070 km²) and includes Sabine River (9,330 mi²; 24,165 km²), Low Bayou (88 mi²; 215 km²), Neches River (20,593 km²; 7,951 mi²), Village Creek (2,227 km²; 860 mi²), and Pine Island Bayou (870 km²; 336 mi²). Most of the inflow is from the Sabine and Neches Rivers which represent 93% of the gauged drainage area. The total average monthly gauged freshwater inflow to Sabine Lake is often (33% of the time) less than 91 cms (3,200 cfs) during October and November. The minimum gauged inflow of 23 cms (812 cfs) occurred in November 1967. Figure 3-5 is the flow-duration curve for Sabine Lake based on the total monthly average gauged inflow for the period 1967-1981. It can be observed that the gauged flow into Calcasieu Lake is about 20% of the gauged flow into Sabine Lake. The shape of the flow-duration curve for Sabine Lake is considerably different from that of Calcasieu Lake. Approximately 57% of the Sabine Lake gauged

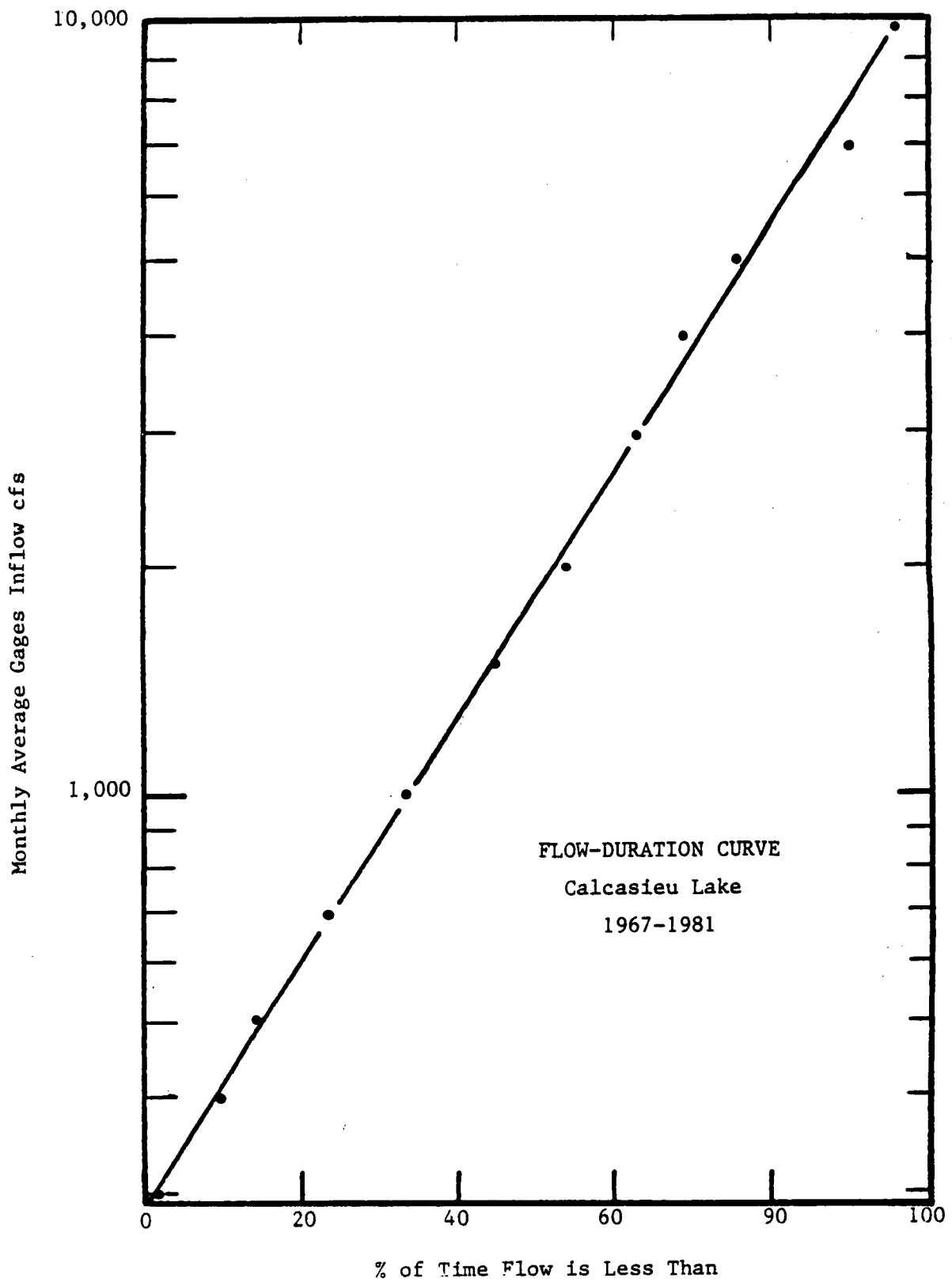


Figure 3-3. Flow-duration curve for Calcasieu Lake, 1967-1981.

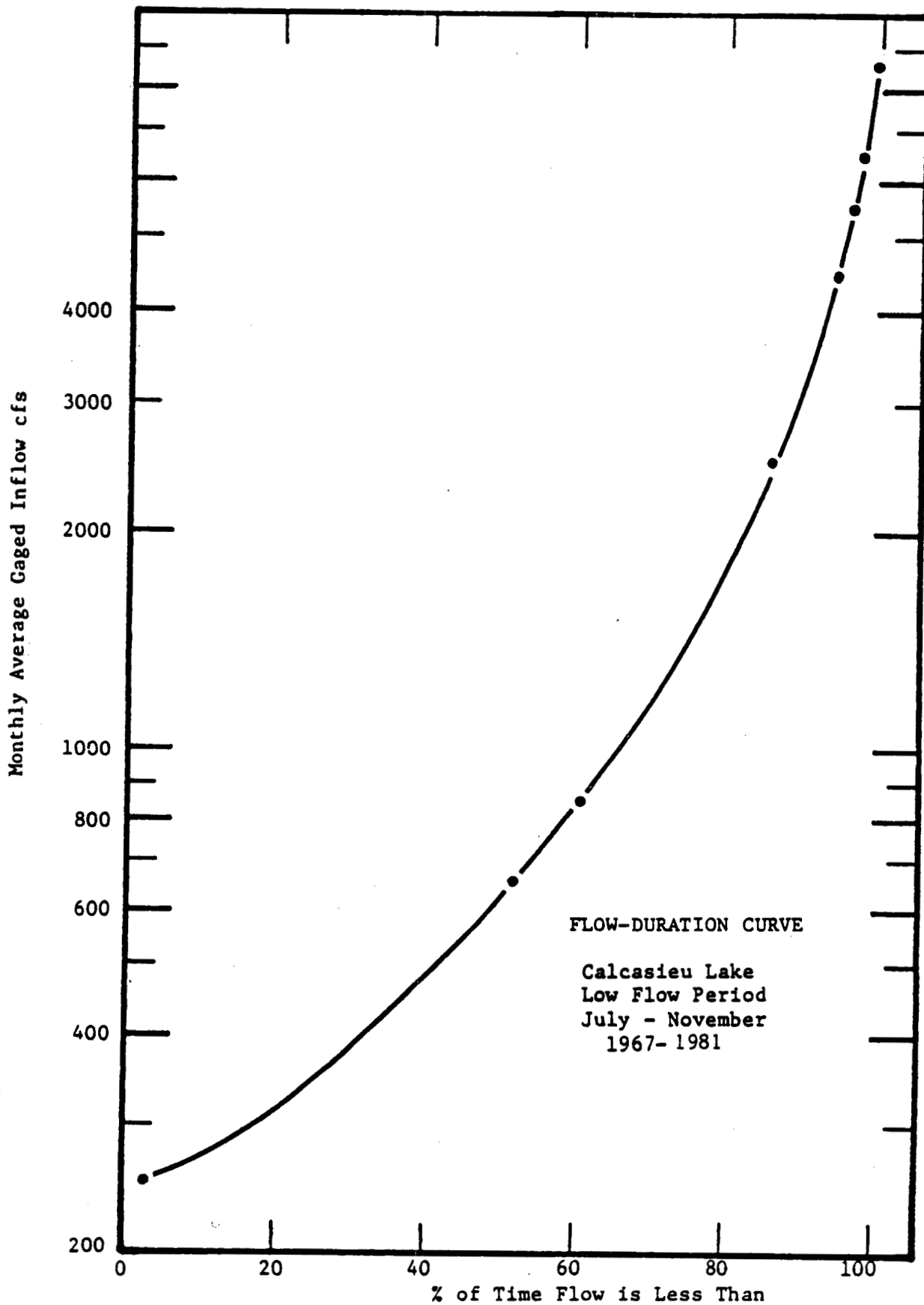


Figure 3-4. Flow-duration curve for Calcasieu Lake during the low flow period from July through November, 1967-1981.

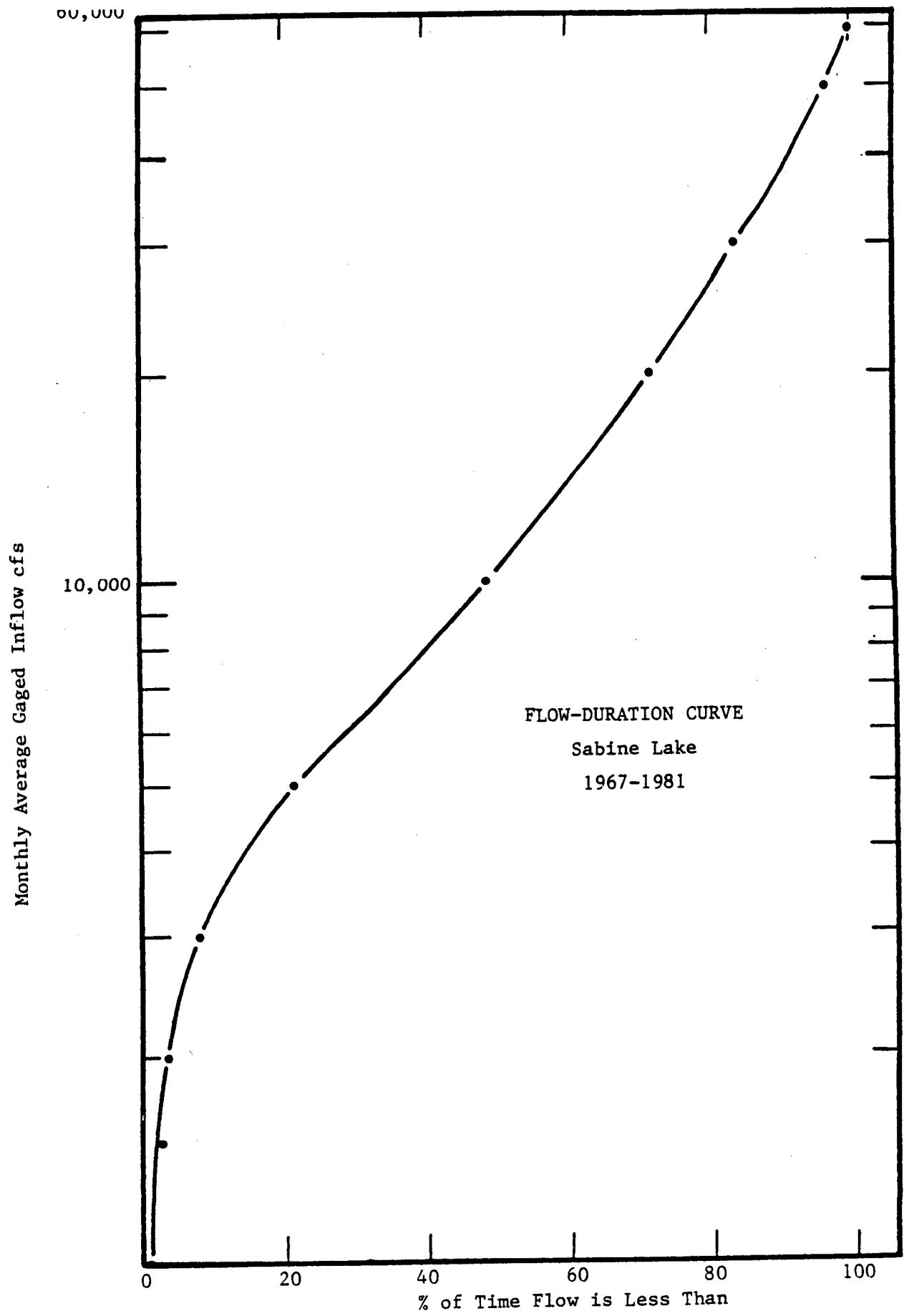


Figure 3-5. Flow-duration curve for Sabine Lake, 1967-1981.
3-12

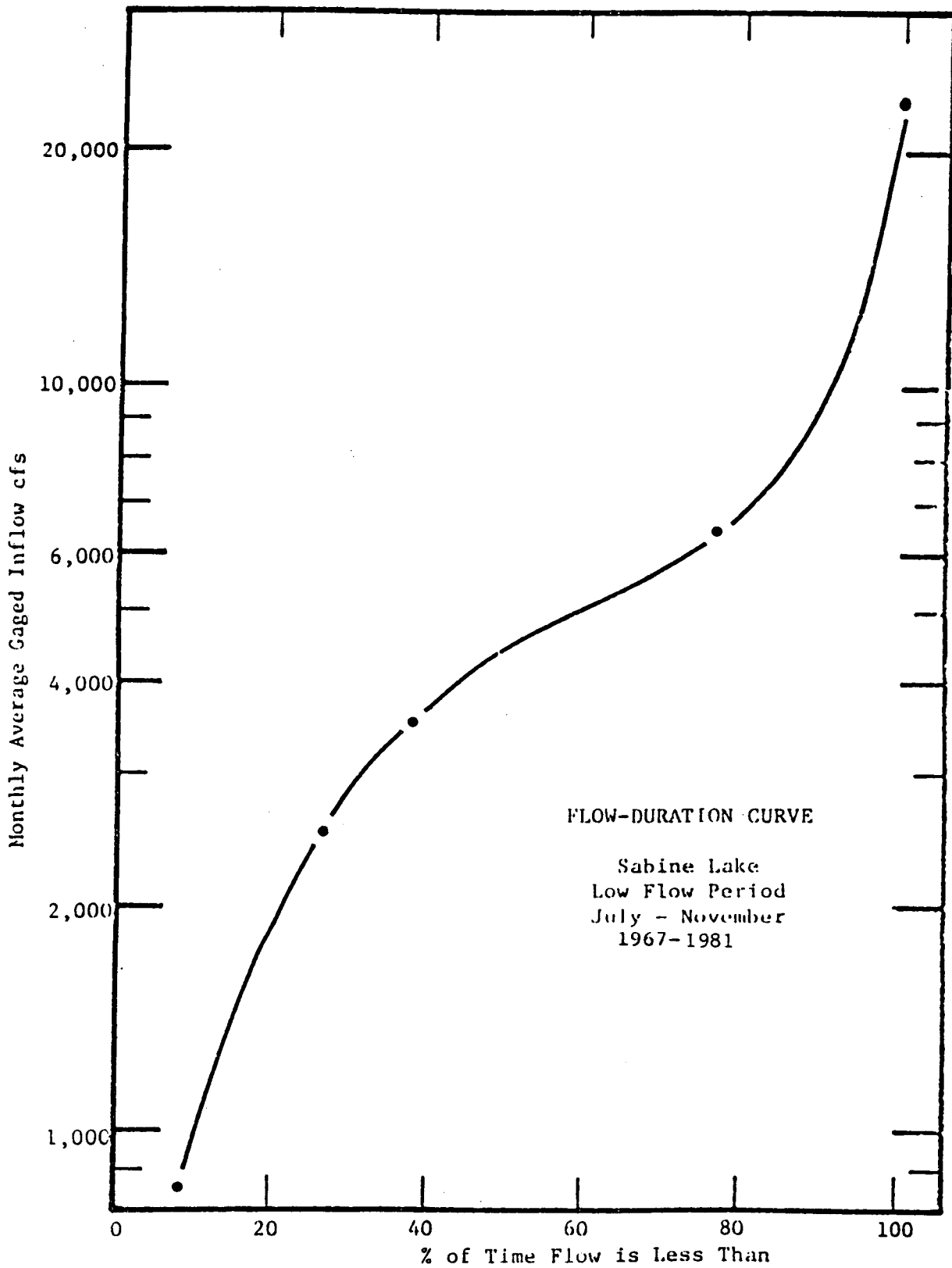


Figure 3-6. Flow-duration curve for Sabine Lake during the low flow period from July through November, 1967-1981.

drainage area is controlled by Toledo Bend and Sam Rayburn reservoirs. Flood waters stored in the winter and early spring are released during the late spring and summer. As a result the low flow period for Sabine Lake is shorter than the low flow period for Sabine Lake is shorter than the low flow period for Calcasieu Lake. The flow-duration curve for the low flow period of October and November is given in Figure 3-6. The average monthly gauged freshwater inflow during the period 1967-1981 ranged from 24 to 660 cms (860 to 23,400 cfs). The average monthly gauged freshwater inflow during the low flow period was less than 4,000 cfs (114 cms) 50% of the time.

3.2.2.2 Ungauged Flow

Ungauged flow into the Calcasieu-Sabine system includes surface runoff from the drainage area below the stream gauging stations, groundwater discharge, direct lake precipitation, lake evaporation, wetland evapotranspiration, irrigation-industrial-municipal return flows, and diversions.

3.2.2.2.1 Surface Water

Large drainage areas around Calcasieu and Sabine Lakes contribute freshwater inflow into the system that is not measured at the gauging stations. The areas or subbasins contributing ungauged inflow to the Calcasieu-Sabine system are shown in Figure 3-2 and are tabulated in Table 3-2. The gauged inflow into Calcasieu Lake is from a drainage area of 5,245 km² (2,025 mi²) while the ungauged drainage area contributing to freshwater inflow in Calcasieu Lake is 4,825 km² (1,863 mi²). The gauged drainage area represents 52% of the total drainage area of Calcasieu Lake. The gauged inflow to Sabine Lake is

Table 3-2. Drainage area contributing to ungauged surface runoff.

Ungauged Watershed Areas*	Area (sq mi)	Area (sq km)
Calcasieu Lake	1863	4825
Coastal Wetlands	420	1088
Subbasin 16	420	1088
Upland	1443	3737
Subbasin 5	187	484
Subbasin 6	267	691
Subbasin 7	304	787
Subbasin 9	196	508
Subbasin 10	176	456
Subbasin 11	62	161
Subbasin 12	251	650
Sabine Lake	2400	6216
Coastal Wetlands	640	1658
Subbasin 14	328	850
Subbasin 15	312	808
Upland	1760	4558
Subbasin 1	864	2238
Subbasin 2	555	1437
Subbasin 3	104	269
Subbasin 4	162	420
Subbasin 8	75	194
Gulf of Mexico	136	352
Subbasin 13	136	352

* See Figure 3-2 for the location of subbasins.

from a drainage area of 48,070 km² (18,560 mi²) representing 89% of the total drainage area of 54,286 km² (20,960 mi²). The ungauged inflow to Sabine Lake is from a drainage area of 6,216 km² (2,400 mi²). According to a study of the influence of freshwater inflows on the Sabine-Neches Estuary by the Texas Department of Water Resources (1981), the gauged freshwater inflow represents an average of 85% of the total freshwater inflow.

Average monthly ungauged inflow values for Calcasieu and Sabine Lakes are tabulated in Appendix Tables C-3 and C-4. Precipitation records from 1968-1981 were obtained for Beaumont and Lake Charles. A runoff model was developed for the ungauged drainage area. The U.S. Soil Conservation Service (SCS) curve number procedure was used to estimate the runoff. Curve numbers were estimated for each subbasin. They were based on the soil type, land cover or land use, hydrologic condition, and antecedent soil moisture. Evaporation from the lakes and evapotranspiration were included in the model for the wetland areas. As a result, during the dry summer months the net runoff could be negative. The runoff from the ungauged drainage area for Calcasieu Lake was based on the precipitation at Lake Charles while the runoff from the ungauged drainage area for Sabine Lake was based on the precipitation at Beaumont. Negative runoff indicates that the sum of the lake evaporation and marsh evapotranspiration is greater than the runoff from the the ungauged drainage area.

Municipal-industrial-irrigation monthly diversions and return flows for Sabine Lake were obtained from the study of the influence of freshwater inflows on the Sabine-Neches Estuary by the Texas Department of Water Resources (1981). Monthly diversions and return

flows for Calcasieu Lake were estimated from the Sabine data. It was assumed that the diversions and return flows at Calcasieu Lake would be similar to those at Sabine Lake but proportional to upland ungauged drainage area.

3.2.2.2.2 Groundwater

The Chicot aquifer is the primary source of groundwater in southwestern Louisiana. Most of the groundwater pumped is used for rice irrigation and by industry in the Lake Charles area. As shown in Figure 3-7, the Chicot aquifer can be separated into three units named 200-ft, 500-ft, and 700-ft sands. The 500-ft and 700-ft sands are hydraulically connected while the 200-ft and 500-ft sands are not hydraulically connected. In the Lake Charles area most of the groundwater is pumped from the 500-ft sand unit (Zack 1971). The Chicot formation outcrops about 32 km (20 mi) north of Lake Charles in Beauregard and Allen Parishes. The aquifer is recharged by rainfall on the sandy outcrop area and by streams crossing the recharge area. The Chicot formation is confined above and below by clay layers and artesian pressures are developed in the aquifer.

Groundwater pumpage in the Lake Charles industrial area has resulted in considerable drawdown in the piezometric surfaces of both the 200-ft and 500-ft sand units. Water level in wells completed in the 500-ft sand unit has declined as much as 4.3 m (14 ft) per year. As shown in Figure 3-7, The piezometric surface in the 500-ft sand unit was at the ground surface in 1903, was 61 m (200 ft) below ground in 1980, and is projected to be 91 m (300 ft) below ground surface in the year 2000 (Zack, 1971).

Because of the decrease in piezometric pressure in the Chicot

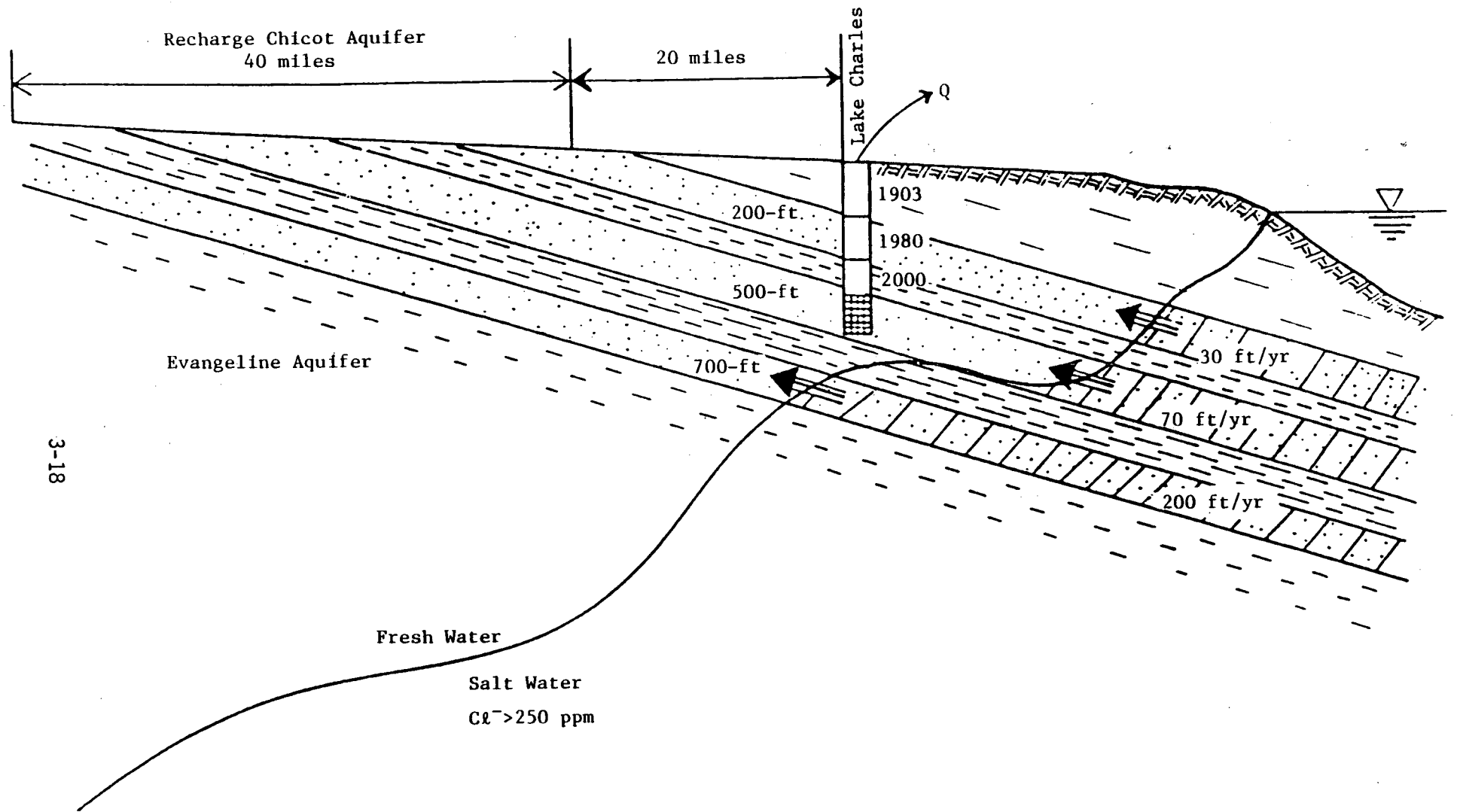
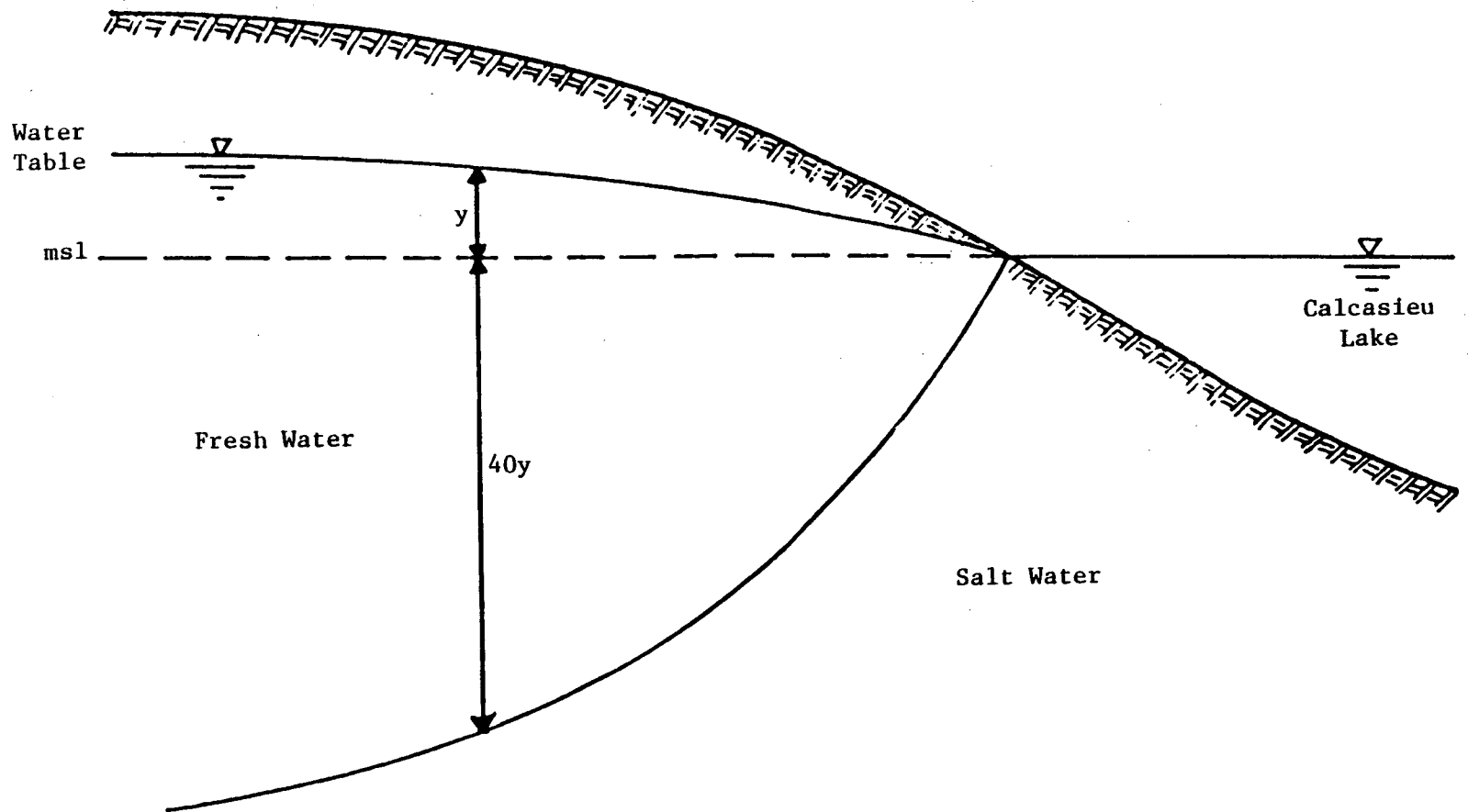


Figure 3-7. Water levels and salt water intrusion for the confined aquifers near Lake Charles, Louisiana.

aquifer the salt water interface is moving northward at a rate of 9 m/yr (30 ft/yr) in the 200-ft sand unit, 21 m/yr (70 ft/yr) in the 500-ft sand unit, and 61 m/yr (200 ft/yr) in the 700-ft sand unit. The salt water intrusion in the Chicot aquifer is caused by over pumping the aquifer. The Sabine River Diversion Canal was completed in May 1981 to provide about 7.4 cms (260 cfs) of water to industries in the Lake Charles area. This should reduce the demand for groundwater in the area. In 1969 the total groundwater pumpage in Calcasieu Parish was estimated at 9.1 cms (320 cfs) (Zack, 1971).

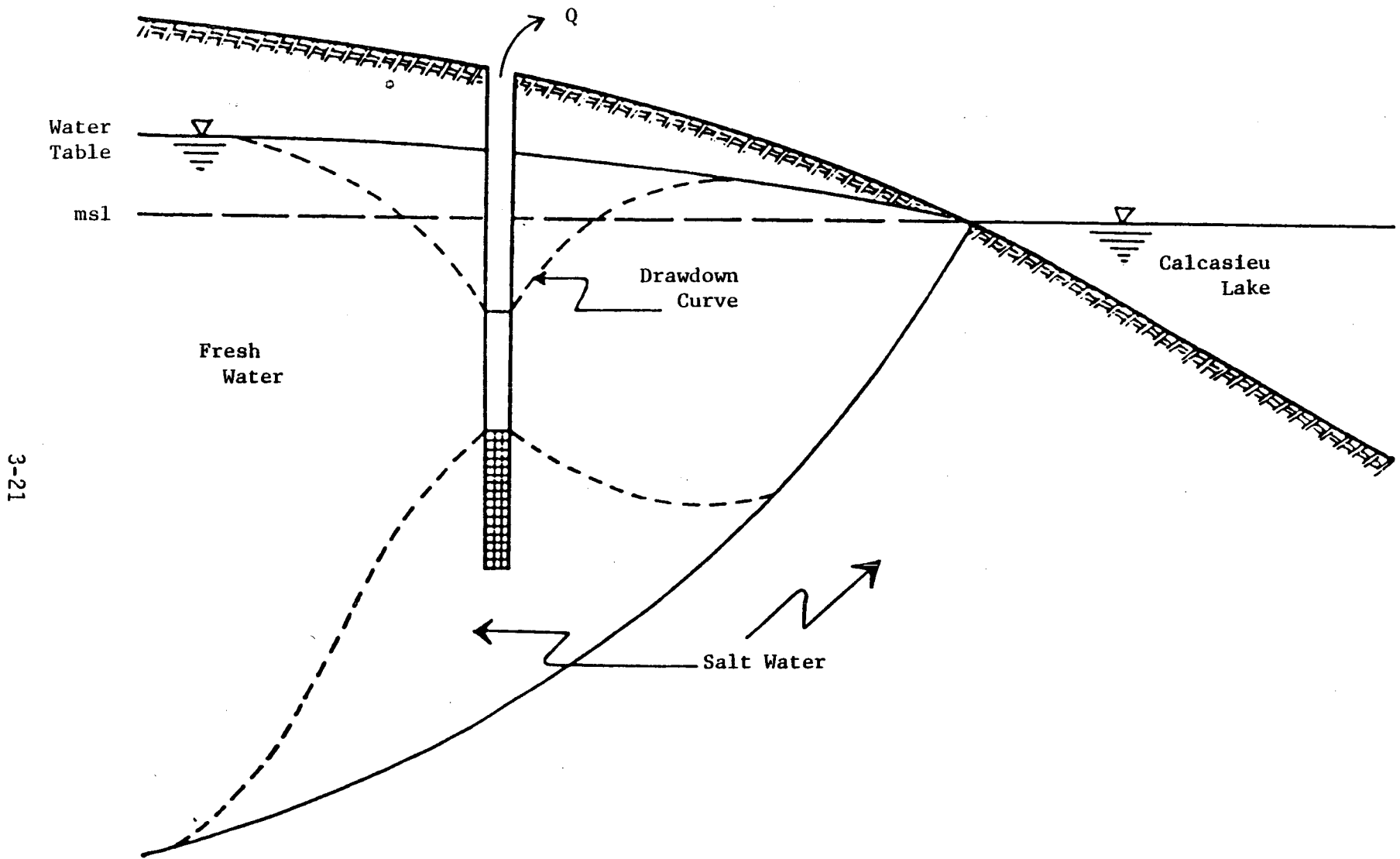
There are some small capacity shallow wells along the Gulf coast. As shown in Figure 3-8, salt water is prevented from intruding into the coastal water table aquifer by the freshwater hydrostatic pressure. Because of the density difference between freshwater and sea water, freshwater will extend below sea level. If the freshwater table level is at an elevation y above mean sea level (msl) then the freshwater will extend to a depth of about $40y$ below msl. For example if ground elevation is 1.5 m (5 ft) msl and the water table is 0.9 m (3 ft) below the ground surface, the fresh water should extend to a depth of 26 m (85 ft) below the ground surface. However, if a well is installed and pumped continuously for an extended period of time with the drawdown at the well below sea level, salt water will intrude into the well (see Figure 3-9). The position of the salt/fresh water interface depends on the elevation of the fresh water table which in turn depends on the recharge and discharge rates. The water table can also be lowered by evapotranspiration of fresh water vegetation during periods of low precipitation (see Figure 3-10).

In order to estimate the total freshwater inflow into the



3-20

Figure 3-8. Coastal water table aquifer.



3-21

Figure 3-9. Salt water intrusion caused by pumping groundwater from coastal water table aquifer.

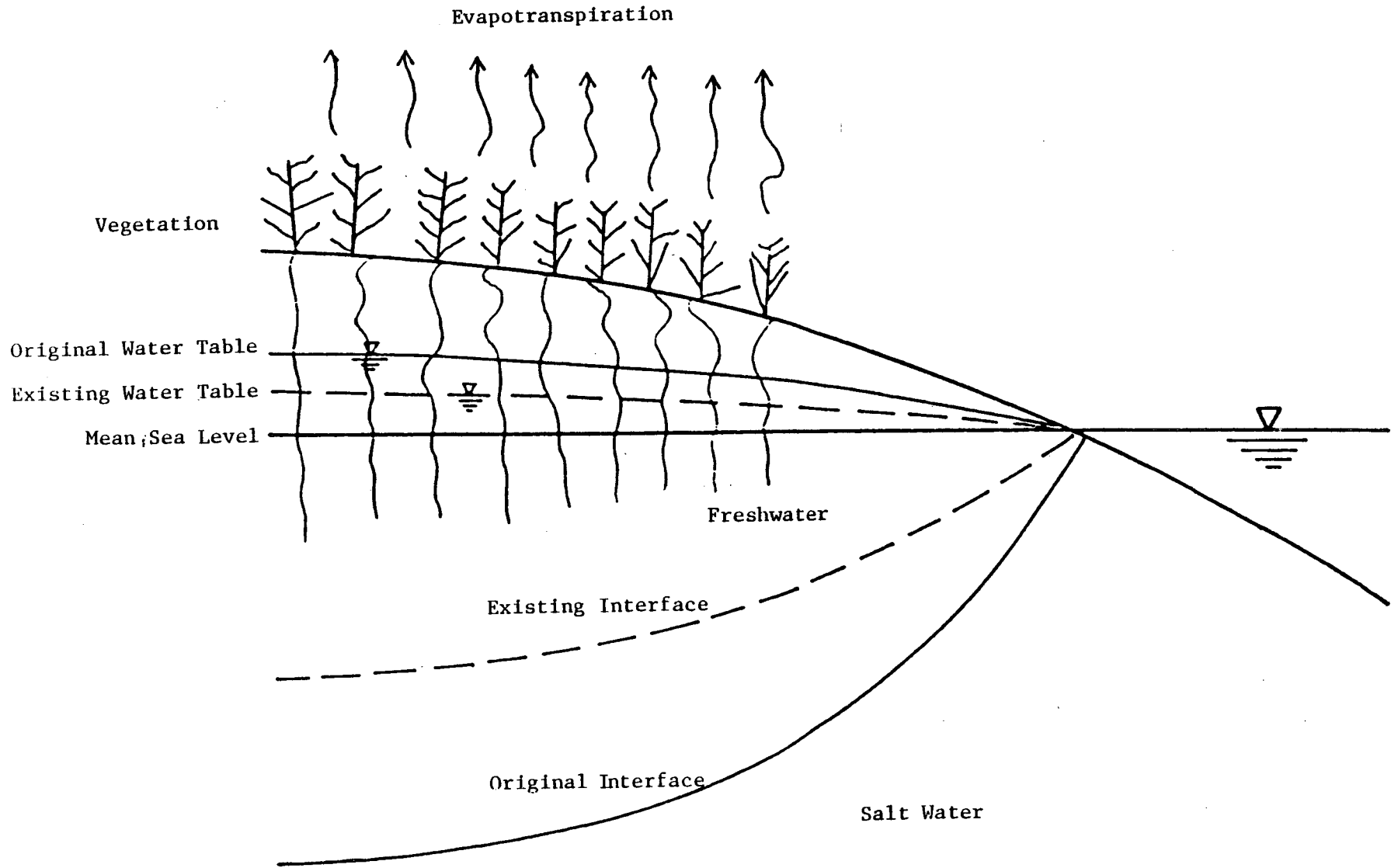


Figure 3-10. Salt water intrusion caused by evapotranspiration in the wetlands.

Calcasieu-Sabine system, it was necessary to estimate the groundwater discharge into Calcasieu Lake, the Intercoastal Waterway, and Sabine Lake. Well driller's geological logs for the Chenier Coastal Plain west of Sabine Lake were reviewed. A typical profile consists of alternating layers of clay and sand. The layers are usually 1.5 to 9.1 m (5 to 30 ft) thick. Generally at the surface, there is about a 9.1 m (30 ft) thick clay layer over a 3.0 m (10 ft) thick sand layer (Texas Water Development Board, 1971). From the Soil Survey Report of Jefferson County, Texas (Soil Conservation Service, 1965), the surface soils in the Chenier Coastal Plain tend to be poorly drained clay with a permeability in the order of 0.025 cm/hr (0.01 in/hr). The permeability of the sand outcrops is generally in the order of 25.4 cm/hr (10 in/hr). To evaluate the approximate discharge of groundwater into Calcasieu Lake, the groundwater flow net was developed as shown in Figure 3-11. The flow net was based on the assumption that the water table is at an elevation of 0.9 m (3 ft) msl. Darcy's equation was used to estimate the discharge rate. This equation is:

$$Q = KAS$$

where Q = discharge in cms (cfs),

K = permeability in m/sec (ft/sec),

A = cross-sectional area of flow in m^2 (ft^2), and

S = slope of water table.

K is the permeability and is assumed equal to 7.0×10^{-8} m/sec (0.01 in/hr or 2.3×10^{-7} ft/sec). Referring to the equipotential line in Figure 3-11 with a value of 0.6 m (2.1 ft) msl, the width of flow is 4 times ℓ where ℓ is the length of one side of the flow net square. The shoreline length of Calcasieu Lake is about 129 km (80 mi). The slope

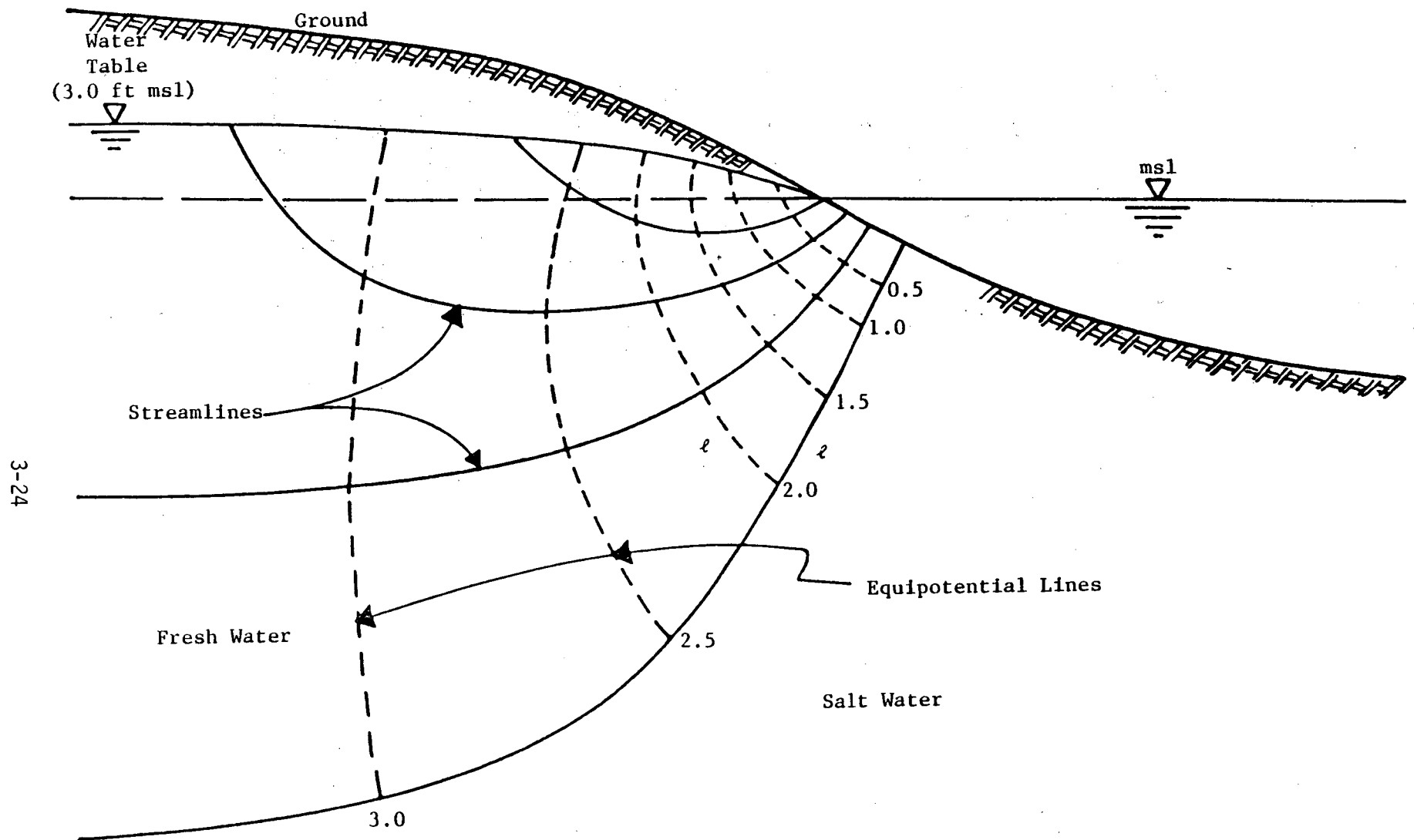


Figure 3-11. Groundwater seepage into Calcasieu Lake.

of the water table is equal to $0.5/\ell$ where 0.06 m (0.5 ft) is the difference between two equipotential lines. The discharge into Calcasieu Lake is estimated at

$$\begin{aligned} Q &= (2.3 \times 10^{-7}) (4 \ell \times 80 \times 5280) (0.5/\ell) \\ &= 0.006 \text{ cms (0.2 cfs)} \end{aligned}$$

A groundwater flow net for a north-south section through the Intracoastal Waterway is shown in Figure 3-12. The flow net was based on the assumption that there was a 10-ft sand layer under 9.1 m (30 ft) of clay. The Intracoastal Waterway is approximately 61 m (200 ft) wide and 6.1 m (20 ft) deep. The flow net was used to estimate the slope of the water table. The computations indicate that the groundwater seepage into the Intracoastal Waterway will approximately be 0.17 cms (6 cfs).

An accurate estimate of groundwater seepage into the system would require installation and observation of piezometers in the field. In this study, we are interested in a rough estimate of groundwater contribution to the freshwater inflow to the Calcasieu-Sabine system. The computations indicate that groundwater does not contribute a significant amount of freshwater inflow to the system.

The ungauged freshwater inflow expresses as a percent of the total freshwater inflow is tabulated in Table 3-3 for the years 1968 through 1981. This table was developed from the data in Appendix Tables C-3 and C-4. The average ungauged freshwater inflow is 30% of the total freshwater inflow to Calcasieu Lake and 18% of the total freshwater inflow to Sabine Lake.

3.2.3 Freshwater Inflow and Salinity Relations

Salinity patterns in the Calcasieu/Sabine system are influenced

Table 3-3. Ungaged freshwater inflow expressed as a percent of total freshwater inflow.

Year	Calcasieu	Sabine
1968	23.0	21.9
1969	35.3	10.8
1970	44.1	38.3
1971	22.2	24.5
1972	30.6	15.6
1973	30.7	14.2
1974	28.4	7.7
1975	15.2	14.0
1976	0.0	11.1
1977	30.9	12.5
1978	21.3	20.6
1979	39.1	15.5
1980	43.2	19.0
1981	51.7	23.1
	Average	17.8
		29.7

primarily by freshwater inflows, tidal mixing, wind induced mixing, and the salinity of Gulf water. The mean tidal range at Sabine and Calcasieu passes is approximately 0.6 m (2 ft). While this is small compared to the tidal ranges on the East and West Coast of the United States, the estuaries are large in area but shallow (1 to 2 m; 3 to 6 ft) resulting in a significant tidal exchange with the Gulf. The salinity of the offshore water will generally range from 20 to 36 o/oo. Gulf salinity is high during periods of low river discharge and low during periods of high river discharge.

Estuarine salinity near the Gulf passes vary with the stage of the tide. The influence of tidal mixing decreases with the distance away from the pass. The influence of freshwater inflow on estuarine salinity is greatest near the source of the inflow and decreases towards the Gulf. The relation between freshwater inflow and salinity developed for one area of an estuary may not be applicable for another area of the same estuary.

More information on the freshwater inflow-salinity relation was available for Sabine Lake than Calcasieu Lake. As a result the freshwater inflow-salinity relation for Sabine Lake will be discussed first.

The Texas Department of Water Resources (1981) in their report on the Sabine-Neches Estuary developed relationships between average monthly gauged freshwater inflow and the average monthly salinity for upper Sabine Lake. Salinity measurements used in the study were from a site west of station E-8 but they can be considered representative of upper Sabine Lake and of station E-8. Regression equations relating salinity to freshwater inflow were developed for each month of the

year. The equations are listed in Table 3-4. For periods of low inflow, the exponent of Q is approximately -0.6 while for periods of high inflow, the exponent of Q is approximately -1.50.

For the low flow period (July through November) the regression equations and their derivatives are:

$$\text{July } S = 8100 Q^{-0.82} \quad \Delta S/\Delta Q = 6640 Q^{-1.82}$$

$$\text{Aug. } S = 2760 Q^{-0.69} \quad \Delta S/\Delta Q = 1900 Q^{-1.69}$$

$$\text{Sept. } S = 1320 Q^{-0.58} \quad \Delta S/\Delta Q = -766 Q^{-1.58}$$

$$\text{Oct. } S = 1290 Q^{-0.58} \quad \Delta S/\Delta Q = -748 Q^{-1.58}$$

$$\text{Nov. } S = 2500 Q^{-0.64} \quad \Delta S/\Delta Q = -1600 Q^{-1.64}$$

where S is salinity in o/oo, Q is the gauged freshwater inflow in cfs, ΔS is the change in salinity in o/oo, and ΔQ is the change in gauged freshwater inflow in cfs.

The Louisiana Department of Wildlife and Fisheries conducted a study of Louisiana's major estuaries and adjacent offshore waters. The two-year study, published in April 1978, provided monthly salinity observations in the upper and lower Calcasieu Lake for the period October 1974 through September 1976. Salinity observations in upper Calcasieu Lake were taken near station E-2 (Barrett, et al, 1978).

Figure 3-13 is a log-log plot of average monthly gauged freshwater inflow into Calcasieu Lake and salinity in upper Calcasieu Lake for the low flow period of July through November. Sufficient data were not available to develop a relation between salinity and inflow for each month. The relation between salinity (S) in o/oo and inflow (Q) in cfs expressed by the straight line in the plot is:

$$S = 380 Q^{-0.52}$$

The derivative of this expression is:

Table 3-4. Salinity/Freshwater inflow regression analysis for Sabine Lake.

Month	Regression Equation S in o/oo and Q in cfs	Range of Q cfs	Standard Error of Estimate
January	$S = 920,400 Q^{-1.32}$	2,600 - 66,000	0.67
February	$S = 6,695,000 Q^{-1.54}$	4,000 - 73,000	0.73
March	$S = 2,875,000 Q^{-1.46}$	3,500 - 67,000	0.58
April	$S = 4,034,000 Q^{-1.50}$	3,000 - 90,000	0.68
May	$S = 563,000 Q^{-1.28}$	3,000 - 113,000	0.66
June	$S = 1,438,-00 Q^{-1.42}$	2,000 - 65,000	0.62
July	$S = 8,100 Q^{-0.82}$	1,000 - 26,000	0.32
August	$S = 2,760 Q^{-0.69}$	750 - 32,000	0.16
September	$S = 1,320 Q^{-0.58}$	730 - 17,000	0.24
October	$S = 1,290 Q^{-0.58}$	650 - 20,000	0.27
November	$S = 2,500 Q^{-0.64}$	1,000 - 44,000	0.33
December	$S = 93,000 Q^{-1.06}$	2,500 - 92,000	0.65

From SABINE-NECHES ESTUARY: A Study of the Influence of Freshwater Inflows.
Texas Department of Water Resources, LP-116, July 1981.

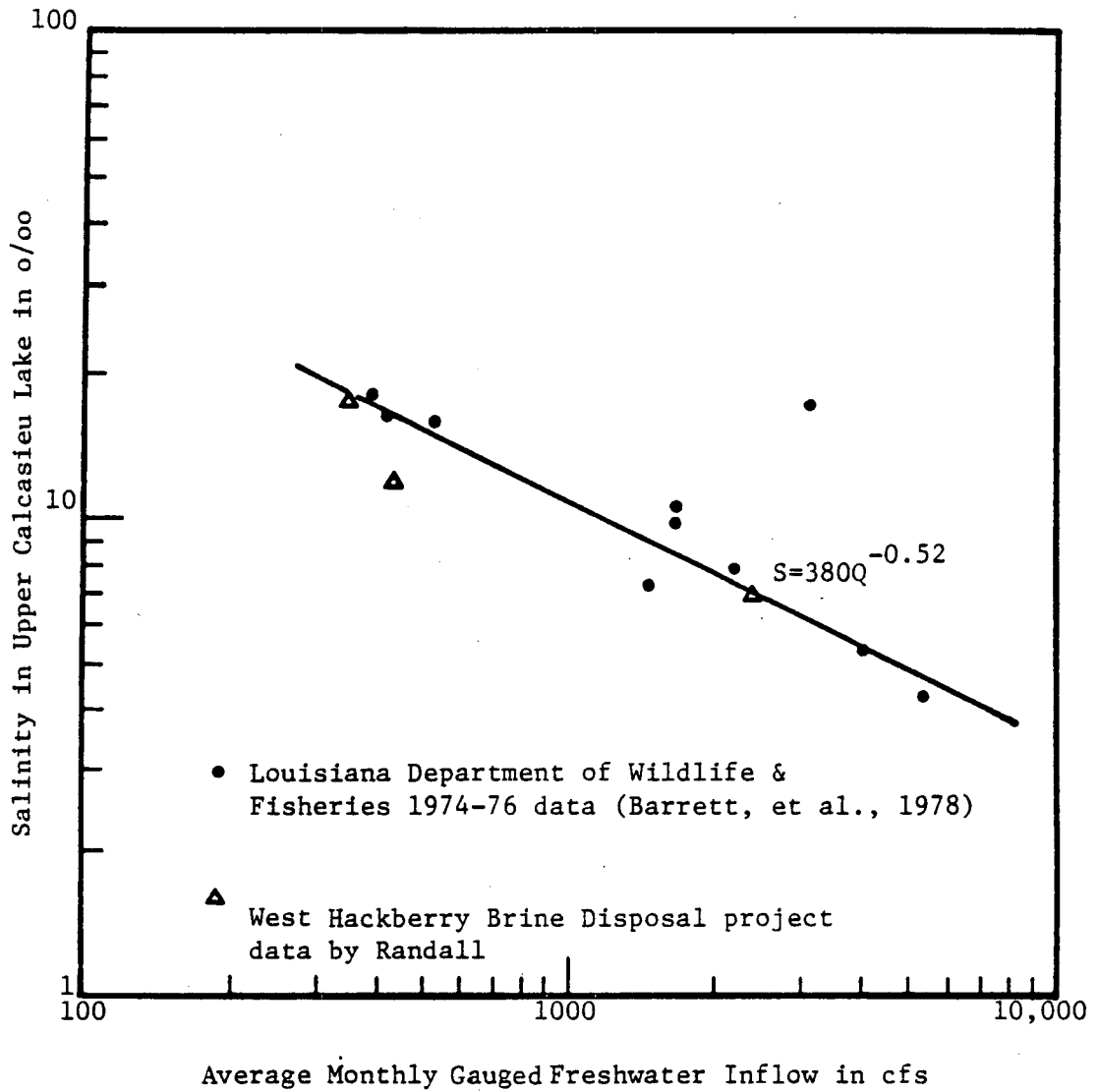


Figure 3-13. Log-log plot of average monthly gauged freshwater inflow into Lake Calcasieu and salinity in upper Calcasieu Lake for the low flow period of July through November.

$$= -198 Q^{-1.52}$$

The West Hackberry project will pump various amounts of freshwater from the Calcasieu/Sabine system. During periods of high freshwater inflow, the project will have no measureable impact on salinity. However, during periods of low freshwater inflow, the project might have an observable impact on salinity.

A significant change in salinity is difficult to define because it depends on many factors. However, for the purpose of this discussion, a significant change in salinity is defined simply as an observable change that could be detected with normal instrumentation.

If 0.1 o/oo change in salinity is considered significant, the critical low freshwater inflow can be computed from the above equations relating change in inflow to change in salinity. Critical low freshwater inflow is defined as the average monthly gauged inflow below which freshwater diversion will cause a significant change in salinity.

Natural salinity variations of several o/oo occur in the estuaries and a change in salinity of 0.1 o/oo may not represent an observable or significant change. Low freshwater inflow rates (Q_L) were computed for several changes in salinity (ΔS) and diversions (ΔQ).

Critical low flows for Calcasieu Lake and Sabine Lake are listed in Tables 3-5 and 3-6, respectively. The critical low flows were computed for freshwater diversions ranging from 0.14 to 1.8 cms (5 to 65 cfs) and changes in salinity of 0.1, 1.0 and 2.0 o/oo. The percent of time during the dry period of the year that the gauged freshwater inflow is less than the critical low flow value is also listed in the

Table 3-5. Critical low flows for Calcasieu Lake and percent of time during the dry period (July-November) that flow is less than critical.

Freshwater Diversion Calcasieu Lake (ΔQ) cms (cfs)	$\Delta S = 0.1$ o/oo		$\Delta S = 1$ o/oo		$\Delta S = 2$ o/oo	
	Low Gaged Inflow ¹ (Q_L) cms (cfs)	% Time July- Nov. Flow < ²	Low Gaged Inflow ¹ (Q_L) cms (cfs)	% Time July- Nov. Flow < ²	Low Gaged Inflow ¹ (Q_L) cms (cfs)	% Time July- Nov. Flow < ²
1.84 (65)	66.7 (2357)	87	14.6 (516)	44	9.2 (326)	26
1.55 (55)	59.7 (2111)	85	13.1 (462)	40	8.3 (292)	18
1.28 (45)	52.3 (1849)	82	11.5 (405)	34	7.2 (256)	8
0.99 (35)	44.3 (1566)	79	9.7 (343)	27	6.1 (217)	0
0.71 (25)	35.5 (1254)	73	7.7 (274)	14	4.9 (174)	0
0.43 (15)	25.3 (895)	64	5.5 (196)	0	3.5 (124)	0
0.14 (5)	12.3 (434)	37	2.7 (95)	0	1.7 (60)	0

$${}^1Q_L = (198 \frac{\Delta Q}{\Delta S})^{0.66} \text{ where flow is in cfs}$$

²From Figure 3-4

Table 3-6. Critical low flows for Sabine Lake and percent of time during the dry period (October-November) that flow is less than critical.

Freshwater Diversion Sabine L. (ΔQ) cms (cfs)	$\Delta S = 0.1$ o/oo		$\Delta S = 1$ o/oo		$\Delta S = 2$ o/oo	
	Low Gaged Inflow ¹ (Q_L) cms (cfs)	% Time Oct.- Nov. Flow < ²	Low Gaged Inflow ¹ (Q_L) cms (cfs)	% Time Oct.- Nov. Flow < ²	Low Gaged Inflow ¹ (Q_L) cms (cfs)	% Time Oct.- Nov. Flow < ²
1.84 (65)	122.7 (4330)	47	29.5 (1040)	11	19.3 (680)	5
1.55 (55)	110.5 (3900)	42	26.6 (940)	9	17.3 (610)	4
1.28 (45)	99.8 (3450)	37	23.5 (830)	8	15.3 (540)	2
0.99 (35)	83.6 (2950)	31	20.1 (710)	6	13.0 (460)	0
0.71 (25)	67.7 (2390)	25	16.2 (570)	2	10.5 (370)	0
0.43 (15)	49.3 (1740)	19	11.9 (420)	0	7.7 (270)	0
0.14 (5)	24.9 (880)	8	6.0 (210)	0	4.0 (140)	0

$${}^1Q_L = 0.5 \left(748 \frac{\Delta Q}{\Delta S} \right)^{0.633} + 0.5 \left(1600 \frac{\Delta Q}{\Delta S} \right)^{0.610}$$

²From Figure 3-6

tables.

3.2.4 Raw Water Diversion from the Intracoastal Waterway

The West Hackberry project will divert various amounts of water from the ICWW at the pumping plant located approximately 12.1 km (7.5 mi) west of Calcasieu Lake and 24.1 km (15 mi) east of Sabine River. The maximum project diversions from the ICWW is expected to be 1.98 cms (70 cfs, 1.08 million barrels per day (MBD)). The amount of water that is diverted from the ICWW is relatively small in comparison to the flow in the ICWW. When the net flow in the ICWW is from Sabine River to Calcasieu Lake, the water that will be diverted from the system is from the Sabine River but this water also represents ungauged inflow that will be diverted primarily from the Calcasieu Estuary. When the pumps are started, the water surface elevation in the ICWW at the pumping station will be drawn down such that the change in flow from the Sabine River plus the change in flow from Calcasieu Lake is equal to the amount of water being pumped. When the flow in the ICWW is from Sabine to Calcasieu, the flow from Sabine River is increased by approximately 35% of the amount of flow being pumped and the flow into Calcasieu Lake is decreased by approximately 65% of the amount of flow being pumped. Thirty-five percent of the pumped water is diverted from the Sabine River and 65% is diverted from Calcasieu Lake. If the net flow in the ICWW is towards the west before the pumps are started, then after the pumps are started, the flow in the ICWW east of the pumping station would be increased by 65% of the pumping rate and the flow in the ICWW west of the pumping station would be decreased by 35% of the pumping rate. Again, approximately 65% of the pumped water will be diverted from the Calcasieu system and 35% from the Sabine system.

The direction of flow in the ICWW should not affect the amount of water being diverted from Calcasieu Lake of the Sabine River.

3.2.5 Impact of Diversions from the ICWW on the Salinity in Upper Calcasieu and Sabine Lakes

Water diverted from the ICWW at the pumping plant will include both freshwater and Gulf water. During the low freshwater inflow period, the salinity of the pumped water will be high. During this period there is little freshwater flowing directly into the ICWW and the salinity at the pump intake is expected to be nearly the same as that in the upper Calcasieu Lake or upper Sabine Lake. The salinity and % freshwater in the diverted water is estimated in Table 3-7. The salinity can be expected to vary from about 3 o/oo to about 24 o/oo during the dry season.

The estimated changes in salinity for the upper Calcasieu Lake and upper Sabine Lake caused by pumping water from the ICWW are listed in Tables 3-8 and 3-9. Table 3-8 is for a diversion of 1.98 cms (70 cfs, 1.08 MBD) and Table 3-9 is for a diversion of 1.42 cms (50 cfs, 0.77 MBD). It can be observed that only in Calcasieu Lake is the change in salinity expected to be more than 0.1 o/oo. The maximum increase in salinity is estimated at 0.45 o/oo and is expected to occur with a diversion of 1.98 cms (70 cfs, 1.08 MBD) and an average monthly gauged freshwater inflow to Calcasieu Lake of 9.07 cms (320 cfs). A gauged inflow of 9.07 cms (320 cfs) or less is expected to occur approximately 20% of the time during the low flow period of July through November. If the diversion is 1.42 cms (50 cfs, 0.77 MBD), the maximum increase in salinity in the upper Calcasieu Lake is estimated at 0.32 o/oo. For a diversion of 1.42 cms (50 cfs, 0.77 MBD), the

Table 3-7. Estimated salinity of the diverted water.

% Time Inflow Less Than ¹	Calcasieu Lake		Sabine Lake		Estimated Salinity of Div. Water (o/oo)	Freshwater ⁶ %
	Inflow ² (cfs)	Salinity ³ (o/oo)	Inflow ⁴ (cfs)	Salinity ⁵ (o/oo)		
10	270	23	1000	27	24	31
20	320	21	1800	19	20	43
30	390	18	2800	14	17	51
40	480	15	3700	12	14	60
50	640	13	4500	11	13	63
60	850	11	5100	10	11	68
70	1170	10	5800	9	10	71
80	1750	8	6800	8	8	77
90	3200	6	9500	7	6	83
100	8500	3	24000	4	3	91

¹Percent of time during the low flow period that the average monthly gaged freshwater inflow is less than the value indicated.

²Average monthly gaged freshwater inflow from Figure 3-4.

³Salinity in Upper Calcasieu Lake = $380 Q^{-0.52}$.

⁴Average monthly gaged freshwater inflow from Figure 3-6.

⁵Salinity in Upper Sabine Lake = $645 Q^{-0.58} + 1250 Q^{-0.64}$.

⁶Percent freshwater based on a Gulf salinity of 35 o/oo.

Table 3-8. Estimated change in salinity caused by pumping 70 cfs water from the Intracoastal Waterway

% Time Gaged Inflow Less Than	Salinity Diverted Water (o/oo)	ΔQ_f (cfs)	ΔQ_g (cfs)	Calcasieu Lake				Sabine Lake			
				Q_{cig} (cfs)	ΔQ_c (cfs)	ΔQ_{cg} (cfs)	ΔS_c (o/oo)	Q_{sig} (cfs)	ΔQ_s (cfs)	ΔQ_{sg} (cfs)	ΔS_s (o/oo)
10	24	21.7	48.3	270	14.1	9.9	0.42	1000	7.6	6.2	0.09
20	20	30.1	39.9	320	19.6	13.7	0.45	1800	10.5	8.6	0.05
30	17	35.7	34.3	390	23.2	16.2	0.39	2800	12.5	10.2	0.02
40	14	42.0	28.0	480	27.3	19.1	0.32	3700	14.7	12.1	0.02
50	13	44.1	25.9	640	28.7	20.1	0.22	4500	15.4	12.6	0.018
60	11	47.6	22.4	850	30.9	21.6	0.15	5100	16.7	13.7	0.016
70	10	49.7	20.3	1170	32.3	22.6	0.10	5800	17.4	14.3	0.014
80	8	53.9	16.1	1750	35.0	24.5	0.06	6800	18.9	15.5	0.012
90	6	58.1	11.9	3200	37.8	26.5	0.02	9500	20.3	16.6	0.007
100	3	63.7	6.3	8500	41.4	29.0	0.006	24000	22.3	18.3	0.002

3-38

Q_{cig} = gaged freshwater inflow to Calcasieu.

Q_{sig} = gaged freshwater inflow to Sabine.

ΔQ_f = amount of freshwater diverted from the ICH.

ΔQ_g = amount of Gulf water diverted from the ICH.

ΔQ_c = amount of freshwater diverted from Calcasieu = $0.65\Delta Q_f$.

ΔQ_{cg} = amount of gaged freshwater diverted from Calcasieu = $0.70\Delta Q_c$.

ΔS_c = $190 \Delta Q_{cg} Q_{cig}^{-1.52}$ = change in salinity in the upper Calcasieu Lake.

ΔQ_g = amount of freshwater diverted from Sabine = $0.35\Delta Q_f$.

ΔQ_{sg} = amount of gaged freshwater diverted from Sabine = $0.82 \Delta Q_g$.

ΔS_s = $374 \Delta Q_{sg} Q_{sig}^{-1.58} + 800 \Delta Q_{sg} Q_{sig}^{-1.64}$ = change in salinity in upper Sabine Lake.

Table 3-9. Estimated change in salinity caused by pumping 50 cfs of water from the Intracoastal Waterway.

% Time Gaged Inflow Less Than	Salinity Diverted Water (o/oo)	ΔQ_f (cfs)	ΔQ_g (cfs)	Calcasieu Lake				Sabine Lake			
				Q_{cig} (cfs)	ΔQ_c (cfs)	ΔQ_{cg} (cfs)	ΔS_c (cfs)	Q_{sig} (cfs)	ΔQ_s (cfs)	ΔQ_{sg} (cfs)	ΔS_s (cfs)
10	24	15.5	34.5	270	10.1	7.1	0.31	1000	5.4	4.4	0.07
20	20	21.5	28.5	320	15.0	10.5	0.32	1800	8.1	6.6	0.04
30	17	25.5	24.5	390	17.6	12.3	0.28	2800	9.5	7.8	0.02
40	14	30.0	20.0	480	19.5	13.7	0.23	3700	10.5	8.6	0.017
50	13	31.5	18.5	640	20.5	14.4	0.15	4500	11.0	9.0	0.013
60	11	34.0	16.0	850	22.1	15.5	0.11	5100	11.9	9.8	0.012
70	10	35.5	14.5	1170	23.1	16.2	0.07	5800	12.4	10.2	0.010
80	8	38.5	11.5	1750	25.0	17.5	0.04	6800	13.5	11.1	0.008
90	6	41.5	8.5	3200	27.0	18.9	0.02	9500	14.5	11.9	0.005
100	3	45.5	4.5	8500	29.6	20.7	0.004	24000	15.9	13.0	0.0013

3-39

Q_{cig} = gaged freshwater inflow to Calcasieu.

Q_{sig} = gaged freshwater inflow to Sabine.

ΔQ_f = amount of freshwater diverted from the ICW.

ΔQ_g = amount of Gulf water diverted from the ICW.

ΔQ_c = amount of freshwater diverted from Calcasieu = $0.65\Delta Q_f$.

ΔQ_{cg} = amount of gaged freshwater diverted from Calcasieu = $0.70\Delta Q_c$.

ΔS_c = $198 \Delta Q_{cg} Q_{cig}^{-1.52}$ = change in salinity in the upper Calcasieu Lake.

ΔQ_s = amount of freshwater diverted from Sabine = $0.35\Delta Q_f$.

ΔQ_{sg} = amount of gaged freshwater diverted from Sabine = $0.82 \Delta Q_s$.

ΔS_s = $374 \Delta Q_{sg} Q_{sig}^{-1.58} + 800 \Delta Q_{sg} Q_{sig}^{-1.64}$ = change in salinity in upper Sabine Lake.

increase in salinity in the upper Calcasieu Lake is expected to be greater than 0.1 o/oo approximately 60% of the time during the low flow period of July through November.

Figure 3-14 shows the expected increase in salinity for upper Calcasieu Lake as a result of pumping 1.98 cms (70 cfs, 1.08 MBD) and 1.42 cms (50 cfs, 0.77 MBD) from the ICWW. When the freshwater inflow is zero, the water pumped from the ICWW is from the Gulf and there is no increase in salinity. Maximum increase in salinity should occur when the average monthly gauged freshwater inflow to Calcasieu Lake is approximately 9.5 cms (300 cfs).

3.2.6 Salinity Model of Calcasieu Lake

A salinity model of Calcasieu Lake was developed to evaluate the change in salinity caused by pumping from the ICWW. A schematic diagram of the model is shown in Figure 3-15. The model includes seven nodes and seven reaches. Node 1 represents the Gulf of Mexico where the Corps of Engineers has a tide gauge. Reach 13 and reach 14 represent Calcasieu Lake and reach 12 represents West Cove. Reaches 11, 15, and 17 represent the ship channel from the Gulf past West Hackberry to the salt water barrier at Lake Charles. The pump is considered a negative lateral inflow to the ICWW (reach 16). The geometry of the system is described by cross-sections in each reach.

Inflow and discharge to the model occur at node 1 (Gulf), node 6 (Sabine River), and node 7 (salt water barrier). Node 3 at the end of West Cove was described as a zero flux node in the model. The USGS daily streamflow records were used to get the freshwater inflow at node 7. Gulf salinity values were measured by the project (Kelly) and along with the Corps of Engineer tidal data were required input for

Percent of Time During the Low Flow Period (July-November) that Inflow is Less Than Indicated Value

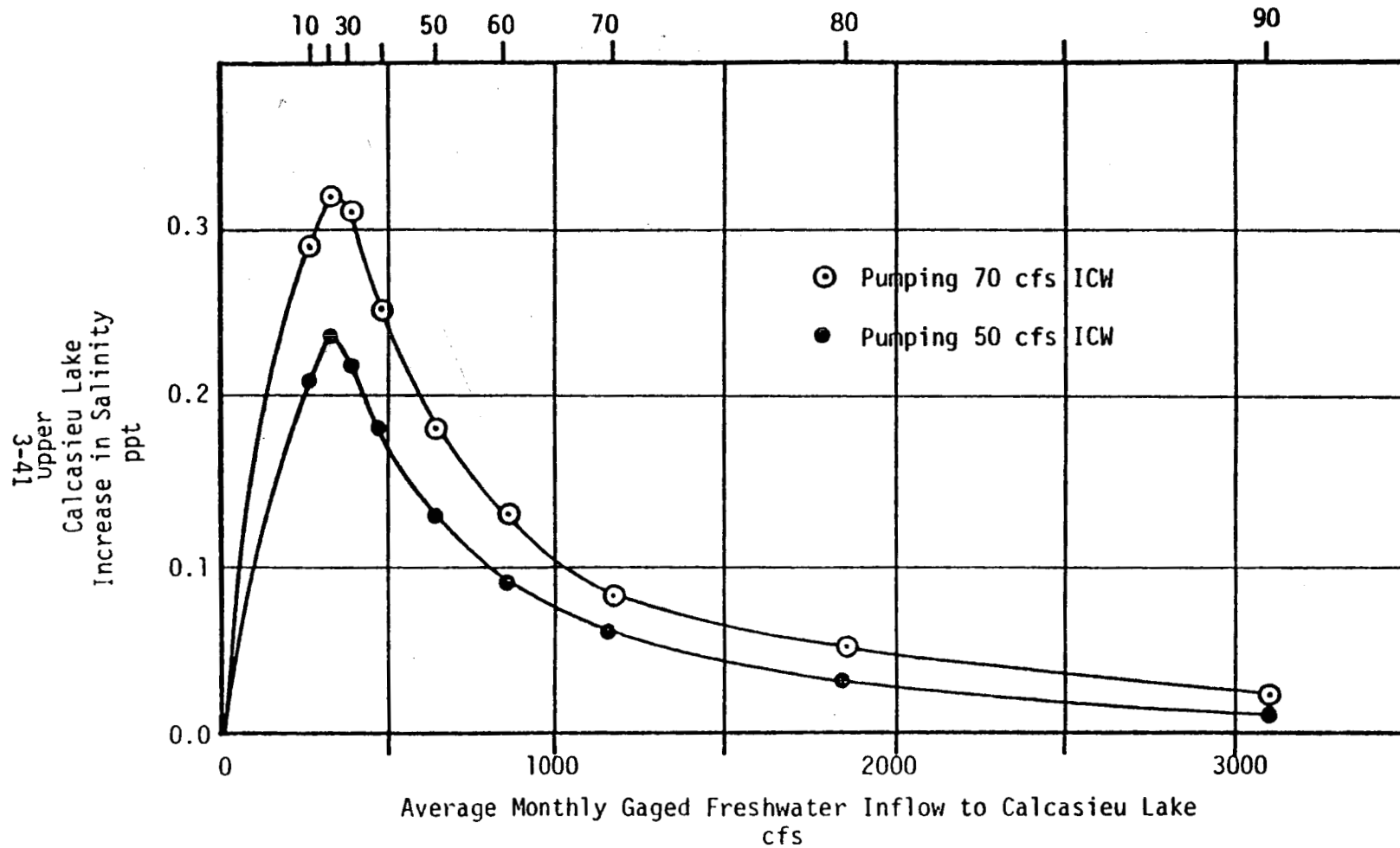


Figure 3-14. Estimated increase in salinity for Upper Calcasieu Lake.

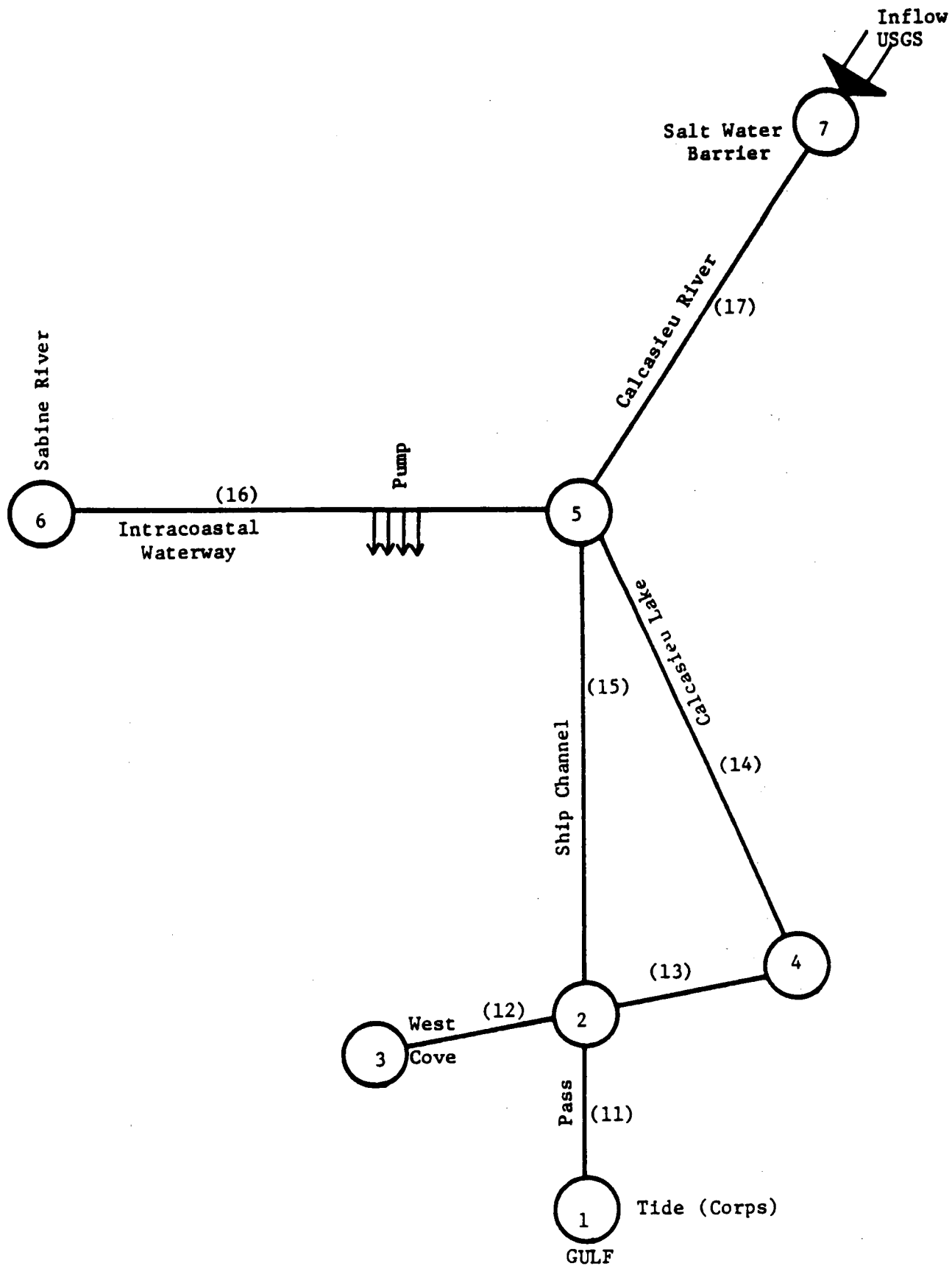


Figure 3-15. Calcasieu Lake salinity model.

node 1. Water level data from our TDR-1 installed at station E-7 provided the tidal data for node 6. Monthly salinity observations by the project (Randall) at E-7 provided salinity data at node 6 for the selected runs of the model included in this report. 1981 Corps of Engineers tidal records for Cameron, West Hackberry, and Calcasieu Locks are included in Appendix Figure C-6.

The model was run for seven days in 1981. The measured (Corps of Engineers data, Appendix Figure C-6) and computed (model) water surface elevations at Calcasieu Locks are plotted in Appendix Figure C-7. The water levels compare reasonably well. The measured (Kelly) and computed (model) current in Calcasieu Pass also compare reasonably well as shown in Appendix Figure C-8. The measured current represents the water current at one point in the pass and may not represent the average current for the cross-section. The computed water current for July 4, 1981, did not compare with the measured current because the tide gauge at Cameron was not operating correctly from July 3 to July 16 (see Appendix Figure C-6).

The computed salinity values with the pump off, pumping 1.42 cms (50 cfs, 0.77 MBD), and pumping 1.98 cms (70 cfs, 1.08 MBD) are tabulated in Table 3-10. In general, the increases in salinity values are greatest at the pump (station E-1) and in the upper ship channel (node 5). The change in salinity in the lower Calcasieu Lake (stations E-3 and E-4) was generally in the order of 0.001 o/oo. The model indicated that the increase in salinity in upper Calcasieu Lake (station E-2) will be less than the value estimated from Figure 3-13 while the increase in salinity for the upper ship channel and ICWW (station E-1 and node 5) will be about equal to that estimated from

Table 3-10. Summary of model results.

Date (1981)	Calcasieu River Inflow (cfs)		cfs	(1) Computed Salinity Values (o/oo)					(2) ICWW Computed Discharge cfs	(3) Estimated Increase in Salinity o/oo
	Daily	Monthly Average		E-1	E-2	E-3	E-4	Node 5		
March 8	5137	1761	0	17.468	13.316	29.415	26.386	13.946	-1064	0.00
			50	17.784	13.398	29.415	26.388	13.936		0.04
			70	17.914	13.432	29.418	26.239	13.937		0.06
May 22	740	791	0	13.652	17.548	25.038	23.019	20.114	1079	0.00
			50	13.817	17.570	25.034	23.002	20.611		0.11
			70	13.904	17.561	25.031	22.995	20.800		0.15
June 12	11446	5291	0	5.941	2.284	18.340	15.461	2.547	-58	0.00
			50	5.929	2.286	18.340	15.465	2.531		0.01
			70	5.930	2.287	18.341	15.466	2.525		0.01
July 4	2328	2494	0	0.987	1.666	10.677	8.594	1.689	1989	0.00
			50	1.010	1.709	10.678	8.597	1.734		0.02
			70	1.021	1.726	10.678	8.599	1.753		0.03
Aug. 8	630	410	0	4.699	4.994	14.572	11.997	7.862	-947	0.00
			50	4.896	4.987	14.574	11.999	7.837		0.25
			70	4.980	4.984	14.574	12.001	7.892		0.35
Sept. 12	341	365	0	18.025	16.679	20.802	19.747	17.789	-1295	0.00
			50	18.418	16.649	20.804	19.750	17.805		0.30
			70	18.570	16.637	20.805	19.751	17.819		0.40
Nov. 11	885	---	0	10.571	13.151	25.801	23.948	16.500	1303	----
			50	10.672	13.126	25.798	23.951	16.895		----
			70	10.719	13.109	25.798	23.951	17.051		----

(1) Average of 96 computed values during 24-hour period.

(2) Average discharge over 24-hour period. Plus is east into Calcasieu Lake.

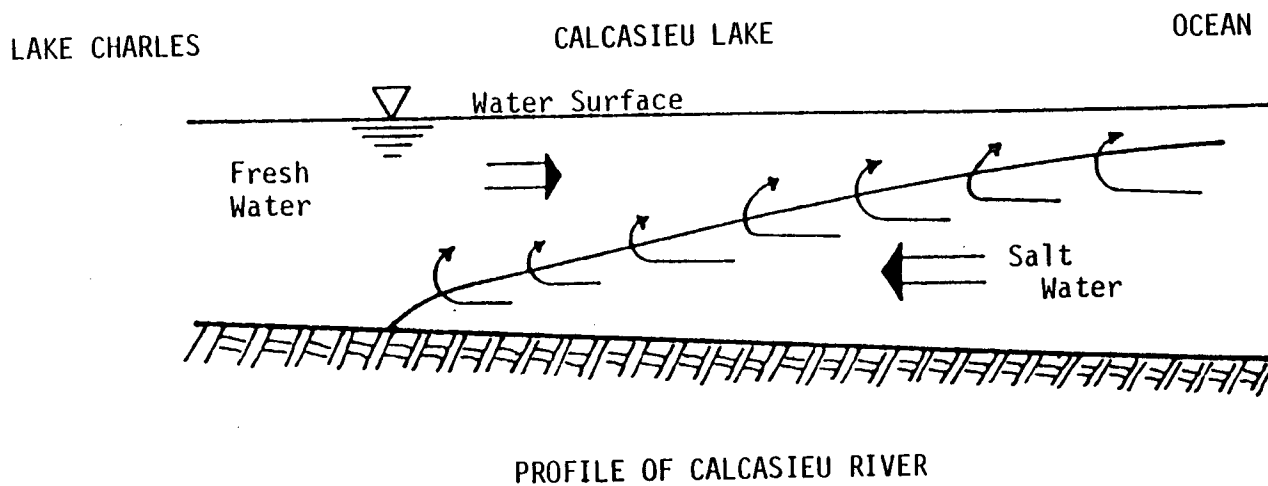
(3) Estimated from Figure 3-13 based on average monthly gaged inflow.

Figure 3-14. Appendix Figure C-9 includes plots of time versus salinity while pumping 0, 1.42, and 1.98 cms (0, 50, and 70 cfs; 0, 0.77, and 1.08 MBD) for lower Calcasieu Lake (stations E-3 and E-4) and upper Calcasieu Lake (stations E-1 and E-2).

3.2.7 Salt Water Wedge in Calcasieu River

As shown in Figure 3-16, the salt water wedge from the Gulf extends up the Calcasieu River. The position of the salt water wedge depends on the size of the channel and the freshwater discharge rate. Salt water intrusion in the Calcasieu River apparently became a problem when the Corps of Engineers completed the 9.1 m deep by 76 m wide (30 ft by 250 ft) wide Calcasieu Ship Channel in 1941. After the channel was enlarged, a freshwater flow of approximately 230 cms (8,000 cfs) was required to hold the salt water wedge below Lake Charles. A salt water barrier was completed in 1968 to prevent the salt water from extending above Lake Charles. The barrier included a gated overflow section and a navigational gate 17 m (56 ft) wide and 4 m (13 ft) deep. The navigational gate is opened for all boat traffic so the barrier is not 100% effective.

The pumping of water from the ICWW should not change the position of the salt water wedge. As the salt water from the Gulf of Mexico moves along the bottom of the ship channel upstream through Calcasieu Lake, some surface water mixes with the bottom water, and the salt water wedge becomes less saline. As a result of pumping from the ICWW, the surface water that mixes with the salt water wedge has a higher salinity and the salt water wedge that reaches the salt water barrier at Lake Charles would have a higher salinity. The increase in salinity of the salt water wedge should be very small.



3-46

Figure 3-16. Salt water intrusion in the Calcasieu River.

The salinity model developed for Calcasieu Lake is a one-dimensional model and cannot be used to evaluate a stratified flow. To provide a rough estimate of the magnitude of the salinity increase, a simplified example follows based on the following assumptions:

1. The salinity of the salt water at Cameron is 30 o/oo.
2. The salinity of the salt water swedge at Lake Charles is 20 o/oo.
3. The salinity of the surface water is as follows:
 - a. Reach 11 (pass) 25 o/oo
 - b. Reach 15 (ship channel) 20 o/oo
 - c. Reach 17 (Calcasieu River) 10 o/oo
4. The mixing rate between the surface water and the salt water wedge is uniform along the length.
5. As a result of pumping from the ICWW, the surface water in the upper half of reach 15 (ship channel) increases from 20.0 o/oo to 20.2 o/oo.
6. The thickness of the salinity wedge decreases from 12 m (40 ft) at node 1 to 10 m (32 ft) at node 2, 4.6 m (15 ft) at node 5, and 2.4 m (8 ft) at node 7.

Based on these assumptions, the salinity of the salt water wedge at Lake Charles would increase 0.01 o/oo as a result of pumping from the ICWW.

3.3 Estuarine Hydrography

3.3.1 General Comments

The estuarine hydrography of Lake Calcasieu, Lake Sabine, and the Intracoastal Waterway was studied prior to brine disposal by

collecting monthly conductivity, temperature, depth, and dissolved oxygen (CTD/DO) data at the ten stations previously shown in Figure 3-1 (Section 3.1) and the results were described in the predisposal report by Randall and James (1981a). CTD/DO data at these same stations have continued to be collected on a monthly basis since the initiation of brine discharge in May of 1981. The purpose of this section is to discuss the results of the estuarine data which were collected during the first twelve-month postdisposal period from May 1981 through April 1982 and to evaluate the impact of the brine discharge on the estuarine system. The instrumentation and sampling procedures are briefly summarized, and a more detailed description may be found in the West Hackberry Field and Laboratory Procedures Manual (Hann and Giamonna, 1981).

3.3.2 Description of Instrumentation

A Hydrolab 8000 CTD/DO instrument (Hydrolab, 1980) has been used for the collection of the estuarine CTD/DO data. This instrument consists of a data transmitter (probe), data bus cable (conductor cable), and a data control unit (remote readout). The probe is capable of measuring conductivity (0-200 mmho/cm), depth (0-200 m), temperature (-5 to +45°C), dissolved oxygen (0-20 mg/l), and pH/ORP.

The accuracy of the conductivity sensor (four electrode type) is +/- 0.5% of full scale which corresponds to +/- 1 mmho/cm or +/- 0.7 o/oo. The conductivity sensor accuracy is improved to at least +/- 0.5 o/oo by calibrating it with standard solutions using a Grundy laboratory salinometer which has an accuracy of +/- 0.003 o/oo (Grundy, 1978). The temperature and depth sensors have an accuracy of +/- 0.2 °C and +/- 1 m. The dissolved oxygen sensor was calibrated

before and after each field trip against water saturated air and Winkler analysis of selected water samples. The remote readout device displays digitally the conductivity to 0.1 mmho/cm, the temperature to 0.1°C, the depth to 0.1 m, and dissolved oxygen to 0.01 mg/l.

3.3.3 Conversion and Calibration of Data

The conductivity data from the CTD/DO instrument are corrected to a temperature of 25°C by an internal compensation circuit. The conductivity data collected were then converted to salinity using

$$S = 1.80655 \times 10^6 \frac{\log_{10} C - 0.57627}{0.892} \quad (3-1)$$

after Weyl (1964), where C is the conductivity in mmho/cm at 25°C. The salinity data were then corrected as required by the calibration results.

The temperature data were used as read from the instrument because calibration checks showed these data were within the manufacturer's accuracy specifications. The depth sensor was adjusted to zero in the laboratory, but the depth measurements frequently required a correction which was determined by a surface measurement and a bottom measurement which was checked with the ship's depth sounder and the marked winch or lifting line.

Selected water samples were taken in conjunction with the dissolved oxygen measurements and these samples were chemically preserved onboard ship. A Winkler analysis of the water samples was completed later in the laboratory, and the results were used to correct the dissolved oxygen data measured with the CTD/DO instrument.

The salinity, temperature, and depth data were used to compute the density of the water column using the equation of LaFond (1951).

These density data are presented in the customary oceanographic form of sigma-t (σ_t) which is defined as

$$\sigma_t = (\rho - 1) \times 10^3 \quad (3-2)$$

where the density (ρ) is expressed in gm/cm³.

3.3.4 Sampling Procedures

The CTD/DO measurements at the estuarine stations E-1 through E-10 were conducted once a month on a one day cruise using the Hydrolab 8000 CTD/DO system. The CTD/DO data were collected at one meter above the bottom, mid-depth, and one meter below the surface except at shallow water stations in the lakes (E-2, E-3, E-4, E-8, E-9 and E-10) where only near bottom and near surface measurements were made. The data were recorded in a bound field data book, and it was returned to the laboratory along with the instrument for further data analysis and calibration.

3.3.5 Estuarine Hydrographic Data Results

3.3.5.1 Calcasieu Lake

The hydrographic data from Calcasieu Lake which were collected from May 1981 through April 1982 are tabulated in Appendix Table C-5. These data were collected at station E2 located in the north end of the lake (Figure 3-1) and at stations E3 and E4 situated in the southern portion of the lake on the east and west side respectively.

In May 1981, the estuarine data was collected on May 22 which was after brine discharge was initiated on May 10. The data show the salinity at E3 and E4 was 26.7 and 26.8 o/oo from top to bottom and at E2 it was 20.9 o/oo. These data show the salinity in the southern portion increased over that measured in April 1981 (Randall and James,

1981), and in the northern portion the water was fresher (20.9 o/oo) and also fresher than that found in April 1981. The temperature increased from nearly 21°C in April 1981 to nearly 23°C. There was no evidence of a thermocline and the warmest water was found at E2 (23.4°C). The dissolved oxygen data was near 7.5 mg/l over the entire lake which was nearly the same as that found in April 1981.

The salinity data collected during the summer months of 1981 from Calcasieu Lake show a freshening trend in June as the salinity in the northern lake (E2) dropped to 16 o/oo while in the southern portion (E3 and E4) the salinity was near 21 o/oo. Again, the salinity was very nearly the same from top to bottom. This freshening trend continued into July when the freshest measurements were made on July 2 with values of 7.2 and 11.6 o/oo at E2 and E4. Station E3 was not measured on the July cruise. In August, the lake showed a trend toward saltier water. Station E2 had a salinity of 11.7 o/oo, and the salinity at E3 was 15.1 o/oo. At station E4, salinity stratification was present with a surface salinity of 13.9 o/oo and bottom salinity of 16.4 o/oo.

The temperature data show the temperature increased to 29.3°C in June and it continued to increase to 30.5°C in August. Station E4 showed the presence of a thermocline on August 5 with a surface temperature of 29.6°C and bottom temperature of 30.3°C. This thermocline was most likely due to the tidal intrusion of Gulf water into the lower lake.

The dissolved oxygen data indicate a trend toward lowered dissolved oxygen in the lake waters. The lake water contained near 6.0 mg/l in June, 5.5 mg/l in July, and back to near 6.0 mg/l in August.

The vertical and horizontal distribution of dissolved oxygen was nearly constant except for station E4 on August 6. On this occasion, the surface waters had 5.7 mg/l while the bottom waters had 1.3 mg/l which indicates anoxic conditions. The low dissolved oxygen reading at this station is attributed to the intrusion of Gulf waters which were experiencing low dissolved oxygen at that time (see Section 2.2). However, the data from Calcasieu Pass did not show the bottom waters were anoxic so it is also possible that the data point is in error.

During the fall of 1981, the overall lake salinity continued to increase with a value near 18 o/oo in September. In October and November, the salinity at E4 (approximately 19.7 o/oo) was less than E2 (21.2 o/oo) and E3 (23.0 o/oo) which is attributed to the intrusion of fresher Gulf waters during this period. The salinity at E3 was also higher than at E4 during this time which may indicate the flushing of the west cove is slower than the east cove.

The temperature of Calcasieu Lake decreased to near 25°C in September and continued this trend through November when the temperature reached 17°C at E2, 15.5°C at E3 and E4 on November 11. The dissolved oxygen remained near 6.0 mg/l in September, and it began to increase in October and reached a value near 8.0 mg/l in November.

During the month of December, the salinity reached a value near 23.5 o/oo in the southern part of the lake and 21.5 o/oo in the northern part. The salinity at all stations decreased to near 18.5 o/oo in January 1982 and then increased to 22 o/oo at E3 and E4 and to 19.5 o/oo at E2 in February.

The temperature in December was nearly the same as that in November, but in January it dropped to 5.0°C at E4 and 8.0°C at E2.

In February, the temperature increased to near 10°C. During the winter months, the vertical temperature distribution was nearly always isothermal, but the horizontal variation showed that the water in the northern part of the lake was warmer than the southern part.

The December dissolved oxygen data show a variation from 7.5 mg/l at E4 and 8.8 mg/l at E3 to 10.2 mg/l at E2. In January, it reached 11.2 mg/l at E4 and was again near 10 mg/l at E2. Dissolved oxygen was near 9.2 mg/l at E2 and E4 and 10.4 mg/l at E3 on February 12. Thus, the dissolved oxygen was highest during the winter months.

The salinity dropped to near 17 o/oo in the southern portion of the lake in March and near 11.7 o/oo in the northern portion which was the beginning of the annual spring freshening of the lake due to runoff. The salinity continued to decrease in April with values of 14.1 o/oo at E3 and near 3 o/oo at E2. At E4, the surface salinity was 10.8 o/oo and the bottom salinity was 17.6 o/oo which is a large variation and attributed to intrusion of Gulf waters at the bottom.

The temperature rose sharply in March to near 21°C with a slight thermocline at each station. The largest temperature difference occurred at E2 where the surface temperature was 20.8°C and the bottom temperature was 19.7°C. In April, the temperature increased slightly to 21°C at E4, 22°C at E3 and 20°C at E2, and the vertical temperature variation was slight (approximately 0.6°C).

The dissolved oxygen varied from near 10 mg/l at E4 and E3 to 7.0 mg/l at E3 in March. Station E2 showed a vertical variation of 8.1 mg/l at the bottom to 10.4 mg/l at the surface. In April, the dissolved oxygen dropped to values near 8.0 mg/l at E3 and E4 and 5.3 mg/l at E2, and the vertical variation was less than that measured in

March.

3.3.5.2 Calcasieu Pass

Monthly CTD/DO measurements were taken at station E5 in the Calcasieu Pass. This station is located on the east side of the ship channel in 7.0 m of water, and it is the same location as site P where continuous CTD data were collected. The results of the continuous CTD data are described in Chapter 2 of this report. The monthly data were collected at 1 m above the bottom, every 3 m, and 1 m below the surface, and the tabulated results are contained in Appendix Table C-6.

After brine discharge was initiated in May 1981, the monthly CTD/DO data at the Calcasieu Pass station was collected on May 22. These data show salinity, temperature, and dissolved oxygen were nearly constant from top to bottom with values of 26.3 o/oo, 23.9°C, and 8.3 mg/l. In June, the data show a vertical variation when the salinity at E5 varied from 19.7 o/oo at the surface to 24.3 o/oo at the bottom, as shown in Figure 3-17. The temperature continued its normal annual increase to 29.0°C at the surface and 28.8°C at the bottom. The dissolved oxygen dropped to 5.5 mg/l at the surface and 4.7 mg/l at the bottom. The July salinity data showed the pass water was fresher with a value of 12.9 o/oo at the surface and 13.7 o/oo near the bottom. The temperature was essentially isothermal at 30.3°C and the dissolved oxygen was 6.1 mg/l at the top and 6.7 mg/l at the bottom. In August, the salinity increased slightly to 16.0 o/oo at the surface and 16.9 o/oo at the bottom (Figure 3-17) and the temperature was again essentially isothermal at 30.5°C. The dissolved oxygen was also constant from top to bottom with a value of 5.7 mg/l. During

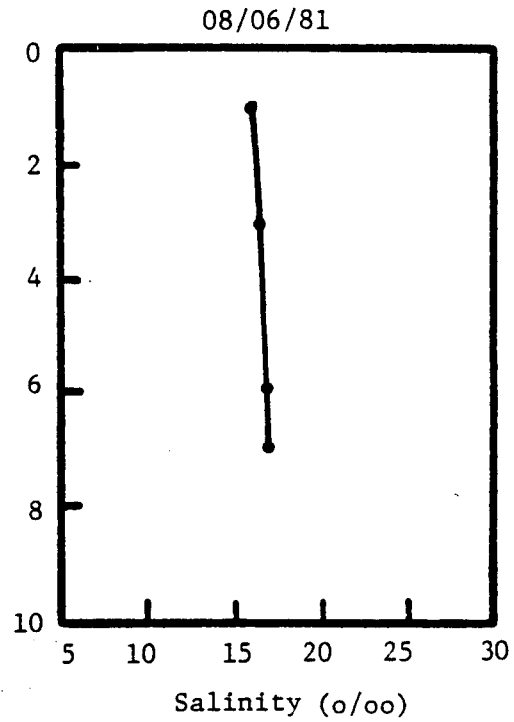
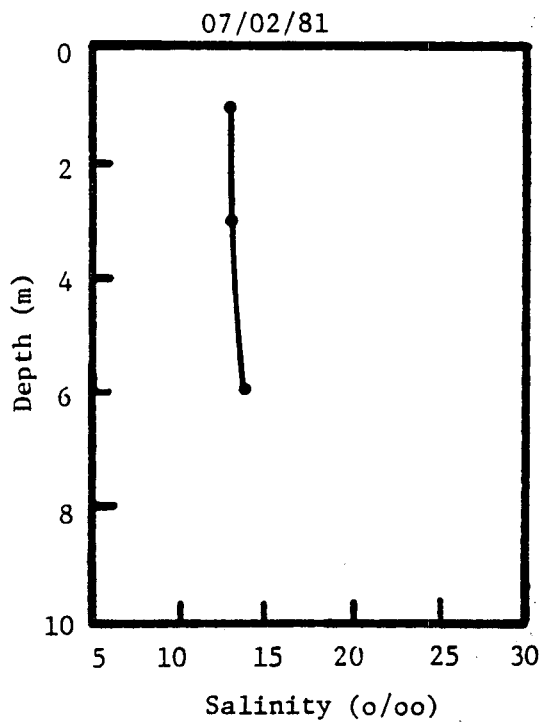
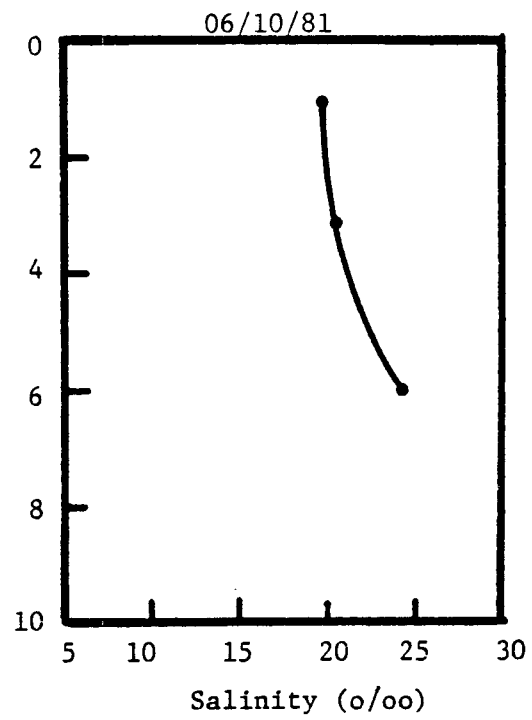
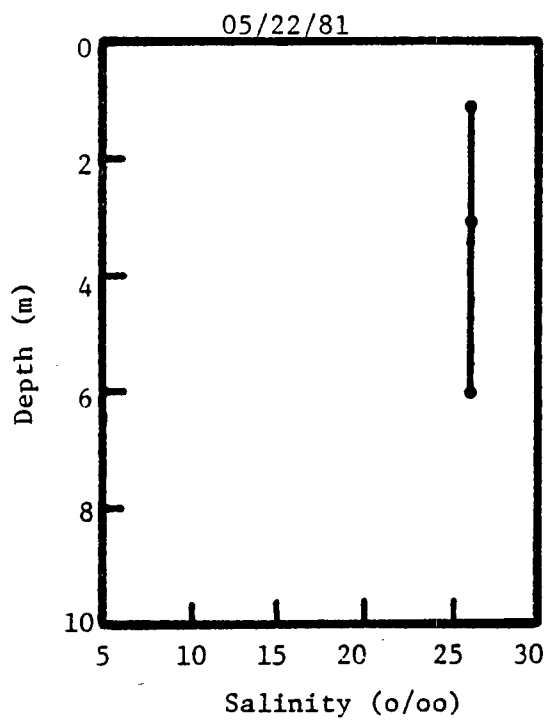


Figure 3-17. Vertical salinity profiles at station E5 in Calcasieu Pass from May through August 1981.

July and August, the dissolved oxygen data in the pass did not indicate an anoxic condition which was observed in the offshore waters as discussed in the monthly offshore hydrographic data discussed in Chapter 2.

During the fall, the vertical distribution of the measured properties of salinity, temperature, and dissolved oxygen in the Calcasieu Pass were nearly constant. The salinity, temperature, and dissolved oxygen measurements on September 10 were 22.7 o/oo, 28.1°C and 6.6 mg/l respectively, which shows the salinity increased, the temperature decreased, and the dissolved oxygen increased over the values measured in August. In October, the pass waters freshened to 19.2 o/oo and the temperature continued to decrease to a value of 26.5°C. The dissolved oxygen remained nearly the same as the previous month at a value of 6.9 mg/l. The freshening trend reversed in November when the salinity increased to 27.8 o/oo (Figure 3-18), but the temperature decrease continued as the temperature dropped to 18.4°C. The dissolved oxygen increased slightly to 7.6 mg/l.

In the winter, the vertical distribution again remained near constant. The December data show the salinity increased to 29.1 o/oo (Figure 3-18), the temperature was 18.2°C, and the dissolved oxygen was 6.1 mg/l. The salinity decreased to near 21 o/oo in January (as shown in Figure 3-19), and the temperature dropped to a value of near 7.0°C. The January dissolved oxygen increased to near 9.0 mg/l which was expected because the low temperature water has a higher dissolved oxygen saturation value. The salinity jumped to 29.2 o/oo on February 12. The pass water began to warm in February as shown by the temperature increase to 10.2°C, and the dissolved oxygen content was

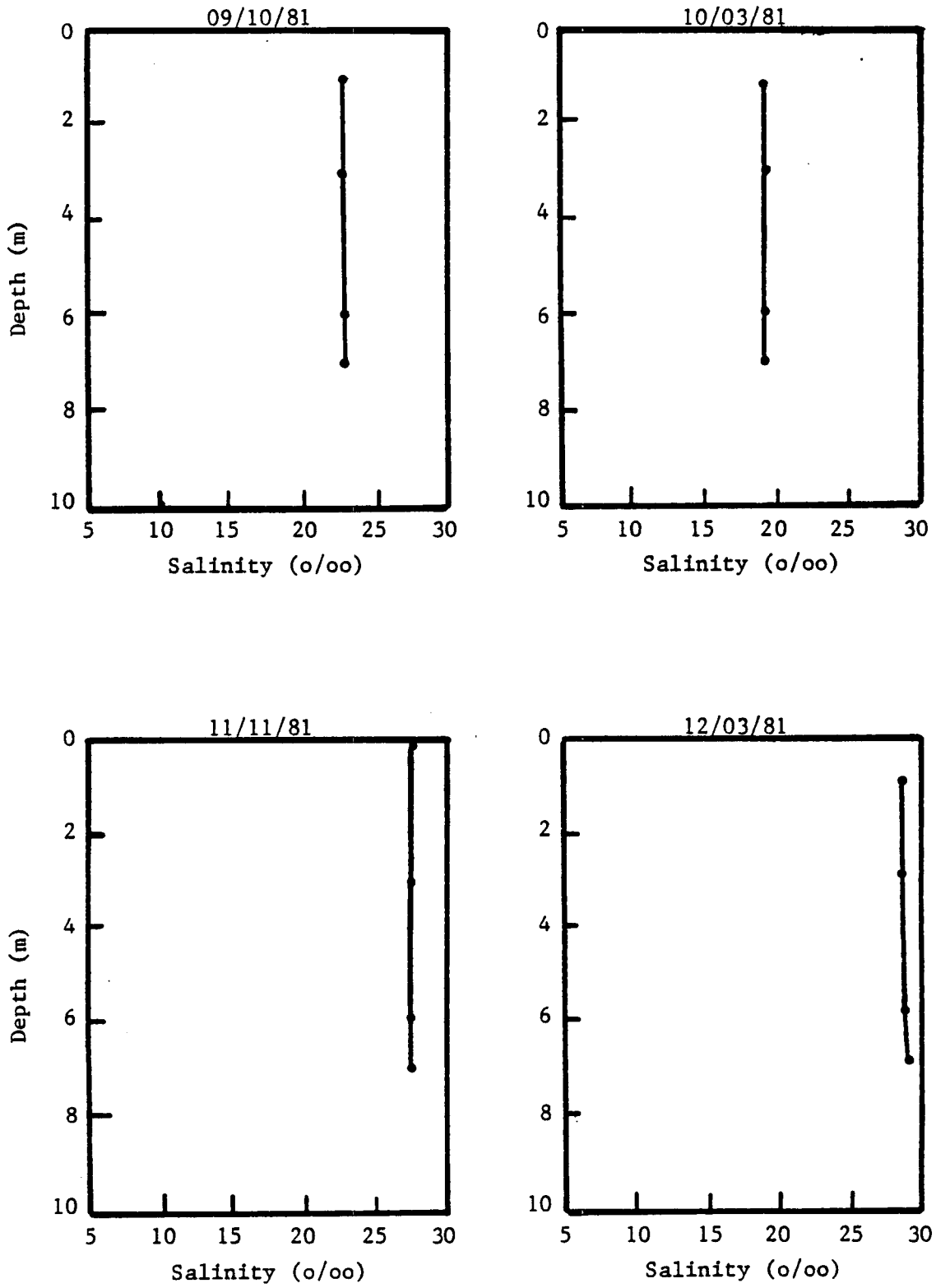


Figure 3-18. Vertical salinity profiles at station E5 in Calcasieu Pass from September through December 1981.

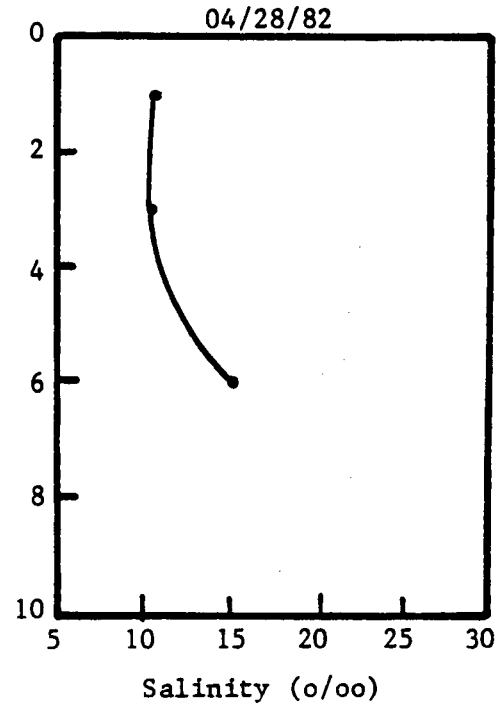
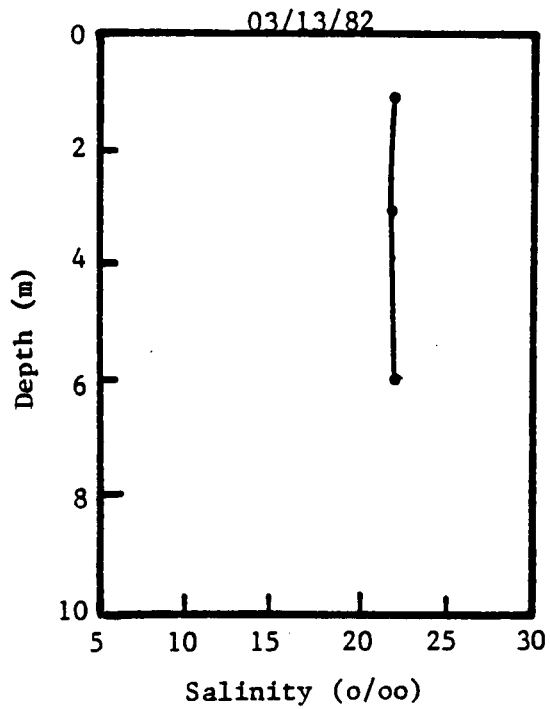
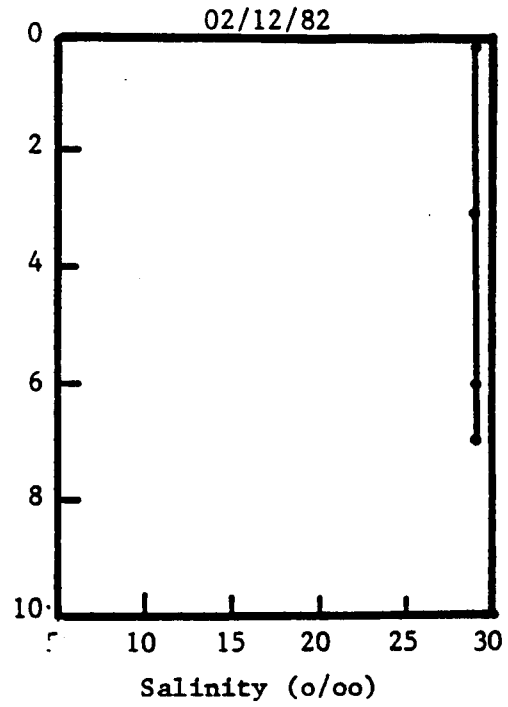
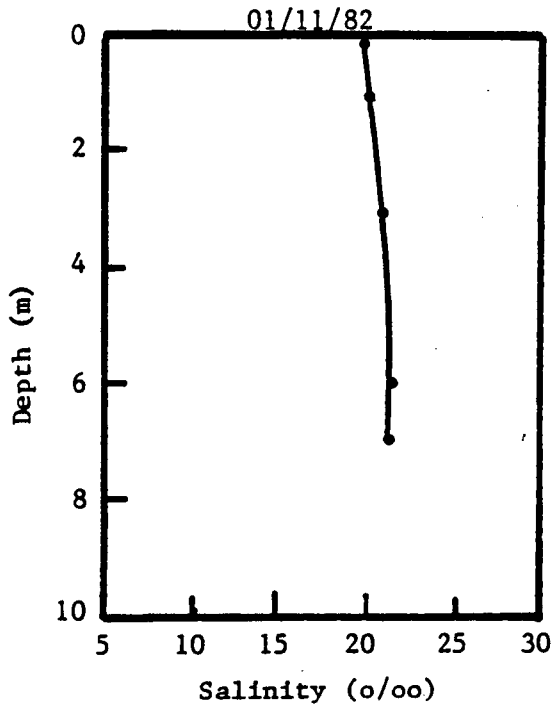


Figure 3-19. Vertical salinity profiles at station E5 in Calcasieu Pass from January through April 1982.

9.8 mg/l.

In the spring of 1982, the March 12 sampling show the salinity decreased to a value of 22.2 o/oo which was essentially isohaline (Figure 3-19). The temperature distribution was isothermal at 16.4°C while the dissolved oxygen decreased to near 9.0 mg/l. In April, the annual temperature increase continued with the pass water temperature rising to a near isothermal value of 20.8°C. The salinity in the pass showed some stratification (Figure 3-19) with a bottom salinity of 15.2 o/oo and a surface salinity of 10.6 o/oo, and these lower salinities also indicated the start of the annual spring runoff. The dissolved oxygen decreased to a value of 7.6 mg/l at the surface and 8.0 mg/l at the bottom.

3.3.5.3 Intracoastal Waterway

Three sampling stations were located in the Intracoastal Waterway. One station (E6) was located at the Ellender Bridge which crosses the waterway just west of the head of Calcasieu Lake and east of the raw water intake which is the location of station E1. The third station (E7) was located near the confluence of the Sabine River and the Intracoastal Waterway. The location of these stations are illustrated in the previous Figure 3-1 (section 3.1), and the hydrographic data recorded at these stations are tabulated in Appendix Table C-7.

On May 22, the salinity at E6 and E1 was 19.8 and 19.0 o/oo from top to bottom respectively, and at E7, it was 7.5 o/oo at the surface and 12.9 o/oo at the bottom. The temperature was 23.3°C at E6 and 24.5°C at E1 with essentially no variation from top to bottom, and it varied from a surface value of 25.0°C to 24.5°C at the bottom for

station E7. The dissolved oxygen was near 6.3 mg/l at E6 and 6.6 mg/l at E1 with nearly constant vertical distribution. Near Sabine Lake (E7), the dissolved oxygen was slightly lower near 5.4 mg/l.

In June, the salinity decreased rapidly, the dissolved oxygen dropped slightly, and the temperature continued its expected seasonal increase. Salinity stratification was evident at E6 where it increased from 5.1 (surface) to 10.9 (bottom) o/oo, and it was nearly isohaline at E1 and E7 with values of 6.6 and 0.2 o/oo respectively. The temperature was warmest (29.8°C) at the raw water intake (E1) and decreased to near 29°C at E6 and E7. The dissolved oxygen was also highest (5.8 mg/l) at E1 and lower at E6 (4.9 mg/l) and E7 (5.1 mg/l). The decrease in salinity is evidence of the beginning of the annual spring runoff period.

The July data show the continuing effects of runoff with salinities of 0.7 o/oo at E6 6.3 o/oo at E1, and 2.0 o/oo at E7. The temperature was vertically isothermal at 30.2°C for E6 and E1 and 29.5°C at E7. The dissolved oxygen remained near 5.0 mg/l at all stations. On August 6, the Intracoastal Waterway data was similar to the July data with salinities of near 4.0 o/oo at E6, 1.2 o/oo at E1, and 1.0 o/oo at E7. The temperature had increased to near 31°C, and the dissolved oxygen remained near 5.0 mg/l. One change which occurred was that the salinity was highest at E1 and E7 and decreased towards E6, but the reversed situation was present in August.

The September data show the salinity increased to near 17.4 o/oo at E6 and was 5.5 o/oo at E1. The water near the Sabine end of the waterway indicated stratification was present with the salinity varying from 3.0 o/oo at the surface to 12.4 o/oo at the bottom. The

overall temperature in the waterway began its annual decrease in September with values of 28.3°C, 27.5°C, and near 29°C at E6, E1, and E7 respectively. The dissolved oxygen was near 6.0 mg/l at the raw water intake (E1) and 5.0 mg/l at E6 and E7.

The temperature continued to decrease in October with values near 27°C, but the salinity and dissolved oxygen were similar to that found in the previous month. A freshening trend was observed in November when the salinity decreased to near 16.0 o/oo, 7.7 o/oo, and 6.0 o/oo at stations E6, E1, and E7. The temperature was warmest at E1 with a value of 18.3°C, and at E6 and E7 it was 17.3°C and 17.8°C respectively. The dissolved oxygen increased to values of near 8.0 mg/l.

The salinity near the Calcasieu Lake end of the waterway (at E6) increased to 20.5 o/oo in December while it was near 8.0 o/oo at E1 and 4.0 o/oo at E7. The temperature was near 17.5°C, and the dissolved oxygen decreased to near 6.5 mg/l at E6 and was near 8.0 mg/l at E1 and 7.2 mg/l at E7. The January data show a large decrease in temperature and an increase in dissolved oxygen. The temperature was 6.9°C at E6, and it was 6.5°C at the surface and 8.8°C at the bottom of E1. Near Sabine Lake (E7), the temperature was 9.3°C. The salinity was highest near Calcasieu Lake with a value of 15.5 o/oo and it decreased towards Sabine Lake with values of near 11.0 o/oo at E1 and 5.0 o/oo at E7.

The temperature in the waterway was nearly the same from E7 to E6 with a value of 10.7°C which was an increase over that measured in January which indicated the minimum temperature occurred in January. The dissolved oxygen decreased to near 8.5 mg/l, and thus the maximum

dissolved oxygen was reached in January coinciding with the temperature minimum. The salinity increase along the waterway from the east end to the west end with values of 18.1 o/oo at E6, 13.0 o/oo at E1, and near 6.0 o/oo at E7.

The onset of spring runoff was indicated by the reduction in the March salinity at all stations with values of 11.7 o/oo, 2.1 o/oo, and 1.8 o/oo at E6, E1, and E7. The temperature increased rapidly to 19.2°C at E6, 17.3°C at E1 and 16.2°C at E7, and the dissolved oxygen was near 8.0 mg/l at E6 and E1 and 7.0 mg/l at E7. The effect of the spring runoff became more evident in April when the salinities further dropped to 2.6 o/oo at E6, 0.4 o/oo at E1, and 0.2 o/oo at E7. The temperature continued to increase as expected with values of 19.4°C, 19.8°C, and 18.8°C at E6, E1, and E7 respectively, but the dissolved oxygen decreased to near 5.0 mg/l at E6 and E7 and 6.0 mg/l at E1.

In summary, the Intracoastal Waterway was more saline near Calcasieu Lake than near Sabine Lake except in July when the reverse situation occurred. The temperature reached a minimum (6.5°C) in January and a maximum (31.3°C) in August, and the dissolved oxygen maximum (11.7 mg/l) coincided with the temperature minimum. The dissolved oxygen minimum spanned over the period from June through August 1981 with values generally near 5.0 mg/l which was well above anoxic values of 2 mg/l or less which were measured in the offshore area during the same period as described in Chapter 2. The maximum measured salinity was 20.5 o/oo in December 1981, and the minimum value was 0.2 o/oo in April 1982.

3.3.5.4 Sabine Lake

Three sampling were also located in Sabine Lake. Station E8 was

at the north end of the lake near the confluence of the Neches River. Stations E9 and E10 were situated in the southern portion of the lake on the west and east side respectively. The previous Figure 3-1 in section 3.1 illustrates the station locations, and the hydrographic data measured at these stations are tabulated in Appendix Table C-8.

The May 1981 hydrographic data from Sabine Lake show the lake was more saline in the southern portion with salinities of 16.4 and 19.2 o/oo at E9 and E10 while the salinity at E8 in the northern half was 13.2 o/oo. The temperature was nearly constant over the lake as indicated by the 24.1°C temperature at E9 and E10 and 24.4°C at E8. The dissolved oxygen was 7.4 mg/l at E8 and a slightly higher value (7.8 mg/l) was measured at E10. The E9 station showed the highest value of 8.8 mg/l.

The lake continued to freshen in June with salinities decreasing at all stations to values of near 10.0, 7.0, and 16.0 o/oo at E8, E9, and E10 respectively. The temperature was isothermal with depth and had increased to 30.0°C at E8, 30.4°C at E9, and 30.6°C at E10. The dissolved oxygen remained essentially the same as that found in May. In July, the lake reached its freshest point as shown by these data. The salinity increased from north to south with values of 1.1 o/oo at E8, 5.6 o/oo at E9, and 8.8 o/oo at E10, and the vertical salinity structure was isohaline. The temperature decreased very slightly to 30.0°C at E8, 29.2°C at E9, and 29.5°C at E10. The dissolved oxygen decreased markedly to near 5.7 mg/l at E8, 6.5 mg/l at E9, and 6.7 mg/l at E10.

Sabine Lake remained relatively fresh in August with salinities between 3.5 and 5.6 o/oo. However, the water temperature increased to

its maximum value with 31.0°C measured at E8 and E9 and 31.7°C at E10. The dissolved oxygen increased to 7.9 mg/l at E8, 6.8 mg/l at E9, and near 7.0 mg/l at E10. These normal dissolved oxygen values were measured at the same time as the anoxic conditions were being found in the offshore waters.

The salinity of the lake increased in September and the highest salinity was measured in the northern half (E8) where the salinity was 10.2 o/oo at the surface and 12.8 o/oo at the bottom. In the southern portion, the salinity was 8.1 o/oo at E9 and 7.3 o/oo at E10. The dissolved oxygen was nearly the same at all three stations with values near 6.4 mg/l, and the temperature began its annual decrease with values near 27.5°C.

The October hydrographic data indicate the lake continued to become more saline, cooler, and richer in dissolved oxygen. The October salinities reached 12.0 and 10.6 o/oo at E9 and E10 respectively, and some salinity stratification was present at E8 where the salinity was 10.8 o/oo at the surface and 13.2 at the bottom. The October temperature was near 26.5°C at all three stations. The dissolved oxygen increased to near 7.5 mg/l at E10, and some vertical variation was measured at E8 and E9 where the values varied from 6.4 to 8.3 mg/l at the bottom and surface respectively. These trends in salinity, temperature, and dissolved oxygen continued through November and December 1981. The salinity reached 14.2 o/oo at E8 and 13.3 o/oo at E9 and E10. The temperature dropped to 18.5°C at E8, 16.8°C at E9, and 16.7°C at E10, and the dissolved oxygen was near 7.8, 10.9, and 9.5 mg/l at E8, E9, and E10 respectively.

During January 1982, station E8 was the only station measured

because of the low water level in the lake. The data at E8 showed the salinity varied from 13.3 o/oo at surface to 15.4 o/oo at the bottom. The temperature reached its lowest value of 9.0°C, and the dissolved oxygen reached a maximum of 1.9 mg/l.

The trends for the hydrographic data reversed in February 1982 when the salinity and dissolved oxygen began to decrease and the temperature started to increase. The salinity at E9 and E10 was 12.0 and 12.9 o/oo respectively, and some vertical salinity variation was present at E8 where it varied from a surface value of 11.6 o/oo to the bottom value of 13.2 o/oo. The temperature increased to near 11.7°C at E8, 10.2°C at E9, and 11.5°C at E10, and the water was slightly warmer on the surface. The dissolved oxygen was near 9.3 mg/l in the southern half of the lake as indicated by the E9 and E10 data, and was near 8.4 mg/l in the northern half (E8).

The March and April data show the effects of spring runoff on the Sabine Lake. The lake freshened to salinities of 0.3 o/oo at E8 and 3.1 o/oo at E10 in April. Station E9 showed a freshening to a salinity of 5.1 o/oo, but in April it became more saline with a value of 11.9 o/oo. No explanation is available for this anomalous behaviour. The temperature increased as expected to values of 19.2°C at E8, 19.7°C at E9, and 22.4°C at E10. The dissolved oxygen continued its annual decrease and reached values of 6.2 mg/l at E8, 5.5 mg/l at E9, and 6.7 mg/l at E10.

3.3.5.5 Average Postdisposal Hydrographic Data for Calcasieu Lake, Raw Water Intake, and Sabine Lake

The average values for the postdisposal hydrographic data for Calcasieu Lake, the raw water intake, and Sabine Lake were computed

from the data collected from May 1981 through April 1982 which are tabulated in Appendix Tables C-5, C-7, and C-8. The resulting average data are tabulated in Table 3-11.

The Calcasieu Lake salinity data show the highest average salinity (24.8 o/oo) occurred in May 1981 and the lowest value (9.4 o/oo) occurred in July 1981. The maximum salinity in May was followed by a decrease to the minimum value in early July, and then the average salinity increased to near 21 o/oo from September through February 1982. In March 1982, the average salinity dropped to 14.9 o/oo and further decreased to 10.4 o/oo in April which coincided with the annual spring runoff period. The average maximum salinity was only 0.4 o/oo higher than that reported in the predisposal study (Randall and James, 1981a) and well within the reported salinity range of 2.4 through 30.1 o/oo. The average salinity data indicate the peak spring runoff in 1981 occurred in June and July, and in 1982 the data show the beginning of runoff occurred in March and April. The average salinity indicate the brine discharge in the offshore waters did not cause the Calcasieu Lake waters to have a salinity above values previously reported, and in fact, during the first year of discharge, the salinities in the lake were well below the maximum value of 30.1 o/oo. This result is not surprising since plume measurements reported in Chapter 4 show the +1 o/oo above ambient plume contours did not reach Calcasieu Pass during the first year of discharge.

The average temperature data for Calcasieu Lake show the maximum average temperature (30.0°C) occurred in August, and it was followed by a gradual decrease to the minimum value of 6.5°C in January 1982. The average dissolved oxygen data show that its highest value (10.6

Table 3-11. Average post-disposal hydrographic data for Calcasieu Lake, raw water intake, and Sabine Lake during the period May 1981 through April 1982.

Date	Conductivity (mmho/cm at 25°C)	Salinity (o/oo)	Temperature (°C)	Dissolved Oxygen (mg/l)	Sigma-t
CALCASIEU LAKE					
05/22/81	38.1	24.8	22.9	7.6	16.3
06/22/81	31.1	19.5	29.3	6.1	10.5
07/02/81	15.6	9.4	29.6	5.6	2.8
08/06/81	23.4	13.9	30.0	5.5	6.1
09/10/81	29.3	18.3	26.2	5.9	10.5
10/03/81	32.8	20.4	24.8	6.7	12.4
11/11/81	33.9	21.2	15.8	8.4	15.3
12/03/81	36.1	22.9	15.9	8.6	16.5
01/11/82	29.6	18.2	6.5	10.6	14.3
02/12/82	33.6	21.3	9.8	9.6	16.3
03/12/82	24.6	14.9	20.4	9.0	9.4
04/28/82	17.5	10.4	20.6	7.2	5.9
RAW WATER INTAKE (Station E1)					
05/22/81	29.9	19.0	24.5	6.7	11.5
06/10/81	11.9	6.6	29.8	5.8	0.7
07/02/81	10.7	6.3	30.2	4.9	0.4
08/06/81	2.3	1.2	31.1	5.6	-3.8
09/10/81	10.1	5.6	27.5	5.9	0.6
10/03/81	19.4	11.4	26.7	6.3	5.2
11/11/81	13.5	7.7	18.3	7.9	4.5
12/03/81	14.9	8.6	16.9	7.8	5.4
01/11/82	18.9	11.1	8.9	10.9	8.5
02/12/82	21.6	13.0	10.6	8.8	9.8
03/12/82	3.9	2.1	17.3	7.8	0.4
04/28/82	0.6	0.4	19.9	6.2	0.0
SABINE LAKE					
05/22/81	26.0	16.3	24.2	8.0	9.5
06/10/81	18.9	11.2	30.4	7.4	3.9
07/02/81	5.2	3.3	29.5	6.4	-1.7
08/06/81	6.9	4.3	30.9	6.7	-1.4
09/10/81	15.5	9.0	27.7	6.2	3.1
10/03/81	19.7	11.6	26.5	7.5	5.4
11/11/81	20.8	12.4	17.5	8.4	8.2
12/03/81	22.6	13.5	17.3	9.5	9.1
01/11/82	22.6	13.5	9.1	10.4	10.4
02/12/82	20.5	12.3	11.1	8.9	9.2
03/12/82	10.6	5.9	18.8	8.6	3.0
04/28/82	10.4	6.1	20.3	6.0	3.2

mg/l) occurred in January 1982 coinciding with the temperature minimum. The minimum average dissolved oxygen (5.5 mg/l) was present in August which coincided with the temperature maximum. These data indicate no anoxic conditions persisted in Calcasieu Lake during the monthly postdisposal measurements. These conditions existed in the lake when anoxic conditions were measured in the offshore water in July and August 1981 as described in Chapter 2.

At the raw water intake in the Intracoastal Waterway, the average salinity was lowest (0.4 o/oo) in April 1982 and highest (19.0 o/oo) in May 1981. The maximum value in May was followed by a rapid decrease to 6.6 o/oo in June coinciding with the 1981 spring runoff and reached a minimum (1.2 o/oo) in August. Subsequently, it reached a value of 11.4 o/oo in October and stayed between 7.7 and 13.0 o/oo through February. The March average salinity dropped rapidly to 2.1 o/oo and reached its lowest value of 0.4 o/oo in April which coincided with the 1982 spring runoff. These values are lower than those reported in the January through April 1981 predisposal period by Randall and James (1981a), and this is attributed to the difference in timing of the spring runoff which varies from year to year. The average temperature maximum (31.1°C) occurred in August and the minimum was measured as 8.9°C in January 1982. The average temperature variation followed the normal annual variation. The average dissolved oxygen data varied from 4.9 mg/l in July 1981 to 10.9 mg/l in January 1982, and it showed no anoxic conditions were measured at the raw water intake during the first year of discharge.

The average hydrographic data for Sabine Lake (Table 3-11) show that the average salinity varied from 16.3 o/oo in May 1981 to 3.3

o/oo in July 1981. The average salinity was reduced from its maximum value of 16.3 o/oo as a result of spring runoff to 11.2 o/oo in June and reached a minimum of 3.3 o/oo in July. After that, it gradually increased to 11.6 o/oo in October and then it varied between 12.3 and 13.5 o/oo from November 1981 through February 1982. The effect of the earlier 1982 spring runoff dropped the average salinity to 5.9 and 6.1 o/oo in March and April 1982. The average temperature variation shows the maximum temperature was 30.9°C in August 1981 and the minimum temperature was 9.1°C in January 1982. The average dissolved oxygen minimum was 6.2 mg/l in September which lagged the temperature maximum by one month, and the maximum average dissolved oxygen was 10.4 mg/l in January 1982 coinciding with the temperature minimum. As was the case for Calcasieu Lake, the average dissolved oxygen data show no anoxic conditions in Sabine Lake were detected.

A comparison of the temporal variation of the average salinity for Calcasieu Lake, Sabine Lake, and the raw water intake during the twelve-month postdisposal period is illustrated in Figure 3-20. This comparison shows that the average salinity in Calcasieu Lake was much higher than that in the Sabine Lake and at the raw water intake (station E1). The average difference in salinity between Calcasieu and Sabine Lake was 8.0 o/oo. These higher salinities in Calcasieu Lake were also reported by Barrett (1971) and in the predisposal study by Randall and James (1981a). The average salinity data at the raw water intake and in Sabine Lake indicate that the Sabine Lake average salinity was on the average 2.3 o/oo higher than that found at the raw water intake. Exceptions to this trend occurred in May 1981, July 1981, and February 1982. The annual salinity trend, Figure 3-20, shows

3-70

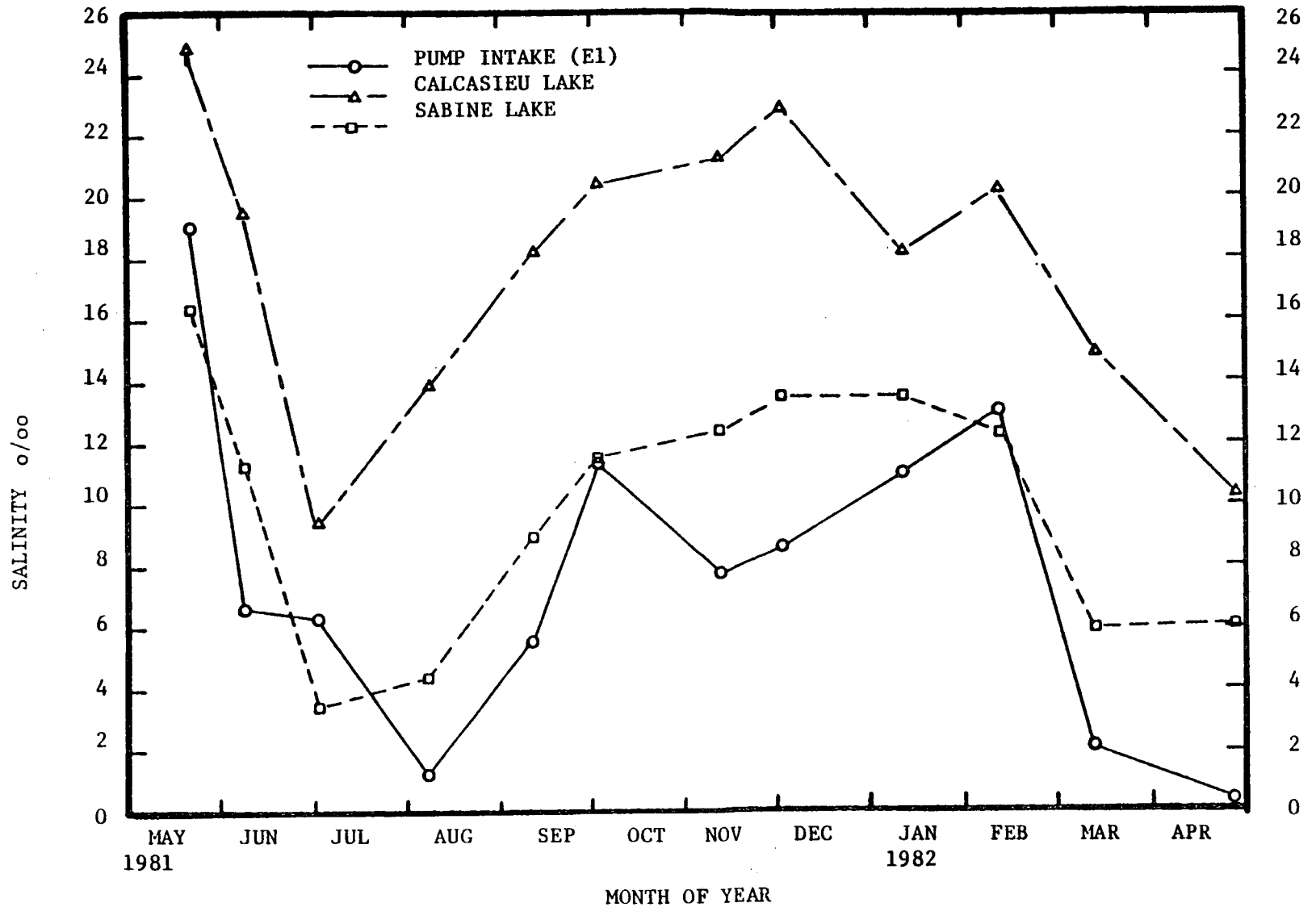


Figure 3-20. Temporal variations of areal salinity for Calcasieu Lake, Sabine Lake, and the pump intake station.

the lakes have a peak salinity prior to spring runoff. Once the spring runoff begins, the salinity drops to a minimum and then slowly returns to a normal salinity condition of approximately 20 o/oo in Calcasieu Lake and 12 o/oo in Sabine Lake in late summer or early fall. The salinity gradually increases to a maximum of approximately 25 o/oo in Calcasieu Lake and 13 o/oo in Sabine Lake over the winter and perhaps early spring depending on the start of the spring runoff.

The temporal variation of average temperature and dissolved oxygen is illustrated in Figures 3-21 and 3-22 respectively. The annual temperature variation of the Calcasieu Lake, Sabine Lake and the Intracoastal Waterway is illustrated in Figure 3-21 where the maximum temperature of 30 to 31°C is reached in August after which it decreases slowly to a minimum near 6 to 9°C in January and then starts increasing again toward the maximum. The average temperature data indicate the Sabine Lake is 1.2°C warmer on the average than the Calcasieu Lake except for March and April 1982. The temperature difference is mostly attributed to the sampling plan which called for the measurements in the Calcasieu and Sabine Lakes to be made in the morning and afternoon respectively, and this plan was reversed in March and April 1982. The temporal variation of the average dissolved oxygen data is shown in Figure 3-22. The results show the dissolved oxygen reached a minimum (between 6 and 8 mg/l) during the summer months coinciding with the temperature maximum and increases to a maximum value between 10 and 11 mg/l in the winter months. Thus, the dissolved oxygen annual variation is nearly a mirror image of the temperature variation. The data also show the dissolved oxygen was higher by approximately 1 mg/l in Sabine Lake from May through

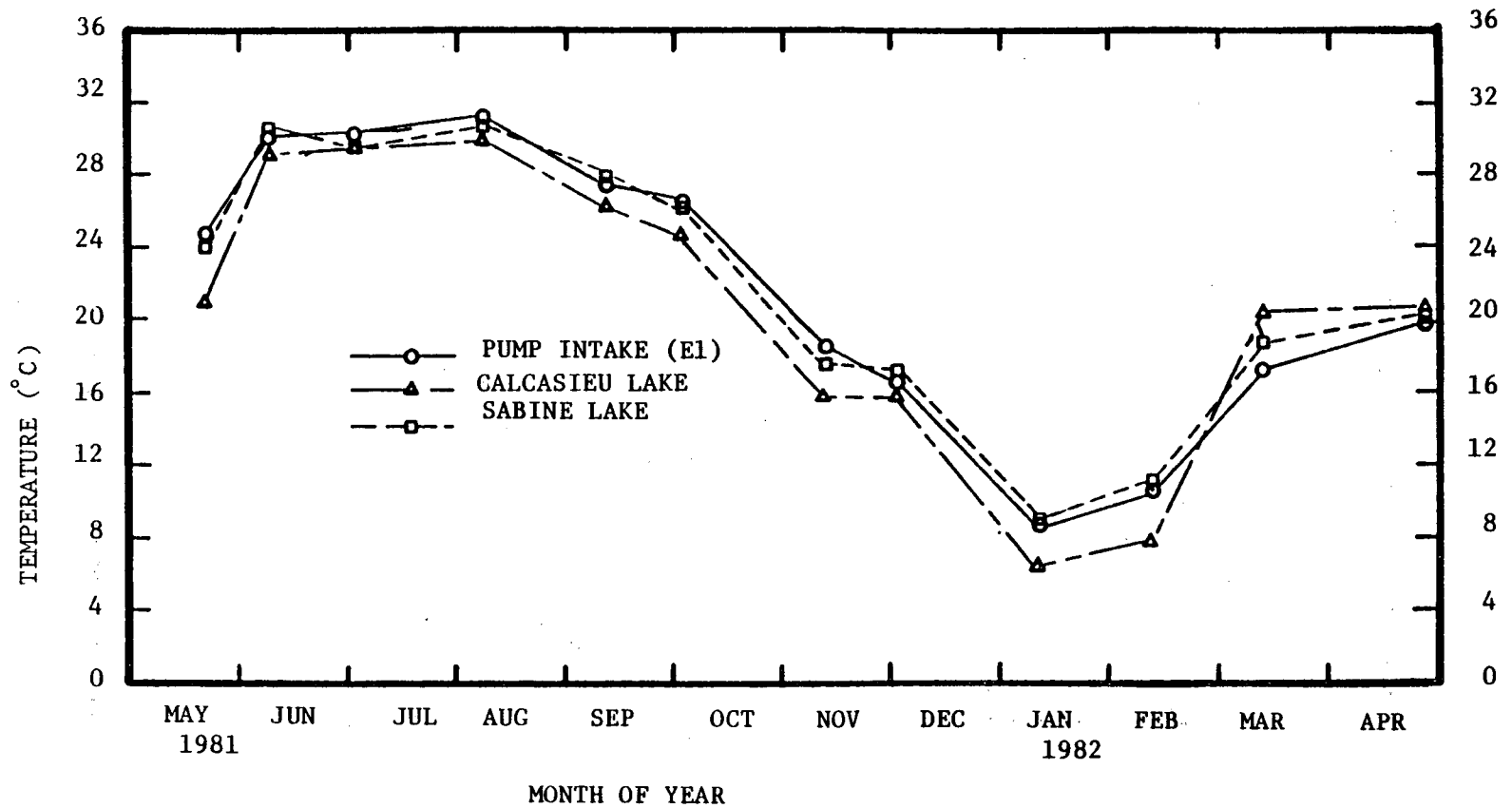


Figure 3-21. Temporal variation of areal average temperature for Calcasieu Lake, Sabine Lake, and the pump intake station.

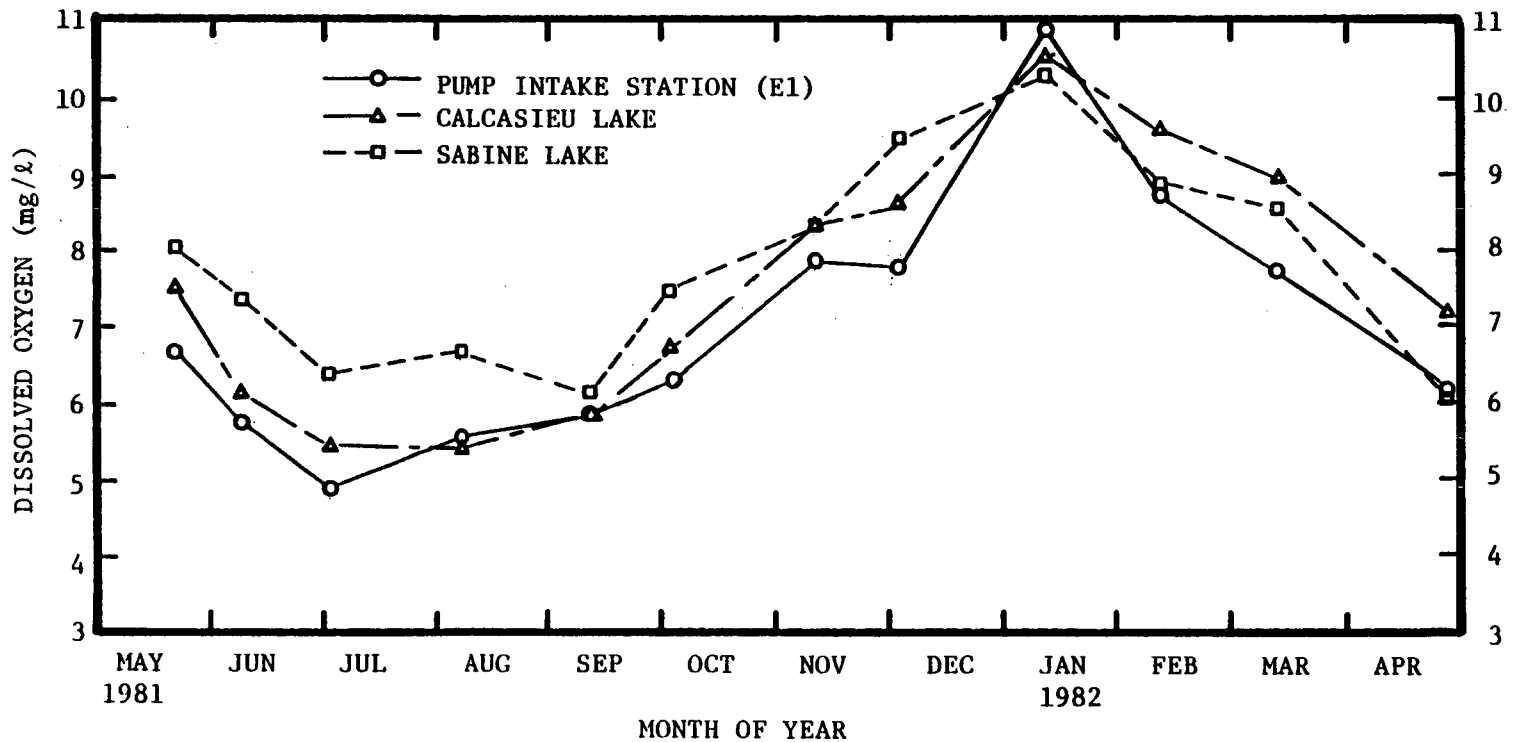


Figure 3-22. Temporal variation of areal average dissolved oxygen for Calcasieu Lake, Sabine Lake, and the pump intake station.

December 1981, and from January through April 1982, it was slightly lower by approximately 0.5 mg/l. The data clearly show no anoxic condition existed in the two lakes or in the Intracoastal Waterway between them during this twelve-month study.

3.4 Summary of Results

The twelve-month postdisposal study of the estuarine hydrography shows that Calcasieu and Sabine Lakes were found to be well mixed estuaries with occasional stratification, and the Intracoastal Waterway connecting the two lakes was also found to be well mixed with occasional stratification. The entrance to Calcasieu Lake, Calcasieu Pass, was likewise found to be well mixed with stratified conditions occurring infrequently.

The salinity data show the salinity in Calcasieu Lake increased from north to south except in October and November 1981 when the salinity on the east side of the south end of the lake was slightly fresher than that at the north end. The south end of Calcasieu Lake is divided into an east and west side, and the salinity in the sides was essentially the same except for these months when the west side was more saline than the east and just the opposite in one other month. In the Intracoastal Waterway, the salinity data show the salinity at the Calcasieu end of the waterway was always more saline except during July 1981 when large freshwater input to the waterway caused the Calcasieu end of the waterway to be less saline than near Sabine Lake. In Sabine Lake, the salinity increased from north to south during May through August 1981 and reversed the trend from September through December. The north to south salinity increase returned during the remainder of the year.

The maximum salinity in the Calcasieu Lake, Intracoastal Waterway, and Sabine Lake was 26.8 o/oo, 20.5 o/oo, and 19.2 o/oo respectively. The Calcasieu Lake, Intracoastal Waterway, and Sabine Lake had minimum salinities of 2.2 o/oo, 0.2 o/oo, and 0.3 o/oo respectively. The average salinity data for Calcasieu Lake, Intracoastal Waterway, and Sabine Lake show Calcasieu Lake was more saline than Sabine Lake by an average of 8.0 o/oo. These data also show the water available at the raw water intake for leaching operations was less saline than that in Sabine Lake by an average of 2.3 o/oo.

The dissolved oxygen data indicate no persistent anoxic conditions were observed. The annual dissolved oxygen cycle consisted of a minimum occurring usually during the summer months and a maximum being reached in the winter months. The average data during this study show the minimum in Calcasieu Lake, Intracoastal Waterway, and Sabine Lake was 5.5, 4.9, and 6.2 mg/l which occurred in August, July and September respectively. The average dissolved oxygen maximum in Calcasieu Lake, Intracoastal Waterway, and Sabine Lake was 10.6, 10.9, and 10.4 mg/l respectively with all of them occurring in January 1982. The three water systems had dissolved oxygen values which were normally within 1 mg/l of each other indicating very little dissolved oxygen variation within the Calcasieu-Sabine estuarine system.

The temperature data illustrated the annual cycle for the Calcasieu-Sabine estuarine system. The maximum average temperature for the Calcasieu Lake, Intracoastal Waterway, and Sabine Lake were 30.0°C, 31.1°C, and 30.9°C respectively with all of them occurring in August. The minimum average temperature in the same order was 6.5°C,

8.9°C, and 9.1°C respectively and each of them, again, occurred in January 1982.

The salinity data show no indication of the brine discharge entering Calcasieu Pass and subsequently increasing the salinity of Calcasieu Lake. The Sabine Lake data also show no indication of the brine discharge entering that lake. This result is further confirmed by the brine plume measurements (Chapter 4) which show the +1 o/oo above ambient salinity contour never reached the entrance to Calcasieu or Sabine Lake.

3.5 Conclusions and Recommendations

The U.S. Geological Survey's daily streamflow records for Calcasieu and Sabine Lakes were obtained for the period October 1967 through October 1981. The streamflow records indicated that the low flow period for Calcasieu Lake extended from July through November. Because of reservoir storage in the drainage area, the low flow period for Sabine Lake included only October and November. It was estimated that the gauged freshwater inflow to Sabine Lake represented 82% of the total freshwater inflow to Sabine and the gauged inflow to Calcasieu Lake represented 70% of the total freshwater inflow to Calcasieu Lake.

Texas Department of Water Resources conducted a study of Sabine Lake and developed equations relating average monthly gauged freshwater inflow to average monthly salinity in upper Sabine Lake. Three years of salinity data were available for Calcasieu Lake and a similar expression was developed for Calcasieu Lake relating average monthly gauged freshwater inflow to salinity in the upper Calcasieu Lake. From these equations, changes in salinity resulting from changes

in gauged freshwater inflow were computed for each lake.

The flow characteristics of the ICWW were evaluated to determine (1) how much water flows in the ICWW from Sabine to Calcasieu or from Calcasieu to Sabine, and (2) how much of the water pumped from the ICWW is from Calcasieu and how much is from Sabine. The raw water intake structure is located closer to Calcasieu Lake than Sabine Lake. It was estimated the 65% of the pumped water would represent a diversion from Calcasieu and 35% of the pumped water would represent a diversion from Sabine regardless of the direction of flow in the ICWW. During the period of low freshwater inflow to the Calcasieu/Sabine system, the salinity of the diverted water increases and much of the pumped water is from the Gulf of Mexico rather than freshwater inflow.

Changes in salinity caused by pumping 1.98 cms (70 cfs, 1.08 MBD) and 1.42 cms (50 cfs, 0.77 MBD) from the ICWW were estimated for upper Calcasieu Lake and upper Sabine Lake. These computations indicated that a diversion of 1.98 cms (70 cfs, 1.08 MBD) from the ICWW would cause a maximum increase in salinity of 0.45 o/oo in the Calcasieu system and 0.09 o/oo in the Sabine system. A diversion of 1.42 cms (50 cfs, 0.77 MBD) from the ICWW would cause a maximum increase in salinity of 0.32 o/oo in Calcasieu and 0.07 o/oo in Sabine. The maximum increases in salinity would occur in the ICWW and the Calcasieu ship channel with smaller salinity increases in upper Calcasieu Lake.

The following conclusions were reached in this part of the study concerning pumping water from the ICWW.

1. The project should not increase salt water intrusion into the groundwater aquifers of the area. Salt water intrusion is

caused by over pumping the aquifers and not the salinity level in Calcasieu Lake.

2. The project should not increase the salt water intrusion into the freshwater marsh areas. Salt water intrusion occurs when the water table is lowered by evapotranspiration during low rainfall periods and/or the recharge has been reduced. The construction of the ICWW has modified the overland flow recharge of the wetlands south of the ICWW and is probably responsible for much of the salt water intrusion into freshwater marsh areas.
3. The project will increase the salinity in upper Calcasieu Lake. Model study indicates the largest change in salinity (0.5 o/oo maximum) will occur in the ship channel and in the ICWW. The increase in salinity in upper Calcasieu Lake will be less (0.2 o/oo maximum).
4. The increase in salinity of the salt water wedge up the Calcasieu River at Lake Charles is expected to be in the order of 0.01 o/oo.

No conclusion was reached as to whether or not the pumping would cause a significant increase in salinity. When these changes are compared to the natural variations that occur in these estuaries, it can be concluded that the project by itself will probably not cause a significant increase in salinity. However, the effects of the diversions are additive and when the effects of all present and future diversions are considered, there will be a significant change in salinity. At some level of diversion, it may be necessary to limit or restrict additional diversions of the system.

As a result of the estuarine hydrography study, it has been shown that the Calcasieu Lake was much more saline than the Sabine Lake and the Intracoastal Waterway by an average of 8 o/oo. In all months of the year except in the fall, both the Calcasieu and Sabine Lakes were more saline in the southern portion of each lake which is nearest the Gulf of Mexico. The measurements at the raw water intake for leaching operations show the water was fresher than that in Sabine Lake by an average of 2.3 o/oo.

The range of salinity for the Calcasieu Lake, Sabine Lake, and Intracoastal Waterway was 26.8 to 2.2 o/oo, 20.5 to 0.2 o/oo, and 19.2 to 0.2 o/oo respectively. The range of temperature for these bodies of water was 30.0 to 6.5°C, 31.1 to 8.9°C, and 30.9 to 9.1°C respectively. The maximum temperatures occurred in August and the minimum temperatures occurred in January. Dissolved oxygen ranged from 5.5 to 10.6 mg/l, 4.9 to 10.9 mg/l, and 6.2 to 10.4 mg/l respectively, and the minimum and maximums occurred in the summer and winter respectively.

The dissolved oxygen data indicate no persistent anoxic conditions were observed during the study.

It is concluded that Calcasieu and Sabine Lakes are well mixed estuaries and that no data collected during this study suggest that the brine discharged from the West Hackberry diffuser entered either of the lakes. Therefore, it is not recommended to continue the present monitoring effort of the lakes unless evidence in the offshore waters indicates that the above ambient brine discharge could possibly be entering the lakes.

CHAPTER 4

BRINE PLUME MEASUREMENTS

Robert E. Randall
Texas A&M University
College Station, Texas 77843

4.1 Introduction

The Department of Energy began pumping brine to the Gulf of Mexico on May 10, 1981 from the West Hackberry site of the Strategic Petroleum Reserve. The brine is being discharged through a multiport diffuser whose seaward end is located at $20^{\circ}39'52''$ N and $93^{\circ}28'35''$ W in 10 m (30 ft) of water approximately 11.5 km (6.2 nm) offshore. A similar brine discharge has been ongoing since March 1980 from the Bryan Mound diffuser offshore of Freeport, Texas, and the results of brine plume measurements have been reported by Randall (1981a, 1981b). As the brine is discharged, it forms a plume near the sea floor where it is advected away and diluted by the ambient sea water. The purpose of this chapter is to describe the results of measuring the areal extent, vertical extent, and the empirical prediction of the plume behavior.

The brine discharge is the result of a solution mining process which is being used to form storage caverns in an underground salt dome near West Hackberry, Louisiana. The brine is first pumped to a

brine pit for temporary storage and settling just before being pumped to the Gulf of Mexico through a buried pipeline as illustrated in Figure 4-1. The last 1006 m (3300 ft) of the pipeline is the multiport diffuser which has 55 diffuser ports extending vertically from the pipeline 1.2 m (4 ft) above the bottom. These ports have an inside diameter of 7.6 cm (3 in) and are spaced 18.3 m (60 ft) apart. As the brine exits from the diffuser ports, it is diluted initially due to jet mixing, and then it falls to the bottom as a result of the greater density and simultaneously spreads laterally. The plume is then dispersed by advection due to currents and diffusion due to turbulence.

The behavior of the brine plume is characterized as a negatively buoyant plume which can be divided into three areas (NOAA, 1977) as shown in Figure 4-2. These three areas depend upon the physical processes by which the plume is being dispersed. The first area is called the near field area where the effluent dilution is affected by turbulent jet mixing which is a function of the ambient current velocity, diffuser design, and water depth. This area is defined as the distance downstream where the individual plumes from each diffuser port merge to form a continuous plume, and this distance has been estimated to be on the order of 30 m (100 ft). In the intermediate field area, the plume experiences buoyant lateral spreading and vertical collapse, and the outer boundary of this area is estimated to be on the order of 305 m (1000 ft) from the diffuser. The final plume area is called the far field which is the largest area and is affected

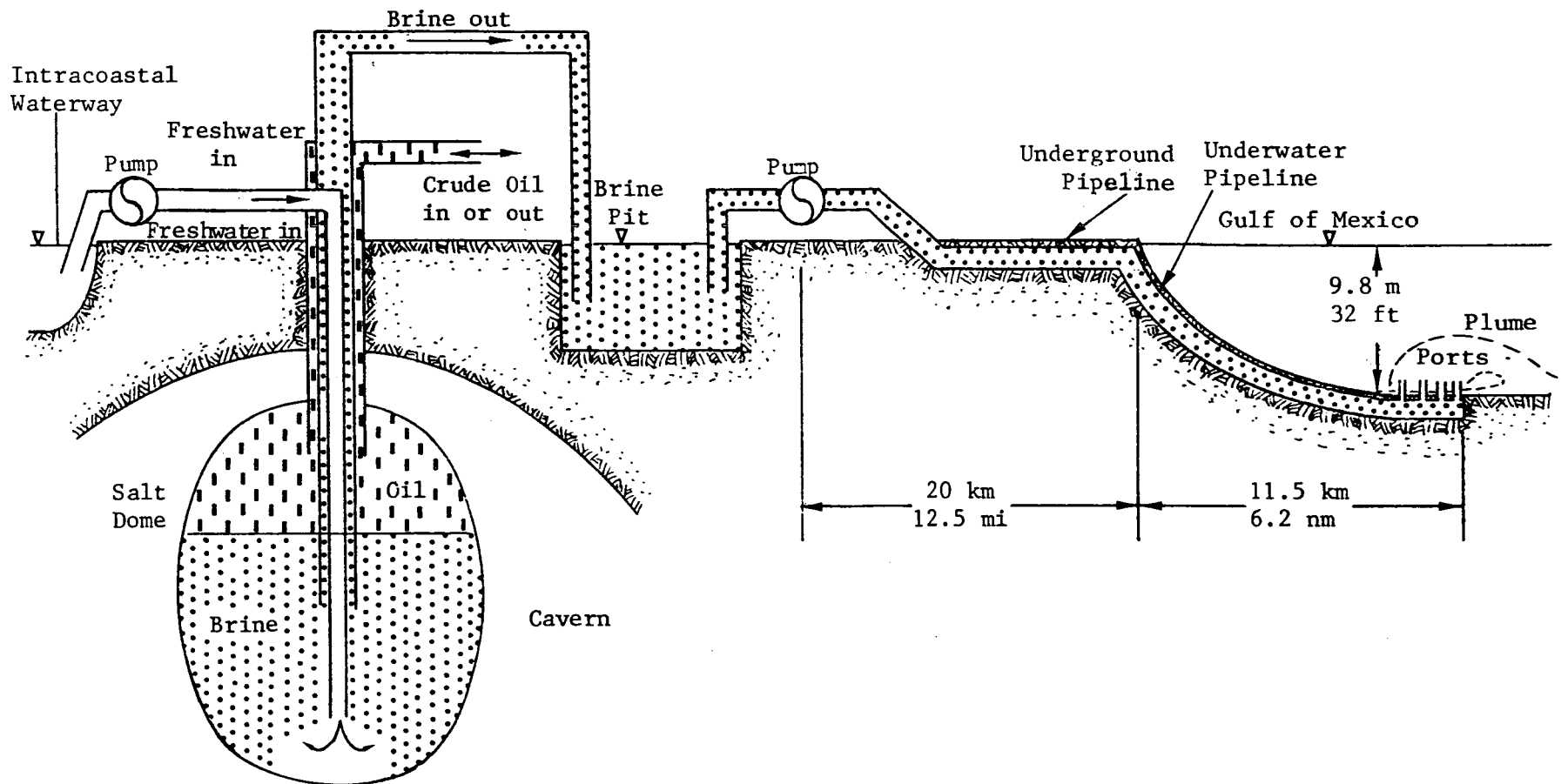


Figure 4-1. Schematic of West Hackberry brine discharge operation.

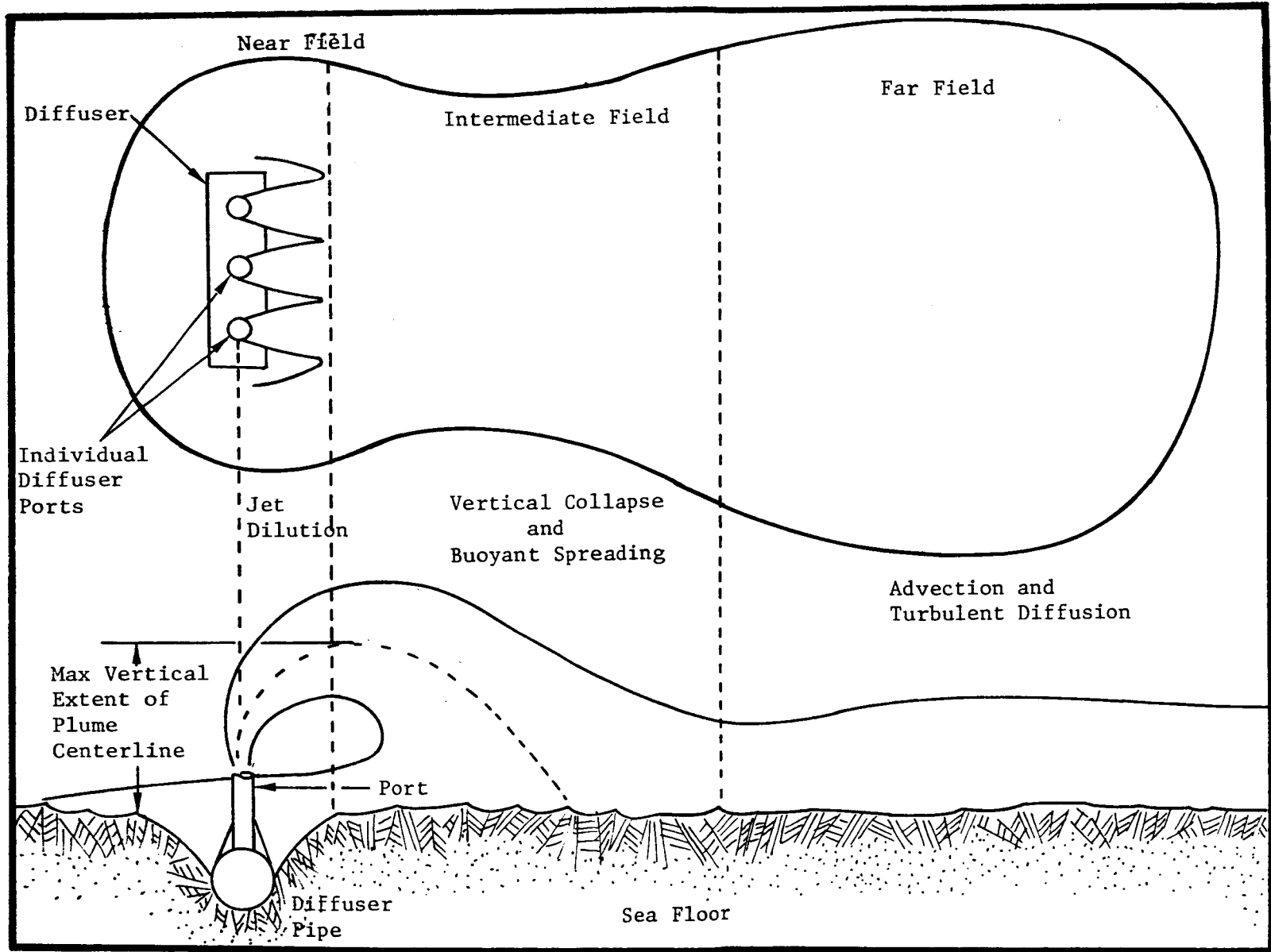


Figure 4-2. Schematic of brine plume characteristics.

most by the physical processes of advection and diffusion.

Initially, the brine was discharged through 32 ports, and 31 of these ports were at the offshore end of the diffuser, and 1 port was the second port at the nearshore end. The discharge rate was near continuous from May 10, 1981 through August 23, 1981 and varied from 21,700 to 29,500 barrels/hr, and the brine pit salinity varied between 76 and 228 o/oo. The brine discharge was stopped from August 24 through September 14, 1981. Brine was discharged in a batching mode from September 15 through October 25, 1981 which means the brine was pumped offshore during only part of the day. For example, on September 25, brine was discharged for only 13 hours at a rate 21,500 barrels/hr with a salinity of 223 o/oo. During this period, the discharge rate varied from 16,000 to 31,900 barrels/hr, and the salinity varied from 219 to 250 o/oo. Near continuous discharge was maintained again from October 26 to January 1, 1982 with the discharge rate between 20,700 and 25,000 barrels/hr and the salinity between 203 and 235 o/oo. From January 2 through February 1, 1982, the discharge returned to the batching mode, and the discharge rate and salinity varied between 21,500 and 23,100 barrels/hr and 222 and 254 o/oo respectively. The period of February 2 through April 30 saw the discharge return to a continuous operation at a rate between 19,000 and 35,400 barrels/hr. The salinity varied from 137 to 250 o/oo. During the period, the number of open ports was increased to 50 on March 18, 1982 and on April 25 the number of open ports was reduced to 42. Thus, the first year of discharge was a period when the brine was

discharged in a batching mode for approximately two months and not discharged at all for approximately one month. The brine salinity during this first year was frequently found to be less than 200 o/oo which was low compared to the maximum brine salinity of 263 o/oo.

Prior to the actual discharge of brine, the above ambient salinity concentration in the far field was predicted using the MIT transient plume model developed by Adams, et al (1975). The predictive results from this model for the West Hackberry diffuser are described in a report by NOAA (1977). Subsequently, another study (NOAA, 1981) was completed to determine the impact of the brine discharge from the West Hackberry diffuser based upon some of the results from the Bryan Mound studies. This study predicted that above ambient salinities of 3 and 4 o/oo would be found near the diffuser and that the brine plume would probably never reach the Calcasieu Pass.

Other studies have been conducted which are directly related to the discharge of a negatively buoyant brine plume. Gaboury and Stolzenbach (1979) discuss the development of a non-dimensional formulation of the MIT transient plume model. This formulation is used to evaluate alternate levels of acceptable impact based on the terms of organism mortality as a function of concentration and exposure time. Vergara and James (1979) describe the results of an experimental study to evaluate the effects of port diameter, exit velocity, and riser height on the resulting brine concentration at the bottom near the diffuser under stagnant conditions.

Tong and Stolzenbach (1979) reported on an analytical and experimental study of the discharge of a negatively buoyant fluid. These experiments were directed toward the investigation of near field dilution of a single port diffuser with varying discharges and cross flow. Procedures were developed for determining a desired near field mixing condition. These procedures were used to design an offshore brine diffuser similar to the one for West Hackberry and Bryan Mound.

This report briefly describes the instrumentation used in tracking the brine plume and the procedures employed to attain the isohaline contours which describe the areal coverage of the plume 25.4 cm (10 in) above the bottom. The results of the plume tracks are described which define the areal extent and the above ambient brine concentrations. Vertical salinity profiles which permit the evaluation of the plume vertical extent are discussed and compared with empirical predictions. Vertical dissolved oxygen profiles are discussed in order to evaluate the effect of the brine discharge on the vertical distribution of dissolved oxygen. The data from the plume tracks during the first year of discharge were also used to develop a procedure for empirically predicting plume contours in the West Hackberry diffuser area. These procedures and some example predictions are discussed and compared with actual field measurements.

4.2 Plume Measurement Equipment

4.2.1 Towing Sled

The plume measurement equipment consists of a conductivity,

temperature, depth, and dissolved oxygen (CTD/DO) sensor which was mounted in a sled and towed on the sea floor by a research vessel as shown in Figure 4-3. Similar equipment (Randall, 1981a) has been used for measuring the brine plume emanating from the Bryan Mound diffuser. The cross-section of the sled is an equilateral triangle and the CTD/DO sensor is located at its centroid. The overall length of the sled is 1.8 m (6 ft), and the runners and braces are 1.9 cm (0.75 in) black iron pipe as shown in Figure 4-4. Flat steel plate skids were attached to the runners such that the sled would stay on top of the thick silt layer which exists in the area of the West Hackberry diffuser. These steel plate skids are 15.2 cm (6.0 in) wide and 0.32 cm (0.125 in) thick. With this design, the CTD/DO sensor is always 25.4 cm (10 in) off the bottom regardless of which set of skids are in contact with the sea floor, and it can tumble without affecting the sensor distance off the bottom.

Since the sled is towed on the sea floor, the possibility of snagging is always present. Therefore, weak links were designed for releasing the sled and sensor from the tow cable and conductor cable respectively. The weak link for the towing cable is connected between the towing wire (Figure 4-3) and the sled, and it releases with a tension of 4893 newtons (N) (1100 lb). The conductor cable is also attached to a weak link which releases with approximately 1344 N (300 lb) of tension. When all the weak links have released, the sled is completely free from the towing vessel and marked with a surface buoy which is attached at all times during the tracking operation. In

4-9

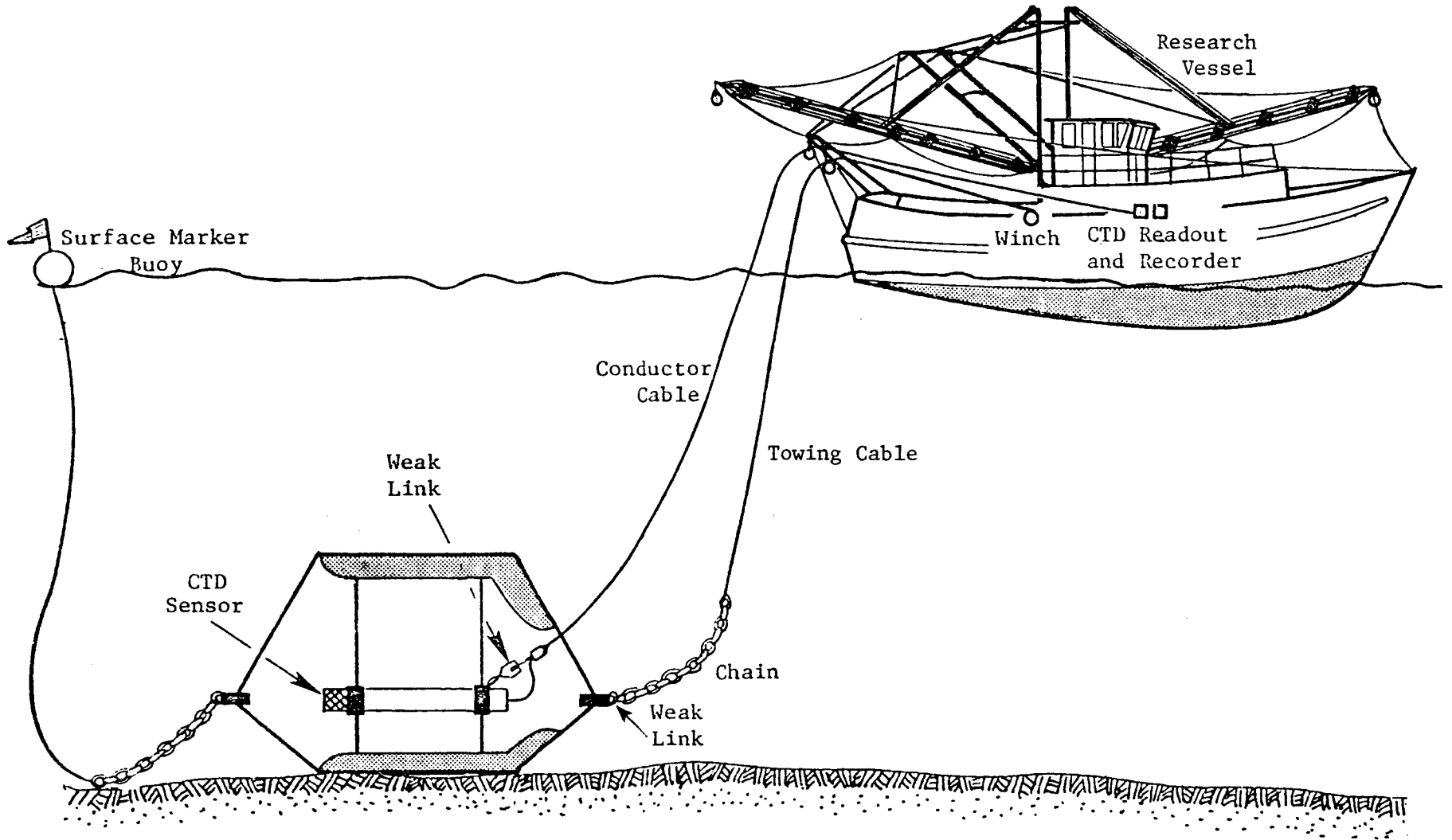
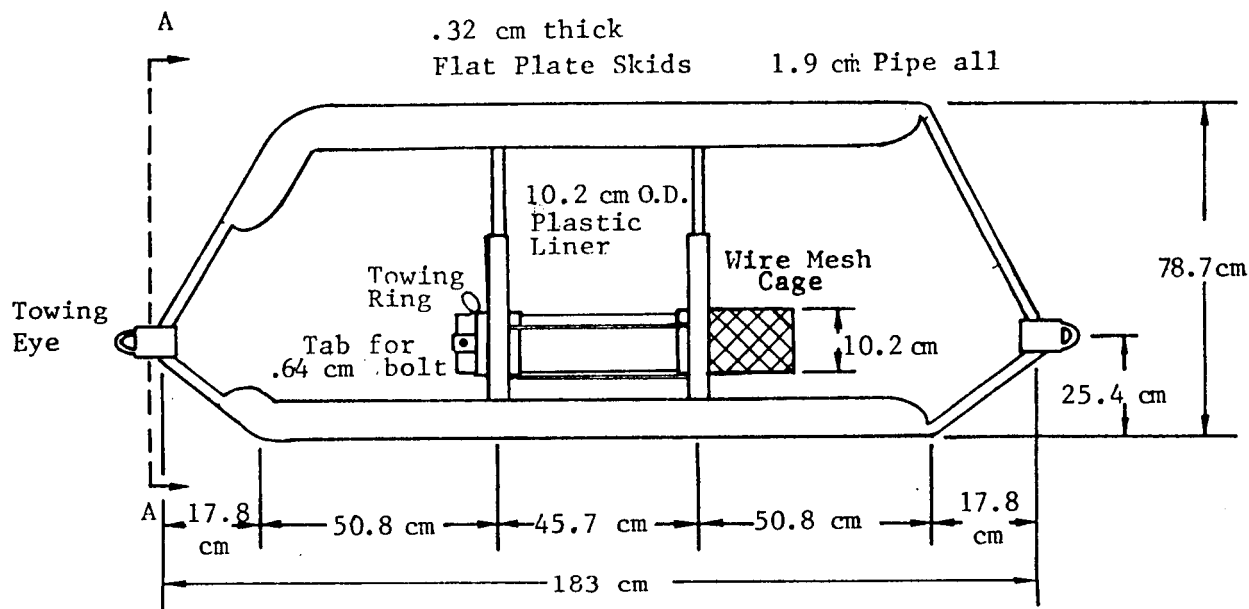


Figure 4-3. Schematic of the plume tracking system.



View A-A

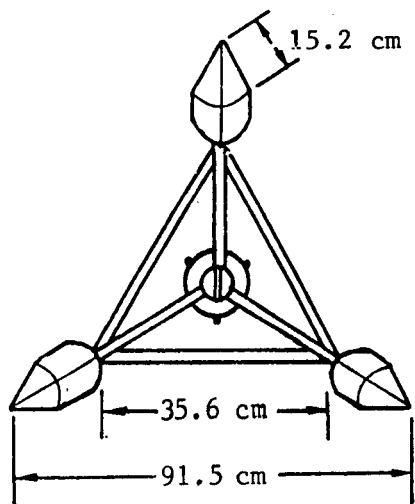


Figure 4-4. Detailed drawing of the towing sled.

order to recover the sled, the research vessel retrieves the surface buoy, and then the buoy line is used to winch the sled to the surface.

4.2.2 Description of Conductivity, Temperature, Depth and Dissolved Oxygen System

The conductivity, temperature, depth, and dissolved oxygen (CTD/DO) system manufactured by the Hydrolab Corporation (Hydrolab, 1980) is used in the plume tracking system which is illustrated in Figure 4-5. The CTD/DO system has three components: the data transmitting unit (sensor), the conductor cable, and the data control unit (readout). The sensor is capable of measuring conductivity (0 to 200 mmho/cm), depth (0 to 200 m), and temperature (-5 to +45°C), dissolved oxygen (0 to 20 mg/l), and pH/ORP. The conductor cable is 150 m (492 ft) long, has 12 conductors, and is 1 cm (3/8 in) in diameter. The data control unit displays selected output digitally, and it is interfaced with a Hewlett Packard Model 85 computer for data parameter selection, recording and presentation. Computer software controls what parameters are measured and at what sampling frequency. The CRT display on the computer provides a continuous update of the CTD/DO data measured by the underwater sensor. This display allows the operator to continually observe the conductivity data which determines when the sensor is in and out of the plume and alerts the operator when sensor problems arise. The computer is programmed such that it automatically records the CTD data at a predetermined interval on cassette tape and prints it on a thermal paper output.

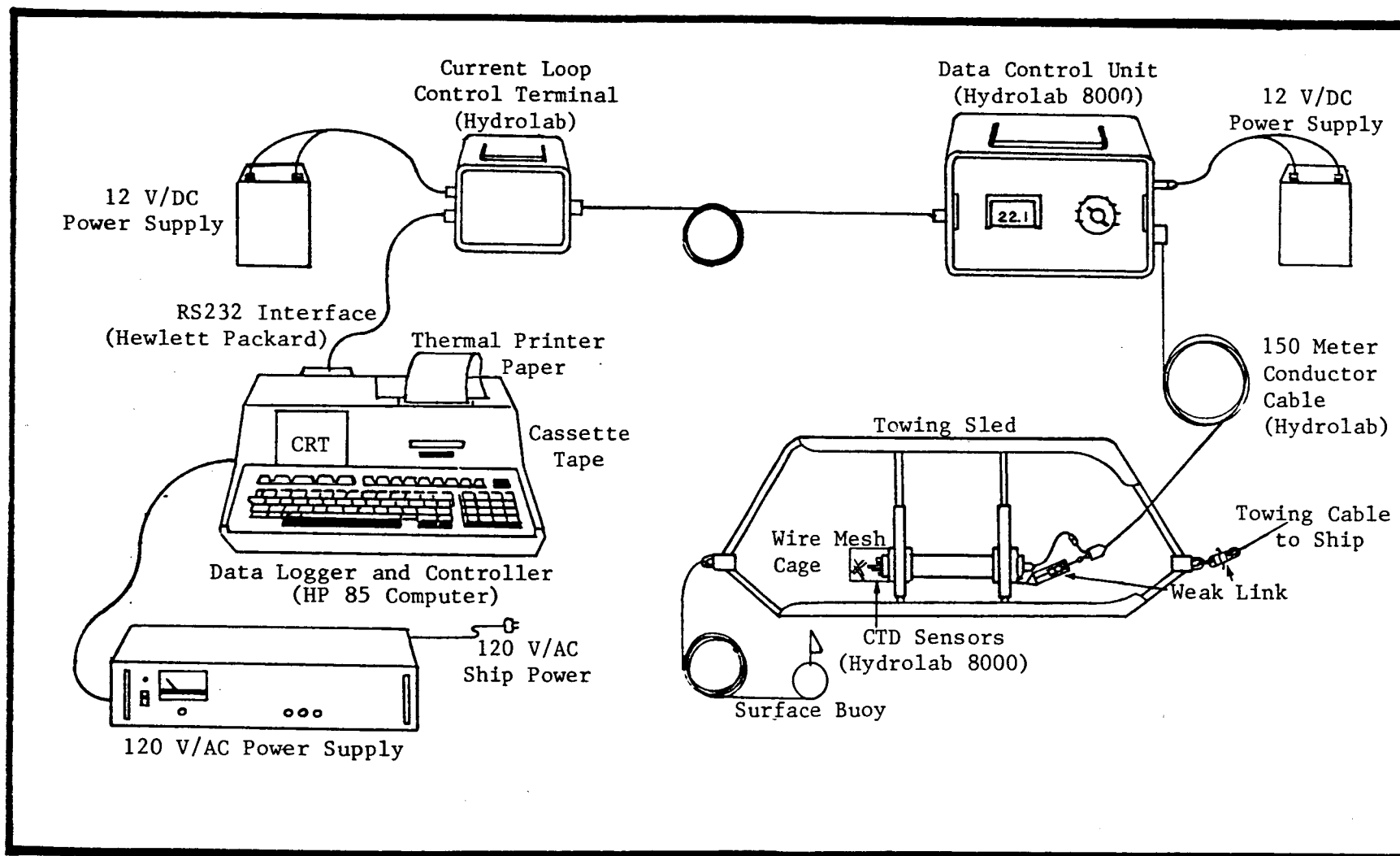


Figure 4-5. Schematic of brine plume measurement equipment.

The accuracy of the conductivity sensor is ± 1.0 mmho/cm, and when the conductivity is converted to salinity the accuracy is ± 0.7 o/oo. The salinity accuracy is improved to at least ± 0.5 o/oo by calibrating with standard solutions using a Grundy laboratory salinometer which has an accuracy of ± 0.003 o/oo, Grundy (1978). The temperature, depth and dissolved oxygen sensors have an accuracy of $\pm 2^\circ\text{C}$, ± 1 m (3 ft), and ± 0.2 mg/l respectively.

4.3 Brine Plume Measurement Procedures

4.3.1 Preliminary Procedures

The CTD/DO system is calibrated in the laboratory before going to the field and the calibration procedures are the same as those described for the Hydrolab 8000 CTD/DO sensor in section 2.2.3 in Chapter 2 of this report. The brine plume measurement system is then loaded on board the R/V Quest and checked for proper operation. The weak links and surface buoy are assembled on the sled and checked for proper assembly. Provided all systems check out satisfactorily, which normally takes approximately 30 minutes, the ship is ready to leave dock.

Upon leaving the dock, the ship heads for the control stations (which are stations 20A, 20, and 20D). Station 20 is located 8.3 km (4.5 nm) east of the diffuser and at the same depth contour, and stations 20A and 20D are 3.7 km (2 nm) north and south of station 20, respectively. A vertical profile of conductivity, temperature, dissolved oxygen, and depth are recorded at a minimum of surface,

mid-depth, and bottom. These data are used to determine the ambient conditions for the sea water in the vicinity of the diffuser. When the vertical profile is completed, the research vessel proceeds to the diffuser area. The ship anchors near TAMU buoy D at the diffuser site, and the currents near the surface and bottom are measured with a remote reading ENDECO Type 923 current meter. The bottom current measurements provide an indication of the expected direction of the plume.

4.3.2 Navigation Procedures

The LORAN C navigation system and a specially constructed LORAN C chart are used for all plume tracking operations. An example of this chart is shown in Figure 4-6. The two secondary transmitting stations used are the X (26000) and the Y (46000) LORAN C stations. The chart is used to plot the ship's track during the plume track and to plot the ship's location and corresponding salinity readings from which the salinity contours are determined.

A Texas Instruments Model 9000 LORAN C receiver is used and it displays the LORAN C coordinates to the nearest 0.1 of a microsecond (μs). For the X (26000) station, a 0.1 μs represents a distance of 15.5 m (51 ft), and a 0.1 μs is 84.1 m (276 ft) for the Y (46000) station. The output from the receiver frequently jumps 0.1 μs , and thus the accuracy is estimated to be +15.5 m (51 ft) and +84.1 m (276 ft) for the two stations used.

The LORAN C coordinates of the diffuser and buoys on the

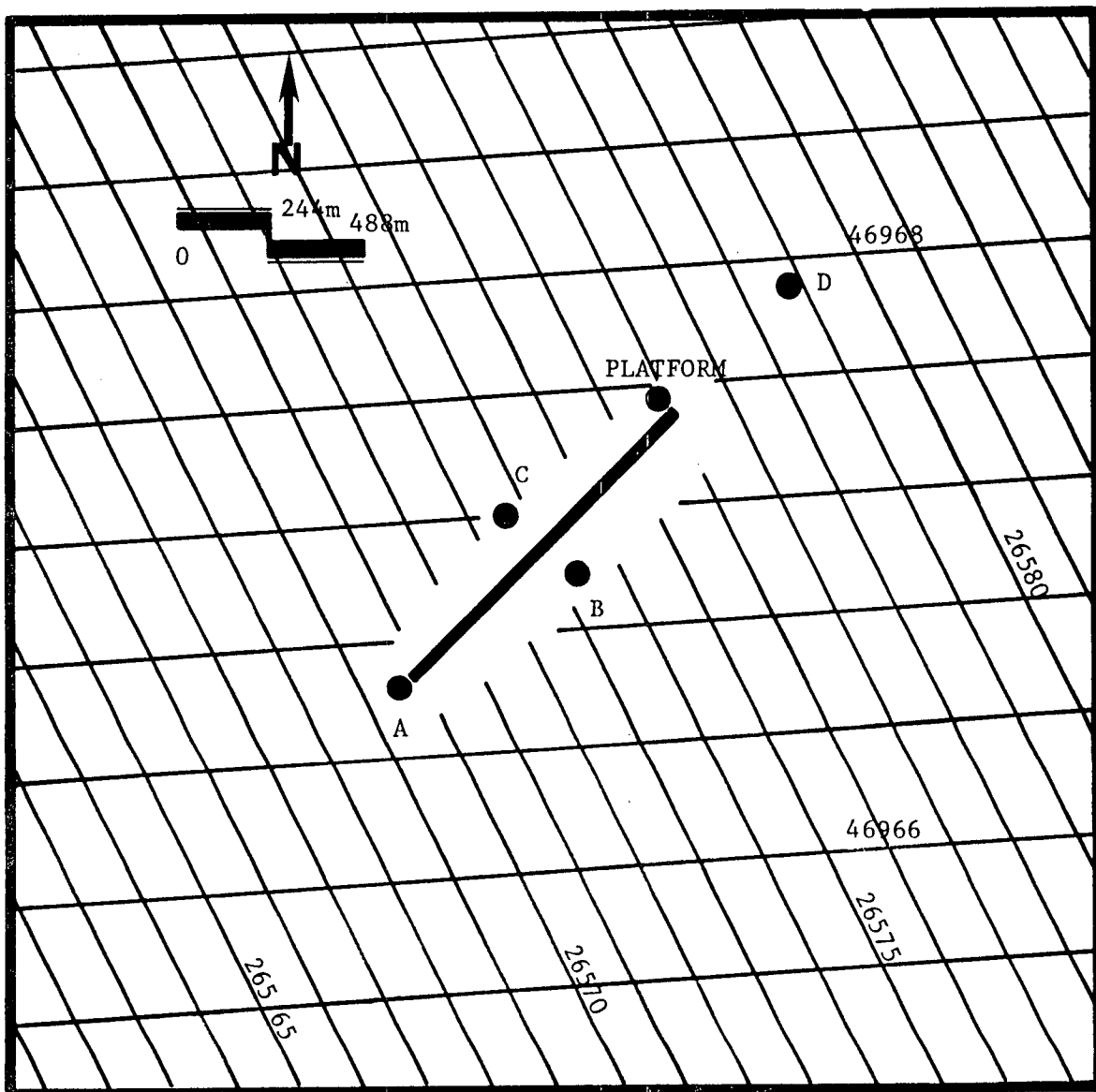


Figure 4-6. Example LORAN C chart used for brine plume measurements.

specially constructed plume tracking chart and the coordinates from the LORAN C receiver are slightly different. Therefore, the LORAN C coordinates of the platform are recorded from the LORAN C receiver before each plume track and compared with those on the chart in order to determine correction factors. The difference between the coordinates are normally constant during the time of plume tracking. These corrections are applied to all data in order to obtain the most accurate ship position.

4.3.3 Selection of Bottom Ambient Salinity

The data collected from June 1978 through June 1979 (Frey et al., 1981) indicate the bottom salinity at the diffuser site varied between 14 and 31 o/oo. Salinity fronts in the vicinity of the diffuser were observed and these fronts tend to move inshore and offshore depending on environmental conditions. It was shown that the largest salinity variation occurred in the cross shelf direction, and the alongshore salinity variation was observed to be less than 1 o/oo over a distance of 16 km (8.6 nm). Thus, the ambient bottom salinity in the diffuser area is very hard to determine exactly, but it is absolutely necessary to be able to make a reasonable estimate in order to evaluate the extent of the brine plume.

Since the alongshore variation of salinity is small, it was decided to select three control stations which are designated stations 20A, 20, and 20D to determine the ambient bottom salinity. Station 20 is a station for the monthly hydrographic data, and it is located 8.3

km (4.5 nm) east of the diffuser (see Figure 2-1 in Chapter 2) and on the same depth contour. Stations 20A and 20D are the same distance from the diffuser, but they are 3.7 km (2 nm) north and south of station 20 respectively. The bottom salinity from these stations are measured and used as the ambient bottom salinity in the diffuser area which was impacted by the brine plume. The cross shelf salinity variation between the ambient stations is assumed to be linear. This procedure is used unless the salinity data collected during the brine plume measurement showed there was a significant difference, and in this case, a transect from the plume measurement data which was furthest away from the diffuser is used. These procedures are slightly different from those used at Bryan Mound where a single control station has usually been found to be satisfactory because the salinity variation is normally not as large due to the increased water depth and distance offshore (Randall, 1981a).

4.3.4 Vertical Profile Measurements

After the research vessel completes the vertical profile measurements at the control stations, it proceeds to TAMU buoy D near the diffuser and anchors. Near surface and bottom current measurements are collected and a vertical profile of conductivity, temperature, depth, and dissolved oxygen is measured.

The bottom current data are used to determine the average direction of the bottom current, and a line is placed on the plume track chart in the direction of the average bottom current and passing

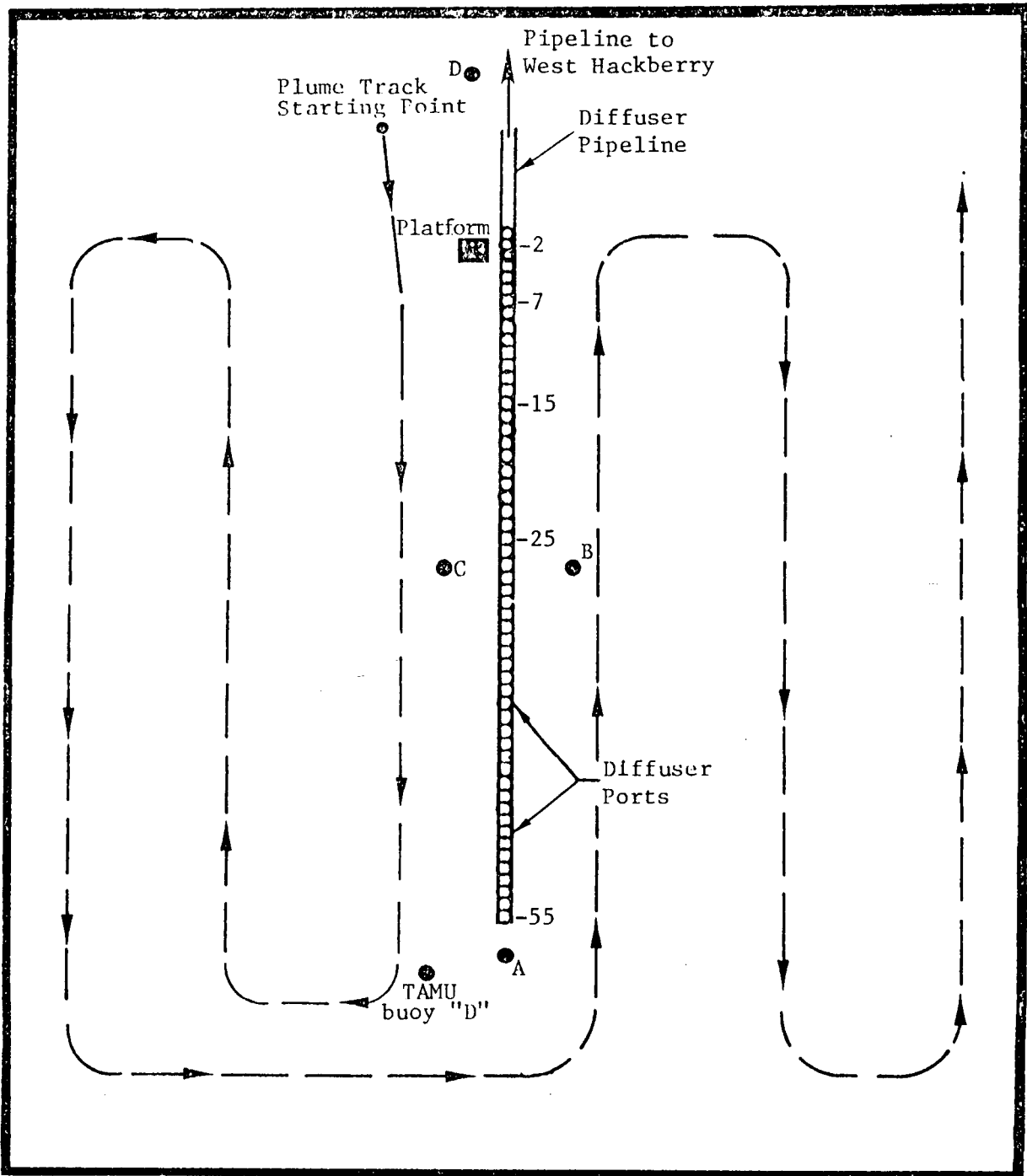


Figure 4-7. Schematic of plume tracking course for the West Hackberry diffuser area. Port numbers 2 and 25 through 55 were open from May 10, 1981 through April 25, 1982. Port numbers 2 and 15 through 55 were open from April 25 through April 30, 1982.

through the center of the diffuser. One station is selected at the intersection of the line and the center of the diffuser, and two additional stations are selected on the upstream and downstream side of the diffuser.

The research vessel weighs anchor and proceeds to the first vertical profile station. These profiles are obtained by lowering the CTD/DO sensor to the bottom and back to the surface while conductivity, temperature, dissolved oxygen, and depth are recorded on cassette tape by the automatic data logger. Water samples near the surface and bottom are collected at each station so that dissolved oxygen concentrations could be compared with measurements determined by Winkler titration procedures. The salinity data is used to evaluate the vertical extent of the brine plume in the immediate vicinity of the diffuser. The dissolved oxygen data is used to evaluate the effects of the brine plume on the vertical distribution of dissolved oxygen.

4.3.5 Areal Extent Measurements

The plume track starting point for measuring the areal extent is normally located inshore and on the west side of the platform as shown on Figure 4-7. At this point, the towing sled is deployed while the ship maintains a slow (3.7 km/hr, 2 kts) headway, and the CTD/DO system is activated. The towing cable and the conductor cable are let out simultaneously until 91 m (300 ft) are in the water. This is the optimum length of cable for towing at a normal speed of 5.6 km/hr (3

cts) while the sled remains on the bottom. The position of the sled on the bottom is confirmed by the depth sensor reading.

The ship steers a course which is nearly parallel to the diffuser and at a distance of approximately 183 m (600 ft) away in order to stay just outside of buoy C and TAMU buoy D as illustrated in Figure 4-7. This course is maintained while the sensor shows the salinity increases as the sled enters the plume and until the salinity decreases to a value indicating the 1 o/oo above ambient salinity contour has been reached. The research vessel makes a slow turn away from the diffuser and proceeds to a reverse course approximately 1 km away. The sled and sensor reenter the plume and this course is maintained until the sensor again shows the 1 o/oo above ambient region has been reached. The research vessel again makes a slow turn away and proceeds to a reverse course approximately 1 km further away. This procedure continues until the 1 o/oo above ambient region has been defined on the upstream side of the diffuser. Next, the research vessel proceeds to the downstream side of the diffuser and follows the same procedure until the 1 o/oo above ambient salinity contour is similarly defined. These plume tracking procedures normally take six to eight hours to complete.

During the tracking procedure, the conductivity, salinity, temperature, and depth data are recorded every minute on cassette tape and thermal printer paper by the automatic data logger. At the same time, the ship's location in terms of LORAN C coordinates is recorded by hand every minute in the LORAN C log book. Watches with sweep

hands are synchronized at the start to insure simultaneous recording of data. The depth data indicate whether the sled is staying on the bottom, and the temperature data are used to determine the presence of any thermal plume resulting from the brine discharge. The conductivity data which are converted to salinity provide the capability of determining isohaline contours that define the areal extent of the brine plume.

The isohaline contours are determined by plotting the location of the sled every minute during the plume tracking period. The conductivity is converted to salinity, and the corresponding salinity values are recorded alongside the location of the sled which is 91 m directly astern of the ship's LORAN C position. Once this is completed for the entire plume track, linear interpolation is used to locate the isohaline contours.

4.4 Areal Extent and Salinity of Measured Brine Plumes

4.4.1 Background

Brine discharge from the West Hackberry diffuser began on May 10, 1981, and plume measurements were planned for once a week during the first month after discharge began, once every two weeks during the second month, and once a month thereafter. All the results of the plume measurements are contained in Appendix D.

The first plume measurement was conducted on May 25, 1981, but the data show no +1 o/oo above ambient contour was detected. No discharge data is available for this date, but it is suspected that

the brine salinity was too low to detect the brine plume. On June 1, 1981, similar results were obtained when the brine salinity was 115 o/oo. The July 17, 1981 plume measurement also showed no indication of an increase in salinity in the vicinity of the diffuser. The discharge data indicated that the brine salinity was 214 o/oo and the rate of discharge was 21,675 barrels/hr. A plume is expected to be detected under these conditions based upon experience from Bryan Mound (Randall, 1981a) and subsequent measurements, and thus, no explanation is given for the results obtained on July 17, 1981.

In September 1981, the brine discharge was shutdown until September 15, but when discharge began again, it was on an intermittent basis. Thus, no plume measurements were made during the month of September and no results are available in Appendix D.

A plume track was completed on March 1, 1982, and again the data showed the salinity did not increase to values which would permit drawing a +1 o/oo above ambient salinity contour. On this date, the brine discharge rate was 35,042 barrels/hr and the average brine salinity was 180 o/oo. The combination of high discharge rate and low brine salinity is believed to be the reason for no closing contours.

The remainder of the plume measurements on June 9, June 17, June 30, August 12, October 28, November 25, and December 16 in 1981 and February 14 and April 30 in 1982 resulted in at least the closing of the +1 o/oo above ambient salinity contour, and these are illustrated in Appendix D. The plume measurement data were collected 25 cm above the sea floor and the salinity contours were drawn for the actual

salinity values to the nearest part per thousand and for increments of 1 o/oo above the ambient salinity. Next, the area inside the closed contours was measured with a polar planimeter. The areal extent and salinity of selected brine plumes measured during first year of discharge are illustrated and described in this section.

4.4.2 June 9, 1981 Brine Plume

The brine plume contours which were determined from the June 9, 1981 data are shown in Figure 4-8. On this date, the brine was being discharged at a rate of 23,580 barrels/hr and the average brine pit salinity was 178 o/oo. The ambient salinity was 29.7 o/oo which was measured at station 20 located 8.3 km (4.5 nm) east of the diffuser and at the same depth contour.

The data in Figure 4-8 show the 30 o/oo contour could be closed around the diffuser and the area inside was measured as 9.4 km². The highest salinity was 30.9 o/oo which was 1.2 o/oo above the ambient salinity. The +1 o/oo above ambient salinity contour is shown in Figure 4-9 and the area inside this contour was 0.3 km². The small above ambient salinities and areal extent of the plume on this date are attributed to the low brine salinity of 178 o/oo.

The average bottom current for the period of plume tracking was determined by vector averaging half-hour data points obtained from the data record of the bottom current meter located 1.8 m (6 ft) above the bottom at instrument site D which is 274 m (900 ft) west of buoy A. The average current speed was 13.4 cm/s in the direction of 037°T as shown by the arrow in Figures 4-8 and 4-9. The bottom current time-series plots for June 9, 1981 and other plume measurement days are illustrated in Appendix B.

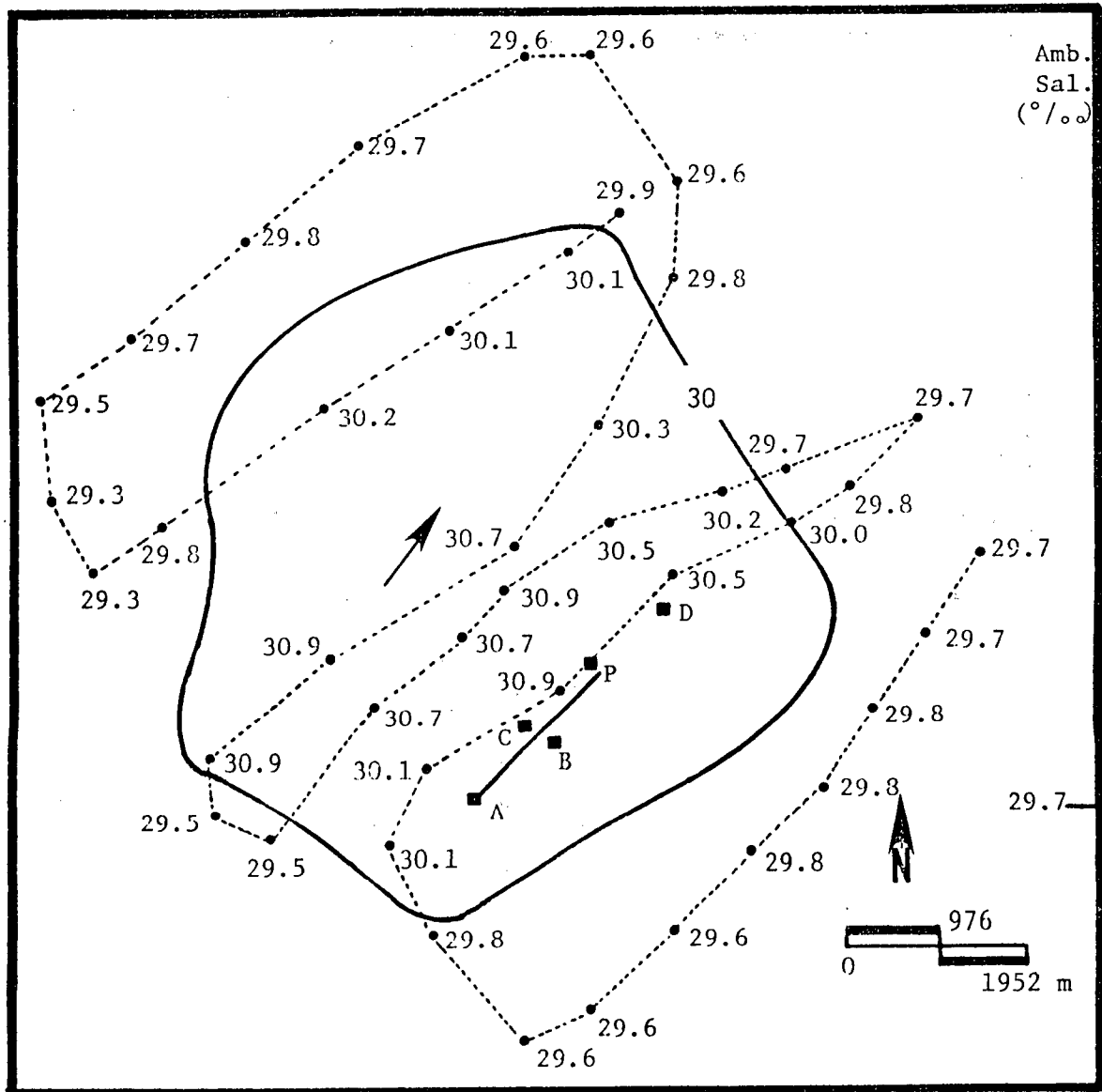


Figure 4-8. Isohaline contours for the West Hackberry brine plume on June 9, 1981. The brine discharge rate and brine pit salinity were 23580 barrels/hr and 178‰ respectively. The average bottom current was 13.4 cm/s in the direction of the arrow. The dashed line indicates the ship's track. Buoys A, B, C and D. (■) mark the diffuser area and P marks the satellite platform near diffuser port number one.

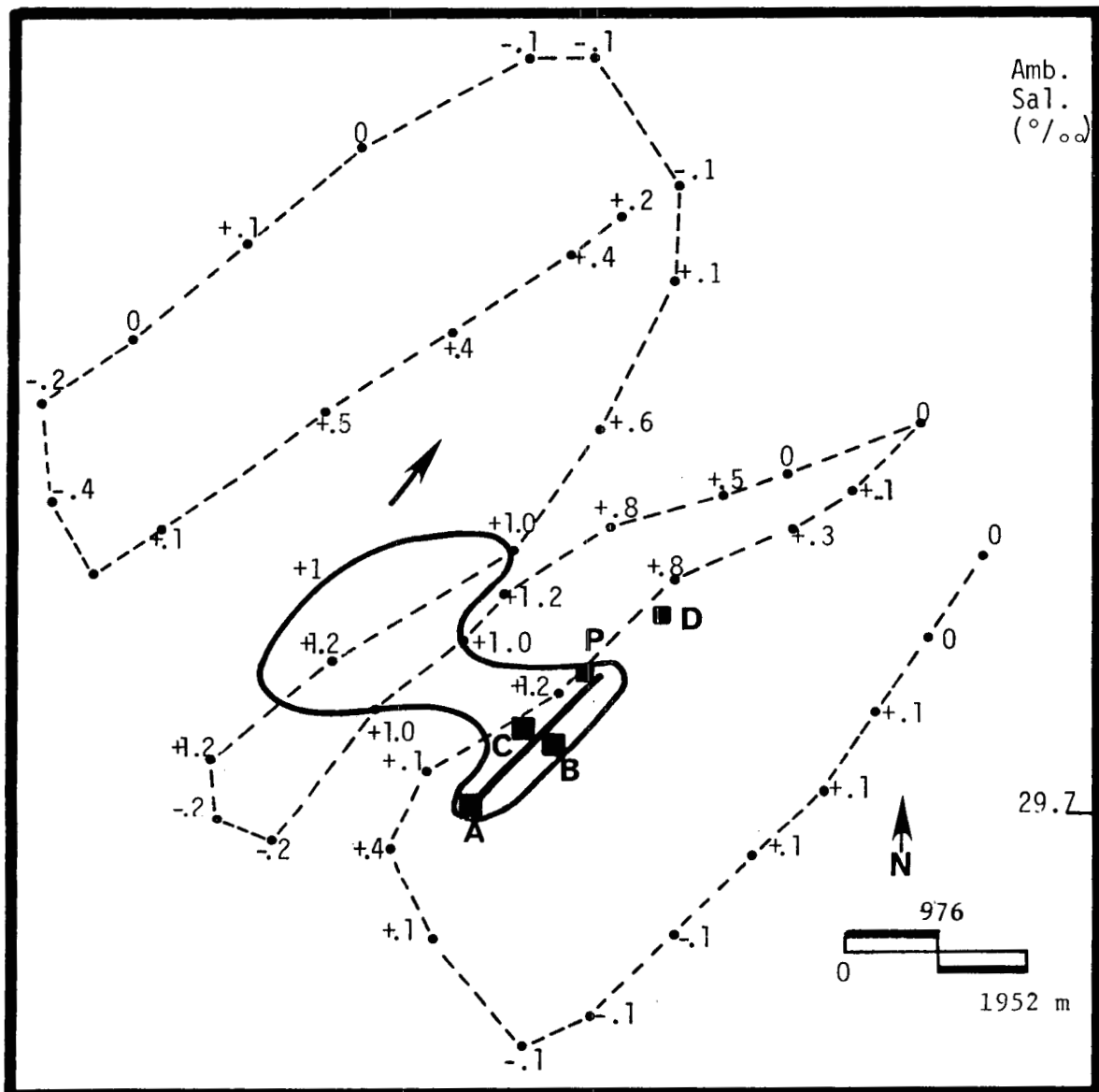


Figure 4-9. Above ambient isohaline contours for the West Hackberry brine plume on June 9, 1981. The brine discharge rate and brine pit salinity were 23,580 barrels/hour and 178 o/oo respectively. The average bottom current was 13.4 cm/s in the direction of the arrow. The dashed line indicates the ship's track. Buoys A, B, C, and D (■) mark the diffuser area and P marks the satellite platform near diffuser port number one.

The time required to track the plume was 6.0 hours, and thus, the isohaline contours shown in Figures 4-8 and 4-9 are a type of average over the time period. During the time of the plume measurements, the bottom current may change and this can distort the plume contours.

The bottom temperature data were measured, and these data show the bottom water was nearly isothermal over the entire brine plume area. The temperature varied between 27.4 and 27.8°C while the brine pit temperature was 31°C, and it was concluded that no detectable thermal plume was present.

4.4.3 August 12, 1981 Brine Plume

On August 12, 1981, the brine was being discharged through 32 ports at a rate of 25,643 barrels/hr and a salinity of 228 o/oo. The average bottom current was 6.8 cm/s in the direction of 208°T as indicated by the arrow in Figures 4-10 and 4-11. The bottom ambient salinity varied from 28.4 to 30.4 o/oo over the cross-shelf distance of the plume as shown at the right hand margin of each contour figure.

The isohaline and the above ambient isohaline contours for the August 12, 1981 plume are illustrated in Figure 4-10 and 4-11 respectively. Figure 4-10 shows that the 32 and 31 o/oo isohalines were closed around the diffuser and that the 29 and 30 o/oo isohalines were distorted indicating the presence of the excess salinity resulting from the brine discharge. The area inside the closed 31 and 32 o/oo contours was 8.1 and 2.0 km² respectively. The highest salinity measured was 32.1 o/oo which was 4.1 o/oo above the ambient salinity.

The above ambient isohaline contours resulted in four closed contours which closely followed the direction of the average bottom

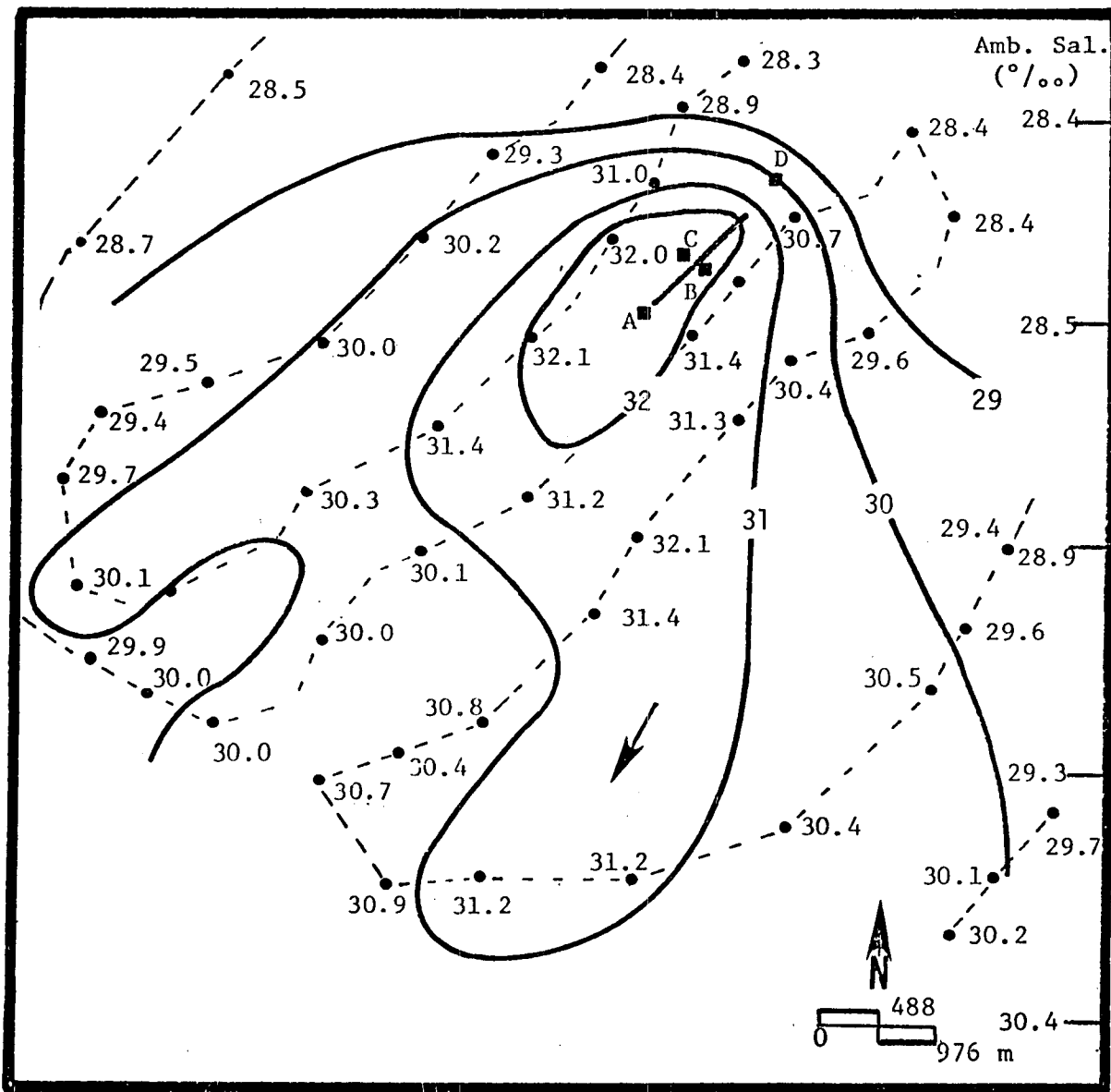


Figure 4-10. Isohaline contours for the West Hackberry brine plume on August 12, 1981. The brine discharge rate and brine pit salinity were 25643 barrels/hr and 228 ‰, respectively. The average bottom current was 6.8 cm/s in the direction of the arrow. The dashed line indicates the ship's track. Buoys A, B, C and D (■) mark the diffuser area and P marks the satellite platform near diffuser port number one.

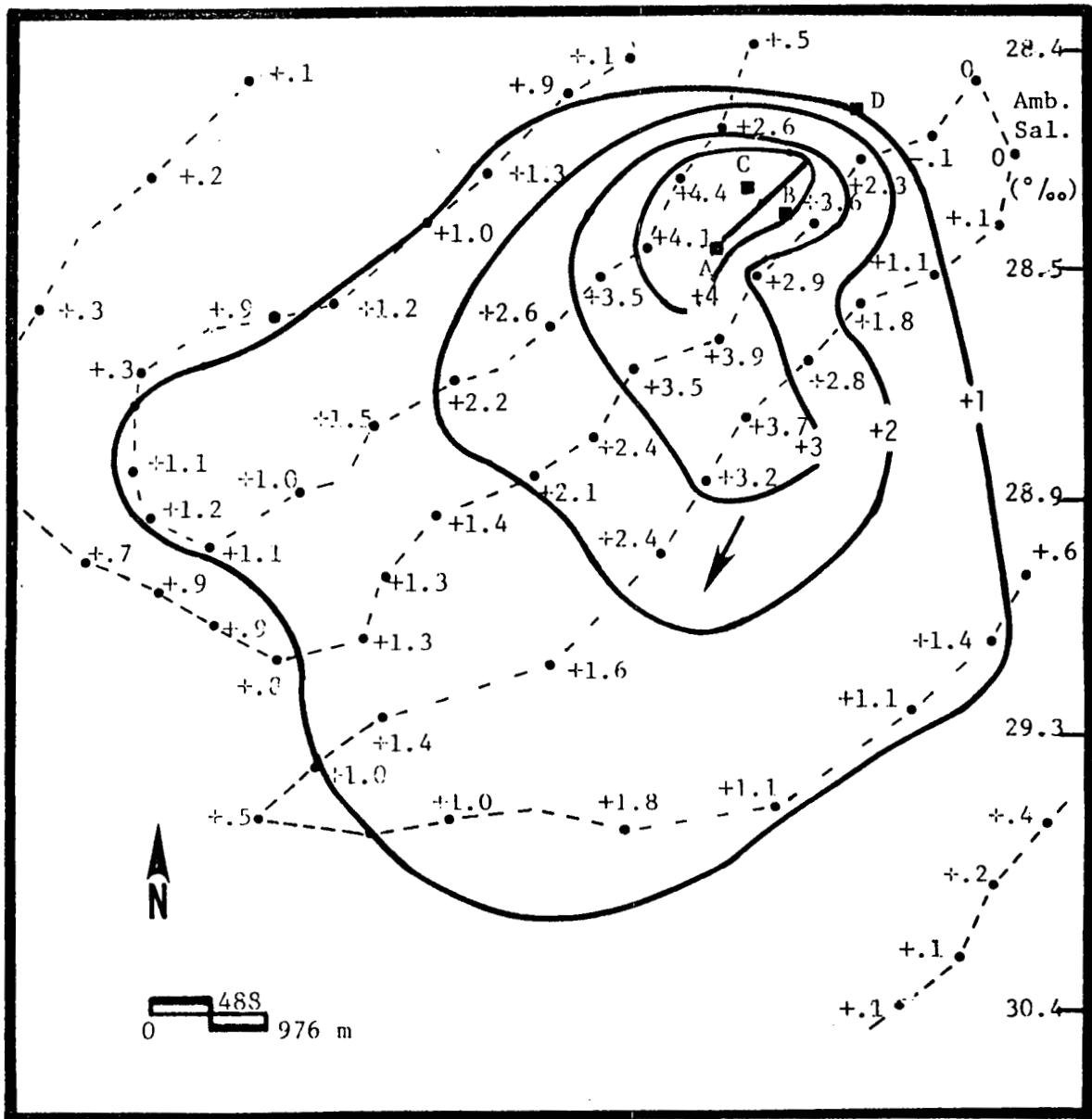


Figure 4-11. Above ambient isohaline contours for the West Hackberry brine plume on August 12, 1981. The brine discharge rate and brine pit salinity were 25643 barrels/hr and 228 ‰, respectively. The average bottom current was 6.8 cm/s in the direction of the arrow. The dashed line indicates the ship's track. Buoys A, B, C and D (●) mark the diffuser area and P marks the satellite platform near diffuser port number one.

current as shown in Figure 4-11. Above ambient isohaline contours of +4, +3, +2, and +1 o/oo were closed, and these contours enclosed an area of 1.1, 4.2, 10.8, and 32.2 km² respectively. The 32.2 km² area inside the +1 contour was the largest area measured during the first year of discharge. The +1 o/oo contours also extended the longest distance from the diffuser which was 5.7 km in the direction of 199°T. A value of +4.4 o/oo was the highest above ambient salinity measured on this date.

The salinity data points for this plume track were collected over a 7-hour period from 1300 to 2000 hours. The bottom temperature varied between 30.1 and 30.7°C while the average brine pit temperature was 34°C so there was no indication of a thermal plume.

4.4.4 November 25, 1981 Brine Plume

The November 25, 1981 brine plume was measured when the brine was being discharged at a rate of 21,680 barrels/hr at an average salinity and temperature of 209 o/oo and 23°C. The average bottom current was 7.6 cm/s in the direction 245°T as shown by the arrow in Figures 4-12 and 4-13. The bottom ambient salinity increased from an inshore value of 29.6 o/oo to an offshore value of 30.6 o/oo as indicated along the right hand margin of each contour figure.

Figures 4-12 and 4-13 illustrate the isohaline and above ambient isohaline contours which were determined from the November 25, 1981 plume measurements. Isohalines of 31, 32, 33, and 34 o/oo were closed around the diffuser as shown in Figure 4-12, and the area within these contours was 26.1, 12.6, 3.9, and 1.1 km² respectively. The highest salinity (34.4 o/oo) was measured near the diffuser and it was 4.4 o/oo above the bottom ambient salinity measured at station 20.

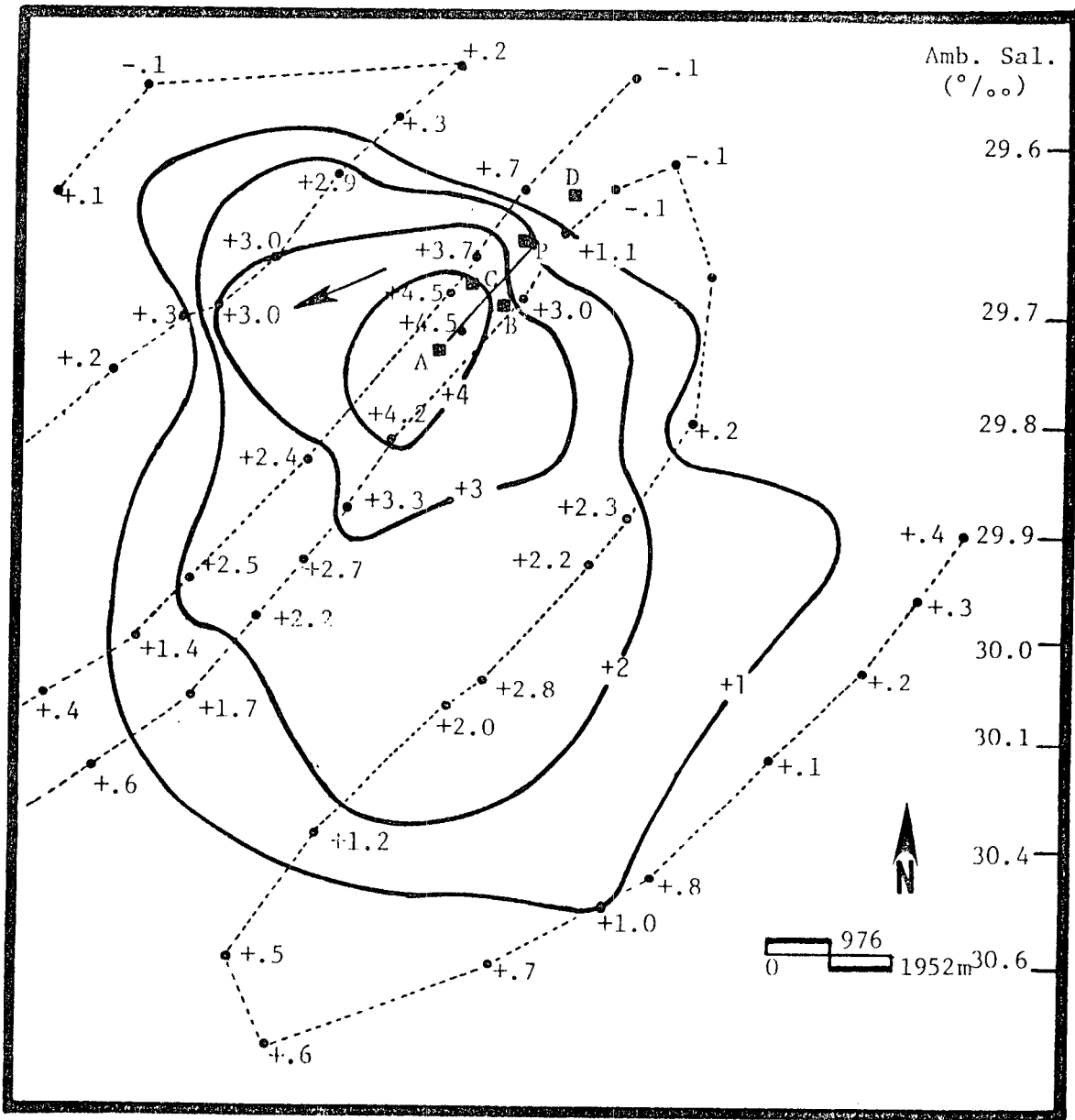


Figure 4-13. Above ambient isohaline contours for the West Hackberry brine plume on November 25, 1981. The brine discharge rate and brine pit salinity were 21680 barrels/hr and 28.9‰ respectively. The average barotropic current was 7.6 cm/s in the direction of the arrow. The dashed line indicates the ship's track. Buoys A, B, C and D (■) mark the diffuser area and P marks the satellite platform near diffuser port number one.

Four above ambient salinity contours are shown in Figure 4-13, and the area within the +4, +3, +2, and +1 o/oo contours was 0.9, 5.2, 12.1, and 20.3 km² respectively. The +1 o/oo contour extended 2.7 km up the coast which was the maximum distance measured up the coast during the first year of discharge. The highest above ambient salinity was +4.5 o/oo which was similar to that measured on August 12, 1981.

The plume measurement was made from 1130 to 1830 hours for a total period of seven hours. The bottom temperature varied between 18.8 and 19.7°C while the average brine temperature was 23°C, and there was no indication of a thermal plume.

4.4.5 February 14, 1982 Brine Plume

The brine was being discharged at a rate of 23,896 barrels/hr on February 14, 1982, and the average brine salinity and temperature were 217 o/oo and 16°C respectively. The average direction of the bottom currents was 259°T at an average speed of 15.2 cm/s. The bottom ambient salinity increased from 31.0 to 31.7 o/oo over the cross-shelf distance of the plume as shown at the right margin of the plume contour figures.

The isohaline and above ambient brine plume contours for February 14, 1982 are illustrated in Figures 4-14 and 4-15. Isohaline contours of 32, 33, 34, and 35 o/oo were closed on this date as shown in Figure 4-14. The 34 o/oo contour broke into two separate contours with one around the diffuser (top) and one offshore of diffuser (bottom). The area inside the top 34 o/oo isohaline contour was 1.6 km² and 2.4 km² inside the bottom contour. The area inside the 35, 33, and 32 o/oo contours was 0.5, 7.9, and 27.3 km² respectively. The salinity

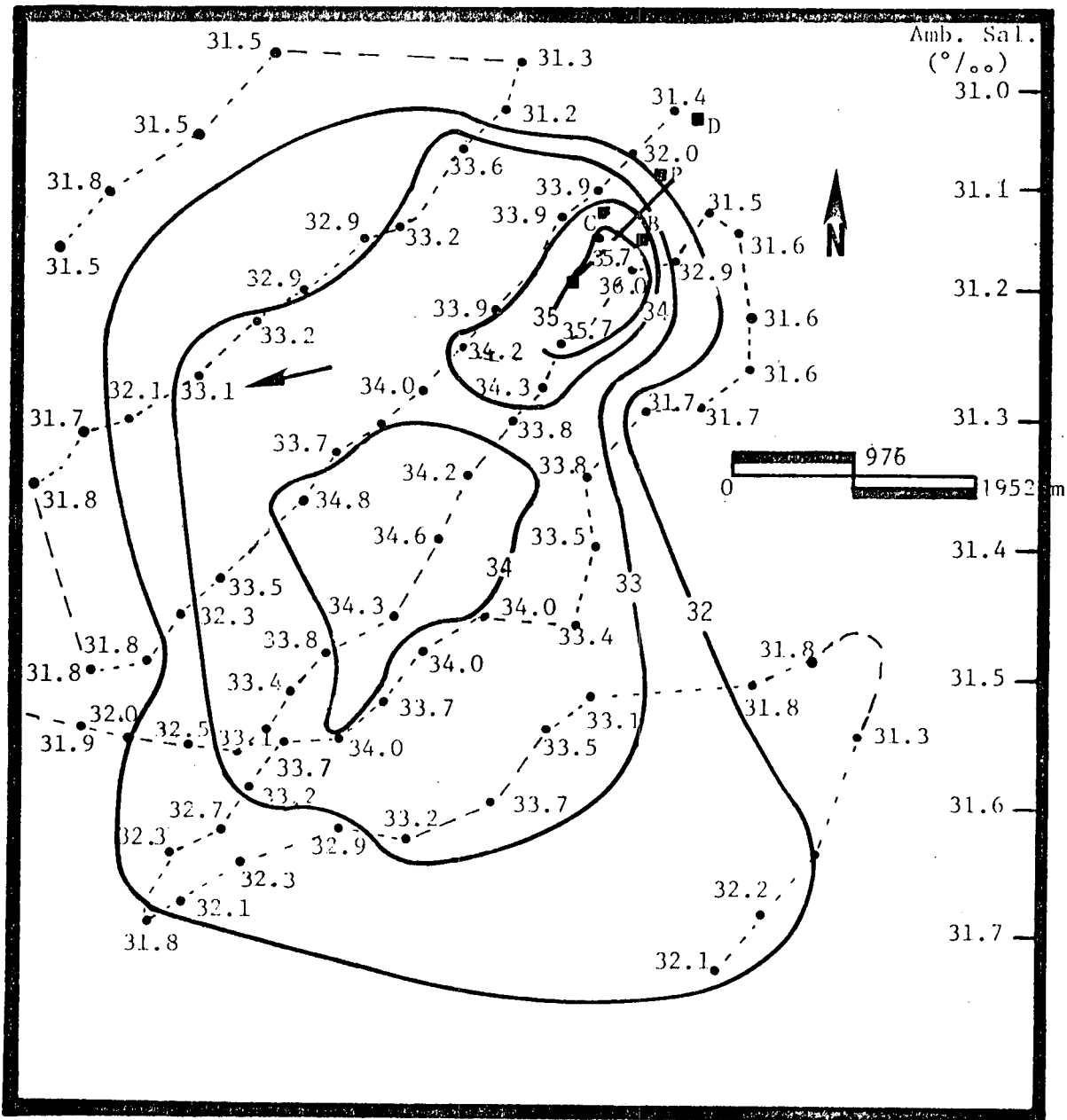


Figure 4-14. Isohaline contours for the West Hackberry brine plume on February 14, 1982. The brine discharge rate and brine pit salinity were 23896 barrels/hr and 217‰ respectively. The average bottom current was 15.2 cm/s in the direction of the arrow. The dashed line indicates the ship's track. Buoys A, B, C and D (■) mark the diffuser area and P marks the satellite platform near diffuser port number one.

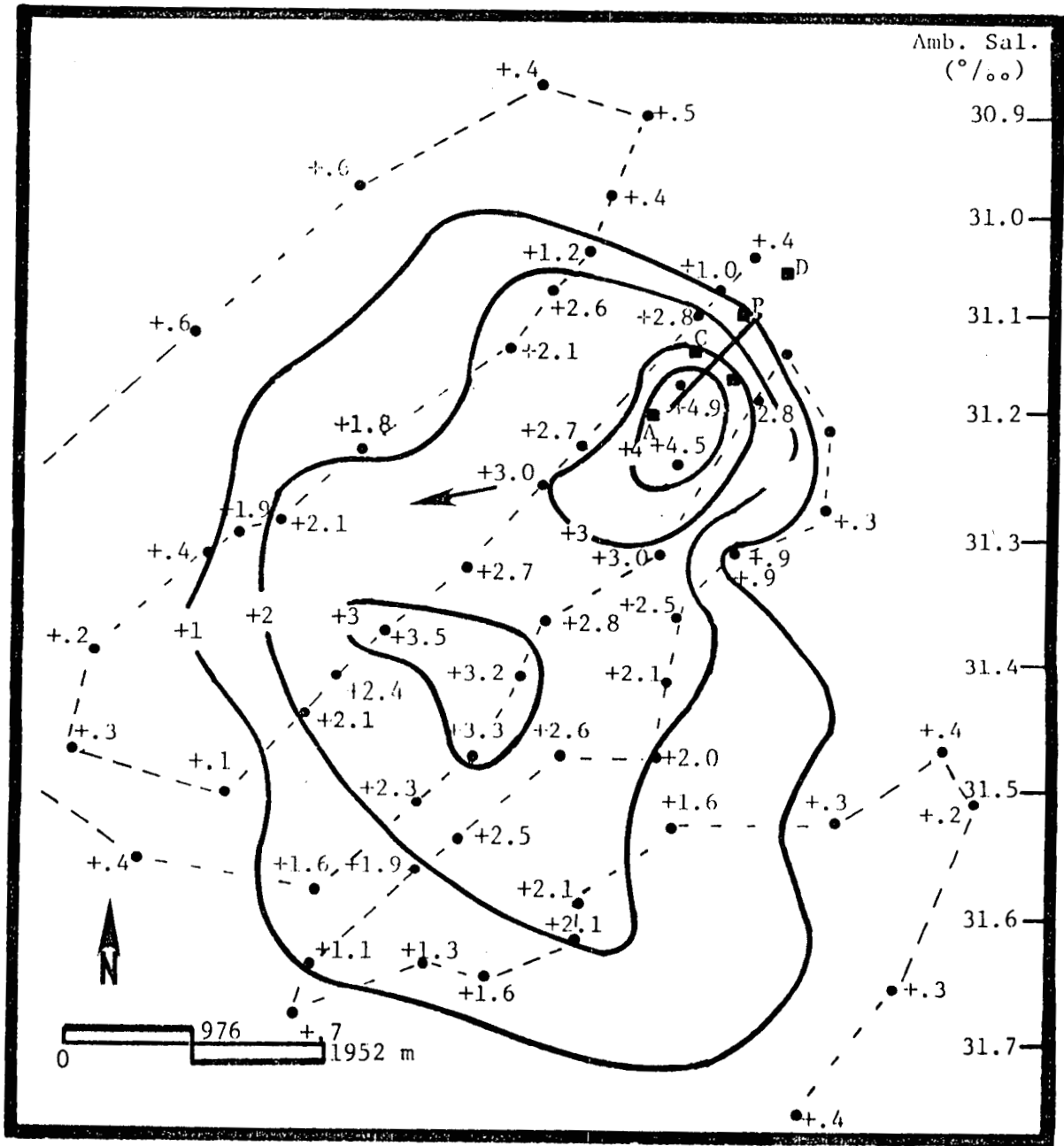


Figure 4-15. Above ambient isohaline contours for the West Hackberry brine plume on February 14, 1982. The brine discharge rate and brine pit salinity were 23896 barrels/hr and 217‰, respectively. The average bottom current was 15.2 cm/s in the direction of the arrow. The dashed line indicates the ship's track. Buoys A, B, C and D (■) mark the diffuser area and P marks the satellite platform near diffuser port number one.

measurements were highest in the vicinity of the diffuser with the highest measurement being 36.0 o/oo which was also the highest value measured during the first year of discharge.

The above ambient salinity contours are shown in Figure 4-15 in which +1, +2, +3, and +4 o/oo contours are closed. Similar to the isohaline contours, the +3 o/oo contour was broken into two locations with areas of 1.4 and 0.5 km² at the top and bottom. The area inside the +1, +2, and +4 o/oo contours was 23.2, 12.4, and 0.5 km² respectively. The +1 contour extended 5.2 km south (offshore), 1.3 km north (inshore), 3.9 km west, and 1 km east of the center of the diffuser. The highest above ambient salinity was +4.9 o/oo which was the maximum above ambient value measured during the first year discharge period. The longest distance from the diffuser center to the +2, +3, and +4 o/oo contours was 4.5, 3.1, and 1.0 km respectively.

The tracking time for this plume was 7.5 hours from 1000 to 1730 hours. The bottom temperature was nearly isothermal over the plume area with maximum and minimum temperatures of 11.6 and 10.7°C. The average brine temperature was 16°C, and again a thermal plume was not observed during the plume measurements.

4.4.6 Summary of Brine Plume Areal Extent and Salinity Results

A summary of the areal extent and salinity data obtained from the plume measurements conducted during the first year of brine discharge are tabulated in Table 4-1. This table shows the average bottom current speed and direction during the plume measurement period, the daily average brine pit salinity and the average brine discharge rate. The ambient bottom salinity at station 20 is tabulated, and the area

Table 4-1. Summary of West Hackberry brine plume areal extent data.

Date	Average Bottom Current		Brine Pit Salinity o/oo	Brine Discharge Rate Barrels/hr	Station 20 Salinity o/oo	Areal Extent			
	Speed cm/s	Direction (True)				Salinity Contours	Area km ²	Above Ambient Sal. Contours	Area km ²
06/09/81	13.4	3.7°	178	23,580	29.7	30	9.4	+1	0.3
06/17/81	5.7	128°	189	26,214	30.5	32	6.0	+1	0.9
06/30/81	7.6	157°	208	28,307	22.1			+1 +2 +3 +4	22.8 9.4 3.9 .6
08/12/81	6.8	208°	228	25,643	28.5	31 32	5.1 2.0	+1 +2 +3 +4	32.2 10.8 4.2 1.1
10/28/81	15.9	293°	225	24,500	30.9	32 33 34 35	5.5 1.4 0.5 0.1	+1 +2 +3 +4	6.6 1.5 0.5 0.1
11/25/81	7.6	245°	209	21,680	29.9	31 32 33 34	26.1 12.6 3.9 1.1	+1 +2 +3 +4	20.3 12.1 5.2 0.9
12/16/81	5.8	206°	202	21,500	31.4	31 32 33 34	28.3 7.9 2.6 0.9	+1 +2 +3	8.4 4.2 1.0
02/14/82	15.2	259°	217	23,896	30.9	32 33 34 top 34 bot 35	27.3 14.9 1.6 2.5 .5	+1 +2 +3 top +3 bot +4	23.2 12.4 1.4 0.5 0.5
04/30/81			229	23,315	28.9	30 31	11.1 6.1	+1 +2 +3	19.9 10.0 4.9

within the normal salinity and above ambient salinity contours are also shown.

In summary, Table 4-1 shows the largest areal extent within the +1, +2, +3, and +4 o/oo above ambient contours was 32.2 km² on 8/12/81, 12.4 km² on 2/14/82, 5.2 km² on 11/25/81, and 1.1 km² on 8/12/81, respectively. The highest above ambient salinity contour was +4 o/oo which occurred on 6/30/81, 8/12/81, 10/28/81, 11/25/81 and 2/14/82. During the first 12 months of discharge, the highest salinity measured during the plume tracks was 36.0 o/oo which was 4.9 o/oo above the ambient salinity measured on February 14, 1982.

Table 4-2 shows a summary of the maximum measured distances from the center of the diffuser to the above ambient salinity contours. It shows the longest distances inshore, offshore, upcoast, downcoast, and the magnitude and direction of the longest distance. The longest distance to the +1 o/oo above ambient contour was 5.7 km (3.1 nm) from the diffuser in the direction of 199°T or southsouthwest of the diffuser. The longest distance to the +2, +3, and +4 o/oo contours was 4.4, 3.4, and 1.7 km (2.4, 1.8, and 0.9 nm) respectively. The maximum inshore and offshore distances for the +1 o/oo above ambient contour were 2.9 km (1.6 nm) and 5.3 km (2.9 nm). In the upcoast and downcoast direction, the longest distances to the +1 o/oo above ambient contour were 2.7 km (1.5 nm) and 4.8 km (2.6 nm) respectively.

4.5 Vertical Salinity Profiles

4.5.1 Background

The vertical extent of the brine plume was determined by measuring the vertical salinity profile directly over the diffuser and at other selected locations. These profiles were then compared to an

Table 4-2. Summary of maximum measured distances from center of diffuser to above ambient salinity contours at the West Hackberry discharge site.

Contour o/oo	Longest Dist. Inshore, 0° (km)	Longest Dist. Offshore, 180° (km)	Longest Dist. Upcoast, 90° (km)	Longest Dist. Downcoast, 270° (km)	Longest Dist. Magnitude (km)	Distance Direction (°T)
+1	2.9 (6/30/81)	5.3 (8/12/81)	2.7 (11/25/81)	4.8 (8/12/81)	5.7 (8/12/81)	199
+2	1.7 (6/30/81)	4.4 (2/14/81)	2.0 (6/30/81)	3.6 (6/30/81)	4.4 (2/14/81)	187
+3	0.9 (6/30/81)	3.0 (2/14/81)	0.8 (8/12/81)	2.8 (6/30/81)	3.4 (2/14/81)	210
+4	0.5 (8/12/81)	1.4 (6/30/81)	0.6 (8/12/81)	0.8 (11/25/81)	1.7 (6/30/81)	210

ambient profile which was taken at station 20. The vertical distance above the bottom at which the salinity profile deviated from the ambient profile was determined to be the vertical extent of the brine plume. After the vertical extent was evaluated, it was compared with the values computed from empirical relationships developed by Tong and Stolzenbach (1979).

The vertical profiles were taken in the plume near field and intermediate field areas which have been estimated to be within 305 m (1000 ft) of the diffuser. The vertical profiles were collected with the same CTD/DO instrument as was used for the plume measurements. For the vertical profiling, the CTD/DO sensor was attached to a weighted line and lowered to the bottom and then raised to the surface while the conductivity and depth were simultaneously recorded on cassette tape using the data logger. The data were recorded at the bottom, 1 m above the bottom, every 3 m, and 1 m below the surface at the control stations 20A, 20, and 20D. More frequent data were collected near the bottom at the vertical profile stations in the plume area. These data were then converted to salinity and plotted to show the vertical distribution of salinity near the diffuser. A minimum of five vertical profile stations were selected along a line intersecting the diffuser center and approximately parallel to the measured bottom current. One station was nearly directly over the diffuser, two were on the west side and the other two were on the east side of the diffuser.

In this section, selected vertical profiles and a comparison of the plume vertical extent as determined from the vertical profiles and as computed from empirical equations are described. These profiles

were collected just prior to the plume measurements described in the previous section. Vertical profiles were measured on the following days: May 25, June 1, June 9, June 17, June 30, July 17, August 12, October 28, November 25 and December 16 in 1981, and on February 14, March 1, and April 30 in 1982. All of these profiles are contained in Appendix D.

4.5.2 June 9, 1981 Vertical Salinity Profiles

The ambient vertical profile at station 20 in Figure 4-16 shows that fresher water (27.0 o/oo) was located in the upper six meters of the water column, and a halocline existed from 6.0 to 7.5 m where the salinity increased from 27.0 to 29.7 o/oo. The salinity was essentially isohaline from 7.5 m to the bottom with a bottom salinity of 30.0 o/oo.

Six vertical profiles were measured on this date and their locations are illustrated on the second page of Figure 4-16. The brine was being discharged at an average rate and salinity of 23,580 barrels/hr and 170 o/oo respectively. Station 1 was located almost directly over the diffuser, and the data show the top six meters were not as fresh as that at station 20 with the salinity varying from 27.4 o/oo at 1.9 m to 28.5 o/oo at 6.3 m. The halocline was also not as sharp as found at the control station, and the salinity varied from 28.5 o/oo at 6.3 m to 29.3 o/oo at 7.8 m. Near 9 m, the salinity at station 1 increased to 30.5 o/oo which was 0.5 o/oo above the bottom ambient salinity. The increase of 0.5 o/oo is attributed to the brine discharge and consequently the vertical extent of the plume was determined to be 0.6 m. The other vertical profiles were very similar to station 1, and the highest bottom salinity was 31.3 o/oo at station

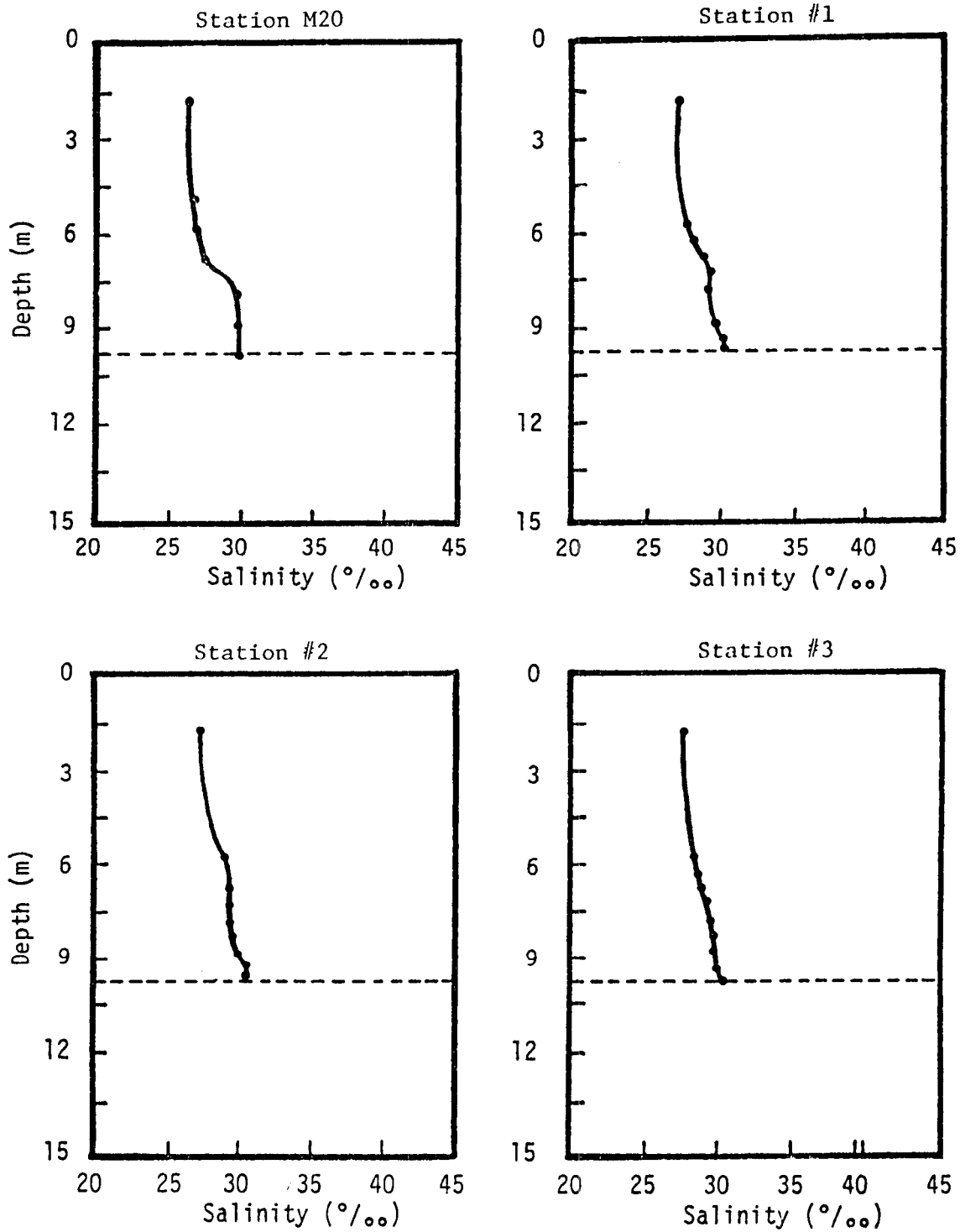


Figure 4-16. Vertical salinity profiles near the diffuser on June 9, 1981. The dashed line represents the depth of the natural bottom (9.6 m). Stations M20A, M20, and M20D are control stations located 7.4 km east of the diffuser, and stations M20A and M20D are 3.7 km north (inshore) and south (offshore) of station 20 respectively. A schematic of the near diffuser station locations is shown on the last page of each figure.

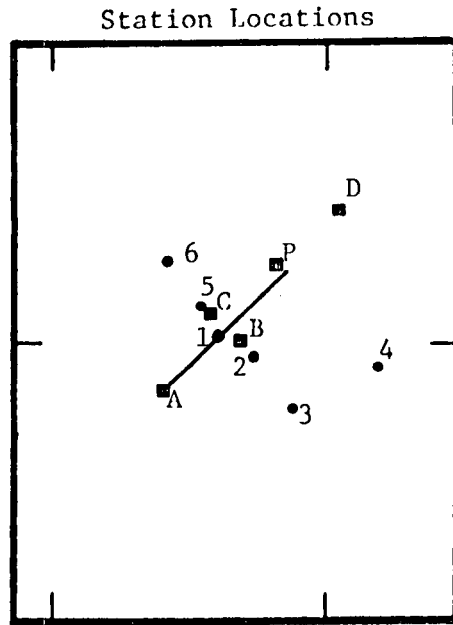
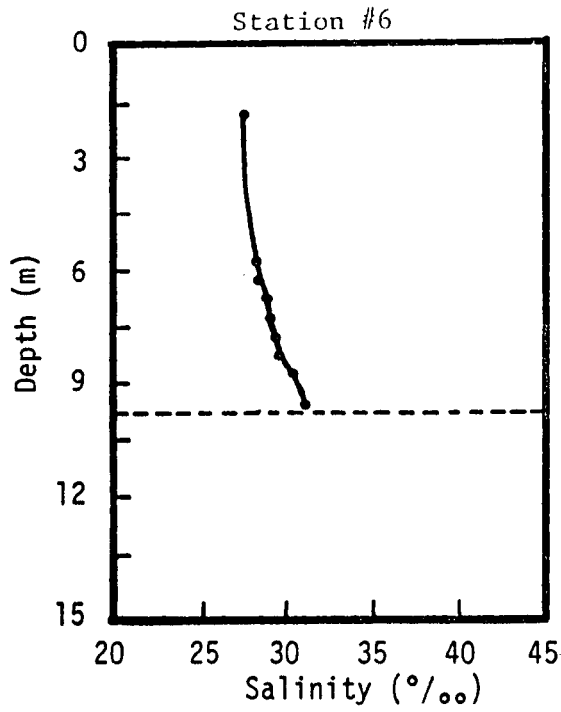
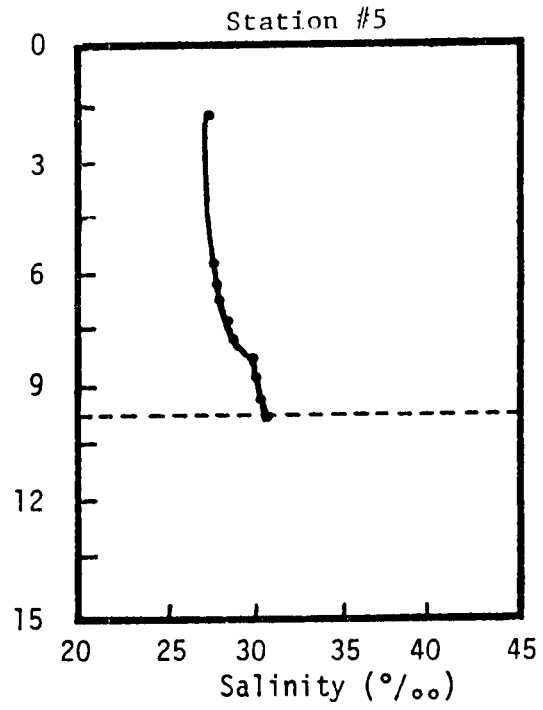
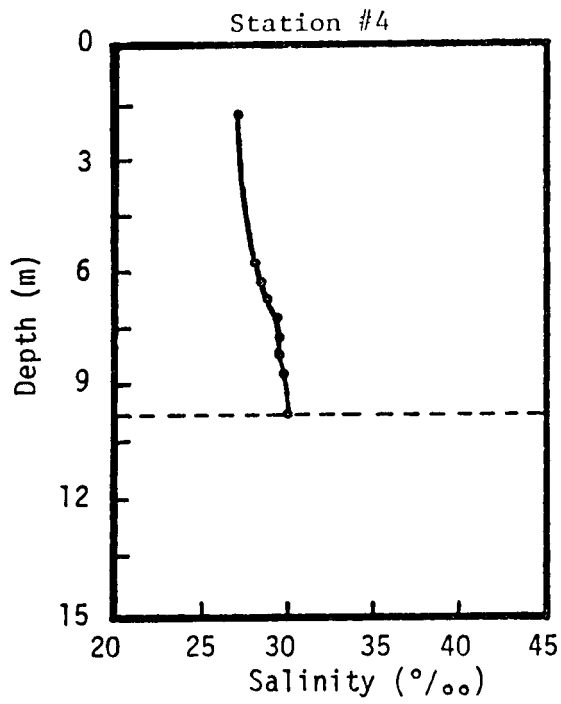


Figure 4-16. Continued

6. The vertical extent was not as apparent on this date as will be shown in some of the later profiles, and the cause was attributed to the relatively low brine salinity.

4.5.3 August 12, 1981 Vertical Salinity Profiles

Station 20 in Figure 4-17 shows the ambient salinity increases from 27.8 o/oo near the surface to 28.3 o/oo at the bottom. This nearly isohaline profile is much more apt to clearly show the extent of the brine plume than those encountered during periods of strong stratification as was found in June and July 1981 and illustrated in Appendix Figures D-22, D-23, and D-24.

Station 2 was located almost directly over the diffuser, and the surface salinity was 28.3 o/oo. The salinity profile, Figure 4-17, was isohaline to a depth of 7.5 m, and then the salinity increased rapidly to a maximum value of 32.0 o/oo at the bottom. Thus, the bottom salinity was 3.7 o/oo above the bottom salinity at station 20, and the vertical extent of the brine plume was 2.2 m as determined by the deviation from the ambient profile at 7.5 m.

The other vertical profile stations in Figure 4-17 show similar results. Station 1 was approximately 300 m east of the diffuser and the bottom salinity was 31.1 o/oo, and its vertical extent was less than that at station 2. The highest bottom salinity was measured at station 3 with a value of 32.8 o/oo. Like station 1, stations 3, 4, and 5 show the plume was very close to the bottom with a vertical extent near 1 m.

4.5.4 November 25, 1981 Vertical Salinity Profile

On November 25, 1981, brine was being discharged at a rate of

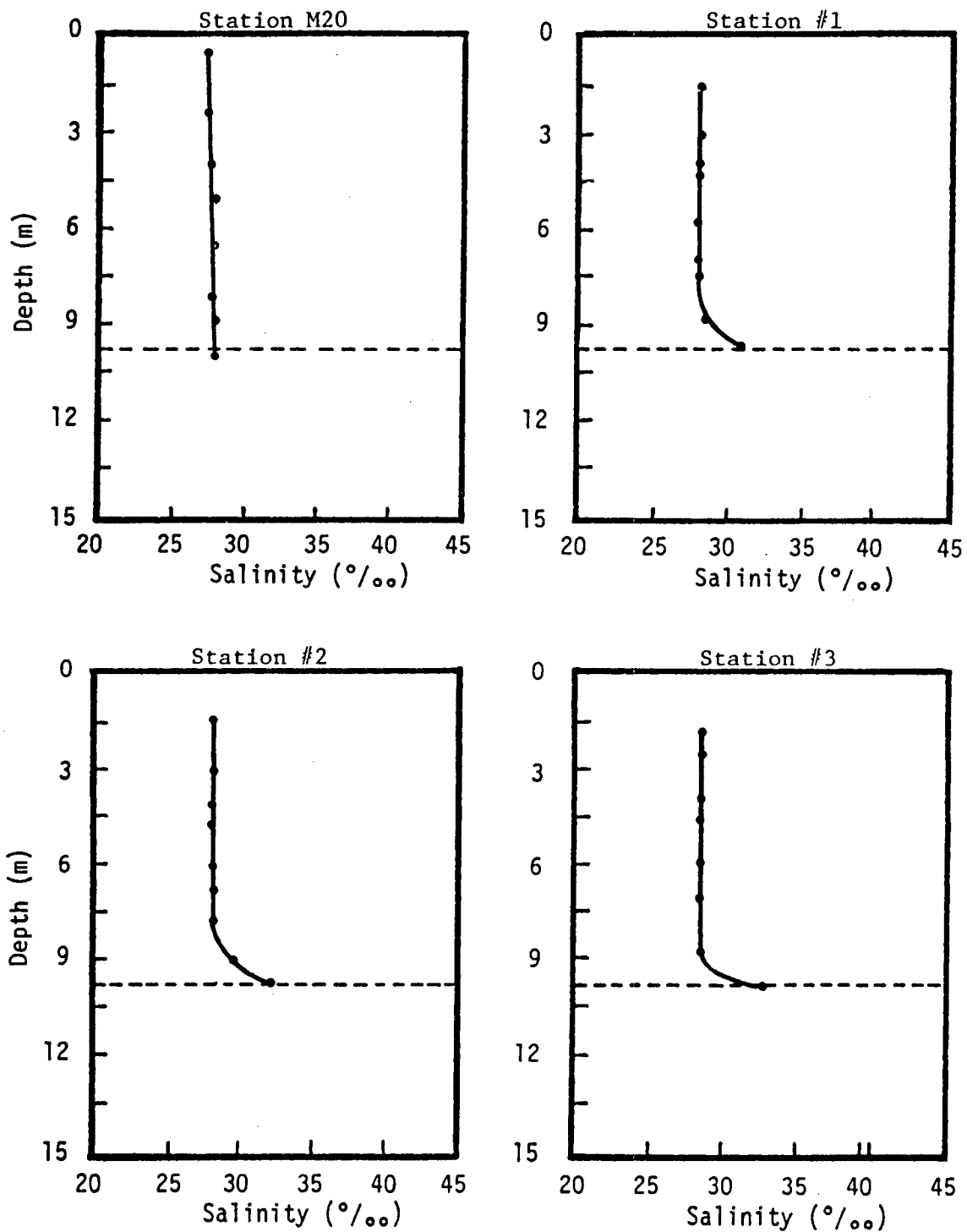


Figure 4-17. Vertical salinity profiles near the diffuser on August 12, 1981. The dashed line represents the depth of the natural bottom (9.6 m). Stations M20A, M20, and M20D are control stations located 7.4 km east of the diffuser, and stations M20A and M20D are 3.7 km north (inshore) and south (offshore) of station 20 respectively. A schematic of the near diffuser station locations is shown on the last page of each figure.

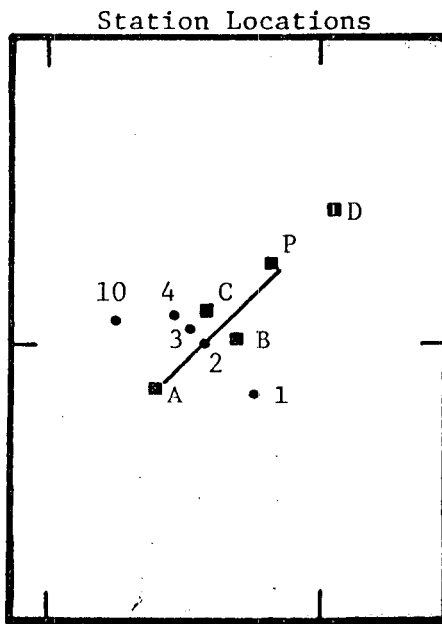
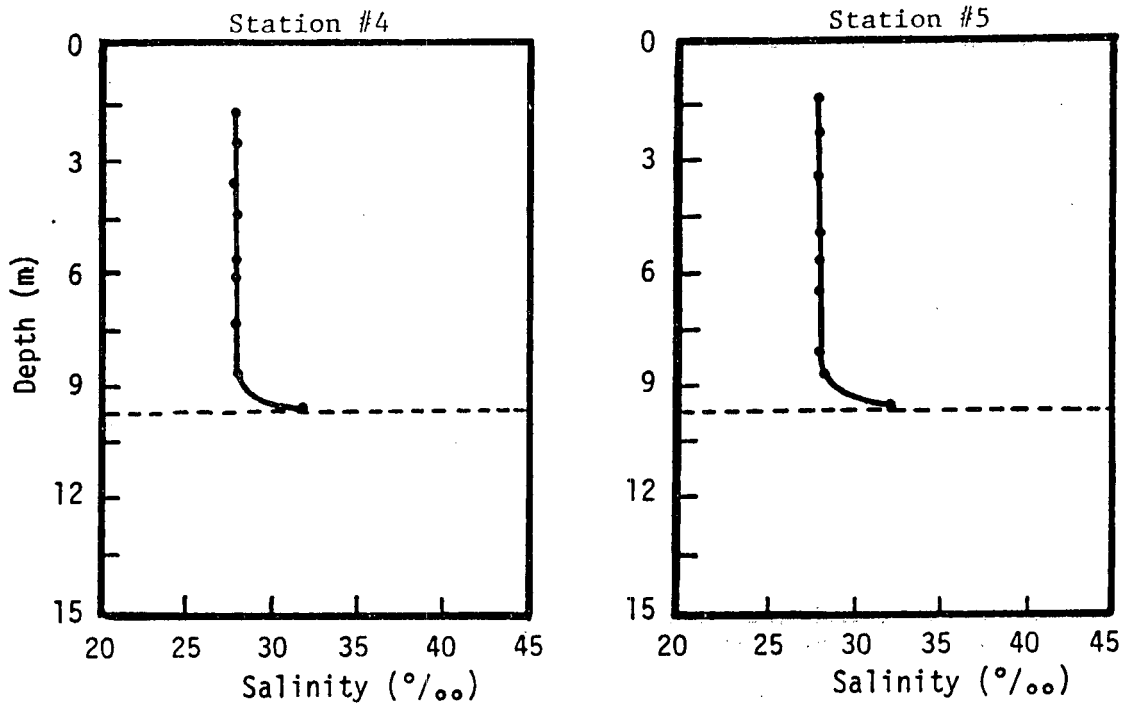


Figure 4-17. Continued.

21,680 barrels/hr and a salinity of 209 o/oo. The ambient salinity profiles at stations 20A, 20, and 20D are shown in Figure 4-18. Ambient stations 20A and 20D were added because of the large cross-shelf variation found in earlier plume measurements. These ambient profiles show the salinity structure was nearly isohaline, and station 20 data show the salinity at the surface was 29.8 o/oo and 30.0 o/oo at the bottom.

Station 3 was measured almost directly over the diffuser, and the data in Figure 4-18 show the surface salinity was 29.6 o/oo which was within 0.2 o/oo of the value at station 20. The salinity was constant to a depth of 7.2 m. At 8.2 m, the salinity was 29.9 o/oo and increased sharply to a maximum value of 34.6 o/oo at the bottom. Again, the deviation from the ambient salinity profile was used to evaluate the vertical extent of the brine plume. The station 3 data show the vertical extent was 1.5 m. The vertical profiles at stations 1, 2, 4, and 5 confirm the vertical extent of the plume and the bottom salinities at these stations were 34.3, 34.6, 34.3, and 34.2 o/oo respectively.

4.5.5 February 14, 1982 Vertical Salinity Profiles

The February 14, 1982 vertical salinity profiles are illustrated in Figure 4-19. Brine was being discharged at a rate and salinity of 23,896 barrels/hr and 217 o/oo respectively. Only two data points were recorded at station 20 because of recording malfunctions. These data indicate the ambient salinity was isohaline with a value of 31.2 o/oo at the surface and bottom.

Vertical profile station number 3 was located almost directly over the diffuser, and the measured data are shown in Figure 4-19.

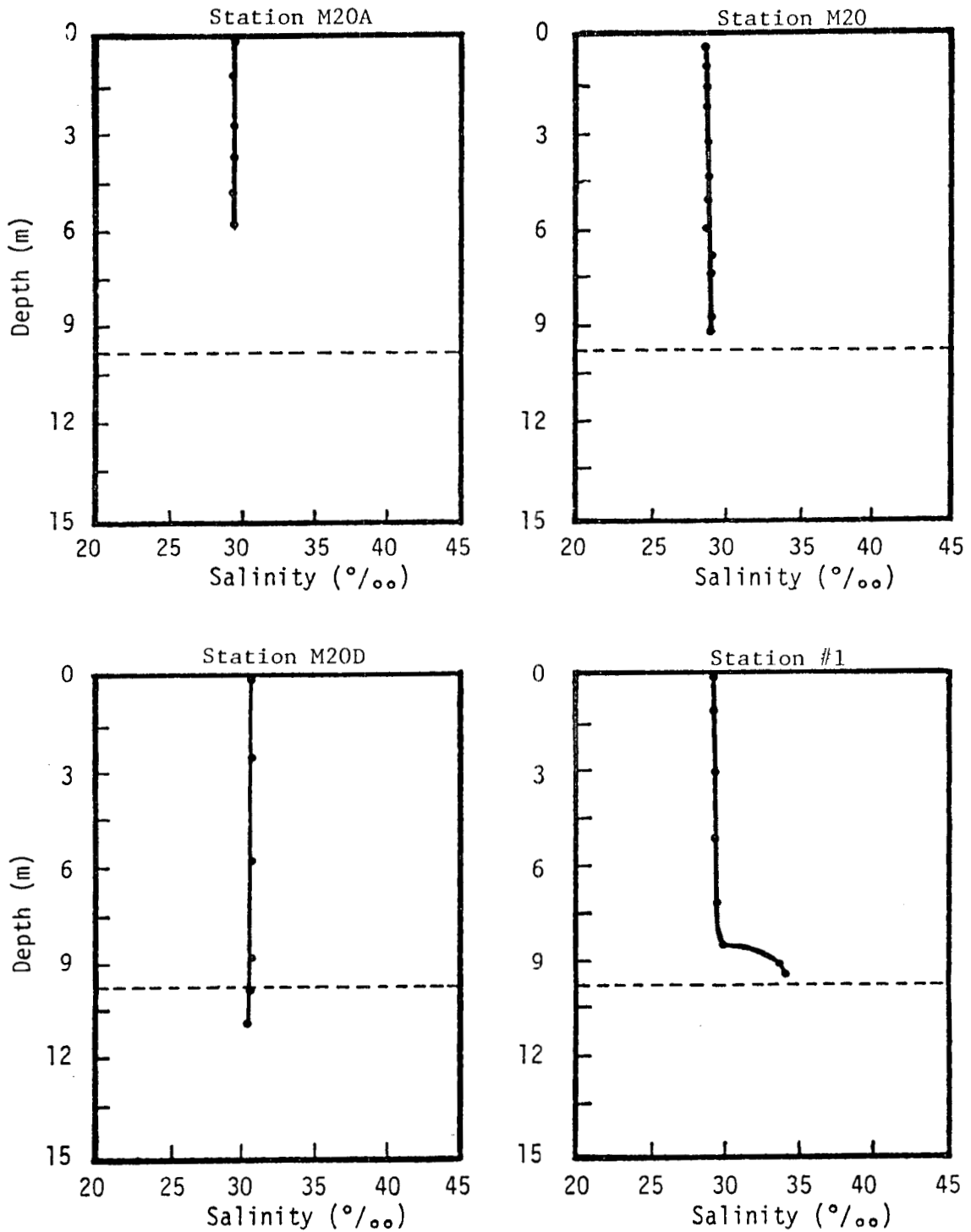


Figure 4-18. Vertical salinity profiles near the diffuser on November 25, 1981. The dashed line represents the depth of the natural bottom (9.6 m). Stations M20A, M20, and M20D are control stations located 7.4 km east of the diffuser, and stations M20A and M20D are 3.7 km north (inshore) and south (offshore) of station 20 respectively. A schematic of the near diffuser station locations is shown on the last page of each figure.

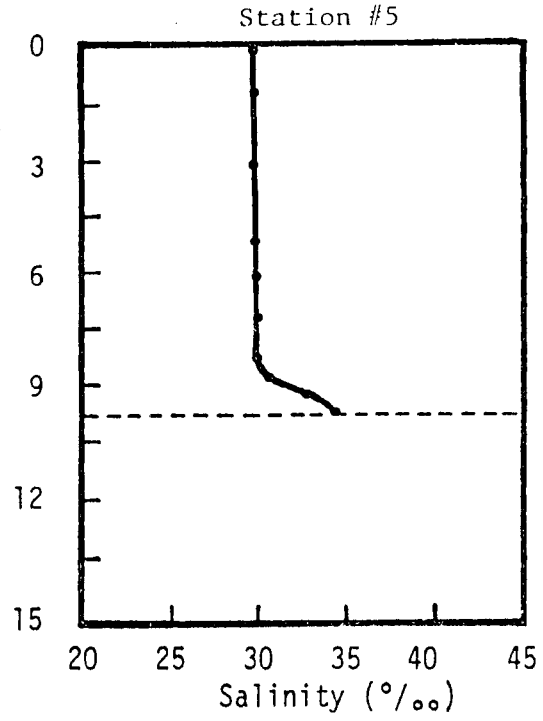
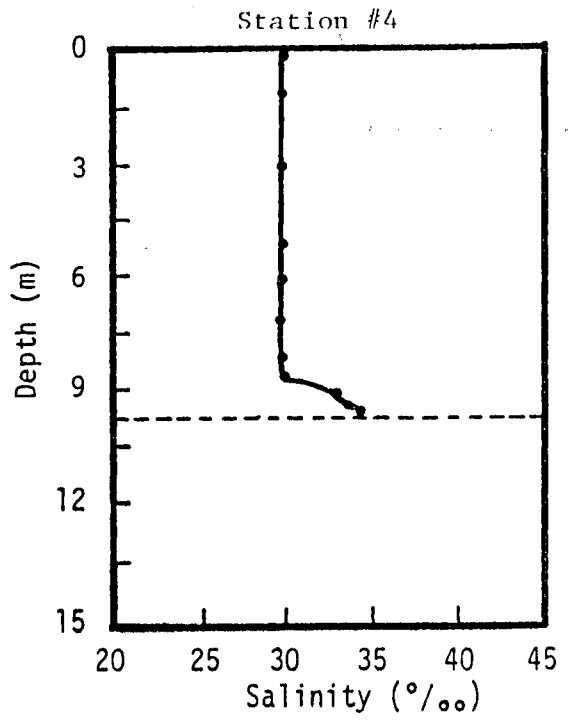
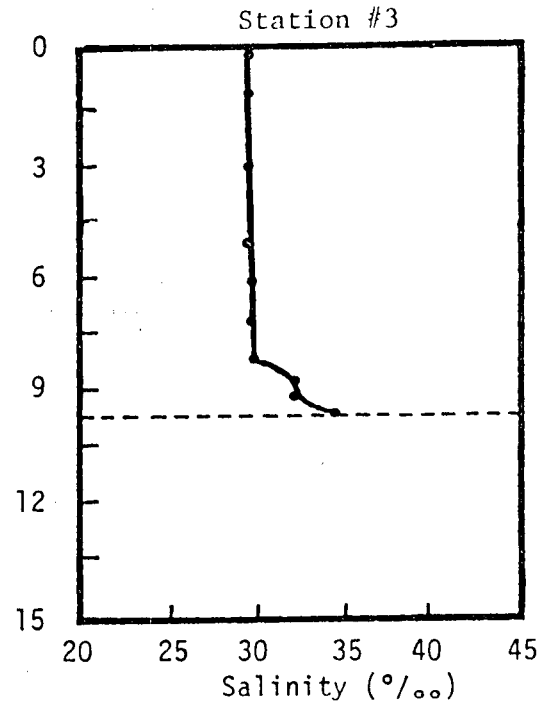
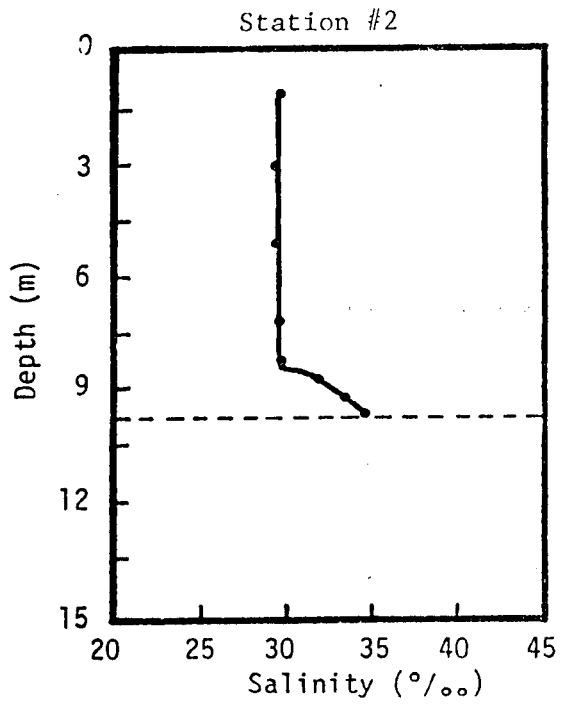


Figure 4-18. Continued.

Station Locations

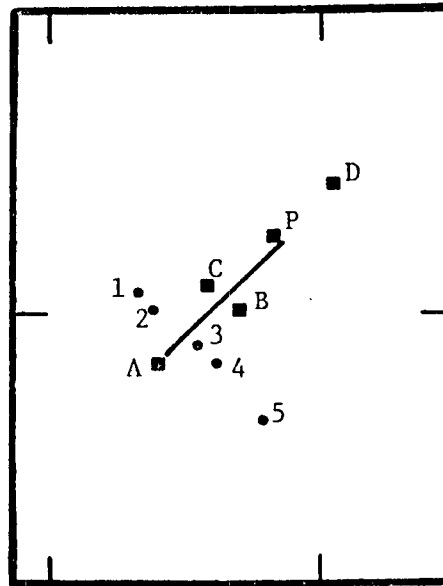


Figure 4-18. Continued.

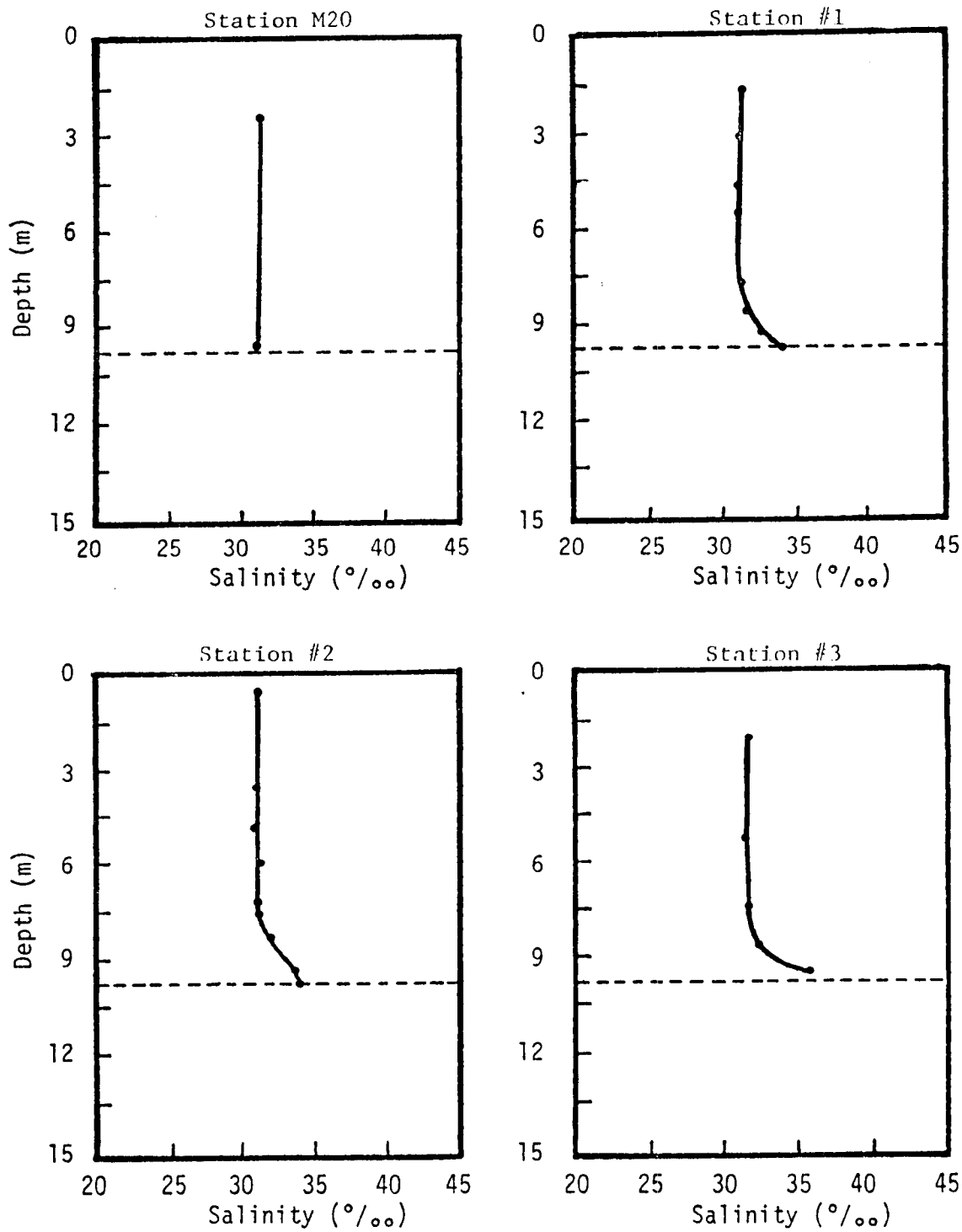


Figure 4-19. Vertical salinity profiles near the diffuser on February 14, 1982. The dashed line represents the depth of the natural bottom (9.6 m). Stations M20A, M20, and M20D are control stations located 7.4 km east of the diffuser, and stations M20A and M20D are 3.7 km north (inshore) and south (offshore) of station 20 respectively. A schematic of the near diffuser station locations is shown on the last page of each figure.

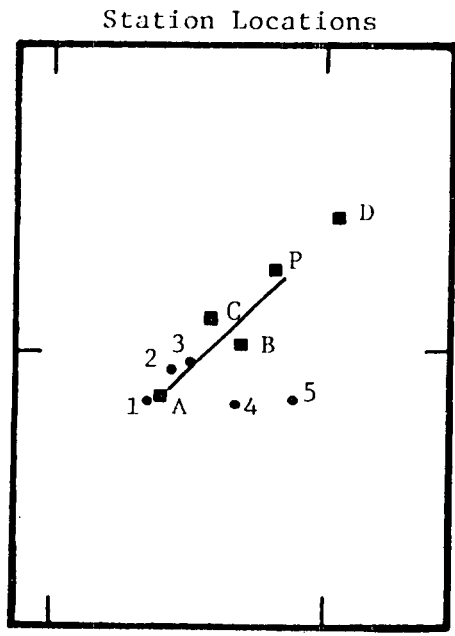
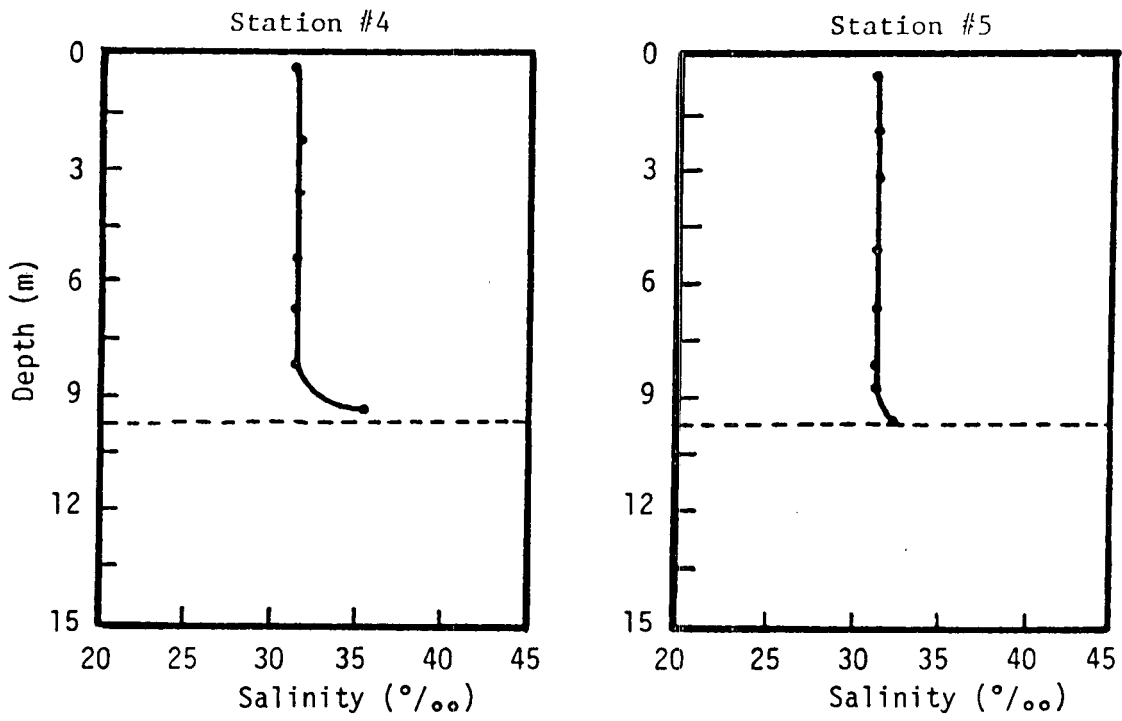


Figure 4-19. Continued.

The station 3 data show the surface salinity was 31.2 o/oo, exactly the same as that measured at station 20, and it was basically isohaline to a depth of 7.5 m. The salinity increased rapidly to a maximum value of 35.7 o/oo on the bottom. The vertical extent of the plume was determined to be 2.2 m based upon the deviation of the salinity profile from the ambient profile at 7.5 m when the bottom depth was 9.7 m. Station 2 was very near station 3 and the salinity profile confirms the vertical extent value, but the bottom salinity only reached 34.1 o/oo. The other vertical profile stations (1, 4, and 5) show the plume was within 1.5 m of the bottom and the bottom salinities were 33.7, 35.3, and 32.6 o/oo respectively.

4.5.6 Comparison of Calculated and Measured Values of the Plume Vertical Extent

An empirical equation was developed by Tong and Stolzenbach (1979) from laboratory experiments to compute the maximum vertical extent of a negatively buoyant plume. This empirical equation is

$$Z_m = 1.7 V [D/(g \Delta\rho_m/\rho_f)]^{1/2} \quad (4-1)$$

where Z_m is the maximum vertical extent of the plume centerline, D is the exit port diameter, V is the exit velocity, ρ_f is the ambient fluid density, $\Delta\rho_m$ is the difference in the density of the brine and ambient sea water, and g is the acceleration due to gravity.

The vertical profiles discussed in the previous sections show the plume vertical extent at specific locations where measurements were taken. Now it is desired to compare the measured plume vertical extent with those values computed from Equation 4-1 using the physical oceanographic data collected during the plume tracking period and the

known diffuser characteristics. The results of the computed and measured values are tabulated in Table 4-3.

The diffuser had 32 open ports for every vertical profile measurement except for April 30, 1982. On June 1, 1981, the measured vertical extent was determined to be 2.6 m while the computed vertical extent was 6.7 m. The June 9 and 30 profiles indicated the vertical extent was 0.6 m and 1.5 m while the computed values were 4.5 and 4.6 m respectively. These data may indicate the measurements were not taken directly over the diffuser ports, and thus the measured data are much lower than the computed values. The August and October vertical profiles were nearly 50 percent of the computed values, and the exit velocity for these dates were 7.8 and 7.4 m/s. The exit velocity dropped to 6.6 m/s on November 25 and December 16, and the measured vertical extent dropped to 1.5 and 2.0 m while the computed values were 3.9 and 4.0 m respectively.

The February 14, 1982 profile showed a 2.2 m vertical extent while the computed value was 4.1 m and the exit velocity was 7.2 m/s. The brine discharge rate increased greatly on March 1, 1982 which resulted in an exit velocity of 10.6 m/s. The computed vertical extent was 6.0 m, but the measured vertical extent was only 0.6 m. The low brine salinity resulted in a small increase in bottom salinity, and consequently, it was very difficult to determine any deviation from the ambient salinity profile. The April 30, 1982 vertical salinity profile clearly shows a departure from the ambient profile at 2.1 m while the computed vertical extent was 3.3 m due to the decreased exit velocity of 5.4 m/s.

In all the vertical profiles, the measured vertical extent was

Table 4-3. Comparison of measured and computed vertical extent of brine plume.

Date	Brine Discharge Rate (Barrels/hr)	Brine Salinity (o/oo)	Ambient Salinity (o/oo)	Ambient Bottom Temp. (°C)	Brine Pit Temp. (°C)	Number of Ports Open	Exit Velocity (m/s)	Computed Vertical Extent (m)	Measured Vertical Extent (m)
6/01/81	29465	108	29.5	26.3	29	32	8.9	6.7	2.6
6/09/81	23580	170	29.7	27.3	31	32	7.1	4.5	0.6
6/17/81	26214	189	30.5	28.8	31	32	7.9	4.6	---
6/30/81	28307	208	22.1	29.0	31	32	8.6	4.6	1.5
7/17/81	21675	214	30.9	28.2	33	32	6.6	3.8	---
8/12/81	25643	228	28.5	29.5	34	32	7.8	4.2	2.2
10/28/81	24500	225	30.9	20.7	29	32	7.4	4.1	2.3
11/25/81	21680	209	29.9	18.5	23	32	6.6	3.9	1.5
12/16/81	21500	202	31.4	16.9	18	32	6.6	4.0	2.0
2/14/82	23896	217	30.9	11.1	16	32	7.2	4.1	2.2
3/01/82	35042	180	28.0	14.3	16	32	10.6	6.0	0.6
4/30/82	23315	229	28.9	20.4	24	42	5.4	3.3	2.1
Average	25401	198	29.3	22.6	26	--	7.6	4.5	1.8

4-54

much less than the computed values indicating the measured vertical data was taken from the plume settling around the diffuser area and apparently not in the immediate vicinity of actual brine jets where the brine is believed to extend much higher and closer to the computed values. Using all the vertical profile data, the average exit velocity was 7.6 m/s and the average computed vertical extent was 4.5 m. The average measured vertical extent was 1.8 m which is 40 percent of the computed value. In the Bryan Mound study (Randall, 1981a), the initial period of discharge (March 10 through July 15, 1980) showed the average exit velocity was 6.7 m/s and the average measured and computed vertical extent was 3.7 and 4.0 m respectively. During the second period from July 15, 1980 through August 24, 1981, the average exit velocity was 8.0 m/s, and the average measured and computed vertical extent was 5.2 and 4.5 m respectively. The low measured vertical extent of the West Hackberry plume is believed to be caused by the inability to keep the CTD/DO sensor near enough to the brine jet, and consequently, the vertical extent of the plume settling to the bottom is measured. The lower brine salinities for the West Hackberry discharge also appear to be a partial cause of the low measured vertical extent.

4.6 Vertical Dissolved Oxygen Profiles

4.6.1 Background

The effect of the brine discharge on the vertical distribution of dissolved oxygen was determined by measuring the vertical dissolved oxygen profile directly over the diffuser and at two intermediate field stations on either side of the diffuser. These profiles were then compared to an ambient profile measured at station 20, and the

deviation from the ambient profile near the bottom was attributed to the brine plume.

The vertical dissolved oxygen profile data were collected simultaneously with the vertical salinity profiles discussed in the previous section. Water samples were collected at selected depths and a Winkler titration procedure was used to determine the dissolved oxygen content. These results were then used to correct the data measured by the CTD/DO sensor.

Vertical dissolved oxygen profiles were measured on June 9, July 17, August 12, October 28, November 25, and December 16 in 1981, and on February 14, March 1, and April 30 in 1982. All of these profiles are contained in Appendix D. Selected vertical dissolved oxygen profiles are discussed in this section to show the effects of the brine discharge on the vertical distribution of dissolved oxygen.

4.6.2 June 9, 1981 Vertical Dissolved Oxygen Profiles

The ambient profile at station 20 in Figure 4-20 shows the dissolved oxygen content was 6.4 mg/l near the surface and decreased slightly to 6.1 mg/l at a depth of 5.8 m. From this depth to the bottom, the dissolved oxygen decreased sharply to 2.8 mg/l. This profile is now compared to the vertical profiles collected in the vicinity of the brine diffuser.

Six vertical profiles were measured on this date, and their locations are shown on the second page of Figure 4-20. The brine was being discharged at an average rate and salinity of 23,580 barrels/hr and 170 o/oo. Station 1 was located almost directly over the diffuser, and the data show the dissolved oxygen was 6.1 mg/l near the surface and it decreased to 5.0 mg/l at a depth of 7.8 m. The

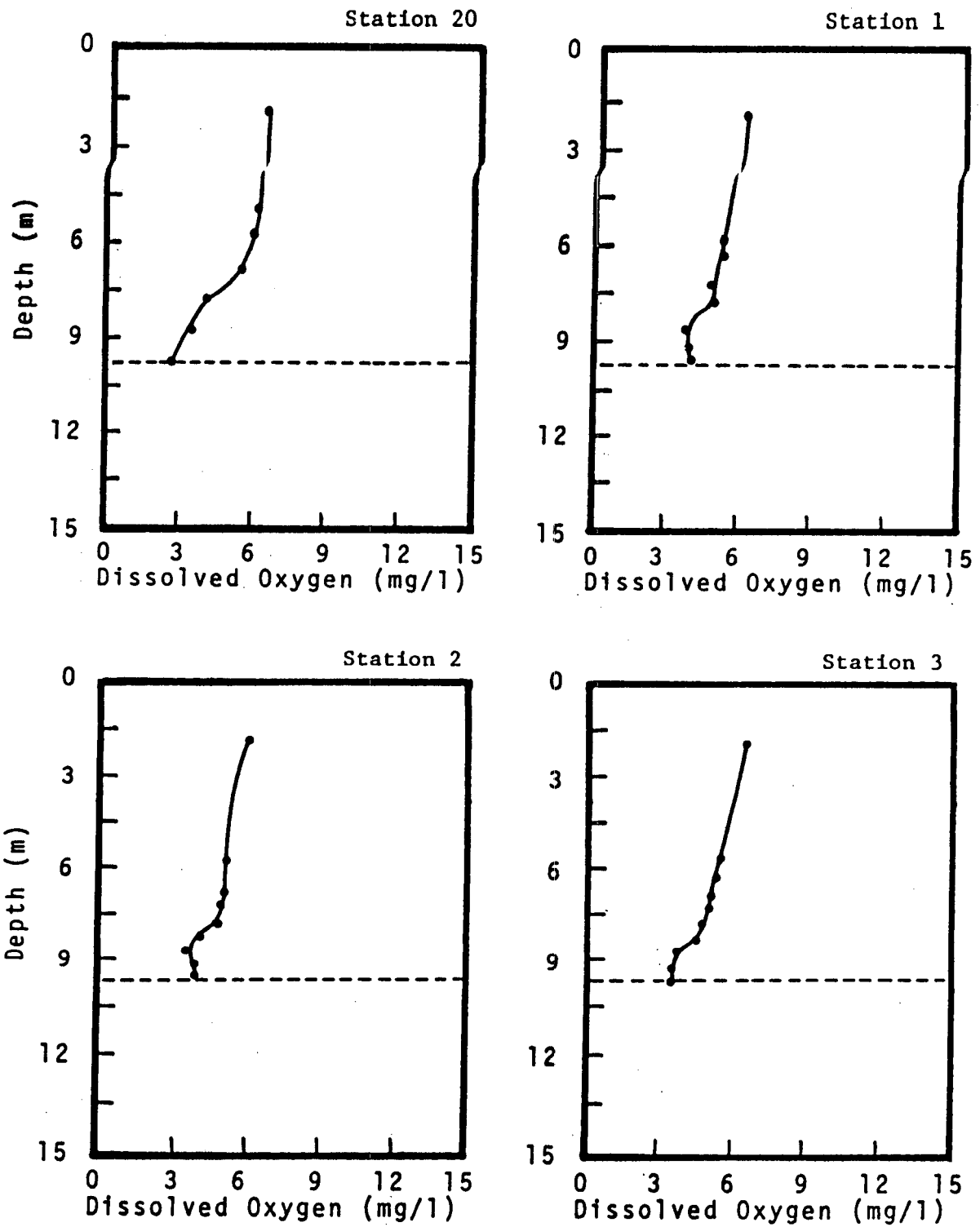


Figure 4-20. Vertical dissolved oxygen profiles near the diffuser on June 9, 1981. The dashed line represents the depth of the natural bottom (9.6 m). Stations 20A, 20, and 20D are control stations located 7.4 km east of the diffuser, and 20A and 20D are 3.7 km north and south of station 20 respectively.

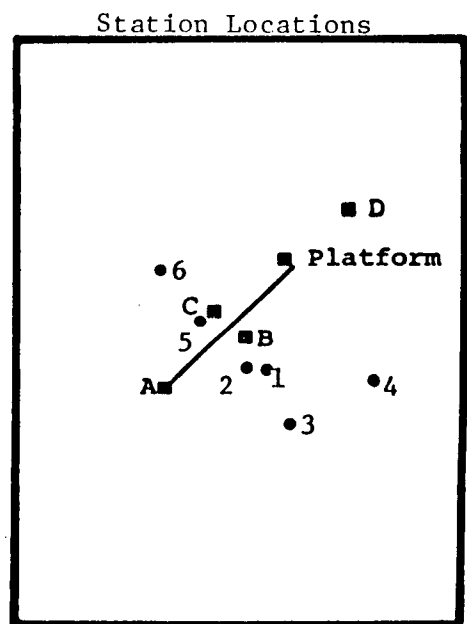
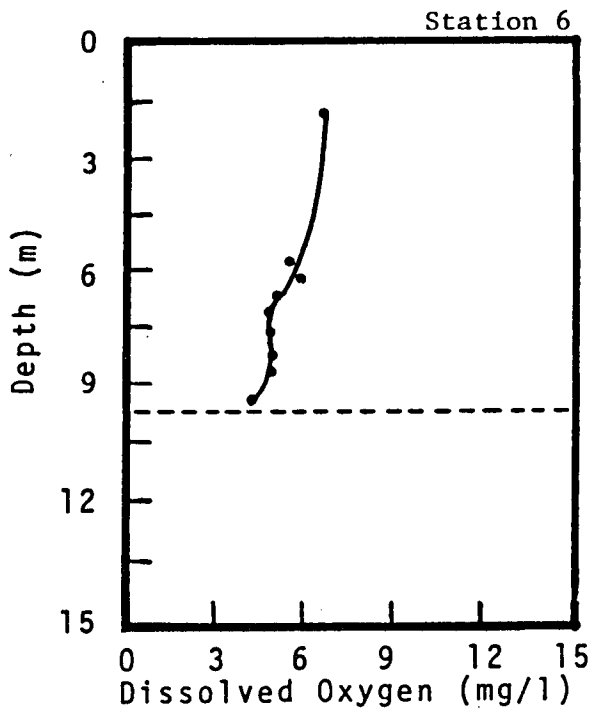
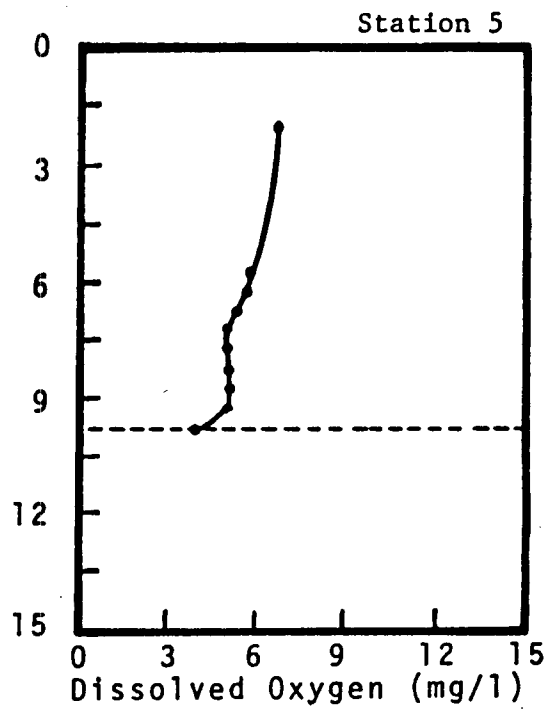
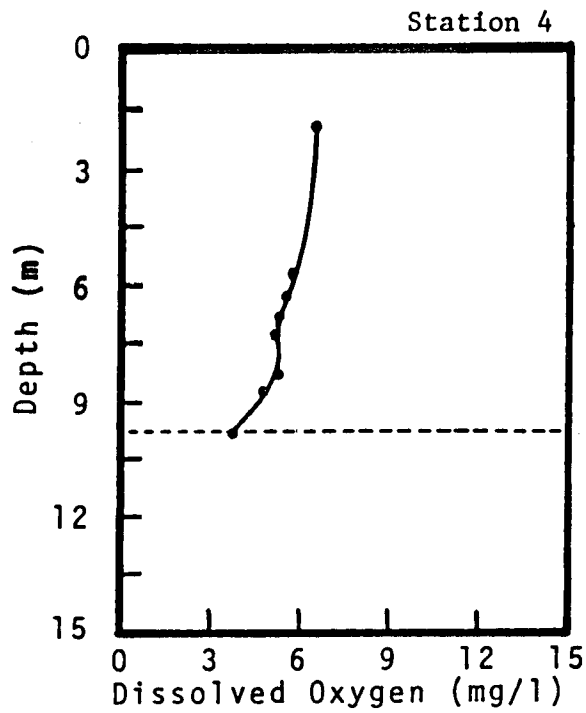


Figure 4-20. Continued.

dissolved oxygen then decreased sharply to 3.9 mg/l at 8.8 m and then increased slightly to 4.2 mg/l at the bottom. The slight increase in dissolved oxygen near the bottom is in contrast to the continued decline of the dissolved oxygen content at station 20. It is believed that the brine discharge is the cause of this increased dissolved oxygen content. The physical mechanism for this increase is believed to be entrainment of the higher oxygenated water in the negatively buoyant brine plume as it falls to the bottom and spreads over the sea floor. The vertical profiles at stations 2 and 3 show a similar trend of increased dissolved oxygen over the ambient data and the breakdown of the sharp decrease in dissolved oxygen in the bottom layer. Stations 4, 5, and 6 show a continuous decrease in dissolved oxygen to a bottom value near 4 mg/l, but it was higher than the bottom value at station 20. These data indicate the brine discharge appears to bring higher oxygenated water to the bottom as the result of entrainment.

4.6.3 July 17, 1981 Vertical Dissolved Oxygen Profiles

The ambient profile at station 20 in Figure 4-21 shows the dissolved oxygen content was near 7.3 mg/l from surface to a depth of 3 m, and it decreased slowly to 6.2 mg/l at 7.0 m. From 7.0 m to the bottom (9.7 m), the dissolved oxygen decreased rapidly to 0.2 mg/l at the bottom. These data indicate the bottom waters were anoxic which has been discussed previously in Chapter 2.

Four vertical profiles were recorded on this date when brine was being discharged at a rate and salinity of 21,675 barrels/hr and 214 o/oo. Station 2 was located almost directly over the diffuser, and the data in Figure 4-21 shows the dissolved oxygen near the surface was 6.4 mg/l. It decreased to 5.9 mg/l at 3.4 m and then started a

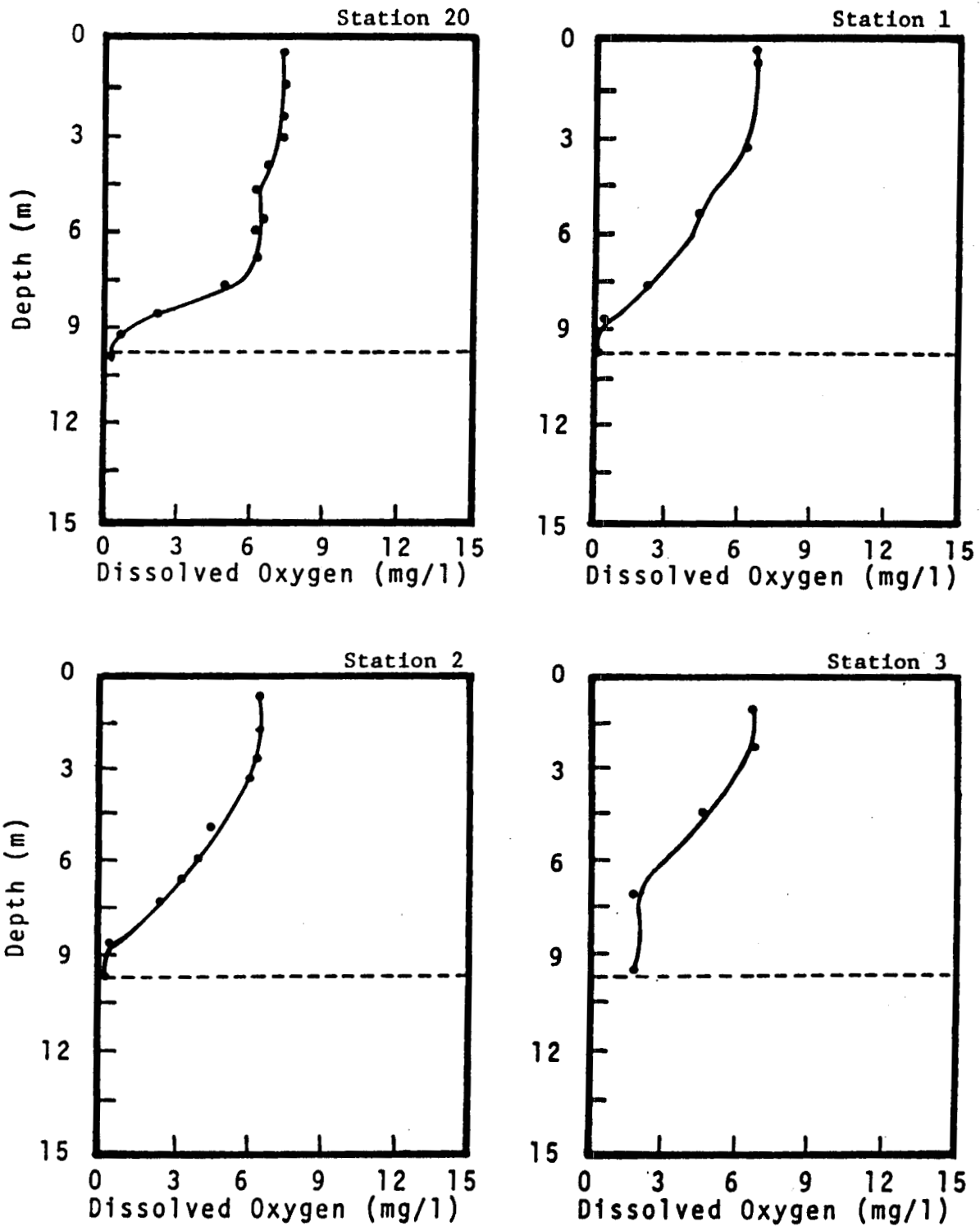


Figure 4-21. Vertical dissolved oxygen profiles near the diffuser on July 17, 1981. The dashed line represents the depth of natural bottom (9.6 m). Stations 20A, 20, and 20D are control stations located 7.4 km east of the diffuser, and 20A and 20D are 3.7 km north and south of stations 20 respectively.

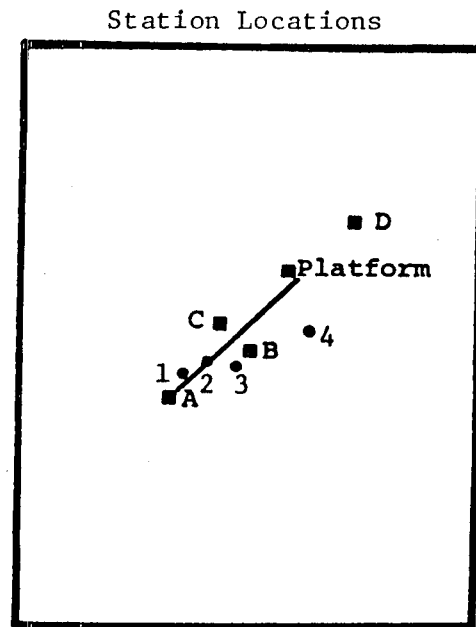
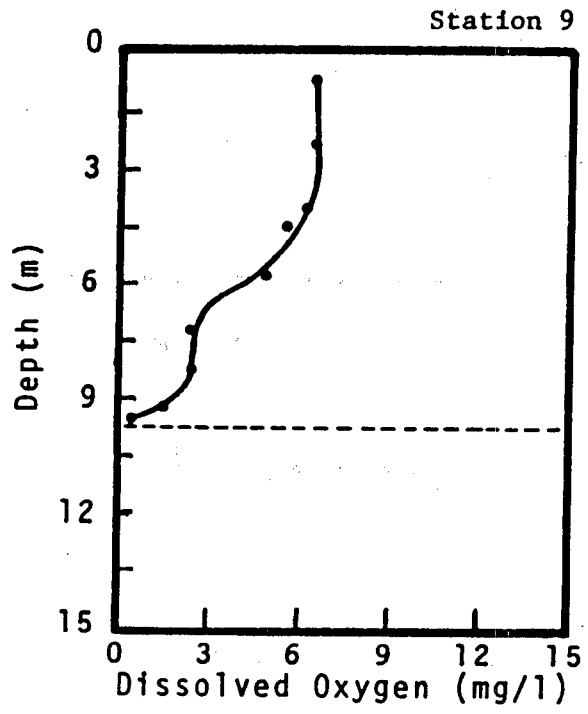


Figure 4-21. Continued.

more gradual decrease to 0.3 mg/l at the bottom. Station 3 shows a similar trend near the surface and a gradual decrease beginning at 3 m. However, the station 3 bottom waters had a dissolved oxygen content of near 2.0 mg/l which was higher than that at station 20 and the other profile stations. Stations 1 and 4 show similar results as that described for station 2. Thus, the July 17 data show the brine appears to have altered the dissolved oxygen gradient and at one station increased the dissolved oxygen content from near 0.5 mg/l to 2.0 mg/l.

4.6.4 August 12, 1981 Vertical Dissolved Oxygen Profiles

On August 12, 1981, the ambient vertical dissolved oxygen profiles at stations 20A, 20, and 20D show the anoxic conditions in July had disappeared. Figure 4-22 shows the dissolved oxygen at station 20 was 5.8 mg/l at the surface and it decreased slightly to 5.1 mg/l at the bottom.

On this date, the brine was being discharged at a rate of 25,643 barrels/hr and at a salinity of 228 o/oo. The vertical profile stations 1 through 4 show the dissolved oxygen profiles in the vicinity of the brine discharge were essentially the same as the ambient profiles. The dissolved oxygen content was nearly the same from top to bottom as a result of the entrained water in the brine plume being the same as that in the bottom water, and consequently there was no apparent effect on the vertical distribution of dissolved oxygen.

4.6.5 November 25, 1981 Vertical Dissolved Oxygen Profiles

Brine was being discharged at a rate of 21,680 barrels/hr at an average salinity of 209 o/oo. Station 20 in Figure 4-23 indicates the

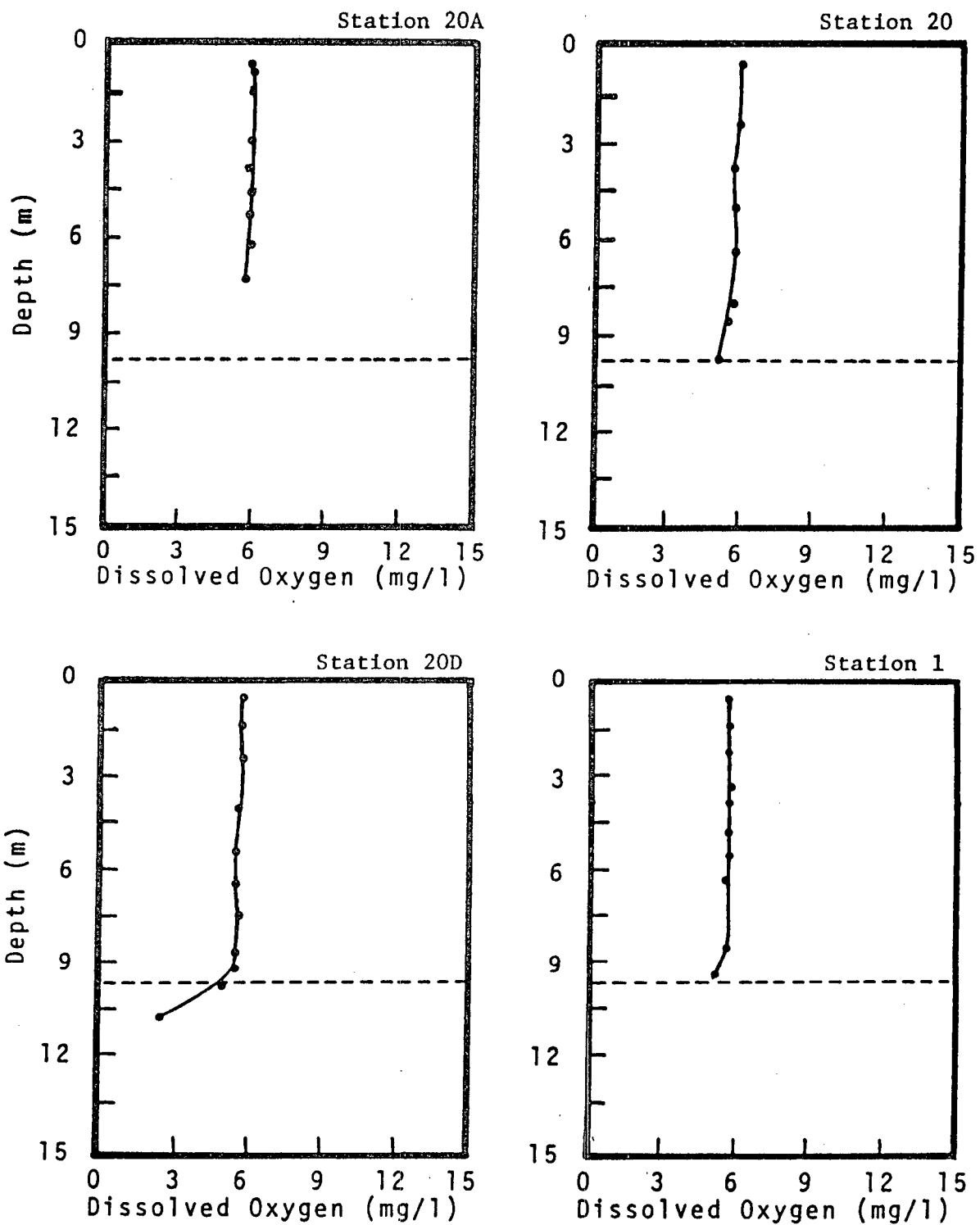


Figure 4-22. Vertical dissolved oxygen profiles near the diffuser on August 12, 1981. The dashed line represents the depth of the natural bottom (9.6 m). Stations 20A, 20, and 20D are control stations, located 7.4 km east of the diffuser, and 20A and 20D are 3.7 km north and south of stations 20 respectively.

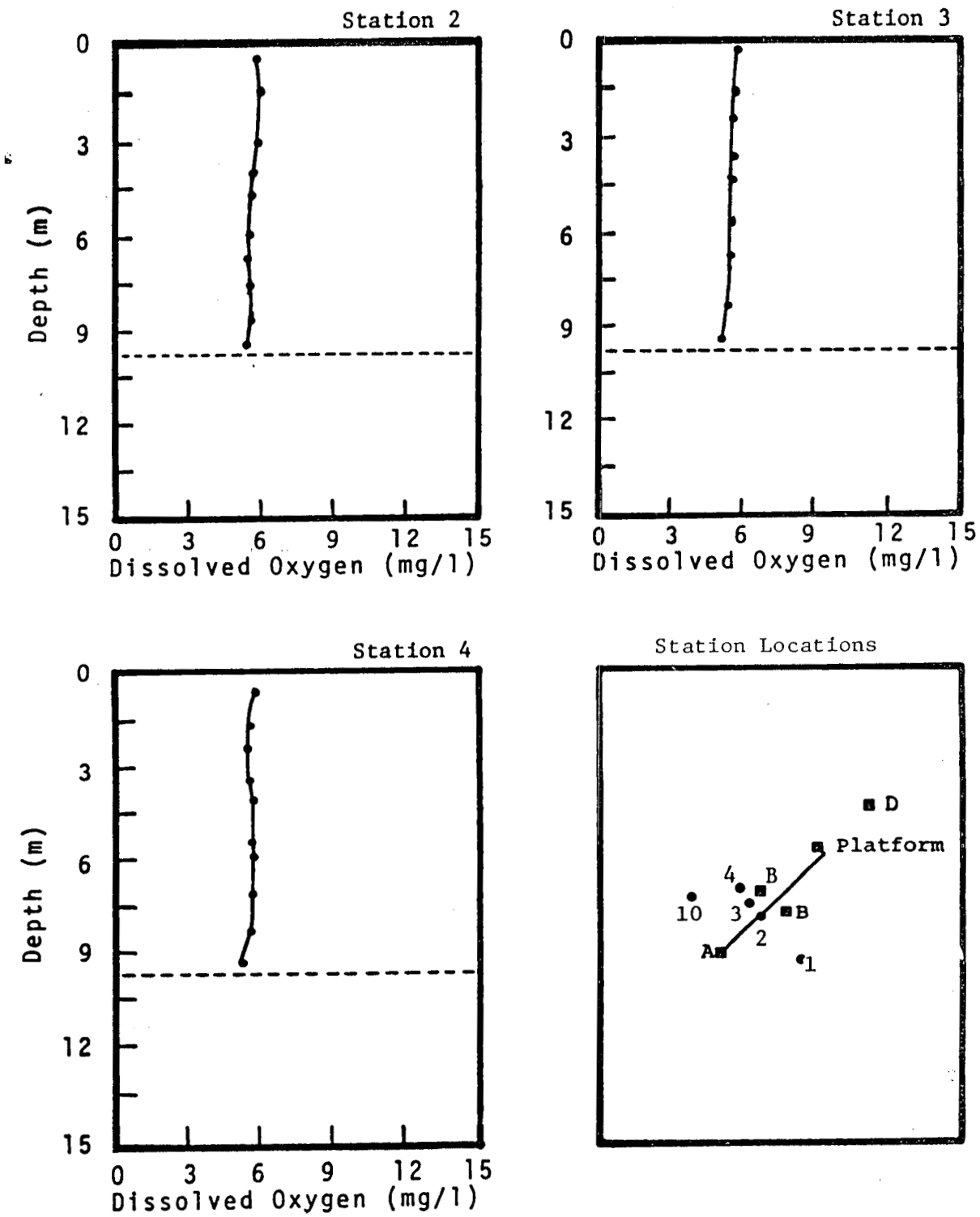


Figure 4-22. Continued.

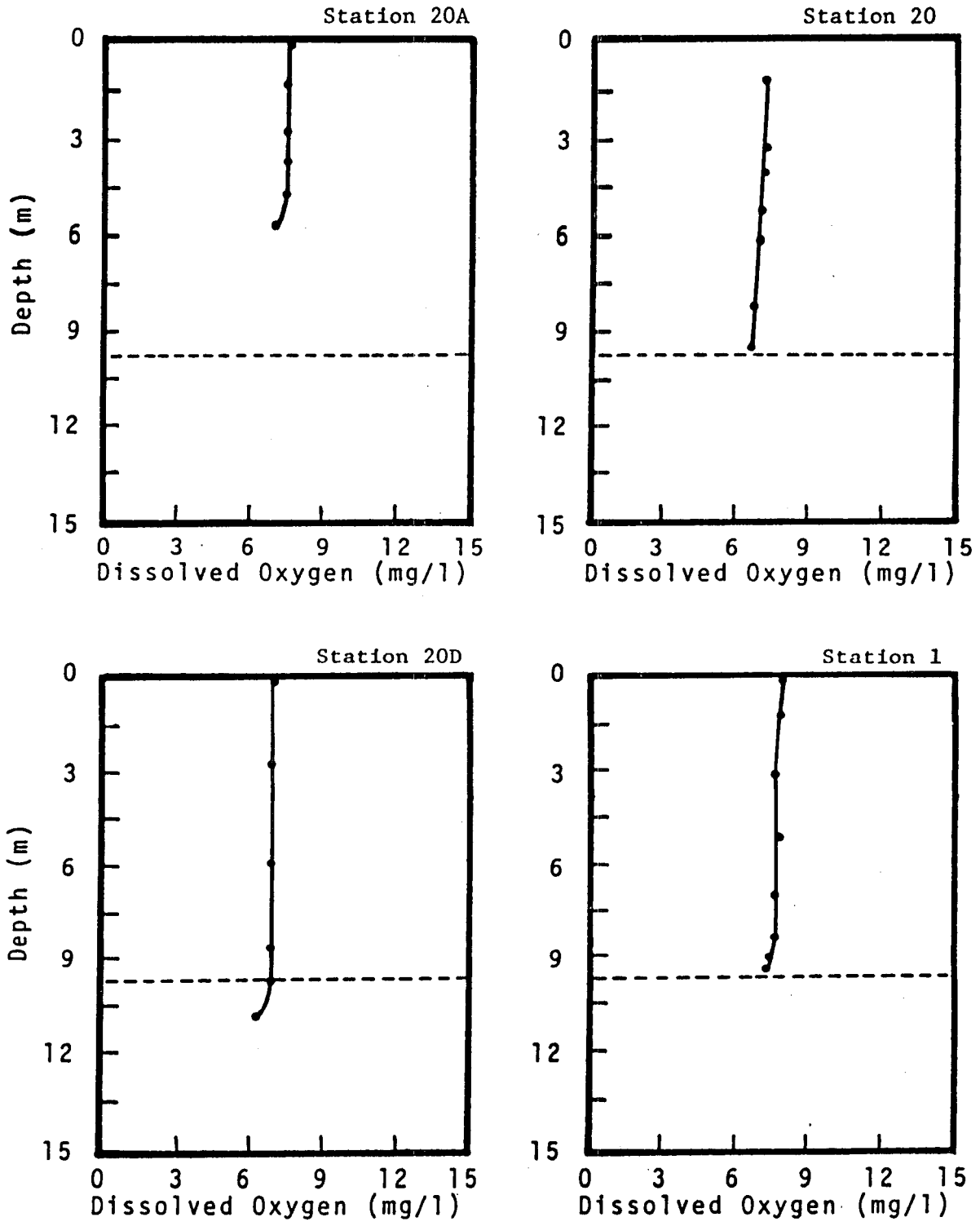


Figure 4-23. Vertical dissolved oxygen profiles near the diffuser on November 25, 1981. The dashed line represents the depth of the natural bottom (9.6 m). Stations 20A, 20, and 20D are control stations located 7.4 km east of the diffuser, and 20A and 20D are 3.7 km north and south of stations 20 respectively.

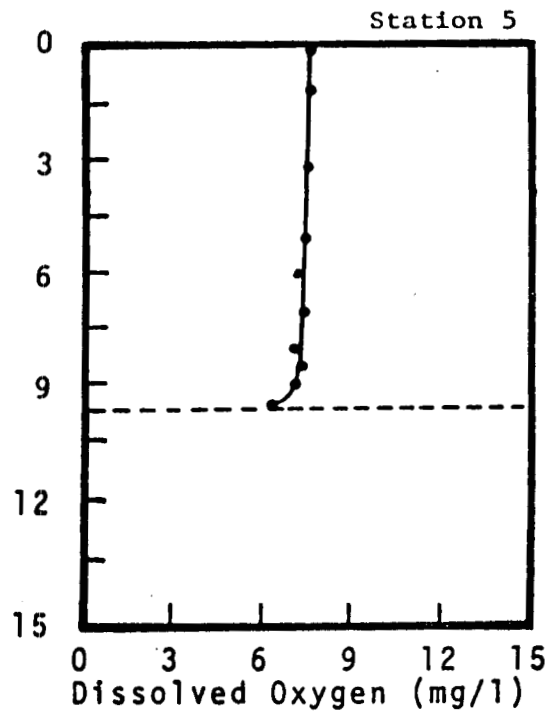
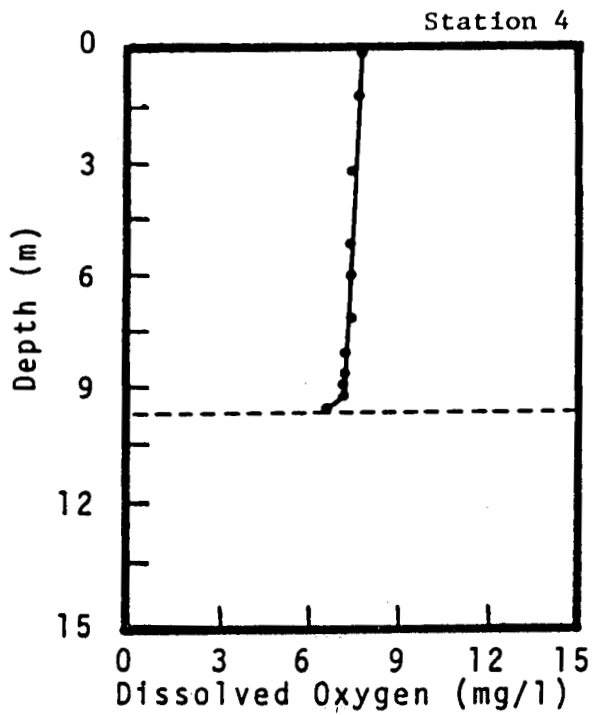
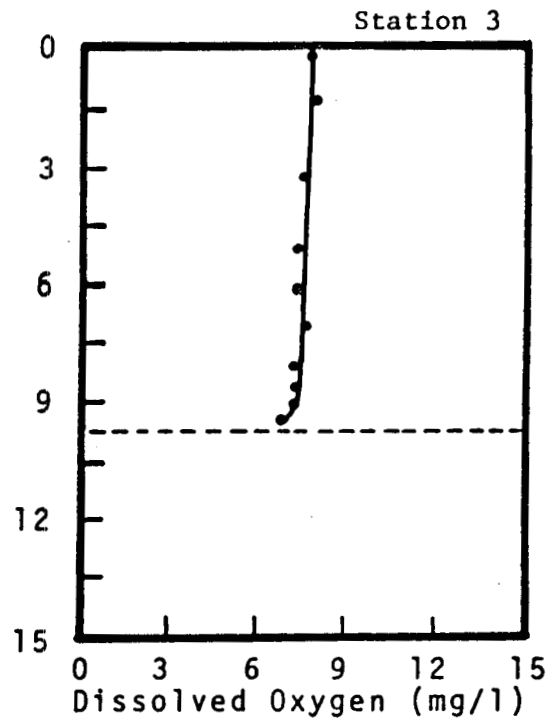
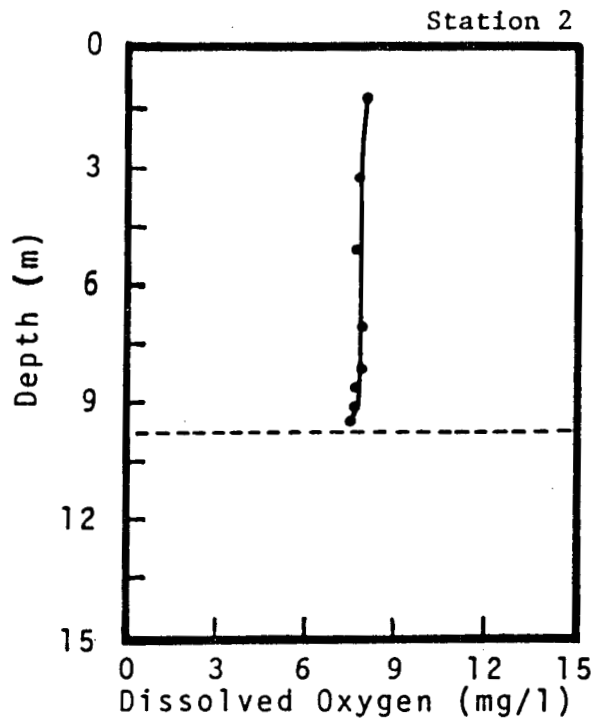


Figure 4-23. Continued.

Station Locations

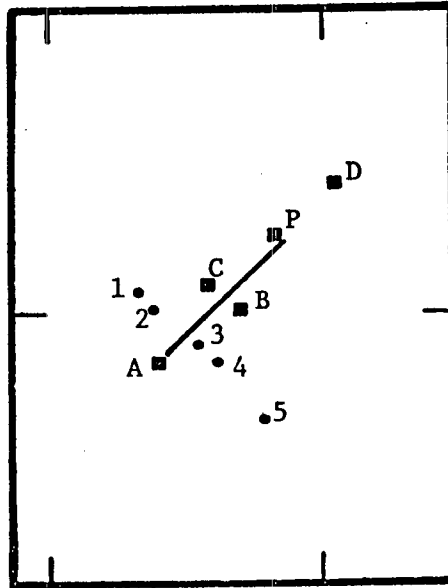


Figure 4-23. Continued.

dissolved oxygen content decreased from 7.4 mg/l at the surface to 6.8 mg/l at the bottom. The vertical profiles at stations 1 through 5 in the diffuser area show the surface to bottom dissolved oxygen behaved similarly to that at the ambient stations. The surface dissolved oxygen was between 7.8 and 8.0 mg/l and it decreased to between 6.4 and 7.6 mg/l at the bottom. These data do not show any effects due to the brine discharge. Similar results were observed during brine plume measurements in December 1981 through March 1982 as shown in figures in Appendix D.

4.6.6 April 30, 1982 Vertical Dissolved Oxygen Profiles

The ambient dissolved oxygen profile at station 20 in Figure 4-24 shows the content of dissolved oxygen was 11.2 mg/l at a depth of 2.3 m, and it decreased gradually to a value of 2.6 mg/l at the bottom. This low bottom dissolved oxygen indicate the probable onset of the anoxic conditions which were observed in the previous summer of 1981.

The vertical profile at station 3 was collected almost directly over the diffuser. As shown in Figure 4-24, these data show the surface dissolved oxygen was 10.8 mg/l, and it decreased gradually to 5.0 mg/l at a depth of 7.8 m. It then increased to a value of 6.4 mg/l at the bottom which is the opposite trend observed at the ambient station. Similar results were obtained at station 5. The other vertical profile stations show the gradual dissolved oxygen content was interrupted in the near bottom waters. This variation in the dissolved oxygen profiles is attributed to the brine discharge as a result of the entrainment of higher oxygenated water in the brine plume which falls to the bottom as a result of its increased density. Similar results were obtained in June and July 1981 as previously

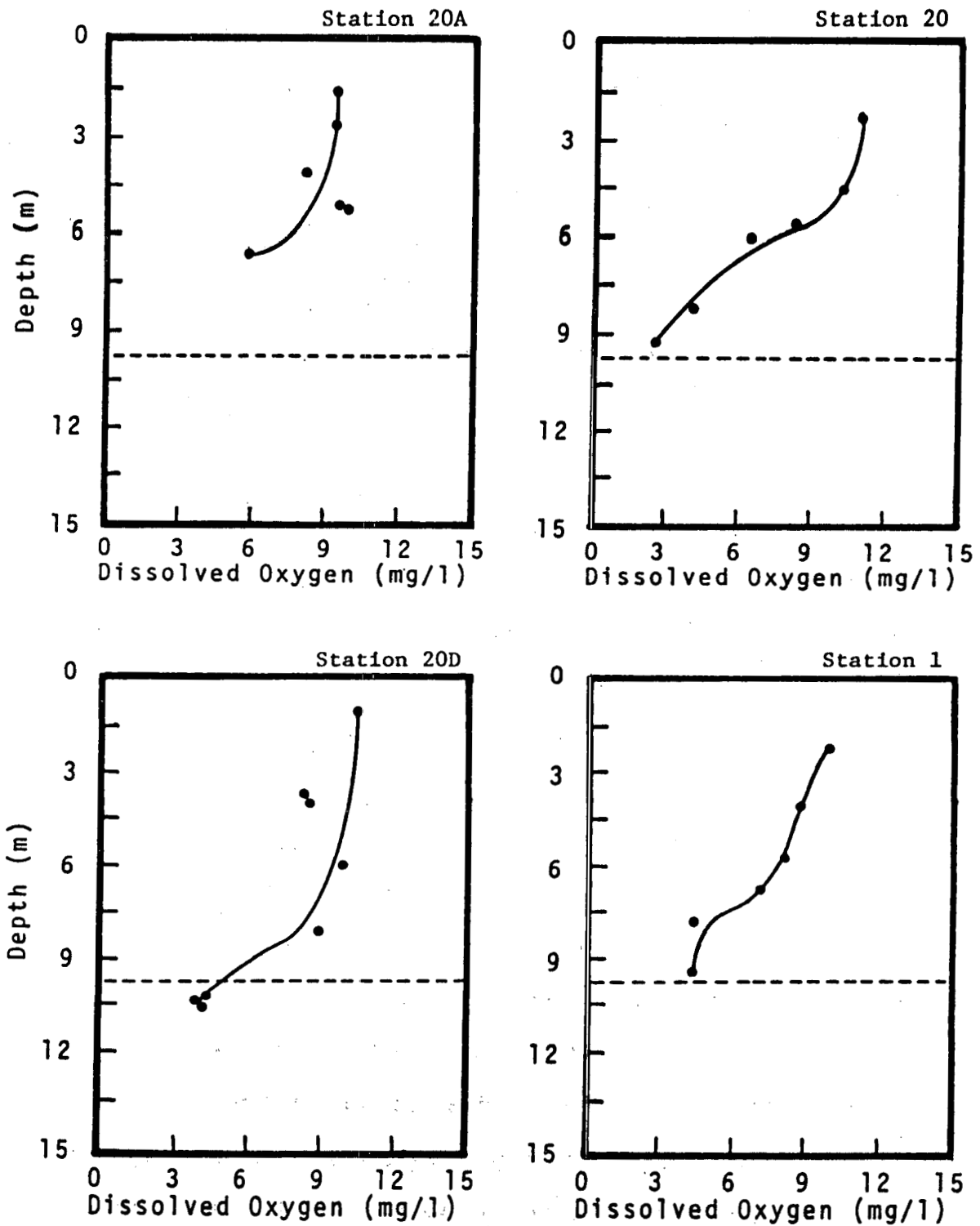


Figure 4-24. Vertical dissolved oxygen profiles near the diffuser on April 30, 1982. The dashed line represents the depth of the natural bottom (9.6 m). Stations 20A, 20, and 20D are control stations located 7.4 km east of the diffuser, and 20A and 20D are 3.7 km north and south of stations 20 respectively.

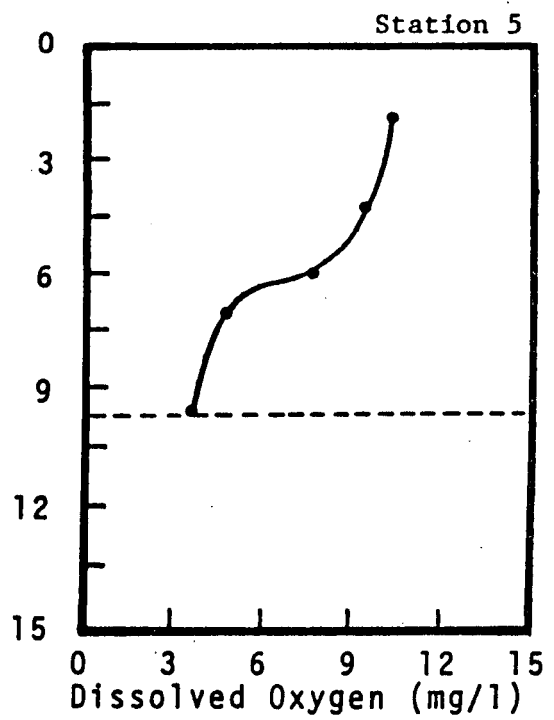
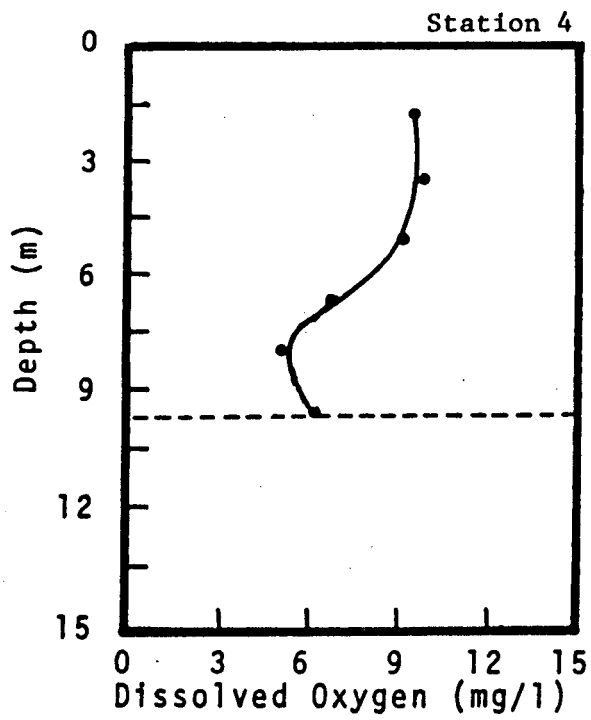
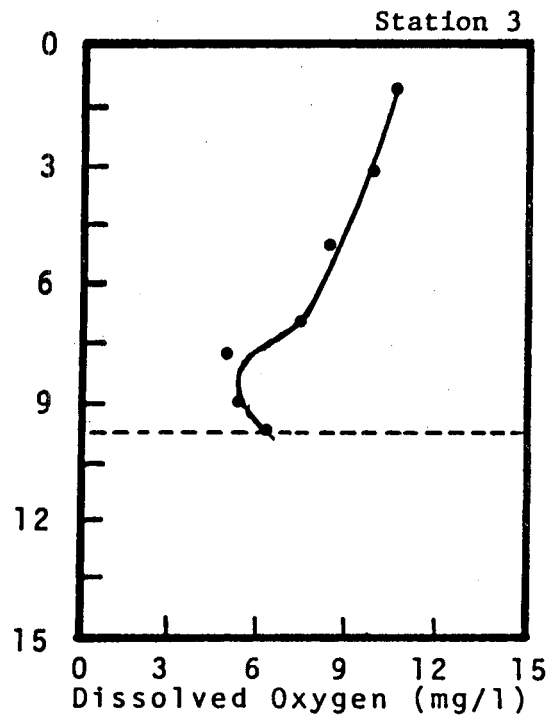
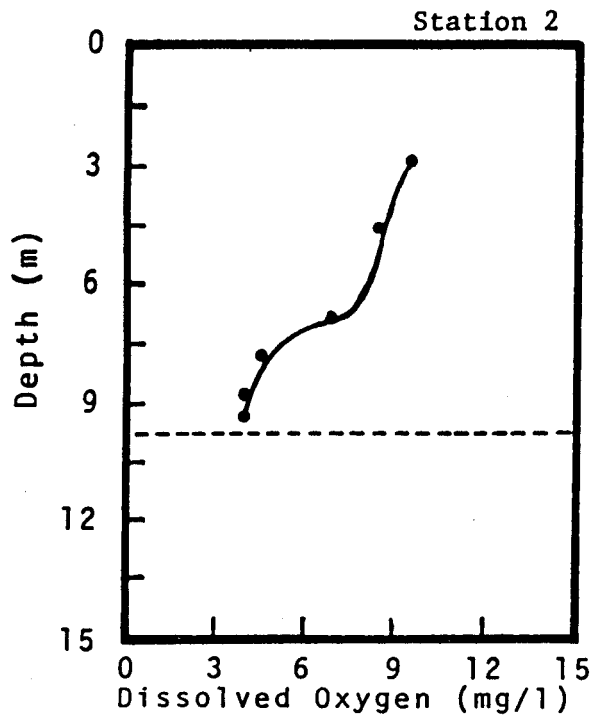


Figure 4-24. Continued..

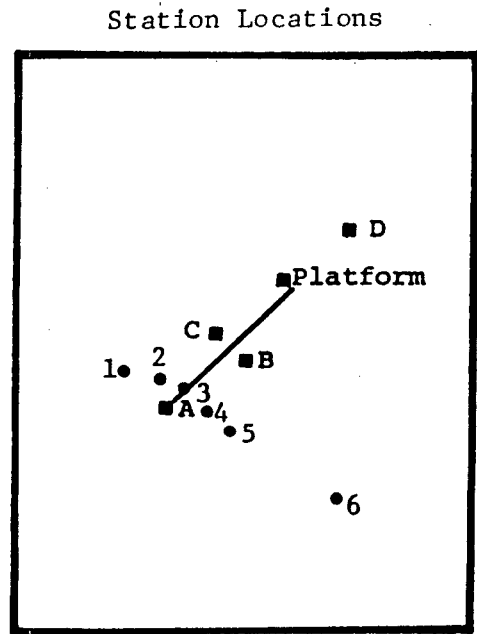
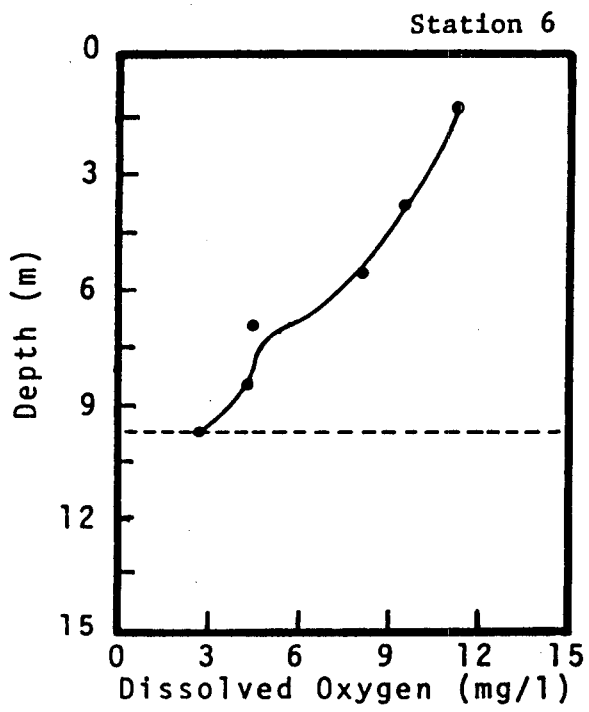


Figure 4-24. Continued.

described.

4.7 Empirical Prediction of Plumes for the West Hackberry Diffuser

4.7.1 Summary of Plume Prediction Procedures

A method for predicting the areal extent of the brine plume emanating from the West Hackberry diffuser was needed during periods when the plume could not be measured. Such a method would aid other investigators who were interested in knowing the areal extent of the brine plume during their sampling cruises. Experimental results of Tong and Stolzenbach (1979), the numerical model of Adams, et al (1975), and field measurements indicated there were certain parameters which are important in describing the plume behavior. These parameters are: bottom current speed (V_c) and direction, brine salinity (S_b), ambient bottom salinity (S_a), and the brine discharge rate (Q). Therefore, empirical equations using dimensionless groupings of the above parameters were developed to estimate the areal extent and the general dimensions of the brine plume. Similar procedures were used to predict the brine plumes for the Bryan Mound diffuser (Randall, 1981).

The measured plumes indicate that an ellipse is a reasonable estimate of the above ambient contours. Therefore, empirical equations were determined which related the upstream length (U_i), downstream length (D_i), and maximum width (W_i) of the plume to the dimensionless groups of physical parameters affecting the plume formation. The two lengths and the width define the axes of an ellipse as illustrated in Figure 4-25. The upstream length (U_i) is measured from the center of the diffuser upstream in the direction of

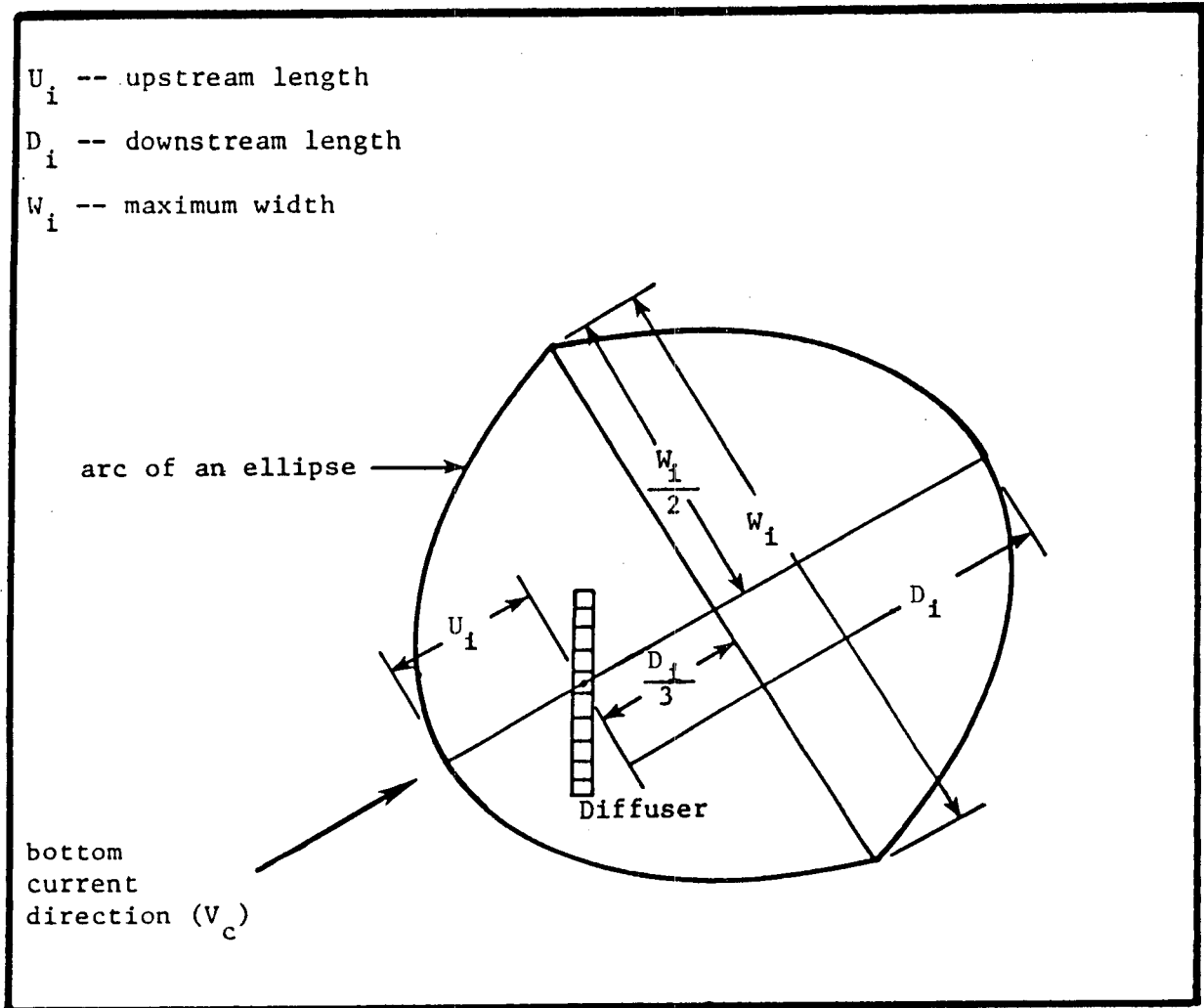


Figure 4-25. Schematic of ellipse used to predict areal extent of brine plume.

the average bottom current to the desired above ambient salinity contour. The downstream length (D_i) is the distance measured in the direction of the bottom current from the center of the diffuser to the desired above ambient contour. The width (W_i) is measured normal to the direction of the bottom current and is bisected by the line extending through the center of the diffuser in the direction of the bottom current. Plume measurements indicate that the maximum width of the plume is usually located approximately 1/3 of the distance downstream of the diffuser, and therefore, the width is displaced a distance $D_i/3$ from the diffuser center. The ends of the lines U_i , D_i , and W_i are then connected with arcs of an ellipse which define the estimated above ambient brine contour.

The empirical relationships which fit the data best are of the form

$$\left. \begin{array}{l} D_i \\ U_i \\ W_i \end{array} \right\} = M \sqrt{\frac{Q}{V_c}} \left[\frac{S_b}{S_a} \right]^e + B \quad (4-2)$$

where Q , V_c , S_b , and S_a are the brine discharge rate (m^3/s), average bottom current (m/s), brine salinity and ambient salinity (o/oo), respectively. The coefficients "M" and "B" and the exponent "e" are determined by curve fits to the measured plume data, the diffuser site D bottom current meter data, and the brine discharge site operating data.

The empirical equations used in this report to estimate the downstream length (D_i) for the +1, +2, and +3 o/oo above ambient

salinity contours and the corresponding correlation coefficient (r) are shown below in Equation 4-3.

$$\begin{aligned}
 D_1 &= 14.5 \sqrt{\frac{Q}{V_c}} \left[\frac{S_b}{S_a} \right]^{2.14} + 84.1 ; r = 0.85 \\
 D_2 &= 2.01 \sqrt{\frac{Q}{V_c}} \left[\frac{S_b}{S_a} \right]^{2.83} + 283.5 ; r = 0.59 \\
 D_3 &= 0.411 \sqrt{\frac{Q}{V_c}} \left[\frac{S_b}{S_a} \right]^{3.39}
 \end{aligned}
 \tag{4-3}$$

Figure 4-26 shows the downstream length (D_i) data measured from the plume tracks during the first 12 months of discharge plotted versus the parameter $Q/V_c(S_b/S_a)$ for the +1, +2, and +3 o/oo above ambient salinity contours. The solid lines in Figure 4-26 were obtained with a least squares curve fit to the first 12 months of data. The data show considerable scatter about the solid line representing the empirical equations which indicates the equations are useful approximations but must be considered only best estimates.

The empirical equations for the plume width (W_i) and the upstream length (U_i) are shown below in Equations 4-4 and 4-5, respectively.

$$\begin{aligned}
 W_1 &= 4.27 \sqrt{\frac{Q}{V_c}} \left[\frac{S_b}{S_a} \right]^{2.53} + 2514 \\
 W_2 &= 111 \sqrt{\frac{Q}{V_c}} \left[\frac{S_b}{S_a} \right]^{.934} + 84.5 ; r = 0.77 \\
 W_3 &= 25.2 \sqrt{\frac{Q}{V_c}} \left[\frac{S_b}{S_a} \right]^{1.37} + 74.3 ; r = 0.68
 \end{aligned}
 \tag{4-4}$$

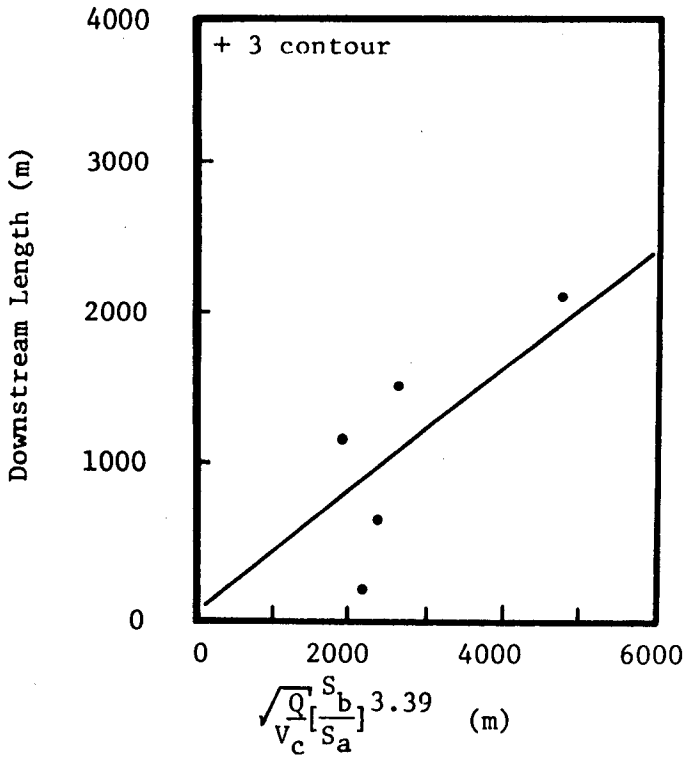
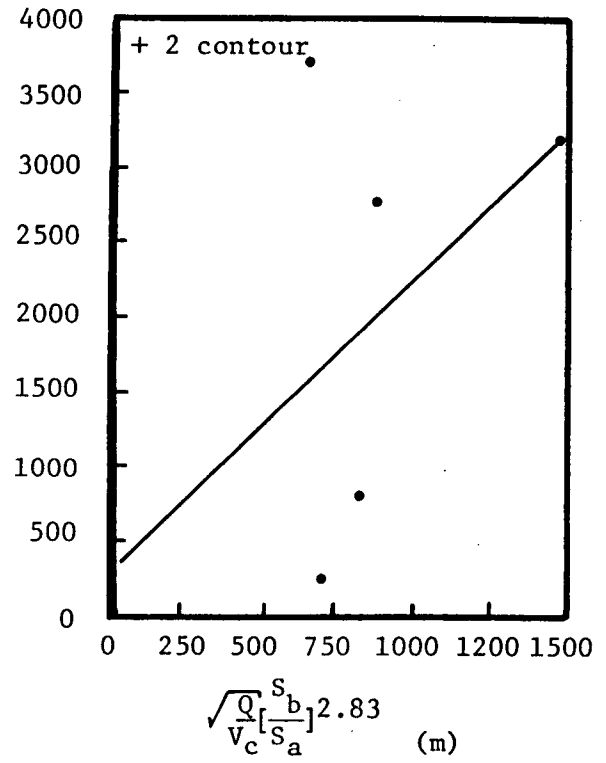
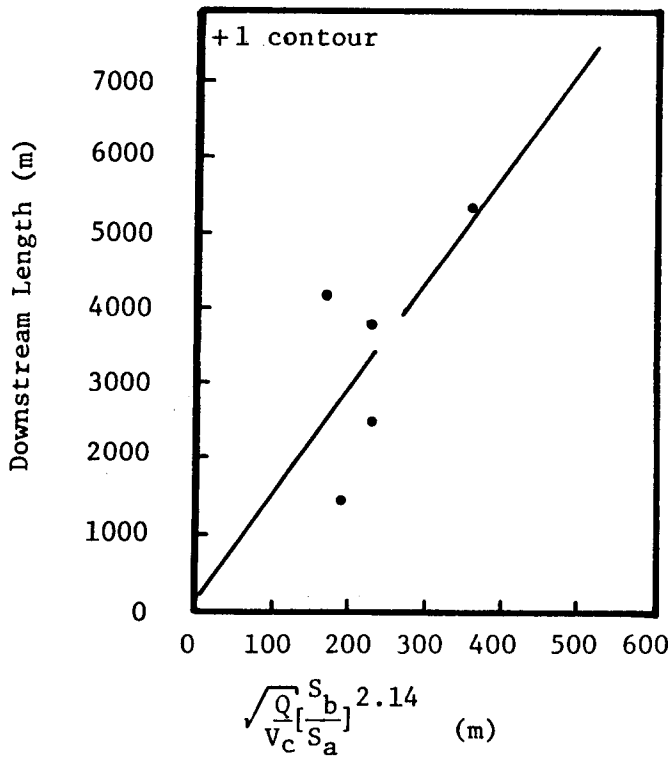


Figure 4-26. The variation of the plume downstream length for the above ambient salinity contours.

$$\begin{aligned}
 C_1 &= 32.6 \sqrt{\frac{Q}{V_c}} \left[\frac{S_b}{S_a} \right]^{0.975} + 219.3 ; r = 0.70 \\
 C_2 &= 37.8 \sqrt{\frac{Q}{V_c}} \left[\frac{S_b}{S_a} \right]^{0.847} + 102.1 ; r = 0.87 \\
 C_3 &= 41.9 \sqrt{\frac{Q}{V_c}} \left[\frac{S_b}{S_a} \right]^{0.7} + 8.9
 \end{aligned}
 \tag{4-5}$$

The width equations are plotted on Figure 4-27 along with the measurements from the first 12 months of plume track data. Figure 4-28 illustrates the variation of the measured upstream length data with the brine discharge and ambient receiving water characteristics. Similar to the downstream length data, these figures show considerable scatter about the empirical equations.

Since the plume tracks normally take 6 to 8 hours, the measured brine plumes are considered an eight-hour average plume. Therefore, an eight-hour average of the bottom current data measured with a continuous recording current meter (see Chapter 2) located 2 m above the bottom in the diffuser area was used for the plume contour predictions. The average brine salinity and average hourly discharge rates were obtained from average daily data reported by the operating facility at West Hackberry. These data were input to the empirical equations (4-3, 4-4, and 4-5) and the lengths and widths were plotted and connected with arcs of an ellipse using an ellipse template. The end result was a prediction of an elliptical plume for the +1, +2, and +3 o/oo contours based upon collected field data.

Empirical equations were also developed for predicting the areal extent of the brine plume, and these are shown below in Equation 4-6.

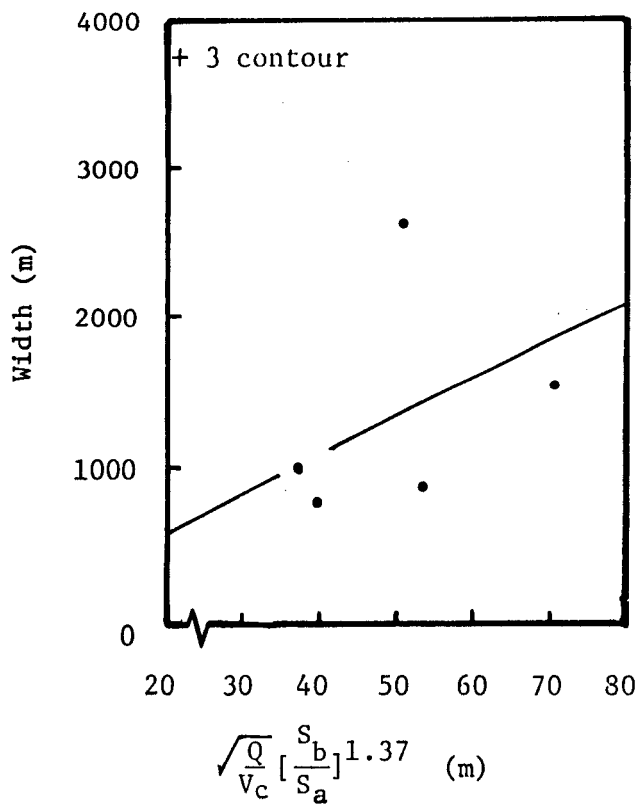
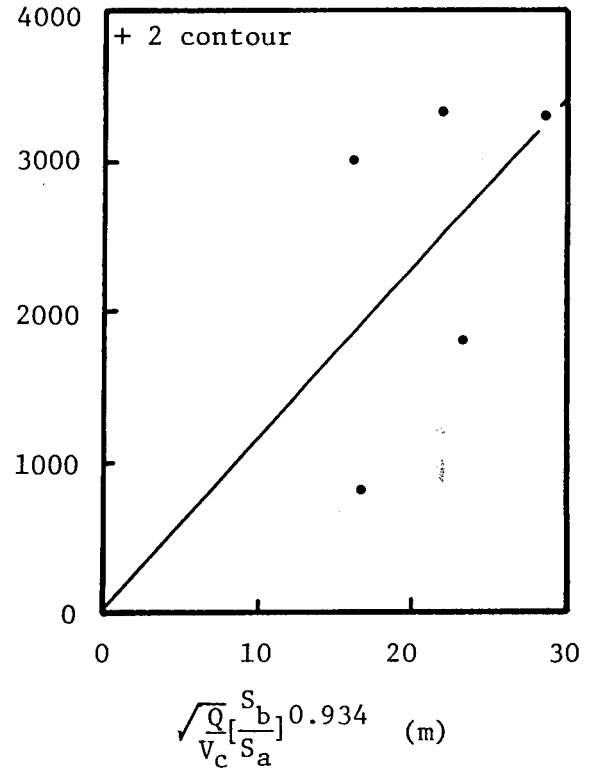
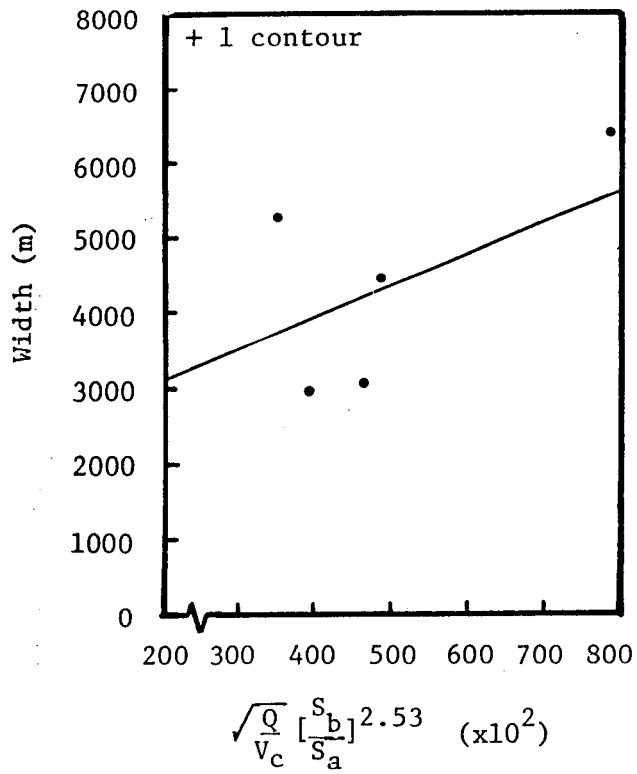


Figure 4-27. The variation of the plume width for the above ambient salinity contours.

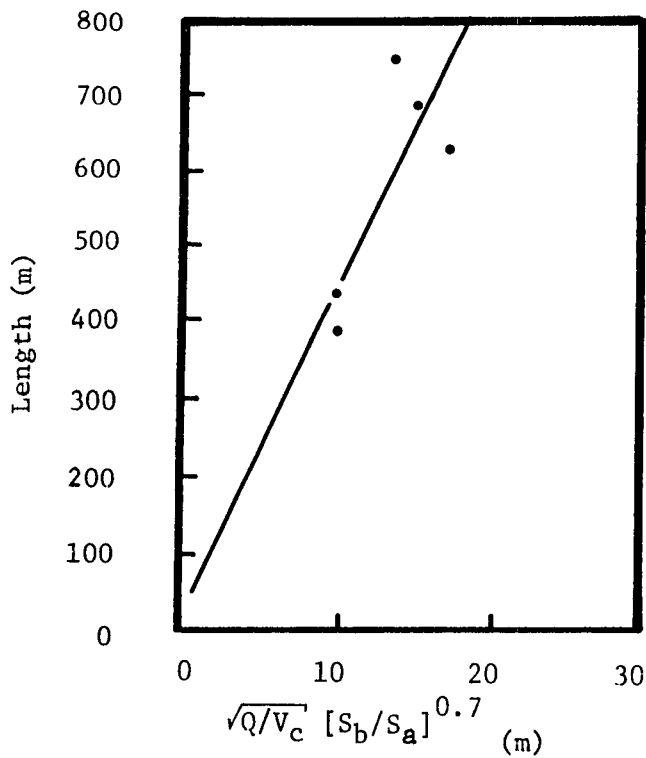
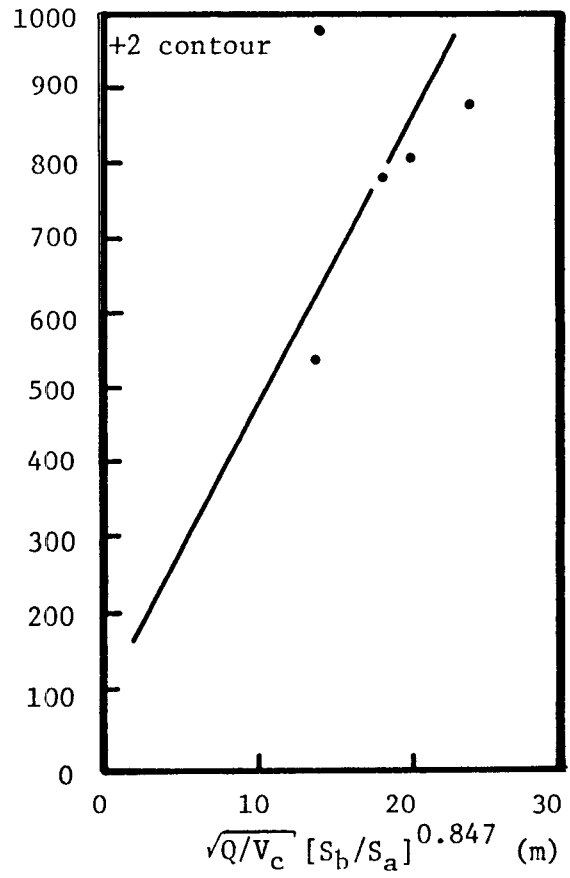
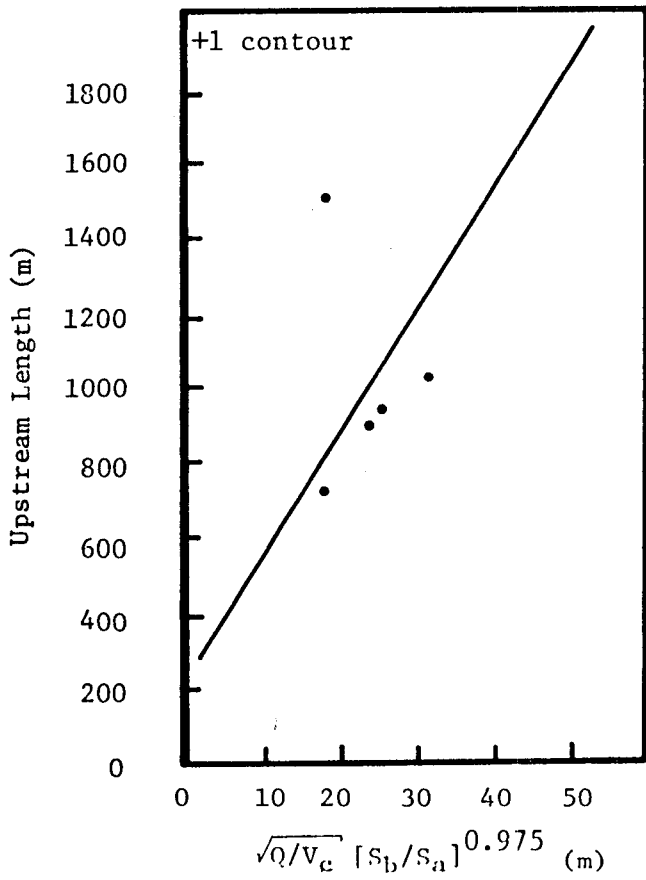


Figure 4-28. The variation of the plume upstream length for the above ambient salinity contours.

$$\begin{aligned}
 A_1 &= 2.96 \times 10^{-4} \sqrt{\frac{Q}{V_c}} \left[\frac{S_b}{S_a} \right]^{4.16} + 3.97 ; r = 0.79 \\
 A_2 &= 4.29 \times 10^{-2} \sqrt{\frac{Q}{V_c}} \left[\frac{S_b}{S_a} \right]^{1.16} + 2.45 ; r = 0.53 \quad (4-6) \\
 A_3 &= 3.41 \times 10^{-5} \sqrt{\frac{Q}{V_c}} \left[\frac{S_b}{S_a} \right]^{4.30} + .35 ; r = 0.69
 \end{aligned}$$

These equations are shown as solid lines on Figure 4-29 along with the area data measured with a polar planimeter and the correlation coefficients (r).

4.7.2 Comparison of Predicted and Measured Plume Contours and Areal Extent

4.7.2.1 Areal Extent Comparison

A comparison of the predicted and measured areas within the +1, +2, and +3 o/oo above ambient contours is illustrated in Figure 4-30. The area inside the +1, +2, and +3 o/oo contours is denoted by the symbols \odot , \triangle , and \square , respectively. If the data fell on the solid line, the measured and predicted values are in exact agreement. The results show that the empirical equations tend to predict larger areas than the measured values except for the measured plume on February 14, 1982.

The areal extent data show considerable scatter, and thus, the empirical equations are only good estimates. Also, only five measured plumes are available for comparison, and more data is desired for establishing the empirical equations. Some of the reasons for the scatter are the bottom current variability, the difficulty in determining the ambient salinity, and the period needed to complete

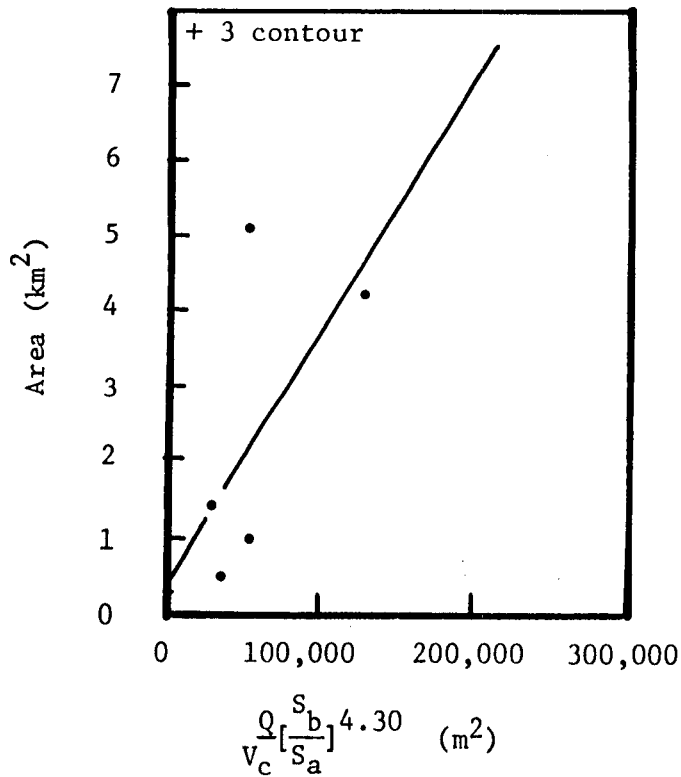
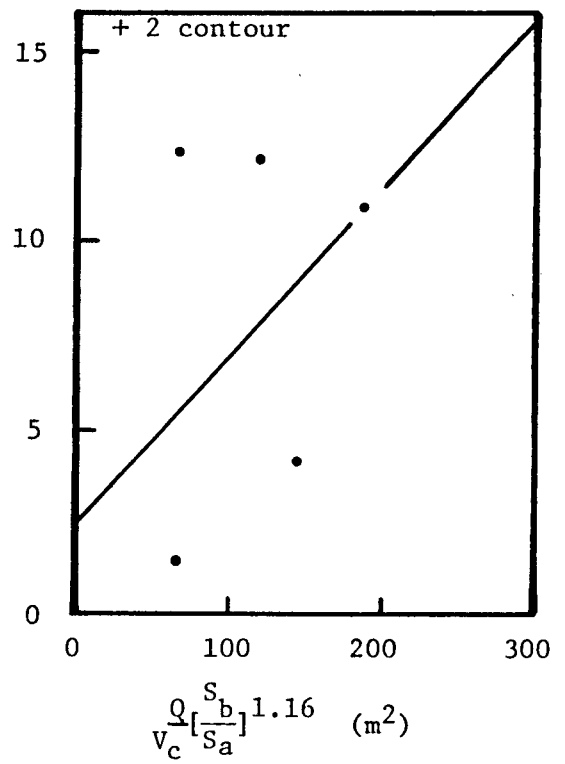
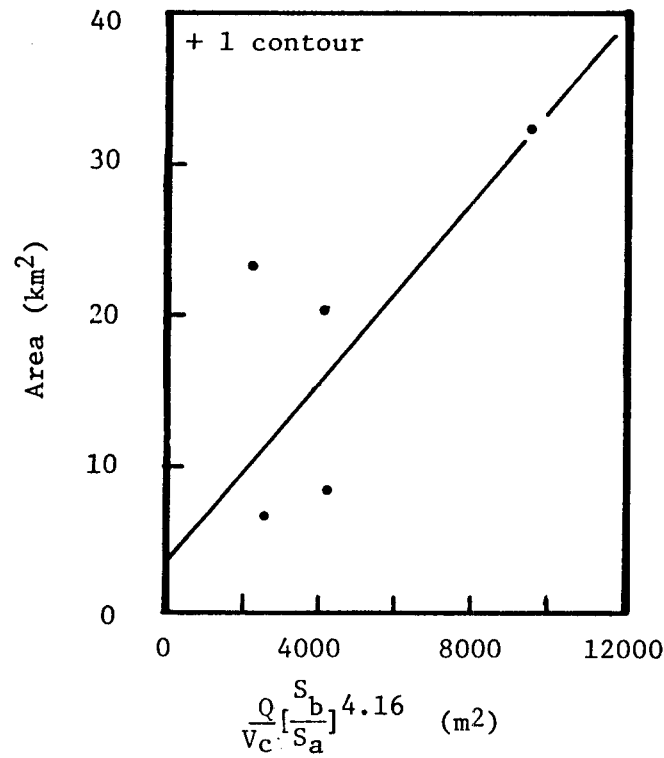


Figure 4-29. The variation of the plume area inside the above ambient salinity contours.

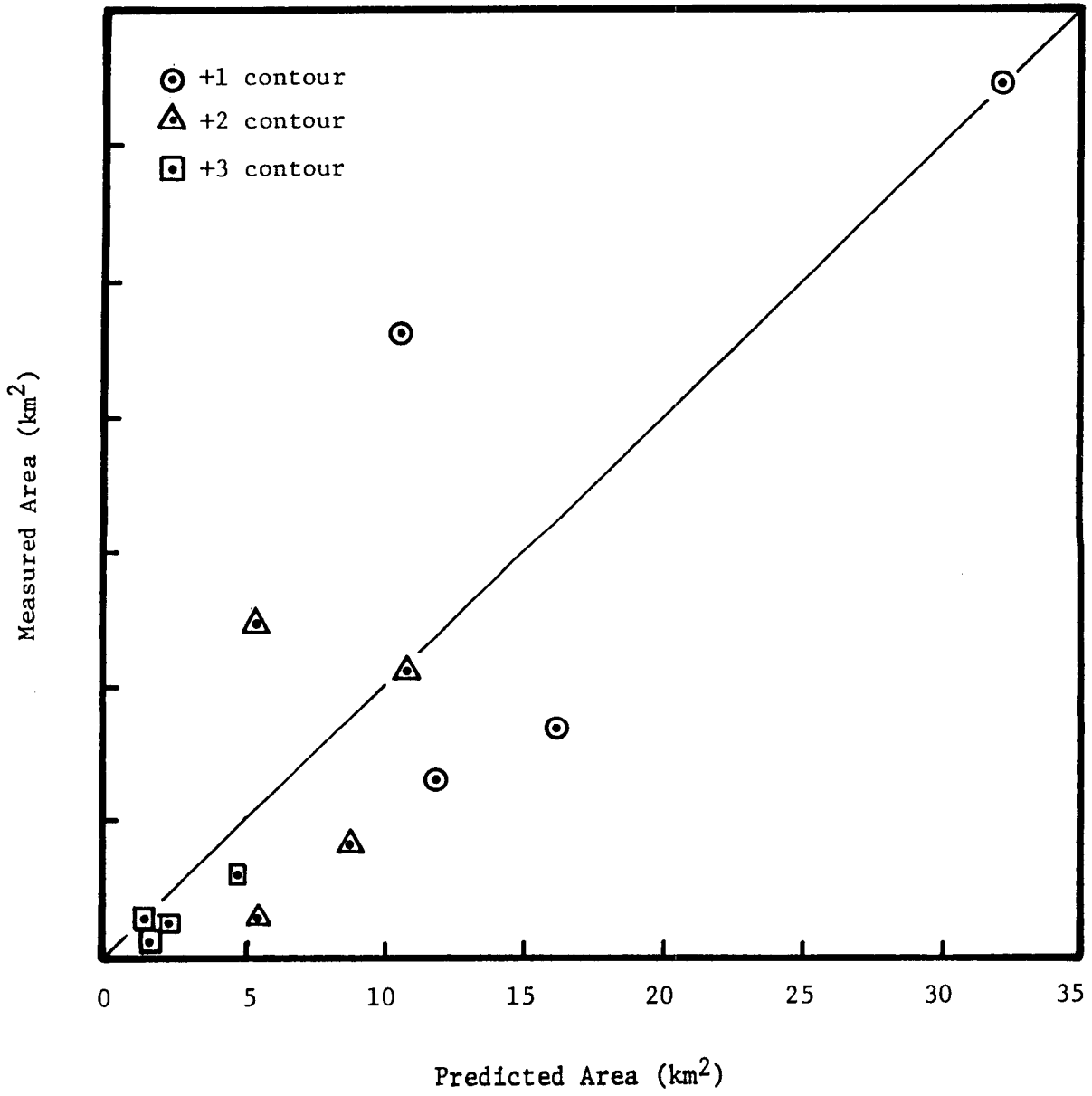


Figure 4-30. The comparison of the measured and predicted areal extent inside the above ambient salinity contours.

the plume measurements.

4.7.2.2 Plume Contour Comparison

The comparison of the measured and predicted plume contours is described to show how well the predicted plumes agree with the measured plumes. The first example is the August 12, 1981 plume and the comparison is illustrated in Figure 4-31. The measured +1, +2, and +3 o/oo above ambient contours are shown as the solid lines, and the dashed lines indicate the predicted plume contours. The direction of the predicted and measured plumes was in excellent agreement. The downstream length and width of the predicted plume contours agreed extremely well, and only the upstream length was underestimated by the prediction techniques. The measured plume had a +4 o/oo above ambient contour but empirical equations for +4 o/oo above ambient were not determined. It was concluded that this prediction was a very good approximation of the actual plume and that the +4 o/oo above ambient contour predictive capability needs to be developed.

A second example is shown in Figure 4-32 for the November 25, 1981 plume measurement. These results show the direction of the predicted plume was more to the south southwest as compared to the apparent southerly direction of the measured plume. The downstream length, upstream length, and width of the predicted plume are all smaller than the measured values. Again, the measured plume shows the existence of a +4 o/oo above ambient salinity contour and a predicted contour is not shown for the reasons previously mentioned. Although this plume prediction is not as good as that obtained for the August 12 data, it is considered a reasonable approximation and a useful tool for predicting the brine plume behavior. The ability to predict the

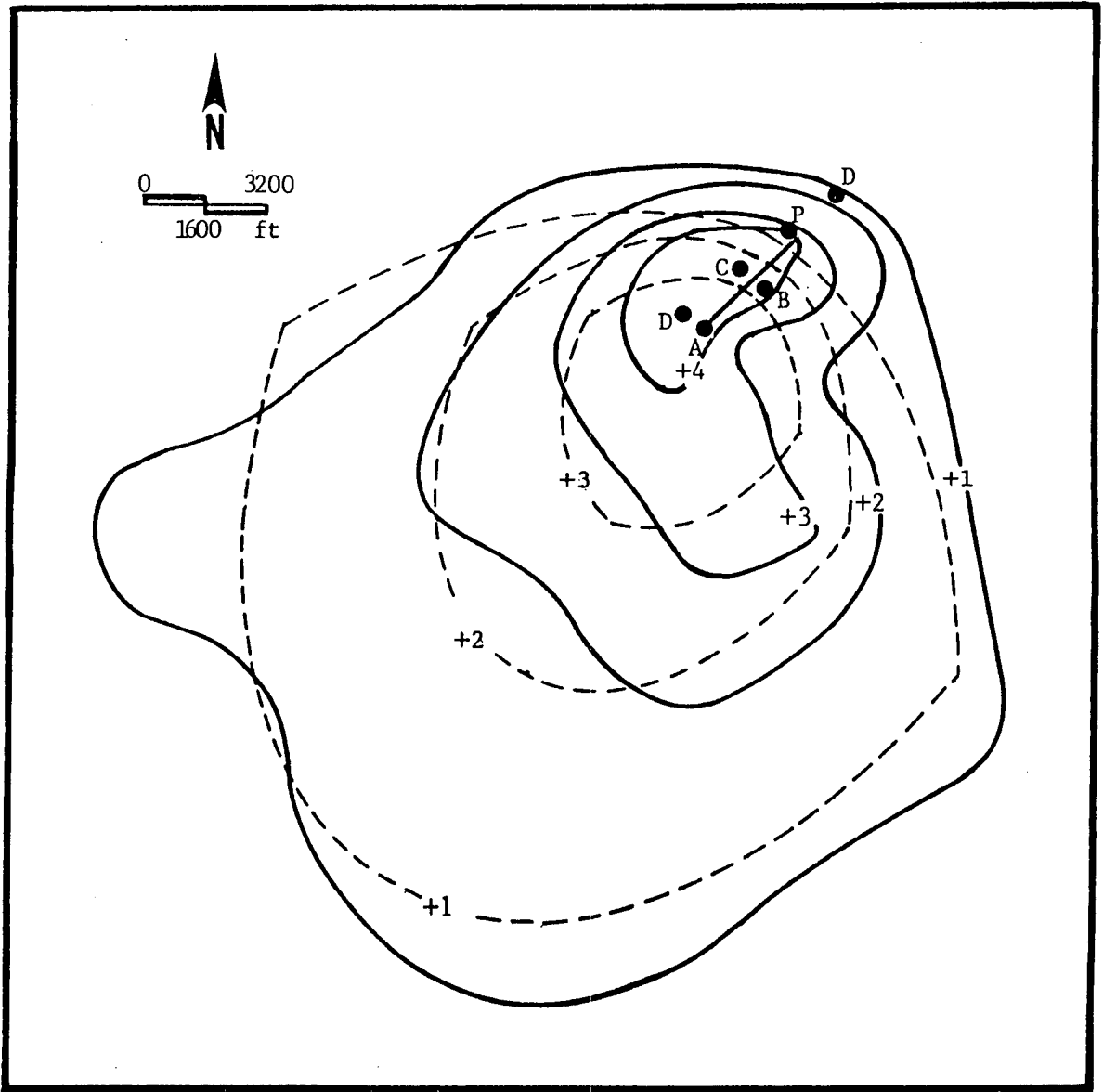


Figure 4-31. Comparison of measured (——) and predicted (-----) salinity plumes on August 12, 1981.

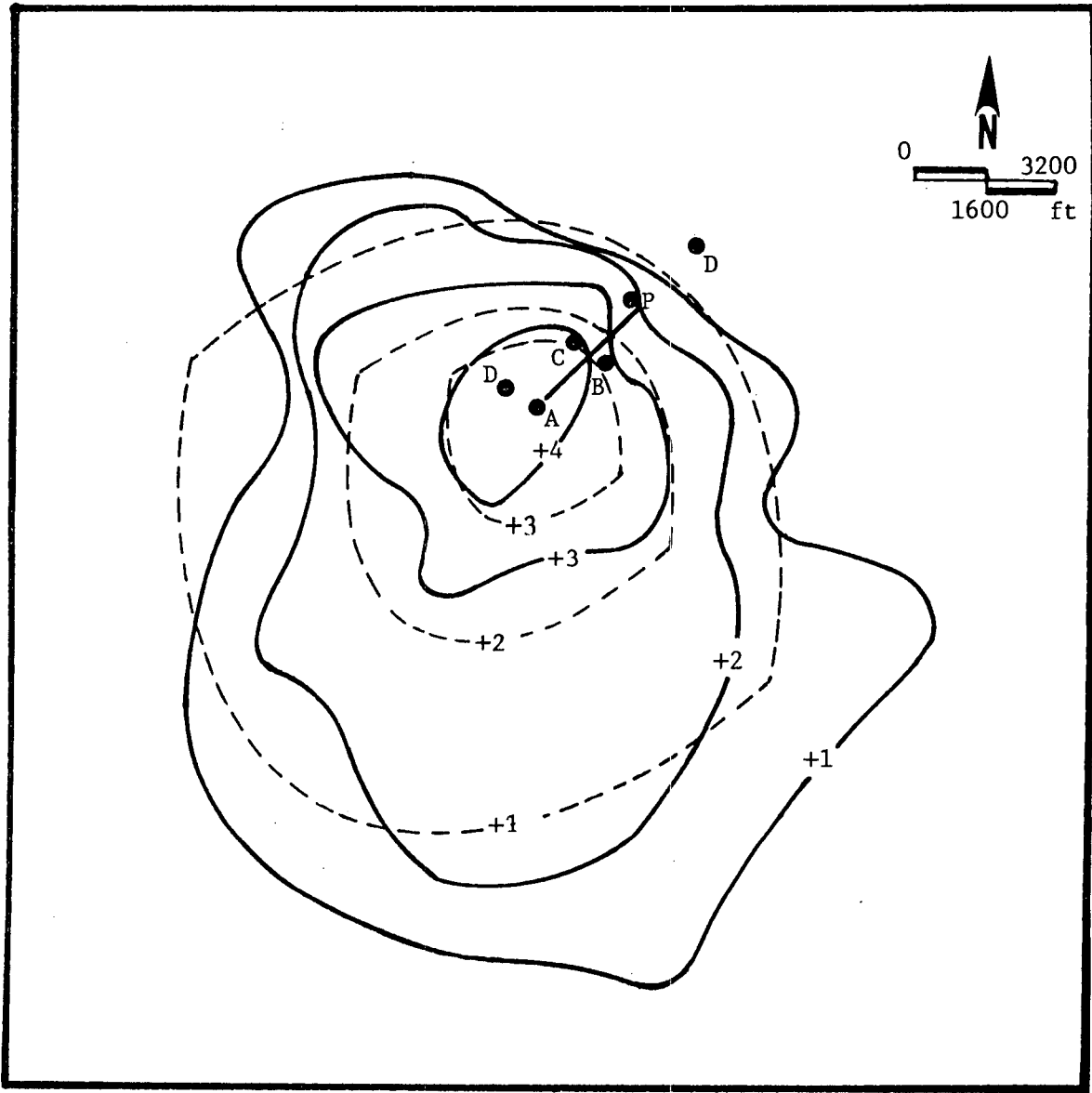


Figure 4-32. Comparison of measured (——) and predicted (-----) salinity plumes on November 25, 1981.

existence of above ambient contours and empirical equations for higher above ambient contours needs to be developed as more data becomes available.

4.7.3 Estimation of Area Exposure Time to Above Ambient Brine Concentrations

The objective of this section is to present results which estimate the percent of time a specific area in the vicinity of the diffuser was exposed to +1, +2, and +3 o/oo above the ambient salinity concentrations. The data necessary for making this estimate are the empirical equations described in section 4.7.1, the bottom current meter data at site D in the diffuser area (Chapter 2), and the brine discharge operating data (Chapter 1). These data were compiled for the entire 12 month postdisposal period and the percent area exposure time for the +1, +2, and +3 o/oo above ambient salinity concentrations was computed.

In order to make these computations, the diffuser area was divided into annular area sectors as shown in Figure 4-33. A polar coordinate system with its origin at the center of the diffuser is shown in Figure 4-33. Concentric circles were drawn at intervals of 0.25, 0.75, 1.25, 1.75, 2.25, 3.25, 4.25, 5.25, and 7.25 km, and each angular sector was a total of 22.5°. The center of each sector lay on a compass direction of North, North Northeast, Northeast, etc.

The next step was to compute the predicted plume contours with the equations described in section 4.7.1. The +1, +2, and +3 o/oo above ambient plume contours were computed for each eight-hour period of the day for which brine discharge data and bottom current data were available. The predicted downstream length, upstream length and width

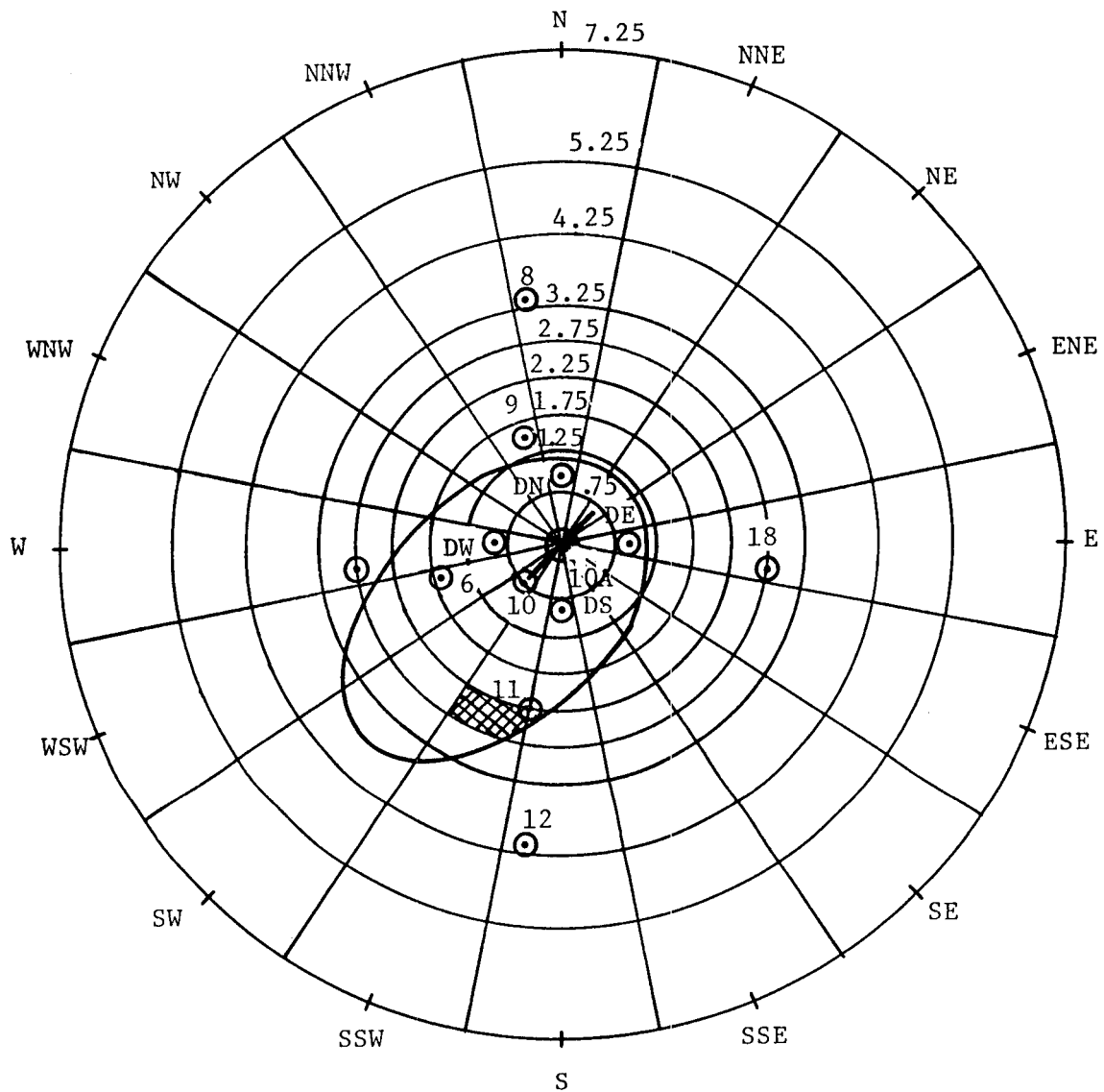
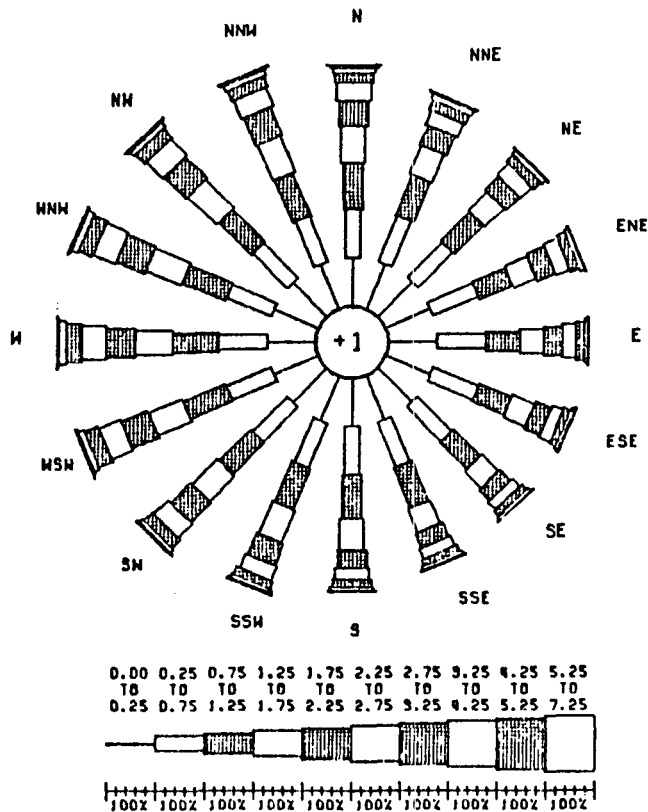


Figure 4-33. Schematic showing division of diffuser area into sectors for use in exposure time computations. Project sampling stations are denoted by ⊙.

were used as the axes of an ellipse. The mathematical expression for the ellipse was determined and used to evaluate the distance to the ellipse boundary. The area bounded by the ellipse contour as shown by the cross hatched area in Figure 4-33 was computed. This area was compared with the annular area of the sector. If the cross hatched area was larger than half the annular sector area, then the entire sector area was considered to be within the above ambient ellipse contour. This procedure was completed for the entire ellipse boundary for each above ambient contour.

A computer program was written which computes (1) the eight-hour average current speed and direction; (2) the upstream length, downstream length, and width of the predicted plume; and (3) the annular sector areas which are inside the predicted plume contour. It does these computations for each eight-hour period and keeps a record of the areas which were impacted by the plume. After all the available data have been analyzed, the results are presented in the form of a rosette diagram and a summary table. These were obtained by altering the physical oceanography (Chapter 2) computer programs which produced the current rosettes and joint frequency distribution of the current meter data.

Figure 4-34 shows the results for the +1 o/oo above ambient area exposure time. The rosette illustrates the percent time of exposure to at least +1 o/oo above ambient salinity in sixteen compass directions. The actual percent exposure time in each annular sector can be determined by the length of the rosette arrow. For example, in the northeast direction the two sectors which are closest to the diffuser (0.00 to 0.25 and 0.25 to 0.75 km) indicate the +1 o/oo above



PERIOD: 06/01/81 TO 03/31/82

NO DISCHARGE OR PHYSICAL DATA: 56.0 DAYS

DIR	DISTANCE FROM DIFFUSER (KM)									
	0.00-0.25	0.25-0.75	0.75-1.25	1.25-1.75	1.75-2.25	2.25-2.75	2.75-3.25	3.25-4.25	4.25-5.25	5.25-7.25
E	100	100	70	50	37	28	17	7	2	0
ENE	100	100	74	50	40	30	19	9	2	0
NE	100	100	84	55	40	32	20	10	3	0
NNE	100	100	91	69	45	31	21	10	4	1
N	100	100	96	78	59	35	21	10	5	1
NNW	100	100	97	82	63	39	24	11	5	1
NW	100	100	97	82	63	47	27	12	4	1
NNW	100	100	97	79	63	49	31	13	4	1
N	100	100	95	75	60	50	34	13	4	1
NSW	100	100	92	73	60	47	31	12	4	1
SW	100	100	91	72	58	40	24	9	4	0
SSW	100	100	90	73	50	31	18	8	4	0
S	100	100	91	64	38	21	16	8	3	0
SSE	100	100	89	53	32	22	14	7	3	0
SE	100	100	79	48	32	22	14	8	3	0
ESE	100	100	72	49	35	24	15	6	3	0

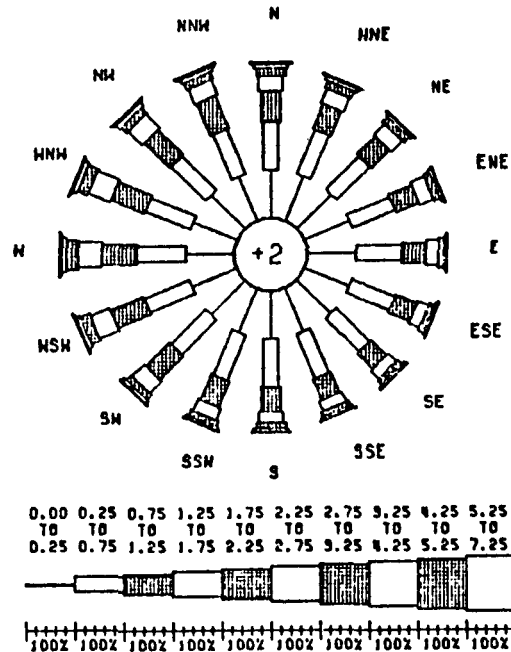
Figure 4-34. Twelve month percent exposure time rosette and distribution table for the +1 o/oo above ambient salinity contour.

ambient contour included these sectors 100% of the time. The annular sector which is 0.75 to 1.25 km NE of the diffuser was inside the +1 contour 84% of the time which is determined by the fact that the cross hatched rectangle is 84% of the length of the value on the scaled arrow below the rosette. The rosette picture is most useful in getting a quick picture of the preferred directions of the brine plume. In the case of the +1 o/oo contour, the percent time of exposure is shown to be pretty evenly distributed in all directions with a slight reduction in percent exposure in the directions SE, ESE, E, and ENE. The table below the rosette diagram has the most information. It gives the values of percent exposure time in each annular sector area. For example, the annular sector west of the diffuser and bounded by the distance of 2.25 to 2.75 km is shown to have an exposure time of 50% for the +1 o/oo contour.

The +1 o/oo above ambient exposure time distribution table shows the longest distance for the +1 o/oo above ambient contour is 7.25 km (3.9 nm) from the diffuser. It shows that the +1 o/oo contour continually envelopes all the area out to 0.75 km (0.45 nm) from the diffuser. For the distance of 0.75 to 1.25 km the highest percent exposure time was 97% in the WNW, NW, and NNW directions and the lowest was 70% in the easterly direction. At a distance of 1.25 to 1.75 km, the highest percent exposure time was 82% in the NW and NNW directions and the lowest was 48% in the SE direction. The WNW, NW, and NNW directions showed the highest percent at a distance of 1.75 to 2.25 km and the lowest was 32% in the SE and SSE directions. The maximum percent exposure time for the distance 2.25 to 2.75 km from the diffuser reduced to 50% in the W direction, and the minimum was

22% SSE and SE of the diffuser. At the distance 2.75 to 3.25 km, the maximum percent exposure time was 34% in the direction W, and the minimum was 14% in the SE and SSE directions. The distance of 3.25 to 4.25 km shows the maximum percent exposure was 13% in the WNW and W directions and the minimum percent exposure was 6% in the direction of ESE. The maximum percent exposure time was 5% for the distance 4.25 to 5.25 km in the directions NNW and N, and the minimum percent exposure was 2% in the directions of ENE and E. Thus, the distribution table for the +1 o/oo contour shows the exposure time was generally the least in the ENE, E, ESE, SE, and SSE directions and the maximum was spread more generally around in the N, NNW, NW, WNW, and W directions.

The percent exposure time for the +2 o/oo above ambient salinity contour for the first 12 months of discharge is shown in Figure 4-35. The rosette shows nearly equal distribution in all directions. The distribution table shows the area within 0.25 km (0.14 nm) of the diffuser center is continually +2 o/oo above the ambient salinity. The area between 0.25 and 0.75 km had an exposure time of 95% to 100% in all directions. The range of percent exposure time for the area between 0.75 and 1.25 km was 74% to 45%, and the NW direction had the maximum value and the SE direction had the minimum value. The percent exposure time for the distance 1.25 to 1.75 km ranged from 48% in the W and WNW directions to 22% in the SSE direction. At the distances of 1.75 to 2.25 km, the maximum percent exposure time was 24% in the W direction and the minimum value was 11% in the S, SSE, SE, and ESE directions. At the distances of 2.25 to 2.75 and 2.75 to 3.25 the percent exposure time was nearly the same in all directions with



PERIOD: 06/01/81 TO 09/31/82
 NO DISCHARGE OR PHYSICAL DATA: 56.0 DAYS

DIR	DISTANCE FROM DIFFUSER (KM)									
	0.00-0.25	0.25-0.75	0.75-1.25	1.25-1.75	1.75-2.25	2.25-2.75	2.75-3.25	3.25-4.25	4.25-5.25	5.25-7.25
E	100	95	49	27	12	5	2	0	0	0
ENE	100	95	51	30	14	6	2	0	0	0
NE	100	96	59	30	16	6	3	0	0	0
NNE	100	97	56	30	15	7	3	1	0	0
N	100	99	69	31	15	8	4	1	0	0
NNW	100	100	73	32	16	8	4	1	0	0
NW	100	100	74	39	17	9	4	1	0	0
WNW	100	100	73	48	22	9	4	1	0	0
W	100	100	73	48	24	8	3	1	0	0
WSW	100	100	72	43	20	7	3	1	0	0
SW	100	100	68	34	14	7	3	0	0	0
SSW	100	99	59	25	19	6	3	0	0	0
S	100	99	52	29	11	5	3	0	0	0
SSE	100	97	47	22	11	6	2	0	0	0
SE	100	96	45	29	11	6	2	0	0	0
ESE	100	95	47	24	11	5	2	0	0	0

Figure 4-35. Twelve month percent exposure time rosette and distribution table for the +2 o/oo above ambient salinity contour.

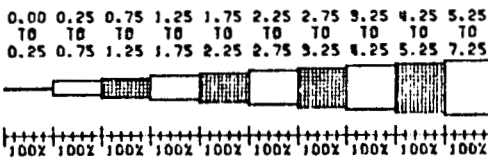
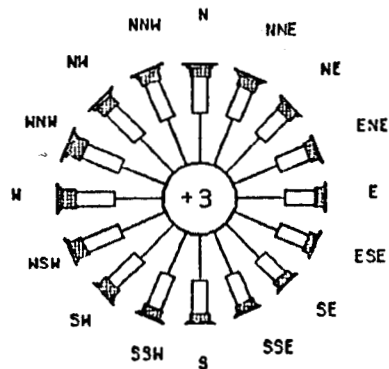
values of near 7% and 3% respectively. The maximum predicted extent of the +2 o/oo above ambient contour was 4.25 km in the N and NNE directions.

The prediction of the percent exposure time for the +3 o/oo above ambient salinity contour is shown in Figure 4-36. The rosette diagram indicates the +3 o/oo contour was generally the same in all directions with a slight decrease in the SE and SSE directions. The distribution table shows that the area within 0.25 km (0.14 nm) of the diffuser center was continually within the +3 o/oo above ambient concentration. The percent exposure time reduced sharply for the distance 0.25 to 0.75 km with a range of 82% to 60%. The maximum value of 82% was in the NW direction. The maximum extent of the +3 o/oo contour was 2.75 km, and the percent exposure time for the distance of 2.25 to 2.75 km was 1% in the directions of WNW, NW, NNW, N, and NNE and 0% in all other directions.

Over the 12 month (approximately 365 days) postdisposal period, of which 56 days could not be analyzed because of lack of data, the percent exposure time to the +1, +2, and +3 o/oo above ambient salinity was predicted in the vicinity of the diffuser. The results indicate that the percent exposure time was fairly evenly distributed in all directions. There was some favoring of the W, WNW, and NW directions, and the least percents of exposure time were usually in the E, ESE, and SE directions. The maximum predicted extent of the +1, +2, and +3 o/oo contours was 7.25, 4.25, and 2.75 km (3.9, 2.3 and 1.5 nm) from the center of the diffuser.

4.8 Summary of Brine Plume Measurement Results

A plume tracking system consisting of a towing sled which housed



PERIOD: 06/01/81 TO 03/31/82
 NO DISCHARGE OR PHYSICAL DATA: 56.0 DAYS

DIR	DISTANCE FROM DIFFUSER (KM)									
	0.00-0.25	0.25-0.75	0.75-1.25	1.25-1.75	1.75-2.25	2.25-2.75	2.75-3.25	3.25-4.25	4.25-5.25	5.25-7.25
E	100	63	17	3	1	0	0	0	0	0
ENE	100	64	18	4	1	0	0	0	0	0
NE	100	66	19	5	1	0	0	0	0	0
NNE	100	68	20	6	1	1	0	0	0	0
N	100	74	18	5	2	1	0	0	0	0
NNW	100	61	19	6	2	1	0	0	0	0
NW	100	62	23	7	2	1	0	0	0	0
WNW	100	61	29	6	2	1	0	0	0	0
W	100	60	30	6	1	0	0	0	0	0
WSW	100	60	26	5	1	0	0	0	0	0
SW	100	70	21	6	1	0	0	0	0	0
SSH	100	72	17	5	1	0	0	0	0	0
S	100	65	16	4	1	0	0	0	0	0
SSE	100	61	16	4	1	0	0	0	0	0
SE	100	60	15	4	1	0	0	0	0	0
ESE	100	63	16	3	1	0	0	0	0	0

Figure 4-36. Twelve month percent exposure time rosette and distribution table for the +3‰ above ambient salinity contour.

a conductivity, temperature, and depth (CTD) probe was towed by a research vessel on a predetermined search course through the expected brine plume area. The probe continuously measured conductivity which was converted to salinity at a distance of 25.4 cm (10 in) above the sea floor. These data were recorded and subsequently used to construct isohaline contour plots which indicate the areal coverage of the plume and the magnitude of the excess salinity concentration. In addition, vertical salinity and dissolved oxygen profiles were measured in the vicinity of the diffuser to evaluate the vertical extent of the plume and the effect of the brine discharge on the vertical distribution of dissolved oxygen.

Brine discharge was scheduled to begin on May 10, 1981, and brine plume measurements were planned for once a week during the first month after discharge began, once every two weeks during the second month, and once a month thereafter. The first two plume measurements were made on May 25 and June 1, 1981, but no contours were closed which was attributed to low brine salinity. The June 9 plume measurement resulted in a closed contour of 30 o/oo which encompassed an area of 9.4 km². The +1 o/oo above ambient contour covered a small area of 0.3 km², and the highest salinity was 30.9 o/oo which was 1.2 o/oo above the ambient salinity. On this date, the brine was being discharged at a rate of 23,580 barrels/hr and a salinity of 178 o/oo.

The June 17 plume measurement resulted in only a +1 o/oo salinity contour encompassing an area of 0.4 km². The first large brine plume was measured on June 30 when the discharge rate was 28,307 barrels/hr and the brine salinity was 208 o/oo. High salinity stratification and large cross-shelf salinity variation were present

on this date which made it very difficult to evaluate the ambient salinity. Results showed the closing of a +4, +3, +2, and +1 o/oo contours with inside areas of 0.6, 3.9, 9.4, and 22.8 km². The July 17 plume measurement completed the initial weekly and biweekly plume tracking cruises, but it did not show any closed contours.

On August 12, 1981, brine was being discharged at a rate of 25,643 barrels/hr and a salinity of 228 o/oo. The highest measured salinity was 32.1 o/oo and the highest above ambient salinity was 4.4 o/oo. There were four closed above ambient salinity contours (+1, +2, +3, and +4 o/oo) and the areal coverage inside these contours was 32.2, 10.8, 4.2, and 1.1 km² respectively. The 32.2 km² area was the largest areal extent measured for the +1 o/oo contour during the first year of discharge, and the longest distance from the diffuser to the +1 contour was 5.7 km in the direction of 199°T.

During September, the brine discharge was stopped and no plume measurements were attempted. The next plume measurement was conducted on October 28 when the brine was being pumped at a rate of 24,500 barrels/hr and a salinity of 225 o/oo. The highest measured salinity was 35.8 o/oo and four above ambient contours were determined with areas of 6.6, 1.5, 0.5, and 0.1 km² inside the +1, +2, +2, and +4 o/oo contours respectively.

The November and December plume measurements were conducted when the brine discharge rate and salinity were near 21,500 barrels/hr and 205 o/oo, respectively. The November data shows that four above ambient contours were measured and the area inside the +1 o/oo contour was 20.3 km². The December data resulted in three above ambient contours with the +1 o/oo contour covering an area of 8.4 km².

The highest salinity measured on these dates was 34.4 o/oo and 34.3 o/oo in November and December respectively.

During January, the brine discharge was being batched which means brine was being pumped to the Gulf of Mexico for only short periods of time (approximately 8 to 12 hours), and consequently, no measurements were attempted. On February 14, 1982, the brine discharge was back to a continuous operation with a rate of 23,892 barrels/hr and salinity of 217 o/oo. The highest salinity (36.0 o/oo) and highest above ambient salinity (+4.9 o/oo) were measured on this date in the immediate vicinity of the diffuser, and four above ambient contours were measured. The areas inside the +1, +2, +3, and +4 o/oo contours was 23.2, 12.4, 2.5, and 0.5 km².

In March 1982, the brine discharge was greatly increased to 35,042 barrels/hr and the salinity was 180 o/oo. The combination of the high discharge rate and low brine salinity resulted in no closed salinity contours. The April 30, 1982 discharge rate was 23,315 barrels/hr and the salinity was 224 o/oo. This plume had three above ambient contours with inside areas of 19.9, 10.0, and 4.9 km² for the +1, +2, and +3 o/oo contours respectively, and the highest salinity was 31.6 o/oo.

Distances were measured from the center of the diffuser to the various above ambient contours. These data indicate the longest distance to the +1 o/oo above ambient contour was 5.7 km (3.1 nm) from the diffuser in the direction of 199°T, or southsouthwest of the diffuser. The longest distance to the +2, +3, and +4 o/oo contours was 4.4, 3.4, and 1.7 km (2.4, 1.8, and 0.9 nm) respectively. The maximum inshore and offshore distances for the +1 o/oo above ambient

contour were 2.9 km (1.6 nm) and 5.3 km (2.9 nm). In the upcoast and downcoast direction, the largest distances to the +1 o/oo above ambient contour were 2.7 km (1.5 nm) and 4.8 km (2.6 nm) respectively.

During the 12 month study, the bottom temperature data collected during the plume measurements show no indication of a significant thermal plume. The maximum difference between the brine temperature measured at the brine pit and the ambient bottom temperature in the offshore area was only 8.3°C. The bottom temperatures measured during the plume tracks varied less than 1°C and were considered nearly isothermal.

The vertical extent of the plume was determined by measuring vertical salinity profiles directly over and in the immediate vicinity of the diffuser. These profiles were then compared to the ambient profile. The vertical distance above the bottom at which the salinity profile deviated from the ambient profile was determined to be the vertical extent of the brine plume, and these values were then compared to the values computed from empirical relationships.

The diffuser had 32 open ports for every vertical profile measurement except for April 30, 1982. On June 1, 1981, the measured vertical extent was 2.5 m while the computed vertical extent was 6.7 m. The June 9 and 30 profiles indicated the vertical extent was 0.6 m and 1.5 m while the computed values predicted 4.5 and 4.6 m respectively. These data indicate the measurements were not taken directly over the diffuser ports and thus, the measured data are much lower than the computed values. The August and October vertical profiles were nearly 50 percent of the computed values, and the exit velocities for these dates were 7.8 and 7.4 m/s. The exit velocity

dropped to 6.6 m/s on November 25 and December 16, and the measured vertical extent dropped to 1.5 and 2.0 m while the computed values were 3.9 and 4.0 m respectively.

The February 14, 1982 profile shows a 2.2 m vertical extent while the computed value was 4.1 m. The brine discharge rate increased greatly on March 1, 1982 which resulted in an exit velocity of 10.6 m/s. The computed vertical extent was 6.0 m, but the measured value was only 0.6 m. The low brine salinity made it very difficult to determine any deviation from the ambient salinity profile. The April 30, 1982 vertical salinity profile clearly shows a rapid departure from the ambient profile at 2.1 m while the computed vertical extent was 3.3 m due to the decreased exit velocity of 5.4 m/s.

In all the vertical profiles, the measured vertical extent was much less than the computed values indicating the measured vertical data was taken from the plume settling around the diffuser area and not from the area directly over the brine jets whose vertical extent is believed to be much higher and closer to the computed values. Using all the vertical profile data, the average exit velocity was 7.6 m/s and the average computed vertical extent was 4.5 m. The average measured vertical extent was 1.8 m which is 40% of the computed value. In the Bryan Mound study (Randall, 1981a), the initial period of discharge (March 10 through July 15, 1980) showed the average exit velocity was 6.7 m/s, and the average measured and computed vertical extent was 3.7 and 4.0 m respectively. During the second period from July 16, 1980 through August 24, 1981, the average exit velocity was 8.0 m/s and the average measured and computed vertical extent was 5.2 and 4.5 m respectively. The low measured vertical extent of the West

Hackberry plume is believed to be caused by the inability to keep the CTD/DO sensor directly over the diffuser, and consequently, the height of the plume settling to the bottom is the value measured. The lower brine salinities for the West Hackberry discharge is also a cause of the low measured vertical extent.

Vertical dissolved oxygen profiles were collected simultaneously with the vertical salinity profiles, and the data collected in the vicinity of the diffuser were compared to that collected at the control stations. A deviation in vertical distribution between the diffuser stations and the control station was interpreted as an effect due to the brine discharge. On June 9, 1981, the vertical profile measured directly over the diffuser showed the dissolved oxygen decreased sharply to 3.9 mg/l at 8.8 m and then increased slightly to 4.2 mg/l at the bottom. The slight increase in dissolved oxygen near the bottom is in contrast to the continued decline of the dissolved oxygen at the control station to a value of 2.8 mg/l. It is believed that the brine discharge entrains the higher oxygenated water in the negatively buoyant plume as it falls to the bottom and spreads over the sea floor.

The July 17 vertical dissolved oxygen profiles were collected during a period of anoxia in the bottom waters which covered an extensive bottom area along the Gulf coast and far exceeded the small area covered by the brine plume. The vertical profile measured directly over the diffuser showed the dissolved oxygen gradient was noticeably less than that at the control station and this was similarly attributed to the brine discharge. The bottom dissolved oxygen value at the control station was 0.2 mg/l, and at the diffuser

site, it was 0.5 mg/l, so the brine discharge apparently affected the gradient, but it didn't remove the anoxic conditions.

The August 12, 1981 vertical dissolved oxygen profiles indicated the anoxic conditions had disappeared and there was only a small decrease in dissolved oxygen from surface to bottom. These same results were obtained at both the diffuser site and control stations. Similar results were obtained for the months of October 1981 through March 1982. However, the April 30, 1982 data showed a stronger dissolved oxygen gradient from surface to bottom, and similar results were obtained as those observed on June 9 which again was attributed to the brine discharge.

The experimental data collected during the plume measurements were used to develop an empirical procedure for predicting the areal extent of the plume. For this procedure, the upstream and downstream distance from the center of the diffuser to the above ambient contours and the maximum width of each contour were measured from actual plume measurements. These data were plotted as a function of a parameter consisting of the average bottom current, discharge rate, brine salinity and ambient salinity. Least squares curve fits were made to the data in order to obtain empirical relationships for the upstream length, downstream length, and width. Thus, the lengths and widths of the above ambient contours were estimated and the end points were connected using arcs of an ellipse. The results of the empirical predictions were compared to actual plume measurements and the procedure provided reasonable estimates of the plume contours. The ability to predict the existence of above ambient salinity contours and empirical equations for higher above ambient salinity contours

needs to be developed as a more extensive data base becomes available. These procedures were used to provide plume estimates for periods when plume measurements were not available provided the average bottom current, brine salinity, and brine discharge rate were known.

The percent of time a specific area in the vicinity of the diffuser was exposed to +1, +2, and +3 o/oo above ambient salinity was estimated for the 12 month study period. The empirical equations for evaluating the size of the brine plume, the bottom current meter data in the diffuser area, and the brine discharge data for the entire 12 month postdisposal period were used for this computation. Over the 12 month (approximately 365 days) postdisposal period, of which 56 days could not be analyzed because of lack of data, the percent exposure time to the +1, +2, and +3 o/oo above ambient salinity was predicted in the vicinity of the diffuser. The results indicate that the percent exposure time was fairly evenly distributed in all directions. There was some favoring of the W, WNW, and NW directions, and the least percents of exposure time were usually in the E, ESE and SE directions. The maximum extent of the +1, +2, and +3 o/oo contours was 7.25, 4.25, and 2.75 km (3.9, 2.3, and 1.5 nm) from the center of the diffuser.

4.9 Conclusions and Recommendations

The highest bottom salinity of 36.0 o/oo was measured on February 14, 1982, and it was 4.9 o/oo above the ambient salinity. The brine was being discharged at a rate of 23,896 barrels/hr and a salinity of 217 o/oo. The highest above ambient salinity contour measured during the year was +4 o/oo which occurred on June 30, August 12, October 28, and November 25 in 1981, and February 14 in 1982. A +3 o/oo contour

was measured on June 30, August 12, October 28, November 25, and December 16 in 1981 and on February 14, and April 30 in 1982. The largest areal extent within the +1 o/oo contour was 32.2 km² which occurred on August 12, 1981. The maximum measured horizontal extent of the salinity plume based on the +1 o/oo above ambient salinity contour was 5.7 km (3.1 nm) from the diffuser. Thus, it is concluded that the diffuser is diluting the brine to 4 to 5 o/oo above the ambient salinity and it is further diluted by advection and turbulence to 1 o/oo above the ambient salinity within 6 km of the diffuser.

An early concern was that the brine plume would enter the Calcasieu Lake through Calcasieu Pass. The Pass is 15.9 km northeast of the diffuser and the longest measured and predicted distances of the +1 contour were 5.7 km and 7.25 km respectively. Thus, it is concluded that the brine did not enter Calcasieu Pass or Calcasieu Lake.

The bottom temperatures measured in the plume area varied less than 1°C, and thus it was concluded that no significant thermal plume was detected during the plume measurements.

The maximum measured vertical extent of the salinity plume was 2.6 m above the sea floor directly over the diffuser. The average vertical extent directly over the diffuser was 1.8 m while the average computed vertical extent was 4.5 m. The low measured vertical extent of the West Hackberry plume is attributed to the inability to keep the CTD/DO sensor directly over the diffuser and to the low brine salinities.

The vertical dissolved oxygen data indicate the brine discharge affects the vertical distribution of dissolved oxygen when a strong

gradient exists such as occurs in the spring and summer months. It is believed that the brine discharge entrains the higher oxygenated water in the negatively buoyant plume as it falls to the bottom and spreads over the sea floor.

An empirical procedure based upon measured plume data was developed to estimate the above ambient salinity contours if the average bottom current, brine salinity, and brine discharge rate were known. The results of this procedure show reasonable agreement with the measured plume tracks. The ability to predict the existence of above ambient contours and empirical equations for higher above ambient contours needs to be developed as a more extensive data base becomes available.

The empirical prediction of plume contours was used in conjunction with physical oceanography data at the diffuser site and brine discharge data to evaluate the percent time a particular annular sector of the sea floor was exposed to +1, +2, and +3 o/oo above ambient salinity. The results show the percent exposure time was near evenly distributed in all directions. The west, west northwest, and northwest directions were slightly favored and the southeast direction was least favored. The maximum predicted extent of the +1, +2, and +3 o/oo contours was 7.25, 4.25, and 2.75 km (3.9, 2.3, and 1.5 nm) from the diffuser, respectively.

It is recommended that near field studies be conducted in order to better evaluate near field plume vertical extent. This study would use a subbottom profiler to evaluate the brine jet vertical extent. Additional vertical profiles using divers should also be used to provide additional information.

Only six satisfactory plume tracks have been completed which limits the ability to make empirical predictions. Discharge operations have not reached the near saturated brine conditions or the expected continuous one million barrels per day discharge rate, and consequently, plume measurements have not been made under these conditions. Therefore, it is recommended that monthly plume tracks be continued.

CHAPTER 5

WATER AND SEDIMENT QUALITY

L. M. Jeffrey, H. E. Murray, and J. F. Slowey
Texas A & M University
College Station, Texas 77843

J. Beck, C. Webre, and G. Grout
McNeese State University
Lake Charles, Louisiana 70609

5.1 Water Quality Studies

5.1.1 Introduction

As part of the Department of Energy's monitoring plan for brine discharge to the Gulf of Mexico from the Strategic Petroleum Reserve Program's West Hackberry site, a regime of monthly and quarterly water and sediment samples were collected at stations shown in Figure 5-1. Fourteen stations were located offshore in the vicinity of the diffuser and five were in the estuary.

Monthly water samples were collected at each station and analyzed for the following parameters:

- 1) total phosphorus
- 2) phosphate
- 3) silicate
- 4) nitrite
- 5) nitrate
- 6) ammonia
- 7) oil and grease
- 8) temperature
- 9) salinity
- 10) dissolved oxygen
- 11) pH

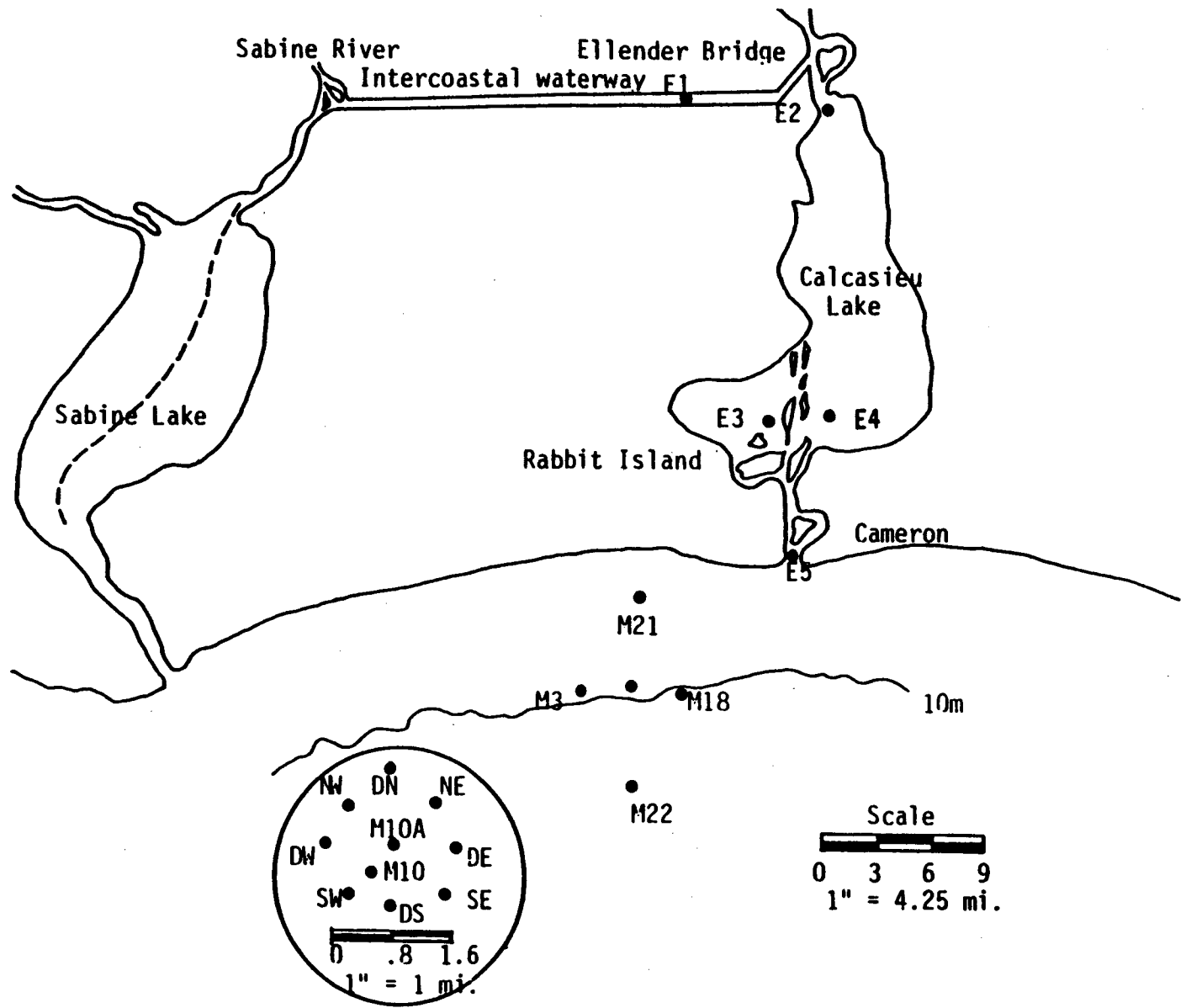


Figure 5-1. Inshore and off shore station locations for postdischarge used in water quality sampling.

12) turbidity

In addition to the above monthly measurements, samples collected at each station on a quarterly basis (June 1981, September 1981, December 1981 and March 1982) were analyzed for major ions present to determine if ionic imbalance has resulted from brine discharge. The ions determined were:

- 1) Ca
- 2) Cl
- 3) K
- 4) Mg
- 5) Na
- 6) SO₄

Furthermore, on a quarterly basis these same major ions were determined in the interstitial or pore waters obtained from sediment samples collected for sediment quality studies. Eh and pH were also measured on sediment samples collected quarterly.

Results of these analyses prior to brine discharge were presented as baseline data in a predisposal report previously submitted to DOE (Slowey et al., 1982).

5.1.2 Sampling and Analytical Methods

All stations were sampled at the surface and bottom depths except for the shallow Calcasieu Lake stations located at E-2, E-3, and E-4. These were sampled only at the surface.

Water samples were collected using 1.8 l Niskin water samplers. Samples were taken from the Niskin samplers and divided into five fractions. About 300 ml were placed in plastic bottles and frozen for nutrient analysis later in the laboratory. Another sample was placed

into 300 ml BOD bottles for dissolved oxygen analysis which was commenced immediately. Samples for oil and grease analyses were placed in glass bottles, acidified and kept refrigerated (iced) until return to the laboratory. About 190 ml were placed into glass bottles which were capped and returned to the laboratory for salinity analysis. The remainder of the sample was placed in one liter plastic Cubitainers and returned to shore for determination of turbidity on a monthly basis and major ions quarterly.

Analytical procedures used in these studies are based upon those contained in the American Public Health Association's Standard Methods for the Examination of Water and Wastewater, 14th edition (APHA, 1975), or in the Environmental Protection Agency's Methods for Chemical Analysis of Water and Wastes, EPA-600/4-79-020 of March 1979, where possible. Specific analytical methods follow.

5.1.2.1 Water Quality Analyses

Analyses of general water and pore water quality parameters were made in accordance with the following methods.

Chloride (Cl) was determined by the mercuric nitrate method described in method #408B of Standard Methods, after a 1:200 volumetric dilution.

Sulfates (SO_4) were determined by the barium sulfate turbidimetric method #427C of Standard Methods, after a 1:50 volumetric dilution.

Orthophosphate phosphorus ($O-PO_4-P$) was measured by the ascorbic acid-molybdate method #425F in Standard Methods. Total phosphorus (T-P) was determined by persulfate digestion to orthophosphate using method #425C-III in Standard Methods followed by analysis of the

produced orthophosphate as described above.

Reactive silica (Si_2) was determined by the molybdosilicate method #426B in Standard Methods.

Both nitrite and nitrate nitrogen ($\text{NO}_2\text{-N}$ and $\text{NO}_3\text{-N}$, respectively) were determined using a Technicon Autoanalyzer II system. The nitrite was first determined by the azo dye colorimetric method and the nitrate was reduced to nitrite using the cadmium reduction method and the resultant nitrite, including the original nitrite, was determined by the azo dye method. Nitrate was obtained by difference. The procedure is described in Method #505 of Standard Methods.

Ammonia nitrogen ($\text{NH}_3\text{-N}$) was determined by a modification of the phenate method (#418C in Standard Methods). Because of difficulties with the manganous sulfate catalyst, this method was modified to use sodium nitroprusside according to the method described for analysis of ammonia in seawater by Strickland and Parsons (1972). In this respect, the method is similar to the automated phenate method described under method #604 in Standard Methods.

Those organic compounds lumped together and referred to under the general term "oil and grease" were measured using the freon extraction, infrared spectrophotometric method contained in method #502B of Standard Methods.

Dissolved oxygen was determined by the modified Winkler Method described under Method #422B of Standard Methods.

Turbidity was determined by the nephelometric method using a Hach Model 2100B turbidity meter (method #214A, Standard Methods).

Pore water for both major cation and anion analyses was obtained by taking a portion of the sediment sample and squeezing it under

nitrogen pressure through a fiberglass filter (0.45 um).

Eh and pH were done on sediments using a standard laboratory meter with platinum electrode, glass electrode and a saturated calomel reference electrode.

5.1.2.2 Major Cation Analyses

All major cations in both the water column and pore waters were determined by atomic absorption spectrophotometry (AAS) using a Perkin-Elmer Model 303 or Model 5000 atomic absorption spectrophotometer equipped with a three-slot burner and using procedures contained under Part 300 of Standard Methods. The major cations (sodium, potassium, calcium and magnesium) were determined by direct flame aspiration after appropriate dilution and treatment. Sodium (Na) required a 1:200 dilution followed by a 1:50 dilution. Potassium (K) required a 1:200 dilution followed by a 1:25 dilution. Calcium (Ca) and magnesium (Mg) both were diluted 1:200 volumetrically prior to analyses.

5.1.3 Results

The general water quality parameters measured on a monthly basis included salinity by conductivity, temperature, dissolved oxygen, pH, turbidity, oil and grease, the nutrients (nitrite, nitrate and ammonia nitrogen, orthophosphate and total phosphorus, and silica). Tabulated results of these analyses for the period May 1981 through April 1982 have been incorporated into Appendix Tables E-1 through E-12.

Changes in nutrient levels are illustrated in Figures 5-2 through 5-7. Concentrations shown compare the average values for surface and bottom offshore waters and inshore waters throughout the year.

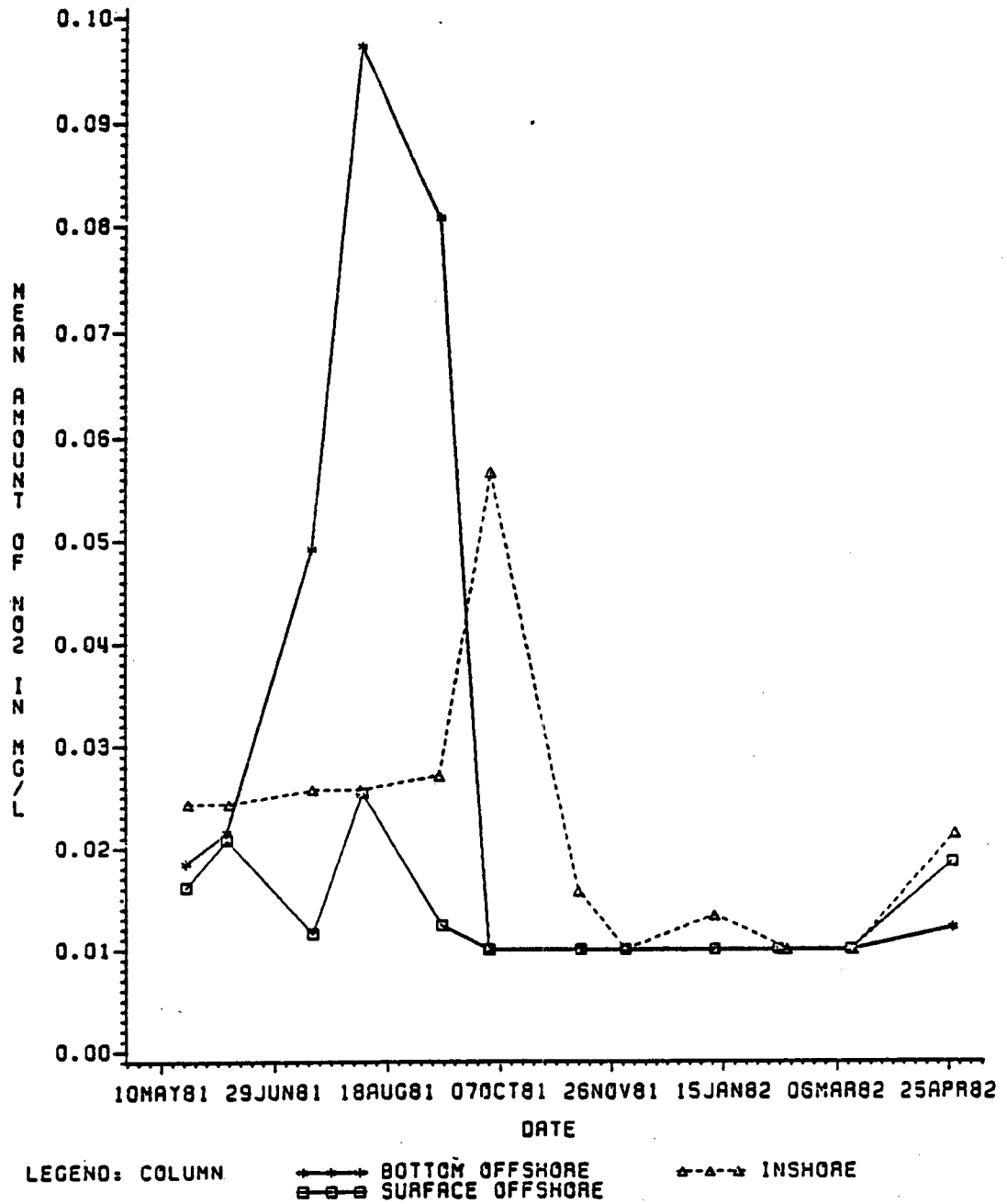


Figure 5-2. Changes in water column nitrite from May 1981 through April 1982.

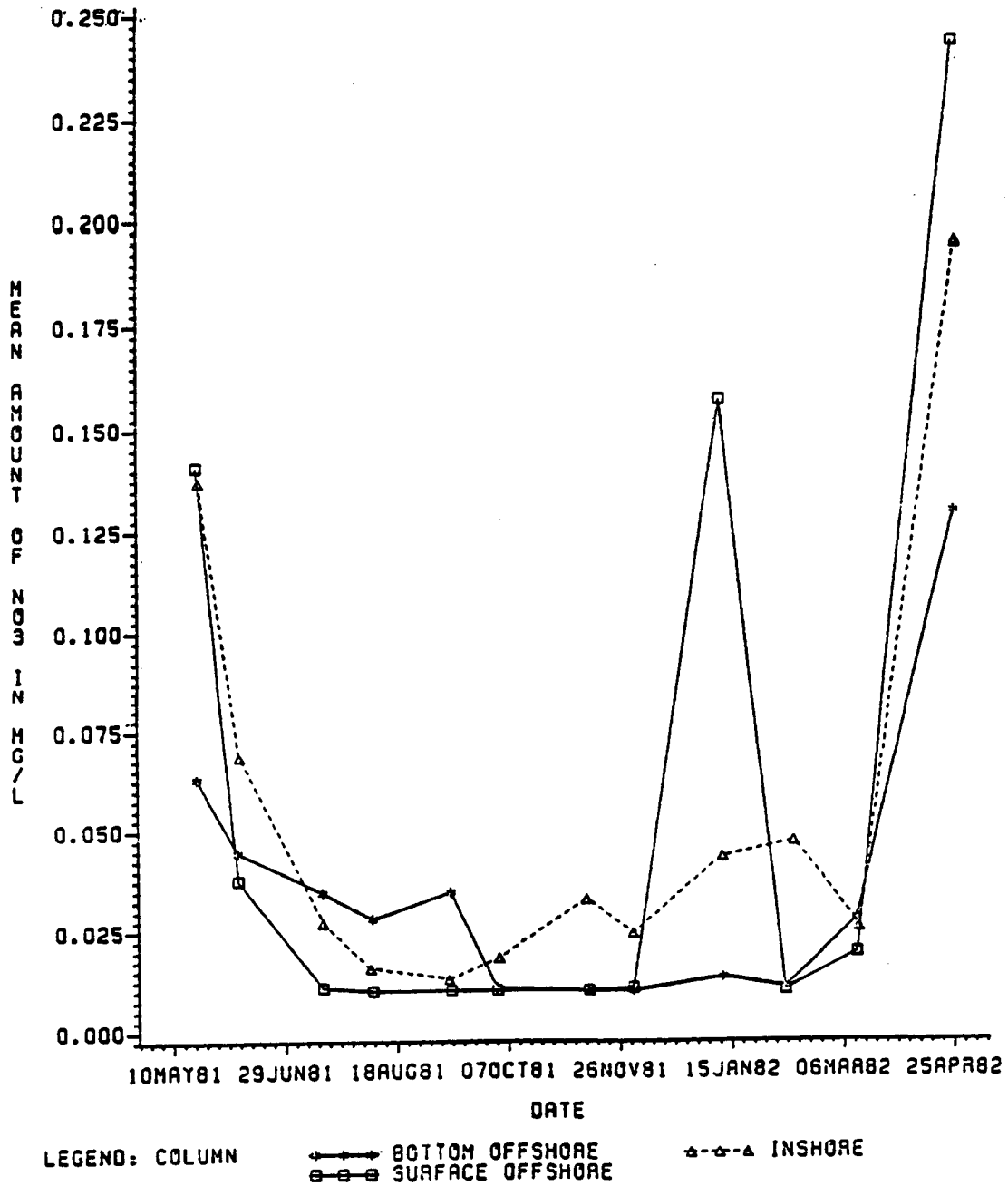


Figure 5-3. Changes in water column nitrate from May 1981 through April 1982.

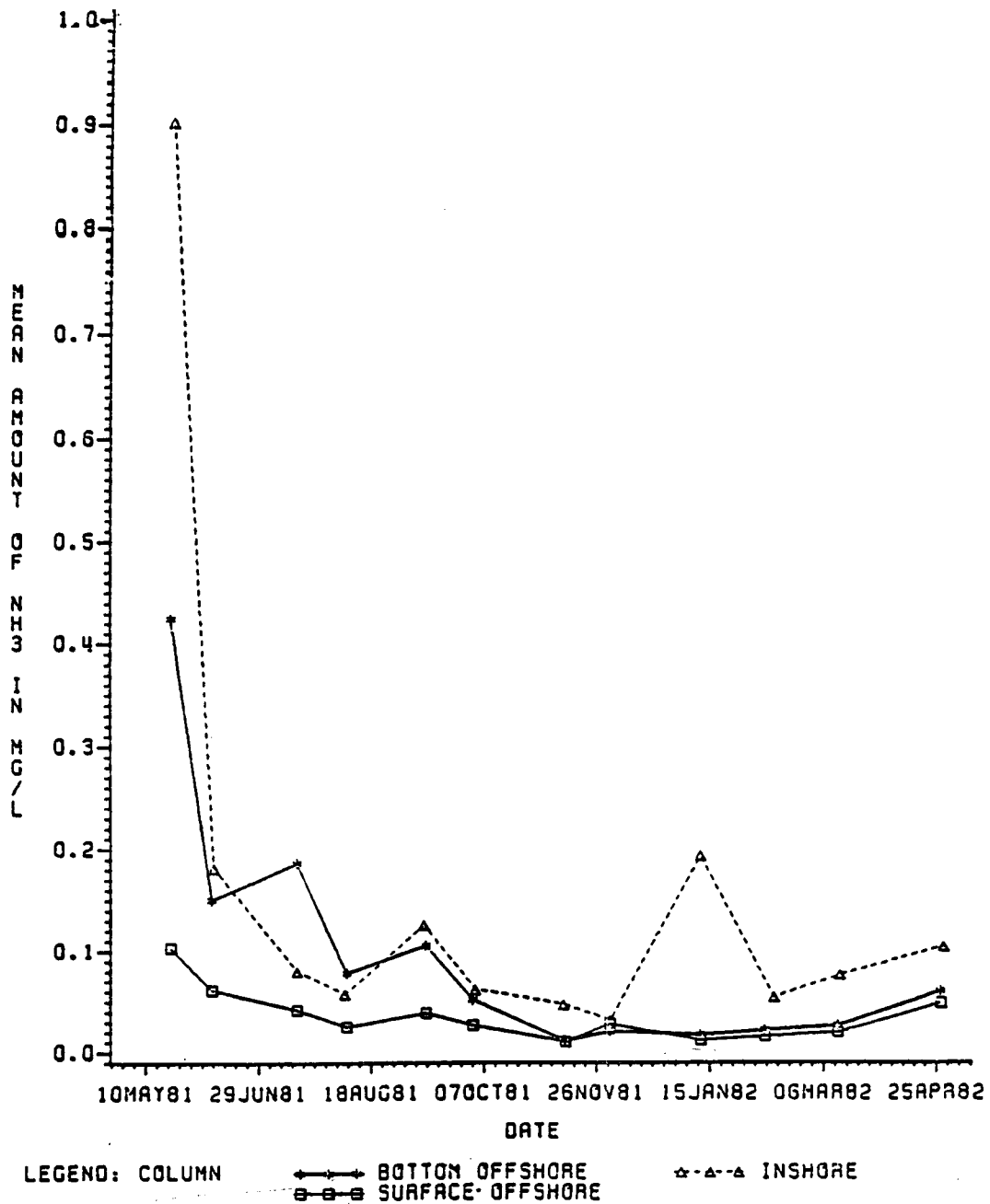


Figure 5-4. Changes in water column ammonia from May 1981 through April 1982.

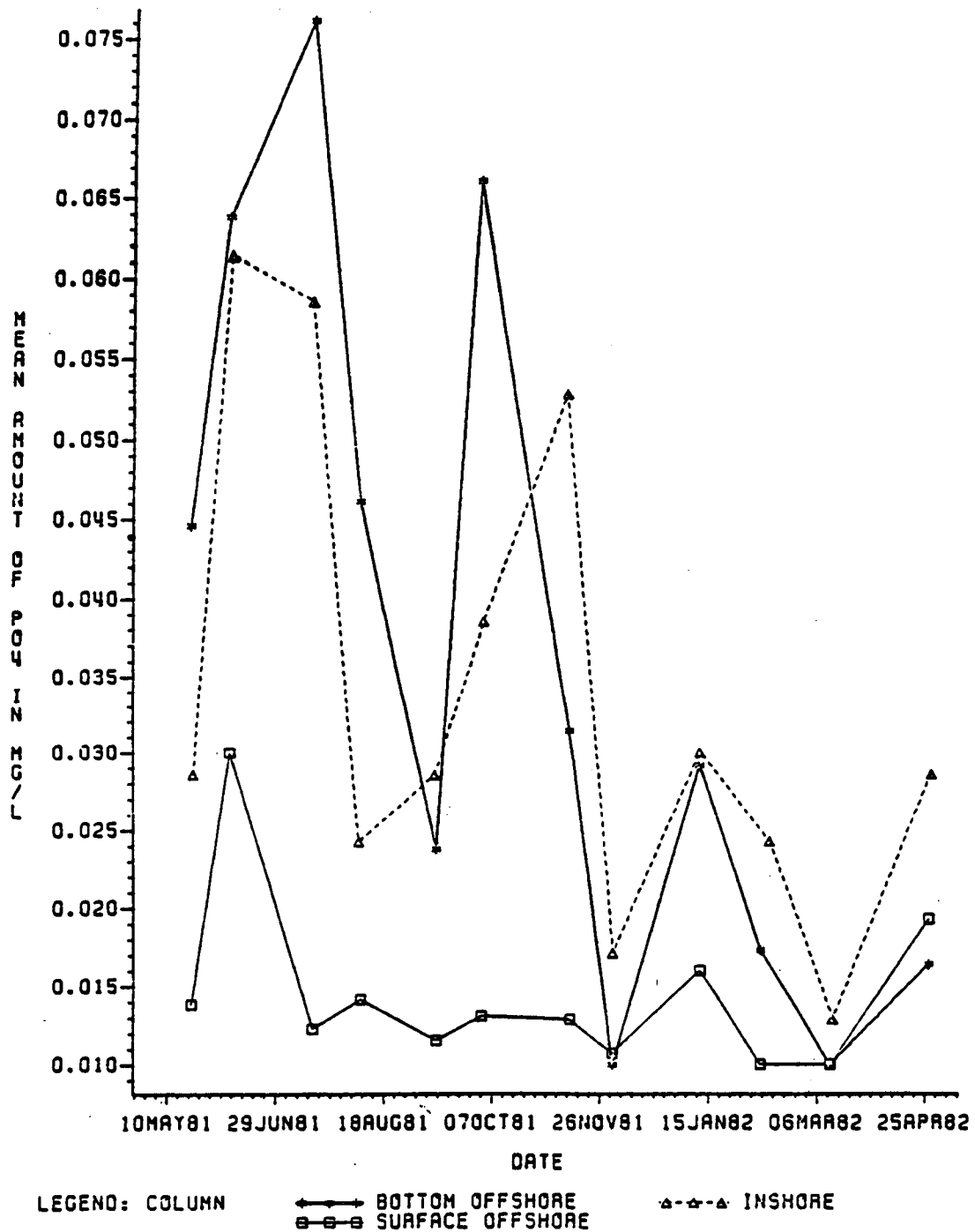


Figure 5-5. Changes in water column phosphate from May 1981 through April 1982.

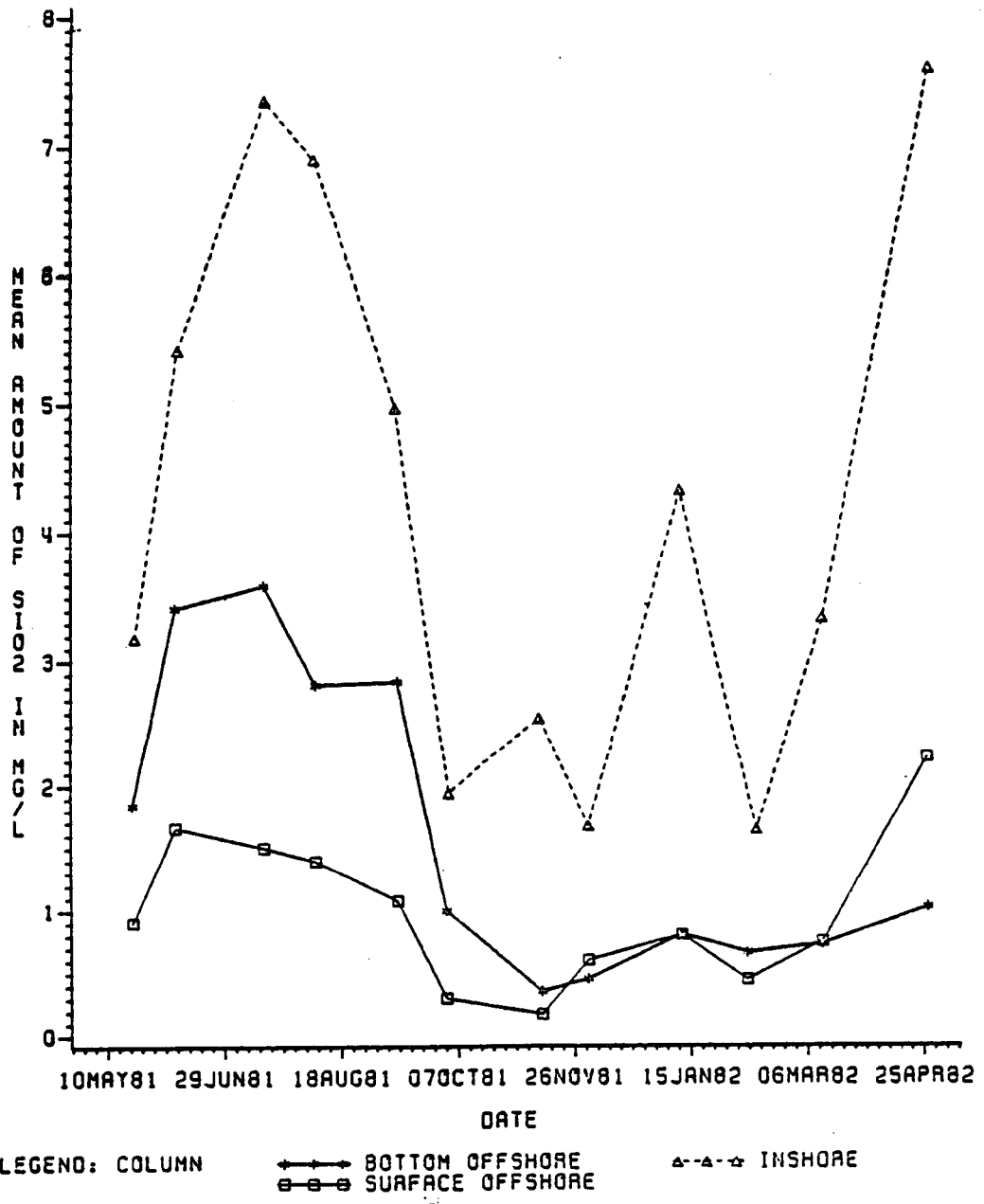


Figure 5-7. Changes in water column silica from May 1981 through April 1982.

Nitrite and nitrate nitrogen concentrations ranged from 0.01 to .15 mg/l and 0.01 to 1.0 mg/l respectively (Appendix Tables E-7 and E-8). Levels for nitrite were higher for offshore bottom samples during the months of June and July 1981 (Figure 5-2). During the remainder of the sampling period levels were generally higher in the inshore samples. For nitrate, however, average concentrations for bottom and surface offshore and inshore samples remained relatively similar in concentration (Figure 5-3). The only exception to this was the relatively high concentration of nitrate found in the surface offshore water during January 1982. This increase was due to the higher concentration found at M-22 (diffuser). Ammonia nitrogen ranged from 0.01 to 1.93 mg/l with inshore stations generally higher. The range of phosphate levels were 0.01 to 0.30 mg/l. Silica levels were between 0.1 to 12.4 mg/l with the inshore stations higher than offshore.

Ammonia nitrogen (Figure 5-4) was highest in May 1981 following the usual spring runoff and its attendant increase in biological activity. This suggests the ammonia increase was a result of the early stages of biological degradation following the spring runoff and plankton growth. Nitrite, the next step after ammonia in nitrogen regeneration, was highest in July and August 1981. Nitrate levels were highest in June 1981, January 1982, and April 1982, all periods of high runoff suggesting that runoff was the predominant control for nitrate levels. Phosphate and total phosphorus were highest in July and October 1981 and January and April 1982. These were all periods of relatively high runoff (Figures 5-5 and 5-6). April is traditionally the month of highest runoff for this area; however,

during the 1981 season, the period of peak runoff was recorded during the month of June. Generally, the pattern observed for the nutrients has followed that reported by other investigators (Barrett, 1971; Barrett, et al., 1978; and Brooks, 1979).

Dissolved oxygen values ranged from 0.5 to 11.0 mg/l and were lower in July 1981 when widespread anoxic conditions were observed (Figures 5-8 and 5-9). This condition probably resulted from organic decay as a result of earlier runoff and was sufficiently widespread to indicate it was not caused by brine discharge. Generally, dissolved oxygen values are typically highest during the winter months. Levels observed during this period follow the seasonal trend. There was no major difference in oxygen levels between the diffuser (stations M10, M10A), near diffuser (stations NW, NE, DW, DE, SW, SE, DN, DS), and controls (stations M21, M22, M3, M18) during this sampling period.

Turbidity values ranged from 1.0 to 99 NTU. The highest mean values occurred in June and October 1981 and January and April 1982 suggesting that this parameter was most influenced by high runoff (Figure 5-10). Bottom offshore and inshore stations demonstrated the most perturbation during this period; surface offshore stations showed relatively little change.

Oil and grease (Figure 5-11) ranged from 0.1 to 63 mg/l; the highest concentration occurred in February 1982. Since it occurred both inshore and offshore, these values are attributed to high runoff at this time.

Overall, salinities ranged from 17.26 o/oo and 35.10 o/oo, and temperatures 7.0°C to 32.5°C. Perturbations observed in the mean salinity levels in Figures 5-12 and 5-13 are a result of seasonal

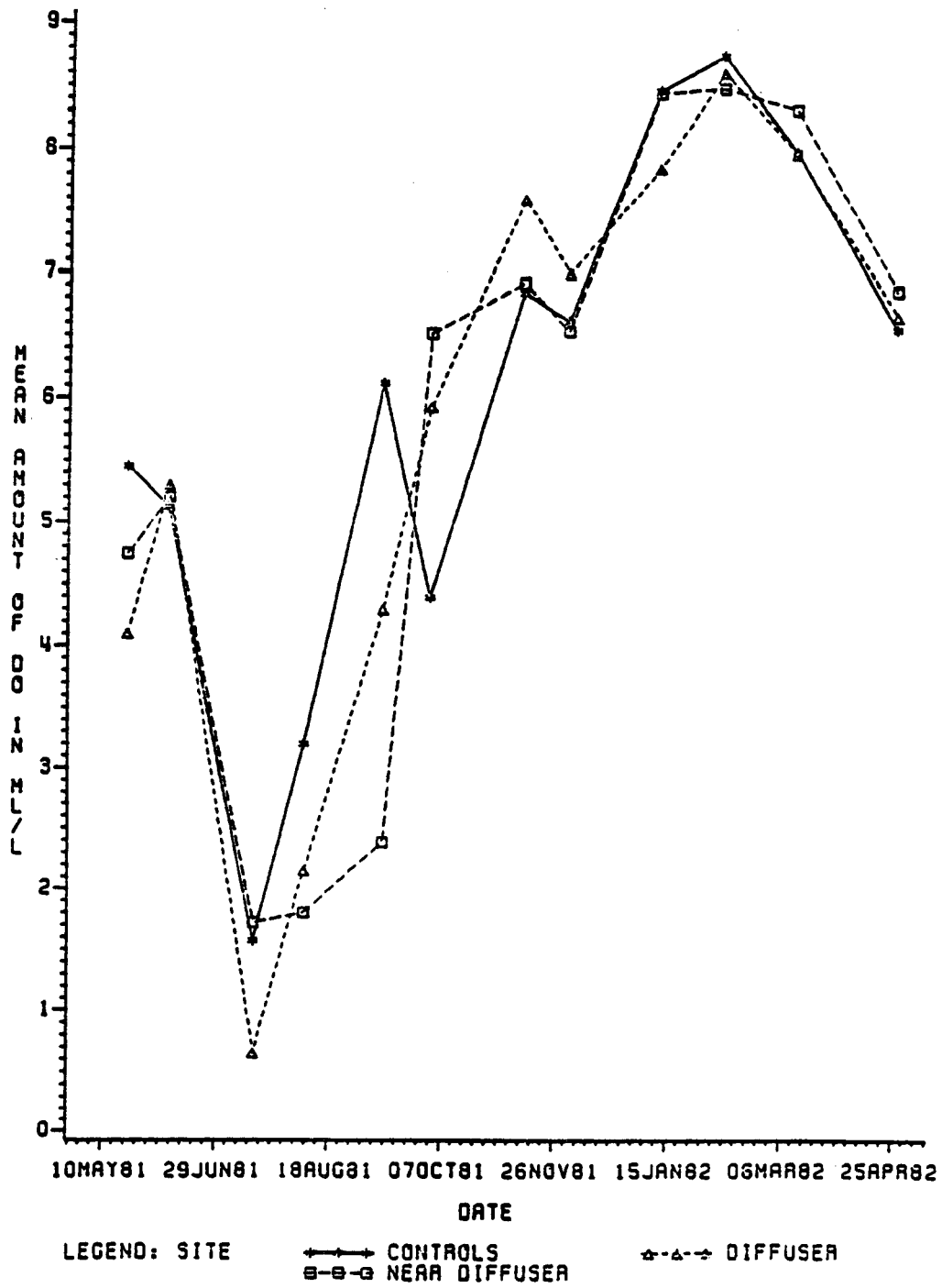


Figure 5-3. Changes in bottom water column dissolved oxygen from May 1981 through April 1982.

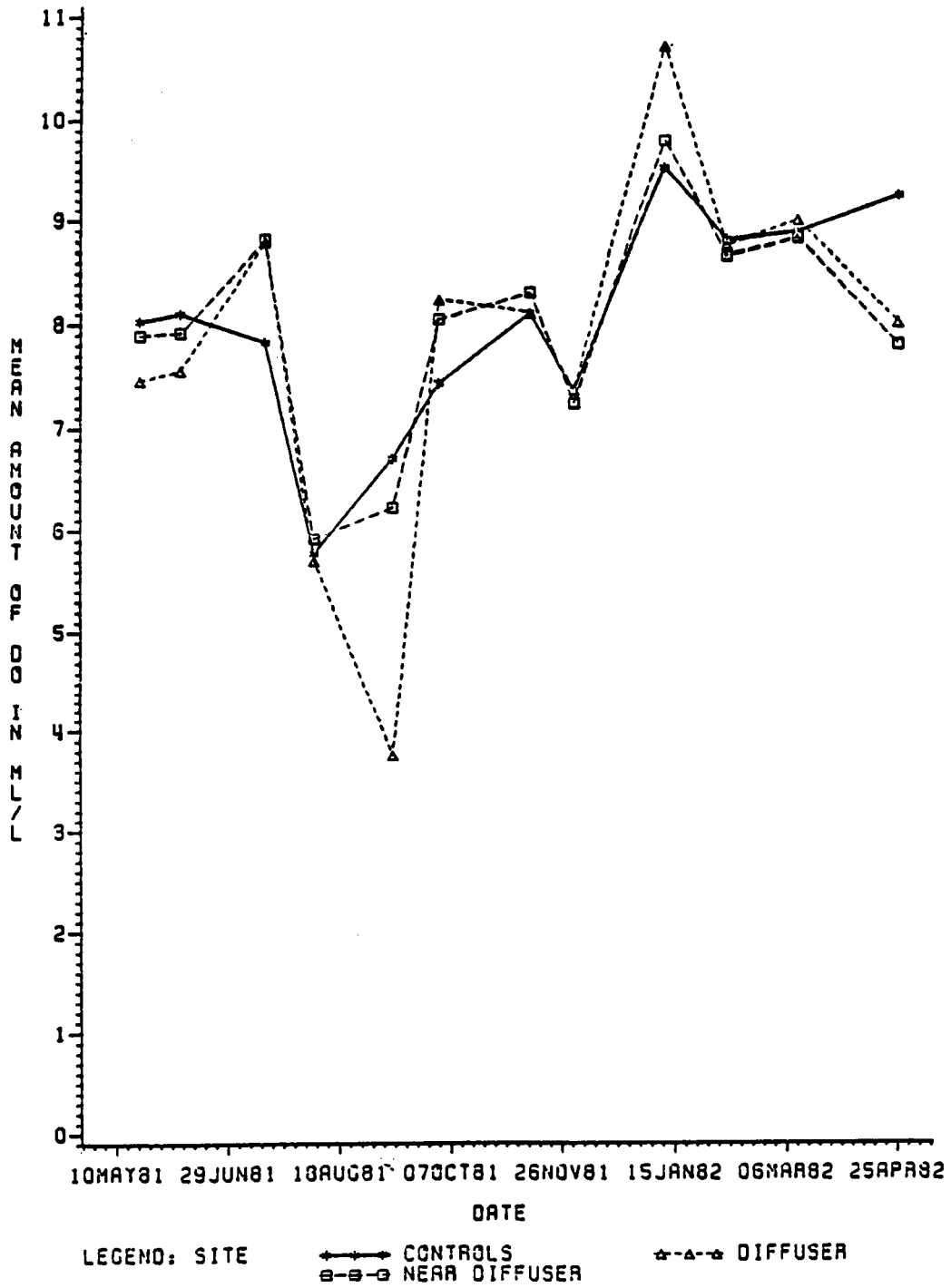


Figure 5-9. Changes in surface water column dissolved oxygen from May 1981 through April 1982.

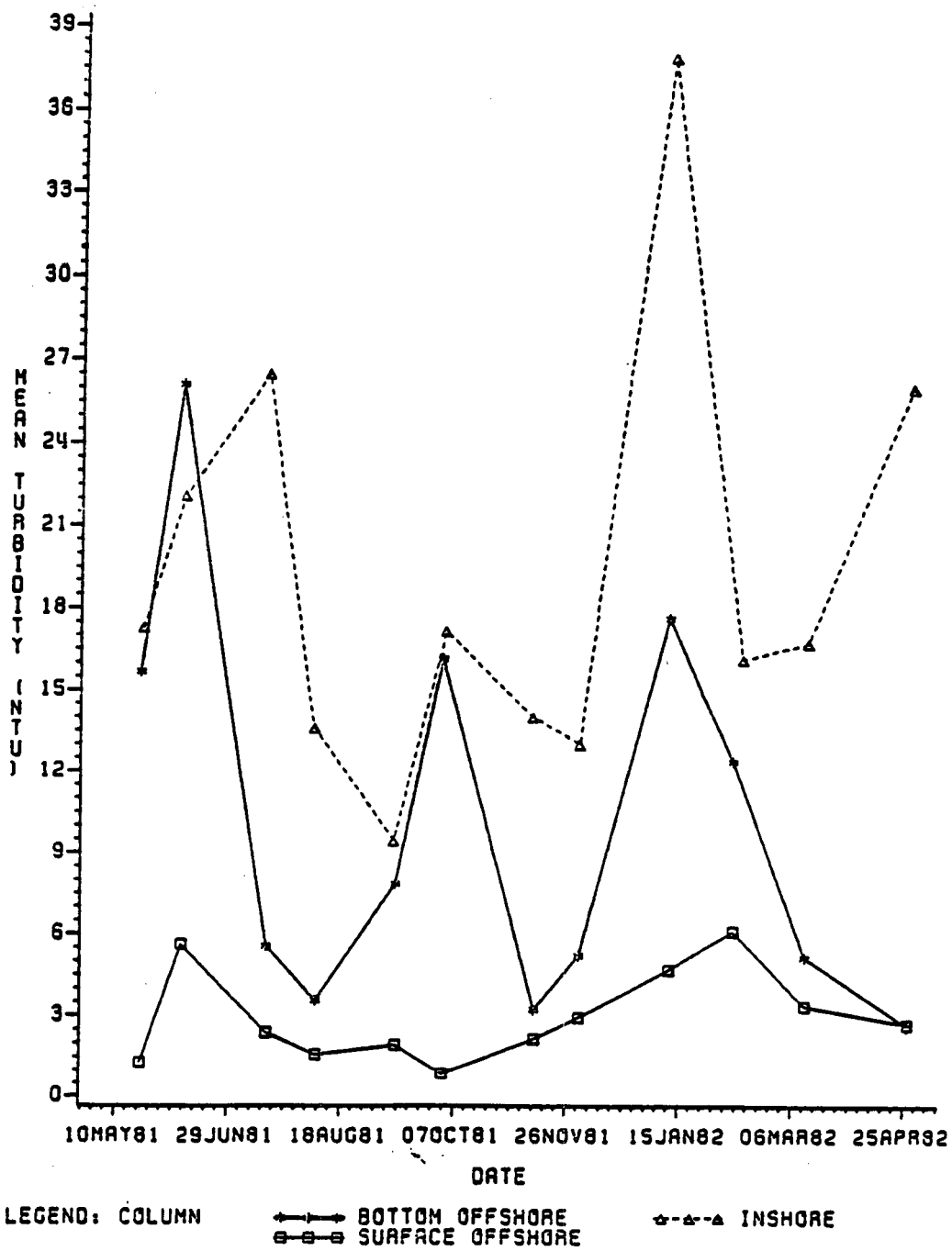


Figure 5-10. Changes in turbidity from May 1981 through April 1982.

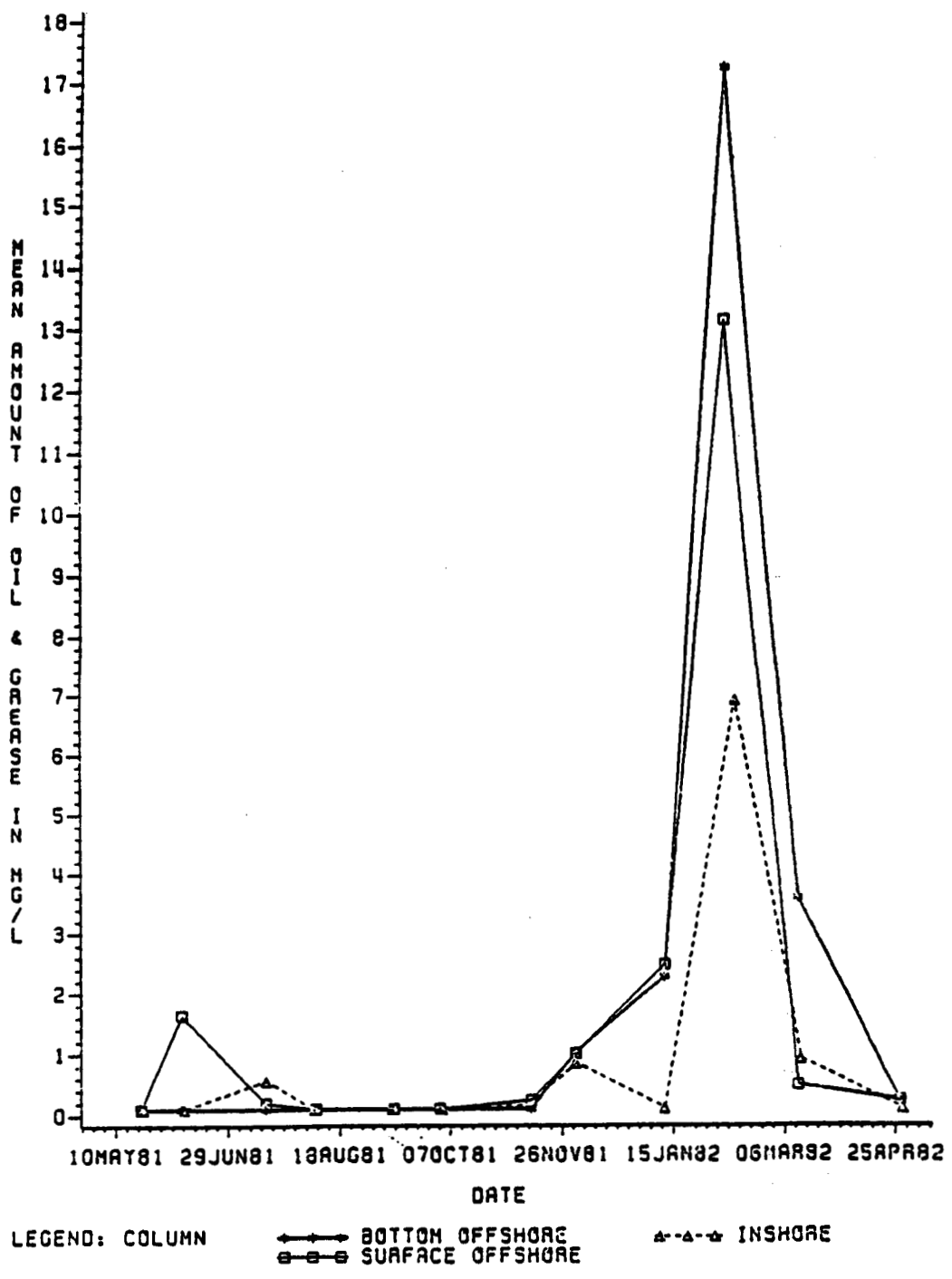


Figure 5-11. Changes in oil and grease from May 1981 through April 1982.

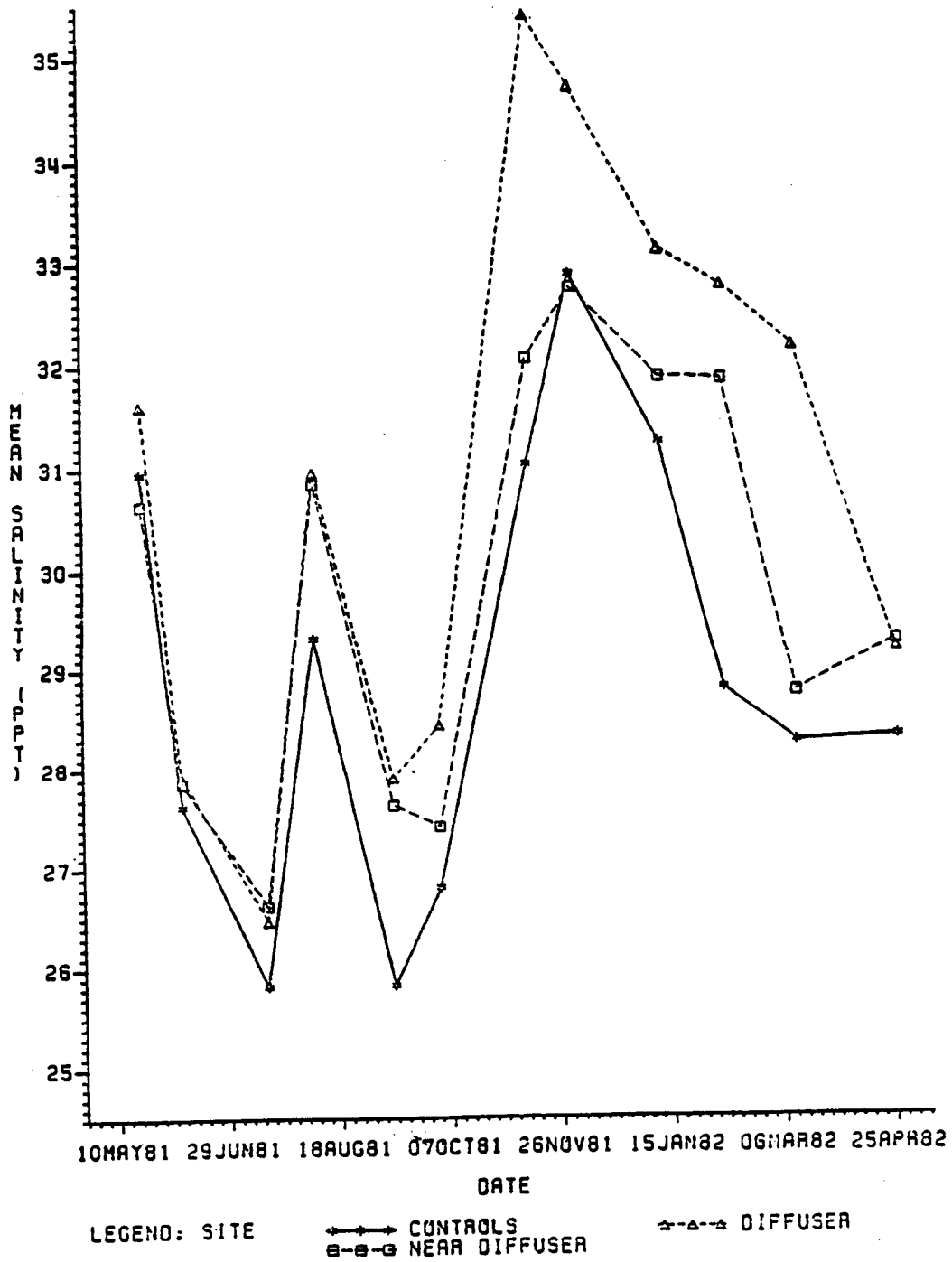


Figure 5-13. Changes in bottom water column salinity from May 1981 through April 1982.

runoff. For example, a sharp salinity drop was observed in July following the unusually high runoff that occurred in June 1981. A second drop in salinity was observed in April 1982 as a result of spring runoff. The higher salinities that occurred in the winter months were due to lower runoff. No difference in surface water salinity was observed between controls, diffuser, and near diffuser stations. However, as shown in Figure 5-13, there was a trend throughout the year for salinities in the bottom waters at the diffuser and near diffuser stations to increase relative to control stations. Differences in bottom water salinities are covered in more detail in the section on plume tracking (Chapter 4). Since water samples used in these water quality studies were collected in Niskin bottles attached to a hydrographic wire, bottom water samples were actually taken at 1/3 to 2/3 m (1 to 2 ft) off the bottom. Results from a previous study (Slowey and Jeffrey, 1981) suggest highest salinities in the diffuser area occur within the bottom 1/3 m (1 ft) of the water column. Therefore, bottom salinities reported here are slightly lower than those actually existing at the sediment-water interface.

Bottom and surface temperatures observed during the year varied only a few tenths of a degree from station to station for any given sampling date; and diffuser stations did not differ from ambient or control stations (Figures 5-14 and 5-15). At diffuser stations where salinity was slightly over ambient suggesting possible brine effect, no corresponding increase in temperature was observed suggesting that under conditions of the past year, brine discharge did not affect bottom temperatures.

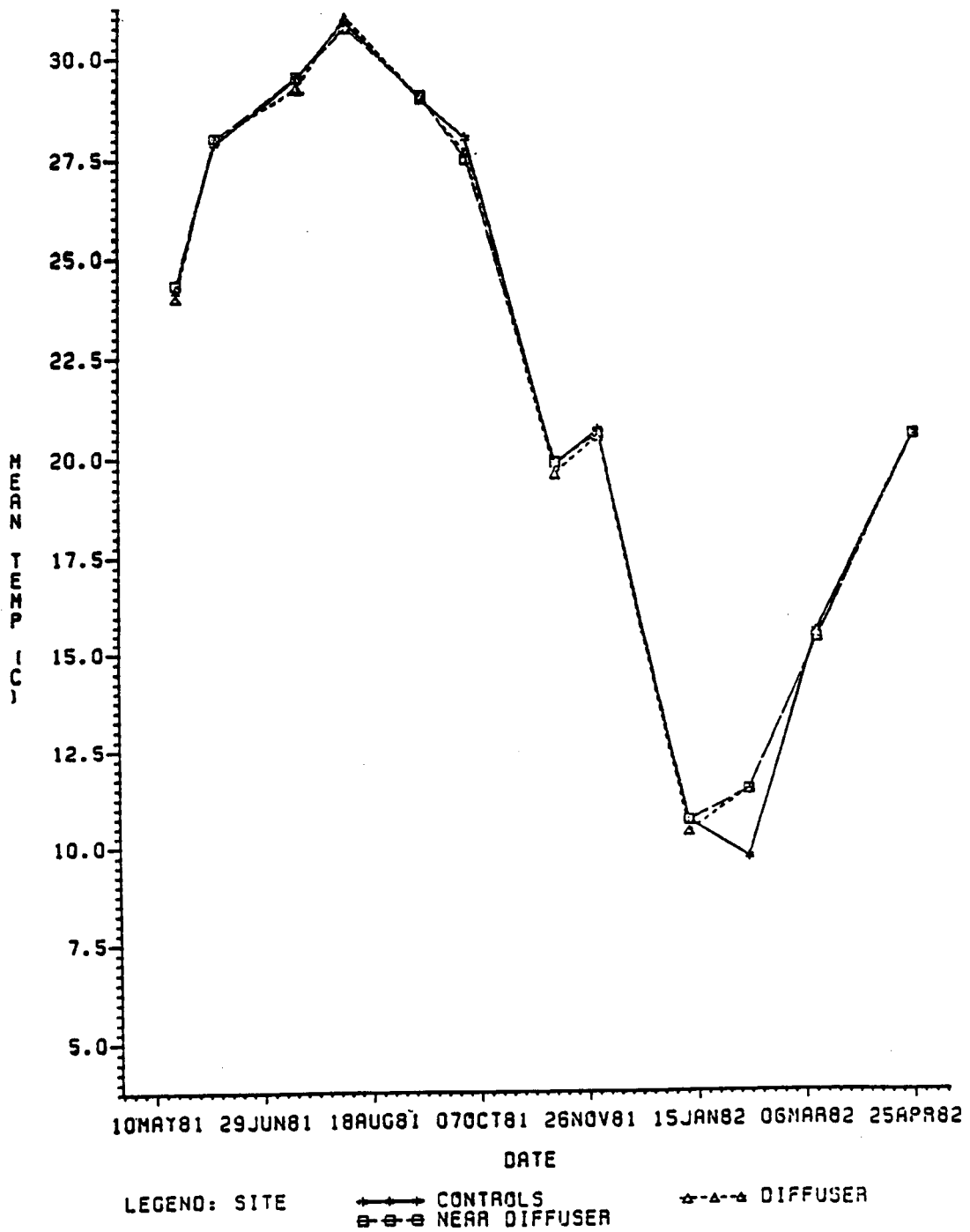


Figure 5-14. Changes in bottom water column temperature from May 1981 through April 1982.

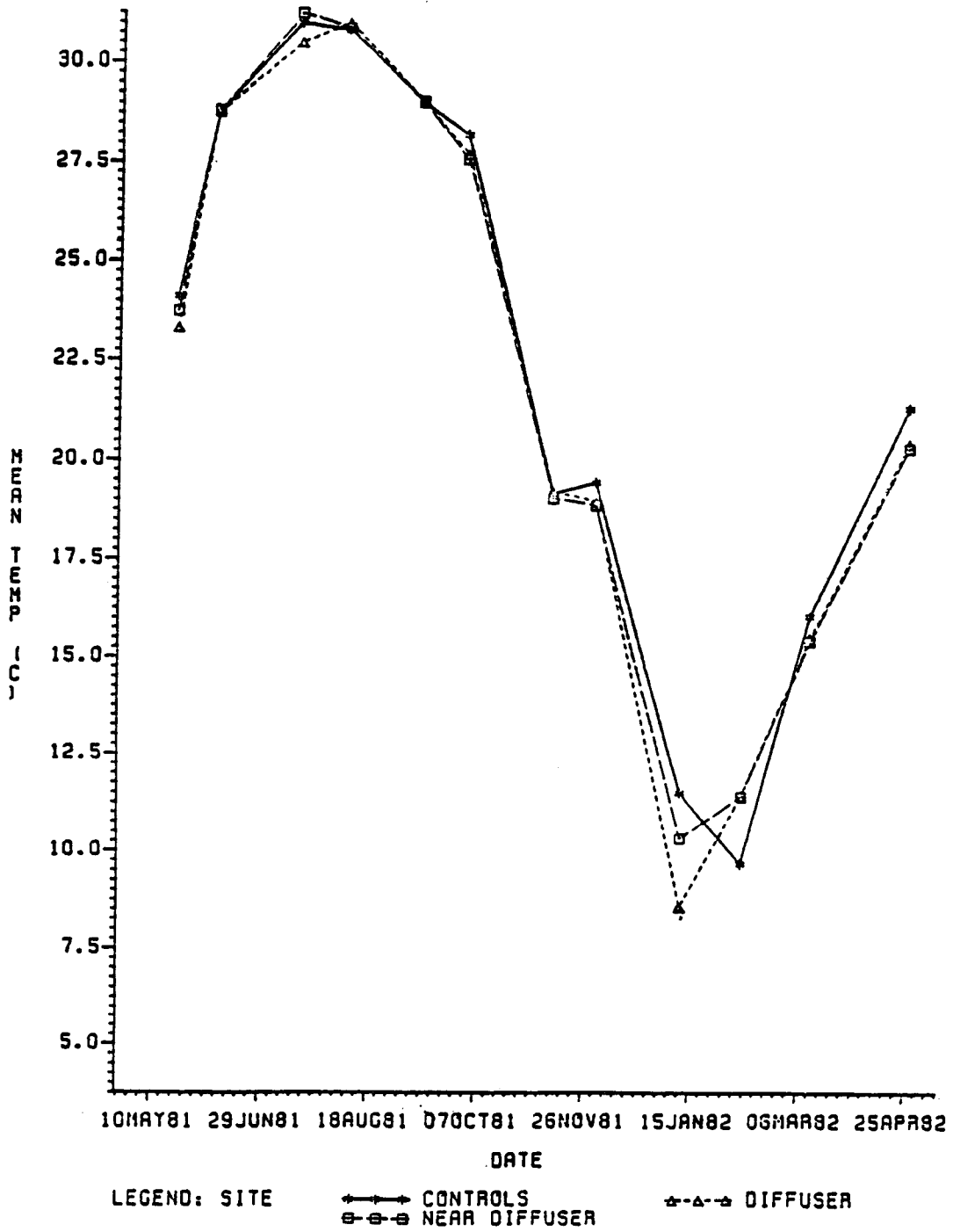


Figure 5-15. Changes in surface water column temperature from May 1981 through April 1982.

Mean pH values were in the range expected for coastal waters (7.5 to 8.5) with the exception of January 1982 and possibly February 1982 data (Figures 5-16 and 5-17). In January, individual pH values ranged from 4.83 to 10.36 indicating probable instrument error during this sample period. Several values below 7.0 measured in February are also probably due to instrument error.

5.1.3.1 Major Ions in the Water Column

Since the first evidence of impact on water quality should be detected in the major constituents of the brine, major ionic species in the water column have been determined on a quarterly basis. Results of major ion analyses for quarterly samplings since June 1981 are presented in Appendix E as Tables E-13 through E-18. If changes in water quality occur as a result of brine discharge, they should show up in these results, especially in the bottom waters.

During early planning stages of the Strategic Petroleum Reserve, concern was raised about the potential adverse effects of ionic imbalance or changes in the ratios of one major ion to another, especially for Ca/Mg (James, 1977). Such imbalance was expected since the relative proportions of the major ions in seawater and the salt dome brine are different. The ratios for some of these ions in typical seawater (35 o/oo) are Na/K = 27.8, Ca/Mg = 0.32, and Cl/SO₄ = 7.14. These ratios in the receiving waters should tend to increase with brine discharge. Changes in these ratios could be used to detect effects of the brine discharge upon the major ion levels.

Ion ratios observed for Na/K, Ca/Mg, and Cl/SO₄ over the past year for the area are presented in Appendix Tables E-19 through E-21, respectively. Although fluctuations exist in these data, there

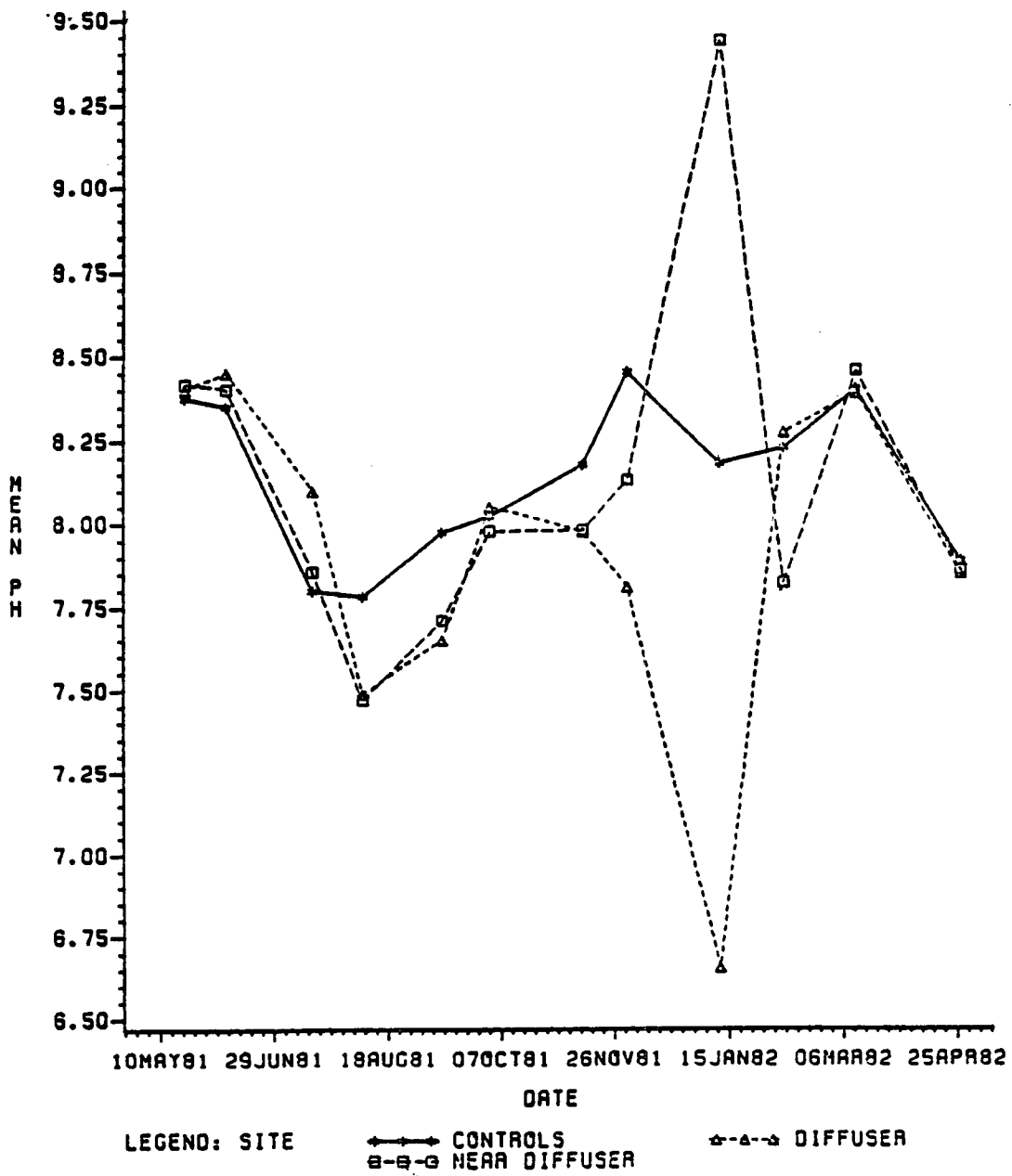


Figure 5-16. Changes in bottom water column pH from May 1981 through April 1982.

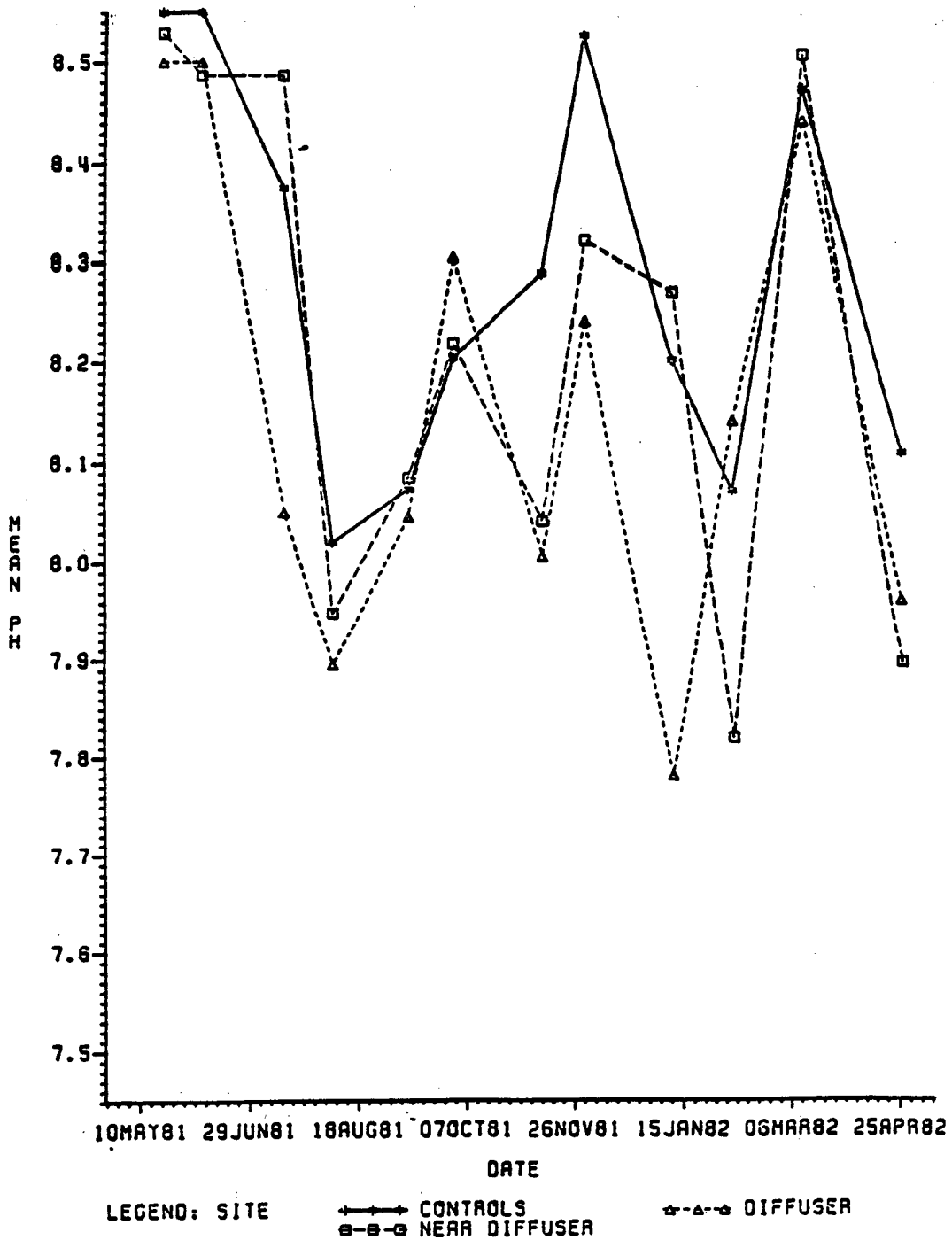


Figure 5-17. Changes in surface water column pH from May 1981 through April 1982.

appears to be no apparent difference between ratios in the diffuser area and the outer control stations over the past year in the water column (see Figures 5-18 through 5-23).

5.1.3.2 Major Ions in Sediment Pore Waters

Major ions were measured in the pore waters taken from the sediments and are presented in Appendix Tables E-22 through E-27. In order to evaluate whether ionic imbalance is occurring in the sediment pore waters, the ratios Na/K, Ca/Mg, and Cl/SO₄ were determined from the above major ion data. These ratios are presented in Appendix Tables E-28 through E-30; Figures 5-24 through 5-26 in the text illustrate these ratios. Values for the ion ratios indicate any changes for these at the diffuser and near diffuser relative to control stations have not been sufficient to detect at this time. Although levels of some major ions (Na⁺, Cl⁻) were slightly elevated near the diffuser relative to controls, fluctuations during the period made it difficult to establish a pattern for these major ions. Similar fluctuations were observed at the Bryan Mound SPR site (Slowey and Jeffrey, 1981), but after the first year a pattern was established showing a continuous increase over time. The trend observed at Bryan Mound would suggest that similar changes may occur at the West Hackberry site with time.

5.1.4 Conclusions

Nutrient levels of offshore and inshore waters were similar when considered for each sampling period. Highest levels were found in inshore and bottom offshore waters. This was true for all nutrients except for the possible exception of nitrate, which was higher in

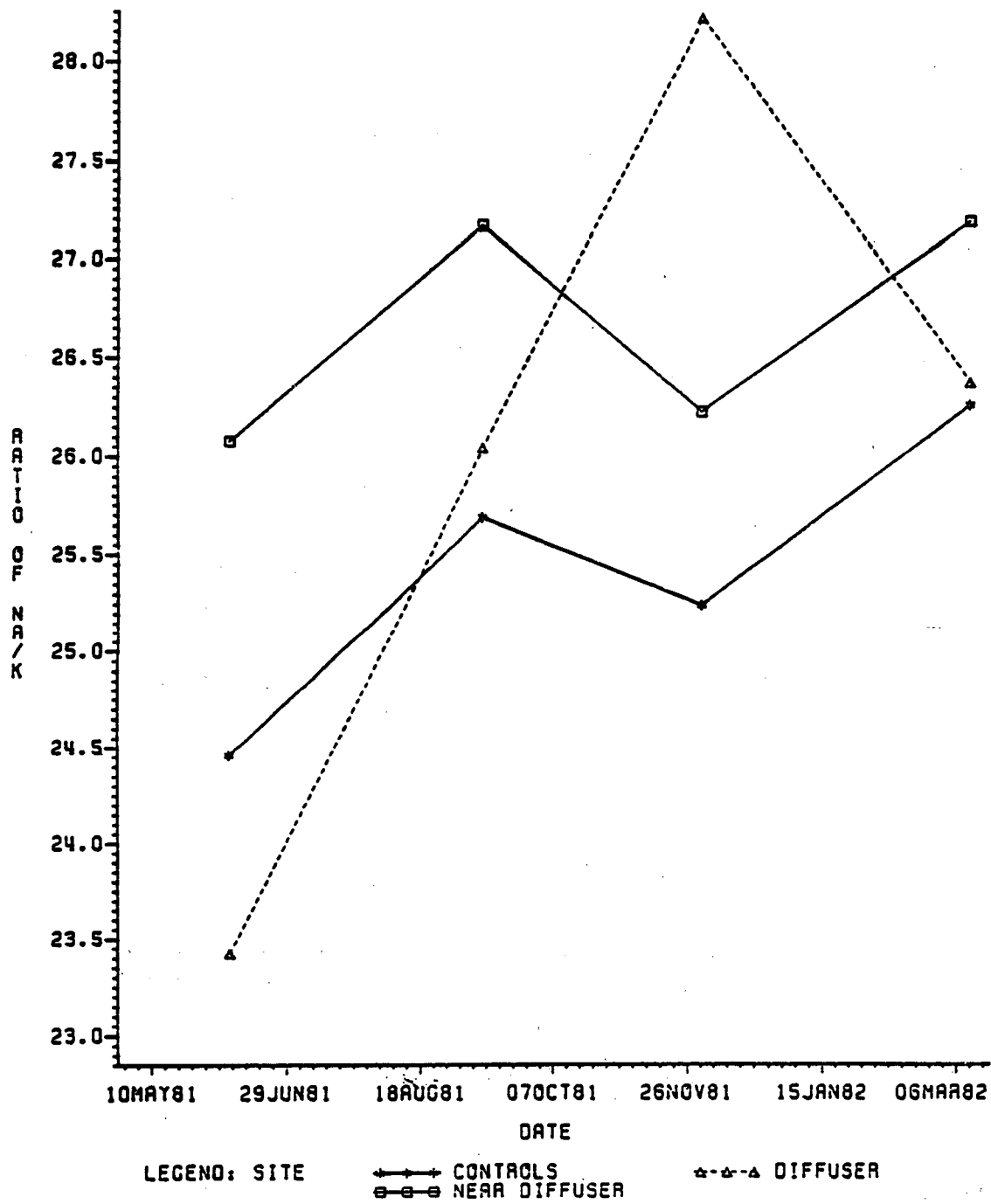


Figure 5-18. Changes in sodium/potassium ion ratios in bottom water samples from May 1981 through April 1982.

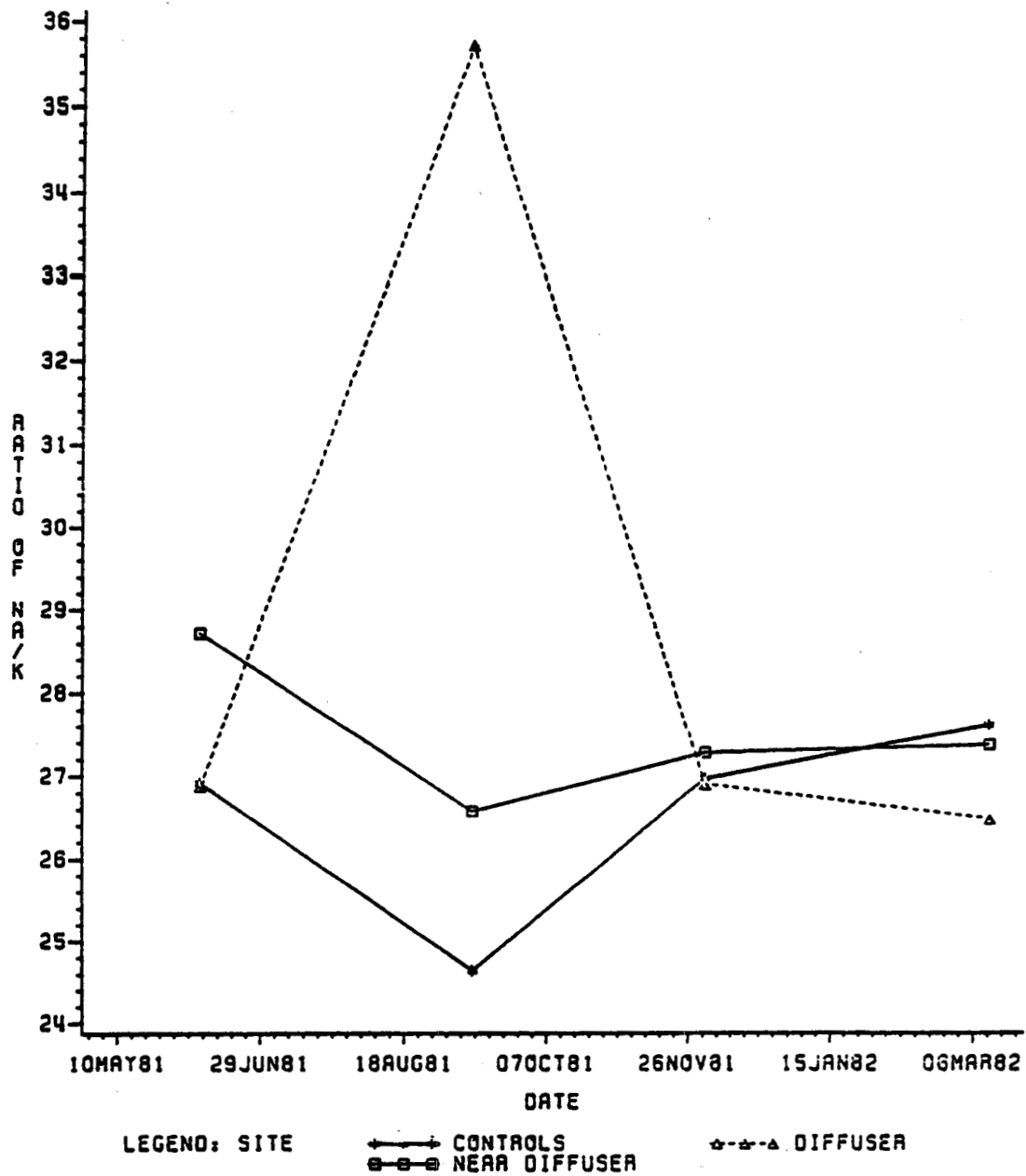


Figure 5-19. Changes in sodium/potassium ion ratios in surface water samples from May 1981 through April 1982.

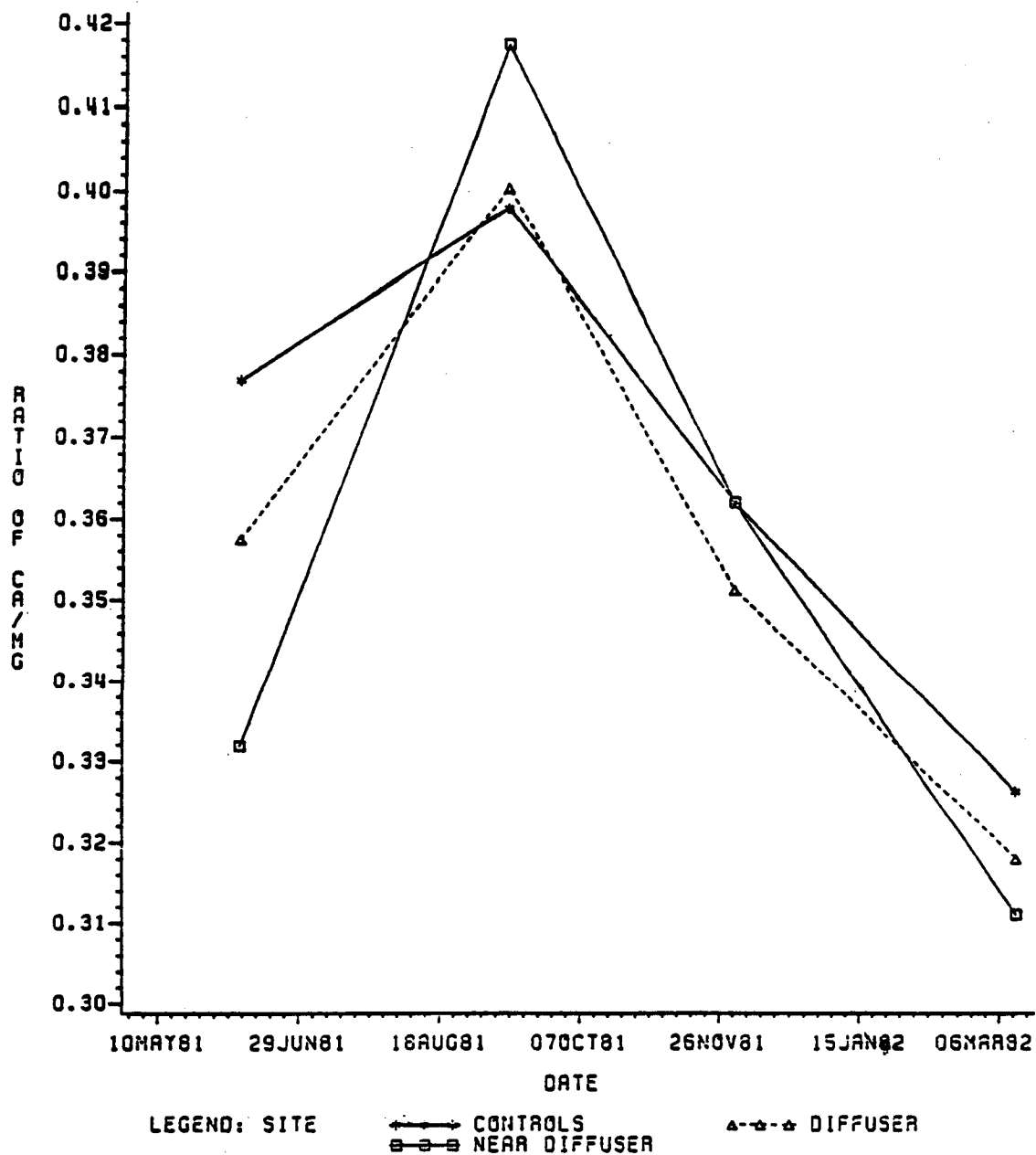


Figure 5-20. Changes in calcium/magnesium ion ratios in bottom water samples from May 1981 through April 1982.

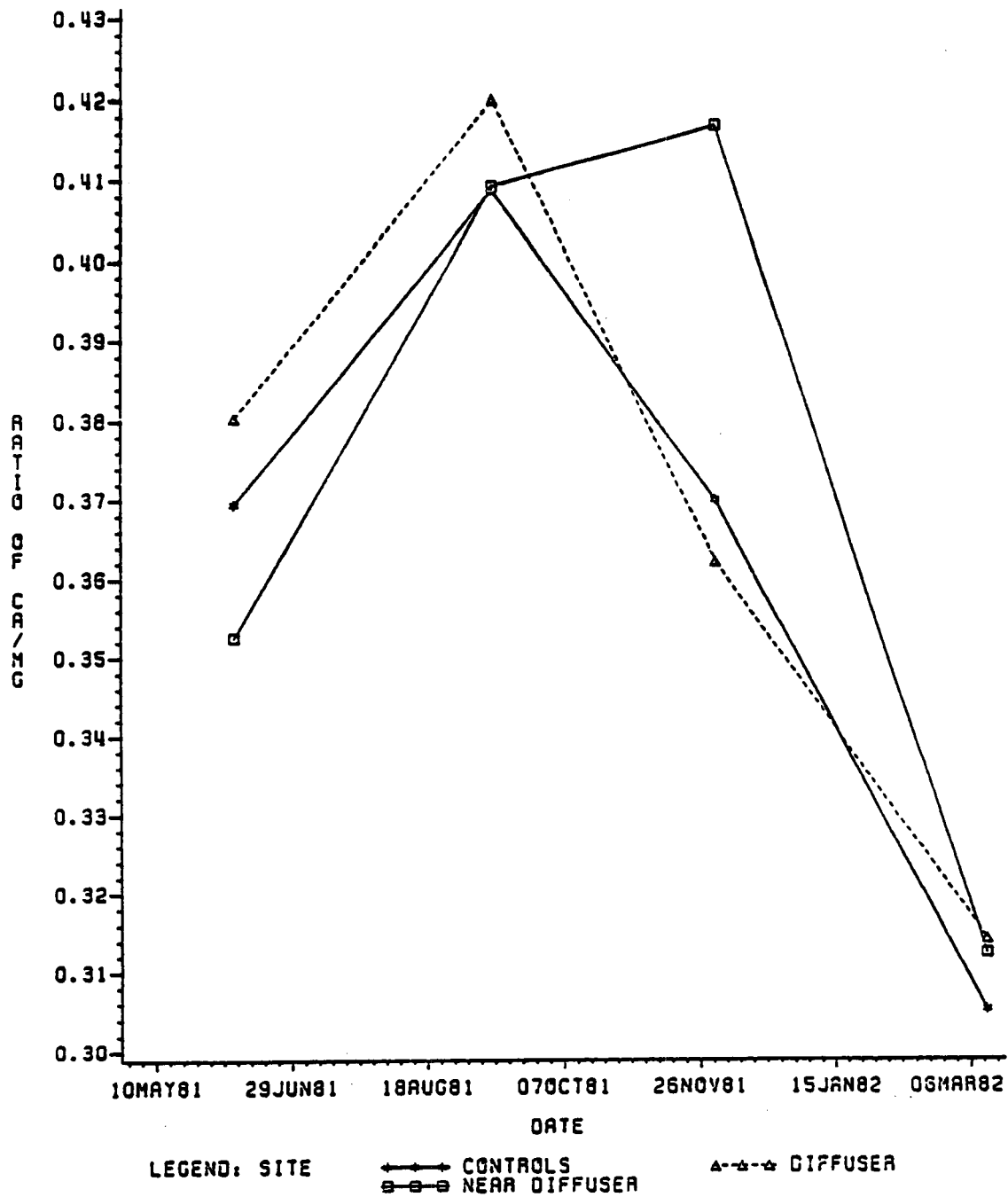


Figure 5-21. Changes in calcium/magnesium ion ratios in surface water samples from May 1981 through April 1982.

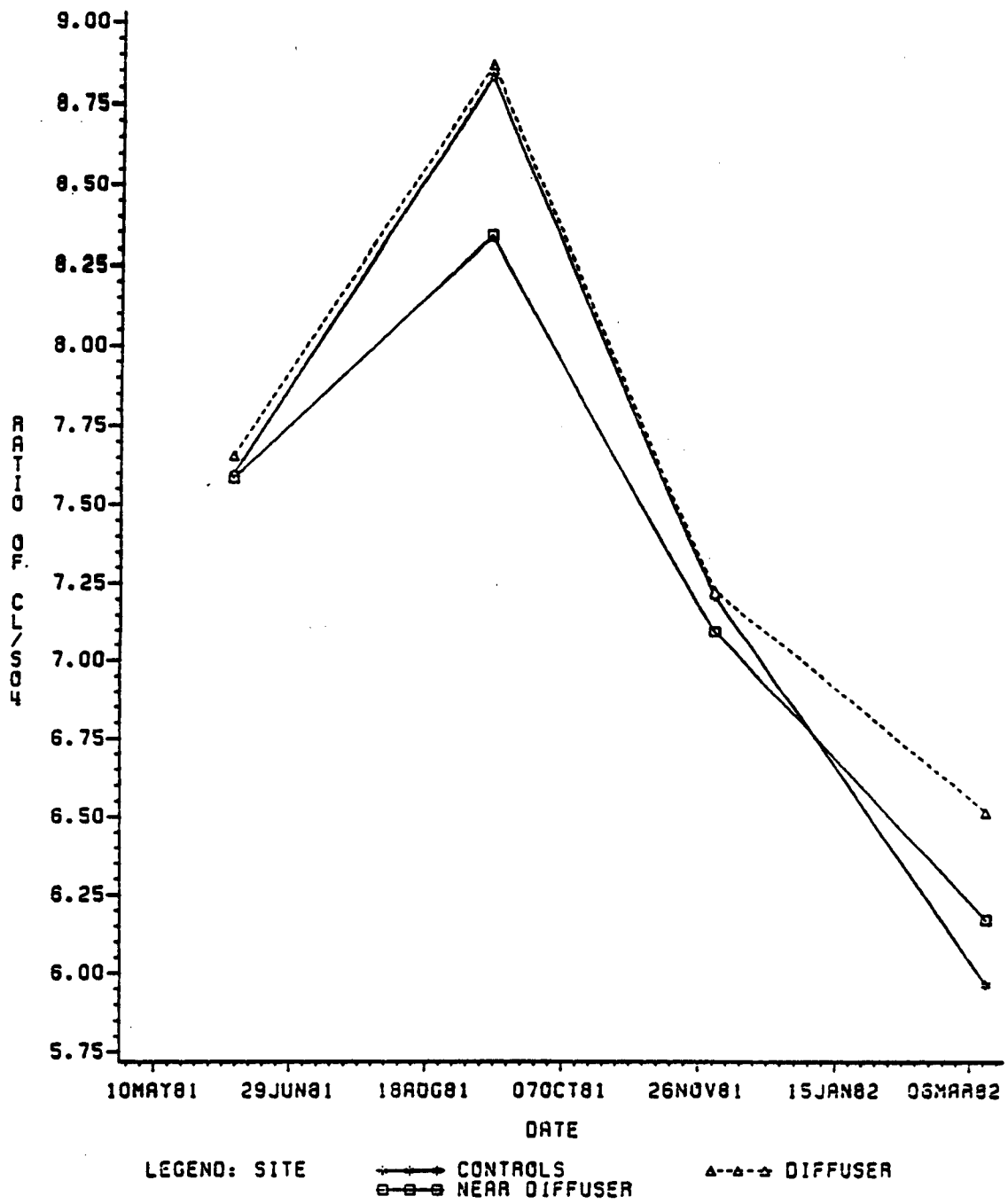


Figure 5-22. Changes in chloride/sulfate ion ratios in bottom water samples from May 1981 through April 1982.

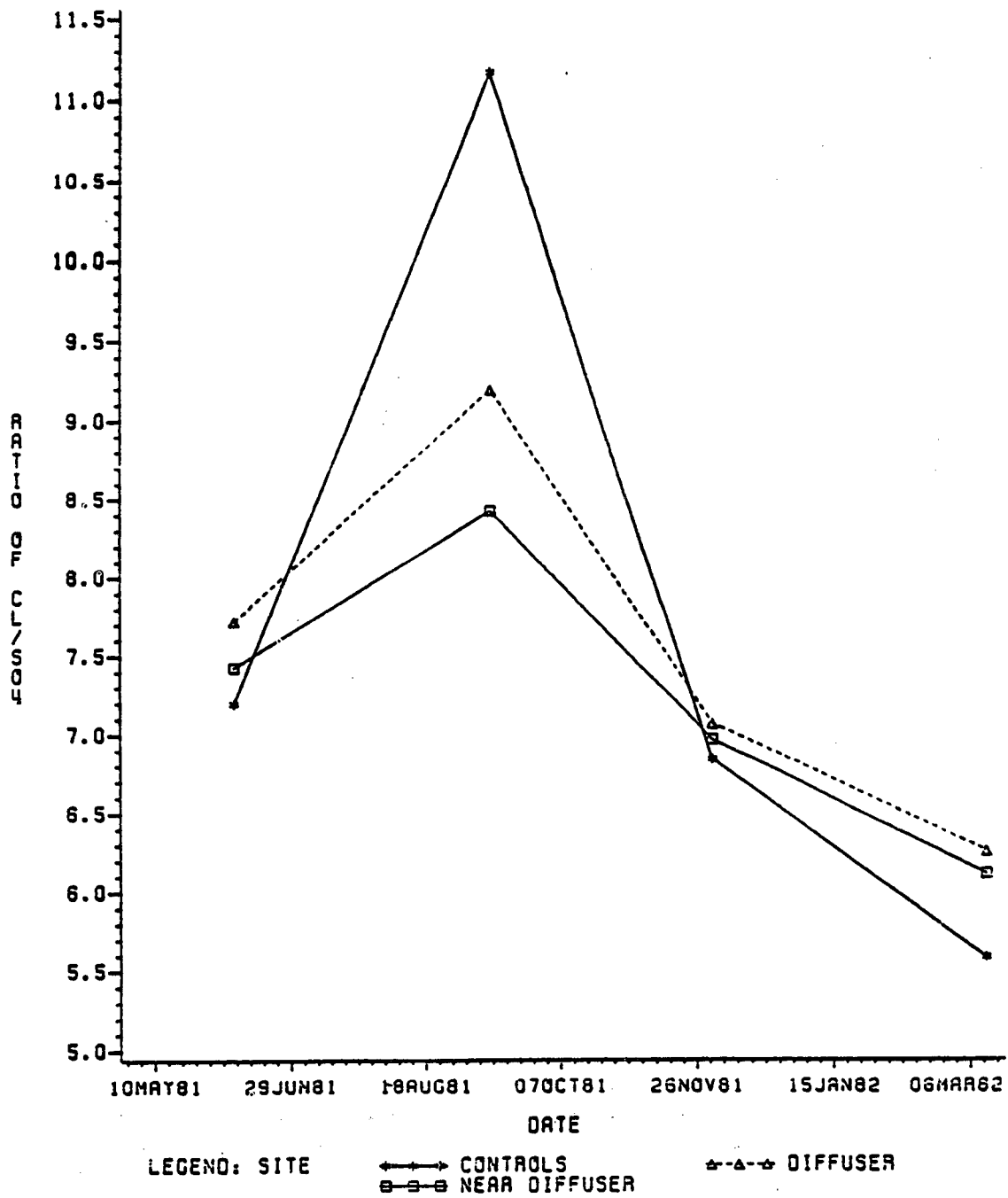


Figure 5-23. Changes in chloride/sulfate ion ratios in surface water samples from May 1981 through April 1982.

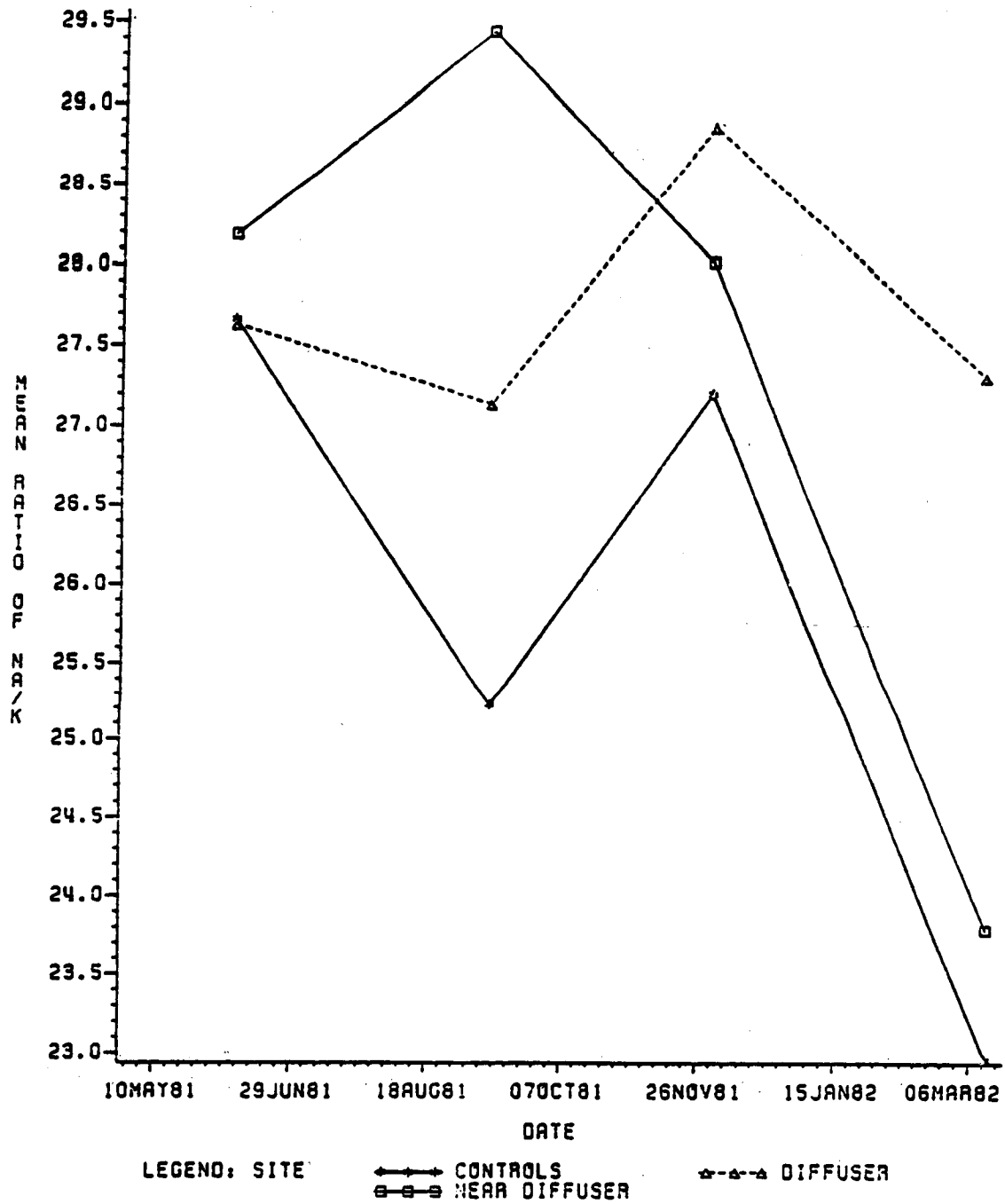


Figure 5-24. Changes in sodium/potassium ion ratios in sediment from May 1981 through April 1982.

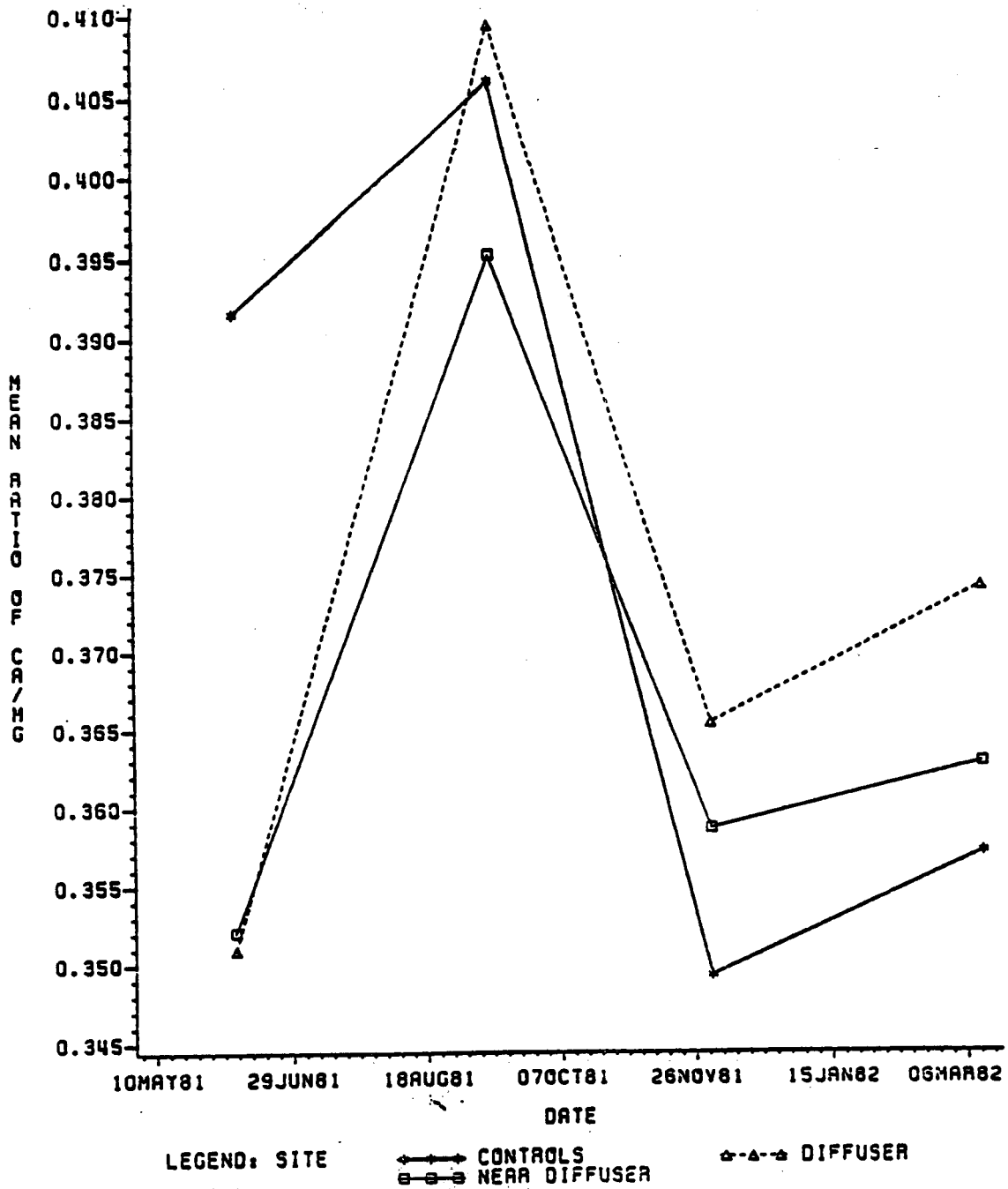


Figure 5-25. Changes in calcium/magnesium ion ratios in sediment from May 1981 through April 1982.

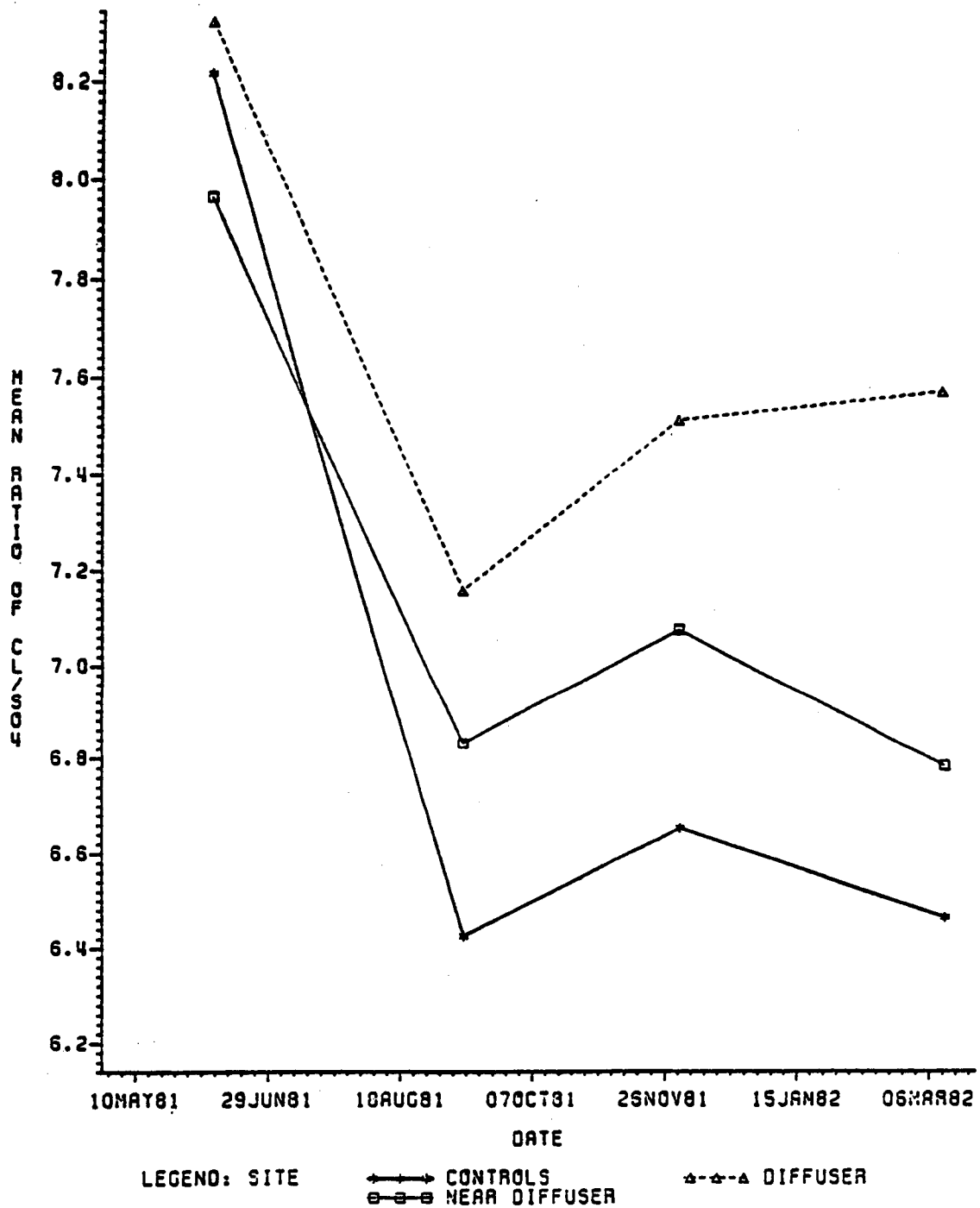


Figure 5-26. Changes in chloride/sulfate ion ratios in sediment from May 1981 through April 1982.

offshore surface water during portions of the year. Water temperature, dissolved oxygen, pH, turbidity, and oil and grease at or near the diffuser compared to controls have shown no adverse change resulting from the discharge of brine. Low dissolved oxygen observed at all stations in early July 1981 appeared to be related to a broader environmental problem rather than to brine discharge. Although some increase in bottom water salinity at the diffuser and near diffuser stations relative to controls was observed, major ions and ion ratios measured in the water column and sediment pore waters indicate that brine discharge had no adverse effect on these parameters during the first year of discharge. Although levels of some major ions (Na^+ , Cl^-) were elevated near the diffuser relative to controls, fluctuations during the period made it difficult to establish a pattern for these major ions. These fluctuations probably resulted from variations in brine salinity and discharge rate during the past year. Similar fluctuations were observed at Bryan Mound during the first year of discharge after which a pattern was established showing an increase in these parameters with time. The trend observed at Bryan Mound would suggest that similar changes might be expected to occur at the West Hackberry site with time.

5.2 Sediment Quality

5.2.1 Grain Size Distribution

5.2.1.1 Estuarine Sediments

Most of the estuarine sediments were poorly sorted clayey silts with average mean diameters in the range of 6.49 to 8.23 ϕ units (see Table 5-1). Percentages of sand, silt and clay, median and mean diameters, sorting, skewness and kurtosis for E1 through E5 are

Table 5-1. Average mean diameters (ϕ units) and standard deviations (S.D.) of sediments in the West Hackberry brine disposal area for May 1981 through April 1982.

Station #	Average Mean Dia. (ϕ)	# Spls.	S.D.
M1	7.08	8	0.97
M3	7.11	12	1.34
M6	8.45	10	0.74
M9	8.94	9	1.44
M10	8.01	12	1.10
M10A	8.94	12	0.64
M11	7.50	8	0.55
M15	8.91	10	0.47
M18	8.89	12	0.62
M20	9.06	10	0.74
M21	9.86	2	0.63
M22	2.91	2	0.72
DN	9.05	10	0.79
DS	8.52	11	1.08
DE	8.61	12	0.71
DW	9.01	12	0.52
NE	7.69	9	2.99
NW	9.29	9	0.55
SE	8.79	9	0.49
SW	8.16	8	1.34
E1	7.36	12	0.55
E2	7.36	12	0.84
E3	8.23	10	1.78
E4	6.79	12	0.68
E5	6.49	12	1.45

tabulated in Appendix E. All the nearshore sediments showed some variability from month to month, but E3 and E5 were highly variable in grain size distribution as is shown in Figure 5-27 where the average grain size diameters are plotted versus time. This variability with time is probably caused by tidal movement of bottom sediments. E1, E2 and E4 were moderately constant with respect to average diameter. Table 5-1 shows the average mean diameters and the standard deviations. (A high standard deviation indicates high variability).

5.2.1.2 Offshore Sediments

Most of the offshore sediments were silty clays with average diameters in the range of 7.08 to 9.86 ϕ units. One exception was M22 with average grain size diameter of 2.91 ϕ (a sandy sediment). Figure 5-28 shows average mean diameters for all stations and their corresponding standard deviations. Appendix E shows, for all stations from May 1, 1981, through April 1982, the median and mean diameters, % sand, silt and clay, sorting skewness and kurtosis. As shown in Table 5-1, stations whose sediments had highly variable mean diameters with time were M1, M3, M9, M10, DS, NE and SW. The remainder of the stations were moderately homogeneous. Figure 5-29 shows a plot of the mean diameter versus time for M18, the control station, M10A, a diffuser station, both moderately homogeneous, and M10, a highly variable station.

The stations with temporally highly variable grain size distributions most probably have inhomogeneous bottoms. The changes with time do not appear to be caused by the action of the brine diffuser.

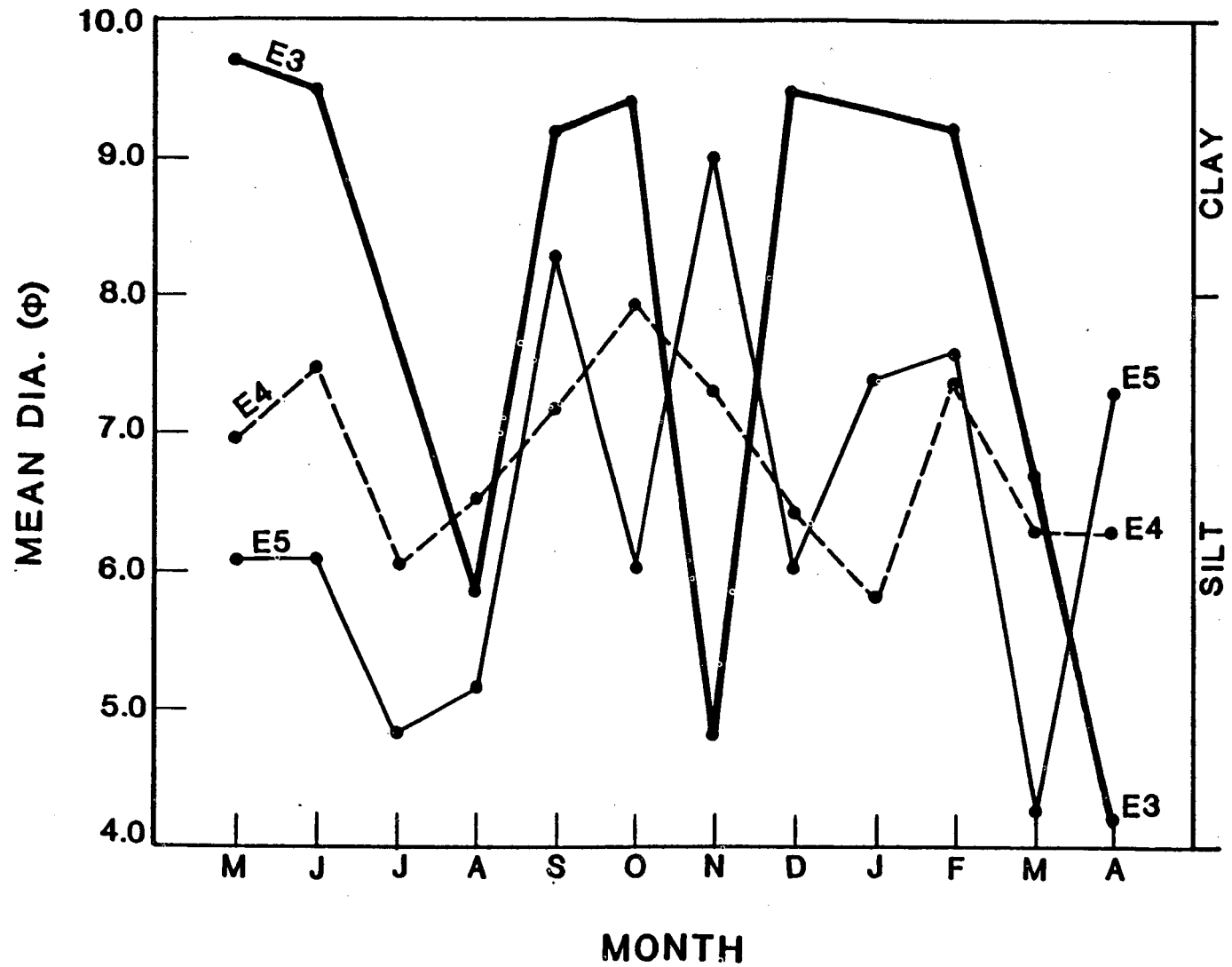


Figure 5-27. Variations of mean diameter of sediments with time in the estuarine area of the West Hackberry brine disposal area from May 1981 through April 1982.

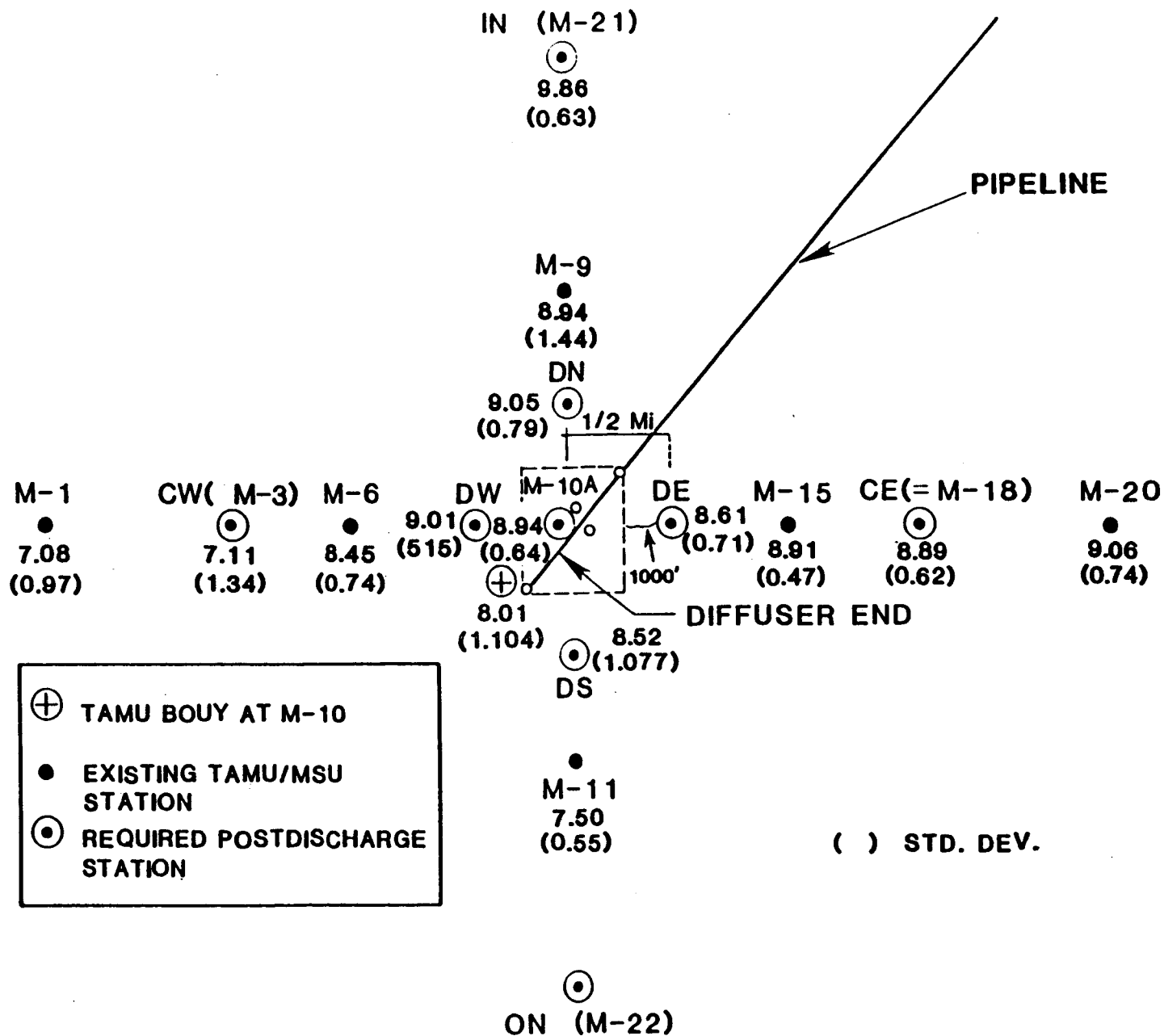


Figure 5-28. Average mean grain size and respective standard deviations for West Hackberry stations from May 1981 through April 1982.

5-42

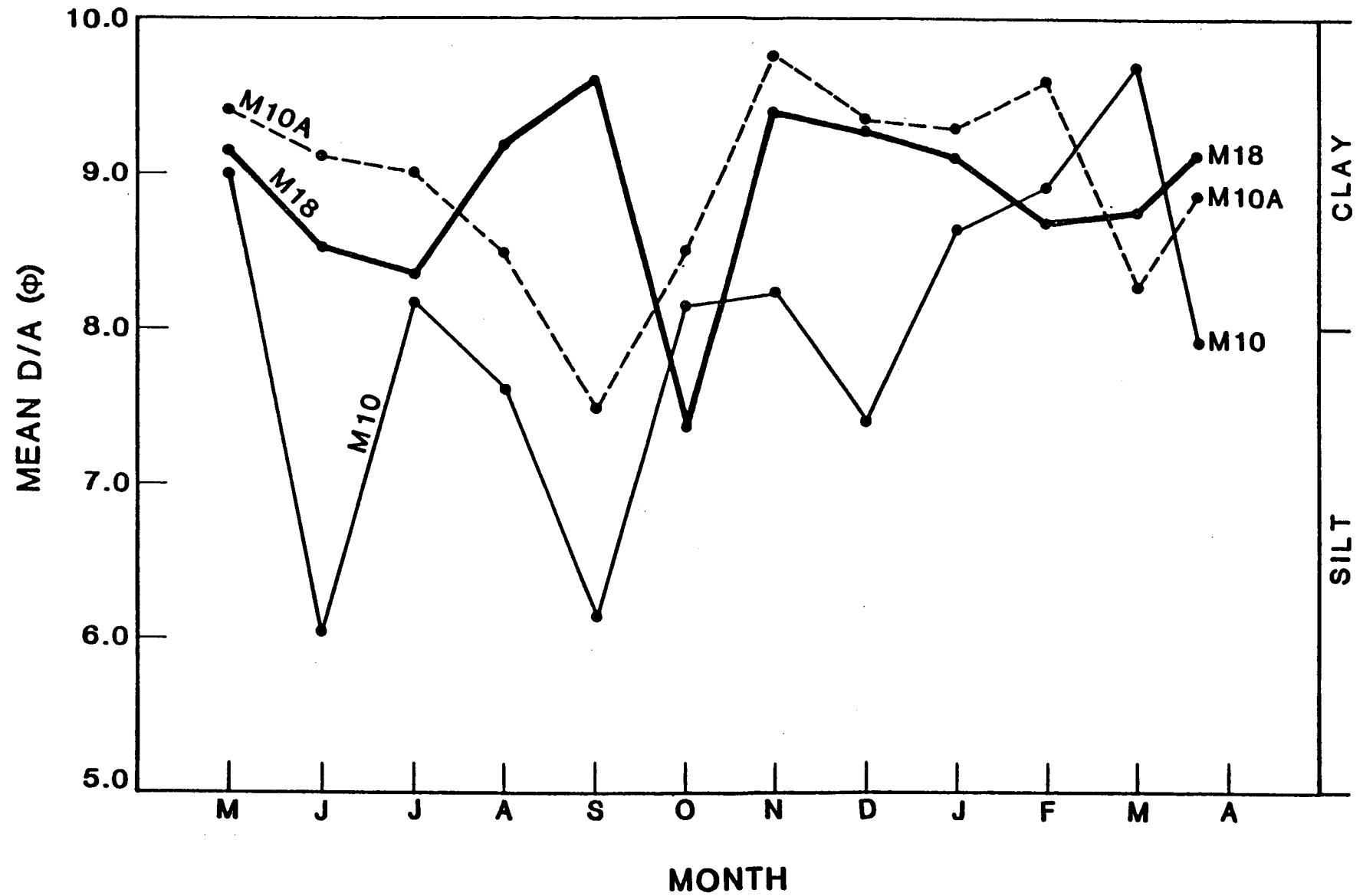


Figure 5-29. Variations of mean diameter of sediments of offshore stations M18, M10A, and M10 in the West Hackberry brine disposal area from May 1981 through April 1982.

5.2.2 Total Organic Carbon

Total organic carbon (TOC) of both nearshore and offshore sediments varied by a factor of two at a given station over the period of May 1981 to April 1982. Table 5-2 shows the monthly concentrations of TOC for each station for the year May 1981 to April 1982. Some of the variations are related to the grain size distribution of the sediments; i.e., the higher the per cent clay and silt, the higher the TOC will be. Other variations may be due to seasonal influx of organic material to the sediments due to differences in river flow.

The range of TOC at the control station M18 was 0.80 to 1.34 mgC/gram dry sediment and at M10A, a station close to the diffuser, a range of 0.62 to 1.55 mgC/gram dry sediment was found. A plot of TOC versus time for M18, M10A and M10 is given in Figure 5-30. The sediments at M10A and M18 are similar in grain size and variability with time, whereas the grain size of the sediments at M10 are considered to be highly variable with time. There is no real evidence that the diffuser has had any impact on the TOC of the sediments around the diffuser. Figure 5-31 shows that TOC is highly variable with time for the inshore stations E1 and E5. E2, E3 and E4 had similar variations in the TOC concentrations with time. Although the sediments in the nearshore area were somewhat coarser in grain size distribution, the concentration levels of TOC of the estuarine sediments were about the same overall.

5.2.3 Pore Water Salinity

5.2.3.1 Offshore Sediments

No substantial increase in pore water salinity of the offshore sediments near the diffuser (M10, M10A, DN, DW, DS, DE, etc.) occurred

Table 5-2. Summary of monthly total organic carbon concentrations in the West Hackberry brine disposal area (May 1981 - April 1982).

Station #	May	June	July	Aug	Sept	Oct	Nov	Dec	Jan	Feb	Mar	Apr
M1	--	--	--	--	0.61	0.81	0.51	0.62	0.58	0.52	0.64	0.93
M3	0.84	0.77	0.86	0.68	0.48	0.92	0.72	0.57	0.38	0.26	0.61	0.71
M6	0.79	0.89	--	--	0.73	1.01	0.77	0.91	0.84	0.48	0.79	0.88
M9	1.14	--	--	--	0.97	1.21	1.07	0.94	1.12	0.92	0.99	1.26
M10	0.78	0.63	0.64	0.64	0.76	0.91	0.55	0.36	0.45	0.84	0.88	0.87
M10A	0.71	0.83	0.62	0.68	0.49	1.17	1.17	0.97	0.95	1.08	1.12	1.55
M11	--	--	--	--	0.96	0.85	0.78	0.65	0.83	0.70	0.49	0.75
M15	0.74	1.13	--	--	1.02	1.09	0.80	1.00	0.84	0.88	1.06	0.55
M18	0.92	0.86	0.97	1.08	1.02	1.19	1.20	0.95	0.88	0.80	1.34	1.13
M20	0.81	1.03	--	--	0.96	1.21	1.23	0.97	1.05	0.60	1.18	0.82
DS	0.86	0.98	--	--	0.81	1.09	0.92	0.93	0.93	0.94	1.04	0.79
DN	1.03	1.11	--	--	0.84	1.19	1.32	0.98	1.07	0.86	0.86	1.22
DE	0.67	0.83	1.04	0.99	0.91	1.19	1.27	1.07	0.98	0.72	0.67	0.86
DW	0.70	0.57	1.03	1.03	0.86	1.17	1.11	0.83	1.02	1.06	1.43	1.10
NE	0.76	--	--	--	0.86	1.13	1.43	--	.17	0.72	1.18	0.61
NW	0.66	--	--	--	0.93	1.21	1.28	1.06	0.75	0.72	1.19	1.05
SE	0.96	--	--	--	0.81	0.86	1.35	1.02	0.94	0.86	0.72	0.67
SW	--	--	--	--	0.73	0.89	0.92	0.79	1.03	1.04	0.70	0.97
E1	0.75	1.36	0.79	1.04	0.84	1.05	0.97	0.91	0.79	0.82	0.82	0.99
E2	1.02	1.10	1.14	1.30	1.25	0.63	1.29	1.08	1.02	0.92	0.73	0.83
E3	0.94	1.51	--	0.59	1.19	1.42	0.50	1.42	--	1.18	0.47	1.10
E4	0.71	0.76	0.83	0.99	0.85	1.06	1.21	1.08	1.20	0.88	1.05	0.65
E5	0.54	0.48	1.02	0.66	0.37	1.92	1.28	0.83	0.85	0.90	0.31	1.86

5-44

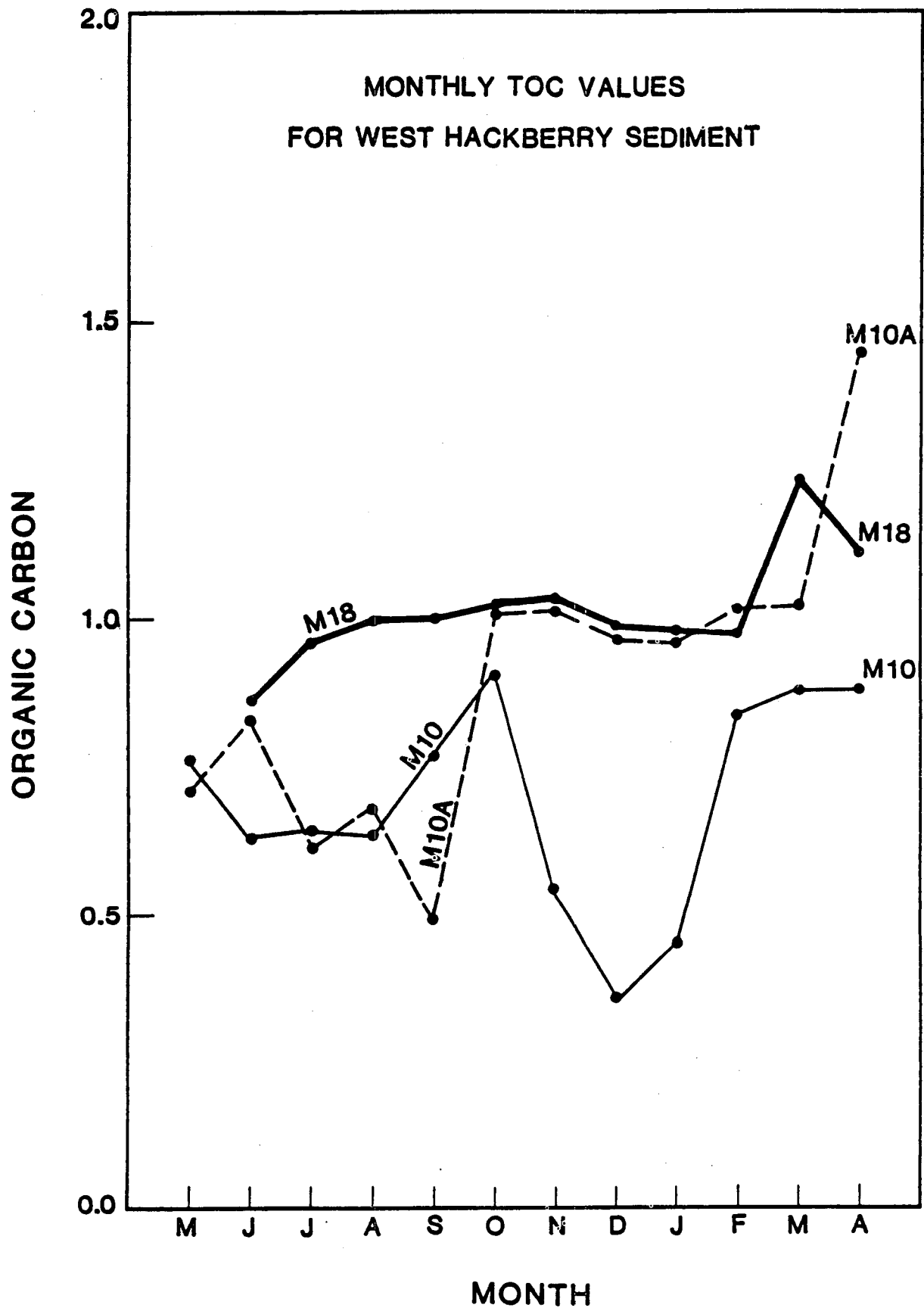


Figure 5-30. Monthly TOC values for West Hackberry sediments at offshore stations M10, M10A, and M18 from May 1981 through April 1982.

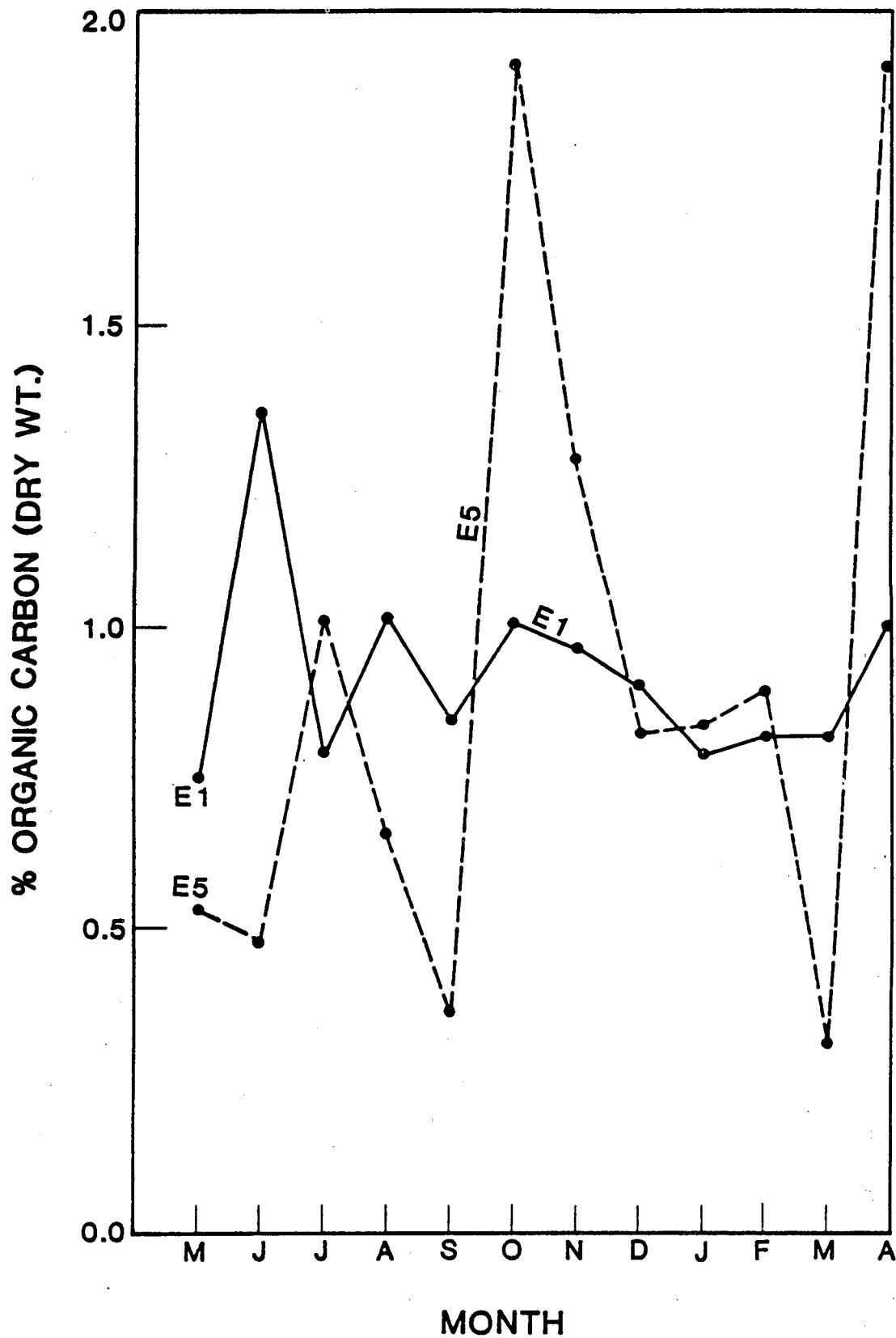


Figure 5-31. Monthly TOC concentrations of estuarine sediments of the West Hackberry area from May 1981 through April 1982.

until August 1981. See Figure 5-32 for a plot of pore water salinity versus time for the control station M18 and the test station M10A. Prior to the August 1981 sampling, the pore water salinity at M10A and other stations around the diffuser were slightly lower than that at M18 (see Figure 5-33). In August and thereafter the sediments at M10A had a pore water salinity 2 to 4% higher than at M18. Table 5-3 shows pore water salinity for all the offshore and estuarine sediments sampled from May 1981 through April 1982.

Besides M10A, other stations which had an elevated pore water salinity consistently with respect to the control station were M10, DW, DS, SE and SW. The maximum pore water salinity during the year was 34.445% at station M10A in November 1981. The corresponding pore water salinity at the control station was 30.46%, thus there was approximately a 4% difference in M10A and the unaffected control station. See Figure 5-34 for a map of the November 1981 offshore pore water salinities. As can be seen in this figure, several stations were impacted by the brine disposal other than the normal ones mentioned above. These were M15, M6, DN and DE. Figure 5-35, showing the April 1982 pore water salinity distribution, is a more normal situation. The bottom water salinities plotted in Figure 5-13 have little relation to the pore water salinity, because the sediments and water samples were collected on different days. For instance, the April 1982 pore water column salinities were collected April 28, 1982.

It should be mentioned here that even though at times pore water salinities become elevated at several stations around the diffuser, they can within a month decrease to a lower value, depending on the overlying water salinity. There does not appear to be a steady

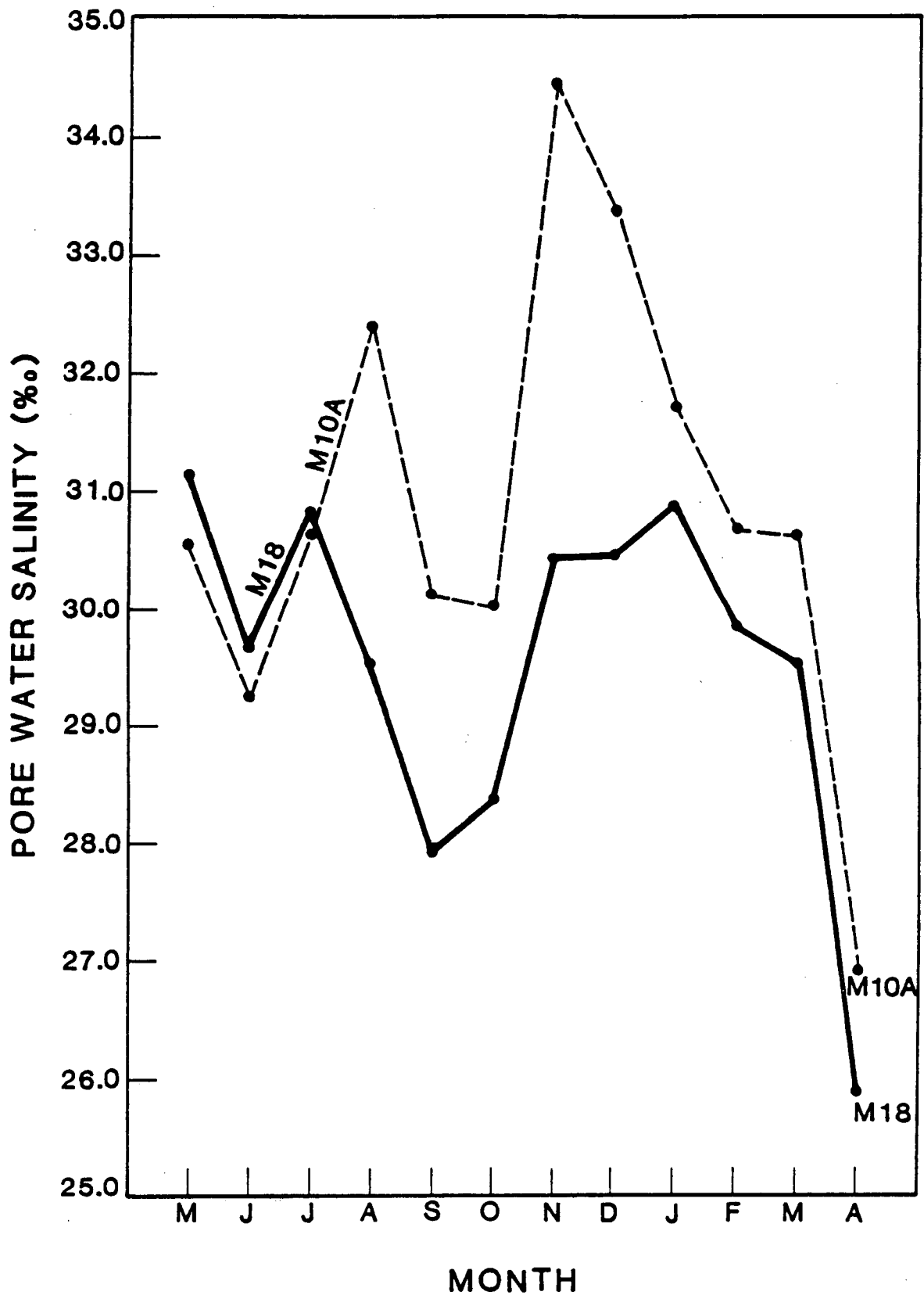


Figure 5-32. Monthly variation of pore water salinity at offshore stations M18 (control) and M10 in the West Hackberry brine disposal area from May 1981 through April 1982.

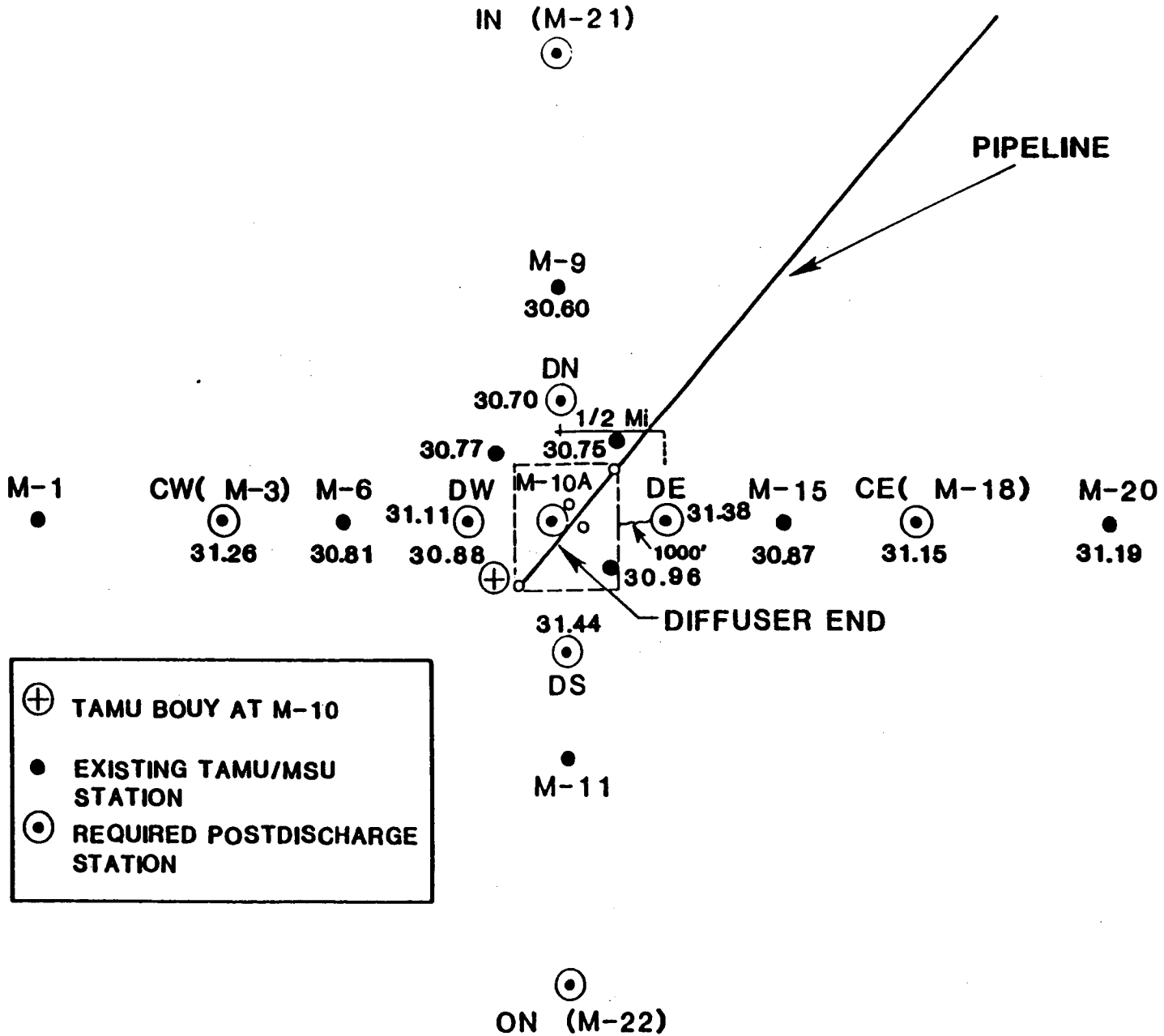


Figure 5-33. Map of May 1981 pore water salinities (o/oo) in the West Hackberry brine disposal area.

Table 5-3. Summary of monthly pore water salinity for sediments in the West Hackberry brine disposal area from May 1981 - April 1982.

Station	May	June	July	Aug	Sept	Oct	Nov	Dec	Jan	Feb	Mar	Apr
E1	17.143	11.528	7.441	3.404	6.385	8.270	8.951	10.929	12.772	14.367	4.527	6.724
E2	21.515	17.459	9.597	12.807	16.989	18.857	20.074	21.368	18.456	18.671	11.369	8.171
E3	26.527	23.481	--	15.419	18.174	20.046	20.841	22.169	--	22.263	18.021	16.122
E4	25.315	22.915	11.934	16.896	19.650	19.930	20.606	22.667	22.765	23.482	18.526	14.101
E5	24.542	26.306	14.801	22.161	21.959	21.933	23.772	24.340	25.053	25.068	20.577	19.429
M1	--	--	--	--	27.792	27.965	30.320	30.847	30.448	29.444	29.250	24.599
M3	31.256	29.296	30.937	30.358	27.948	28.205	30.503	30.986	30.768	29.393	29.515	24.557
M6	30.809	29.242	--	--	28.043	28.462	31.157	31.831	30.928	30.428	29.775	25.521
M9	30.600	--	--	--	27.463	27.010	30.668	30.927	30.145	29.375	28.732	25.033
M10	30.882	29.685	30.908	32.472	29.816	30.149	33.100	32.905	31.406	31.777	30.312	26.969
M10A	30.604	29.291	30.742	32.345	30.156	30.020	34.454	33.419	31.770	30.713	30.655	26.907
M11	--	--	--	--	28.411	29.075	31.797	31.914	31.882	30.803	30.995	25.201
M15	30.870	29.227	--	--	28.541	28.219	32.831	31.399	30.920	30.538	29.754	25.352
M18	31.148	29.670	30.861	29.562	27.982	28.335	30.456	30.456	30.934	29.886	29.512	25.964
M20	31.191	33.376	--	--	27.899	28.016	30.367	31.003	30.614	30.054	29.421	25.705
DN	30.703	30.038	--	--	27.948	28.131	31.747	31.325	30.887	29.825	28.916	23.962
DS	31.443	29.577	31.745	--	29.283	29.603	32.818	32.698	31.849	30.189	30.174	25.994
DE	31.376	30.826	30.529	30.600	28.185	28.001	31.292	31.483	31.079	30.169	29.522	25.255
DW	31.113	29.904	30.618	32.927	29.667	29.375	32.766	32.673	31.277	31.453	29.710	26.067
NE	30.751	--	--	--	27.481	27.997	30.995	31.936	30.042	29.558	28.850	24.079
NW	30.770	--	--	--	27.196	27.510	30.658	31.470	30.350	29.996	29.143	25.381
SE	30.955	--	--	--	28.442	30.365	31.806	31.902	30.011	30.535	29.925	25.052
SW	--	--	--	--	29.364	29.950	32.941	32.206	31.968	30.689	30.449	25.838

5-50

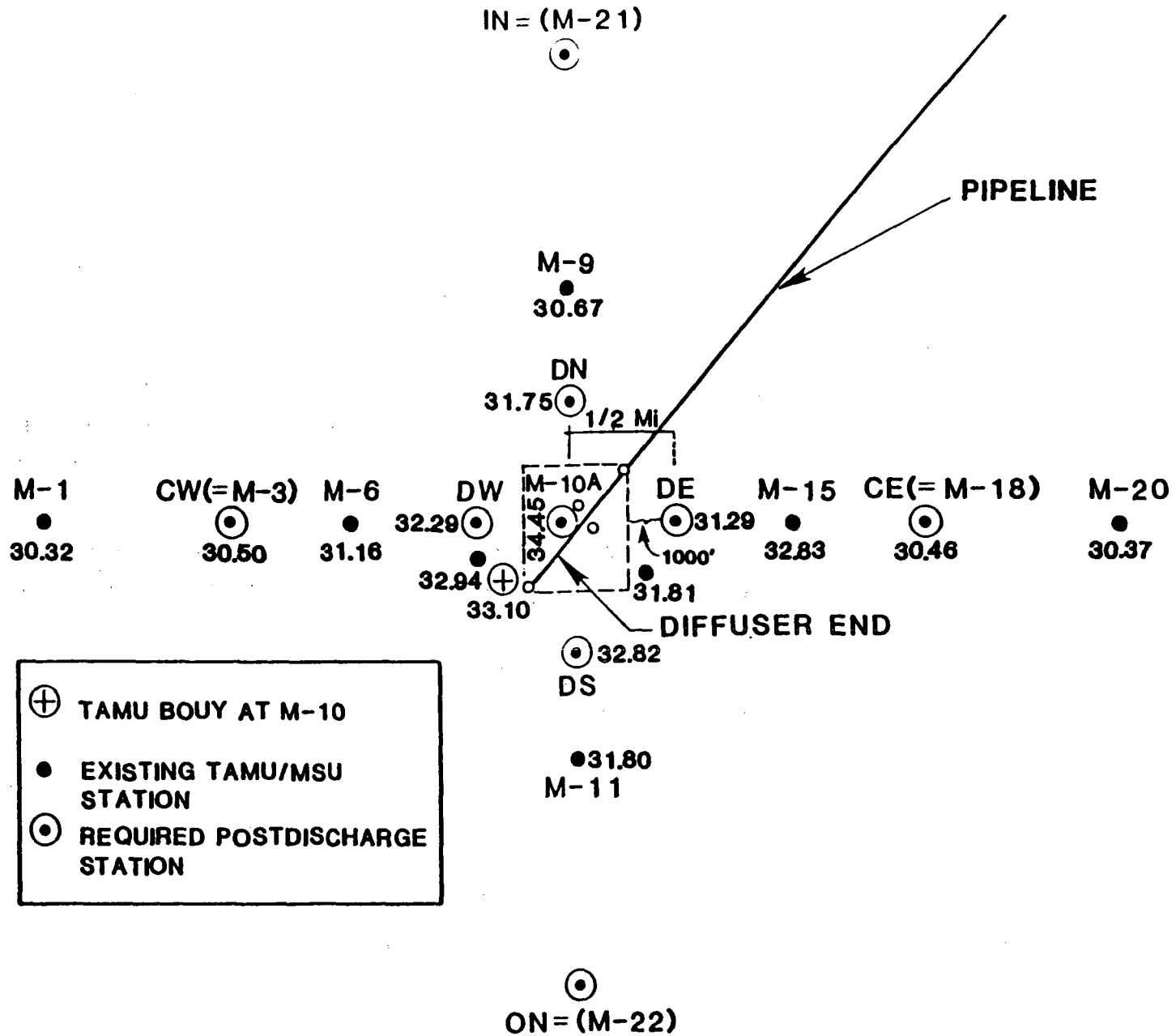


Figure 5-34. Map of November 1981 pore water salinities (o/oo) in the West Hackberry brine disposal area.

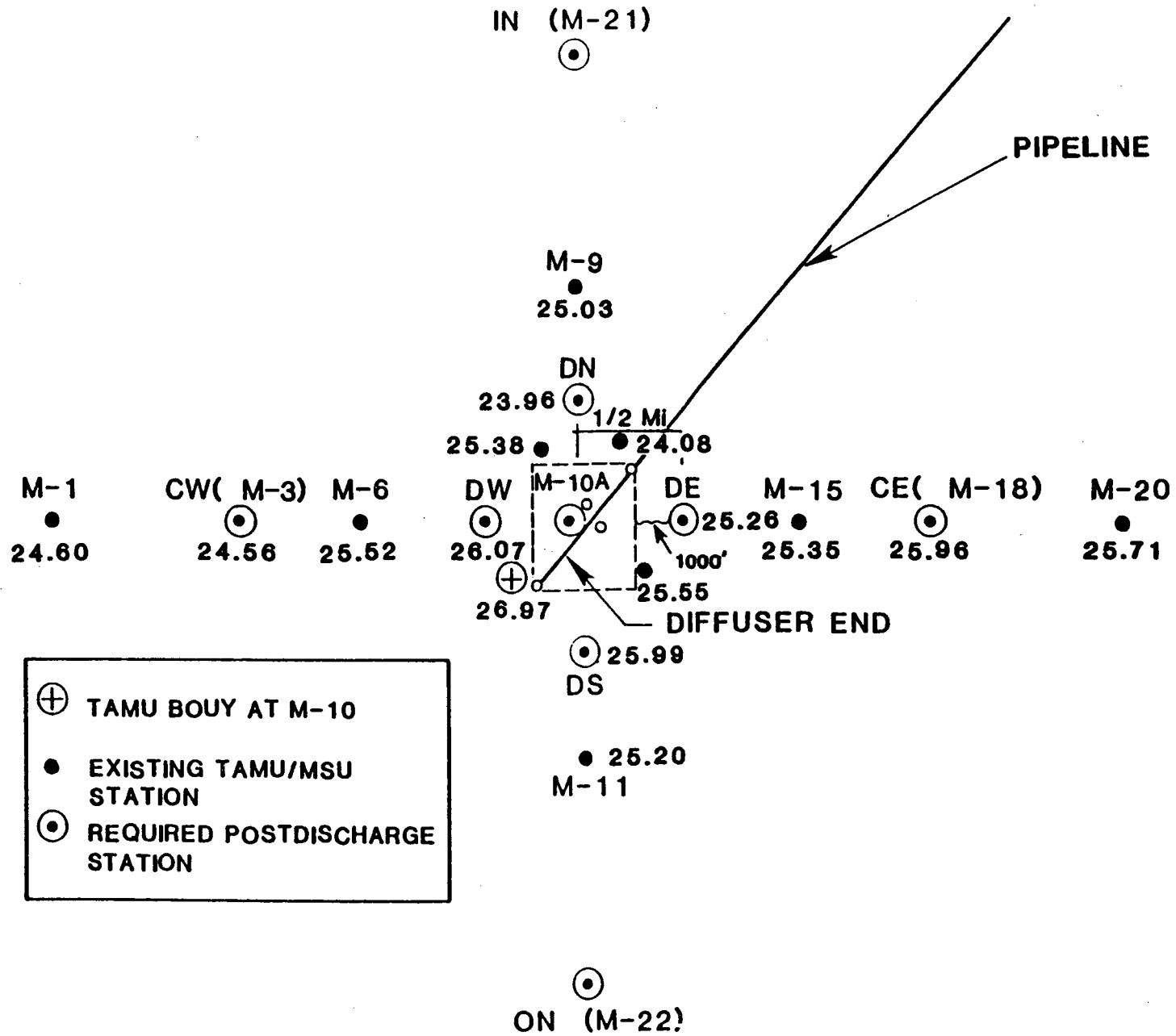


Figure 5-35. Map of April 1982 pore water salinities (o/oo) in the West Hackberry brine disposal area.

accumulation of salt in the upper three inches of sediment at the end of 18 months. It would be of interest to collect cores at stations M10 and M10A and determine the pore water salinity with depth to see how far the diluted brine might extend.

It should be noted also that really excessive pore water salinities have not been found in the impacted stations yet.

5.2.3.2 Estuarine Sediments

The pore water salinity of the sediments at E1, E2, E3, E4, and E5 were lower than the offshore sediments as expected, but also variable with time (see Figures 5-36 and 5-37). There was a gradient of increasing pore water salinity from E1 (the northernmost station) to E5. E3 and E4 had similar pore water salinities (see Figure 5-37). There is no evidence that the operation of the Brine diffuser had any impact on the pore water salinity of the estuarine sediments.

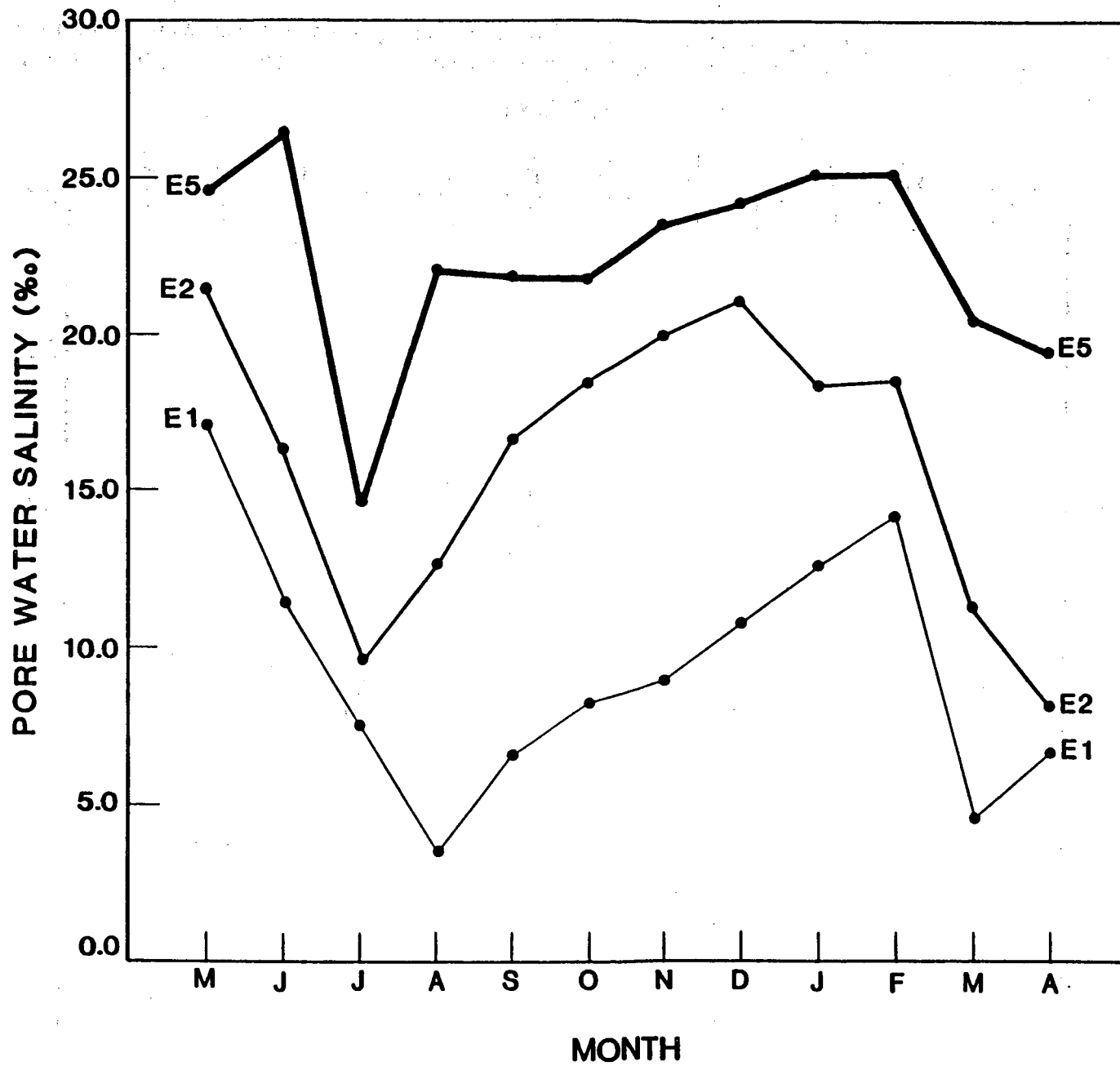


Figure 5-36. Monthly variations of pore water salinities for estuarine stations E1, E2, and E5 in the West Hackberry brine disposal area from May 1981 through April 1982.

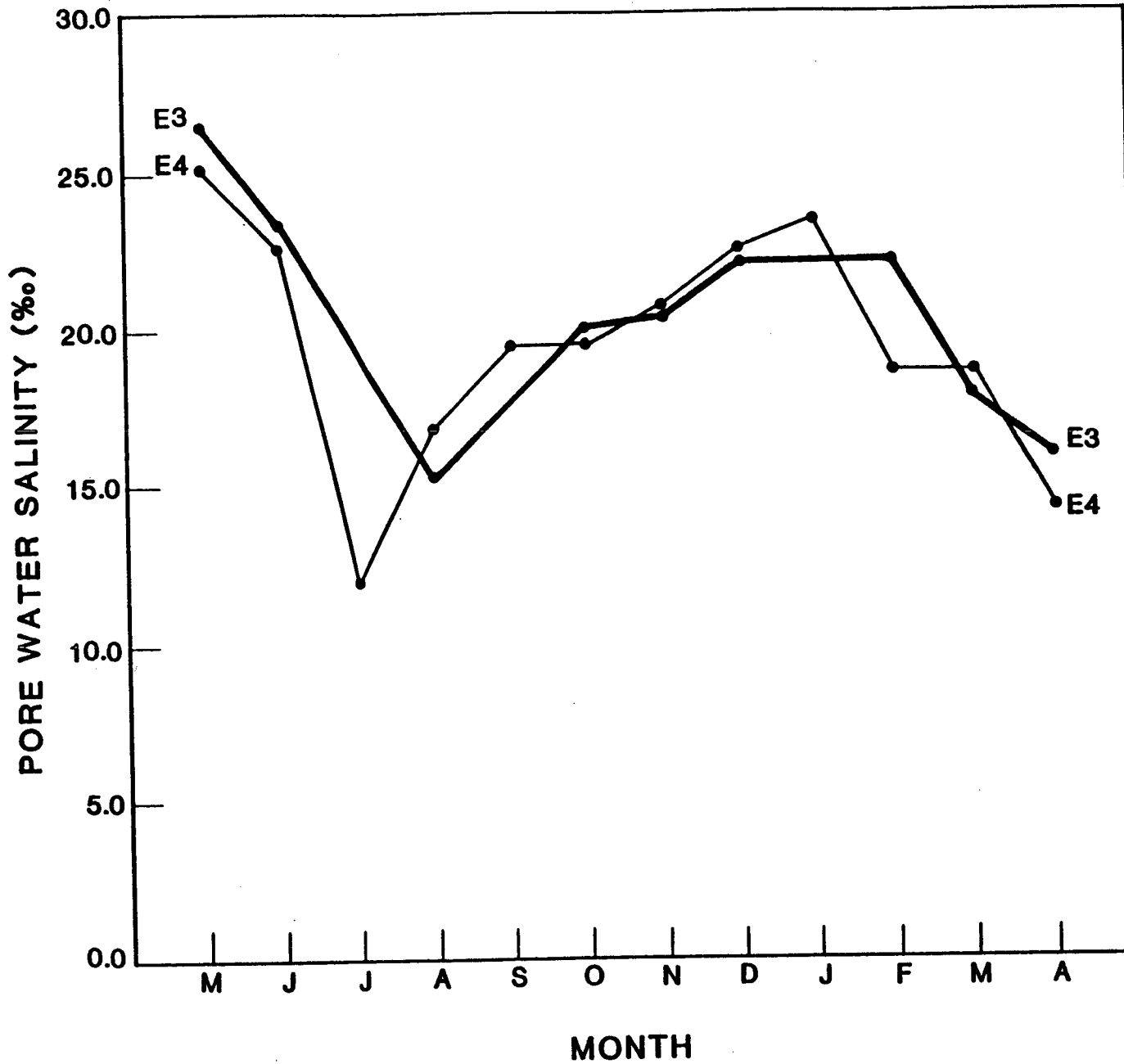


Figure 5-37. Monthly variations of the pore water salinities for estuarine stations E3 and E4 in the West Hackberry brine disposal area from May 1981 through April 1982.

5.3 Special Pollutant Survey

5.3.1 Introduction

The special pollutant survey was undertaken in order to determine:

a) what pollutants may be introduced from the Intracoastal Waterway to the brine pond and finally to the area of the diffuser,

b) what pollutants may be introduced into the area of the diffuser by the brine water produced at the SPR site in West Hackberry and pumped offshore, and

c) to see if significant changes in ionic balance of total metals and major ions have been caused by discharge of brine offshore in the area of the diffuser.

The survey measured the major ions, total metals and the group of pesticides, herbicides and high molecular weight hydrocarbons listed in Table 5-4. These pollutants were determined in samples collected at the intake structure (station E1) located in the Intracoastal Waterway, the brine pond located at the West Hackberry brine pump station and at the diffuser site (station M10A) located 6.2 nm offshore. Water and sediment samples were collected at stations E1 and M10A and in addition, two species of benthic biota were collected at station M10A. Only water samples were collected at the brine pond. The stations were all sampled the same day and were sampled one week prior to discharge, one month after the start of discharge and every six months after the second survey.

Table 5-4. List of parameters to be measured in the Special Pollutant Sampling Tasks.

(1) Eh	Total metals:
(2) pH	(9) As
Major ions:	(10) Cu
(3) Ca	(11) Cr
(4) Cl	(12) Hg
(5) K	(13) Mg
(6) Mg	(14) Zn
(7) Na	(15) Cd
(8) SO ₄	

PESTICIDES, HERBICIDES

AND HIGH MOLECULAR WEIGHT HYDROCARBONS

- (16) Molinate (Ordram)
- (17) Dieldrin
- (18) Propanil (Stam, Propanex)
- (19) 2, 4, - D
- (20) Trifluralin (Treflan)
- (21) Vernolate
- (22) Aldrin
- (23) Total DDT (all isomers)
- (24) Chlordane (and its isomers)
- (25) Silvex
- (26) 2, 4, 5 - T
- (27) Parathion
- (28) Guthion
- (29) Toxaphene
- (30) HCB
- (31) PCB 1232
- (32) PCB 1242
- (33) PCB 1248
- (34) PCB 1254
- (35) PCB 1260
- (36) High Molecular Weight Hydrocarbons (HMWH)
- (37) Identification of top 20 peaks

5.3.2 Sampling Method

Sampling was done at all three stations, the intake structure (E1), the brine pond and diffuser (M10A) on the same day. Surveys were conducted on May 5, 1981, June 1, 1981 and on March 30, 1982. The May 5 survey was done just prior to start of discharge; June 1 corresponded to sampling within one month after start of discharge and March 30 was the six month sampling. The six month survey was conducted originally on November 13, 1981 but problems with the analysis forced a second survey to be resampled on March 30. A discussion of this problem will be made in the discussion section on hydrocarbons.

Water and sediment samples were collected at stations E1 and M10A while a water sample was collected at the brine pond. In addition two species of benthic biota were collected at station M10A. The selected benthic biota were moon snails (Polinicies duplicatus) and white shrimp (Penaeus setiferus). White shrimp was selected due to the possibility of accumulation of pollutants and subsequent transfer to man. The need for the sampling of a predator at a low trophic level with limited mobility and sufficient biomass led to selection of moon snails. Insufficient biomass of moon snails were often found even after repeated trawls so spider crab (Libinia dubia) was selected as an alternate benthic species. As a result, the only complete set of data obtained for this investigation is for white shrimp.

Water samples were collected using a three liter Van Dorn sampler

at mid-depth and were transferred to glass bottles supplied by the subcontractor for pesticide analysis and plastic bottles for metal analysis. The sediment samples were collected at station E1 using a 0.05 m² Ekman grab and at station M10A using a 0.1 m² Smith-McIntyre grab sampler. The upper few centimeters of the grab samples were placed in glass bottles supplied by the subcontractor for pesticide analysis and Whirl-Pak bags for metal and major ion analysis. The benthic biota were collected at the diffuser site (station M10A) during fifteen minute trawls using a 4.9 meter otter trawl with a 1.9 cm bar mesh netting. When insufficient biomass was collected, the trawls were repeated with samples wrapped in aluminum foil.

All samples were labeled with the cruise number, the station number and the date of collection. The biota samples placed in aluminum foil were sealed with freezer tape and labeled. All samples were stored on ice until returned to the laboratory. The water samples for pesticide analysis and all sediment samples were stored at 4°C until transfer to the subcontractor. The water samples for metal analysis were acidified with nitric acid to pH 2.

The samples for pesticide analysis were transferred to the subcontractor using a letter of transmittal with copies going to subcontractor, the principal investigator and the technical director. The letter contained the information: date of transmittal, type(s) of sample(s), type of vehicle used to transport the samples, person(s) handling transfer of sample(s) and to whom the sample(s) were transferred.

5.3.3 Laboratory Analyses

Water and sediment samples were analyzed for major ions, total metals and the pesticides, herbicides and hydrocarbons listed in Table 5-4. Water and sediment samples were analyzed for major ions, total metals, pesticides, herbicides and hydrocarbons. Benthic biota were analyzed for total metals, pesticides, herbicides and hydrocarbons. The following section summarizes the chemical methods used in the analysis of major ions, total metals, herbicides, pesticides and hydrocarbons.

5.3.3.1 Major ions

The concentrations of calcium in water and sediment samples were analyzed by the EDTA titrimetric procedure. Murexide or Eriochrome Blue-Black R were used as indicators in the EDTA titration (Methods for Chemical Analysis of Water and Wastes EPA-600 4-79-020, method 215.2).

The concentration of chloride in water and sediment samples were analyzed by the mercuric nitrate titration of an acidified sample with a mixed diphenylcarbazone-bromophenol blue indicator (Methods for Chemical Analysis of Water and Wastes EPA-600 4-79-020, method 325.3).

The sodium and potassium levels in water and sediment samples were analyzed by the flame photometric method (Standard Methods for the Examination of Water and Wastewater, 14th edition, 1975).

The concentration of magnesium in water and sediment samples were analyzed by the photometric (B & L Spec. 20) method. The magnesium ions in a dechlorinated sample were precipitated as magnesium hydroxide

in the presence of brilliant yellow (Standard Method for the Examination of Water and Wastewater, 14th edition, 1975).

The water and sediment levels of sulfate were analyzed by the turbidimetric method. Sulfate was converted to a barium sulfate suspension under controlled conditions. The resulting turbidity was measured on a spectrophotometer and concentration determined from standard curves (Methods for Chemical Analysis of Water and Wastes EPA-600 4-79-020, method 375.4).

5.3.3.2 Total metals

5.3.3.2.1 Water

The analyses of cadmium, copper, and zinc were done on whole water samples that were acidified to pH 2.4, chealated with ammonium pyrrolidine dithiocarbamate (APDC), extracted with methyl isobutyl ketone (MIBK) and analyzed by flame atomic absorption (Methods for Chemical Analysis of Water and Wastes EPA-600 4-79-020, method 220.1, copper; method 289.1, zinc).

The analyses for arsenic in whole water samples was done by chealating and extracting arsenic by the method presented for copper, magnesium and zinc. The MIBK extracts were evaporated to dryness, the residues dissolved in nitric acid and analyzed by flameless atomic absorption (Methods for Analysis of Water and Wastes EPA-600 4-79-020, method 206.2).

Whole water samples were analyzed for mercury by the cold vapor flameless atomic absorption technique (Methods for Analysis of Water and Wastes EPA-600 4-79-020, method 245.1).

Magnesium was determined by adding lanthanum chloride solution (1:10) to the sample and standards and read directly by atomic absorption (Methods for Chemical Analysis of Water and Wastes EPA-600 4-79-020, Method 242.1).

Chromium was determined in whole water samples by oxidizing with potassium permanganate and sodium azide, chealated with APDC, extracted with MIBK and analyzed by flame atomic absorption (Methods for Analysis of Water and Wastes EPA-600 4-79-020, method 218.3).

5.3.3.2.2 Sediment

Arsenic, cadmium, chromium, copper, magnesium and zinc were extracted with nitric and hydrochloric acids with heat. The extracts were cooled, filtered and analyzed by flame atomic absorption (chromium, copper, magnesium and zinc) or flameless atomic absorption (arsenic) by the methods referenced under the section on water (Interim Method for the Sampling and Analysis of Priority Pollutants in Sediment and Fish tissue, EPA-EMSL-Cincnnati, 1978).

Mercury was determined in sediment samples by digesting in aqua regia, oxidizing with potassium permanganate and analyzed by the cold vapor flameless atomic absorption technique (Methods for Analysis of Water and Wastes EPA-600 4-79-020, method 245.5).

5.3.3.2.3 Tissue

The determination of arsenic in tissue samples was done by digesting nitric and sulfuric acids with gentle heating, refluxed with hydrogen peroxide and analyzed by gaseous hydride flame atomic

absorption (Interim Method for the Sampling and Analysis of Priority Pollutants in Sediments and Fish Tissue, EPA-EMSL - Cincinnati, 1978).

Cadmium, chromium, copper, magnesium, and zinc were determined in tissue samples by charring with sulfuric acid in an oven followed by a muffle furnace. The ash was dissolved in nitric acid and the aqueous solution analyzed by flame atomic absorption (Interim Method for the Sampling and Analysis of Priority Pollutants in Sediments and Fish Tissues, EPA-EMSL - Cincinnati, 1978).

Mercury was determined in tissue samples by digestion in nitric and sulfuric acids with gentle heating, oxidized with potassium permanganate and analyzed by the cold vapor flameless atomic absorption technique (Interim Method for the Sampling and Analysis of Priority Pollutants in Sediments and Fish Tissue, EPA-EMSL - Cincinnati, 1978).

5.3.3.3 Pesticides, herbicides and hydrocarbons

The pesticides, herbicides and hydrocarbon samples were analyzed on a Hewlett Packard 5985 microprocessor controlled dual source electron impact/chemical ionization mass spectrometer interfaced with a Model 5840 gas chromatograph. GC columns: J & W 25 meter SE 54 fused silica, Temperature Program: 60°C for 2 min. to 300°C at 10°C per minute, hold at 300°C for 15 min., injection: 1 ul sample and 100 mg d-10 anthracene as internal standard.

5.3.3.3.1 Water

Water samples were extracted with methylene chloride, at pH 9-11 and 2. The extracts were dried over anhydrous sodium sulfate and cleaned up by florisil column chromatography. The fractions were

concentrated by Kuderna-Danish and the herbicide extracts derivitized. The concentrated extracts were analyzed by total scan and selective ion monitoring GC/MS runs (Federal Register, December 3, 1979, methods 608, 614, 615 and 625; Analysis of Pesticide Residues in Human and Environmental Samples Industrial Environmental Research Laboratory, Edison, N.J.).

5.3.3.3.2 Sediment

Sediment samples were air dried, and extracted on a Soxhlet apparatus with an acetone-hexane (1:1) mixture overnight. The extracts were washed with sodium sulfate solution and extracted into hexane at pH 9 and 2. The hexane extracts were concentrated, analyzed by GC/MS (Federal Register, December 3, 1979, methods 608 and 625; Analysis of Pesticide Residues in Human and Environmental Samples, Industrial Environmental Research Laboratory, Edison, N.J.).

5.3.3.3.3 Biota

Samples of biota were ground with dry ice and the dry ice allowed to sublime in the freezer and the ground tissue extracted in a Soxhlet apparatus with acetonitrile overnight. The extracts were washed with sodium sulfate solution and extracted into hexane at pH 9 and 2. The hexane extracts were concentrated and analyzed by GC/MS (Federal Register, December 3, 1979, methods 608 and 625; Analysis of Pesticide Residues in Human and Environmental Samples, Industrial Environmental Research Laboratory, Edison, N.J.).

5.3.4 Results

Table 5-5 gives the concentrations of the major ions in water and

Table 5-5. Major ion concentrations in water and sediment at the intake structure, brine pond, and diffuser site

Date of Collection	Station	Eh	pH	Ca	Cl	K	Mg	Na	SO ₄
<u>Water (mg l⁻¹)</u>									
3-13-81	E1	+0.088	7.36	180	7260	210	435	4300	1050
5-05-81	E1	+0.182	7.19	250	10600	308	635	5200	1800
6-01-81	E1	+0.161	6.93	195	7570	268	310	4250	825
3-30-82	E1	+0.241	7.63	85	5600	178	173	2390	750
5-05-81	Brine Pond	NA*	NA	570	149000	95	90	99500	1580
6-01-81	Brine Pond	NA	NA	915	67500	177	347	33500	2710
3-30-82	Brine Pond	NA	NA	827	168000	314	163	101000	3700
3-13-81	M10A	+0.165	8.05	550	16100	310	1530	10500	2200
5-05-81	M10A	+0.171	8.15	355	15100	465	950	8300	2480
6-01-81	M10A	+0.160	8.11	380	16500	370	1030	10200	2680
3-30-82	M10A	+0.300	8.17	161	12200	407	405	5600	1560
<u>SEDIMENT (ug g⁻¹ dry weight)</u>									
3-13-81	E1	+0.078	7.30	4700	2810	800	1160	1700	<50
5-05-81	E1	+0.170	7.25	2300	8000	780	5920	6600	440
6-01-81	E1	+0.175	7.11	1920	4200	600	3580	3000	145
3-30-82	E1	+0.205	7.42	2530	4000	870	3100	3080	110
3-13-81	M10A	+0.167	8.04	5500	18900	3100	13260	11800	<50
5-05-81	M10A	NA	NA	5200	23300	2960	13200	18600	780
6-01-81	M10A	+0.160	7.40	8600	20200	2420	13120	17200	250
3-30-82	M10A	+0.255	7.85	6520	11580	1310	7680	7280	300

* NA - the analysis was not done for the parameters listed

sediment samples collected during the four surveys conducted during this study. Data for the cruise conducted during the pre-discharge phase on March 13, 1981 are included for comparison purposes (Beck et al., 1981). The remaining data are for the current study with cruises on May 5, 1981, June 1, 1981 and March 30, 1982. Samples were collected at the intake structure (station E1), brine pond and diffuser site (station M10A). The major ions measured included calcium (Ca), chlorine (Cl), potassium (K), magnesium (Mg), sodium (Na) and sulfate (SO_4) as well as the physical parameters Eh and pH.

Table 5-6 presents the concentrations of the total metals in water and sediment samples. Table 5-7 gives the total metal concentrations in the benthic biota samples. Water samples were collected at stations E1 and M10A as well as the brine pond, sediments at stations E1 and M10A and two species of benthic biota at station M10A. The selected benthic biota included white shrimp (Penaeus setiferus), and moon snails (Polinicies duplicatus). However, moon snails are often not found in sufficient biomass to allow pesticide analysis. As a result, spider crab (Libinia dubia) was selected as an alternate source of benthic biota. The total metals analyzed included arsenic (As), cadmium (Cd), chromium (Cr), copper (Cu), mercury (Hg) and zinc (Zn).

Table 5-8 shows hydrocarbon data measured in sediments at station E1 and M10A. No high molecular weight hydrocarbons have been found in water or biota samples and these samples are not included in

Table 5-6. Total metal concentrations in water at the intake structure, brine pond, and diffuser structure and sediments at the intake structure and diffuser site.

Date of Collection	Station	As	Cd	Cr	Cu	Hg	Mg	Zn
<u>WATER</u> ($\mu\text{g l}^{-1}$)								
3-13-81	E1	< 2.0	< 2.0	< 10	1.4	< .1	435000	< 20
5-05-81	E1	< 2.0	< 2.0	< 10	1.2	1.0	635000	< 20
6-01-81	E1	< 2.0	< 2.0	< 10	1.4	2.0	310000	< 20
3-30-82	E1	< 2.0	< 2.0	< 10	0.5	2.6	173000	< 20
5-05-81	Brine Pond	< 2.0	< 2.0	< 10	0.7	< .1	90000	135
6-01-81	Brine Pond	< 2.0	< 2.0	< 10	0.9	< .1	347000	80
3-30-82	Brine Pond	< 2.0	< 2.0	70	4.3	6.0	163000	180
3-13-81	M10A	< 2.0	< 2.0	< 10	1.4	< .1	1530000	< 20
5-05-81	M10A	< 2.0	< 2.0	< 10	0.9	< .1	950000	< 20
6-01-81	M10A	< 2.0	< 2.0	< 10	1.4	< .1	1030000	< 20
3-30-82	M10A	< 2.0	< 2.0	< 10	< .1	0.6	405000	50
<u>SEDIMENT</u> ($\mu\text{g kg}^{-1}$ dry weight)								
3-13-81	E1	< 1.0	< .5	12.8	10.8	0.2	3920	55.4
5-05-81	E1	< 1.0	< .5	12.1	14.4	< .1	5920	60.6
6-01-81	E1	< 1.0	< .5	10.5	12.2	< .1	3580	55.0
3-30-82	E1	< 1.0	< 1.2	12.7	13.9	0.3	3100	70.5
3-13-81	M10A	< 1.0	< .5	25.0	25.0	0.2	13260	110.2
5-05-81	M10A	< 1.0	< .5	24.0	25.6	0.1	13160	112.2
6-01-81	M10A	< 1.0	< .5	25.0	22.0	< .1	13120	82.0
3-30-82	M10A	< 1.0	< .5	22.7	25.1	0.2	7680	77.7

Table 5-7. Total metal concentrations in selected benthic biota at the diffuser site.

Date of Collection	As	Cd	Cr	Cu (concentration)	Hg	Mg	Zn
<u>Penaeus setiferus</u> ($\mu\text{g kg}^{-1}$ wet weight)							
3-03-81	< 1.0	< .5	< 1.0	8.2	0.05	580	13.6
5-05-81	< 1.0	< .5	< 1.0	14.6	0.06	575	18.4
6-01-81	< 1.0	< .5	< 1.0	13.7	0.05	710	19.5
3-30-82	< 1.0	< .5	1.7	18.4	0.10	890	16.5
<u>Polinicies duplicatus</u> ($\mu\text{g kg}^{-1}$ wet weight)							
5-05-81	< 1.0	< .5	< 1.0	9.0	0.03	1080	26.0
6-01-81	< 1.0	< .5	< 1.0	4.8	0.04	1370	14.5
<u>Libinia dubia</u> ($\mu\text{g kg}^{-1}$ wet weight)							
5-05-81	< 1.0	< .5	< 1.0	12.0	0.05	4580	44.0
3-30-82	< 1.0	1.6	1.0	17.5	0.20	3230	29.7

Table 5-8. Concentrations of hydrocarbons in sediments collected at the intake structure and diffuser site in the units of $\mu\text{g kg}^{-1}$

STATION	E1				M10			
Date of Collection	3-13-81/5-5-81/6-1-81/3-30-82 / 3-13-81/5-5-81/6-1-81/3-3-82							
COMPOUND								
pentadecane	320	ND*	ND	ND	ND	ND	ND	ND
hexadecane	480	ND	ND	ND	ND	ND	ND	ND
heptadecane	640	ND	ND	ND	ND	ND	ND	ND
octadecane	520	ND	ND	ND	160	ND	ND	ND
nonadecane	480	ND	ND	ND	160	ND	ND	ND
eicosane	480	ND	ND	ND	ND	1520	ND	ND
heneicosane	280	ND	ND	ND	ND	ND	ND	ND
docosane	280	ND	ND	ND	ND	600	ND	ND
tricosane	240	ND	ND	ND	ND	ND	ND	ND
tetracosane	ND	ND	ND	ND	200	ND	ND	ND
pentacosane	240	ND	ND	ND	120	ND	ND	ND
heptacosane	320	ND	ND	ND	ND	ND	ND	ND
octacosane	ND	ND	ND	ND	120	ND	ND	ND
nonacosane	160	ND	ND	ND	ND	ND	ND	ND
hentriacontane	80	ND	ND	ND	ND	ND	ND	ND
hentriacontene	80	ND	ND	ND	ND	ND	ND	ND
large alkanes (greater than hentriacontane)	120	ND	ND	ND	160	ND	ND	ND

* ND - below the detection limit of $50 \mu\text{g kg}^{-1}$

Table 5-8. Table 5-9 presents the pesticides and herbicides measured in water, sediment and biota samples. Analyses of all pesticides presented in Table 5-4 were attempted, however, only the compounds given in Table 5-9 have been identified during this survey.

5.3.5 Discussion

The water and sediment samples collected at station E1 and M10A showed positive Eh values throughout the study period. This would indicate the presence of oxidizing conditions in samples collected during special pollutant cruises. The pH values measured during these cruises showed values expected for sea water (~ 8) and lower values for samples collected in the Intracoastal Waterway. Eh and pH measurements were not attempted at the brine pond.

The data presented for major ions in Table 5-5 for water samples collected offshore at station M10A showed wide variations during this study. The data obtained for the March 13, and June 1, 1981 surveys agree well with the expected values for seawater. For example, Riley and Skirow (1965) reported that typical seawater would have the concentrations: Na = 10,500 mg l⁻¹, K = 380 mg l⁻¹, Ca = 400 mg l⁻¹, Cl = 19,000 mg l⁻¹ and SO₄ = 2,920 mg l⁻¹. The surveys of May 5, 1981 and March 30, 1982, however, show deviations from values expected for seawater. These variations occurred after heavy fresh water runoff and produced lowered concentrations of total metals at station M10A. This effect is very evident after the March 30, 1982 survey. It is also noted that total metals concentrations

Table 5-9. Pesticides and herbicides in water, sediment and selected biota at the intake structure, brine pond and diffuser site in the units $\mu\text{g l}^{-1}$ for water and $\mu\text{g kg}^{-1}$ for sediment and selected biota.

Date of Collection	Station	PCB 1242	HCB	Silvex	Parathion (concentration)	d-BHC	BEHP**	DNBP**
WATER								
3-13-81	E1	ND *	ND	ND	ND	ND	ND	ND
5-05-81	E1	ND	ND	ND	ND	ND	ND	ND
6-01-81	E1	ND	ND	ND	ND	ND	ND	ND
3-30-82	E1	0.2	0.01	ND	ND	0.1	ND	ND
3-13-81	Brine Pond	ND	ND	ND	ND	ND	ND	ND
5-05-81	Brine Pond	ND	ND	ND	ND	ND	ND	ND
6-01-81	Brine Pond	ND	ND	ND	ND	ND	ND	ND
3-30-82	Brine Pond	0.4	0.02	ND	ND	ND	ND	ND
3-13-81	M10A	ND	ND	ND	ND	ND	ND	ND
5-05-81	M10A	ND	ND	ND	ND	ND	ND	ND
6-01-81	M10A	ND	ND	ND	ND	ND	ND	ND
3-30-82	M10A	0.2	0.02	ND	ND	ND	ND	ND
SEDIMENT								
3-13-81	E1	ND	ND	ND	ND	ND	ND	ND
5-05-81	E1	ND	ND	ND	ND	ND	ND	ND
6-01-81	E1	ND	ND	ND	ND	ND	ND	ND
3-30-82	E1	180	6.4	100	120	ND	>18000	ND
3-13-81	M10A	ND	ND	ND	ND	ND	ND	ND
5-05-81	M10A	ND	ND	ND	ND	ND	ND	ND
6-01-81	M10A	ND	ND	ND	ND	ND	ND	ND
3-30-82	M10A	100	4.4	ND	70	ND	>150000	230
BIOTA								
3-13-81		ND	ND	ND	ND	ND	ND	ND
5-05-81	<u>Penaeus setiferus</u>	ND	ND	ND	ND	ND	ND	ND
6-01-81		ND	ND	ND	ND	ND	ND	ND
3-30-82		190	7.5	ND	ND	ND	>31000	ND
5-05-81	<u>Libinia dubia</u>	ND	ND	ND	ND	ND	ND	ND
3-30-82		210	8.2	ND	ND	ND	33000	ND
5-05-81	<u>Polinicies duplicatus</u>	ND	ND	ND	ND	ND	ND	ND
6-01-81		ND	ND	ND	ND	ND	ND	ND

* ND - the detection limit for PCB-1242 was $0.02 \mu\text{g l}^{-1}$, d-BHC was $0.006 \mu\text{g l}^{-1}$ measured in a composite chlorinated pesticide and PCB standard analyzed by GC/ECD. The detection limit for parathion is expected to be similar to PCB-1242 since it was extracted from similar medium. All other detection limits for compounds analyzed in water, sediments and tissue samples were expected to meet or exceed the limits stated in Federal Register (December 3, 1979) Vol. 44, No. 233, pages 69464-69575.

** The two compounds are BEHP - bis (2-ethyl hexyl) phthalate and DNBP - di-nbutyl phthalate.

measured at station E1 were also lowered significantly during March 1982 due to heavy rainfall upriver during February and March 1982.

It is clear from the data presented in Table 5-5 that the brine water pumped offshore has not altered the major ion concentrations or ionic ratios at station M10A. Elevated concentrations of Na and Cl are expected from the discharge of brines but Table 5-5 shows that the discharged brine contains higher Ca and lower Mg concentrations when compared to seawater. These major ions could possibly be used to identify changes in the water column at the diffuser. However, only average or lower values of Ca and Mg have been found at M10A suggesting the absence of change. The largest effect on major ions observed in the current study appears to be due to runoff of fresh water in the coastal area.

Sediment samples were collected at stations E1 and M10A with the major ions determined from 1 N HNO_3 leachates. The major ion concentrations were higher in the marine sediments compared to samples collected at E1. The concentrations of major ions decreased significantly during the March 30, 1982 survey at M10A and this appears to be related to reduced concentrations of major ions in the water column. The sediments at E1 would not appear to introduce major ions that would alter the concentrations of major ions in the diffuser area.

Tables 5-6 and 5-7 present data for total metals measured in water, sediment and biota samples collected in this survey. The data

for total metals measured in water samples indicate low concentrations for most metals with some below detection limits (As, Cd, Cr and Zn). The brine pond water differed from other samples due to higher concentrations of zinc, copper and mercury during the March 1982 cruise.

Total metal concentrations in the 1 N HNO₃ leachates from sediments continue to disagree with the evaluation of the West Hackberry site measured by Tillery (1980). Tillery (1980) reported the values: Cd = 0.060 ug g⁻¹, Cr = 6.3 ug g⁻¹, Cu = 7.4 ug g⁻¹, Hg = 0.059 ug g⁻¹ and Zn = 38 ug g⁻¹ as dry weight for sediments collected during the winter months. The current study shows higher concentrations of Cr, Cu and Hg by factors of about 4 when compared to Tillery's results. However, our values agree well with other studies along the Gulf Coast (Hann et al, 1980, 1981 a, b; Science Applications, Inc., 1978) using 1 N HNO₃ leachates. The results reported above can only be compared to the diffuser site (M10A) data in Table 5-6. No prior data appears to exist for sediments collected at the intake structure so no comparisons can be made. It is clear from the results presented in Table 5-6 that concentrations of total metals are not changing with time at either sampling site. It is unlikely that total metals leaching from sediments at E1 would introduce metals to offshore waters, since the concentrations of total metals are not significantly different between sediments collected at E1 and M10A.

Table 5-7 presents total metal concentrations in three species of benthic biota: Penaeus setiferus (white shrimp), Polinicies duplicatus

(moon snails), and Libinia dubia (spider crab). The moon snail and spider crab are alternate biota to insure collection of sufficient biomass for chemical analysis. The total metals found in biota at M10A are in good agreement with previous studies done by Tillery (1980). There is little variation in metal concentrations for each species or between species. The only changes found in the study are the increased concentrations of Cr in white shrimp and Cd in the spider crab for the March 30, 1982 survey. However, there does not appear to be a trend toward changing metal concentrations in biota collected in the vicinity of the diffuser.

The results of the pesticide, herbicide and high molecular weight hydrocarbons analysis of water, sediment and benthic biota samples are presented in Tables 5-8 and 5-9. Table 5-4 presents the list of pollutants that were analyzed in the current study. Tables 5-8 and 5-9 presents only those compounds that have been identified to the present time.

The water and biota samples collected during the current investigation contained no detectable levels of high molecular weight hydrocarbons. The sediments collected at stations E1 and M10A contained the hydrocarbons listed in Table 5-8. These hydrocarbons ranged from pentadecane to hydrocarbons larger than hentriacontene in the March 13 and May 5, 1981 surveys. During the last two surveys none of these compounds have been identified. The high molecular weight hydrocarbons found in this survey do not have their origins in petroleum related activities.

Table 5-9 presents the pesticides and herbicides that have been

identified to date in water and sediment samples collected at stations E1 and M10A, water collected at the brine pond and biota samples at station M10A. No pesticides or herbicides had been identified in the sample area until the survey of March 30, 1982. The March 1982 data analysis included the use of electron capture detector (ECD) while in the previous three surveys only the results of repeated GC/MS scans were reported. The use of repeated GC/MS scans preclude observation of the polychlorinated compounds due to very poor sensitivity of the method. The pollutants identified in the March 1982 cruise included the compounds: PCB-1242, HCB, silvex, parathion, delta-BHC, bis (2-ethyl hexyl) phthalate (BEHP) and di-n-butyl phthalate (DNBP). PCB-1242 and HCB were found in all samples collected during the March cruise and appear to show a biological enrichment in the biota. BEHP was found in extremely high concentrations in sediments at E1 and M10A and biota at M10A while DNBP in sediments at M10A. The other compounds are generally found only in sediment samples.

The March 1982 cruise was originally scheduled for November 13, 1981 but poor results for the analysis of pesticides, herbicides and hydrocarbons as well as failure to identify spiked compounds forced a change in subcontractors. The analysis of spiked samples by the second subcontractor was adequate and gives confidence in results presented for the March survey. Blanks were carried through the entire analysis for all water samples and no pollutants were identified in the blanks run prior to or following the analysis of our samples reducing the possibility of contamination of samples by the subcontractor.

The data presented in Table 5-9 for PCB-1242 and HCB would indicate that these pollutants are wide spread and do not appear to be the result of the leaching of salt from the West Hackberry site. It may be possible that these pollutants are being transported from the Intracoastal Waterway through the brine pond. Future sampling should be able to ascertain the significance of this problem. It is interesting to note that the U.S. Army Corps of Engineers (1976) during a study of the impact of dredging operations on the Calcasieu River found PCB-1242 at levels ranging from 30 to 360 $\mu\text{g kg}^{-1}$ in sediment samples. These values agree well with the results found in the current study. The extremely high concentrations of the phthalate compounds are difficult to interpret and may be the result of sample contamination or a recent spill of these compounds in the Intracoastal Waterway. Future surveys should be able to determine the significance of these results.

5.3.6 Conclusions

The brine that has been transported offshore has not altered the major ion concentrations or ionic ratios with the largest observed effect on major ion concentrations during the current study being decreases due to runoff of freshwater. No changes in major ions or total metals concentrations in sediment samples or for total metals in biota have been found to date. The following organic compounds have been identified during the current years effort: PCB-12842 HCB, parathion, silvex, delta-BHC, bis-(2-ethyl hexyl) phthalate and

di-n-butyl phthalate. The data suggest these compounds were transported offshore from the Intracoastal Waterway via the pipeline.